

Springer Proceedings in Mathematics & Statistics

Colin C. Adams
Cameron McA. Gordon
Vaughan F. R. Jones
Louis H. Kauffman
Sofia Lambropoulou
Kenneth C. Millett
Jozef H. Przytycki
Renzo Ricca
Radmila Sazdanovic *Editors*

Knots, Low- Dimensional Topology and Applications

Knots in Hellas, International Olympic
Academy, Greece, July 2016

 Springer

Springer Proceedings in Mathematics & Statistics

Volume 284

Springer Proceedings in Mathematics & Statistics

This book series features volumes composed of selected contributions from workshops and conferences in all areas of current research in mathematics and statistics, including operation research and optimization. In addition to an overall evaluation of the interest, scientific quality, and timeliness of each proposal at the hands of the publisher, individual contributions are all refereed to the high quality standards of leading journals in the field. Thus, this series provides the research community with well-edited, authoritative reports on developments in the most exciting areas of mathematical and statistical research today.

More information about this series at <http://www.springer.com/series/10533>

Colin C. Adams · Cameron McA. Gordon ·
Vaughan F. R. Jones · Louis H. Kauffman ·
Sofia Lambropoulou · Kenneth C. Millett ·
Jozef H. Przytycki · Renzo Ricca ·
Radmila Sazdanovic
Editors

Knots, Low-Dimensional Topology and Applications

Knots in Hellas, International Olympic
Academy, Greece, July 2016

 Springer

Editors

Colin C. Adams
Department of Mathematics
Williams College
Williamstown, MA, USA

Cameron McA. Gordon
Department of Mathematics
University of Texas at Austin
Austin, TX, USA

Vaughan F. R. Jones
Department of Mathematics
Vanderbilt University
Nashville, TN, USA

Louis H. Kauffman
Department of Mathematics, Statistics
and Computer Science
University of Illinois at Chicago
Chicago, IL, USA

Sofia Lambropoulou
School of Applied Mathematical
and Physical Sciences
National Technical University of Athens
Athens, Greece

Kenneth C. Millett
Department of Mathematics
University of California, Santa Barbara
Santa Barbara, CA, USA

Jozef H. Przytycki
Department of Mathematics, Columbian
College of Arts & Sciences
George Washington University
Washington, DC, USA

Renzo Ricca
Department of Mathematics
and Applications
University of Milano-Bicocca
Milan, Italy

University of Gdańsk
Gdańsk, Poland

Radmila Sazdanovic
Department of Mathematics
North Carolina State University
Raleigh, NC, USA

ISSN 2194-1009

ISSN 2194-1017 (electronic)

Springer Proceedings in Mathematics & Statistics

ISBN 978-3-030-16030-2

ISBN 978-3-030-16031-9 (eBook)

<https://doi.org/10.1007/978-3-030-16031-9>

Library of Congress Control Number: 2019935549

Mathematics Subject Classification (2010): 90B05, 90B06, 90B10, 90B15, 90B18, 90B20, 90B22, 90B25, 90B30, 90B35, 90B36, 90B40, 90B50, 90B60, 90B70, 90B80, 90B85, 90B90, 90B99

© Springer Nature Switzerland AG 2019

This work is subject to copyright. All rights are reserved by the Publisher, whether the whole or part of the material is concerned, specifically the rights of translation, reprinting, reuse of illustrations, recitation, broadcasting, reproduction on microfilms or in any other physical way, and transmission or information storage and retrieval, electronic adaptation, computer software, or by similar or dissimilar methodology now known or hereafter developed.

The use of general descriptive names, registered names, trademarks, service marks, etc. in this publication does not imply, even in the absence of a specific statement, that such names are exempt from the relevant protective laws and regulations and therefore free for general use.

The publisher, the authors and the editors are safe to assume that the advice and information in this book are believed to be true and accurate at the date of publication. Neither the publisher nor the authors or the editors give a warranty, expressed or implied, with respect to the material contained herein or for any errors or omissions that may have been made. The publisher remains neutral with regard to jurisdictional claims in published maps and institutional affiliations.

This Springer imprint is published by the registered company Springer Nature Switzerland AG
The registered company address is: Gewerbestrasse 11, 6330 Cham, Switzerland

Preface

This collection of papers originates from the conference: *International Conference on Knots, Low-Dimensional Topology and Applications—Knots in Hellas 2016*. The conference was held at the International Olympic Academy, Ancient Olympia, Greece from July 17–23, 2016. The conference was an occasion to celebrate the 70th birthday of Louis H. Kauffman.

The website for the conference is: <https://toce27.wixsite.com/knotsinhellas2016>.

The link includes detailed information on the organization of the conference, such as copies of talks given at the conference, photos and videos, as well as the members of the International and Local Committees, to all of whom, as well as to the staff of the International Olympic Academy, we are indebted for their work toward the realization and the success of the Conference.

The goal of this international cross-disciplinary conference was to enable exchange of methods and ideas as well as exploration of fundamental research problems in the fields of knot theory and low-dimensional topology, from theory to applications in sciences like biology and physics, and to provide high-quality interactions across fields and generations of researchers, from graduate students to the most senior researchers. In this sense, this volume is one of the few published books covering and combining these topics.

This volume features cutting-edge research papers written by conference participants. The authors were asked to include illuminating state-of-the-art surveys and overviews of their research fields and of the topics they presented in the conference. The book is expected to be most useful for researchers who wish to expand their research to new directions, to learn about new tools and methods in the area, and need to find relevant and recent bibliography.

The focal topics include the wide range of classical and contemporary invariants of knots and links and related topics such as three- and four-dimensional manifolds, braids, virtual knot theory, quantum invariants, braids, skein modules and knot algebras, link homology, quandles, and their homology; hyperbolic knots and

geometric structures of three-dimensional manifolds; and the mechanism of topological surgery in physical processes, knots in nature in the sense of physical knots with applications to polymers, DNA enzyme mechanisms, and protein structure and function.

We proceed now to give summaries of the chapters.

The chapter “[A Survey of Hyperbolic Knot Theory](#)” by David Futer, Efstratia Kalfagianni, and Jessica S. Purcell surveys tools and techniques for determining geometric properties of a link complement from a link diagram. In particular, it examines the tools used to estimate geometric invariants in terms of basic diagrammatic link invariants. The focus is on determining when a link is hyperbolic, estimating its volume, and bounding its cusp shape and cusp area. Sample applications are given, and open questions and conjectures are discussed.

The chapter “[Spanning Surfaces for Hyperbolic Knots in the 3-Sphere](#)” by Colin Adams studies surfaces with boundary a given knot in the 3-sphere. The paper considers such surfaces, both embedded and singular, for hyperbolic knots and discusses how the hyperbolic invariants affect the surfaces and how the surfaces affect the hyperbolic invariants.

The chapter “[On the Construction of Knots and Links from Thompson’s Groups](#)” by Vaughan F. R. Jones reviews recent developments in the theory of Thompson group representations related to knot theory. It is a readable introduction to the topology of these new relationships.

The chapter “[Virtual Knot Theory and Virtual Knot Cobordism](#)” by Louis H. Kauffman is an introduction to virtual knot theory and virtual knot cobordism. Nontrivial examples of virtual slice knots are given and determinations of the four-ball genus of positive virtual knots are explained in relation to joint work with Dye and Kaestner. The paper studies the affine index polynomial, proves that it is a concordance invariant, shows that it is invariant also under certain forms of labeled cobordism, and studies a number of examples in relation to these phenomena. In particular, the paper shows how a mod-2 version of the affine index polynomial is a concordance invariant of flat virtual knots and links, and explores a number of examples in this domain.

The chapter “[Knot Theory: From Fox 3-Colorings of Links to Yang–Baxter Homology and Khovanov Homology](#)” by Józef H. Przytycki is an introduction to knot theory from the historical perspective. The chapter describes how the work of Ralph H. Fox was generalized to distributive colorings (rack and quandle) and eventually in the work of Jones and Turaev to link invariants via Yang–Baxter operators. By analogy to Khovanov homology, the paper builds homology of distributive structures (including homology of Fox colorings) and generalizes it to homology of Yang–Baxter operators.

The chapter “[Algebraic and Computational Aspects of Quandle 2-Cocycle Invariant](#)” by W. Edwin Clark and Masahico Saito studies quandle homology theories. These theories have been developed and their cocycles have been used to

construct invariants in state-sum form for knots using colorings of knot diagrams by quandles. In this chapter, recent developments in these matters, as well as computational aspects of the invariants, are reviewed. Problems and conjectures pertinent to the subject are discussed.

The chapter “[A Survey of Quantum Enhancements](#)” by Sam Nelson is a survey article that summarizes the current state of the art in the nascent field of quantum enhancements, a type of knot invariant defined by collecting values of quantum invariants of knots with colorings by various algebraic objects over the set of such colorings. This class of invariants includes classical skein invariants and quandle and biquandle cocycle invariants as well as new invariants.

The chapter “[From Alternating to Quasi-Alternating Links](#)” by Nafaa Chbili introduces the class of quasi-alternating links and reviews some of their basic properties. In particular, the paper discusses the obstruction criteria for link quasi-alternateness introduced recently in terms of quantum link invariants.

The chapter “[Hoste’s Conjecture and Roots of the Alexander Polynomial](#)” by Alexander Stoimenov studies the Alexander polynomial. The Alexander polynomial remains one of the most fundamental invariants of knots and links in 3-space. Its topological understanding has led a long time ago to a complete understanding about what (Laurent) polynomials can occur as the Alexander polynomial of an arbitrary knot. Ironically, the question to characterize the Alexander polynomials of alternating knots turns out to be far more difficult, even though in general alternating knots are much better understood. Hoste, based on computer verification, made the following conjecture about 15 years ago: If z is a complex root of the Alexander polynomial of an alternating knot, then $\operatorname{Re} z \geq -1$. This paper discusses some results toward this conjecture, about 2-bridge (rational) knots or links, 3-braid alternating links, and Montesinos knots.

The chapter “[A Survey of Grid Diagrams and a Proof of Alexander’s Theorem](#)” by Nancy Scherich studies grid diagrams in relation to classical knot theory and computer coding of knots and links. Grid diagrams are a representation of knot projections that are particularly useful as a format for algorithmic implementation on a computer. This paper gives an introduction to grid diagrams and demonstrates their programmable viability in an algorithmic proof of Alexander’s theorem. Throughout, there are detailed comments on how to program a computer to encode the diagrams and algorithms.

The chapter “[Extending the Classical Skein](#)” by Louis H. Kauffman and Sofia Lambropoulou summarizes the skein-theoretic and combinatorial approaches to the new generalizations of skein polynomials for links. The first one of these generalizations, the invariant Θ that generalizes the HOMFLYPT polynomial, was discovered by Chlouveraki, Juyumaya, Karvounis, and the second author, and it has its roots in the Yokonuma–Hecke algebra of type A and a Markov trace defined on this algebra. The authors gave a skein-theoretic proof of the existence of Θ , while W.B. R. Lickorish gave a closed combinatorial formula for Θ . The authors also extend the Kauffman (Dubrovnik) polynomial to a new skein invariant for links and provide a Lickorish-type closed formula for this extension.

The chapter “[From the Framisation of the Temperley–Lieb Algebra to the Jones Polynomial: An Algebraic Approach](#)” by Maria Chlouveraki proves that the Framisation of the Temperley–Lieb algebra is isomorphic to a direct sum of matrix algebras over tensor products of classical Temperley–Lieb algebras. This result is used to obtain a closed combinatorial formula for the invariant for classical links obtained from a Markov trace on the Framisation of the Temperley–Lieb algebra. For a given link L , this formula involves the Jones polynomials of all sublinks of L , as well as linking numbers.

The chapter “[A Note on \$\mathfrak{gl}_{m|n}\$ Link Invariants and the HOMFLY–PT Polynomial](#)” by Hoel Queffelec and Antonio Sartori presents a short and unified representation-theoretical treatment of type A link invariants (that is, the HOMFLY–PT polynomials, the Jones polynomial, the Alexander polynomial, and, more generally, the $\mathfrak{gl}_{m|n}$ quantum invariants) as link invariants with values in the quantized oriented Brauer category.

The chapter “[On the Geometry of Some Braid Group Representations](#)” by Mauro Spera reports on recent differential geometric constructions that can produce representations of braid groups, together with applications in different domains of mathematical physics. The classical Kohno construction for the 3- and 4-strand pure braid groups is explicitly implemented by resorting to the Chen–Hain–Tavares nilpotent connections and to hyperlogarithmic calculus, yielding unipotent representations able to detect Brunnian and nested Brunnian phenomena. Physically motivated unitary representations of Riemann surface braid groups are then described, relying on Bellingeri’s presentation and on the geometry of Hermitian–Einstein holomorphic vector bundles on Jacobians, via representations of Weyl–Heisenberg groups.

The chapter “[Towards a Version of Markov’s Theorem for Ribbon Torus-Links in \$\mathbb{R}^4\$](#) ” by Celeste Damiani studies ribbon torus-links embedded in \mathbb{R}^4 . In classical knot theory, Markov’s theorem gives a way of describing all braids with isotopic closures as links in \mathbb{R}^3 . This paper presents a version of Markov’s theorem for extended loop braids with closure in $B^3 \times S^1$, as a first step toward a Markov’s theorem for extended loop braids and ribbon torus-links in \mathbb{R}^4 .

The chapter “[An Alternative Basis for the Kauffman Bracket Skein Module of the Solid Torus via Braids](#)” by Ioannis Diamantis gives an alternative basis for the Kauffman bracket skein module of the solid torus. The new basis is obtained with the use of the Temperley–Lieb algebra of type B and it is appropriate for computing the Kauffman bracket skein module of the lens spaces $L(p, q)$ via braids.

The chapter “[Knot Invariants in Lens Spaces](#)” by Bostjan Gabrovsek and Eva Horvat summarizes results regarding the Kauffman bracket skein module, the HOMFLYPT skein module, and the Alexander polynomial of links in lens spaces, represented as mixed link diagrams. These invariants generalize the classical Kauffman bracket, the HOMFLYPT, and the Alexander polynomials, respectively. We compare the invariants by means of their ability to distinguish between some difficult cases of knots with certain symmetries.

The chapter “[Identity Theorem for Pro- \$p\$ -groups](#)” by Andrey M. Mikhovich studies algebra related to knot theory and combinatorial group theory. The concept of schematization consists in replacing simplicial groups by simplicial affine group schemes. A schematic approach makes it possible to consider the problems of pro- p -group theory through the prism of Tannaka duality, concentrating on the category of representations.

The chapter “[A Survey on Knotoids, Braidoids and Their Applications](#)” by Neslihan Gügümcü, Louis H. Kauffman, and Sofia Lambropoulou is a survey of knotoids and braidoids, their theory and invariants, as well as their applications in the study of proteins. Knotoids were introduced by Turaev and they are represented by knot diagrams with ends such that the ends can inhabit different regions in the diagram. Equivalence is generated by Reidemeister moves that do not slide arcs across these free ends. New invariants of knotoids are constructed using the virtual closure and corresponding invariants in virtual knot theory. A version of the theory of braids is formulated for knotoids and applications of these structures to the study of proteins are described.

The chapter “[Regulation of DNA Topology by Topoisomerases: Mathematics at the Molecular Level](#)” by Rachel E. Ashley and Neil Osheroff studies the topology of DNA. Even though genetic information is encoded in a one-dimensional array of nucleic acid bases, three-dimensional relationships within DNA play a major role in how this information is accessed and utilized by living organisms. Because of the intertwined nature of the DNA 2-braid and its extreme length and compaction in the cell, some of the most important three-dimensional relationships in DNA are topological in nature. This article reviews the mathematics of DNA topology, describes the different classes of topoisomerases, and discusses the mechanistic basis for their actions in both biological and mathematical terms. It also discusses how topoisomerases recognize the topological states of their DNA substrates and products and how some of these enzymes distinguish supercoil handedness during catalysis and DNA cleavage.

The chapter “[Topological Entanglement and Its Relation to Polymer Material Properties](#)” by Eleni Panagiotou reviews recent results that show how measures of topological entanglement can be used to provide information relevant to dynamics and mechanics of polymers. The paper uses molecular dynamics simulations of coarse-grained models of polymer melts and solutions of linear chains in different settings. The paper applies the writhe to give estimates of the entanglement length and to study the disentanglement of polymer melts in an elongational flow.

The chapter “[Topological Surgery in the Small and in the Large](#)” by Stathis Antoniou, Louis H. Kauffman, and Sofia Lambropoulou directly connects topological changes that can occur in mathematical three-space via surgery, with black hole formation, the formation of wormholes, and new generalizations of these phenomena. This work enhances the bridge between topology and natural sciences and creates a new platform for exploring geometrical physics.

We hope the reader finds in this small collection of excellent papers a sense of the spirit of our conference and of the creativity of this topological subject.

Williamstown, USA
Austin, USA
Nashville, USA
Chicago, USA
Athens, Greece
Santa Barbara, USA
Washington, USA
Milan, Italy
Raleigh, USA

Colin C. Adams
Cameron McA. Gordon
Vaughan F. R. Jones
Louis H. Kauffman
Sofia Lambropoulou
Kenneth C. Millett
Jozef H. Przytycki
Renzo Ricca
Radmila Sazdanovic

Contents

A Survey of Hyperbolic Knot Theory	1
David Futer, Efstratia Kalfagianni and Jessica S. Purcell	
Spanning Surfaces for Hyperbolic Knots in the 3-Sphere	31
Colin C. Adams	
On the Construction of Knots and Links from Thompson’s Groups	43
Vaughan F. R. Jones	
Virtual Knot Theory and Virtual Knot Cobordism	67
Louis H. Kauffman	
Knot Theory: From Fox 3-Colorings of Links to Yang–Baxter Homology and Khovanov Homology	115
Józef H. Przytycki	
Algebraic and Computational Aspects of Quandle 2-Cocycle Invariant	147
W. Edwin Clark and Masahico Saito	
A Survey of Quantum Enhancements	163
Sam Nelson	
From Alternating to Quasi-Alternating Links	179
Nafaa Chbili	
Hoste’s Conjecture and Roots of the Alexander Polynomial	191
Alexander Stoimenov	
A Survey of Grid Diagrams and a Proof of Alexander’s Theorem	207
Nancy C. Scherich	
Extending the Classical Skein	225
Louis H. Kauffman and Sofia Lambropoulou	

From the Framisation of the Temperley–Lieb Algebra to the Jones Polynomial: An Algebraic Approach 247
 Maria Chlouveraki

A Note on $\mathfrak{gl}_{m|n}$ Link Invariants and the HOMFLY–PT Polynomial 277
 Hoel Queffelec and Antonio Sartori

On the Geometry of Some Braid Group Representations..... 287
 Mauro Spera

Towards a Version of Markov’s Theorem for Ribbon Torus-Links in \mathbb{R}^4 309
 Celeste Damiani

An Alternative Basis for the Kauffman Bracket Skein Module of the Solid Torus via Braids 329
 Ioannis Diamantis

Knot Invariants in Lens Spaces 347
 Boštjan Gabrovšek and Eva Horvat

Identity Theorem for Pro- p -groups 363
 Andrey M. Mikhovich

A Survey on Knotoids, Braidoids and Their Applications 389
 Neslihan Gügümcü, Louis H. Kauffman and Sofia Lambropoulou

Regulation of DNA Topology by Topoisomerases: Mathematics at the Molecular Level 411
 Rachel E. Ashley and Neil Osheroff

Topological Entanglement and Its Relation to Polymer Material Properties 435
 Eleni Panagiotou

Topological Surgery in the Small and in the Large 449
 Stathis Antoniou, Louis H. Kauffman and Sofia Lambropoulou

Conference Program 457

List of Participants 467

A Survey of Hyperbolic Knot Theory



David Futer, Efstratia Kalfagianni and Jessica S. Purcell

Abstract We survey some tools and techniques for determining geometric properties of a link complement from a link diagram. In particular, we survey the tools used to estimate geometric invariants in terms of basic diagrammatic link invariants. We focus on determining when a link is hyperbolic, estimating its volume, and bounding its cusp shape and cusp area. We give sample applications and state some open questions and conjectures.

Keywords Hyperbolic knot · Hyperbolic link · Volume · Slope length · Cusp shape · Dehn filling

2010 Mathematics Subject Classification 57M25 · 57M27 · 57M50

1 Introduction

Every link $L \subset S^3$ defines a compact, orientable 3-manifold boundary consisting of tori; namely, the link exterior $X(L) = S^3 \setminus N(L)$, where $N(L)$ denotes an open regular neighborhood. The interior of $X(L)$ is homeomorphic to the link complement $S^3 \setminus L$. Around 1980, Thurston proved that link complements decompose into pieces that admit locally homogeneous geometric structures. In the most interesting scenario, the entire link complement has a hyperbolic structure, that is a metric of constant curvature -1 . By Mostow–Prasad rigidity, this hyperbolic structure is

D. Futer

Department of Mathematics, Temple University, Philadelphia, PA 19122, USA

e-mail: dfuter@temple.edu

E. Kalfagianni (✉)

Department of Mathematics, Michigan State University, East Lansing, MI 48824, USA

e-mail: kalfagia@math.msu.edu

J. S. Purcell

School of Mathematical Sciences, Monash University, Clayton, VIC 3800, Australia

e-mail: jessica.purcell@monash.edu

© Springer Nature Switzerland AG 2019

C. C. Adams et al. (eds.), *Knots, Low-Dimensional Topology*

and Applications, Springer Proceedings in Mathematics & Statistics 284,

https://doi.org/10.1007/978-3-030-16031-9_1

unique up to isometry, hence geometric invariants of $S^3 \setminus L$ give topological invariants of L that provide a wealth of information about L to aid in its classification.

An important and difficult problem is to determine the geometry of a link complement directly from link diagrams, and to estimate geometric invariants such as volume and the lengths of geodesics in terms of basic diagrammatic invariants of L . This problem often goes by the names *WYSIWYG topology*¹ or *effective geometrization* [60]. Our purpose in this paper is to survey some results that effectively predict geometry in terms of diagrams, and to state some open questions. In the process, we also summarize some of the most commonly used tools and techniques that have been employed to study this problem.

1.1 Scope and Aims

This survey is primarily devoted to three main topics: determining when a knot or link is hyperbolic, bounding its volume, and estimating its cusp geometry. Our main goal is to focus on the methods, techniques, and tools of the field, in the hopes that this paper will lead to more research, rather than strictly listing previous results.

This focus overlaps significantly with the list of topics in Adams' survey article *Hyperbolic knots* [2]. That survey, written in 2003 and published in 2005, came out just as the pursuit of effective geometrization was starting to mature. Thus, although the topics are quite similar, both the results and the underlying techniques have advanced to a considerable extent. This is especially visible in efforts to predict hyperbolic volume (Sect. 4), where only a handful of the results that we list were known by 2003. The same pattern asserts itself throughout.

As with all survey articles, the list of results and open problems that we can address is necessarily incomplete. We are not addressing the very interesting questions on the geometry of embedded surfaces, lengths and isotopy classes of geodesics, exceptional Dehn fillings, or geometric properties of other knot and link invariants. Some of the results and techniques we have been unable to cover will appear in a forthcoming book in preparation by Purcell [76].

1.2 Originality, or Lack Thereof

With one exception, all of the results presented in this survey have appeared elsewhere in the literature. For all of these results, we point to references rather than giving rigorous proofs. However, we often include quick sketches of arguments to convey a sense of the methods that have been employed.

The one exception to this rule is Theorem 4.11, which has not previously appeared in writing. Even this result cannot be described as truly original, since the proof works by assembling a number of published theorems. We include the proof to indicate how to assemble the ingredients.

¹WYSIWYG stands for “what you see is what you get”.

1.3 Organization

We organize this survey as follows: Sect. 2 introduces terminology and background that we will use throughout. Section 3 is concerned with the problem of determining whether a given link is hyperbolic. We summarize some of the most commonly used methods used for this problem, and provide examples. In Sects. 4 and 5, we address the problem of estimating important geometric invariants of hyperbolic link complements in terms of diagrammatic quantities. In Sect. 4, we discuss methods for obtaining two sided combinatorial bounds on the hyperbolic volume of link complements. In Sect. 5, we address the analogous questions for cusp shapes and for lengths of curves on cusp tori.

1.4 Acknowledgements

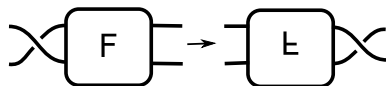
Futer is supported in part by NSF grant DMS–1408682. Kalfagianni is supported in part by NSF grants DMS–1404754 and DMS–1708249. Purcell is supported in part by the Australian Research Council. All three authors acknowledge support from NSF grants DMS–1107452, 1107263, 1107367, “RNMS: Geometric Structures and Representation Varieties” (the GEAR Network).

2 Definitions

In this section, we gather many of the key definitions that will be used throughout the paper. Most of these definitions can be found (and are better motivated) in standard textbooks on knots and links, and on 3–manifolds and hyperbolic geometry. We list them briefly for ease of reference.

2.1 Diagrams of Knots and Links

Some of the initial study of knots and links, such as the work of Tait in the late 1800s, was a study of *diagrams*: projections of a knot or link onto a plane $\mathbb{R}^2 \subset \mathbb{R}^3$, which can be compactified to $S^2 \subset S^3$. We call the surface of projection the *plane of projection* for the diagram. We may assume that a link has a diagram that is a 4-valent graph on S^2 , with over-under crossing information at each vertex. When studying a knot via diagrams, there are obvious moves that one can make to the diagram that do not affect the equivalence class of knot; for example these include *flips* studied by Tait, shown in Fig. 1, and Reidemeister moves studied in the 1930s. Without going

Fig. 1 A flype

into details on these moves, we do want our diagrams to be “sufficiently reduced,” in ways that are indicated by the following definitions.

Definition 2.1 A diagram of a link is *prime* if for any simple closed curve $\gamma \subset S^2$, intersecting the diagram transversely in exactly two points in the interior of edges, γ bounds a disk $D^2 \subset S^2$ that intersects the diagram in a single arc with no crossings.

Two non-prime diagrams are shown in Fig. 2, left. The first diagram can be simplified by removing a crossing. The second diagram cannot be reduced in the same way, because the knot is composite; it can be thought of as composed of two simpler prime diagrams by joining them along unknotted arcs. Prime diagrams are seen as building blocks of all knots and links, and so we restrict to them.

Definition 2.2 Suppose K is a knot or link with diagram D . The *crossing number* of the diagram, denoted $c(D)$, is the number of crossings in D . The *crossing number* of K , denoted $c(K)$, is defined to be the minimal number of crossings in any diagram of K .

Removing a crossing as on the left of Fig. 2 gives a diagram that is more reduced. The following definition gives another way to reduce diagrams.

Definition 2.3 Let K be a knot or link with diagram D . The diagram is said to be *twist reduced* if whenever γ is a simple closed curve in the plane of projection intersecting the diagram exactly twice in two crossings, running directly through the crossing, then γ bounds a disk containing only a string of alternating bigon regions in the diagram. See Fig. 2, right.

Any diagram can be modified to be twist reduced by performing a sequence of flypes and removing unnecessary crossings.

Definition 2.4 Two crossings in a diagram D are called *twist equivalent* if they are connected by a string of bigons, as in the far right of Fig. 2. A *twist region* in D is

**Fig. 2** Left: two diagrams that are not prime. Right: a twist reduced diagram

an equivalence class. We always require twist regions to be alternating (otherwise, D can be simplified by removing crossings).

The number of twist regions in a prime, twist reduced diagram is the *twist number* of the diagram, and is denoted $t(D)$. The minimum of $t(D)$ over all diagrams of K is denoted $t(K)$.

2.2 The Link Complement

Rather than study knots exclusively via diagrams and graphs, we typically consider the *knot complement*, namely the 3–manifold $S^3 \setminus K$. This is homeomorphic to the interior of the compact manifold $X(K) := S^3 \setminus N(K)$, called the *knot exterior*, where $N(K)$ is a regular neighborhood of K . When we consider knot complements and knot exteriors, we are able to apply results in 3–manifold topology, and consider curves and surfaces embedded in them. The following definitions apply to such surfaces.

Definition 2.5 An orientable surface S properly embedded in a compact orientable 3–manifold \overline{M} is *incompressible* if whenever $E \subset \overline{M}$ is a disk with $\partial E \subset S$, there exists a disk $E' \subset S$ with $\partial E' = \partial E$. S is *∂ -incompressible* if whenever $E \subset \overline{M}$ is a disk whose boundary is made up of an arc α on S and an arc on $\partial \overline{M}$, there exists a disk $E' \subset S$ whose boundary is made up of the arc α on S and an arc on ∂S .

Definition 2.6 Let \overline{M} be a compact orientable 3–manifold. A two–sphere $S \subset M$ is called *essential* if it does not bound a 3–ball.

Consider a (possibly non-orientable) properly embedded surface $S \subset \overline{M}$. Let \tilde{S} be the boundary of a regular neighborhood $N(S) \subset \overline{M}$. If $S \neq S^2$, it is said to be *essential* if \tilde{S} is incompressible and ∂ -incompressible.

We will say that \overline{M} is *Haken* if it is irreducible and contains an essential surface S . In this case, we also say the interior M is Haken.

Finally, we will sometimes consider knot complements that are fibered, in the following sense.

Definition 2.7 A 3–manifold M is said to be *fibered* if it can be written as a fiber bundle over S^1 , with fiber a surface. Equivalently, M is the mapping torus of a self-homeomorphism f of a (possibly punctured) surface S . That is, there exists $f : S \rightarrow S$ such that

$$M = S \times I / (x, 0) \sim (f(x), 1).$$

The map f is called the *monodromy* of the fibration.

2.3 Hyperbolic Geometry Notions

The knot and link complements that we address in this article also admit geometric structures, as in the following definition.

Definition 2.8 A knot or link K is said to be *hyperbolic* if its complement admits a complete metric of constant curvature -1 . Equivalently, it is hyperbolic $S^3 \setminus K = \mathbb{H}^3 / \Gamma$, where \mathbb{H}^3 is hyperbolic 3-space and Γ is a discrete, torsion-free group of isometries, isomorphic to $\pi_1(S^3 \setminus K)$.

Thurston showed that a prime knot in S^3 is either hyperbolic, or it is a *torus knot* (can be embedded on an unknotted torus in S^3), or it is a *satellite knot* (can be embedded in the regular neighborhood of a non-trivial knot) [81]. This article is concerned with hyperbolic knots and links.

Definition 2.9 Suppose \overline{M} is a compact orientable 3-manifold with ∂M a collection of tori, and suppose the interior $M \subset \overline{M}$ admits a complete hyperbolic structure. We say M is a *cusped manifold*.

Moreover, M has ends of the form $T^2 \times [1, \infty)$. Under the covering projection $\rho : \mathbb{H}^3 \rightarrow M$, each end is geometrically realized as the image of a horoball $H_i \subset \mathbb{H}^3$. The preimage $\rho^{-1}(\rho(H_i))$ is a collection of horoballs. By shrinking H_i if necessary, we can ensure that these horoballs have disjoint interiors in \mathbb{H}^3 . For such a choice of H_i , $\rho(H_i) = C_i$ is said to be a *horoball neighborhood* of the *cusps* C_i , or *horocusp* in M .

Definition 2.10 The boundary of a horocusp inherits a Euclidean structure from the hyperbolic structure on M . This Euclidean structure is well defined up to similarity. The similarity class is called the *cusps shape*.

Definition 2.11 For each cusp of M there is an 1-parameter family of horoball neighborhoods obtained by expanding the horoball H_i while keeping the same limiting point on the sphere at infinity. In the preimage, expanding H_i expands all horoballs in the collection $\rho^{-1}(C_i)$. Expand each cusp until the collection of horoballs $\rho^{-1}(\cup C_i)$ become tangent, and cannot be expanded further while keeping their interiors disjoint. This is a choice of *maximal cusps*. The choice depends on the order of expansion of cusps C_1, \dots, C_n . If M has a single end C_1 then there is a unique choice of expansion, giving a unique maximal cusp referred to as the *the maximal cusp* of M .

Definition 2.12 For a fixed set of embedded horoball neighborhoods C_1, \dots, C_n of the cusps of a cusped hyperbolic 3-manifold M , we have noted that the torus ∂C_i inherits a Euclidean metric. Any isotopy class of simple closed curves on the torus is called a *slope*. The *length of a slope* s , denoted $\ell(s)$, is defined to be the length of a geodesic representative of s on the Euclidean torus ∂C_i .

3 Determining Hyperbolicity

Given a combinatorial description of a knot or link, such as a diagram or braid presentation, one of the first things we would often like to ascertain is whether the link complement admits a hyperbolic structure. In this section, we describe the currently available tools to check this and give examples of knots to which they apply.

There are three main tools used to prove a link or family of links is hyperbolic. The first is direct calculation, for example using gluing and completeness equations, often with the help of a computer. The second is Thurston's geometrization theorem for Haken manifolds, which says that the only obstruction to $X(K)$ being hyperbolic consists of surfaces with non-negative Euler characteristic. The third is to perform a long Dehn filling on a manifold that is already known to be hyperbolic, for instance by one of the previous two methods.

3.1 Computing Hyperbolicity Directly

From Riemannian geometry, a manifold M admits a hyperbolic structure if and only if $M = \mathbb{H}^3 / \Gamma$, where $\Gamma \cong \pi_1(M)$ is a discrete subgroup of $\text{Isom}^+(\mathbb{H}^3) = \text{PSL}(2, \mathbb{C})$. See Definition 2.8.

Therefore one way to find a hyperbolic structure on a link complement is to find a discrete faithful representation of its fundamental group into $\text{PSL}(2, \mathbb{C})$. This is usually impractical to do directly. However, note that if a manifold M can be decomposed into simply connected pieces, for example a triangulation by tetrahedra, then these lift to the universal cover. If this cover is isometric to \mathbb{H}^3 , then the lifted tetrahedra will be well-behaved in hyperbolic 3-space. Conversely, if the lifted tetrahedra fit together coherently in \mathbb{H}^3 , in a group-equivariant fashion, one can glue the metrics on those tetrahedra to obtain a hyperbolic metric on M . This gives a condition for determining hyperbolicity, which is often implemented in practice.

Gluing and Completeness Equations for Triangulations

The first method for finding a hyperbolic structure is direct, and is used most frequently by computer, such as in the software SnapPy that computes hyperbolic structures directly from diagrams [29]. The method is to first decompose the knot or link complement into ideal tetrahedra, as in Definition 3.1, and then to solve a system of equations on the tetrahedra to obtain a hyperbolic structure. See Theorem 3.6.

This method is most useful for a single example, or for a finite collection of examples. For example, it was used by Hoste, Thistlethwaite, and Weeks to classify all prime knots with up to 16 crossings [55]. Of the 1, 701, 903 distinct prime knots with at most 16 crossings, all but 32 are hyperbolic.

We will give a brief description of the method. For further details, there are several good references, including notes of Thurston [80] where these ideas first appeared, and papers by Neumann and Zagier [71], and Futer and Guéritaud [35]. Purcell is developing a book with full details and examples [76].

Definition 3.1 An *ideal tetrahedron* is a tetrahedron whose vertices have been removed. When a knot or link complement is decomposed into ideal tetrahedra, all ideal vertices lie on the link, hence have been removed.

There are algorithms for decomposing knot and link complements into ideal tetrahedra. For example, Thurston decomposes the figure–8 knot complement into two ideal tetrahedra [80]. Menasco generalizes this, describing how to decompose a link complement into two ideal polyhedra, which can then be subdivided into tetrahedra [67]. Weeks uses a different algorithm in his computer software SnapPea [84].

Assuming we have a decomposition of a knot or link complement into ideal tetrahedra, we now describe how to turn this into a complete hyperbolic structure. The idea is to associate a complex number to each ideal edge of each tetrahedron encoding the hyperbolic structure of the ideal tetrahedron. The triangulation gives a complete hyperbolic structure if and only if these complex numbers satisfy certain equations: the *edge gluing* and *completeness* equations.

Consider \mathbb{H}^3 in the upper half space model, $\mathbb{H}^3 \cong \mathbb{C} \times (0, \infty)$. An ideal tetrahedron $\Delta \subset \mathbb{H}^3$ can be moved by isometry so that three of its vertices are placed at 0, 1, and ∞ in $\partial\mathbb{H}^3 \cong \mathbb{C} \cup \{\infty\}$. The fourth vertex lies at a point $z \in \mathbb{C} \setminus \{0, 1\}$. The edges between these vertices are hyperbolic geodesics.

Definition 3.2 The parameter $z \in \mathbb{C}$ described above is called the *edge parameter* associated with the edge from 0 to ∞ . It determines Δ up to isometry.

Notice if z is real, then the ideal tetrahedron is flat, with no volume. We will prefer to work with z with positive imaginary part. Such a tetrahedron Δ is said to be *geometric*, or positively oriented. If z has negative imaginary part, the tetrahedron Δ is negatively oriented.

Given a hyperbolic ideal tetrahedron embedded in \mathbb{H}^3 as above, we can apply (orientation–preserving) isometries of \mathbb{H}^3 taking different vertices to 0, 1, ∞ . By taking each edge to the geodesic from 0 to ∞ , we assign edge parameters to all six edges of the ideal tetrahedron. This leads to the following relations between edge parameters:

Lemma 3.3 *Suppose Δ is a hyperbolic ideal tetrahedron with vertices at 0, 1, ∞ , and z . Then the edge parameters of the six edges of Δ are as follows:*

- Edges $[0, \infty]$ and $[1, z]$ have edge parameter z .
- Edges $[1, \infty]$ and $[0, z]$ have edge parameter $1/(1 - z)$.
- Edges $[z, \infty]$ and $[0, 1]$ have edge parameter $(z - 1)/z$.

In particular, opposite edges in the tetrahedron have the same edge parameter.

Suppose an ideal tetrahedron Δ with vertices at 0, 1, ∞ and z is glued along the triangle face with vertices at 0, ∞ , and z to another tetrahedron Δ' . Then Δ' will have vertices at 0, ∞ , z and at the point zw , where w is the edge parameter of Δ' along the edge $[0, \infty]$. When we glue all tetrahedra in \mathbb{H}^3 around an ideal edge of the triangulation, if the result is hyperbolic then the product of all edge parameters must be 1 with arguments summing to 2π . More precisely, the sum of the logs of the edge parameters must be $0 + 2\pi i$.

Definition 3.4 (*Gluing equations*) Let e be an ideal edge of a triangulation of a 3-manifold M , for example a knot or link complement. Let z_1, \dots, z_k be the edge parameters of the edge of the tetrahedra identified to e . The *gluing equation* associated with the edge e is:

$$\prod_{i=1}^k z_i = 1 \quad \text{and} \quad \sum_{i=1}^k \arg(z_i) = 2\pi. \tag{1}$$

Writing this in terms of logarithms, (1) is equivalent to:

$$\sum_{i=1}^k \log(z_i) = 2\pi i. \tag{2}$$

A triangulation may satisfy all gluing equations at all its edges, and yet fail to give a complete hyperbolic structure. To ensure the structure is complete, an additional condition must be satisfied for each torus boundary component.

Definition 3.5 (*Completeness equations*) Let T be a torus boundary component of a 3-manifold M whose interior admits an ideal triangulation.

Truncate the tips of all tetrahedra to obtain a triangulation of T . Let μ be an oriented simple closed curve on T , isotoped to meet edges of the triangulation transversely, and to avoid vertices. Each segment of μ in a triangle cuts off a single vertex of the triangle, which comes from an edge of the ideal triangulation and so has an associated edge parameter z_i . If the vertex lies to the right of μ , let $\varepsilon_i = +1$; otherwise let $\varepsilon_i = -1$. The *completeness equation* associated to μ is:

$$\sum_i \varepsilon_i \log(z_i) = 0, \quad \text{which implies} \quad \prod_i z_i^{\varepsilon_i} = 1. \tag{3}$$

With these definitions, we may state the main theorem.

Theorem 3.6 *Suppose \overline{M} is a 3-manifold with torus boundary, equipped with an ideal triangulation. Suppose for some choice of positively oriented edge parameters $\{z_1, \dots, z_n\}$, the gluing equations are satisfied for each edge, and the completeness equations are satisfied for homology generators μ, λ on each component of $\partial\overline{M}$. Then the interior of \overline{M} , denoted by M , admits a complete hyperbolic structure. Furthermore, the unique hyperbolic metric on M is given by the geometric tetrahedra determined by the edge parameters.*

In fact, the hypotheses of Theorem 3.6 are stronger than necessary. If \overline{M} has k torus boundary components, then only $n - k$ of the n gluing equations are necessary (see [71] or [28]). In addition, only one of μ or λ is required from each boundary component [28].

Some classes of 3-manifolds that can be shown to be hyperbolic using Theorem 3.6 include the classes of once-punctured torus bundles, 4-punctured sphere bundles, and 2-bridge link complements [49]. (In each class, some low-complexity

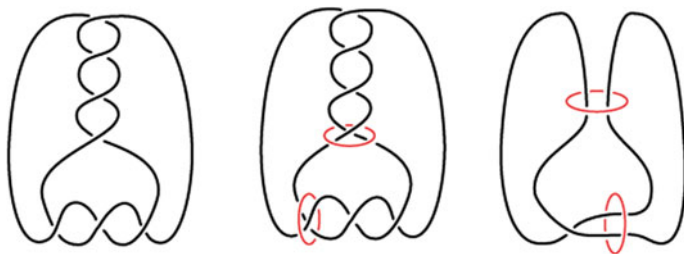


Fig. 3 Left: a diagram of a knot K . Center: adding a crossing circles for each twist region of K produces a link J . Right: removing full twists produces a *fully augmented link* L with the property that $S^3 \setminus J$ is homeomorphic to $S^3 \setminus L$

examples must be excluded to ensure hyperbolicity.) These manifolds have natural ideal triangulations guided by combinatorics. In the case of 2-bridge knot and link complements, the triangulation is also naturally adapted to a planar diagram of the link [78]. Once certain low-complexity cases (such as $(2, q)$ torus links) have been excluded, one can show that the gluing equations for these triangulations have a solution. This gives a direct proof that the manifolds are hyperbolic.

Circle Packings and Right Angled Polyhedra

Certain link complements have very special geometric properties that allow us to compute their hyperbolic structure directly, but with less work than solving nonlinear gluing and completeness equations as above. These include the Whitehead link, which can be obtained from a regular ideal octahedron with face-identifications [80]. They also include an important and fairly general family of link complements called *fully augmented links*, which we now describe.

Starting with any knot or link diagram, identify *twist regions*, as in Definition 2.4. The left of Fig. 3 shows a knot diagram with two twist regions. Now, to each twist region, add a simple unknotted closed curve encircling the two strands of the twist region, as shown in the middle of Fig. 3. This is called a *crossing circle*. Because each crossing circle is an unknot, we may perform a full twist along a disk bounded by that unknot without changing the homeomorphism type of the link complement.

This allows us to remove as many pairs of crossings as possible from twist regions. An example is shown on the right of Fig. 3. The result is the diagram of a fully augmented link.

Provided the original link diagram before adding crossing circles is sufficiently reduced (prime and twist reduced; see Definitions 2.1 and 2.3), the resulting fully augmented link will be hyperbolic, and its hyperbolic structure can be completely determined by a circle packing. The procedure is as follows.

Replace the diagram of the fully augmented link with a trivalent graph by replacing each neighborhood of a crossing circle (with or without a bounded crossing) by a single edge running between knot strands, closing the knot strands. See Fig. 4, left. Now take the dual of this trivalent graph; this is a triangulation of S^2 . Provided the original diagram was reduced, there will be a circle packing whose nerve is this

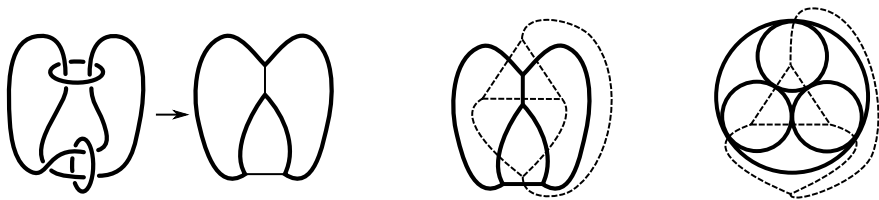


Fig. 4 Left: Obtain a 3-valent graph by replacing crossing circles with edges. Middle: The dual is a triangulation of S^2 . Right: The nerve of the triangulation defines a circle packing that cuts out a polyhedron in \mathbb{H}^3 . Two such polyhedra glue to form $S^3 \setminus L$

triangulation of S^2 . The circle packing and its orthogonal circles cut out a right angled ideal polyhedron in \mathbb{H}^3 . The hyperbolic structure on the complement of the fully augmented link is obtained by gluing two copies of this right angled ideal polyhedron. More details are in [44, 75].

3.2 Geometrization of Haken Manifolds

The methods of the previous section have several drawbacks. While solving gluing and completeness equations works well for examples, it is difficult to use the methods to find hyperbolic structures for infinite classes of examples. The method that has been most useful to show infinite examples of knots and links are hyperbolic is to apply Thurston’s geometrization theorem for Haken manifolds, which takes the following form for manifolds with torus boundary components.

Theorem 3.7 (Geometrization of Haken manifolds) *Let M be the interior of a compact manifold \overline{M} , such that $\partial\overline{M}$ is a non-empty union of tori. Then exactly one of the following holds:*

- \overline{M} admits an essential torus, annulus, sphere, or disk, or
- M admits a complete hyperbolic metric.

Thus the method to prove M is hyperbolic following Theorem 3.7 is to show \overline{M} cannot admit embedded essential surfaces of nonnegative Euler characteristic. Arguments ruling out such surfaces are typically topological or combinatorial in nature.

Some sample applications of this method are as follows. Menasco used the method to prove any alternating knot or link, aside from a $(2, q)$ -torus link, is hyperbolic [68]. Adams and his students generalized Menasco’s argument to show that almost alternating and toroidally alternating links are hyperbolic [8, 9]. There are many other generalizations, e.g. [43].

Menasco’s idea was to subdivide an alternating link complement into two balls, above and below the plane of projection, and crossing balls lying in a small neighborhood of each crossing, with equator along the plane of projection. An essential

surface can be shown to intersect the balls above and below the plane of projection in disks only, and to intersect crossing balls in what are called *saddles*. These saddles act as fat vertices on the surface, and can be used to obtain a bound on the Euler characteristic of an embedded essential surface. Combinatorial arguments, using properties of alternating diagrams, then rule out surfaces with non-negative Euler characteristic.

More generally, classes of knots and links can be subdivided into simpler pieces, whose intersection with essential surfaces is then examined. Typically, surfaces with nonnegative Euler characteristic can be restricted to lie in just one or two pieces, and then eliminated.

Thurston's Theorem 3.7 can also be used to show that manifolds with certain properties are hyperbolic. For example, consider again the gluing equations. This gives a complicated nonlinear system of equations. If we consider only the imaginary part of the logarithmic gluing equation (2), the system becomes linear: the sums of dihedral angles around each edge must be 2π . It is much easier to solve such a system of equations.

Definition 3.8 Suppose M is the interior of a compact manifold with torus boundary, with an ideal triangulation. A solution to the imaginary part of the (logarithmic) gluing equations (2) for the triangulation is called a *generalized angle structure* on M . If all angles lie strictly between 0 and π , the solution is called an *angle structure*. See [35, 66] for background on (generalized) angle structures.

Theorem 3.9 (Angle structures and hyperbolicity) *If M admits an angle structure, then M also admits a hyperbolic metric.*

The proof has been attributed to Casson, and appears in Lackenby [62]. The idea is to consider how essential surfaces intersect each tetrahedron of the triangulation. These surfaces can be isotoped into *normal form*. A surface without boundary in normal form intersects tetrahedra only in triangles and in quads. The angle structure on M can be used to define a combinatorial area on a normal surface. An adaptation of the Gauss–Bonnet theorem implies that the Euler characteristic is a negative multiple of the combinatorial area. Then one shows that the combinatorial area of an essential surface must always be strictly positive, hence Euler characteristic is strictly negative. Then Theorem 3.7 gives the result.

Knots and links that can be shown to be hyperbolic using the tools of Theorem 3.9 include arborescent links, apart from three enumerated families of non-hyperbolic exceptions. This can be shown by constructing an ideal triangulation (or a slightly more general ideal decomposition) of the complement of an arborescent link, and endowing it with an angle structure [34].

Conversely, every hyperbolic knot or link complement in S^3 admits *some* ideal triangulation with an angle structure [52]. However, this triangulation is not explicitly constructed, and need not have any relation to the combinatorics of a diagram.

3.3 Hyperbolic Dehn Filling

Another method for proving that classes of knots or links are hyperbolic is to use Dehn filling. Thurston showed that all but finitely many Dehn fillings on a hyperbolic manifold with a single cusp yield a closed hyperbolic 3-manifold [80].

More effective versions of Thurston's theorem have been exploited to show hyperbolicity for all but a bounded number of Dehn fillings. Results in this vein include the 2π -theorem that yields negatively curved metrics [21], and geometric deformation theorems of Hodgson and Kerckhoff [51]. The sharpest result along these lines is the 6-Theorem, due independently to Agol [11] and Lackenby [62]. (The statement below assumes the geometrization conjecture, proved by Perelman shortly after the papers [11, 62] were published.)

Theorem 3.10 (6-Theorem) *Suppose M is a hyperbolic 3-manifold homeomorphic to the interior of a compact manifold \bar{M} with torus boundary components T_1, \dots, T_k . Suppose s_1, \dots, s_k are slopes, with $s_i \subset T_i$. Suppose there exists a choice of disjoint horoball neighborhoods of the cusps of M such that in the induced Euclidean metric on T_i , the slope s_i has length strictly greater than 6, for all i . Then the manifold obtained by Dehn filling along s_1, \dots, s_k , denoted $M(s_1, \dots, s_k)$, is hyperbolic.*

Theorem 3.10 can be used to prove that a knot or link is hyperbolic, as follows. First, show the knot complement $S^3 \setminus K$ is obtained by Dehn filling a manifold Y that is known to be hyperbolic. Then, prove that the slopes used to obtain $S^3 \setminus K$ from Y have length greater than 6 on a horoball neighborhood of the cusps of Y . See also Sect. 5 for ways to prove that slopes are long.

Some examples of links to which this theorem has been applied include *highly twisted links*, which have diagrams with 6 or more crossings in every twist region. (See Definition 2.4.) These links can be obtained by surgery, as follows. Start with a fully augmented link as described above, for instance the example shown in Fig. 3. Performing a Dehn filling along the slope $1/n$ on a crossing circle adds $2n$ crossings to the twist region encircled by that crossing circle, and removes the crossing circle from the diagram. When $|n| \geq 3$, the result of such Dehn filling on each crossing circle is highly twisted.

Using the explicit geometry of fully augmented links obtained from the circle packing, we may give a lower bound on the lengths of the slopes $1/n_i$ on crossing circles. Then Theorem 3.10 shows that the resulting knots and links must be hyperbolic [44].

Other examples can also be obtained in this manner. For example, Baker showed that infinite families of Berge knots are hyperbolic by showing they are Dehn fillings of minimally twisted chain link complements, which are known to be hyperbolic, along sequences of slopes that are known to grow in length [18].

The 6-Theorem is sharp. This was shown by Agol [11], and by Adams and his students for a knot complement [5]. The pretzel knot $P(n, n, n)$, which has 3 twist regions, and the same number of crossings in each twist region, has a toroidal Dehn filling along a slope with length exactly 6.

3.4 *Fibered Knots and High Distance Knots*

We finish this section with a few remarks about other ways to prove manifolds are hyperbolic, and give references for further information. However, these methods seem less directly applicable to knots in S^3 than those discussed above, and the full details are beyond the scope of this paper.

Recall Definition 2.7 of a fibered knot. When the monodromy is pseudo-Anosov, the knot complement is known to be hyperbolic [82]. The figure-8 knot complement can be shown to be hyperbolic in this way; see for example [80, p. 70]. Certain links obtained as the complement of closed braids and their braid axis have also been shown to be hyperbolic using these methods [50]. It seems difficult to apply these methods directly to knots, however.

Another method is to consider bridge surfaces of a knot. Briefly, there is a notion of distance that measures the complexity of the bridge splitting of a knot. Bachman and Schleimer proved that any knot whose bridge distance is at least 3 must be hyperbolic [17]. It seems difficult to bound bridge distance for classes of examples directly from a knot diagram. Recent work of Johnson and Moriah is the first that we know to obtain such bounds [61].

4 Volumes

As mentioned in the introduction, the goal of effective geometrization is to determine or estimate geometric invariants directly from a diagram. As volume is the first and most natural invariant of a hyperbolic manifold, the problem of estimating volume from a diagram has received considerable attention. In this section, we survey some of the results and techniques on both upper and lower bounds on volume.

4.1 *Upper Bounds on Volume*

Many bounds in this section involve constants with geometric meaning. In particular, we define

$$v_{\text{tet}} = \text{volume of a regular ideal tetrahedron in } \mathbb{H}^3 = 1.0149\dots$$

and

$$v_{\text{oct}} = \text{volume of a regular ideal octahedron in } \mathbb{H}^3 = 3.6638\dots$$

These constants are useful in combinatorial upper bounds on volume because every geodesic tetrahedron in \mathbb{H}^3 has volume at most v_{tet} , and every geodesic octahedron has volume at most v_{oct} . See e.g. Benedetti and Petronio [19].

Bounds in Terms of Crossing Number

The first volume bounds for hyperbolic knots are due to Adams [1]. He showed that, if $D = D(K)$ is a diagram of a hyperbolic knot or link with $c \geq 5$ crossings, then

$$\text{vol}(S^3 \setminus K) \leq 4(c(D) - 4)v_{\text{tet}}. \tag{4}$$

Adams’ method of proof was to use the knot diagram to divide $S^3 \setminus K$ into tetrahedra with a mix of ideal and material vertices, and to count the tetrahedra. Since the subdivision contains at most $4(c(D) - 4)$ tetrahedra, and each tetrahedron has volume at most v_{tet} , the bound follows.

In a more recent paper [3], Adams improved the upper bound of (4):

Theorem 4.1 *Let $D = D(K)$ be a diagram of a hyperbolic link K , with at least 5 crossings. Then*

$$\text{vol}(S^3 \setminus K) \leq (c(D) - 5)v_{\text{oct}} + 4v_{\text{tet}}.$$

Again, the method is to divide the link complement into a mixture of tetrahedra and octahedra, and to bound the volume of each polyhedron by v_{tet} or v_{oct} respectively. The subdivision into octahedra was originally described by D. Thurston.

The upper bound of Theorem 4.1 is known to be asymptotically sharp, in the sense that there exist diagrams of knots and links K_n with $\text{vol}(S^3 \setminus K_n)/c(K_n) \rightarrow v_{\text{oct}}$ as $n \rightarrow \infty$; see [26]. On the other hand, this upper bound can be arbitrarily far from sharp. A useful example is the sequence of twist knots K_n depicted in Fig. 5. Since the number of crossings is $n + 2$, the upper bound of Theorem 4.1 is linear in n . However, the volumes of K_n are universally bounded and only increasing to an asymptotic limit:

$$\text{vol}(S^3 \setminus K_n) < v_{\text{oct}}, \quad \lim_{n \rightarrow \infty} \text{vol}(S^3 \setminus K_n) = v_{\text{oct}}$$

This holds as a consequence of the following theorem of Gromov and Thurston [80, Theorem 6.5.6].

Theorem 4.2 *Let M be a finite volume hyperbolic manifold with cusps. Let $N = M(s_1, \dots, s_n)$ be a Dehn filling of some cusps of M . Then $\text{vol}(N) < \text{vol}(M)$.*

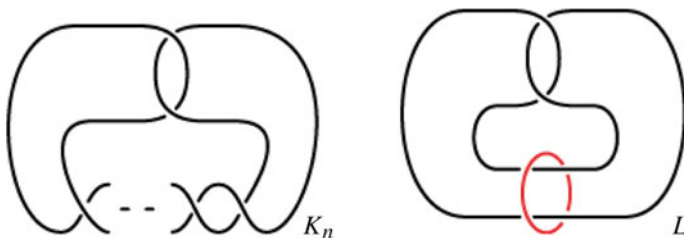


Fig. 5 Every twist knot K_n has two twist regions, consisting of 2 and n crossings. Every K_n can be obtained by Dehn filling the red component of the Whitehead link L , depicted on the right

Returning to the case of twist knots, every K_n can be obtained by Dehn filling on one component of the Whitehead link L , depicted in Fig. 5, right. Thus Theorem 4.2 implies $\text{vol}(S^3 \setminus K_n) < \text{vol}(S^3 \setminus L) = v_{\text{oct}}$.

Bounds in Terms of Twist Number

Following the example of twist knots in Fig. 5, it makes sense to seek upper bounds on volume in terms of the twist number $t(K)$ of a knot K (see Definition 2.4), rather than the crossing number alone.

The following result combines the work of Lackenby [63] with an improvement by Agol and D. Thurston [63, Appendix].

Theorem 4.3 *Let $D(K)$ be a diagram of a hyperbolic link K . Then*

$$\text{vol}(S^3 \setminus K) \leq 10(t(D) - 1)v_{\text{tet}}.$$

Furthermore, this bound is asymptotically sharp, in the sense that there exist knot diagrams $D_n = D(K_n)$ with $\text{vol}(S^3 \setminus K_n)/t(D_n) \rightarrow 10v_{\text{tet}}$.

The method of proof is as follows. First, one constructs a *fully augmented link* L , by adding an extra component for each twist region of $D(K)$ (see Fig. 3). As described in Sect. 3.1, the link complement $S^3 \setminus L$ has simple and explicit combinatorics, making it relatively easy to bound $\text{vol}(S^3 \setminus L)$ by counting tetrahedra. Then, Theorem 4.2 implies that the same upper bound on volume applies to $S^3 \setminus K$.

As a counterpart to the asymptotic sharpness of Theorem 4.3, there exist sequences of knots where $t(K_n) \rightarrow \infty$ but $\text{vol}(S^3 \setminus K_n)$ is universally bounded. One family of such examples is the *double coil knots* studied by the authors [40].

Subsequent refinements or interpolations between Theorems 4.1 and 4.3 have been found by Dasbach and Tsvietkova [30, 31] and Adams [4]. These refinements produce a smaller upper bound compared to that of Theorem 4.3 when the diagram $D(K)$ has both twist regions with many crossings and with few crossings. However, the worst case scenario for the multiplicative constant does not improve due to the asymptotic sharpness of Theorems 4.1 and 4.3.

4.2 Lower Bounds on Volume

By results of Jorgensen and Thurston [80], the volumes of hyperbolic 3-manifolds are well-ordered. It follows that every family of hyperbolic 3-manifolds (e.g. link complements; fibered knot complements, knot complements of genus 3, etc.) contains finitely many members realizing the lowest volume. Gabai, Meyerhoff, and Milley [46] showed that the three knot complements of lowest volume are the figure-8 knot, the 5_2 knot, and the $(-2, 3, 7)$ pretzel, whose volumes are

$$\text{vol}(4_1) = 2v_{\text{tet}} = 2.0298\dots, \quad \text{vol}(5_2) = \text{vol}(P(-2, 3, 7)) = 2.8281\dots \quad (5)$$

Agol [12] showed that the two multi-component links of lowest volume are the Whitehead link and the $(-2, 3, 8)$ pretzel link, both of which have volume $v_{\text{oct}} = 3.6638\dots$. Yoshida [86] has identified the smallest volume link of 4 components, with volume $2v_{\text{oct}}$. Beyond these entries, lower bounds applicable to *all* knots (or *all* links) become scarce. Not even the lowest volume link of 3 components is known to date.

Nevertheless, there are several practical methods of obtaining diagrammatic lower bounds on the volume of a knot or link, each of which applies to an infinite family of links, and each of which produces *scalable* lower bounds that become larger as the complexity of a diagram becomes larger. We survey these methods below.

Angle Structures

Suppose that $S^3 \setminus K$ has an ideal triangulation τ supporting an angle structure θ . (Recall Definition 3.8.) Every ideal tetrahedron of τ , supplied with angles via θ , has an associated volume. As a consequence, one may naturally define a volume $\text{vol}(\theta)$ by summing the volumes of the individual tetrahedra.

Conjecture 4.4 (Casson) *Let τ be an ideal triangulation of a hyperbolic manifold M , which supports an angle structure θ . Then*

$$\text{vol}(\theta) \leq \text{vol}(M),$$

with equality if and only if θ solves the gluing equations and gives the complete hyperbolic structure on M .

While Conjecture 4.4 is open in general, it is known to hold if the triangulation τ is *geometric*, meaning that some (possibly different) angle structure θ' solves the gluing equations on τ . In this case, a theorem of Casson and Rivin [35, 77] says that θ' uniquely maximizes volume over all angle structures on τ , implying in particular that $\text{vol}(\theta) \leq \text{vol}(\theta') = \text{vol}(M)$.

In particular, the known case of Conjecture 4.4 has been applied to the family of 2-bridge links. In this case, the link complement has a natural angled triangulation whose combinatorics is closely governed by the link diagram [49, Appendix]. It follows that, for a sufficiently reduced diagram D of a 2-bridge link K ,

$$2v_{\text{tet}}(D) - 2.7066 \leq \text{vol}(S^3 \setminus K) \leq 2v_{\text{oct}}(t(D) - 1), \quad (6)$$

which both sharpens the upper bound of Theorem 4.3 and proves a comparable lower bound.

There are rather few other families where this method has been successfully applied. One is the weaving knots studied by Champanerkar, Kofman, and Purcell [27].

In the spirit of open problems, we mention the family of fibered knots and links. Agol showed that these link complements admit combinatorially natural *veering triangulations* [13], which have angle structures with nice properties [36, 53]. A proof of Conjecture 4.4, even for this special family, would drastically expand the list

of link complements for which we have practical, combinatorial volume estimates. See Worden [85] for more on this problem.

Guts

One powerful method of estimating the volume of a Haken 3–manifold was developed by Agol, Storm, and Thurston [14], building on previous work of Agol [10].

Definition 4.5 Let M be a Haken hyperbolic 3–manifold and $S \subset M$ a properly embedded essential surface. We use the symbol $M \setminus \setminus S$ to denote the complement in M of a collar neighborhood of S . Following the work of Jaco, Shalen, and Johannson [58, 59], there is a canonical way to decompose $M \setminus \setminus S$ along essential annuli into three types of pieces:

- I –bundles over a subsurface $\Sigma \subset S$,
- Seifert fibered pieces, which are necessarily solid tori when M is hyperbolic,
- All remaining pieces, which are denoted guts (M, S) .

Thurston’s hyperbolization theorem (a variant of Theorem 3.7) implies that guts (M, S) admits a hyperbolic metric with totally geodesic boundary. By Miyamoto’s theorem [70], this metric with geodesic boundary has volume at least $v_{\text{oct}} |\chi(\text{guts}(M, S))|$, where χ denotes Euler characteristic.

Agol, Storm, and Thurston showed [14]:

Theorem 4.6 *Let M be a Haken hyperbolic 3–manifold and $S \subset M$ a properly embedded essential surface. Then*

$$\text{vol}(M) \geq v_{\text{oct}} |\chi(\text{guts}(M, S))|.$$

The proof of Theorem 4.6 relies on geometric estimates due to Perelman. Agol, Storm, and Thurston double $M \setminus \setminus S$ along its boundary and apply Ricci flow with surgery. They show that the metric on guts (M, S) converges to the one with totally geodesic boundary, while volume decreases, and while the metric on the remaining pieces shrinks away to volume 0.

Theorem 4.6 has been applied to several large families of knots. For alternating knots and links, Lackenby computed the guts of checkerboard surfaces in an alternating diagram [63]. Combined with Theorems 4.3 and 4.6, this implies:

Theorem 4.7 *Let D be a prime alternating diagram of a hyperbolic link K in S^3 . Then*

$$\frac{v_{\text{oct}}}{2}(t(D) - 2) \leq \text{vol}(S^3 \setminus K) \leq 10v_{\text{tet}}(t(D) - 1),$$

Thus, for alternating knots, the combinatorics of a diagram determines $\text{vol}(S^3 \setminus K)$ up to a factor less than 6. Compare (6) in the 2–bridge case. The authors of this survey have extended the method from alternating links to the larger family of *semi-adequate* links, and the even larger family of *homogeneously adequate* links. We refer to [41] and the survey paper [42] for definitions of these families and for the

precise theorem statements. The method gives particularly straightforward estimates in the same vein as Theorem 4.7 for positive braids [41, 47] and for Montesinos links [33, 41]. In another direction, Howie and Purcell generalized the method from alternating links in S^3 to alternating links on surfaces in any compact 3-manifold and obtained generalizations of Theorem 4.7 in this setting [57].

Question 4.8 Does every knot $K \subset S^3$ admit an essential spanning surface S such that the Euler characteristic $\chi(\text{guts}(S^3 \setminus K, S))$ can be computed directly from diagrammatic data?

The answer to Question 4.8 is “yes” whenever K admits a *homogeneously adequate* diagram in the terminology of [41]. However, it is not known whether K always admits such a diagram. This is closely related to [41, Question 10.10].

Dehn Filling Bounds

A powerful method for proving lower bounds on the volume of $N = S^3 \setminus K$ involves two steps: first, prove a lower bound on $\text{vol}(M)$ for some surgery parent M of N , using one of the above methods; and second, control the change in volume as we Dehn fill M to recover N .

The following theorem, proved in [37], provides an estimate that has proved useful for lower bounds on the volume of knot complements.

Theorem 4.9 *Let M be a cusped hyperbolic 3-manifold, containing embedded horocusps C_1, \dots, C_k (plus possibly others). On each torus $T_i = \partial C_i$, choose a slope s_i , such that the shortest length of any of the s_i is $\ell_{\min} > 2\pi$. Then the manifold $M(s_1, \dots, s_k)$ obtained by Dehn filling along s_1, \dots, s_k is hyperbolic, and its volume satisfies*

$$\text{vol}(M(s_1, \dots, s_k)) \geq \left(1 - \left(\frac{2\pi}{\ell_{\min}}\right)^2\right)^{3/2} \text{vol}(M).$$

Earlier results in the same vein include an asymptotic estimate by Neumann and Zagier [71], as well as a cone-deformation estimate by Hodgson and Kerckhoff [51].

The idea of the proof of Theorem 4.9 is as follows. Building on the proof of the Gromov–Thurston 2π -Theorem, construct explicit negatively curved metrics on the solid tori added during Dehn filling. This yields a negatively curved metric on $M(s_1, \dots, s_k)$ whose volume is bounded below in terms of $\text{vol}(M)$. Then, results of Besson, Courtois, and Gallot [20, 22] can be used to compare the volume of the negatively curved metric on $M(s_1, \dots, s_k)$ with the true hyperbolic volume.

Theorem 4.9 leads to diagrammatic volume bounds for several classes of hyperbolic links. For example, the following theorem from [37] gives a double-sided volume bound similar to Theorem 4.7.

Theorem 4.10 *Let $K \subset S^3$ be a link with a prime, twist-reduced diagram $D(K)$.*

Assume that $D(K)$ has $t(D) \geq 2$ twist regions, and that each region contains at least 7 crossings. Then K is a hyperbolic link satisfying

$$0.70735 (t(D) - 1) < \text{vol}(S^3 \setminus K) < 10 v_{\text{tet}} (t(D) - 1).$$

The strategy of the proof of Theorem 4.10 is to view $S^3 \setminus K$ as a Dehn filling on the complement of an augmented link obtained from the highly twisted diagram $D(K)$. The volume of augmented links can be bounded below in terms of $t(D)$ using Miyamoto’s theorem [70]. The hypothesis that each region contains at least 7 crossings ensures that the filling slopes are strictly longer than 2π , hence Theorem 4.9 gives the result.

Similar arguments using Theorem 4.9 have been applied to links obtained by adding alternating tangles [38], closed 3–braids [39] and weaving links [27].

Knots with Symmetry Groups

We close this section with a result about the volumes of symmetric knots. Suppose $K \subset S^3$ is a hyperbolic knot, and G is a group of symmetries of K . That is, G acts on S^3 by orientation–preserving homeomorphism that send K to itself. It is a well-known consequence of Mostow rigidity that G is finite and acts on $M = S^3 \setminus K$ by isometries [80, Corollary 5.7.4]. Furthermore, G is cyclic or dihedral [55].

Define $n = n(G)$ to be the smallest order of a subgroup $\text{Stab}_G(x)$ stabilizing a point $x \in S^3 \setminus K$, or else $n = |G|$ if the group acts freely. While this definition depends on how G acts, it is always the case that $n(G)$ is at least as large as the smallest prime factor of $|G|$.

The following result follows by combining several statements in the literature. Since it has not previously been recorded, we include a proof.

Theorem 4.11 *Let $K \subset S^3$ be a hyperbolic knot. Let G be a group of orientation–preserving symmetries of S^3 that send K to itself. Define $n = n(G)$ as above. Then*

$$\text{vol}(S^3 \setminus K) \geq |G| \cdot x_n,$$

where $x_n = 2.848$ if $n > 10$ and $n \neq 13, 18, 19$ and x_n takes the following values otherwise.

$v_{\text{oct}}/12 = 0.30532 \dots$	$n = 2$	2.16958	$n = 7, 8$
$v_{\text{tet}}/2 = 0.50747 \dots$	$n = 3$	2.47542	$n = 9$
0.69524	$n = 4$	2.76740	$n = 10$
1.45034	$n = 5$	$\text{vol}(m011) = 2.7818 \dots$	$n = 13$
2.00606	$n = 6$	$\text{vol}(m016) = 2.8281 \dots$	$n = 18, 19$

Proof First, suppose that G acts on $M = S^3 \setminus K$ with fixed points. Then the quotient $\mathcal{O} = M/G$ is a non-compact, orientable hyperbolic 3–orbifold whose torsion orders are bounded below by n . We need to check that $\text{vol}(\mathcal{O}) \geq x_n$. If $n = 2$, this result is due to Adams [7, Corollary 8.2]. If $n = 3$, the result is essentially due to Adams and Meyerhoff; see [15, Lemma 2.2] and [16, Lemma 2.3]. If $n \geq 4$, the result is due to Atkinson and Futer [16, Theorem 3.8]. In all cases, it follows that $\text{vol}(M) \geq |G| \cdot x_n$.

Next, suppose that G acts freely on $M = S^3 \setminus K$. Then the quotient $N = M/G$ is a non-compact, orientable hyperbolic 3–manifold. If $\text{vol}(N) \geq 2.848$, then the

theorem holds automatically because $x_n \leq 2.848$ for all n . If $\text{vol}(N) < 2.848$, then Gabai, Meyerhoff, and Milley showed that N is one of 10 enumerated 3-manifolds [46, Theorem 1.2]. In SnapPy notation, these are `m003`, `m004`, `m006`, `m007`, `m009`, `m010`, `m011`, `m015`, `m016`, and `m017`. We restrict attention to these manifolds.

Since G acts freely on M , the solution to the Smith conjecture implies that G also acts freely on S^3 . By a theorem of Milnor [69, p. 624], G contains at most one element of order 2, which implies that it must be cyclic. Thus $P = S^3/G$ is a lens space obtained by a Dehn filling on N .

An enumeration of the lens space fillings of the 10 possible manifolds N appears in the table on [38, p. 243]. This enumeration can be used to show that all possibilities satisfy the statement of the theorem.

Suppose that a lens space $L(p, q)$ is a Dehn filling of N . If N actually occurs as a quotient of $M = S^3 \setminus K$, then M must be a cyclic p -fold cover of N . We may rigorously enumerate all cyclic p -fold covers using SnapPy [29]. In almost all cases, homological reasons show that these covers are not knot complements. For instance, $N = \text{m003}$ has two lens space fillings: $L(5, 1)$ and $L(10, 3)$. This manifold has six 5-fold and six 10-fold cyclic covers, none of which has first homology \mathbb{Z} . Thus `m003` is not a quotient of a knot complement. The same technique applies to 8 of the 10 manifolds N .

The two remaining exceptions determine several values of x_n . The manifold `m011` has 9-fold and 13-fold cyclic covers that are knot complements in S^3 . The value of x_9 is already smaller than $\text{vol}(\text{m011})$, but the value of x_{13} is determined by this example. Similarly, the manifold `m016`, which is the $(-2, 3, 7)$ pretzel knot complement, has 18-fold and 19-fold cyclic covers that are knot complements, determining the values of x_{18} and x_{19} . \square

5 Cusp Shapes and Cusp Areas

Several results discussed above, such as Theorems 3.10 and 4.9, require the slopes used in Dehn filling along knot or link complements to be long. To obtain lower bounds for lengths of slopes, we consider an additional invariant of hyperbolic knots and links, namely their cusp shapes and cusp areas.

Definition 5.1 Let C_1, \dots, C_n be a fixed choice of maximal cusps for a link complement M , as in Definition 2.11. The *cusp area* of a component C_i , denoted by $\text{area}(\partial C_i)$, is the Euclidean area of ∂C_i . The *cusp volume*, denoted by $\text{vol}(C_i)$, is the volume of C_i . Note that $\text{area}(\partial C_i) = 2 \text{vol}(C_i)$. When M has multiple cusps, the cusp area and cusp volume depend on the choice of maximal cusp.

This section surveys some methods for estimating the area of a maximal cusp and the length of slopes on it, and poses some open questions.

5.1 Direct Computation

Similar to the techniques in Sect. 3, if we can explicitly determine a geometric triangulation of a hyperbolic 3–manifold, then we can determine its cusp shape and cusp area. This is implemented in SnapPy [29].

For fully augmented links, whose geometry is completely determined by a circle packing, the cusp shape is also determined by the circle packing. The cusp area can be computed by finding an explicit collection of disjoint horoballs in the fully augmented link, as in [44].

Under very strong hypotheses, it is possible to apply the cone deformation techniques of Hodgson and Kerckhoff [51] to bound the change in cusp shape under Dehn filling. Purcell carried this out in [74], starting from a fully augmented link. However, the results only apply to knots with at least two twist regions and at least 116 crossings per twist region.

To obtain more general bounds for larger classes of knots and links, additional tools are needed. The main tools are pleated surfaces and packing techniques.

5.2 Upper Bounds and Pleated Surfaces

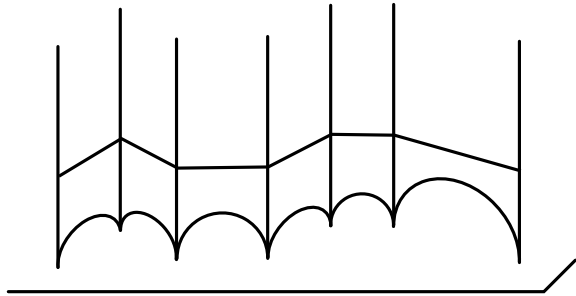
If M is a hyperbolic link complement, then for any choice of maximal cusp, there is a collection of slopes whose Dehn fillings gives S^3 . These are the *meridians* of M . Because S^3 is not hyperbolic, the 6–Theorem implies that in any choice of maximal cusp for M , one or more of these slopes must have length at most 6. Indeed, the 6–Theorem is proved by considering punctured surfaces immersed in M and using area arguments to bound the length of a slope.

Definition 5.2 Let M be a hyperbolic 3–manifold with cusps a collection of cusps C , and let S be a hyperbolic surface. A *pleated surface* is a piecewise geodesic, proper immersion $f : S \rightarrow M$. Properness means that any cusps of S are mapped into cusps of M . The surface S is cut into ideal triangles, each of which is mapped into M by a local isometry. In M , there may be bending along the sides of the triangles. See Fig. 6.

An essential surface S in a hyperbolic 3–manifold M can always be homotoped into a pleated form. The idea is to start with an ideal triangulation of S , then homotope the images of the edges in M to be ideal geodesics in M . Similarly, homotope the ideal triangles to be totally geodesic, with sides the geodesic edges in M . This gives S a pleating. See [25, Theorem 5.3.6] or [62, Lemma 2.2] for proofs.

The main result on slope lengths and pleated surfaces is the following, which is a special case of [11, Theorem 5.1] and [62, Lemma 3.3]. The result is used in the proof of the 6–Theorem.

Fig. 6 The lift of a pleated surface to the universal cover \mathbb{H}^3 of M . The piecewise linear zig-zag lies in a single horosphere



Theorem 5.3 Let $M = S^3 \setminus K$ be a hyperbolic knot complement with a maximal cusp C . Suppose that $f : S \rightarrow M$ is a pleated surface, and let $\ell_C(S)$ denote the total length of the intersection curves in $f(S) \cap \partial C$. Then

$$\ell_C(S) \leq 6|\chi(S)|.$$

The idea of the proof of Theorem 5.3 is to find disjoint horocusp neighborhoods $H = \cup H_i$ in S such that $f(H_i) \subset C$, and such that $\ell(\partial H_i)$ is at least as big as the length of $f(\partial H_i)$ measured on C . This allows us to compute as follows:

$$\ell_C(S) \leq \sum_{i=1}^s \ell(\partial H_i) = \sum_{i=1}^s \text{area}(H_i) \leq \frac{6}{2\pi} \text{area}(S) = \frac{6}{2\pi} \cdot 2\pi|\chi(S)|.$$

Here, the first inequality is by construction. The second equality is a general fact about hyperbolic surfaces, proved by a calculation in \mathbb{H}^2 . The third inequality is a packing theorem due to Böröczky [23]. The final equality is the Gauss–Bonnet theorem.

Sample Applications

As noted above, the 6–Theorem implies that the length of a meridian is at most 6. Theorem 5.3 has also been used to estimate the lengths of other slopes. For example, a λ –curve is defined to be a curve that intersects the meridian μ exactly once. The knot-theoretic longitude, which is null-homologous in $S^3 \setminus K$, is one example of a λ –curve, and need not be the shortest λ –curve. There may be one or two shortest λ –curves. For any λ –curve λ , note that $\ell(\mu)\ell(\lambda)$ gives an upper bound on cusp area.

By applying Theorem 5.3 to a singular spanning surface in a knot complement, the authors of [6] obtain the following upper bounds on meridian, λ –curve, and cusp area.

Theorem 5.4 Let K be a hyperbolic knot in S^3 with crossing number $c = c(K)$. Let C denote the maximal cusp of $S^3 \setminus K$. Then, for the meridian μ and for the shortest λ –curve,

$$\ell(\mu) \leq 6 - \frac{7}{c}, \quad \ell(\lambda) \leq 5c - 6, \quad \text{and} \quad \text{area}(\partial C) \leq 9c \left(1 - \frac{1}{c}\right)^2.$$

Another instance where Theorem 5.3 applies is to knots with a pair of essential spanning surfaces S_1 and S_2 ; in this case the surface S is taken to be the disjoint union of the two spanning surfaces. The following appears in [24].

Theorem 5.5 *Let K be a hyperbolic knot with maximal cusp C . Suppose that S_1 and S_2 are essential spanning surfaces in $M = S^3 \setminus K$ and let $i(\partial S_1, \partial S_2) \neq 0$ denote the minimal intersection number of $\partial S_1, \partial S_2$ in ∂C . Finally, let $\chi = |\chi(S_1)| + |\chi(S_2)|$. Then, for the meridian μ and the shortest λ -curve,*

$$\ell(\mu) \leq \frac{6\chi}{i(\partial S_1, \partial S_2)}, \quad \ell(\lambda) \leq 3\chi, \quad \text{and} \quad \text{area}(\partial C) \leq \frac{18\chi^2}{i(\partial S_1, \partial S_2)}.$$

Theorem 5.5 is useful because the checkerboard surfaces of many knot diagrams are known to be essential. For instance, the checkerboard surfaces of alternating diagrams are essential. Indeed, in [6] the authors use pleated checkerboard surfaces to prove the meridian of an alternating knot satisfies $\ell(\mu) < 3 - 6/c$. Other knots with essential spanning surfaces include *adequate knots*, which arose in the study of Jones type invariants. Ozawa first proved that two surfaces in such links are essential [73]; see also [41]. More generally, Theorem 5.5 applies to knots that admit alternating projections on surfaces so that they define essential checkerboard surfaces. These have been studied by Ozawa [72] and Howie [56].

All the results above indicate that meridian lengths should be strictly less than 6. For knots in S^3 , no examples are known with length more than 4.

Question 5.6 Do all hyperbolic knots in S^3 satisfy $\ell(\mu) \leq 4$?

For links in S^3 , Goerner showed there exists a link in S^3 with 64 components, and a choice of cusps for which each meridian length is $\sqrt{21} \approx 4.5826$ [48].

Question 5.7 Given a hyperbolic link $L \subset S^3$, consider the shortest meridian among the components of L . What is the largest possible value of the shortest meridian? Is it $\sqrt{21}$?

The 6–Theorem gives a bound on the length of any non-hyperbolic Dehn fillings. By geometrization, non-hyperbolic manifolds are either *reducible* (meaning they contain an essential 2–sphere), or *toroidal* (meaning they contain an essential torus), or small Seifert fibered. The 6–Theorem is only known to be sharp on toroidal fillings. Thus one may ask about the maximal possible length for the other types of fillings. See [54] for related questions and results.

Upper Bounds on Area Via Cusp Density

The *cuspidal density* of a cusped 3–manifold M is the volume of a maximal cusp divided by the volume of M . Böröczky [23] showed that cuspidal density is universally bounded by $\sqrt{3}/2v_{\text{tet}}$, with the figure–8 knot complement realizing this

bound. Recall from Theorem 4.3 that every hyperbolic knot $K \subset S^3$ satisfies $\text{vol}(S^3 \setminus K) \leq 10 v_{\text{tet}}(t - 1)$, where $t = t(D)$ is the twist number of any diagram. Combining this with Böröczky's theorem shows that a maximal cusp $C \subset S^3 \setminus K$ satisfies

$$\text{area}(\partial C) \leq 10\sqrt{3} \cdot (t - 1) \approx 17.32 \cdot (t - 1).$$

We note that this bound can be arbitrarily far from sharp. This is already true for Theorem 4.3. In addition, Eudave-Muñoz and Luecke [32] showed that the cusp density of a hyperbolic knot complement can be arbitrarily close to 0.

5.3 Lower Bounds via Horoball Packing

Theorems 5.3 and 5.4 give methods for bounding cusp area from above. To give lower bounds on slope lengths, for example to apply the 6–Theorem, we must bound cusp area or cusp volume from below. The main tool for this is to use *packing arguments*: find a disjoint collection of horoballs with Euclidean diameters bounded from below in a fundamental region of the cusp. Take their shadows on the cusp torus. The area of the cusp torus must be bounded below by the areas of the shadows.

One sample result that has been used to bound cusp shape is the following, from [64].

Lemma 5.8 *Suppose that a one-cusped hyperbolic 3–manifold M contains at least p homotopically distinct essential arcs, each with length at most L measured with respect to the maximal cusp H of M . Then the cusp area $\text{area}(\partial H)$ is at least $p\sqrt{3}e^{-2L}$.*

Similar techniques were also used to bound cusp areas in [39] and in [45].

The idea of the proof is that an arc from the cusp to itself of length L lifts to an arc in the universal cover between two horoballs. We may identify the universal cover of M with the upper half-space model of \mathbb{H}^3 , so that the boundary of one cusp in M lifts to a horosphere at Euclidean height 1. The Euclidean metric on this horosphere coincides with the hyperbolic metric. Arcs of bounded length lead to horoballs whose diameter is not too small, and whose shadows have a definite area.

At this writing there is no general lower bound of cusp shapes for all hyperbolic knots. However, for alternating knots, Lackenby and Purcell found a collection of homotopically distinct essential arcs of bounded length, then applied Lemma 5.8 to show the following [64].

Theorem 5.9 *Let D be a prime, twist reduced alternating diagram of some hyperbolic knot K and let $t = t(D)$ be the twist number of D . Let C be the maximal cusp of $M = S^3 \setminus K$. Then*

$$A(t - 2) \leq \text{area}(\partial C) \leq 10\sqrt{3}(t - 1),$$

where A is at least 2.278×10^{-9} .

For 2–bridge knots there is a much sharper lower bound [39]:

$$\frac{8\sqrt{3}}{147}(t-1) \leq \text{area}(\partial C) \leq \frac{\sqrt{3}v_{\text{oct}}}{v_{\text{tet}}}(t-1).$$

Note that Theorem 5.9, along with Theorem 4.7 implies that the cusp density of alternating knots is universally bounded below. This is not true for non-alternating knots [32]. It would be interesting to study the extent to which Theorem 5.9 can be generalized.

In general, we would like to know how to obtain many homotopically distinct arcs that can be used in Lemma 5.8. The arcs used in the proof of Theorem 5.9 lie on complicated immersed essential surfaces, described in [65]. It is conjectured that much simpler *crossing arcs* should play this role.

Definition 5.10 Let K be a knot with diagram $D(K)$. A *crossing arc* is an embedded arc α in S^3 with $\partial\alpha \subset K$, such that in $D(K)$, α projects to an unknotted embedded arc running from an overstrand to an understrand in a crossing.

The following conjecture is due to Sakuma and Weeks [78].

Conjecture 5.11 *In a reduced alternating diagram of a hyperbolic alternating link, every crossing arc is isotopic to a geodesic.*

Conjecture 5.11 is known for 2–bridge knots [49, Appendix] and for classes of closed alternating braids [83].

Computer experiments performed by Thistlethwaite and Tsvietkova [79] also support the following conjecture, which would give more information on the lengths of crossing arcs, hence more information on cusp areas.

Conjecture 5.12 *Crossing arcs in alternating knots have length universally bounded above by $\log 8$.*

References

1. C. Adams, *Hyperbolic Structures on Link Complements* (University of Wisconsin, Madison, 1983). Ph.D. thesis
2. C. Adams, *Hyperbolic Knots*, Handbook of knot theory (Elsevier B. V., Amsterdam, 2005), pp. 1–18. MR 2179259
3. C. Adams, Triple crossing number of knots and links. *J. Knot Theory Ramif.* **22**(2), 1350006 (2013). MR 3037297
4. C. Adams, Bipyramids and bounds on volumes of hyperbolic links. *Topology Appl.* **222**, 100–114 (2017). MR 3630197

5. C. Adams, H. Bennett, C. Davis, M. Jennings, J. Kloke, N. Perry, E. Schoenfeld, Totally geodesic Seifert surfaces in hyperbolic knot and link complements. II. *J. Differ. Geom.* **79**(1), 1–23 (2008). MR 2414747 (2009b:57032)
6. C. Adams, A. Colestock, J. Fowler, W. Gillam, E. Katerman, Cusp size bounds from singular surfaces in hyperbolic 3-manifolds. *Trans. Am. Math. Soc.* **358**(2), 727–741 (electronic) (2006). MR MR2177038 (2006k:57041)
7. C.C. Adams, Limit volumes of hyperbolic three-orbifolds. *J. Differ. Geom.* **34**(1), 115–141 (1991). MR 1114455 (92d:57029)
8. C.C. Adams, Toroidally alternating knots and links. *Topology* **33**(2), 353–369 (1994)
9. C.C. Adams, J.F. Brock, J. Bugbee, T.D. Comar, K.A. Faigin, A.M. Huston, A.M. Joseph, D. Pesikoff, Almost alternating links. *Topology Appl.* **46**(2), 151–165 (1992)
10. I. Agol, Lower bounds on volumes of hyperbolic Haken 3-manifolds (1999). [arXiv:math/9906182](https://arxiv.org/abs/math/9906182)
11. I. Agol, Bounds on exceptional Dehn filling. *Geom. Topol.* **4**, 431–449 (2000). MR 1799796 (2001j:57019)
12. I. Agol, The minimal volume orientable hyperbolic 2-cusped 3-manifolds. *Proc. Am. Math. Soc.* **138**(10), 3723–3732 (2010). MR 2661571
13. I. Agol, *Ideal triangulations of pseudo-Anosov mapping tori*. *Topol. Geom. Dimens. Three, Contemp. Math.* 560, Amer. Math. Soc. (Providence, 2011), pp. 1–17. MR 2866919
14. I. Agol, P.A. Storm, W.P. Thurston, Lower bounds on volumes of hyperbolic Haken 3-manifolds. *J. Am. Math. Soc.* **20**(4), 1053–1077 (2007). with an appendix by Nathan Dunfield
15. C.K. Atkinson, D. Futer, Small volume link orbifolds. *Math. Res. Lett.* **20**(6), 995–1016 (2013). MR 3228616
16. C.K. Atkinson, D. Futer, The lowest volume 3-orbifolds with high torsion. *Trans. Am. Math. Soc.* **369**(8), 5809–5827 (2017). MR 3646779
17. D. Bachman, S. Schleimer, Distance and bridge position. *Pac. J. Math.* **219**(2), 221–235 (2005). MR 2175113 (2007a:57028)
18. K.L. Baker, Surgery descriptions and volumes of Berge knots. II. Descriptions on the minimally twisted five chain link. *J. Knot Theory Ramif.* **17**(9), 1099–1120 (2008). MR MR2457838
19. R. Benedetti, C. Petronio, *Lectures on Hyperbolic Geometry* (Universitext, Springer, Berlin, 1992). MR MR1219310 (94e:57015)
20. G. Besson, G. Courtois, S. Gallot, Entropies et rigidités des espaces localement symétriques de courbure strictement négative. *Geom. Funct. Anal.* **5**(5), 731–799 (1995). MR 1354289
21. S.A. Bleiler, C.D. Hodgson, Spherical space forms and Dehn filling. *Topology* **35**(3), 809–833 (1996)
22. J. Boland, C. Connell, J. Souto, Volume rigidity for finite volume manifolds. *Am. J. Math.* **127**(3), 535–550 (2005). MR 2141643
23. K. Böröczky, Packing of spheres in spaces of constant curvature. *Acta Math. Acad. Sci. Hungar.* **32**(3–4), 243–261 (1978). MR MR512399 (80h:52014)
24. S.D. Burton, E. Kalfagianni, Geometric estimates from spanning surfaces. *Bull. Lond. Math. Soc.* **49**(4), 694–708 (2017)
25. R.D. Canary, D.B.A. Epstein, P.L. Green, Notes on notes of Thurston, in *Fundamentals of hyperbolic geometry: selected expositions*, vol. 328, London Mathematical Society Lecture Note series (Cambridge University Press, Cambridge, 2006), pp. 1–115. With a new foreword by Canary. MR 2235710
26. A. Champanerkar, I. Kofman, J.S. Purcell, Geometrically and diagrammatically maximal knots. *J. Lond. Math. Soc. (2)* **94**(3), 883–908 (2016). MR 3614933
27. A. Champanerkar, I. Kofman, J.S. Purcell, Volume bounds for weaving knots. *Algebr. Geom. Topol.* **16** (6), 3301–3323 (2016). MR 3584259
28. Y.-E. Choi, Positively oriented ideal triangulations on hyperbolic three-manifolds. *Topology* **43**(6), 1345–1371 (2004). MR 2081429
29. M. Culler, N.M. Dunfield, M. Goerner, J.R. Weeks, SnapPy, a computer program for studying the geometry and topology of 3-manifolds (2017). <http://snappy.computop.org>

30. O. Dasbach, A. Tsvietkova, A refined upper bound for the hyperbolic volume of alternating links and the colored Jones polynomial. *Math. Res. Lett.* **22**(4), 1047–1060 (2015). MR 3391876
31. O. Dasbach, A. Tsvietkova, Simplicial volume of links from link diagrams. *Math. Proc. Camb. Phil. Soc.* **166**(1), 75–81 (2019). MR 3893305
32. M. Eudave-Muñoz, J. Luecke, Knots with bounded cusp volume yet large tunnel number. *J. Knot Theory Ramif.* **8**(4), 437–446 (1999). MR 1697382 (2000g:57007)
33. K. Finlinson, J.S. Purcell, Volumes of Montesinos links. *Pac. J. Math.* **282**(1), 63–105 (2016). MR 3463425
34. D. Futer, F. Guéritaud, Angled decompositions of arborescent link complements. *Proc. Lond. Math. Soc.* (3) **98**(2), 325–364 (2009). MR 2481951
35. D. Futer, F. Guéritaud, From angled triangulations to hyperbolic structures, in *Interactions between hyperbolic geometry, quantum topology and number theory*, vol. 541, Contemporary Mathematics (American Mathematical Society, Providence, 2011), pp. 159–182. MR 2796632
36. D. Futer, F. Guéritaud, Explicit angle structures for veering triangulations. *Algebr. Geom. Topol.* **13**(1), 205–235 (2013). MR 3031641
37. D. Futer, E. Kalfagianni, J.S. Purcell, Dehn filling, volume, and the Jones polynomial. *J. Differ. Geom.* **78**(3), 429–464 (2008). MR 2396249
38. D. Futer, E. Kalfagianni, J.S. Purcell, Symmetric links and Conway sums: volume and Jones polynomial. *Math. Res. Lett.* **16**(2), 233–253 (2009). MR 2496741
39. D. Futer, E. Kalfagianni, J.S. Purcell, Cusp areas of Farey manifolds and applications to knot theory. *Int. Math. Res. Not. IMRN* **2010**(23), 4434–4497 (2010)
40. D. Futer, E. Kalfagianni, J.S. Purcell, On diagrammatic bounds of knot volumes and spectral invariants. *Geom. Dedicata* **147**, 115–130 (2010). MR 2660569
41. D. Futer, E. Kalfagianni, J.S. Purcell, *Guts of Surfaces and the Colored Jones Polynomial*, vol. 2069, Lecture Notes in Mathematics (Springer, Heidelberg, 2013)
42. D. Futer, E. Kalfagianni, J.S. Purcell, Jones polynomials, volume and essential knot surfaces: a survey, in *Knots in Poland. III. Part I*, Banach Center Publication, vol. 100, Polish Academy Science Institute of Mathematics, (Warsaw, 2014), pp. 51–77. MR 3220475
43. D. Futer, E. Kalfagianni, J.S. Purcell, Hyperbolic semi-adequate links. *Commun. Anal. Geom.* **23**(5), 993–1030 (2015). MR 3458811
44. D. Futer, J.S. Purcell, Links with no exceptional surgeries. *Comment. Math. Helv.* **82**(3), 629–664 (2007). MR 2314056
45. D. Futer, S. Schleimer, Cusp geometry of fibered 3-manifolds. *Am. J. Math.* **136**(2), 309–356 (2014). MR 3188063
46. D. Gabai, R. Meyerhoff, P. Milley, Minimum volume cusped hyperbolic three-manifolds. *J. Am. Math. Soc.* **22**(4), 1157–1215 (2009). MR 2525782
47. A. Giambrone, Combinatorics of link diagrams and volume. *J. Knot Theory Ramif.* **24**(1), 1550001, 21 (2015). MR 3319678
48. M. Goerner, Regular tessellation links (2014). [arXiv:1406.2827](https://arxiv.org/abs/1406.2827)
49. F. Guéritaud, On canonical triangulations of once-punctured torus bundles and two-bridge link complements. *Geom. Topol.* **10**, 1239–1284 (2006). With an appendix by David Futer. MR 2255497
50. E. Hironaka, E. Kin, A family of pseudo-Anosov braids with small dilatation. *Algebr. Geom. Topol.* **6**, 699–738 (2006). MR 2240913
51. C.D. Hodgson, S.P. Kerckhoff, Universal bounds for hyperbolic Dehn surgery. *Ann. Math.* (2) **162**(1), 367–421 (2005). MR MR2178964
52. C.D. Hodgson, J.H. Rubinstein, H. Segerman, Triangulations of hyperbolic 3-manifolds admitting strict angle structures. *J. Topol.* **5**(4), 887–908 (2012). MR 3001314
53. C.D. Hodgson, J.H. Rubinstein, H. Segerman, S. Tillmann, Veering triangulations admit strict angle structures. *Geom. Topol.* **15**(4), 2073–2089 (2011). MR 2860987
54. N.R. Hoffman, J.S. Purcell, Geometry of planar surfaces and exceptional fillings. *Bull. Lond. Math. Soc.* **49**(2), 185–201 (2017). MR 3656288
55. J. Hoste, M. Thistlethwaite, J. Weeks, The first 1,701,936 knots. *Math. Intell.* **20**(4), 33–48 (1998). MR MR1646740 (99i:57015)

56. J.A. Howie, Surface-alternating knots and links, Ph.D. thesis, University of Melbourne, 2015
57. J.A. Howie, J.S. Purcell, Geometry of alternating links on surfaces (2017). [arXiv:math/1712.01373](https://arxiv.org/abs/math/1712.01373)
58. W.H. Jaco, P.B. Shalen, Seifert fibered spaces in 3-manifolds. *Mem. Am. Math. Soc.* **21**(220), viii+192 (1979). MR MR539411 (81c:57010)
59. K. Johannson, *Homotopy Equivalences of 3-Manifolds with Boundaries*, vol. 761, Lecture Notes in Mathematics (Springer, Berlin, 1979)
60. J. Johnson, WYSIWYG Hyperbolic knots, Low Dimensional Topology Blog. <https://ldtopology.wordpress.com/2007/11/18/temporary/>
61. J. Johnson, Y. Moriah, Bridge distance and plat projections. *Algebr. Geom. Topol.* **16**(6), 3361–3384 (2016). MR 3584261
62. M. Lackenby, Word hyperbolic Dehn surgery. *Invent. Math.* **140**(2), 243–282 (2000)
63. M. Lackenby, The volume of hyperbolic alternating link complements. *Proc. Lond. Math. Soc.* (3) **88**(1), 204–224 (2004). With an appendix by Ian Agol and Dylan Thurston
64. M. Lackenby, J.S. Purcell, Cusp volumes of alternating knots. *Geom. Topol.* **20**(4), 2053–2078 (2016). MR 3548463
65. M. Lackenby, J.S. Purcell, Essential twisted surfaces in alternating link complements. *Algebr. Geom. Topol.* **16**(6), 3209–3270 (2016). MR 3584257
66. F. Luo, S. Tillmann, Angle structures and normal surfaces. *Trans. Am. Math. Soc.* **360**(6), 2849–2866 (2008). MR 2379778
67. W.W. Menasco, Polyhedra representation of link complements, in *Low-dimensional Topology (San Francisco, Calif., 1981)*, vol. 20, Contemporary Mathematics (American Mathematical Society, Providence, 1983), pp. 305–325. MR MR718149 (85e:57006)
68. W.W. Menasco, Menasco, closed incompressible surfaces in alternating knot and link complements. *Topology* **23**(1), 37–44 (1984)
69. J. Milnor, Groups which act on S^n without fixed points. *Am. J. Math.* **79**, 623–630 (1957). MR 0090056
70. Y. Miyamoto, Volumes of hyperbolic manifolds with geodesic boundary. *Topology* **33**(4), 613–629 (1994). MR 1293303
71. W.D. Neumann, D. Zagier, Volumes of hyperbolic three-manifolds. *Topology* **24**(3), 307–332 (1985). MR 815482
72. M. Ozawa, Non-triviality of generalized alternating knots. *J. Knot Theory Ramif.* **15**(3), 351–360 (2006)
73. M. Ozawa, Essential state surfaces for knots and links. *J. Aust. Math. Soc.* **91**(3), 391–404 (2011)
74. J.S. Purcell, Cusp shapes under cone deformation. *J. Differ. Geom.* **80**(3), 453–500 (2008). MR 2472480
75. J.S. Purcell, An introduction to fully augmented links, in *Interactions Between Hyperbolic Geometry, Quantum Topology and Number Theory*, Contemporary Mathematics (American Mathematical Society, Providence, 2011), pp. 205–220. MR 2796634
76. J.S. Purcell, Hyperbolic knot theory (2017). <http://users.monash.edu/~jpurcell/hypknottheory.html>
77. I. Rivin, Euclidean structures on simplicial surfaces and hyperbolic volume. *Ann. Math.* (2) **139**(3), 553–580 (1994). MR 1283870
78. M. Sakuma, J. Weeks, Examples of canonical decompositions of hyperbolic link complements. *Jpn. J. Math. (N.S.)* **212**, 393–439 (1995). MR 1364387
79. M. Thistlethwaite, A. Tsvietkova, An alternative approach to hyperbolic structures on link complements. *Algebr. Geom. Topol.* **14**(3), 1307–1337 (2014). MR 3190595
80. W.P. Thurston, *The Geometry and Topology of Three-manifolds*, Princeton Univ. Math. Dept. Notes (1979). <http://www.msri.org/communications/books/gt3m>
81. W.P. Thurston, Three-dimensional manifolds, Kleinian groups and hyperbolic geometry. *Bull. Am. Math. Soc. (N.S.)* **6**(3), 357–381 (1982)
82. W.P. Thurston, Hyperbolic structures on 3-manifolds II: surface groups and 3-manifolds which fiber over the circle (1998). [arXiv:math/9801045](https://arxiv.org/abs/math/9801045)

83. A. Tsvietkova, Determining isotopy classes of crossing arcs in alternating links. *Asian J. Math.* **22**(6), 1005–1024 (2018)
84. J. Weeks, Computation of hyperbolic structures in knot theory, *Handbook of knot theory* (Elsevier B. V., Amsterdam, 2005), pp. 461–480. MR 2179268
85. W. Worden, Experimental statistics of veering triangulations. *Exp. Math.* (to appear). [arXiv:1710.01198](https://arxiv.org/abs/1710.01198). <https://doi.org/10.1080/10586458.2018.1437850>
86. K. Yoshida, The minimal volume orientable hyperbolic 3-manifold with 4 cusps. *Pac. J. Math.* **266**(2), 457–476 (2013). MR 3130632

Spanning Surfaces for Hyperbolic Knots in the 3-Sphere



Colin C. Adams

Abstract We consider results and questions related to both the geometry and topology of surfaces that span hyperbolic knots, including embedded orientable and nonorientable surfaces as well as singular punctured surfaces.

Keywords Hyperbolic knot complement · Seifert surface · Totally geodesic surface · Quasi-Fuchsian surface

2010 Mathematics Subject Classification 57M25 · 57M50

1 Introduction

In the 1970s, W. Thurston proved that knots in the 3-sphere fall into three disjoint classes: torus knots, satellite knots and hyperbolic knots. A torus knot $T_{p,q}$ lives on the surface of an unknotted torus, wrapping p times meridianally and q times longitudinally. A satellite knot K lives in a tubular neighborhood of another nontrivial knot K' such that it cannot be isotoped within the neighborhood to miss any meridional disks of the tube neighborhood. Note that all composite knots fall into the satellite knot category by using the so-called swallow-follow torus that swallows one factor knot and follows the other.

A knot K is *hyperbolic* if its complement possesses a metric of constant curvature -1 . This is equivalent to there being a covering map from hyperbolic 3-space \mathbb{H}^3 to $S^3 \setminus K$ such that the covering transformations form a discrete group of fixed-point free isometries of \mathbb{H}^3 . By the Mostow-Prasad Rigidity Theorem, the hyperbolic knots have a unique hyperbolic volume associated with the complement. Moreover, one can also obtain a variety of hyperbolic invariants, each uniquely determined for the knot.

C. C. Adams (✉)

Williams College, Bascom Hall, Williamstown, MA 01267, USA
e-mail: cadams@williams.edu

© Springer Nature Switzerland AG 2019

C. C. Adams et al. (eds.), *Knots, Low-Dimensional Topology and Applications*, Springer Proceedings in Mathematics & Statistics 284, https://doi.org/10.1007/978-3-030-16031-9_2

Thurston's groundbreaking result revolutionized knot theory. In this paper, we discuss its implications for spanning surfaces, which are surfaces in S^3 such that their boundary is a given knot. In particular, most of the time, we will look at Seifert surfaces, which are embedded orientable surfaces in S^3 with boundary equal to the knot, and the nonorientable versions, known as nonorientable Seifert surfaces, though we will also discuss certain singular punctured spanning surfaces as well. We do not in general distinguish between isotopy classes of surfaces and a given representative of the isotopy class except where necessary for clarity.

Note that when a knot K is hyperbolic, we can think of its complement $S^3 \setminus K$ as the hyperbolic manifold M . We can also consider the manifold $M' = S^3 \setminus N(K)$, where $N(K)$ is an open neighborhood of K . Then M' has a single torus boundary and the interior of M' is homeomorphic to M . When considering spanning surfaces, it is often convenient to think of them as living in M' so we can talk about them being properly embedded. We will jump back and forth between these viewpoints as appropriate. A *cuspl* of a hyperbolic knot complement is a neighborhood of the missing knot that lifts to a collection of horoballs in hyperbolic space \mathbb{H}^3 . A maximal cusp is a cusp that has been expanded until it touches itself on the boundary. Throughout this paper, $c(K)$ denotes the minimal number of crossings in any projection of K . If R is a submanifold of M or M' of dimension 1, 2, or 3, $N(R)$ denotes an open regular neighborhood.

In Sect. 2, we discuss Seifert surfaces and nonorientable Seifert surfaces, including state surfaces and checkerboard surfaces. In Sect. 3, we delineate the three possibilities for spanning surfaces with regard to hyperbolic knots: virtual fibers, accidental parabolic surfaces and quasi-Fuchsian surfaces. We then focus on totally geodesic (Fuchsian) surfaces, which are special cases of quasi-Fuchsian surfaces. Section 4 is devoted to quasi-Fuchsian surfaces and a measure of how far they are from being Fuchsian. Section 5 discusses singular punctured disks with boundary the knot, and how they impact hyperbolic invariants. A method for generating these surfaces from D. Thurston's octahedral decomposition of a knot complement is included.

2 Seifert Surfaces

Given any knot in S^3 , one can obtain a Seifert surface by applying Seifert's algorithm to an oriented projection. Traveling along the knot, we split it at each crossing and reglue so that the orientations of the resulting strands match. Then each of the disjoint simple closed curves that result is spanned with a disk. Half-twisted bands are attached to the boundaries of the disk at each crossing. One can check this always results in an orientable surface. We call a surface obtained in this manner a *canonical Seifert surface* for the knot.

In fact, the resulting surface is not uniquely determined. If, for instance the Seifert circles are nested, one can place the disks that span them at certain alternative heights relative to one another and obtain non-isotopic surfaces. And of course, different projections of the same knot can result in additional surfaces.

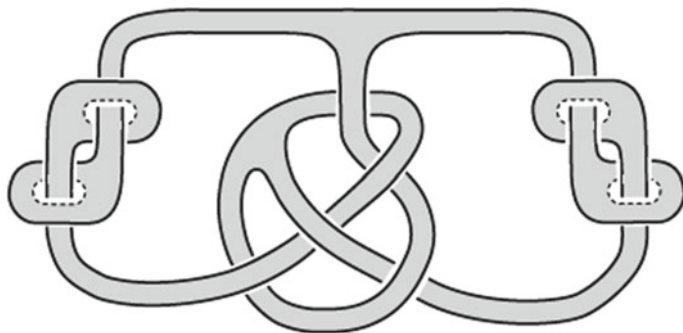


Fig. 1 A knot that has both a totally knotted Seifert surface and a disjoint semi-free Seifert surface. (Figure from [8], used with permission)

For any canonical Seifert surface S , $S^3 \setminus (N(S) \cup N(K))$ is a handlebody. More generally, we can define any Seifert surface to be *free* if $S^3 \setminus (N(S) \cup N(K))$ is a handlebody. (We call it free since the fundamental group of a handlebody is free.)

We can now define three invariants. The *canonical genus* $g_c(K)$ is the least genus of any canonical Seifert surface for K . The *free genus* $g_f(K)$ is the least genus of any free Seifert surface. And the *genus* $g(K)$ is the least genus of any Seifert surface for K . It is immediate that $g(K) \leq g_f(K) \leq g_c(K)$. Although for many knots, they are all equal, there are examples of knots where they can be arbitrarily far apart.

We define a *totally knotted Seifert surface* to be the opposite extreme from a free Seifert surface in the sense that $\partial(N(S) \cup N(K))$ is incompressible in $S^3 \setminus (N(S) \cup N(K))$. We define a *semi-free Seifert surface* to be one where $\partial(N(S) \cup N(K))$ is compressible in $S^3 \setminus (N(S) \cup N(K))$. So a free Seifert surface is also semi-free.

We will be particularly interested in minimal genus Seifert surfaces. Such a surface must be incompressible or we could compress and lower genus.

In 1992, Kakimizu [13] defined the *Kakimizu complex* associated to a knot, which is a simplicial complex that has a vertex for every isotopy class of a minimal genus Seifert surface and an n -simplex spanning $n + 1$ vertices if the corresponding collection of Seifert surfaces can be made pairwise disjoint. In the case that a knot is hyperbolic, it is known that the Kakimizu complex is finite (due to Jaco–Sedgwick (see [14, 19]), connected [13, 16] and contractible [15].

In [8], it was shown that there exist hyperbolic knots that have n pairwise disjoint totally knotted surfaces for any positive integer n . There are also hyperbolic knots with one semi-free Seifert surface and n totally knotted surfaces, again all pairwise disjoint. As an example of the techniques for proving this, in Fig. 1, we see a knot and a spanning surface with four punctures. We then glue in either of the two surfaces from Fig. 2 at the punctures. This generates both a totally knotted Seifert surface and a disjoint semi-free Seifert surface. We will see later that if we restrict the geometry of the surfaces, this cannot happen.

A generalization of Seifert’s algorithm allows us to make an arbitrary choice of how to split each crossing in either of the two possible ways. The resulting collection of circles is called a state. Again, by adding a disk spanning each circle and adding

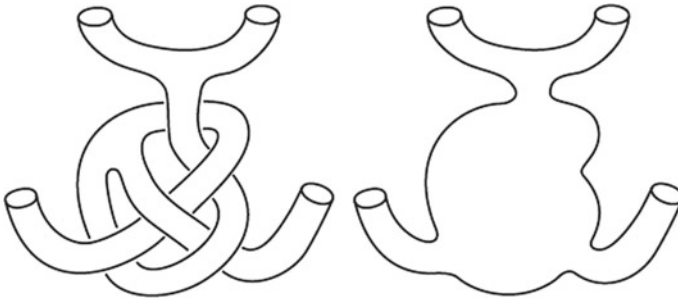


Fig. 2 Gluing on two options to create the two surfaces. (Figure from [8], used with permission)

twisted bands at each crossing, we obtain what is called the corresponding *state surface*, again keeping in mind that the surface is not uniquely determined if there is nesting of state circles. A state surface need not be orientable.

Another type of spanning surface is obtained by taking a projection of the knot and shading in alternate regions, to obtain a *checkerboard surface*. Each projection yields two such. The two checkerboard surfaces correspond to two particular states, both with no nested circles and with opposite choice of splittings at each crossing. These are usually not orientable, and it can never be the case that both are orientable. In fact a checkerboard surface S is orientable if and only if all complementary regions in the projection have an even number of edges.

3 The Trichotomy of Surfaces in Hyperbolic 3-Manifolds

For a hyperbolic knot, work of [17] (see also [4, 5]) implies that a Seifert surface of minimal genus must have one of the following three behaviors:

1. S is a virtual fiber, meaning that a finite cover of the manifold is fibered with S as a fiber. This causes a connected lift of the surface to \mathbb{H}^3 to have limit set the entire boundary of \mathbb{H}^3 .
2. There is an accidental parabolic in S , which is to say, a simple closed loop in S that is not parallel to the boundary of S but can be homotoped into the boundary of M .
3. S is quasi-Fuchsian, meaning that the limit set of a connected lift of S to hyperbolic 3-space is a quasi-circle.

In [10] (see also [7]), it was proved that in a non-fibered hyperbolic knot complement, a minimal genus Seifert surface cannot possess accidental parabolics and hence must be quasi-Fuchsian. We now focus on this case.

We are particularly interested in the subset of quasi-Fuchsian spanning surfaces called either *Fuchsian* or *totally geodesic surfaces*. Such a surface lifts to a collection

Table 1 Table of rigid 2-orbifolds

Hyperbolic rigid 2-orbifolds	Exceptions (these are not hyperbolic)
$S^2(n, m, p)$	$S^2(2, 2, n), S^2(2, 3, 3), S^2(2, 3, 4), S^2(2, 3, 5), S^2(2, 3, 6), S^2(2, 4, 4), S^2(3, 3, 3)$
$D^2(n; m)$	$D^2(2; n), D^2(3; 2), D^2(3; 3), D^2(4; 2)$
$D^2(; n, m, p)$	$D^2(; 2, 2, n), D^2(; 2, 3, 3), D^2(; 2, 3, 4), D^2(; 2, 3, 5), D^2(; 2, 3, 6), D^2(; 2, 4, 4), D^2(; 3, 3, 3)$

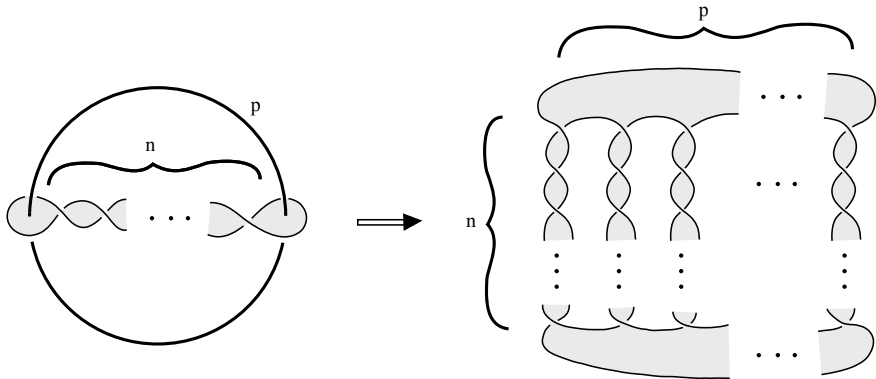


Fig. 3 A totally geodesic Seifert surface for the (n, n, \dots, n) -pretzel knot

of geodesic planes in hyperbolic 3-space. In [2, 3], examples of such surfaces were produced using the following method. Certain hyperbolic 2-orbifolds are rigid, as appear in Table 1. This means that they have a unique hyperbolic structure and they are themselves totally geodesic. The integers before the semi-colon are the orders of cone points in the interior of the 2-orbifold, and the integers after the semi-colon are the orders of corners on the boundary of the 2-orbifold.

If one can find a knot or link in the 3-sphere with a spanning surface, such that they have certain symmetries, the quotient under which is a spherical 3-orbifold such that the surface projects to a rigid 2-orbifold, then the surface must be totally geodesic in the hyperbolic structure on the knot or link complement.

Example 1

The (n, n, \dots, n) -pretzel knot possesses a totally geodesic Seifert surface. On the left in Fig. 3, we see a spherical 3-orbifold with a single circular singular set of order p . We have removed a knot from it that bounds a rigid 2-orbifold of type $S^2(p, p, \infty)$, such that the 2-orbifold lifts to the totally geodesic Seifert surface for the knot on the right.

Example 2

We can also obtain totally knotted totally geodesic Seifert surfaces as in Fig. 4.

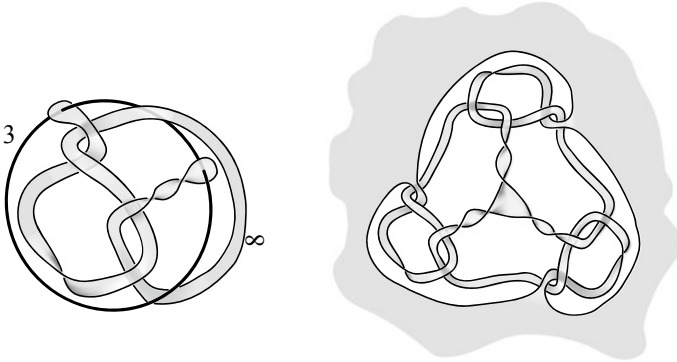


Fig. 4 A totally knotted totally geodesic Seifert surface

Example 3

If we allow ourselves to leave the category of knots in the 3-sphere momentarily, we note that there are examples of links such that both checkerboard surfaces are totally geodesic (Fig. 5).

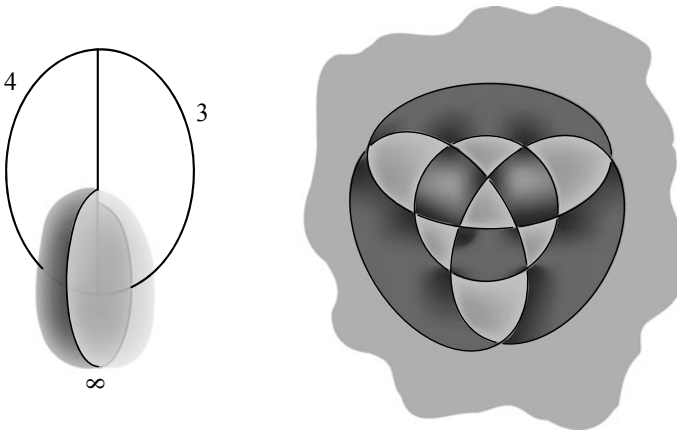


Fig. 5 A link with two embedded totally geodesic checkerboard surfaces

It remains an open question as to whether any knot has a projection with both checkerboard surfaces totally geodesic. See also the comment after the next example.

Note that in [6], the authors provide examples of two links living in $T \times I$ where T is the torus, namely the triaxial link and the square-weave link, such that both checkerboard surfaces on the torus are totally geodesic.

Example 4

Again leaving the category of knots for just another moment, an example of a nonorientable totally geodesic checkerboard surface in a link complement is found in the Whitehead link, shown in Fig. 6. This construction generalizes to $(2p, 2q + 1, 2p)$ -pretzel links. It is not known whether nonorientable totally geodesic Seifert surfaces exist in knot complements.

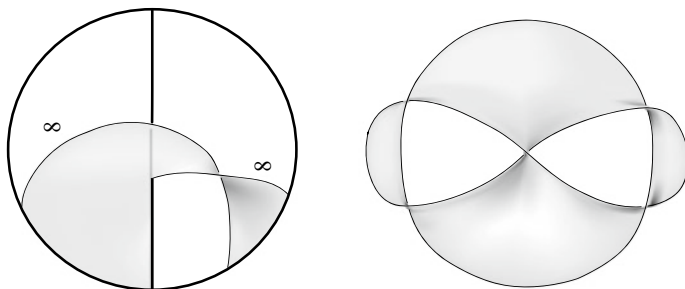


Fig. 6 A rigid 2-orbifold yielding a nonorientable totally geodesic spanning surface for the Whitehead link

Note that for any knot, at least one of the two checkerboard surfaces must be nonorientable. (This follows by showing via Euler characteristic that at least one of the faces in the projection plane has an odd number of edges, forcing the checkerboard surface that does not contain that face to be nonorientable.)

Although knots can have arbitrarily many different Seifert surfaces, when we restrict to certain kinds of totally geodesic surfaces, this is no longer true. For instance, in [2], it was proved that when a semi-free totally geodesic surface exists for a given knot in S^3 , it must be the only totally geodesic Seifert surface for the knot. In particular, this means that if there is a vertex of the Kakimizu complex corresponding to a semi-free totally geodesic Seifert surface, then no other vertex can correspond to a totally geodesic Seifert surface. Thus a (n, n, \dots, n) -pretzel knot has exactly one totally geodesic Seifert surface.

Totally geodesic Seifert surfaces appear to be relatively rare. For example, in [3], it was proved that 2-bridge knots never have totally geodesic Seifert surfaces.

One method for restricting totally geodesic surfaces utilizes a new invariant. Given a nontrivial, minimal length closed curve γ representing the boundary of a surface S on the boundary of a maximal cusp C of the complement of a hyperbolic knot K , we call the length of the shortest path in ∂C which starts and ends on γ , but which is not isotopic into γ , the *width* of S , denoted $w(S)$. In the case that the surface is orientable, γ will be a longitude, and we say this width is the width of the knot $w(K)$.

In [2], it is proved that for a totally geodesic Seifert surface in a knot complement to exist, $1 \leq w(K)$. Moreover, if such a surface is semi-free, then $w(K) < 2$. This upper bound cannot be improved as the widths of the (p, p, p) -pretzel knots approach 2 as p grows.

Then, if two oppositely oriented strands in a knot projection are twisted around each other to obtain a sequence of bigons, and if the resulting sequence of knots is hyperbolic, the widths of these knots approach 0. Thus, all but finitely many of the knots in the sequence cannot possess totally geodesic Seifert surfaces.

4 Quasi-Fuchsian Seifert Surfaces

Assuming a given hyperbolic knot is not fibered, it must possess at least one quasi-Fuchsian Seifert surface. So it is useful to understand such surfaces. We would like to have a measure of how far a given quasi-Fuchsian Seifert surface is from being Fuchsian.

Given a properly embedded quasi-Fuchsian Seifert surface S for a hyperbolic knot K and a maximal cusp C for the complement of K , lift to the upper-half-space model of \mathbb{H}^3 such that ∂C lifts to a horosphere H centered at ∞ , which appears as a horizontal plane. A topological plane P covering S has a limit point at ∞ . The limit set L of P is a quasi-line in the xy -plane. Let P_1 and P_2 be two vertical planes such that they sandwich the limit set L between them and the Euclidean distance between their boundary lines in the xy -plane is as small as possible. Note that their boundary lines will be parallel. The *cuspidal thickness* of S , denoted $ct(S)$, is then defined to be the distance between P_1 and P_2 as measured in the horizontal plane H covering the boundary of the cusp C , as in Fig. 7.

There is no corresponding measure in the case of a closed quasi-Fuchsian surface. Note that if S is Fuchsian (totally geodesic), then $ct(S) = 0$. In [1], the previously mentioned results on width of Fuchsian surfaces are extended to quasi-Fuchsian surfaces. In particular, $w(S) + ct(S) \geq 1$ and if S is semi-free, then $w(S) - ct(S) < 2$. This allows one to restrict the types of quasi-Fuchsian surfaces that can be present in a given hyperbolic knot complement.

In [11], it is proved that for a hyperbolic alternating link, the checkerboard surfaces are quasi-Fuchsian. (The proof that appears in [1] is incomplete.) From additional results in [1], this implies that every hyperbolic alternating knot or link possesses a quasi-Fuchsian spanning surface, which is one of the checkerboard surfaces, with $w(S) - ct(S) \leq 1$.

In [9], cusp thicknesses of certain checkerboard surfaces were approximated. In Fig. 8, the limit set for a checkerboard surface S for the figure-eight knot is shown with a cusp thickness of approximately 1.06824. (The checkerboard surfaces for the figure-eight are equivalent under a symmetry, so they both have the same cusp thickness.) The width of this checkerboard surface is $w(S) \approx 0.65465$. Hence $w(S) - ct(S) < 1$. In fact, in this case, it is less than 0, which will always be the case whenever there is a bigon in the complement of the checkerboard surface in the projection sphere.

5 Punctured Immersed Spanning Surfaces

In [12], the author introduced an immersed punctured disk with boundary equal to the knot or link obtained in the following manner. We take a projection of the knot or link and we cone the projection up to a point U above the projection plane. The result is a singular disk that is punctured by the knot at each crossing. The singular set consists of double point arcs running from the top of each crossing to U . A similar construction works if we cone to a point D below the projection plane.

Z.-X. He used these surfaces to obtain lower bounds on the crossing number of satellite knots of hyperbolic knots. In [2], these surfaces were used to find bounds on cusp invariants for hyperbolic manifolds. For example, it was proved that the meridian length of a hyperbolic knot as measured in a maximal cusp is at most $6 - 7/c(K)$ and the longitude length is at most $5c(K) - 6$.

We now provide an alternative method for obtaining these surfaces. A construction originally due to D. Thurston [18] allows the decomposition of a knot or link complement into octahedra, with a mixture of ideal and finite vertices. Again, we choose points U and D above and below the projection plane. Then we insert an octahedron between the top and bottom strand at each crossing as in Fig. 9.

Of the equatorial vertices, two are lifted up to the finite point U above the projection plane, causing the identification of two edges of the octahedron, and two are pulled down to the vertex D below the projection plane, again identifying two edges of the octahedron. Gluing the faces of the various octahedra at each crossing together

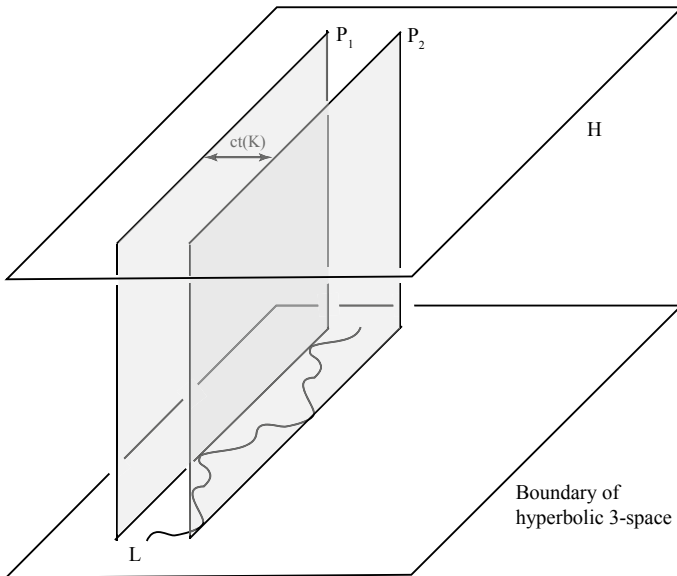


Fig. 7 The cusp thickness of a quasi-Fuchsian surface

Fig. 8 The limit set for a checkerboard surface of the figure-eight knot. (Figure from [9], used with permission)



appropriately, as demonstrated in Fig. 10 for two octahedra sharing a bigon, yields the knot complement.

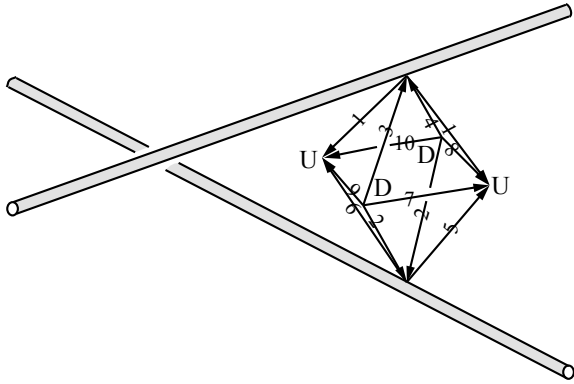


Fig. 9 Insert an octahedron at each crossing, with a mix of finite and ideal vertices

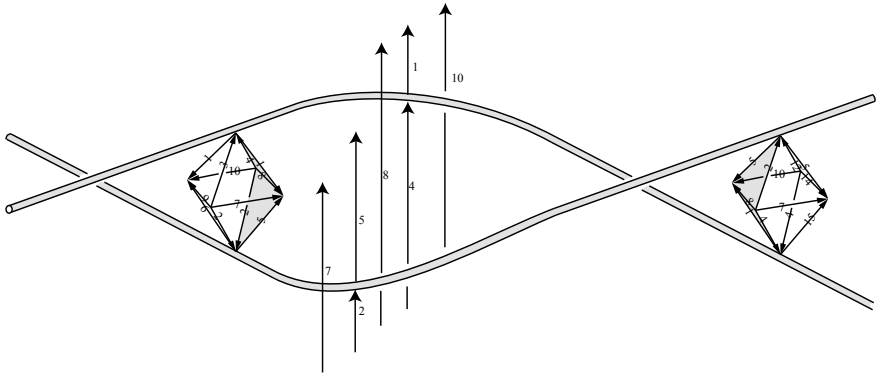
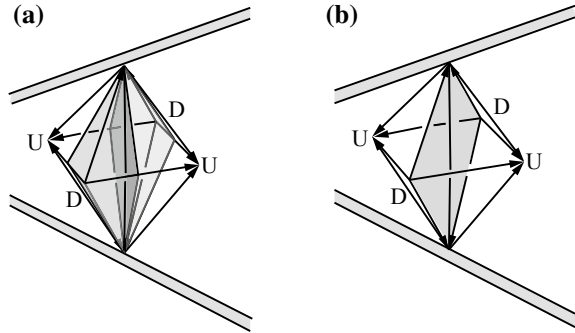


Fig. 10 Glue adjacent octahedra together along the appropriate faces

Fig. 11 Cross sections of octahedra that yield interesting surfaces



This construction has been helpful in proving the Volume Conjecture for a handful of knots, which relates the hyperbolic volume to the asymptotic behavior of the colored Jones polynomial. It also gives an upper bound on volume for knots.

$$vol(K) < c(K)(3.6638\dots)$$

This follows because any hyperbolic octahedron has volume at most the volume of an ideal regular tetrahedron, which is $3.6638\dots$

But now, we consider some surfaces that come out of this octahedral construction. We first take the surfaces that result by taking the two vertical cross sections of each octahedron as shown in Fig. 11a.

Clearly, the result is a surface that self intersects along the vertical edges that connect the top strand of a crossing to the bottom strand of a crossing. In fact, this results in two embedded surfaces intersecting along these edges, those being the checkerboard surfaces of the projection. So we see that the checkerboard surfaces are a natural byproduct of the octahedral decomposition.

Now take the the vertical cross section of each octahedron that passes through the top and bottom ideal vertices and through the two vertices labelled D as in Fig. 11b.

If we glue these cross sections of all of the octahedra together, we obtain the punctured immersed disk obtained in He’s construction by coning the projection to the point D . If instead, we take vertical cross sections that contain the two points labelled U , then they glue up to form the immersed disk in He’s construction obtained by coning the projection to the point U . So once again, we see an important surface as a natural byproduct of the octahedral decomposition.

There are still many interesting open questions as to the geometric behavior of surfaces in hyperbolic knot complements. Understanding their behavior will lead to further understanding of hyperbolic knots.

References

1. C. Adams, Noncompact Fuchsian and quasi-Fuchsian surfaces in hyperbolic 3-manifolds. *Algebr. Geom. Top.* **7**, 565–582 (2007)
2. C. Adams, H. Bennett, C. Davis, M. Jennings, J. Novak, N. Perry, E. Schoenfeld, Totally geodesic Seifert surfaces in hyperbolic knot complements II. *J. Diff. Geom.* **79**, 1–23 (2008)
3. C. Adams, E. Schoenfeld, Totally geodesic Seifert surfaces in hyperbolic knot complements I. *Geom. Dedicata* **116**, 237–247 (2005)
4. F. Bonahon, Bouts des variétés hyperboliques de dimension 3. *Ann. Math.* **124**, 71–158 (1986)
5. R. Canary, D.B.A. Epstein, P. Green, Notes on notes of Thurston, in *Analytic and Geometric Aspects of Hyperbolic Space*. LMS Lecture Notes, vol. 111, ed. by D.B.A. Epstein (Cambridge University Press, Cambridge, 1987)
6. A. Champanerkar, I. Kofman, J. Purcell, Geometry of biperiodic alternating links (2018), [arXiv:1802.05343](https://arxiv.org/abs/1802.05343)
7. D. Cooper, D. Long, Some surface subgroups survive surgery. *Geom. Topol.* **5**, 347–367 (2001)
8. T. Crawford, Totally knotted and semi-free pairwise disjoint Seifert surfaces in knot complements, Williams College thesis (2012)
9. B. DeMeo, Cusp thicknesses of checkerboard surfaces for a family of links, Williams College thesis (2015)
10. S. Fenley, Quasifuchsian Seifert surfaces. *Math. Zeit.* **228**, 221–227 (1998)
11. D. Futer, E. Kalfagianni, J. Purcell, Quasifuchsian state surfaces. *Trans. AMS* **366**, 4323–4343 (2014)
12. Z.-X. He, On the crossing number of high degree satellites of hyperbolic knots. *Math. Res. Lett.* **5**, 235–245 (1998)
13. O. Kakimizu, Finding disjoint incompressible spanning surfaces for a link. *Hiroshima Math. J.* **22**, 225–236 (1992)
14. U. Oertel, On the existence of infinitely many essential surfaces of bounded genus. *Pac. J. Math* **202**, 449–458 (2002)
15. P. Przytycki, J. Schultens, Contractibility of the Kakimizu complex and symmetric Seifert surfaces. *Trans. Am. Math. Soc.* **364**, 1489–1508 (2012)
16. M. Scharlemann, A. Thompson, Finding disjoint Seifert surfaces. *Bull. LMS* **20**, 61–64 (1988)
17. W. Thurston, *The Geometry and Topology of 3-Manifolds*. Lecture Notes (Princeton University, Princeton, 1978)
18. D. Thurston, Hyperbolic volume and the Jones polynomial, lecture notes, Grenoble summer school. *Invariants des noeuds et de variétés de dimension 3* (1999)
19. R. Wilson, Knots with infinitely many incompressible Seifert surfaces. *J. Knot Theory Ramif.* **17**, 537–551 (2008)

On the Construction of Knots and Links from Thompson's Groups



Vaughan F. R. Jones

Abstract We review recent developments in the theory of Thompson group representations related to knot theory.

Keywords Thompson group · Knot · Link · Braid · Representation · Skein theory

2010 Mathematics Subject Classification 57M25 · 57M27 · 20F36 · 20F38 · 22D10

1 Introduction

The Thompson group F is the group of all piecewise linear homeomorphisms g of $[0, 1]$ with $g(0) = 0$, $g(1) = 1$, which are smooth except at finitely many dyadic rationals, and whose slopes, when defined, are powers of 2. The bigger Thompson group T has the same definition except that its elements act on the circle \mathbb{R}/\mathbb{Z} and need not preserve 0 or 1. A few years ago in [17] a method of geometric origin was introduced for constructing representations of F and T . The construction involved a target category which was in the first instance a tensor category. Applying this construction to the category of Conway tangles gave a way of constructing a link from a Thompson group element. It was shown in [17] that all links arise in this fashion. The knot theoretic outcome of this construction can be summed up by a four step procedure going from an element $g \in F$ to an unoriented link $L(F)$. Let us describe this procedure.

As in [7] any element $g \in F$ can be represented as a pair of binary planar rooted trees with the same number of leaves. Let us explain how. By successively splitting in half intervals of $[0, 1]$ according to the tree, the leaves of such a tree are naturally identified with intervals with dyadic rational endpoints of the form $[\frac{a}{2^n}, \frac{a+1}{2^n}]$.

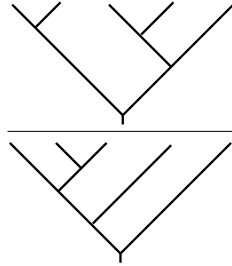
V. F. R. Jones (✉)

Department of Mathematics, Vanderbilt University, Nashville, TN, USA
e-mail: vaughan.f.jones@Vanderbilt.Edu

© Springer Nature Switzerland AG 2019

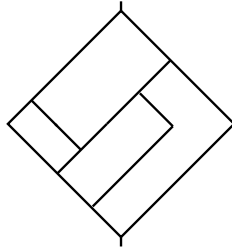
C. C. Adams et al. (eds.), *Knots, Low-Dimensional Topology and Applications*, Springer Proceedings in Mathematics & Statistics 284, https://doi.org/10.1007/978-3-030-16031-9_3

The g defined by such a pair of trees sends the intervals/leaves of the first tree to the intervals/leaves of the second tree (from left to right), with constant slope. For reasons explained in this paper we will draw the pair of trees as a fraction—an example is given below:

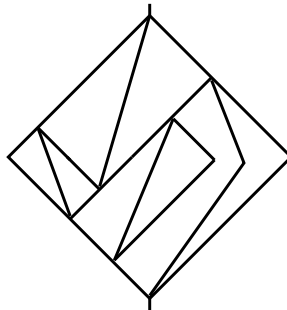


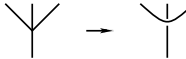
(Just to make sure what we have said is clear, the leaves (from left to right) of the denominator tree correspond to the intervals $[0, \frac{1}{8}]$, $[\frac{1}{8}, \frac{3}{16}]$, $[\frac{3}{16}, \frac{1}{4}]$, $[\frac{1}{4}, \frac{1}{2}]$, and $[\frac{1}{2}, 1]$, and for the numerator tree, $[0, \frac{1}{4}]$, $[\frac{1}{4}, \frac{1}{2}]$, $[\frac{1}{2}, \frac{5}{8}]$, $[\frac{5}{8}, \frac{3}{4}]$, and $[\frac{3}{4}, 1]$.)

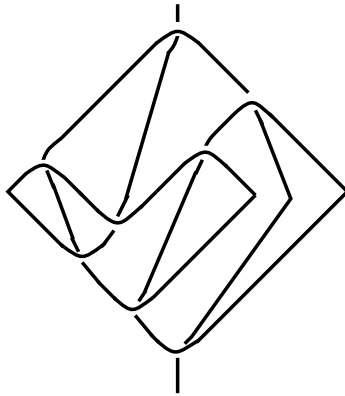
The first step in the construction of $L(g)$ is to flip the numerator upside down and join its leaves to those of the denominator:



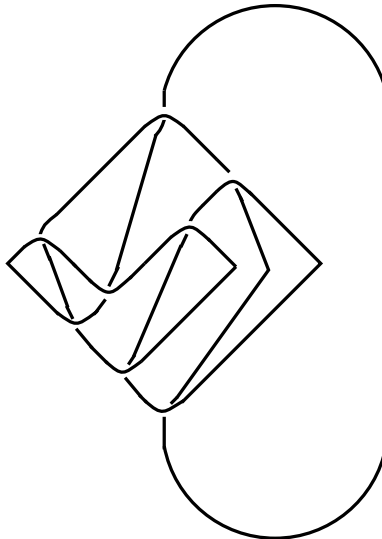
Now each vertex of the top tree shares a region with a unique vertex of the bottom tree. Join them with an edge in that region:



All vertices are now 4-valent. Replace them all with crossings with the vertical edges going under:  which gives:



Finally tie the top edge to the bottom to obtain the link $L(g)$:



Note that the pair of trees defining g is not quite unique but there is a unique pair with no “cancelling carets” so for $L(g)$ to be well defined, use this pair. Cancelling carets are quite innocent on the knot theory side, they just give unknots which do not link with the rest of the diagram.

For details consult [17].

Our example fairly visibly gives a 2 component unlink and the reader is likely to struggle to obtain a nontrivial knot. Indeed even the number of components of

the link determined by the pair of trees is obscure. However we have the following result:

Theorem 1.1 *Let R be the ring of formal linear combinations (over \mathbb{Z}) of isotopy classes of unoriented link diagrams with multiplication given by distant union and conjugation given by mirror image. There is an R -module \mathcal{V} with R -valued sesquilinear inner product $\langle \cdot, \cdot \rangle$, together with a privileged element $\Omega \in \mathcal{V}$, and a $\langle \cdot, \cdot \rangle$ -preserving R -linear action π of Thompson’s group F on \mathcal{V} such that for $g \in F$,*

$$\langle \pi(g)\Omega, \Omega \rangle = L(g)$$

Moreover any unoriented link in \mathbb{R}^3 can be realised as $L(g)$ for some $g \in F$.

Since [17] this construction has been better understood, considerably simplified and generalised, though admittedly at the cost of geometric understanding. In this largely expository paper we will first describe the new simplified version of the construction of the action of the Thompson groups with a few new examples. We will then explain the particular context that leads to the theorem above—further simplified by the use of the Thompson groups F_3 and T_3 rather than F_2 and T_2 . Finally we will list a few obvious questions that remain open at this stage.

2 The Directed Set/Functor Method

A planar k -forest is the isotopy class of a disjoint union of planar rooted trees all of whose vertices are adjacent to $k + 1$ edges, embedded in the strip $(\mathbb{R}, [0, 1]) \subset \mathbb{R}^2$ with roots lying on $(\mathbb{R}, 0)$ and leaves lying on $(\mathbb{R}, 1)$. Edges connected to roots and leaves meet the boundaries of the strip transversally and only the leaves and the roots meet the boundary. The isotopies preserve the strip but may act nontrivially on the boundary. Planar k -forests form a category in the obvious way with objects being \mathbb{N} (whose elements are identified with isotopy classes of sets of points on a line) and whose morphisms are the planar k -forests themselves, which can be composed by stacking a forest in $(\mathbb{R}, [0, 1])$ on top of another, lining up the leaves of the one on the bottom with the roots of the other by isotopy then rescaling the y axis to return to a forest in $(\mathbb{R}, [0, 1])$.

We will call this category \mathcal{F}_k . For $k = 2$ and $k = 3$ we will use the terms binary and ternary forest respectively.

The set of morphisms from 1 to n in \mathcal{F}_k is the set of k -ary planar rooted trees \mathfrak{T}_k and is a *directed set* with $s \leq t$ iff there is and $f \in \mathcal{F}$ with $t = fs$.

It is useful to know the number of k -ary planar rooted trees.

Proposition 2.1 *There are $FC(k, n)$ k -ary planar rooted trees with n vertices where $FC(k, n)$ is the Fuss–Catlan number $\frac{1}{(k - 1)n + 1} \binom{kn}{n}$.*

Proof By attaching k new trees to the root vertex we see that the number of k -ary planar rooted trees with n vertices satisfies the same recursion relation:

$$FC(k, n + 1) = \sum_{\ell_1, \ell_2, \dots, \ell_k, \sum \ell_i = n} \prod_{i=1}^n FC(k, \ell_i).$$

See [10] for details about the Fuss–Catalan numbers. □

Given a functor $\Phi : \mathcal{F} \rightarrow \mathcal{C}$ to a category \mathcal{C} whose objects are sets, we define the direct system S_Φ which associates to each $t \in \mathfrak{T}, t : 1 \rightarrow n$, the set $\Phi(\text{target}(t)) = \Phi(n)$. For each $s \leq t$ we need to give t'_s . For this observe that there is an $f \in \mathcal{F}$ for which $t = fs$ so we define

$$t'_s = \Phi(f)$$

which is an element of $Mor_{\mathcal{C}}(\Phi(\text{target}(s)), \Phi(\text{target}(t)))$ as required. The t'_s trivially satisfy the axioms of a direct system.

As a slight variation on this theme, given a functor $\Phi : \mathcal{F} \rightarrow \mathcal{C}$ to any category \mathcal{C} , and an object $\omega \in \mathcal{C}$, form the category \mathcal{C}^ω whose objects are the sets $\overline{Mor}_{\mathcal{C}}(\omega, obj)$ for every object obj in \mathcal{C} , and whose morphisms are composition with those of \mathcal{C} . The definition of the functor $\Phi^\omega : \mathcal{F} \rightarrow \mathcal{C}^\omega$ is obvious. Thus the direct system S_{Φ^ω} associates to each $t \in \mathfrak{T}, t : 1 \rightarrow n$, the set $Mor_{\mathcal{C}}(\omega, \Phi(n))$. Given $s \leq t$ let $f \in \mathcal{F}$ be such that $t = fs$. Then for $\kappa \in Mor_{\mathcal{C}}(\omega, \Phi(\text{target}(s)))$,

$$t'_s(\kappa) = \Phi(f) \circ \kappa$$

which is an element of $Mor_{\mathcal{C}}(\omega, \Phi(\text{target}(t)))$.

As in [14] we consider the direct limit:

$$\varinjlim S_\Phi = \{(t, x) \text{ with } t \in \mathfrak{T}, x \in \Phi(\text{target}(t))\} / \sim$$

where $(t, x) \sim (s, y)$ iff there are $r \in \mathfrak{T}, z \in \Phi(\text{target}(z))$ with $t = fr, s = gr$ and $\Phi(f)(x) = z = \Phi(g)(y)$.

We use $\frac{t}{x}$ to denote the equivalence class of $(t, x) \text{ mod } \sim$.

The limit $\varinjlim S_\Phi$ will inherit structure from the category \mathcal{C} . For instance if the objects of \mathcal{C} are Hilbert spaces and the morphisms are isometries then $\varinjlim S_\Phi$ will be a pre-Hilbert space which may be completed to a Hilbert space which we will also call the direct limit unless special care is required.

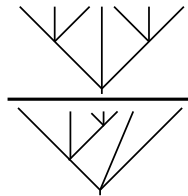
As was observed in [14], if we let Φ be the identity functor and choose ω to be the tree with one leaf, then the inductive limit consists of equivalence classes of pairs $\frac{t}{x}$ where $t \in \mathcal{T}$ and $x \in \Phi(\text{target}(t)) = Mor(1, \text{target}(t))$. But $Mor(1, \text{target}(t))$ is nothing but $s \in \mathcal{T}$ with $\text{target}(s) = \text{target}(t)$. So a fraction $\frac{s}{t}$ is an equivalence

class of **pairs of trees with the same number of leaves**. Thus the inductive limit is nothing but the (Brown-)Thompson group F_k if we equip it with the group law

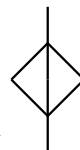
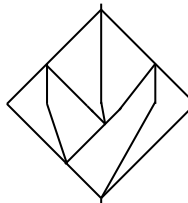
$$\frac{r \ s}{s \ t} = \frac{r}{t}.$$

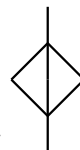
(Just as with the multiplication of the rational numbers as fractions of integers, it is important to note that it is the equivalence class $\frac{s}{t}$ that is used in the above formula. Particular pairs of trees representing the equivalence classes will not in general have the denominator of the first pair equal to the numerator of the second, but they can be stabilised so that this is true.)

For instance the following tree fraction gives an element of F_3 :



This explains the notation we used for F in the introduction. The equivalence class $\frac{s}{t}$ for a pair of trees s and t is the set of all other pairs which are related to s and t by cancelling carets as in [7]. It is part of the philosophy of this paper to think of $\frac{s}{t}$ also as the diagram obtained by flipping the numerator upside down and attaching its leaves to those of the denominator so that, for instance, the above element can equally be written



For F_3 cancelling a caret is just the removal of  from a diagram consisting of the “upside down numerator” picture of a pair of trees.

(Geometrically this makes sense- F_3 is a group of piecewise linear homeomorphisms constructed from intervals which are sent by scaling transformations to other intervals. If we associate an interval with each leaf of a tree by the rule that each

vertex of the tree splits an interval up into three adjacent intervals of equal width, then the element of F_3 given by a diagram as above maps an interval of a leaf of the bottom tree to the interval of the leaf of the top tree to which it is attached. A pair of cancelling carets is just the subdivision of an interval on which the homeomorphism is already linear into intervals of equal length, which obviously does not change the homeomorphism coded for by the pair of trees.)

With this definition of the group we may construct actions in a simple way. For any functor Φ , $\lim_{\rightarrow} S_{\Phi}$ carries a natural action of F_k defined as follows:

$$\frac{s}{t} \left(\frac{t}{x} \right) = \frac{s}{x}$$

where $s, t \in \mathfrak{T}_k$ with $target(s) = target(t) = n$ and $x \in \Phi(n)$. A Thompson group element given as a pair of trees with m leaves, and an element of $\lim_{\rightarrow} S_{\Phi}$ given as a pair (tree with n leaves, element of $\Phi(n)$), may not be immediately composable by the above formula, but they can always be “stabilised” to be so within their equivalence classes.

The Thompson group action preserves the structure of $\lim_{\rightarrow} S_{\Phi}$ so for instance in the Hilbert space case the representations are unitary.

3 The Connection with Knots

A Conway tangle is an isotopy class of rectangles with m “top” and n “bottom” boundary points, containing smooth curves called strings with under and over crossings which meet the boundary transversally in the $m + n$ boundary points. The isotopies are considered to contain the three Reidemeister moves but must fix the top and bottom edges of the rectangles. Conway tangles form a category whose objects are $0 \cup \mathbb{N}$ with the non-negative integer n being identified with isotopy classes of sets of n points in an interval. The morphisms are then the Conway tangles with the obvious stacking as composition:



A morphism in \mathfrak{C} from 3 to 5 :

Of course the set of morphisms from m to n is empty if $m + n$ is odd.

Definition 3.1 The Conway tangles defined above will be called the category of tangles \mathfrak{C} .

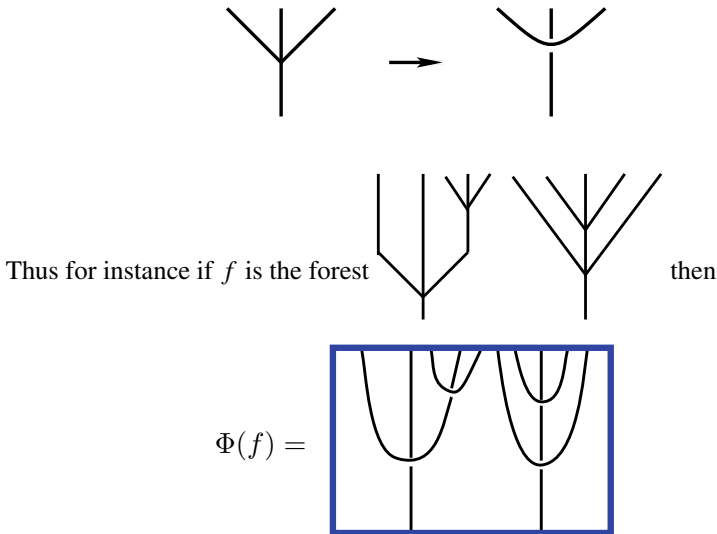
We will apply the construction of the previous section to the ternary Thompson group F_3 to obtain actions of it on spaces of tangles. We distinguish three slightly different ways to do this.

(1) Set theoretic version:

To perform the construction of the previous section we need to define a functor from ternary forests to \mathcal{C} .

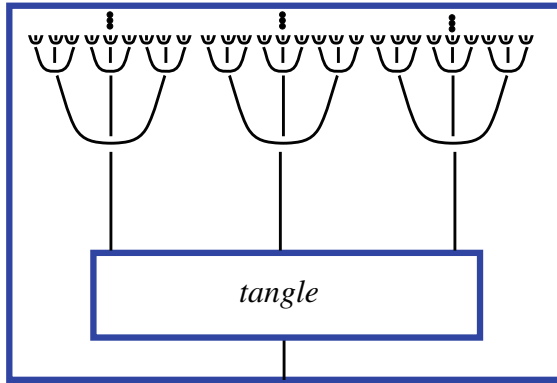
Definition 3.2 The functor $\Phi : \mathcal{F}_3 \rightarrow \mathcal{C}$ is defined as follows:

- (a) On objects $\Phi(n) = n$ so that the roots of a planar forest are sent to the boundary points at the bottom of a tangle, from left to right.
- (b) On morphisms (i.e. forests), $\Phi(f)$ is defined to be the tangle obtained by isotoping the forest to be in a rectangle with roots on the bottom edge and leaves on the top edge, and replacing each vertex of the forest with a crossing thus:



The well definedness and functoriality of Φ are obvious.

By the machinery of the previous section we obtain an action of F_3 on a set $\tilde{\mathcal{C}}$, the direct limit of sets of tangles. An element of the set $\tilde{\mathcal{C}}$ is the equivalence class of a pair (t, T) where t is a ternary planar rooted tree with n leaves and T is a $(1, n)$ Conway tangle. Adding a single vertex to t corresponds to adding a single crossing to T and this generates the equivalence relation. Thus an element of $\tilde{\mathcal{C}}$ can be thought of as an infinite tangle with one boundary point at the bottom and eventually ending up with a lot of simple crossings organised as below:



The original geometric intuition of our construction was to think of a Thompson group element as giving a piecewise linear foliation of a rectangle attaching points at the bottom to their images on the top, and stacking it on top of the above picture to give a new such picture. See [15].

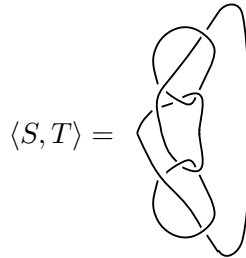
(2) Linearised version:

Recall that R is the ring of formal linear combinations (over \mathbb{Z}) of (three dimensional) isotopy classes of unoriented links with distant union as multiplication. An unoriented link acts on a tangle simply by inserting a diagram for it in any region of the tangle containing no strings.

Definition 3.3 We use δ to denote the element of R given by a single unknotted circle.

One may alter construction 1 by replacing the set of $(1, 2k + 1)$ tangles by the free R -module $R\mathcal{C}_{1,k}$ having those tangles as a basis. This way the direct limit V is also an R -module. More importantly mirror image defines an involution on R and there is a sesquilinear form $\langle S, T \rangle$ on each $R\mathcal{C}_{1,k}$ obtained by reflecting the tangle T about the top side of its rectangle, then placing it above S and connecting all the boundary points in the obvious way to obtain an element of R .





Unfortunately the connecting maps i_s^t of the direct system do not preserve \langle, \rangle . But this is easily remedied by adjoining a formal square root $\sqrt{\delta}$ and its inverse to R to obtain $R[\sqrt{\delta}, \frac{1}{\sqrt{\delta}}]$. One then modifies the functor Φ by multiplying the $R[\sqrt{\delta}, \frac{1}{\sqrt{\delta}}]$ -linear map induced by Φ in (i) above (by its action on a the basis of tangles) by $(\frac{1}{\sqrt{\delta}})^p$ where p is the number of vertices in the forest. Then the connecting maps preserve the sesquilinear form which thus passes to a sesquilinear form on the direct limit $R[\sqrt{\delta}, \frac{1}{\sqrt{\delta}}]$ -module which is tautologically preserved by the action of F_3 . To simplify notation we will continue to use R for $R[\sqrt{\delta}, \frac{1}{\sqrt{\delta}}]$.

Now we are finally at the interesting bit. Given a representation of a group G on an R -module V , $g \mapsto u_g$, preserving a sesquilinear form \langle, \rangle , the *coefficients* of the representation are the functions

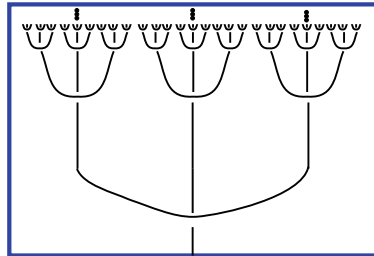
$$g \mapsto \langle u_g(\xi), \eta \rangle$$

as ξ and η vary in V .

But our construction of the direct limit gives us a *privileged vector* $\Omega \in V$, namely the equivalence class of the $(1, 1)$ tangle ω consisting of a single straight string connecting the boundary points of a rectangle with two boundary points, one at the bottom and one at the top. (Recall that the $(1, 1)$ tangles span the space right at the bottom of the direct limit-namely the space assigned by the functor to the object 1.) We will call this vector Ω . With the notation we have established,

$$\Omega = \frac{1}{\omega}.$$

Intuitively, if we want to think of Ω as an element of V thought of as an infinite tangle, it is just:



(normalised by the appropriate power of δ for a given finite approximation).

Since Ω is a privileged vector, we would like to know the function on F_3 given by the coefficient $\langle u_g(\Omega), \Omega \rangle$, g being an element of F_3 and u_g being the representation we have constructed. It is tempting to call the vector Ω the “vacuum vector” so that by analogy with physics (strengthened by the next section on topological quantum field theory) we offer the following:

Definition 3.4 The element $\langle u_g(\Omega), \Omega \rangle$ of $R[\sqrt{\delta}, \frac{1}{\sqrt{\delta}}]$ is called the *vacuum expectation value* of $g \in F_3$. (It is just a power of δ times a tangle.)

It is not hard to calculate this element of R if we follow the definitions carefully.

Let $g = \frac{s}{t}$ be an element of F_3 where s and t are planar rooted ternary trees with the same number of leaves. $\Omega \in V$ is given by $\frac{1}{\omega}$ where 1 is the tree with no vertices. To calculate $u_g(\Omega)$ we need to stabilise 1 so that we can apply the formula defining the representation. Thus we write $\frac{1}{\omega} = \frac{t}{\Phi(t)(\omega)}$ -recall that $\Phi(t)$, for a tree with n leaves, is defined by changing all the vertices to crossings to get a tangle then using the stacking of tangles to go from $\Phi(1)$ to $\Phi(n)$. (One must also multiply by a power of δ .) Thus by definition

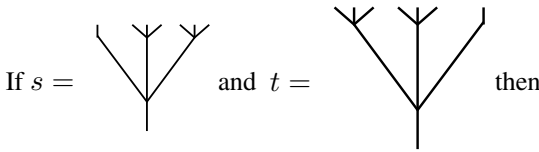
$$u_g(\Omega) = \frac{s}{\Phi(t)(\omega)}.$$

To evaluate the sesquilinear form we must write Ω in the form $\frac{s}{something}$ and by what he have just said, that something is $\Phi(s)(\omega)$.

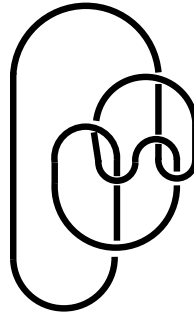
We conclude that

$$\langle u_g(\Omega), \Omega \rangle = \langle \Phi(s)(\omega), \Phi(t)(\omega) \rangle.$$

More explicitly the coefficient is obtained by attaching s to an upside down copy of t , joining the top vertex to the bottom one and replacing vertices by crossings, thus:



$$\langle u_g \Omega, \Omega \rangle = \frac{1}{\delta^2}$$



The factor $\frac{1}{\delta^2}$ comes innocently from the normalisation of the functor Φ . The picture is fairly obviously a trefoil.

Definition 3.5 If $g \in F_3$ we call $L(g)$ the link $\delta^n \langle u_g \Omega, \Omega \rangle$ for the unique representation of g as a pair of trees each with a minimal number n of vertices.

Then we have:

Theorem 3.1 Any knot or link can be obtained as $L(g)$ for some $g \in F_3$.

These vacuum expectation values are inherently unoriented. There are two ways to handle oriented links, the most powerful of which is presented in [5]. But the easiest way is to use the following.

Definition 3.6 Let $\vec{F}_3 < F_3$ be the subgroup of elements for whose pair of trees presentation the checkerboard shading gives a Seifert surface.

For F_2 this subgroup was identified in [9] as being isomorphic to F_3 ! See also [20].

(3) Skein theory version.

In the simple linearised version one may easily specialise δ to some non-zero number and use the complex numbers as coefficients. But each approximating space to the inductive limit is infinite dimensional. This can be remedied by taking a skein theory relation [8, 19] and applying it to the approximating vector spaces spanned by tangles. This is entirely compatible with the Thompson group action. The vacuum expectation value will then be (up to a power of δ) the link invariant of the skein theory for the link $L(g)$ of Definition 3.5. Since we are dealing with an unoriented theory the skein theories will have to be unoriented

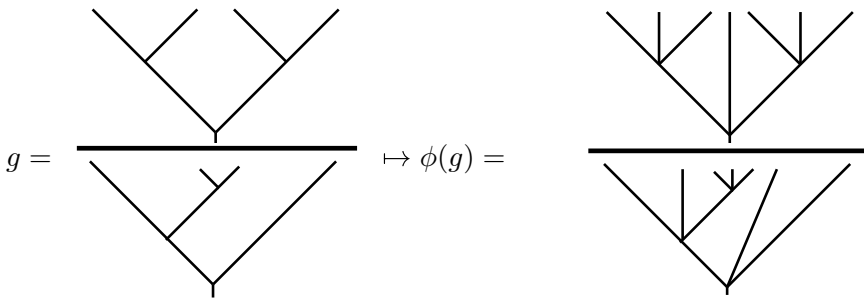
also and we will have to play the usual regular isotopy game. Indeed the vacuum expectation value will be an invariant of regular isotopy if we use the Kauffman bracket or the Kauffman polynomial. Moreover the diagram for $L(g)$ can be considered up to regular isotopy. Since the proof below of the realisation of all links as $L(g)$ actually uses a lot of type I Reidemeister moves, one may ask whether all *regular isotopy classes* of link diagrams actually arise as $L(g)$.

- (4) TQFT version: We may “apply a (unitary) TQFT” at any stage in the above procedures, provided it is unoriented. This means that the approximating subspaces for the direct limit are finite dimensional Hilbert spaces and the connecting maps i_s^t are isometries so the direct limit vector space is a pre-Hilbert space on which the Thompson group acts by isometries so we can complete and obtain a *unitary* representation of the Thompson group.

The vacuum expectation values of the unitary representation can then always be calculated as statistical mechanical sums as in [16].

4 Relationship with the Original Construction-Proof of Theorem 3.1.

It is possible to understand the construction of [17], which we gave in the introduction, in terms of a natural embedding ϕ of F_2 in F_3 . Take a binary rooted planar tree and simply attach another leaf to the middle of each vertex thus:

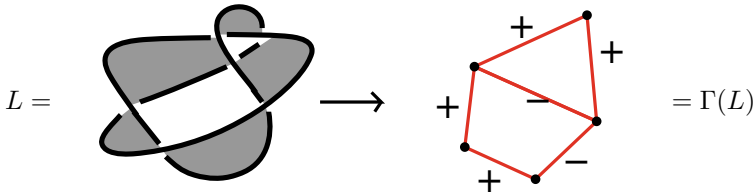


By construction $\langle u_{\phi(g)}\Omega, \Omega \rangle$ is the same as the coefficient of $g \in F_2$ defined in [17]. When there is no ambiguity we will identify F_2 with $\phi(F_2)$ as a subgroup of F_3 .

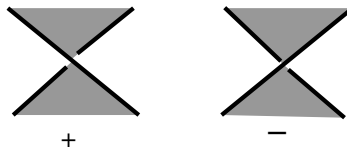
Since F_3 is much bigger than F_2 it should be possible to find a simpler proof of the “Alexander” Theorem 3.1 that all links can be obtained as vacuum expectation values for elements of F_3 . We will see that, if we try to imitate the proof of [17] we run into a problem with signs so that the proof of the weaker theorem seems harder than that of the stronger one! So we will sketch a slightly improved version of the proof of [17], pointing out the difference between the F_2 and F_3 cases.

Proof of Theorem 3.1:

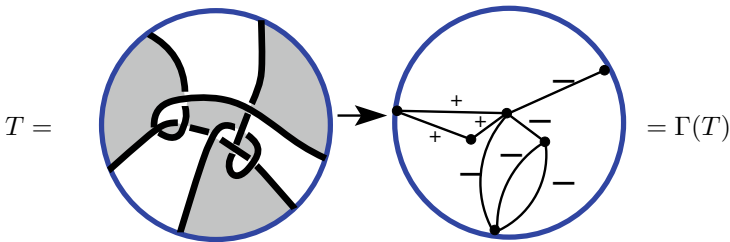
Proof Given a link diagram L for an unoriented link L we start by forming the edge-signed planar graph $\Gamma(L)$ given by a checkerboard shading of L as usual, thus:



Where we have adopted the sign convention of [17]:

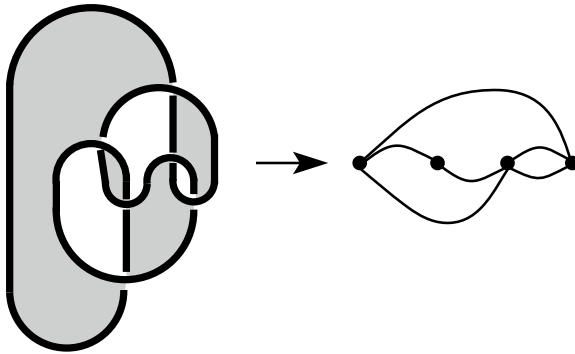


This process may be extended to Conway tangles, moving the vertices for boundary-touching faces to the boundary thus:



It is important to note that this process is *reversible*, a tangle can be obtained from any planar graph Γ with some vertices on the boundary, by putting little crossings in the middle of the edges of Γ and connecting them up around the faces of Γ with the faces meeting the boundary having two points on the boundary rather than a little crossing. (Or equivalently define the tangle as the intersection of some smooth disc with the link defined by Γ .) This means that the map from Conway tangles to planar graphs in a disc is injective.

Observe that if the link diagram is of the form $L(g)$ (see Definition 3.5) then $\Gamma(L)$ has a special form, e.g.



The diagram consists of two (not necessarily ternary) trees, one above and one below the line where the two (ternary) trees of g meet. The strategy of the proof is to take a link diagram L and modify it by planar isotopies and Reidemeister moves so that $\Gamma(L)$ looks like a graph as above.

Definition 4.1 A rooted planar/linear n -tree will be the isotopy class of a planar tree with all vertices being points on the x -axis, the isotopies being required to preserve the x axis. The root is then the leftmost point on the straight line which might as well be taken as 0.

We see that an element $g \in F_3$ (defined as a pair of ternary trees) has trees T^+ and T^- above and below the x axis respectively with the x axis as boundary. The signed graphs $\Gamma(T^+)$ and $\Gamma(T^-)$ are both rooted planar/linear n -trees where the trees defining g have $2n - 1$ leaves.

Remark 4.1 Here there is a new phenomenon compared to the F_2 case of [17]. If $g \in F_2 < F_3$ (and there are no cancelling carets) all the edges of $\Gamma(T^+)$ have a plus sign and all the edges of $\Gamma(T^-)$ have a minus sign. This is no longer true for a general element of F_3 . In fact each edge of $\Gamma(T^+)$ and $\Gamma(T^-)$ can be oriented pointing away from the root of the tree. For $\Gamma(T^+)$, if the x co-ordinate of the first vertex of the edge is less than the x co-ordinate of the second then the sign of the edge is plus, and in the opposite case it is minus. And the other way round for $\Gamma(T^-)$.

(*) The diagrams of elements of F_2 are characterised among all those of F_3 by the fact that the x coordinate increases along the oriented edges.

Proposition 4.1 There are $FC(3, n - 1) = \frac{1}{2n - 1} \binom{3n - 3}{n - 1}$ rooted planar/linear n -trees with n vertices.

Proof We need to establish the recurrence relation in the proof of Proposition 2.1 for $k = 3$. Let pl_n be the number of rooted planar/linear n -trees and take a rooted planar/linear n -tree t with 2 vertices. Then given 3 rooted planar/linear n -trees t_1, t_2 and t_3 one may form another rooted planar/linear n -tree by attaching t_1 to the right of the root of t , the reflection of t_2 in the y axis to the left of the non-root vertex of

t and t_3 to the right of the non-root vertex of t . Moreover any rooted planar/linear $n + 1$ -tree can be decomposed in this way. Thus $pl_{n+1} = \sum_{\ell_1+\ell_2+\ell_3=n} pl_{\ell_1}pl_{\ell_2}pl_{\ell_3}$. \square

By Propositions 2.1, 4.1 and the injectivity of the map from trees to tangles, or directly, there are the same number of rooted planar/linear $n + 1$ -trees as there are ternary n -trees, and given two rooted planar/linear $n + 1$ -trees Γ_{\pm} we can construct an element of F_3 by flipping Γ_- upside down and attaching it underneath Γ_+ to form a planar graph and signing all the edges according to whether their end points have smaller or larger x coordinate, we obtain a signed planar graph $\Gamma_+ \cup \Gamma_-$ from which we get a link L with $\Gamma(L) = \Gamma_+ \cup \Gamma_-$.

By Remark 4.1, if $g \in F_2$, any tree in $\Gamma_+ \cup \Gamma_-$ that arises at this point were rooted planar/linear n -trees of a special kind-namely any vertex is connected by exactly one edge to a vertex to the left of it. Such trees are counted by the usual Catalan numbers.

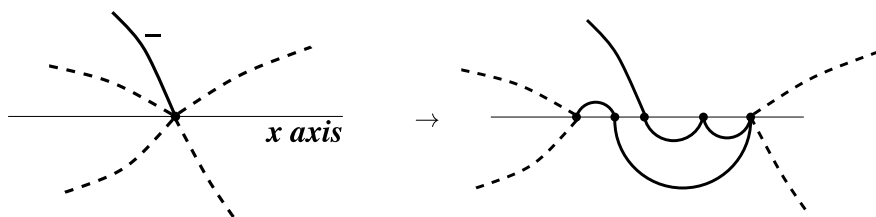
To prove Theorem 3.1, we see that it suffices to find rooted planar/linear $n + 1$ -trees Γ_{\pm} so that $\Gamma_+ \cup \Gamma_-$ differs from $\Gamma(L)$ by planar isotopies and Reidemeister moves. We will give a slightly improved version of the argument of [17] which will give us elements of F_2 . Surprisingly, we will only use Reidemeister moves of types I and II.

Note that we may suppose the link diagram L is connected so that $\Gamma(L)$ is too.

First isotope $\Gamma(L)$ so that all its vertices are on the x axis. Unless there is a Hamiltonian path through the vertices of $\Gamma(L)$, there will be edges of $\Gamma(L)$ crossing the x axis. Taking care of these edges is very simple and is described in lemma 5.3.6 of [17], but some previous versions of [17] are missing this point. Near where the offending edge cross the x axis, just add two vertices to $\Gamma(L)$ on the x axis and join them with an edge signed \pm according to the sign of the offending edge. Continue to call this graph $\Gamma(L)$. See [17].

At this stage we have a lot of the ingredients of an edge-signed rooted planar/linear graph of the form $\Gamma(L(g))$. $\Gamma(L)$ consists of two graphs, $\Gamma(L)^+$ and $\Gamma(L)^-$ in the upper and lower half-planes respectively, with vertices all lying on the x axis. The root is the vertex with smallest x coordinate. We will make a series of modifications and continue to call the graph $\Gamma(L)$ after each modification since it will represent the same link.

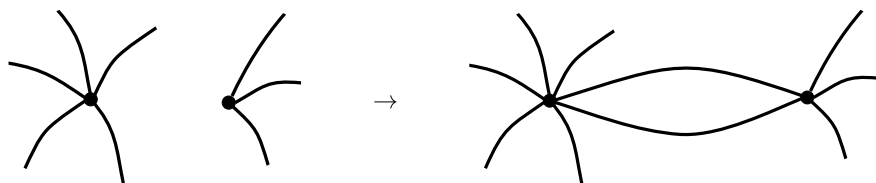
The first thing we will take care of is the signs. Since we are trying to produce an element of F_2 , we must end up with all $\Gamma(L)^+$ signs positive and all $\Gamma(L)^-$ signs negative. This may not yet be the case. But we may change $\Gamma(L)$ by type II Reidemeister moves so as to correct the bad signs one at a time. Here is how-in the diagram below the dashed lines are edges of indeterminate sign, the solid lines with no signs are positive edges if they are above the x axis and negative if below, except for a solid line with a sign next to it which is an edge with that sign.



Here we have started with a “bad” edge above the x axis and changed the graph near one end of that edge. The two small added edges in the lower half plane cancel (type II Reidemeister move) with the solid edge above to recreate the bad edge. The other two added edges just cancel to return the picture to its original form. Thus that part of the graph $\Gamma(L)$ shown on the left gives the same link after being replaced by the figure on the right.

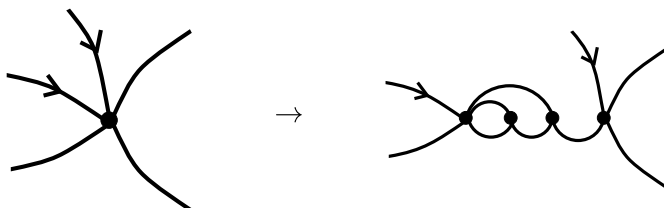
We now need to alter the graph so that if we orient the edges away from the root then the x coordinate of their sources are less than that of their targets. We can say this informally as: “each vertex is hit exactly once from the left”, top and bottom. If we do this with local changes in accordance with our convention that edges in the upper and lower half planes are positive and negative respectively, we will be done.

First let us make sure that every (non root) vertex is hit from the left, top and bottom. If there is one that is not, simply join it to its neighbour on the left with a pair of cancelling edges thus:



(Recall that the edges all get their signs from being in the upper or lower half plane.)

Now our only remaining problem is that vertices may have multiple hits from the left. We only need to show how to get rid of the leftmost one at each vertex, wlog in the upper half plane. Proceed thus:



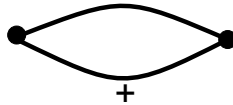
The two edges hitting the vertex from the left have been replaced by one. A lot of type I and II Reidemeister moves shows that replacing the picture on the left by

the one on the right preserves the link L . And all the added vertices are hit exactly once, top and bottom, from the left.

Continuing in this way one obtains a $\Gamma(L)$ consisting of two rooted planar/linear n -trees top and bottom from which an element of F_3 (in fact it's in F_2) may be reconstructed by the method we described for going from a signed planar graph back to a link diagram.

This ends the proof of Theorem 3.1. □

The algorithm for constructing Thompson group elements from links in the above proof is of theoretical interest only. In particular the sign correcting move is very inefficient. Even for the Hopf link, if one starts with the following $\Gamma(L)$ and applies the algorithm, the Thompson group element is very complicated (remember that the top edge is a positive one by convention):



5 The Annular Version, Thompson's Groups T_n

There are two other well known versions of the Thompson groups F_n , namely T_n and V_n . T_n is a group of PL homeomorphisms of the circle (rather than the interval) with slopes all powers of n and non smooth points all of the form $\frac{a}{n^b}$ where a and b are integers. T_n contains an obvious copy of F_n and can be obtained from it by adding rotations of the circle by angles $\frac{2\pi a}{n^b}$. V_n is even bigger, allowing discontinuous permutations of the intervals on the circle.

Both T_n and V_n can be constructed from our category of forests method by suitably decorating the forests with cyclic and general permutations respectively-see [14]. But the functor to tangles only works for T_n because of the discontinuities in V_n . Obviously all knots and links can be obtained from T_3 from this functor since they can already be made from F_3 , but some links may be much easier to realise using T_3 .

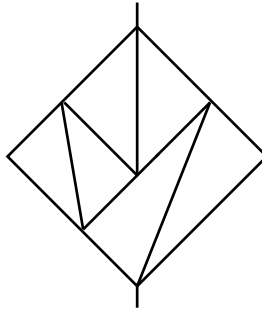
There is a bigger group called the "braided Thompson group" [12] which should have all the advantages of both braids and the Thompson groups.

6 The Group Structure-Analogy with Braid Groups

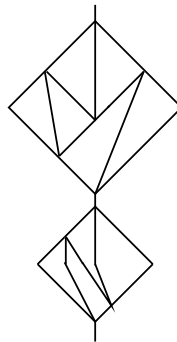
We are promoting the Thompson groups as groups from which links can be constructed, like the braid groups. In this section we will establish a strong, albeit not always straightforward, analogy between the two groups and their relationships with links.

The most obvious first thing missing from our construction of the Thompson groups in Sect. 2, which is front and centre in the braid groups, is a geometric understanding of the group law. But this is supplied by work of Guba and Sapir in [13] and Belk in [6]. Here is how to compose two F_3 elements, given as pairs of rooted planar ternary trees $\frac{s}{t}$ as usual, from this point of view.

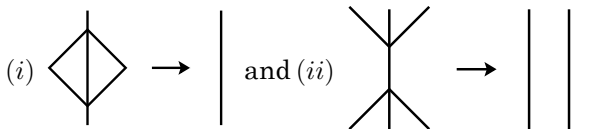
Given $\frac{r}{s}$ and $\frac{s}{t}$, draw them as we have with the denominator on the bottom and the numerator, upside down, on the top, joined at the leaves, thus:



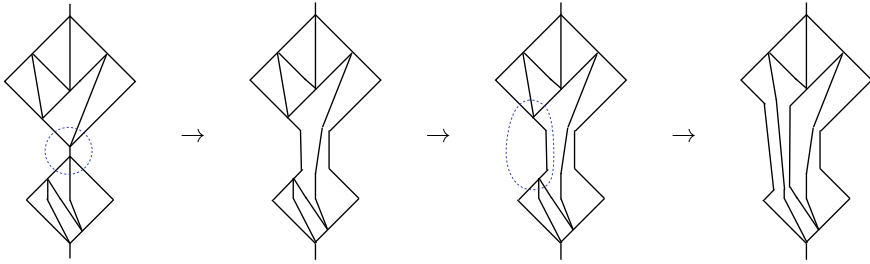
Now arrange the picture of $\frac{s}{t}$ underneath that of $\frac{r}{s}$ with the top vertices aligned, and fuse the top edges thus:



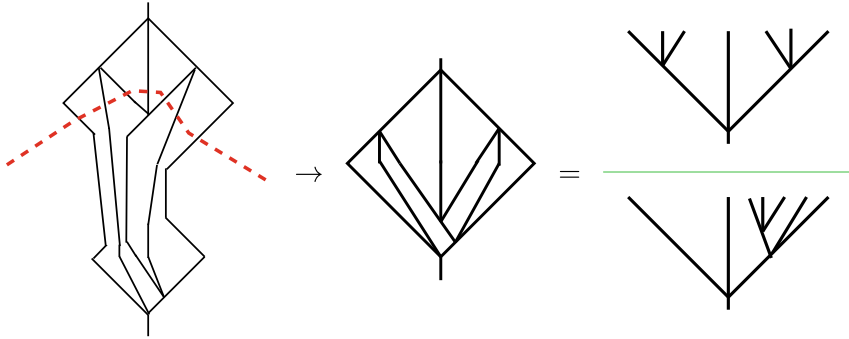
Now apply the following two cancellation moves:



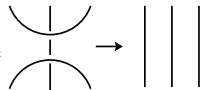
until they can no longer be applied. It is easy enough to see that at this point the remaining diagram can be decomposed into a pair of ternary planar trees, thus another element of F_3 . We illustrate with the above example:



Now we draw in a curve showing the split between the top and bottom trees, and redraw as a standard picture.



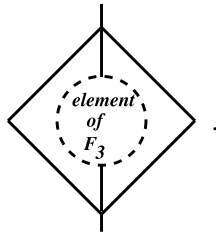
N.B. It is important to note that of the vacuum expectation value of the composition- by replacing the vertices of the diagrams by crossings- cannot be done until all the cancellations have been made.

This is because the knot theoretic move  is NOT an isotopy. It is what we call an “elementary cobordism”.

Definition 6.1 Changing $) ($ to \frown in a link diagram is called an “elementary cobordism”.

Thus each time we apply the cancellation move (ii) above we are changing the underlying link by an elementary cobordism. In particular we see that the first cancellation applied in the sequence of moves in the Guba-Sapir-Belk composition method actually transforms the underlying link almost into the connect sum-it differs from it by a single elementary cobordism.

Let us call H the subgroup of F_3 consisting of all elements of the form



(Obviously $H \cong F_3$.) For $h \in H$, $L(h)$ always contains a distant unknot sitting on top of another link. Let $\widetilde{L}(h)$ be $L(h)$ with this distant unknot removed. Let us also define the size $|g|$ of an element $g \in F_3$ to be the number of vertices in a tree of a minimal pair of trees picture of g , not counting the root vertex. Then $|gh| \leq |g| + |h|$ with equality only if there is only the first cancellation when using the Guba–Sapir–Belk composition.

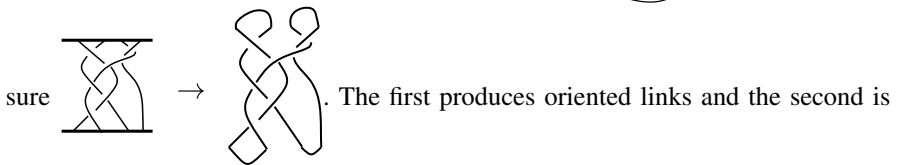
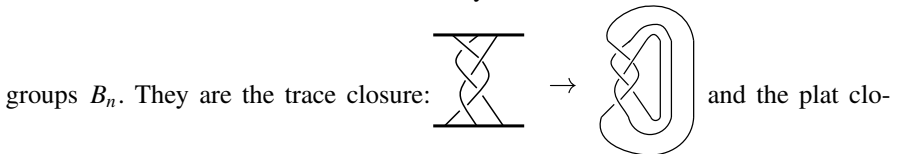
Proposition 6.1 *Let g and h be elements of $H < F_3$ with $|gh| = |g| + |h|$. Then*

$$\widetilde{L}(gh) = \widetilde{L}(g) \# \widetilde{L}(h)$$

Proof This is immediate on drawing a picture of gh . □

Thus group composition in F_3 can be *directly* related to the connected sum of the links.

We now remind the reader of the two ways links can be obtained from the braid



inherently unoriented. (We call the first the “Trace” closure rather than just the closure to distinguish it from the plat closure. Both closures will produce an arbitrary link for a sufficiently large n . (The closure result is a theorem of Alexander [2], the plat closure existence follows fairly obviously from an n -bridge picture of a link.) In both cases it is known exactly when two different braids give the same link-for the closure this is a theorem of Markov (see [3]) and for the plat closure a theorem of Birman [4].

We can now create a table comparing and contrasting the braid groups and Thompson group as link constructors:

One could argue that it is the inductive limit B_∞ of the braid groups that is the correct analogue of a Thompson group, but even then there is a strong contrast in that B_∞ is not finitely generated. Also the annular version of B_∞ is not clear.

Braid groups	Thompson group
Two versions: Unoriented (Plat closure)	Two versions Unoriented (all of F_3)
Oriented (Trace closure)	Oriented (The subgroup $\vec{F}_3 < F_3$ of definition 3.6.)
All knots and links as closure: Alexander theorem	All knots and links as $L(g)$: "Alexander theorem". Theorem 3.1
Braid index, plat index (=bridge number)	\vec{F}_3 index, F_3 index, \vec{F}_2 index, F_2 index
Markov, Birman theorems, conjugation, double cosets, stabilisation	??,??,??
Group law: Many cobordisms applied to - connected sum No changes but isotopy after these cobordisms	Group law: Connected sum directly More cobordisms needed after connected sum
??	$L(gh) = L(g)\#L(h) \iff gh = g + h $
All B_n 's needed to get all knots and links.	One finitely presented group gives all knots and links.
Contains free groups	Doesn't contain free groups
Non-amenable	??
Annular version available see [11]	Annular version available

7 Questions

We give a list of questions which arise naturally in this work. Some are probably quite easy to answer.

- (1) "Markov theorem."

Our theorems concerning the realisation of all links from Thompson group elements are analogous to Alexander's theorem [2] which asserts that any (oriented) link may be obtained by closing a braid. Markov's theorem answers the question of exactly when two braids give the same closure, in terms of simple changes on the braid group elements. It should be possible to give such a theorem for the Thompson groups F_3 and F_2 . It is easy enough to get moves on group elements that preserve the link, but proving sufficiency of these moves has not yet been achieved.

- (2) A detail about oriented links.

Theorem 3.1 is very precise-one obtains links without any ambiguity up to distant unlinks (or powers of δ). But the oriented version, as proved in [17], produces in general links that differ from the desired one by distant unlinks. So is it true that the Alexander-type theorem for oriented links from a subgroup of F_2 or F_3 is true on the nose?

- (3) A detail about regular isotopy.

Do all *regular* isotopy classes of link diagrams arise as $L(g)$? (See item 3 of Sect. 3.)

- (4) Number of components.

The number of components of the trace of a braid is just the number of orbits of

the corresponding permutation. One way to extract the number of components of $L(g)$ is to apply the TQFT functor for $q = 1$ and take the logarithm of the vacuum expectation value. Is there a simple group theoretic formula for the number of components of $L(g)$?

(5) Other Thompson groups.

It is possible to represent links as plane projections with singularities higher than double points (see, e.g. [1]), e.g. triple and quadruple points. Such projections naturally arise if one considers the Thompson groups F_{2k-2} as coming from the category of forests \mathcal{F}_{2k-1} . Does Theorem 3.1 extend to all k ?

(6) Proof of Theorem 3.1.

Find a proof more adapted to F_3 , making the different sign configurations a virtue rather than a vice.

(7) Thompson index.

The F_k index of a link L is the smallest number of vertices of a tree such that L is represented as the vacuum expectation value of an element of F_k given by a pair of trees with n leaves. Given that the number of trees with n leaves is finite and the identification of links is algorithmically solvable, this is a *finite problem* for a given L . Problem: calculate the F_3 and F_2 indices of the Borromean rings. (The diagram just before Definition 3.5 shows that the F_3 index of the trefoil is 3, its F_2 index is more than 3 as can be seen by enumerating all the 25 pairs of binary planar rooted trees with 3 vertices each. So the F_3 and F_2 indices are different in general.)

(8) Irreducibility.

When are the unitary representations of the Thompson groups coming from unitary TQFT's irreducible? (On the closed F_n -linear span of the vacuum.) Some progress was made on this in [18] where a family of unitary representations using the construction of Sect. 2 for a TQFT with a slightly different functor Φ were shown to be irreducible.

(9) Flat connections.

TQFT braid group representations are known to come from monodromy of flat connections on a classifying space (KZ connection). Can we exhibit the representations of this paper, or at least some of them, as coming from flat connections on Belk's (or some other) classifying space [6]?

References

1. C. Adams, Quadruple crossing number of knots and links, *emph Math. Proc. Camb. Philos. Soc.* **156**, 241–253 (2014)
2. J. Alexander, A lemma on a system of knotted curves. *Proc. Natl. Acad. Sci. USA* **9**, 93–95 (1923)
3. J. Birman, *Braids, Links and Mapping Class Groups*. *Annals of Mathematics Studies*, vol. 82 (Princeton University Press, Princeton, 1975)
4. J. Birman, On the stable equivalence of Heegaard splittings of plat presentation of links. *Canad. J. Math.* **XXVIII**(2), 264–290 (1976)

5. V. Aiello, R. Conti, V. Jones, The Homflypt polynomial and the oriented Thompson group. *Quantum Topol.* **9**, 461–472 (2018)
6. J. Belk, Thompson’s group F. Ph.D. Thesis (Cornell University) (2007). [arXiv:0708.3609](https://arxiv.org/abs/0708.3609)
7. J.W. Cannon, W.J. Floyd, W.R. Parry, Introductory notes on Richard Thompson’s groups. *L’Enseignement Mathématique* **42**, 215–256 (1996)
8. J.H. Conway, An enumeration of knots and links, and some of their algebraic properties, in *Computational Problems in Abstract Algebra (Proc. Conf., Oxford, 1967)* (1970), pp. 329–358
9. G. Golan, M. Sapir, On Jones’ subgroup of Thompson group F. *J. Algebra* **470**, 122–159 (2017)
10. R. Graham, D. Knuth, O. Patashnik, *Concrete Mathematics*, 2nd edn. (Addison-Wesley Publishing Company, Boston, 1994)
11. J.J. Graham, G.I. Lehrer, The representation theory of affine Temperley Lieb algebras. *L’Enseignement Mathématique* **44**, 1–44 (1998)
12. P. Greenberg, V. Sergiescu, An acyclic extension of the braid group. *Comment. Math. Helv.* **66**, 109–138 (1991)
13. V. Guba, M. Sapir, Diagram groups. *Mem. Am. Math. Soc.* **130** (1997)
14. V. Jones, A no-go theorem for the continuum limit of a periodic quantum spin chain. *Commun. Math. Phys.* **357**, 295–317 (2018)
15. V.F.R. Jones, Planar Algebras I, preprint, [arXiv:math/9909027](https://arxiv.org/abs/math/9909027)
16. V. Jones, On knot invariants related to some statistical mechanical models. *Pac. J. Math.* **137**, 311–334 (1989)
17. V. Jones Some unitary representations of Thompson’s groups F and T. *J. Comb. Algebra* **1**, 1–44 (2017)
18. V. Jones, Irreducibility of the wysiwyg representations of the Thompson group. Preprint (2018)
19. L. Kauffman, State models and the Jones polynomial. *Topology* **26**, 395–407 (1987)
20. Y. Ren, From skein theory to presentations for Thompson group (2016), [arXiv:1609.04077](https://arxiv.org/abs/1609.04077)

Virtual Knot Theory and Virtual Knot Cobordism



Louis H. Kauffman

Abstract This paper is an introduction to virtual knot theory and virtual knot cobordism [37, 39]. Non-trivial examples of virtual slice knots are given and determinations of the four-ball genus of positive virtual knots are explained in relation to joint work with Dye and Kaestner [12]. We study the affine index polynomial [38], prove that it is a concordance invariant, show that it is invariant also under certain forms of labeled cobordism and study a number of examples in relation to these phenomena. In particular we show how a mod-2 version of the affine index polynomial is a concordance invariant of flat virtual knots and links, and explore a number of examples in this domain.

Keywords Knot · Link · Virtual knot · Graph · Invariant · Bracket polynomial · Parity bracket polynomial · Arrow polynomial · Affine index polynomial · Cobordism · Concordance

AMS Subject Classification 57M25

1 Introduction

This paper is an introduction to virtual knot theory and to virtual knot cobordism. It is organized as follows. In Sect. 2 we include a description of basics in virtual knot theory and the problems that arise from it. This section includes different interpretations of virtual knot theory including flat virtual knot theory, problems related to the Kauffman bracket and Jones polynomial for the theory, a discussion of parity, the odd writhe and a description of the parity bracket polynomial formulated by Manturov

L. H. Kauffman (✉)

Department of Mathematics, Statistics and Computer Science (m/c 249),
University of Illinois, 851 South Morgan Street, Chicago, IL 60607-7045, USA
e-mail: kauffman@uic.edu

Department of Mechanics and Mathematics, Novosibirsk State University,
Novosibirsk, Russia

© Springer Nature Switzerland AG 2019

C. C. Adams et al. (eds.), *Knots, Low-Dimensional Topology and Applications*, Springer Proceedings in Mathematics & Statistics 284,
https://doi.org/10.1007/978-3-030-16031-9_4

[48] and a small introduction to quandles and virtual quandles. All of this background material is used in the remainder of the paper where we apply these ideas and techniques to virtual knot cobordism. Section 3 gives the definitions for cobordism of virtual knots and the definition of virtual Seifert surfaces. We define the (virtual) four-ball genus $g_4(K)$ for virtual knots and links, and show that every virtual link K bounds a virtual surface that is a natural generalization of the Seifert surface for a classical link. We state our result [12] determining the four-ball genus for positive virtual knots. We give many properties of a key example, the virtual stevedore's knot. We then discuss the affine index polynomial [38], prove that it and a relative of it for flat virtual knots are concordance invariants. Many examples are given.

This paper describes a study of knot cobordism at the level of virtual knot theory. One can develop other combinatorial variants of virtual knot theory by giving up more structure. One can use Gauss codes or Gauss diagrams to represent virtual knots, and release certain structures related to the codes to make combinatorial theories (such as free knots) that inform the virtual knot theory. Such work has been initiated by Turaev [57] and carried further by Manturov [21, 49, 50]. We should also mention the following papers on virtual knot theory that provide useful background, but not cited directly in the present paper [5, 8, 11, 18, 19, 31, 33, 35, 37, 37, 38, 46, 53]. In particular, we mention the following papers related to the theory of virtual braids, a topic fundamental to virtual knots and links that is not covered in the present paper. The interested reader will enjoy consulting these papers [1, 41–45].

Note that the work [50] can be used to prove that many virtual knots are not concordant to any slice classical knot. That paper is focused on the cobordism of free knots. Results about free knots (undecorated Gauss diagrams taken up Reidemeister move equivalence) are often applicable to standard virtual knots by simply forgetting some of the structure. An important question about our formulation of virtual knot cobordism is: If two classical knots are concordant in the virtual category, are they concordant in the usual sense? This is now answered in the affirmative by Boden, Chrisman and Gaudreau in [4].

2 Virtual Knot Theory

Virtual knot theory [31–33, 37] studies a generalization of classical knot theory described by diagrams that include a virtual crossing (see Fig. 1) that is neither over nor under. Such a diagram can be regarded as an abstract knot diagram, determined by the cyclic ordered structure of its crossing data. Virtual crossings are the result of immersing the abstract diagram into the plane. A diagrammatic theory with generalized Reidemeister moves defines this virtual theory. Virtual knots can be studied by examining embeddings of curves in thickened surfaces of arbitrary genus, up to the addition and removal of empty handles from the surface. Surface representations of this kind give topological meaning to the theory. This paper will concentrate on the diagrammatic point of view and will utilize the combinatorics of the virtual crossing structure. Classical knot theory embeds in virtual knot theory. The theory of virtual cobordism developed here is formulated in terms of diagrams.

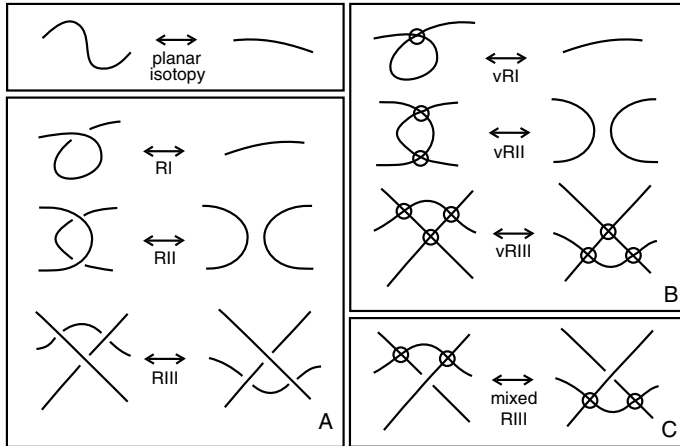


Fig. 1 Virtual moves

Moves on virtual diagrams generalize the Reidemeister moves for classical knot and link diagrams. See Fig. 1. Classical crossings interact with one another according to the usual Reidemeister moves, while virtual crossings are artifacts of the structure of the diagram in the plane. Adding the global detour move to the Reidemeister moves completes the description of moves on virtual diagrams. In Fig. 1 we illustrate a set of local moves involving virtual crossings. The global detour move is a consequence of moves (B) and (C) in Fig. 1. The detour move is illustrated in Fig. 2. Virtual knot and link diagrams that can be connected by a finite sequence of these moves are said to be *equivalent* or *virtually isotopic*. Figure 5 illustrates how a virtual knot can be interpreted in terms of the Gauss code (indicating a sequence of over and under crossings with signs that determine the diagram) and via an embedded curve in a thickened surface.

We also study *flat virtual knots and links* where the structure of the virtual crossings is the same, but the classical crossings are transverse intersection points of locally immersed curves in the plane without over or under crossing data. These are referred to as *flat crossings*. As we shall see, the theory of flat virtual knots and links governed by the moves in Fig. 3 is highly non-trivial and worth a study in parallel with the regular theory of virtual knots and links.

Virtual knot diagrams are usually represented as diagrams in the plane, but the theory is not changed if one regards the diagram as drawn on the surface of a two dimensional sphere. Moves that swing an arc around the two-sphere can be accomplished in the plane by using the detour move. Again, we refer to the reference papers at the beginning of this section for the reader who is interested in more details about the foundations of virtual knot and link theory.

Another way to understand virtual diagrams is to regard them as representatives for oriented Gauss codes [17], [31, 32] (Gauss diagrams). Such codes do not always have planar realizations. An attempt to embed such a code in the plane leads to the production of the virtual crossings. The detour move makes the particular choice of virtual crossings irrelevant. *Virtual isotopy is the same as the equivalence relation*

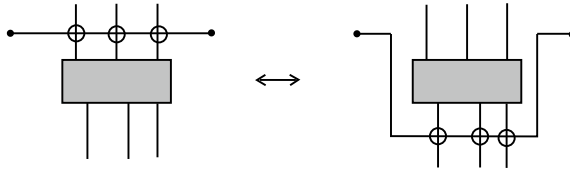


Fig. 2 Detour move

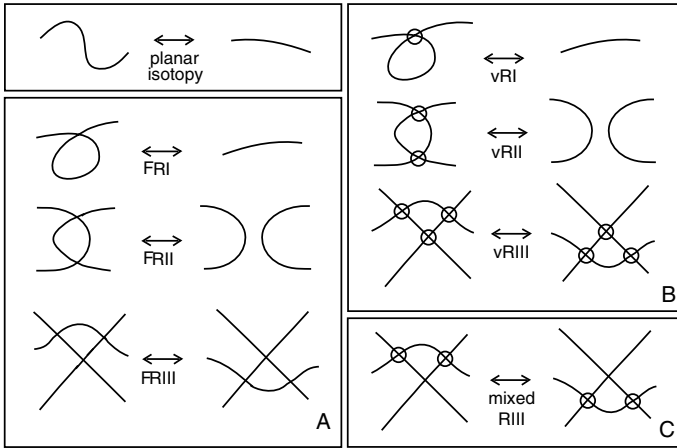
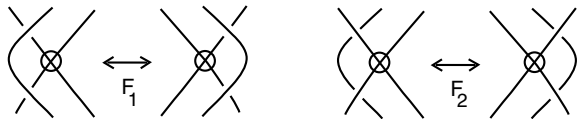


Fig. 3 Flat virtual moves

Fig. 4 Forbidden moves



generated on the collection of oriented Gauss codes by abstract Reidemeister moves on these codes. Similar remarks hold for flat virtual diagrams.

Figure 4 illustrates the two *forbidden moves*. Neither of these follows from Reidemeister moves plus detour move, and indeed it is not hard to construct examples of virtual knots that are non-trivial, but will become unknotted on the application of one or both of the forbidden moves. The forbidden moves change the structure of the Gauss code and, if desired, must be considered separately from the virtual knot theory proper.

2.1 Interpretation of Virtuals Links as Stable Classes of Links in Thickened Surfaces

There is a useful topological interpretation [31, 33] for virtual knot theory in terms of embeddings of links in thickened surfaces (equivalently, diagrams for links drawn on surfaces without the use of virtual crossings). One way to represent the virtual

Fig. 5 Surface representation

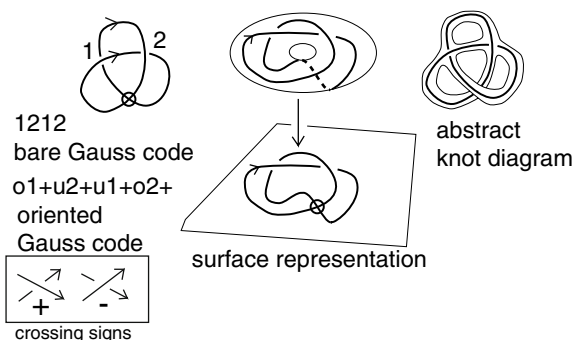


diagram on a surface is to regard each virtual crossing as a shorthand for a detour of one of the arcs in the crossing through a 1-handle that has been attached to the 2-sphere of the original diagram. By interpreting each virtual crossing in this way, we obtain an embedding of a collection of circles into a thickened surface $S_g \times R$ where g is the number of virtual crossings in the original diagram L , S_g is a compact oriented surface of genus g and R denotes the real line.

Another way to put the virtual diagram in a surface is shown in Fig. 5. There we illustrate how to construct an *abstract knot diagram* associated with the virtual diagram. The abstract knot diagram is a surface with boundary that forms a neighborhood of the diagram, lifting the virtual crossings into disjoint ribbons that locally project to the virtual crossing in the plane. A closed surface is obtained by adding disks to the boundary components of the abstract link diagram. The result is a surface of least genus supporting that initial diagram.

We say that two such surface embeddings are *stably equivalent* if one can be obtained from another by isotopy in the thickened surfaces, homeomorphisms of the surfaces and the addition or subtraction of empty handles. Equivalently, the stabilization can be obtained by taking an abstract knot diagram neighborhood of the given knot or link diagram K in a given surface. Remove this abstract diagram and add any orientable surfaces with boundary to the boundary circles of the abstract diagram. Let K' denote this new knot or link in the resulting closed surface. Then K' is stably equivalent to the original knot or link K , and this notion of cutting out the knot and reembedding it is equivalent to the handles definition of stable equivalence.

Theorem 1 ([31, 33, 55]) *Two virtual link diagrams are isotopic if and only if their corresponding surface embeddings are stably equivalent.*

The reader will find more information about this correspondence [31, 33] in other papers by the author and in the literature of virtual knot theory. Flat virtual knots and links correspond to stabilized classes of immersed curves in surfaces in a form exactly analogous to our statements about the virtual knot theory.

2.2 Review of the Bracket Polynomial for Virtual Knots

In this section we recall how the bracket state summation model [28] for the Jones polynomial is defined for virtual knots and links.

The bracket polynomial [28] model for the Jones polynomial [22–24, 58] is usually described by the expansion

$$\langle \diagdown \diagup \rangle = A \langle \smile \rangle + A^{-1} \langle \rangle \langle \rangle \tag{1}$$

and we have

$$\langle K \bigcirc \rangle = (-A^2 - A^{-2}) \langle K \rangle \tag{2}$$

$$\langle \diagdown \diagup \rangle = (-A^3) \langle \smile \rangle \tag{3}$$

$$\langle \diagup \diagdown \rangle = (-A^{-3}) \langle \smile \rangle \tag{4}$$

We call a diagram in the plane *purely virtual* if the only crossings in the diagram are virtual crossings. Each purely virtual diagram is equivalent by the virtual moves to a disjoint collection of circles in the plane.

A state S of a link diagram K is obtained by choosing a smoothing for each crossing in the diagram and labelling that smoothing with either A or A^{-1} according to the convention indicated in the bracket expansion above. Then, given a state S , one has the evaluation $\langle K|S \rangle$ equal to the product of the labels at the smoothings, and one has the evaluation $\|S\|$ equal to the number of loops in the state (the smoothings produce purely virtual diagrams). One then has the formula

$$\langle K \rangle = \sum_S \langle K|S \rangle d^{\|S\|-1}$$

where the summation runs over the states S of the diagram K , and $d = -A^2 - A^{-2}$. This state summation is invariant under all classical and virtual moves except the first Reidemeister move. The bracket polynomial is normalized to an invariant $f_K(A)$ of all the moves by the formula $f_K(A) = (-A^3)^{-wr(K)} \langle K \rangle$ where $wr(K)$ is the *writhe* of the (now) oriented diagram K . The writhe is the sum of the orientation signs (± 1) of the crossings of the diagram. To fix the convention of orientation sign, note that the signs of crossings are indicated in Fig. 5. Letting $sgn(c) = \pm 1$ denote the sign of a classical crossing in an oriented link diagram, we have the formula for the writhe:

$$wr(K) = \sum_{c \in Cr(K)} sgn(c)$$

where $Cr(K)$ denotes the collection of classical crossings of the diagram K .

The Jones polynomial, $V_K(t)$ is given in terms of this model by the formula

$$V_K(t) = f_K(t^{-1/4}).$$

This definition is a direct generalization to the virtual category of the state sum model for the original Jones polynomial. It is straightforward to verify the invariances stated above. In this way one has the Jones polynomial for virtual knots and links.

We have [33] the

Theorem 2 *To each non-trivial classical knot diagram of one component K there is a corresponding non-trivial virtual knot diagram $Virt(K)$ with unit Jones polynomial.*

The main ideas behind this Theorem are indicated in Figs. 6 and 7. In Fig. 6 we indicate the *virtualization* operation that replaces a given classical crossing by using two virtual crossings and changing the implicit orientation of the classical crossing. We also show how the bracket polynomial sees this operation as though the crossing had been switched in the classical knot. (Take the formulas in Fig. 6 as exercises in applying the expansion formula for the bracket.) If we virtualize a set of classical crossings whose switching will unknot the knot, then the virtualized knot will have unit Jones polynomial.

To see that the resulting virtualized knot is non-trivial, we use the *involutory quandle* of K , denoted $IQ(K)$. When we write the word quandle below, it will refer to the involutory quandle. This is an algebraic invariant (of all three Reidemeister moves) with one binary operation. The quandle was invented by David Joyce [25] and independently by Sergei Matveev [51]. See Fig. 7 for an illustration of the formalism of the quandle. Each arc in the diagram is assigned a generator of the quandle. If a and c are undercrossing arcs at a crossing, and b is an overcrossing arc at the crossing, then $ab = c$ and $cb = a$. Multiplication in the quandle is not associative and it satisfies the rules $aa = a$, $(ab)b = a$ and $(ab)c = (ac)(bc)$ for all elements a, b, c in the quandle. It is known that the involutory quandle of a non-trivial knot is itself non-trivial. That is, it is not isomorphic with the quandle of the unknot. The involutory quandle detects the unknot. The involutory quandle is extended to virtual knots by using the same relations on the classical crossings and introducing no new relations at the virtual crossings. The virtualization operation does not change this extended quandle, as is shown in Fig. 7. This implies that virtual knots obtained by virtualization from classical non-trivial knots will themselves be non-trivial.

It is an open problem whether there are classical knots (actually knotted) having unit Jones polynomial. (There are linked links whose linkedness is unseen by the Jones polynomial [13].) We do know that the knots $Virt(K)$ produced by this Theorem for non-trivial classical knots K are never isotopic to a classical knot. Such examples are guaranteed to be non-trivial, and are not classical [12].

The involutory quandle is generalized to the *quandle*, an algebraic structure with two binary operations that are inverses of each other and satisfying the axioms indicated in Fig. 8. In this Figure we illustrate how the operations and labellings are associated with the classical and virtual crossings to form the *virtual quandle* of an

Fig. 6 Virtualizing a crossing and crossing switches

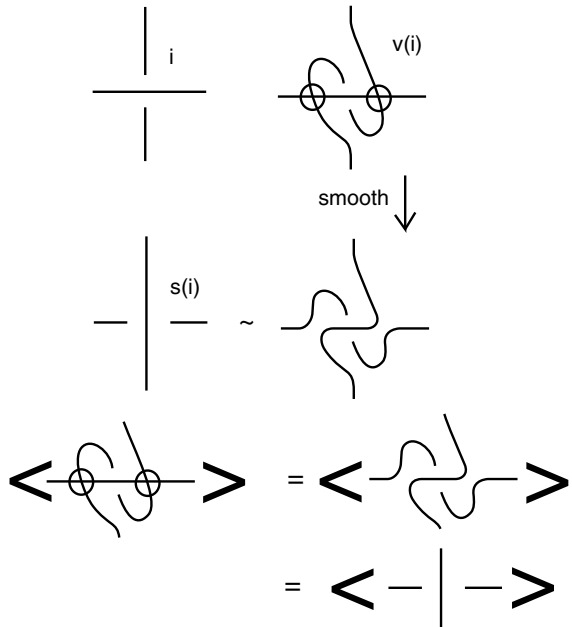


Fig. 7 Quandle invariance under virtualization

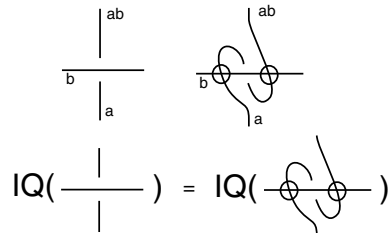
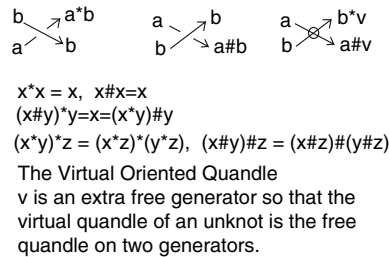
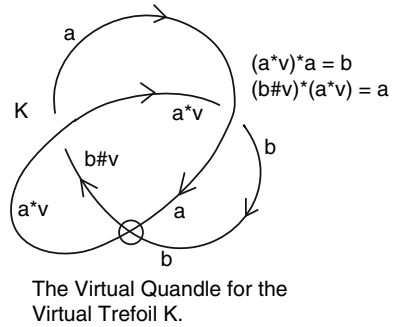


Fig. 8 The virtual oriented quandle



oriented virtual knot of link diagram. The virtual quandle has an extra free generator v that acts at the virtual crossings in the diagram. One can define just the *quandle* of a virtual diagram, but the virtual quandle is a stronger invariant of virtual knots and links. See [2, 47] for more information about the virtual quandle. *At this writing it is not known whether the virtual quandle detects the virtual unknot.* In [3] it is

Fig. 9 The virtual quandle of the virtual trefoil



shown that the Kishino knot (see the next section) is detected by the group associated with the virtual quandle. This proves that the Kishino knot is detected by the virtual quandle. More examples need to be explored in this domain.

There are many examples of virtual knots with trivial ordinary quandles. For example, the virtual trefoil in Figs. 5 and 9 has a trivial standard quandle, but a non-trivial virtual quandle. In Fig. 9 we illustrate the equations for the relations in the virtual quandle of the virtual trefoil knot K . One way to see the non-triviality of this virtual quandle is to use the *Alexander representation* given by $x * y = tx + (1 - t)y$, $x \# y = t^{-1}x + (1 - t^{-1})y$ with $x * v = sx + (1 - s)v$, $x \# v = s^{-1}x + (1 - s^{-1})v$. This defines a Generalized Alexander Module over $Z[t, t^{-1}, s, s^{-1}]$. The relations then reduce it to a module generated by a and v with relation

$$((1 - s^2) + (s - 1)t + (s^2 - s)t^{-1})(a - v) = 0.$$

The polynomial $S_K(s, t) = (1 - s^2) + (s - 1)t + (s^2 - s)t^{-1}$ is the Sawollek polynomial [54] of the virtual knot K . For more information about the Sawollek polynomial and for other approaches to algebraic invariants of virtual knots such as the *biquandle* and the definitions of these structures, see the papers [14, 15]. These papers discuss unsolved problems in virtual knot theory and combinatorial knot theory.

2.3 Parity, Odd Writhe and the Parity Bracket Polynomial

Parity is an important theme in virtual knot theory and figures in many investigations of this subject. In a virtual knot diagram there can be both even and odd crossings. A crossing is *odd* if it flanks an odd number of symbols in the Gauss code of the diagram. A crossing is *even* if it flanks an even number of symbols in the Gauss code of the diagram. For example, in Fig. 5 we illustrate the virtual knot K with bare Gauss code 1212. Both crossings in the diagram K are odd. In any classical knot diagram all crossings are even.

In [34] we introduced a numerical invariant of virtual knots, the *odd writhe* $J(K)$ defined for any virtual knot diagram K . $J(K)$ is the sum of the signs of the odd crossings. Classical diagrams have zero odd writhe. Thus if $J(K)$ is non-zero, then K is not equivalent to any classical knot. For the mirror image K^* of any diagram K , we have the formula $J(K^*) = -J(K)$. Thus, when $J(K) \neq 0$, we know that the knot K is not classical and not equivalent to its mirror image. Parity does all the work in this simple invariant. For example, if K is the virtual knot in Fig. 5, then we have $J(K) = 2$. Thus K , the simplest virtual knot, is non-classical and it is chiral (inequivalent to its mirror image).

In this section we introduce the Manturov Parity Bracket [48]. This is a form of the bracket polynomial defined for virtual knots and for free knots (unlabeled Gauss diagrams taken up to abstract Reidemeister move equivalence) that uses the parity of the crossings. To compute the parity bracket, we first make all the odd crossings into graphical vertices. Then we expand the resulting diagram on the remaining even crossings. The result is a sum of graphs with polynomial coefficients.

More precisely, let K be a virtual knot diagram. Let $E(K)$ denote the result of making all the odd crossings in K into graphical nodes as illustrated in Fig. 10. Let $SE(K)$ denote the set of all bracket states of $E(K)$ obtained by smoothing each classical crossing in $E(K)$ in one of the two possible ways. Then we define the *parity bracket*

$$\langle K \rangle_p = (1/d) \sum_{S \in SE(K)} A^{i(S)} [S]$$

where $d = -A^2 - A^{-2}$, $i(S)$ denotes the product of A or A^{-1} from each smoothing site according to the conventions of Fig. 10, and $[S]$ denotes the reduced class of the virtual graph S . The graphs are subject to a reduction move that eliminates bigons as in the second Reidemeister move on a knot diagram as shown in Fig. 10. Thus $[S]$ represents the unique minimal representative for the virtual graph S under virtual graph isotopy coupled with the bigon reduction move. A graph that reduces to a circle (the circle is a graph for our purposes) is replaced by the value d above. Thus $\langle K \rangle_p$ is an element of a module generated by reduced graphs with coefficients Laurent polynomials in A .

Fig. 10 Parity bracket expansion

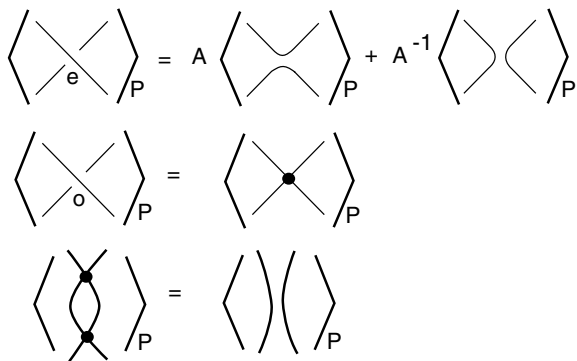


Fig. 11 Kishino diagram

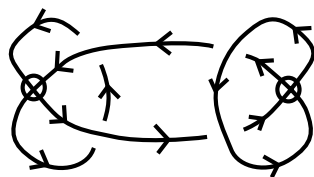
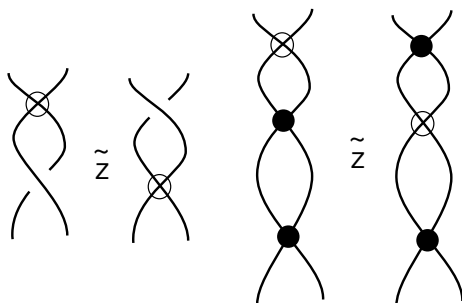


Fig. 12 Z-move and graphical Z-move



With the usual bracket polynomial variable A , the parity bracket is an invariant of standard virtual knots. With $A = \pm 1$ it is an invariant of flat virtual knots. Even more simply, with $A = 1$ and taken modulo two, we have an invariant of flat knots with loop value zero. See Fig. 11 for an illustration of the application of the parity bracket to the Kishino diagram illustrated there. The Kishino diagram is notorious for being hard to detect by the usual polynomial invariants such as the Jones polynomial. It is a perfect example of the power of the parity bracket. All the crossings of the Kishino diagram are odd. Thus there is exactly one term in the evaluation of the Kishino diagram by the parity bracket, and this term is the Kishino diagram itself, with its crossings made into graphical nodes. The resulting graph is irreducible and so the Kishino diagram becomes its own invariant. We conclude that this diagram will be found from any isotopic version of the Kishino diagram. This allows strong conclusions about many properties of the diagram. For example, it is easy to check that the least surface on which this diagram can be represented (with the given planar cyclic orders at the nodes) is genus two. Thus we conclude that the least genus for a surface representation of the Kishino diagram as a flat knot or virtual knot is two.

In Fig. 12 we illustrate the *Z-move* and the *graphical Z-move*. We say that two virtual link diagrams K and K' are *Z-equivalent* if K' can be obtained from K by some finite sequence of Reidemeister moves, detour moves and Z-moves. Two virtual knots or links that are related by a Z-move have the same standard bracket polynomial. This follows directly from our discussion in the previous section. We would like to analyze the structure of Z-moves using the parity bracket. In order to do this we need a version of the parity bracket that is invariant under the Z-move. In order to accomplish this, we need to add a corresponding Z-move in the graphical reduction process for the parity bracket. This extra graphical reduction is indicated in Fig. 12 where we show a graphical Z-move. The reader will note that graphs that are irreducible

Fig. 13 A knot KS with unit Jones polynomial

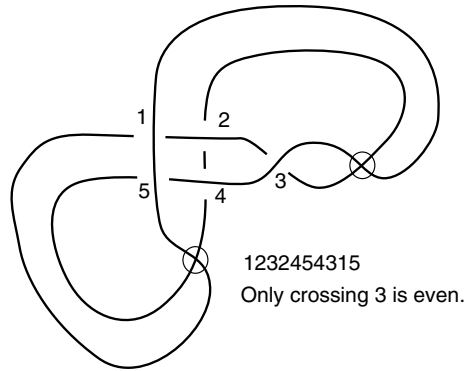
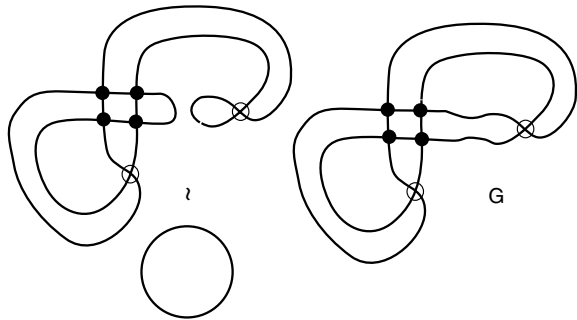


Fig. 14 Parity bracket states for the knot KS



without the graphical Z-move can become reducible if we allow graphical Z-moves in the reduction process. For example, the graph associated with the Kishino knot is reducible under graphical Z-moves. However, there are examples of graphs that are not reducible under graphical Z-moves and Reidemeister two moves. An example of such a graph occurs in the parity bracket of the knot KS shown in Figs. 13 and 14. This knot has one even classical crossing and four odd crossings. One smoothing of the even crossing yields a state that reduces to a loop with no graphical nodes, while the other smoothing yields a state that is irreducible even when the Z-move is allowed. The upshot is that this knot KS is not Z-equivalent to any classical knot. Since one can verify that KS has unit Jones polynomial, this example is a counterexample to a conjecture of Fenn, Kauffman and Maturov [14] that suggested that a knot with unit Jones polynomial should be Z-equivalent to a classical knot.

Some further remarks should be made about the structure of the parity bracket for flat virtual knots. In Fig. 15 we illustrate the structure of the flat virtual two-move in the framework of a Gauss diagram. The move requires oppositely oriented arcs (chords of the Gauss diagram) in the pattern shown where the endpoints of the paired arcs are adjacent along the circle of the Gauss diagram. Then Fig. 16 illustrates that there is no such two-move available in the flat Kishino diagram. It is on this basis that we know that the graph diagram for the parity bracket of the flat Kishino knot is irreducible and so can conclude that this is a non-trivial flat virtual knot. The same

Fig. 15 Flat Gauss two move

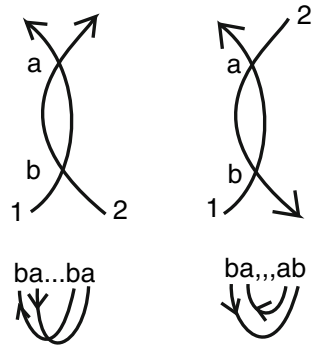
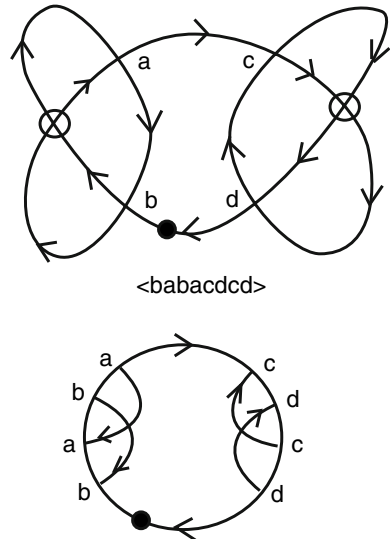


Fig. 16 Flat Kishino



kind of argument applies to other examples. In Figs. 17 and 18 we show examples of flat virtual knots with all odd crossings such that the graph diagrams are irreducible.

In the Fig. 18 an infinite class of examples is indicated by recursively continuing the indicated construction. Since the graphs of these examples are distinct, the corresponding flat virtuals are distinct. These examples are of interest in relation to *pass equivalence*, an equivalence relation on oriented knot and link diagrams generated by isotopy and the pass-move indicated in Fig. 19 [27, 39]. In classical knot theory any knot is pass equivalent either to the trefoil knot or to the unknot. Via the structure of the generating pass move, it follows that the *flat projection* $F(K)$, for any virtual knot or link K , is an invariant (as a flat virtual link) of the pass equivalence class of K . It follows that there are an infinite number of distinct pass classes among virtual knots.

Fig. 17 Odd crossing flat example with Gauss diagram

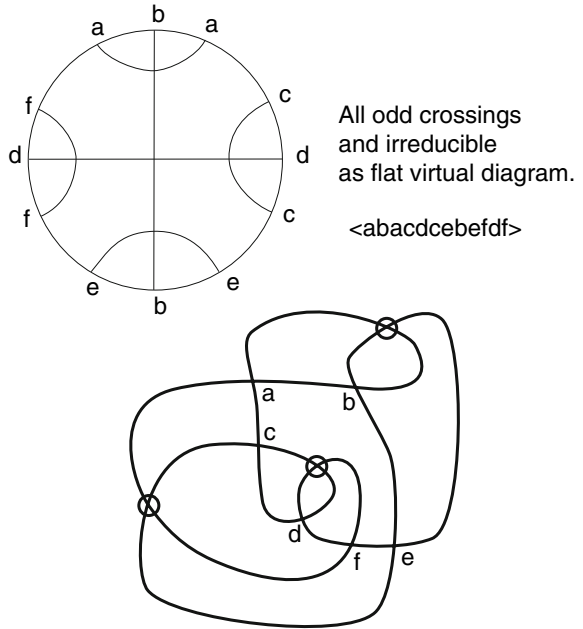


Fig. 18 Gauss diagram from an infinite class of examples

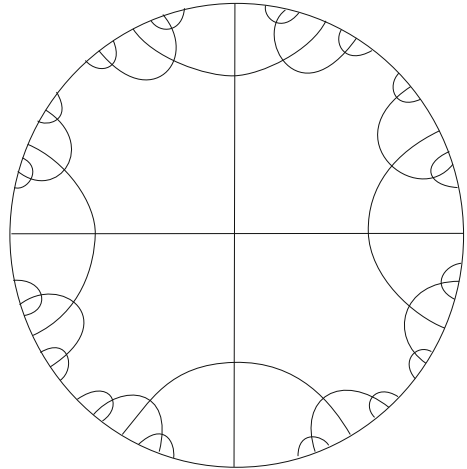
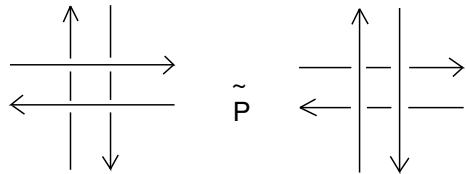


Fig. 19 Pass equivalence



2.4 The Arrow Polynomial for Virtual and Flat Virtual Knots and Links

This section describes an invariant for oriented virtual knots and links, and for flat oriented virtual knots and links that we call the *arrow polynomial* [11, 37]. This invariant is considerably stronger than the Jones polynomial for virtual knots and links, and is a natural extension of the Jones polynomial, using the oriented diagram structure of the state summation. The construction of the arrow polynomial invariant begins with the oriented state summation of the bracket polynomial. This means that each local smoothing is either an oriented smoothing or a *disoriented smoothing* as illustrated in Figs. 20 and 21. In [11] we show how the arrow polynomial can be used to estimate virtual crossing numbers.

In Fig. 20 we illustrate the oriented bracket expansion for both positive and negative crossings in a link diagram. An oriented crossing can be smoothed in the oriented fashion or the disoriented fashion as shown in Fig. 20. We refer to these smoothings as *oriented* and *disoriented* smoothings. To each smoothing we make an associated configuration that will be part of the arrow polynomial state summation. The configuration associated to a state with oriented and disoriented smoothings is obtained by applying the reduction rules described below. See Fig. 21. The arrow polynomial state summation is defined by the formula:

$$\mathcal{A}[K] = \sum_S \langle K|S \rangle d^{\|S\|-1} [S]$$

where S runs over the oriented bracket states of the diagram, $\langle K|S \rangle$ is the usual product of vertex weights as in the standard bracket polynomial, and $[S]$ is a product of extra variables K_1, K_2, \dots associated with the state S . These variables are explained below.

Due to the oriented state expansion, the loops in the resulting states have extra combinatorial structure in the form of paired *cusps* as shown in Fig. 20. Each disoriented smoothing gives rise to a cusp pair where each cusp has either two oriented lines going into the cusp or two oriented lines leaving the cusp. We reduce this structure according to a set of rules that yields invariance of the state summation under

Fig. 20 Oriented bracket expansion for the arrow polynomial

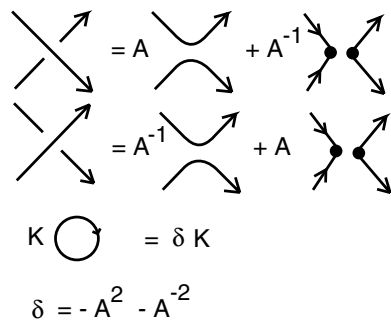
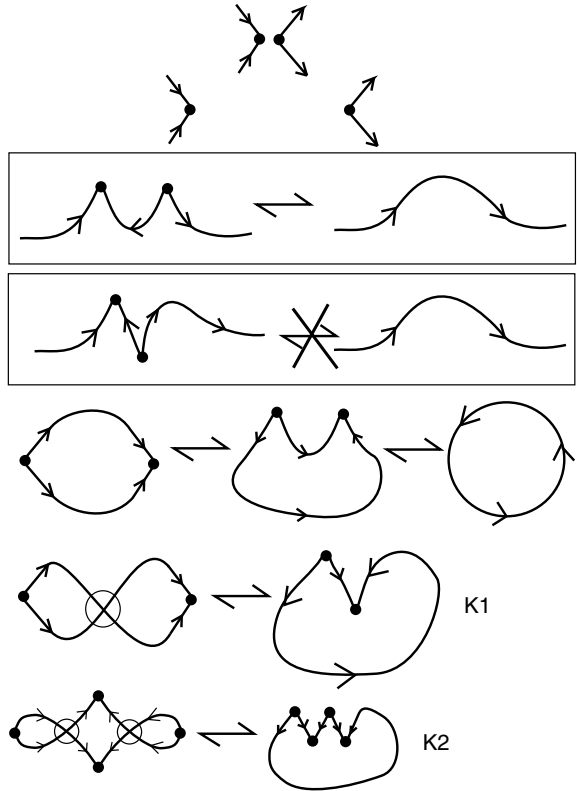


Fig. 21 Reduction relation for the arrow polynomial



the Reidemeister moves. The basic conventions for this simplification are shown in Fig. 21. Each cusp is denoted by an angle with arrows either both entering the vertex or both leaving the vertex. Furthermore, the angle locally divides the plane into two parts: One part is the span of an acute angle; the other part is the span of an obtuse angle. We refer to the span of the acute angle as the *inside* of the cusp.

Remark on State Reduction. Figure 21 illustrates the basic reduction rule for the arrow polynomial. The reduction rule allows the cancellation of two adjacent cusps when they have *insides on the same side* of the segment that connects them. When the insides of the cusps are on opposite sides of the connecting segment (a “zig-zag”), then no cancellation is allowed. Each state circle is seen as a circle graph with extra nodes corresponding to the cusps. All graphs are taken up to virtual equivalence, as explained earlier in this paper. Figure 21 illustrates the simplification of two circle graphs. In one case the graph reduces to a circle with no vertices. In the other case there is no further cancellation, but the graph is equivalent to one without a virtual crossing. The state expansion for $\mathcal{A}[K] = \ll K \gg$ is exactly as shown in Fig. 20, but we use the reduction rule of Fig. 21 so that each state is a disjoint union of reduced circle graphs. Since such graphs are planar, each is equivalent to an embedded graph

(no virtual crossings) via the detour move, and the reduced forms of such graphs have $2n$ cusps that alternate in type around the circle so that n are pointing inward and n are pointing outward. The circle with no cusps is evaluated as $d = -A^2 - A^{-2}$ as is usual for these expansions, and the circle is removed from the graphical expansion. We let K_n denote the circle graph with $2n$ alternating cusps types as shown in Fig. 21 for $n = 1$ and $n = 2$. Each circle graph contributes $d = -A^2 - A^{-2}$ to the state sum and the graphs K_n for $n \geq 1$ remain in the graphical expansion. Each K_n is an extra variable in the polynomial. Thus a product of the K_n 's corresponds to a state that is a disjoint union of copies of these circle graphs. By evaluating each circle graph as $d = -A^2 - A^{-2}$ (as well as taking its arrow variable K_n) we guarantee that the resulting polynomial will reduce to the original bracket polynomial when each of the new variables K_n is set equal to unity. Note that we continue to use the caveat that an isolated circle or circle graph (i.e. a state consisting in a single circle or single circle graph) is assigned a loop value of unity in the state sum. This assures that $\mathcal{A}[K]$ is normalized so that the unknot receives the value one.

We have the following Proposition, showing that the phenomenon of cusped states and extra variables K_n only occurs for virtual knots and links.

Proposition 1 *In a classical knot or link diagram, all state loops reduce to loops that are free from cusps.*

Proof See [11, 37].

Theorem 3 *With the above conventions, the arrow polynomial $\mathcal{A}[K]$ is a polynomial in A, A^{-1} and the graphical variables K_n (of which finitely many will appear for any given virtual knot or link). $\mathcal{A}[K]$ is a regular isotopy invariant of virtual knots and links. The normalized version*

$$\mathcal{W}[K] = (-A^3)^{-wr(K)} \mathcal{A}[K]$$

is an invariant virtual isotopy. If we set $A = 1$ and $d = -A^2 - A^{-2} = -2$, then the resulting specialization

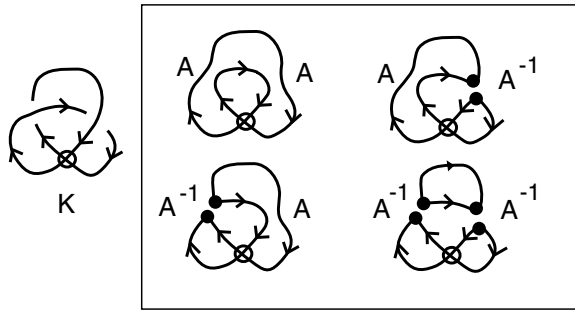
$$\mathcal{F}[K] = \mathcal{A}[K](A = 1)$$

is an invariant of flat virtual knots and links.

Proof [11, 37].

Here is a first example of a calculation of the arrow polynomial invariant. View Fig. 22. The virtual knot K in this figure has two crossings. One can see that this knot is a non-trivial virtual knot by simply calculating the odd writhe $J(K)$ (defined in Sect. 2.3). We have that $J(K) = 2$, proving that K is non-trivial and non-classical. This is the simplest virtual knot, the analog of the trefoil knot for virtual knot theory. The arrow polynomial gives an independent verification that K is non-trivial and non-classical.

Fig. 22 Arrow polynomial of the virtual trefoil knot



$$\langle\langle \text{Virtual Trefoil} \rangle\rangle = A^2 + (2 + A^{-2} d) K1$$

Fig. 23 Arrow polynomial for the virtualized trefoil

$$\langle\langle \text{Virtualized Trefoil} \rangle\rangle = (A^3 + Ad + 2A^{-1} + A^{-3} d) + (Ad + A^{-1}d^2 + Ad) K1^2$$

Fig. 24 Arrow polynomial for the Kishino diagram

$$\begin{aligned} \langle\langle \text{Kishino Diagram} \rangle\rangle &= 1 + A^4 + A^{-4} + 2 \text{ (diagram)} \\ &+ (A^2 d + A^{-2} d) \text{ (diagram)} + \text{ (diagram)} \\ &+ d^2 \text{ (diagram)} \\ &= 1 + A^4 + A^{-4} + 2 K2 - (A^4 + A^{-4} + 2) K1^2 \end{aligned}$$

The next example is given in Fig. 23. Here we calculate the arrow polynomial for a non-trivial virtual knot with unit Jones polynomial. Specialization of the calculation to $A = 1$ shows that the corresponding flat knot is non-trivial as well.

Figure 24 exhibits the calculation of the arrow polynomial for the Kishino diagram, showing once again that the Kishino knot is non-trivial and that its underlying flat diagram is also non-trivial.

Fig. 25 The 1-virtualization of a classical diagram (A)

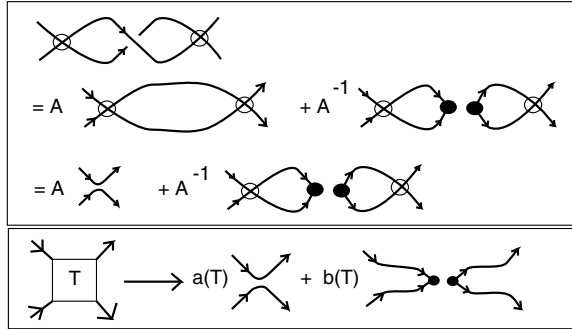
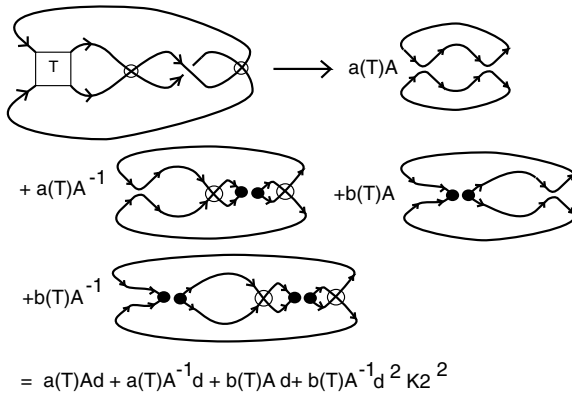


Fig. 26 The 1-virtualization of a classical diagram (B)



The example shown in Figs. 25 and 26 shows the result of expanding a virtualized classical crossing using the arrow polynomial state sum. Virtualization of a crossing was described in Sect. 2.2. In a virtualized crossing, one sees a classical crossing that is flanked by two virtual crossings. In Sect. 2.2 we showed that the standard bracket state sum does not see virtualization in the sense that it has the same value as the result of smoothing both flanking virtual crossings that have been added to the diagram. The result is that the value of the bracket polynomial of the knot with a virtualized classical crossing is the same as the value of the bracket polynomial of the original knot after the same crossing has been *switched* (exchanging over and under crossing segments).

As one can see from the formula in Fig. 25, this smoothing property of the bracket polynomial will not generally be the case for the arrow polynomial state sum. In Fig. 28 we show that this difference is indeed the case for an infinite collection of examples. In that figure we use a tangle T that is assumed to be a classical tangle. Arrow polynomial expansion of this tangle is necessarily of the form shown in that figure: a linear combination of an oriented smoothing and a reverse oriented smoothing with respective coefficients $a(T)$ and $b(T)$ in the Laurent polynomial ring $Q[A, A^{-1}]$. We leave the verification of this fact to the reader. In Fig. 26 we show a

generic diagram that is obtained by a *single* virtualization from a classical diagram, and we illustrate the calculation of its arrow polynomial invariant. As the reader can see from this Figure, there is a non-trivial graphical term whenever $b(T)$ is non-zero. Thus we conclude that the single virtualization of any classical link diagram (in the form shown in this figure) will be non-trivial and non-classical whenever $b(T)$ is non-zero. This is an infinite class of examples, and the result can be used to recover the results about single virtualization that we obtained in a previous paper with Heather Dye [10] using the surface bracket polynomial.

For more information about the arrow polynomial, we refer the reader to our paper [11] where we prove that the maximal monomial degree in the K_n variables is a lower bound for the virtual crossing number of the virtual knot or link. There are many open problems associated with this estimate for the virtual crossing number. Also the reader of [11] will encounter examples of virtual knots and links that are undetectable by the arrow polynomial.

3 Virtual Knot Cobordism and Concordance

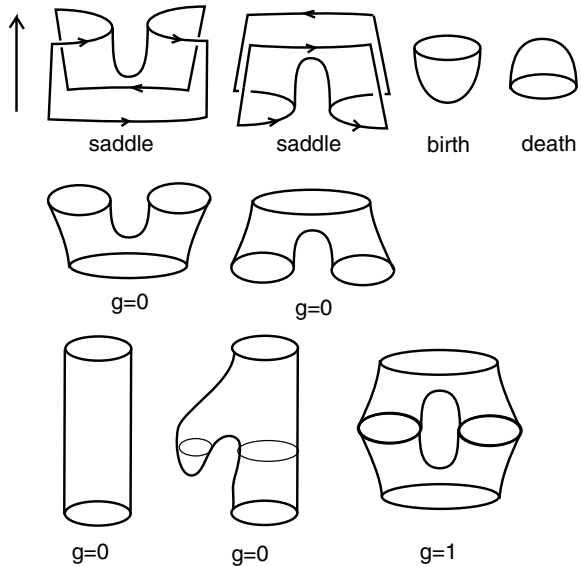
Definition 1 Two oriented virtual knots or links K and K' are *virtually cobordant* if one may be obtained from the other by a sequence of virtual isotopies (Reidemeister moves plus detour moves) plus births, deaths and oriented saddle points, as illustrated in Fig. 27. A *birth* is the introduction into the diagram of an isolated unknotted circle. A *death* is the removal from the diagram of an isolated unknotted circle. A saddle point move results from bringing oppositely oriented arcs into proximity and resmoothing the resulting site to obtain two new oppositely oriented arcs.

See Fig. 27 for an illustration of the process. Figure 27 also illustrates the *schema* of surfaces that are generated by cobordism process. These are abstract surfaces with well defined genus in terms of the sequence of steps in the cobordism. In the Figure we illustrate two examples of genus zero, and one example of genus 1. We say that a cobordism has genus g if its schema has genus g . Two virtual knots or links are *virtually concordant* if there is a cobordism of genus zero connecting them. Note that virtual concordance is a special case of virtual cobordism. We shall often just say *cobordant* or *concordant* with the word virtual assumed.

Definition 2 A virtual knot is said to be a *slice* knot if it is virtually concordant to the unknot, or equivalently if it is virtually concordant to the empty knot (The unknot is concordant to the empty knot via one death). As we shall see below, *every virtual knot or link is cobordant to the unknot*. Another way to say this, is to say that there is a *virtual surface* (schema) whose boundary is the given virtual knot. The reader should note that when we speak of a virtual surface, we mean a surface schema that is generated by saddle moves, maxima and minima as described above.

The reader should note the sharp difference between the concepts of *cobordism* of virtual knots and *concordance* of virtual knots. Two knots that are cobordant can

Fig. 27 Saddles, births and deaths

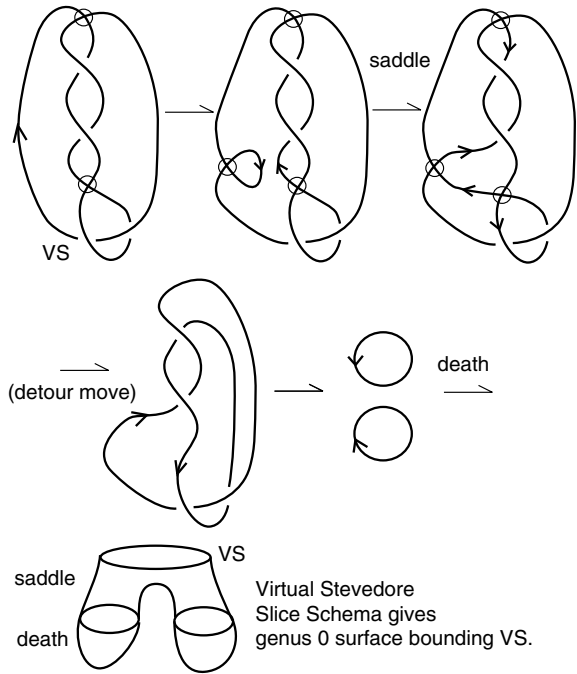


mutually bound a virtual surface of arbitrary genus. Two knots that are concordant must mutually bound a surface of genus zero. Just as in the classical case of knot concordance, this is a highly restricted relationship and one wants to be able to determine whether two knots are concordant, whereas any two knots are cobordant. On the other hand, the least genus for a cobordism surface between two knots or between a knot and the unknot is of great interest.

Definition 3 The *four-ball genus* $g_4(K)$ of a virtual knot or link K is the least genus among all virtual surfaces obtained by virtual cobordism that bound K . As we shall see below, there is a simple upper bound on the four-ball genus for any virtual knot or link and a definite result for the four-ball genus of positive virtual knots [12]. Note that in this definition of four-ball genus we have not made reference to an embedding of the surface in the four-ball D^4 . The surface constructed by a virtual cobordism is, for this paper, an abstract surface with a well-defined genus. This same surface can be given the structure of virtual surface diagram analogous to a virtual knot or link diagram (see [56]) but we will not discuss this aspect of virtual surfaces in the present paper. Note that virtual slice knots are virtual knots K with $g_4(K) = 0$.

In Fig. 28 we illustrate the *virtual stevedore's knot* that we will denote by VS , and show that it is a slice knot in the sense of the above definition. This figure illustrates how the surface schema whose boundary in the virtual stevedore is evolved via the saddle point that produces two virtually unlinked curves that are isotopic to a pair of curves that can undergo deaths to produce the genus zero slicing surface. We will use this example to illustrate our theory of virtual knot cobordism, and the questions that we are investigating.

Fig. 28 Virtual Stevedore is slice



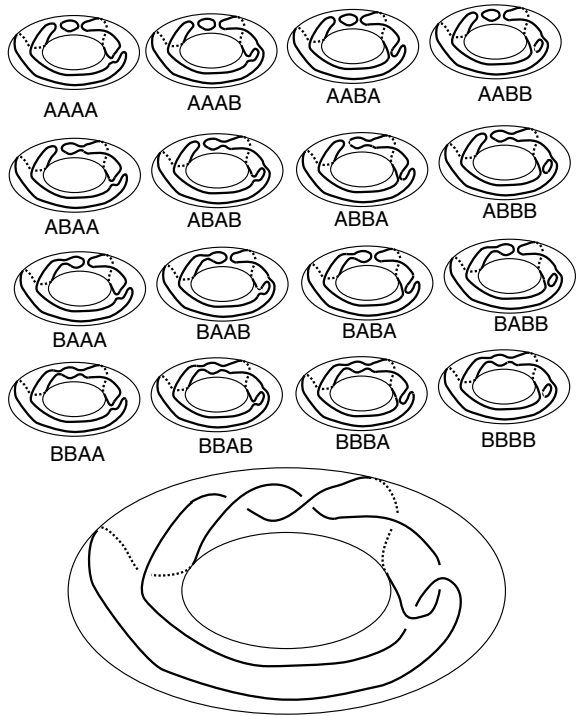
We prove that VS is not classical by showing that it is represented on a surface of genus one and no smaller. The reader should note the difference between representation of a virtual knot or link *on* a surface (as an embedding into the thickened surface) and the concept of spanning surface that will be discussed in the next section.

The technique for finding this virtual surface genus for the virtual stevedore is to use the bracket expansion on a toral representative of VS and examine the structure of the state loops on that surface. See Fig. 29. Note that in this figure the virtual crossings correspond to parts of the diagram that loop around the torus, and do not weave on the surface of the torus. An analysis of the homology classes of the state loops shows that the knot cannot be isotoped off the handle structure of the torus. See [10, 36] for more information about using the surface bracket.

Next we examine the bracket polynomial of the virtual stevedore, and show by a direct calculation (omitted here) that it has the same bracket polynomial as the classical figure eight knot. This calculation shows that VS is not a connected sum of two virtual knots. Thus we know that VS is a non-trivial example of a virtual slice knot.

In Fig. 30 we illustrate a connected sum of a virtual knot K and its *vertical mirror image* $K^!$. The vertical mirror image is obtained by reflecting the diagram in a plane perpendicular to the plane of the diagram *and reversing the orientation of the resulting diagram*. We indicate this particular connected sum by $K \sharp K^!$. While connected sum of virtual knots is not in general defined except by a diagrammatic choice, we do

Fig. 29 Virtual Stevedore is not classical



have a diagrammatic definition of this connected sum and it is the case that $K \sharp K^1$ is a slice knot for any virtual diagram K . The idea behind the proof of this statement is illustrated in Fig. 31. Saddle points can be made by pairing arcs across the mirror and the diagram resolves into a collection of virtual trivial circles. We omit the detailed proof of this fact about virtual concordance. This result is a direct generalization of the corresponding result for classical knots and links [16].

3.1 Spanning Surfaces for Knots and Virtual Knots and the Four-Ball Genus of Positive Virtual Knots

Every oriented classical knot or link bounds an embedded orientable surface in three-space. A representative surface of this kind can be obtained by Seifert’s algorithm (See [27, 29, 30]). We illustrate Seifert’s algorithm for a trefoil diagram in Fig. 32. The algorithm proceeds as follows: At each oriented crossing in a given diagram K , smooth that crossing in the oriented manner (reconnecting the arcs locally so that the crossing disappears and the connections respect the orientation). The result operation is a collection of oriented simple closed curves in the plane, usually called the *Seifert*

Fig. 30 Vertical mirror image

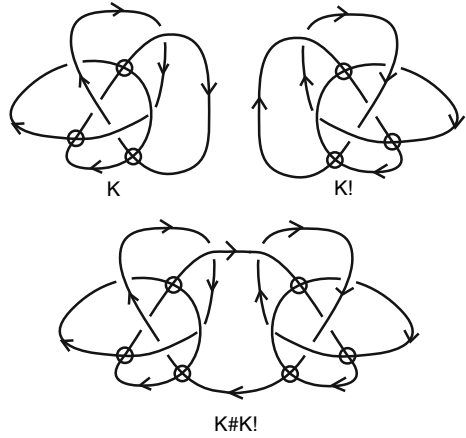
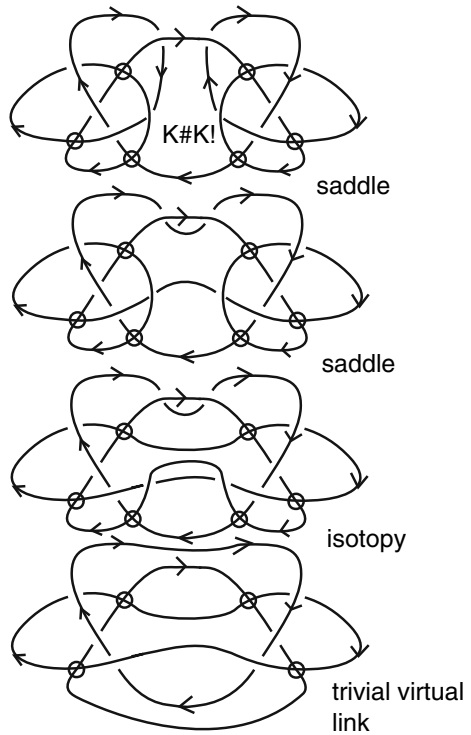
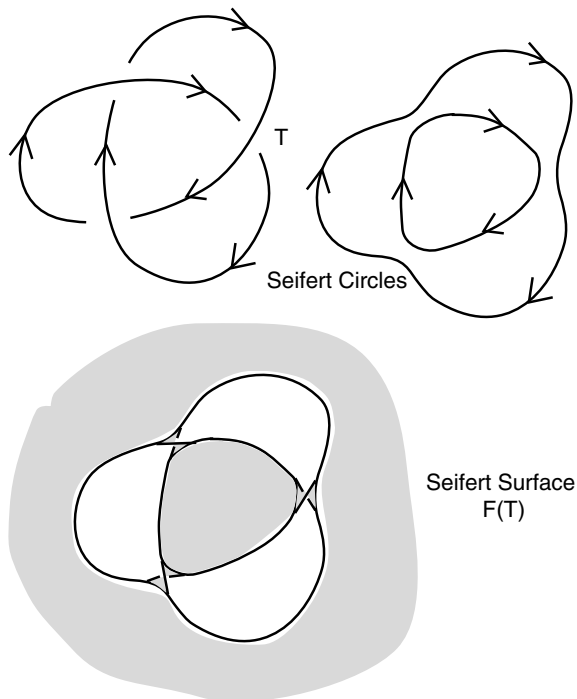


Fig. 31 Connected sum with vertical mirror image is slice



circles. To form the *Seifert surface* $F(K)$ for the diagram K , attach disjoint discs to each of the Seifert circles, and connect these discs to one another by local half-twisted bands at the sites of the smoothing of the diagram. This process is indicated in Fig. 32. In that figure we have not completed the illustration of the outer disc.

Fig. 32 Classical Seifert surface



Lemma 1 *Let K be a classical knot diagram with n crossings and r Seifert circles. Then the genus of the Seifert surface $F(K)$ is given by the formula*

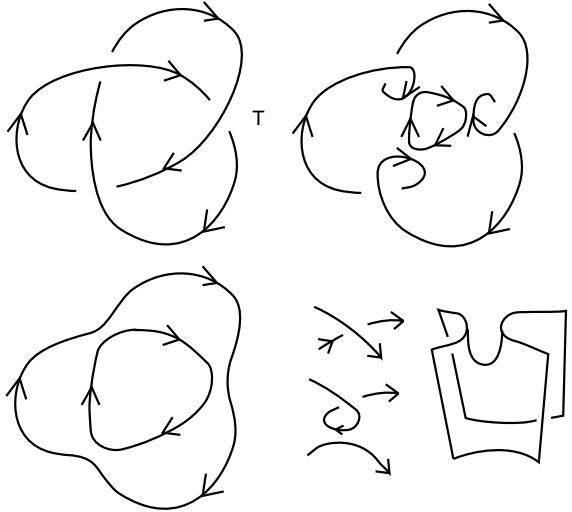
$$g(F(K)) = (1/2)(-r + n + 1).$$

Proof See [39].

For any classical knot K , there is a surface bounding that knot in the four-ball that is homeomorphic to the Seifert surface. One constructs this surface by pushing the Seifert surface into the four-ball keeping it fixed along the boundary. A different description of this surface is indicated in Fig. 33. We perform a saddle point transformation at every crossing of the diagram. The result of these operations is a collection of unknotted and unlinked curves. We then bound each of these curves by discs (via deaths of circles) and obtain a surface $S(K)$ embedded in the four-ball with boundary K . As the reader can easily see, the curves produced by the saddle transformations are in one-to-one correspondence with the Seifert circles for K and $S(K)$ is homeomorphic with the Seifert surface $F(K)$. Thus $g(S(K)) = (1/2)(-r + n + 1)$.

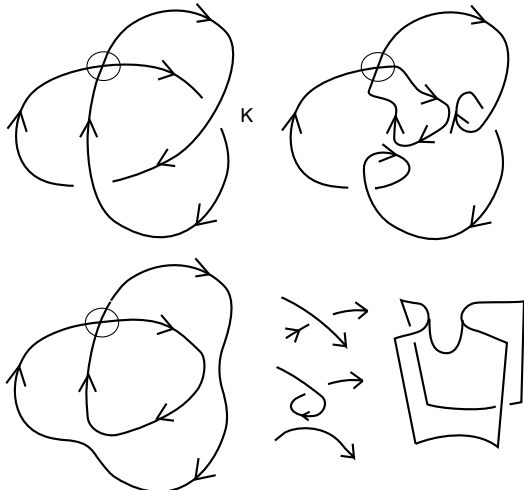
We generalize the Seifert surface to a surface $S(K)$ for virtual knots K by performing exactly these saddle moves at each classical crossing of the virtual knot. View Fig. 34. The result of these operations is a collection of unknotted curves that are isotopic (by the first classical Reidemeister move) to curves with only virtual cross-

Fig. 33 Classical cobordism surface



Every classical knot diagram bounds a surface in the four-ball whose genus is equal to the genus of its Seifert Surface.

Fig. 34 Virtual cobordism Seifert surface



Seifert Circle(s) for K

Every virtual diagram K bounds a virtual orientable surface of genus $g = (1/2)(-r + n + 1)$ where r is the number of Seifert circles, and n is the number of classical crossings in K .

This virtual surface is the cobordism Seifert surface when K is classical.

ings. Once the first Reidemeister moves are performed, these curves are identical with the *virtual Seifert circles* obtained from the diagram K by smoothing all of its classical crossings. We can isotope these circles into a disjoint collection of circles and cap them with discs in the four-ball. The result is a virtual surface $S(K)$ whose boundary is the given virtual knot K . We will use the terminology *virtual surface in the four-ball* for this surface schema. In the case of a virtual slice knot, the knot bounds a virtual surface of genus zero. We have the following lemma.

Lemma 2 *Let K be a virtual knot, then the virtual Seifert surface $S(K)$ constructed above has genus given by the formula*

$$g(S(K)) = (1/2)(-r + n + 1)$$

where r is the number of virtual Seifert circles in the diagram K and n is the number of classical crossings in the diagram K .

Proof See [39].

Remark. Note that it follows from the above discussion that if a diagram K' is obtained from a diagram K by replacing a crossing in K by its oriented smoothing, then K' is cobordant to K via a single saddle point move. We will use this observation repeatedly in the rest of the paper.

Remark. For the virtual stevedore in Fig. 35 there is a lower genus surface (genus zero as we have already seen) than can be produced by cobordism using the virtual Seifert surface. In that same figure we have illustrated a diagram D with the same projected diagram as the virtual stevedore, but D has all positive crossings. In this case we can prove that there is no virtual surface for this diagram D of four-ball genus less than 1. In fact, we have the following result. This theorem is a generalization of a corresponding result for classical knots due to Rasmussen [52].

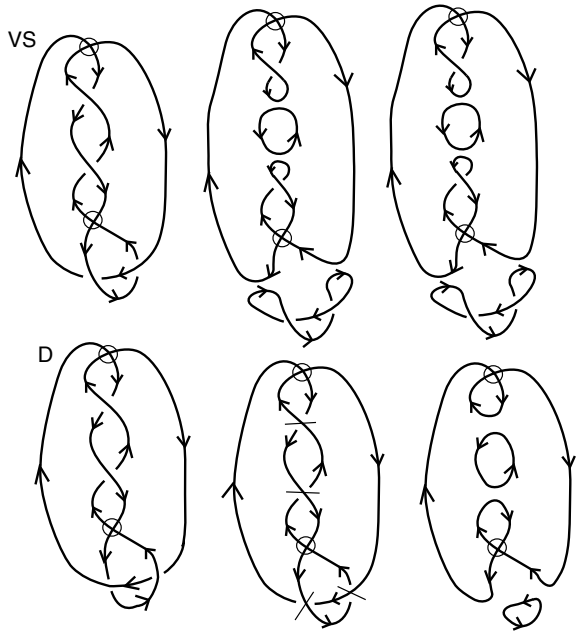
Theorem 4 (On Four-Ball Genus for Positive Virtual Knots [12]) *Let K be a positive virtual knot (i.e. all classical crossings in K are positive), then the four-ball genus $g_4(K)$ is given by the formula*

$$g_4(K) = (1/2)(-r + n + 1) = g(S(K))$$

where r is the number of virtual Seifert circles in the diagram K and n is the number of classical crossings in this diagram. In other words, the virtual Seifert surface for K represents its minimal four-ball genus.

Remark. This theorem is proved by using a generalization of integral Khovanov homology to virtual knot theory originally devised by Manturov [49]. In [12] we reformulate this theory and show that it generalizes to the Lee homology theory (a variant of Khovanov homology) as well. With this theorem, we know the genus for an infinite class of virtual knots and can begin the deeper exploration of genus for non-positive virtual knots and links.

Fig. 35 Virtual Stevedore cobordism Seifert surface



$$g = (1/2)(-r + n + 1) = (1/2)(-3 + 4 + 1) = 1.$$

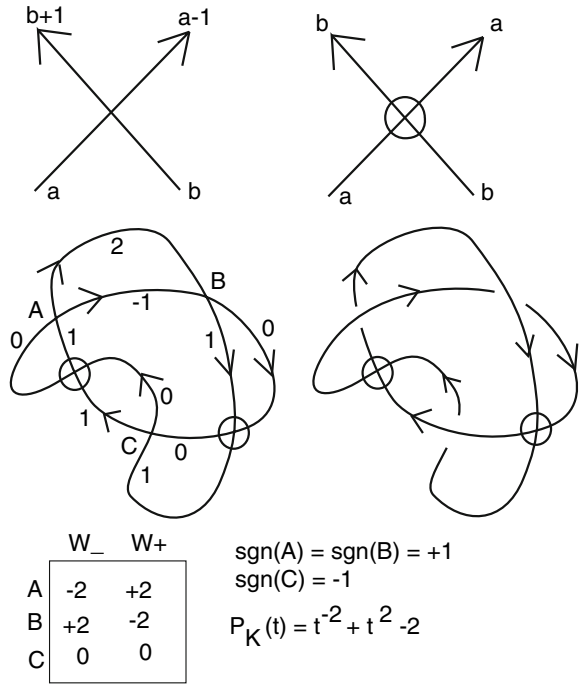
Seifert Cobordism for the Virtual Stevedore and for a corresponding positive diagram D.

3.2 The Affine Index Polynomial Invariant

The purpose of this section is to show that the affine index polynomial invariant [38] of virtual knots is a concordance invariant (see Definition 3.1), and to extend this invariant and its properties to virtual links. To this purpose, we begin by reviewing the definition of the affine index polynomial and recall its basic properties. We use the diagrammatic point of view in this section and do not use Gauss codes for the definitions and constructions.

We first describe how to calculate the affine index polynomial, then prove invariance under virtual link equivalence, and then prove concordance invariance. Calculation begins with a flat oriented virtual knot diagram (the classical crossings in a flat diagram do not have choices made for over or under). An *arc* of a flat diagram is an edge of the 4-regular graph that represents the diagram. An edge extends from one classical crossing to the next in orientation order. An arc may have many virtual crossings, but it begins at a classical crossing and ends at another classical crossing. We label each arc c in the diagram with an integer $\lambda(c)$ so that an arc that meets a classical crossing and crosses to the left increases the label by one, while an arc that meets a classical crossing and crosses to the right decreases the label by one. See Fig. 36 for an illustration of this rule. Such integer labeling can always be done for any virtual or classical link diagram [38]. In a virtual diagram the labeling is unchanged

Fig. 36 Labeled flat crossing and an example



at a virtual crossing, as indicated in Fig. 36. One can start by choosing some arc to have an arbitrary integer label, and then proceed along the diagram labeling all the arcs via this crossing rule. We call such an integer labeling of a diagram an *affine labeling* of the diagram and sometimes just a *labeling* of the diagram. In [38] we use the equivalent term *Cheng labeling* for the affine labeling.

Remark. We discuss the algebraic background to this invariant in [38]. Once we have a labeled flat diagram, we assign two *weights*, W_+ and W_- to each of its crossings according to the definition below. Then given a diagram with classical crossings j we assign a weight $W(j)$ to be W_+ if c is a positive classical crossing, and W_- if j is a negative classical crossing.

Definition 4 Given a labeled flat diagram we define two numbers at each classical crossing: W_- and W_+ as shown in Fig. 36. If we have a labeled classical crossing with left incoming arc a and right incoming arc b then the right outgoing arc is labeled $d = a - 1$ and the left outgoing arc is labeled $c = b + 1$ as shown in Fig. 36. We then define $W_+ = a - (b + 1)$ and $W_- = b - (a - 1)$. Note that $W_- = -W_+$ in all cases.

Definition 5 Given a crossing c in a diagram K , we let $\text{sgn}(c)$ denote the sign of the crossing. The sign of the crossing is plus or minus one according to the convention shown in Fig. 37. The *writhe*, $wr(K)$, of the diagram K is the sum of the signs of all its crossings. For a virtual link diagram, labeled in the integers according to the scheme above, and a crossing c in the diagram, define *the weight of the crossing*

Fig. 37 Crossing signs

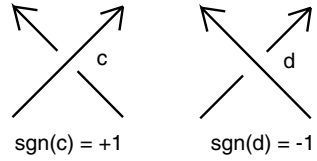
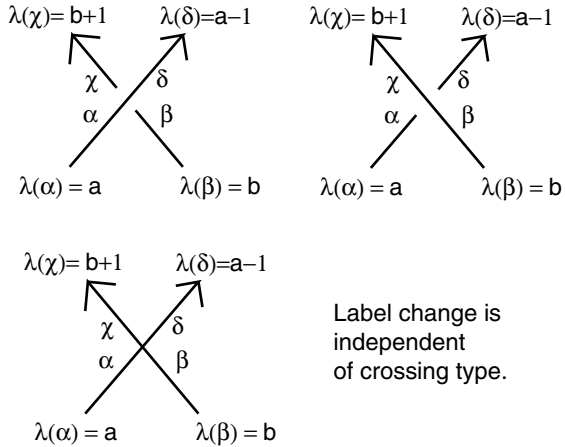


Fig. 38 Labels for crossings



$W_K(c)$ by the equation (Fig. 38)

$$W_K(c) = W_{sgn(c)}(c)$$

where $W_{sgn(c)}(c)$ refers to the underlying flat diagram for K . Thus $W_K(c)$ is $W_{\pm}(c)$ according as the sign of the crossing is plus or minus. We shall often indicate the weight of a crossing c in a knot diagram K by $W(c)$ rather than $W_K(c)$.

Remark. Note that in Fig. 36 we have flat crossings A, B, C and corresponding crossings in the virtual knot K . The Figure illustrates that $W_K(A) = -2, W_K(B) = +2, W_K(C) = 0$.

Definition 6 Let K be a virtual knot diagram. Define the *Affine Index Polynomial* of K by the equation

$$P_K = \sum_c sgn(c)(t^{W_K(c)} - 1) = \sum_c sgn(c)t^{W_K(c)} - wr(K)$$

where the summation is over all classical crossings in the virtual knot diagram K . The Laurent polynomial P_K is an invariant of virtual knots, as we shall recall below, and we shall show that it is a concordance invariant. Note that we can rewrite this definition as follows:

$$P_K = \sum_{n=1}^{\infty} wr_n(K)(t^n - 1)$$

where

$$wr_n(K) = \sum_{c:W_K(c)=n} sgn(c).$$

We can think of these numbers $wr_n(K)$ as special writhes for the virtual knot diagram, similar in spirit to the odd writhe. Each $wr_n(K)$ for $n = 1, 2, \dots$ is an invariant of the virtual knot K . Note also that a crossing c in K is odd (by our previous definition) if and only if $W_K(c)$ is odd. Thus, if $J(K)$ denotes the odd writhe of K , then

$$J(K) = \sum_{c:W_K(c) \text{ odd}} sgn(c) = \sum_{n \text{ odd}} wr_n(K).$$

Definition 7 In a flat virtual link the classical crossings are immersion crossings, neither over nor under, Reidemeister moves are allowed independent of over and under, but virtual crossings still take detour precedence over classical crossings [31] (See Sect. 2 of the present paper). We define the *Flat Affine Index Polynomial*, PF_K , for a flat virtual knot K by the formula

$$PF_K(t) = \sum_c (t^{|W_K(c)|} + 1)$$

where the polynomial is taken over the integers modulo two, but the exponents (the absolute values of the weights at the crossings) are integral. It is not hard to see that $PF_K(t)$ is an invariant of flat virtual knots, and that the concordance results of the present paper hold in the flat category for this invariant.

Remark. In Figs. 39 and 40 we indicate the affine index polynomials for examples of links. In this case the exponents in the polynomials contain a generic integer N that can be taken to be much greater than zero. Then the corresponding flat affine polynomial for Fig. 39 is $PF = t^{N-1} + t^N + t + 1 \pmod{2}$, and in Fig. 40 it is $PF = t^M + t^N + t^{M-1} + t^{N-1} \pmod{2}$. This shows that the flat versions of these links are non-trivial and that they are (using the results of the next section) not cobordant to the corresponding unlinks. See also Figs. 54 and 56 for examples of non-trivial flat affine polynomials, and the later discussion related to these figures.

Remark. In Fig. 36 we show the computation of the weights for a given flat diagram and the computation of the polynomial for a virtual knot K with this underlying diagram. The knot K is an example of a virtual knot with unit Jones polynomial. The polynomial P_K for this knot has the value

$$P_K = t^{-2} + t^2 - 2,$$

showing that this knot is not isotopic to a classical knot.

Fig. 39 Affine index invariant of a virtual link

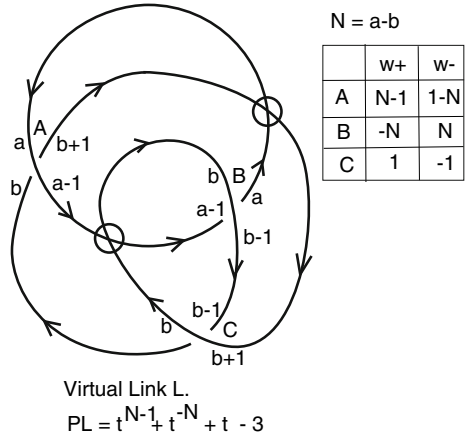
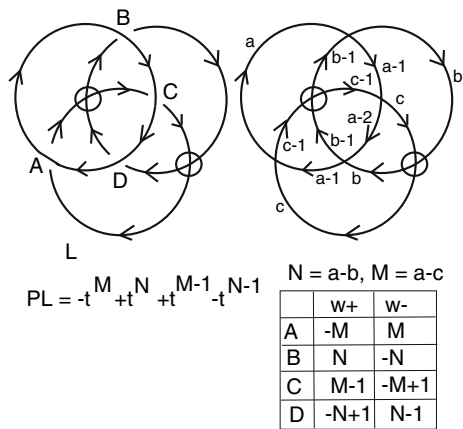


Fig. 40 Affine index invariant of a virtual Borromean rings



3.3 Invariance of $P_K(t)$

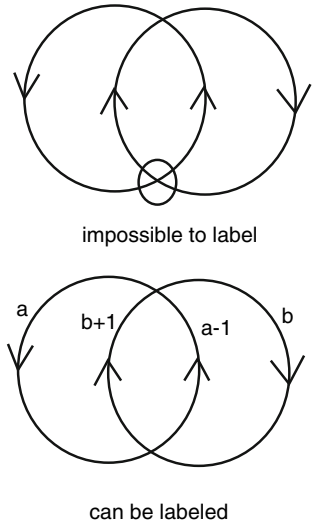
In order to show the invariance and well-definedness of $P_K(t)$ we must first show the existence of affine labelings of flat virtual knot diagrams. We do this by showing that any virtual knot diagram K that overlies a given flat diagram D can be so labeled.

Proposition 2 Any flat virtual knot diagram has an affine labeling.

Proof This proposition is proved in [38]. The main point is that on traversing the entire diagram, one goes through each crossing twice. The combination of these two operations results in a total change of zero. Hence, whatever label one begins with, the return label after a complete circuit of a diagram component will be the same as the start label.

Definition 8 Not all multi-component virtual diagrams can be labeled. See Fig. 41 for such an example. We call a multi-component diagram D compatible if every

Fig. 41 Possible and impossible labels for links



component of the diagram has algebraic intersection number zero (taking signed intersection numbers in the plane) with the other components in D .

We observe the following

Lemma 3 *Let D be a multi-component virtual diagram. Then D can be given an affine labeling if and only if it is compatible.*

Proof In any traverse of a given component of D one will meet external crossings each once, and increment or decrement the labeling according as the crossing has positive or negative sign with respect to this component. Self-crossings are met twice, once as an increment and once as a decrement. Thus the total traverse will not change the initial label if and only if the algebraic intersection number of the given component with the rest of the diagram is zero. Since this must hold for each component of the diagram D , we conclude that D can be labeled if and only if D is compatible.

Remark. If we follow the algorithm described in Fig. 36 to compute a labeling, using a different starting value, the resulting labeling will differ from the first labeling by a constant integer at every label. Since the polynomial is defined in terms of the differences $W_{\pm}(c)$ at each classical crossing c of K , it follows that the weights W_{\pm} as described above are well-defined. We can now state a result about the weights. See [38] for the proof. Let \bar{K} denote the diagram obtained by reversing the orientation of K and let K^* denote the diagram obtained by switching all the crossings of K . \bar{K} is called the *reverse* of K , and K^* is called the *flat mirror image* of K . We let K^{\dagger} denote the *vertical mirror image* of K as shown in Fig. 30.

The following proposition and its proof will be mostly found in [38] except for the statements about the vertical mirror image K^{\dagger} . These statements are easily seen from the discussion here and so we do not give a proof of this proposition here.

Proposition 3 *Let K be a virtual knot diagram and $W_{\pm}(c)$ the crossing weights as given in Definitions 5 and 6. If α is an arc of K , let $\bar{\alpha}$ denote the corresponding arc of \bar{K} , the result of reversing the orientation of K .*

1. *Let c be a crossing of K and let \bar{c} denote the corresponding crossing of \bar{K} , then $W(\bar{c}) = -W(c)$. Hence,*

$$P_{\bar{K}}(t) = P_K(t^{-1}).$$

Similarly, for the flat mirror image we have

$$P_{K^*}(t) = -P_K(t^{-1}),$$

and for the vertical mirror image

$$P_{K^!}(t) = -P_K(t).$$

Thus this invariant changes t to t^{-1} when the orientation of the knot is reversed, and it changes global sign and t to t^{-1} when the knot is replaced by its flat mirror image.

2. *If K is a classical knot diagram, then for each crossing c in K , $W(c) = 0$ and $P_K(t) = 0$.*
3. *If $K \# L$ denotes a connected sum (the diagrams are joined by removing an arc from each, and connecting them) of K and L , then*

$$P_{K \# L} = P_K + P_L.$$

Thus, if $K \# K^!$ denotes a connected sum of a virtual knot with its vertical mirror image (see Fig. 30), then it follows from the above that

$$P_{K \# K^!} = P_K - P_{K^!} = 0.$$

We will now state the invariance of $P_K(t)$ under virtual isotopy. The reader will recall that virtual isotopy consists in the classical Reidemeister moves plus virtual moves that are all generated by one generic detour move. The (unoriented) virtual isotopy moves are illustrated in Figs. 1 and 2. In Figs. 42 and 43 we show the relevant information for verifying that $P_K(t)$ is an invariant of oriented virtual isotopy. The reader can find the details of this proof for virtual knots in [38].

Theorem 5 *Let K be a virtual knot diagram. Then the polynomial $P_K(t)$ is invariant under oriented virtual isotopy and is hence an invariant of virtual knots.*

Proof See [38].

Generalization of the Affine Index Polynomial from Knots to Links. We are now in a position to generalize the invariant $P_K(t)$ to cases of virtual and classical link diagrams. Some of the material in this discussion can be found in embryonic form in

Fig. 42 Reidemeister moves II and II

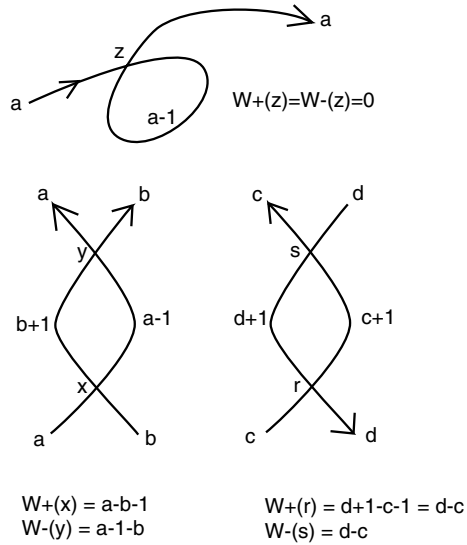
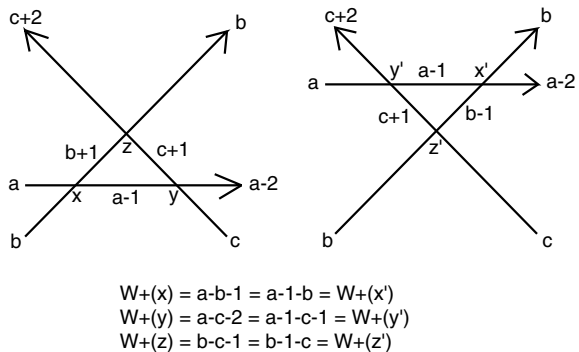


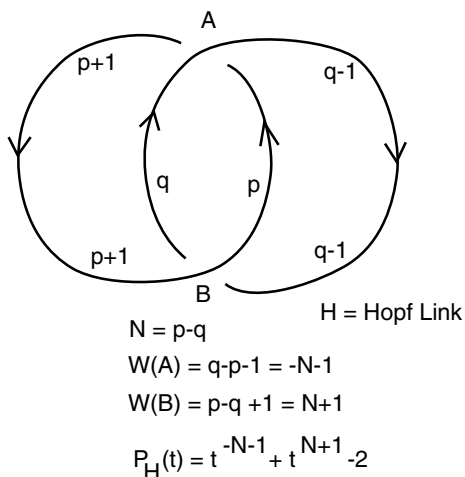
Fig. 43 Reidemeister move III



[38]. Special link diagrams can be affine colored according to our rules. For example, view Fig. 44 to see a labeling of the classical Hopf link. Before analyzing this figure, consider the proof for the invariance of the polynomial $P_K(t)$. Affine coloring is uniquely inherited under Reidemeister moves and the weights at the three crossings of the third Reidemeister move are permuted under the move. See Figs. 42 and 43. These properties are true for the polynomial that we write for any affine-colored link. Thus we can conclude that *if we are given a pair (L, C) where L is a link diagram and C is an affine-coloring of this diagram, then the polynomial $P_L(t)$, defined just as before, is an invariant of the pair (L, C) where a Reidemeister move applied to (L, C) produces (L', C') where L' is the diagram obtained from L by the move, and C' is the coloring uniquely obtained from C by the move. The resulting polynomial is an invariant of the link itself.*

Now go back to Fig. 44 and note that we have given arbitrary labels p and q to arcs on the two components and obtained weights of the form $-N - 1$ and $-N + 1$

Fig. 44 Invariant for the Hopf link



where $N = p - q$. If we regard N as an integer variable in the polynomial $P_H = t^{-N-1} + t^{N+1} - 2$ (H is a positive Hopf link), then this polynomial is an invariant of the link. This can be verified by applying Reidemeister moves to the link and showing that the value of N is preserved.

In working with the invariant for a link we choose an *algebraic* starting value for each component of the link, using a different algebraic symbol for each component. It is convenient in displaying the weights to use new variables corresponding to the differences between algebraic labels. Thus in Fig. 39 we have a two component virtual link with labels a and b for each component and we define $N = a - b$. At a crossing between two components the weights will be expressed uniquely in terms of N (the difference between their algebraic labels). The invariant polynomial for the link has algebraic exponents involving these differences. In Fig. 39 the polynomial is $P_K = t^{N-1} + t^{-N} + t - 3$.

In Fig. 40 we illustrate a link L that is a virtual Borromean rings. No two components are linked but the triple is linked. The algebraically weighted affine index polynomial detects the linkedness of these rings. Note that in this case we have two algebraic exponents N and M . We leave it to the reader to examine Fig. 40 for more details about this example.

We have defined *compatibility* (Definition 8) of multi-component diagrams above and proved that a multi-component diagram can be affine labeled if and only if it is compatible (Lemma 3). Therefore compatible links have affine index polynomials. Just as we have remarked, such polynomials will in general have exponents that are new variables and that can be specialized to polynomials of labeled pairs. It is useful to have both the absolute link invariants and the labeled pair invariants. We shall use both types of invariant in the discussion to follow.

3.4 Concordance Invariance of the Affine Index Polynomial

We now study the concordance invariance of the affine index polynomial following our work in [40]. This invariant is also called the *writhe polynomial*, $W_K(t)$, in the context of Gauss diagrams, see [4] where the W notation is used and where a proof of the concordance invariance in the case of knots is given using Gauss diagrams. The main result of this section is the

Theorem 6 *The affine index polynomial $P_K(t)$ is a concordance invariant of virtual knots K and compatible virtual links (the links for which the invariant is defined). In the case of links we use integral affine labelings for the link, just as in the case of knots. For links, the genus zero concordance is restricted to one where all critical points can be paired in canceling maxima and saddles and canceling saddles and minima. Note that this condition is automatically satisfied in the case of concordance of knots.*

Proof This proof is given in [40]. We include it here for the sake of completeness. Suppose that K is concordant to K' . Then there is a genus zero sequence of births deaths and saddles connecting K to K' . Genus zero implies that the core structure of this sequence is a tree of saddles, births and deaths. The genus zero surface is constructed from a sequence of pairings of births with saddles, and saddles with deaths. In other words, the basic operation that constructs the concordance consists in the splitting off from, or amalgamation of a trivial knot with the body of the concordance via a birth and saddle, or a saddle and a death. Thus we can consider an elementary genus zero concordance consisting in a virtual knot K and a trivial circle C , disjoint from K , such that the link diagram L consisting of the disjoint union of K and C undergoes virtual isotopy to a diagram D . One oriented saddle point move on D forms a new knot K' . It is sufficient to prove that $P_K = P_{K'}$. To prove this fact, note that by taking a constant labeling of C , we have a defined polynomial P_L with $P_K = P_L$. Then L is isotopic to D , and so by invariance of the affine index polynomial, $P_K = P_L = P_D$. At the place of the saddle point move there is a label a on the K component of D and a label b on the C component of D . We can add $a - b$ to the labels on all arcs of the C component of D and retain a legal coloring of D that does not change its polynomial evaluation (This is a general property of the labelings—they can always be shifted by a constant). Thus we may assume that D is prepared with a labeling so that $P_K = P_D$, and the labels at the saddle point are the same. Then the saddle move can be performed, and the new diagram K' inherits the same labeling. Hence $P_D = P_{K'}$. We have proved that $P_K = P_{K'}$. This completes the proof of the case of a birth followed by a saddle point. The remaining case is a saddle point followed by a death. In this case the link obtained after the saddle point inherits a labeling from the original knot and, given that the resulting link is isotopic to a disjoint union of a knot and a trivial circle, the argument proceeds as before. For links the criterion for the invariant to be defined is the existence of a labeling for the link diagram. Once we know that the labeling exists, the above arguments apply equally well to the case of links.

Fig. 45 Single saddle genus one surface

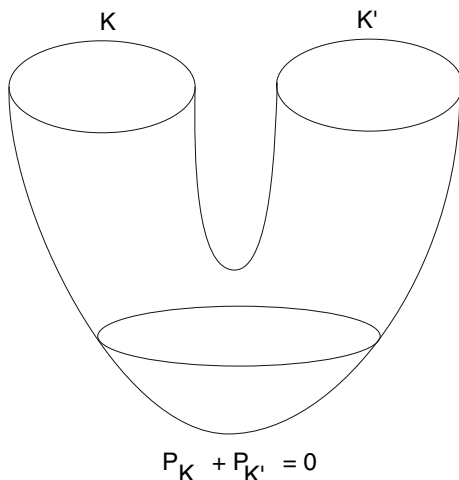
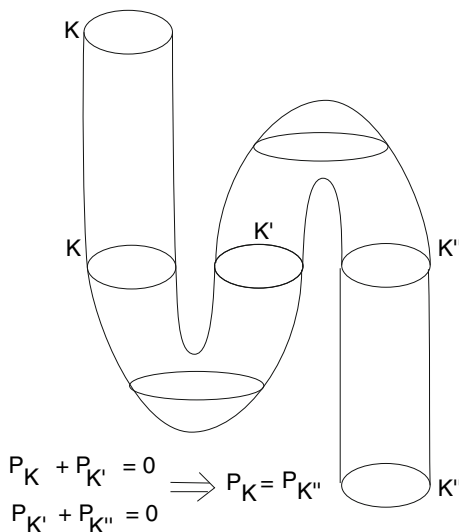
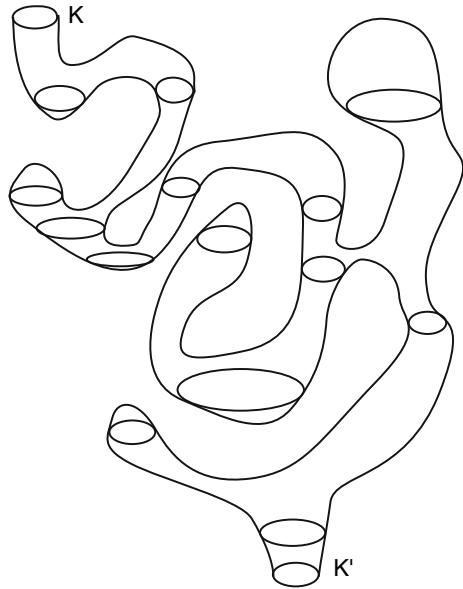


Fig. 46 Double saddle genus zero concordance



To complete the proof, we note that an elementary genus zero concordance from a link L of two components K and K' with one saddle point as shown in Fig. 45 has the property that $P_L = P_K + P_{K'} = 0$. The proof is by a labeling amalgamation argument as above. Similarly, if a concordance from knots K to K' consists in two saddle points as shown in Fig. 46, then $P_K = P_{K'}$ by two applications of the one saddle point observation. These two types of saddle point interaction combined with the maximum and minimum cancellations with saddle points discussed above constitute a complete list of the possibilities in an arbitrary concordance. See Fig. 47 for a typical example of a concordance schema. One sees, using the facts we have indicated here,

Fig. 47 Concordance schema



that on passing through a critical level in the concordance, the value of the polynomial sum of the components of the link at that level is not changed. Thus the value of P at the beginning of the concordance and the value of P at the end are equal. This completes the proof that the affine index polynomial is an invariant of concordance of virtual knots and links.

Remark. In Fig. 48 we illustrate an elementary concordance, as discussed in the proof above. The diagram K' is transformed by a single saddle point move to the diagram D , which is isotopic to a diagram that is the disjoint union of K and C where C is an unknotted circle. Letting C undergo death, we have a concordance from K' to K . We leave labeling this figure to the reader. It is clear that the crossings of the component of D that becomes C in the isotopy will have a total contribution of zero to the polynomial and that their contribution to D is identical to their contribution to K' . Thus we see directly in this case how $P_K = P_{K'}$. In Fig. 49 we show the weight calculation for the first part of the concordance in the previous figure. Note that the total weight contribution to the affine index polynomial from the unknotted and unlinked component (after the saddle move) is zero. This is in accord with our proof of concordance invariance.

Remark. Any virtual slice knot K will have $P_K(t) = 0$ since K is concordant to the unknot. In the case of the virtual stevedore knot, we see in Fig. 50 that all the weights are zero. We can ask when a virtual knot will have all of its weights equal to zero. It is certainly not the case that any virtual slice knot will have null weights. For example, view Fig. 51 where we show the knot $K \sharp K'$ where K is the virtual trefoil, and K' denotes the vertical mirror image of K . We know that $P_{K'}(t) = -P_K(t)$ for any virtual knot K . And so $P_{K \sharp K'} = 0$ for any virtual knot K . In fact, as remarked

Fig. 50 Virtual Stevedore has a null labeling

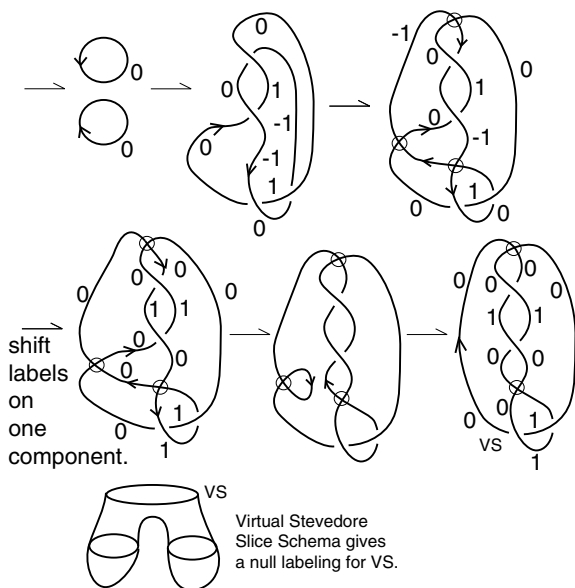
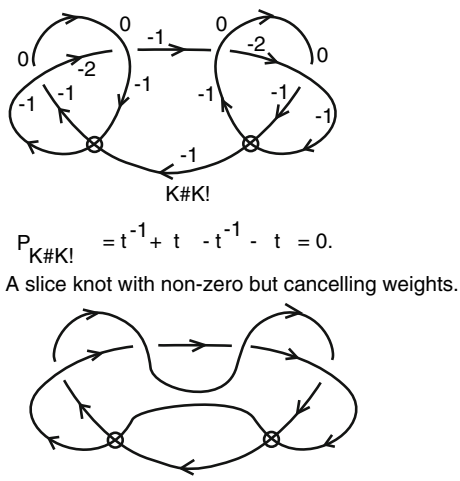


Fig. 51 A virtual slice knot with non-zero but canceling weights



in the previous section, it is the case that $K\sharp K^!$ is virtually slice for any virtual knot K . In such examples it is often the case that P_K is non-trivial and so the diagram has canceling but non-null weights. This is the case in this specific example, where $P_K = t^{-1} + t - 2$.

We finish this paper with a process that applies to most examples of the affine index polynomial. Taking a knot or link diagram K with a labeling, some of the weights

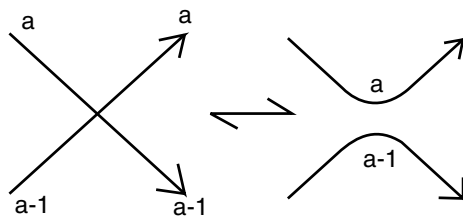


Fig. 52 Basic labeled cobordism

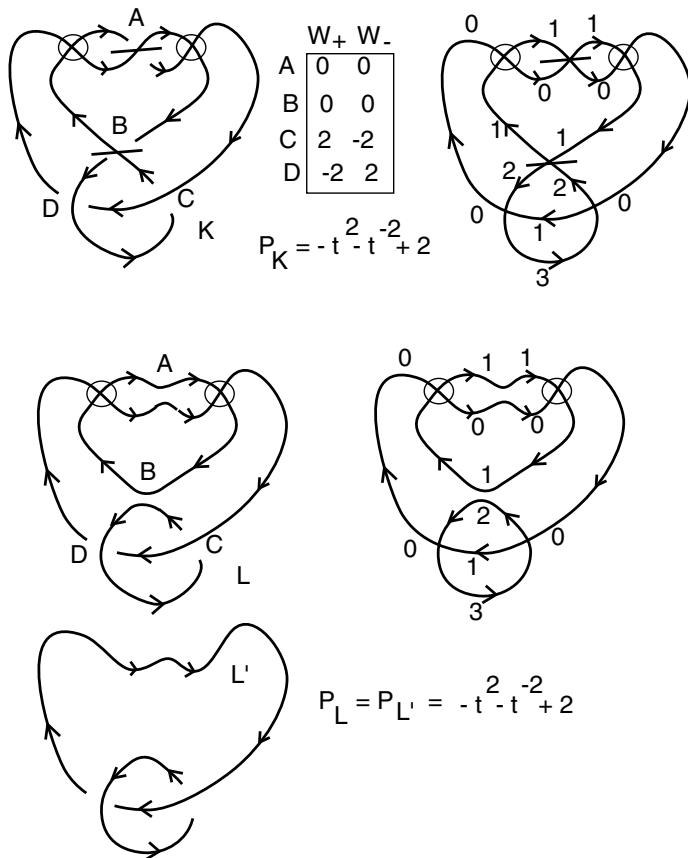


Fig. 53 Labeled cobordism of a knot to a link

may be zero. At each crossing with weight zero, we can smooth the crossing to obtain a link L that is cobordant to K (recall that smoothing a crossing can be accomplished by one saddle move). Thus we can smooth all crossings with null weights and obtain a knot or link K' such that K is cobordant to K' , K' has only non-zero weights (or it is an unknot or unlink) and $P_K = P_{K'}$. This process of removing crossings and

Fig. 54 Polynomial calculation for two knots

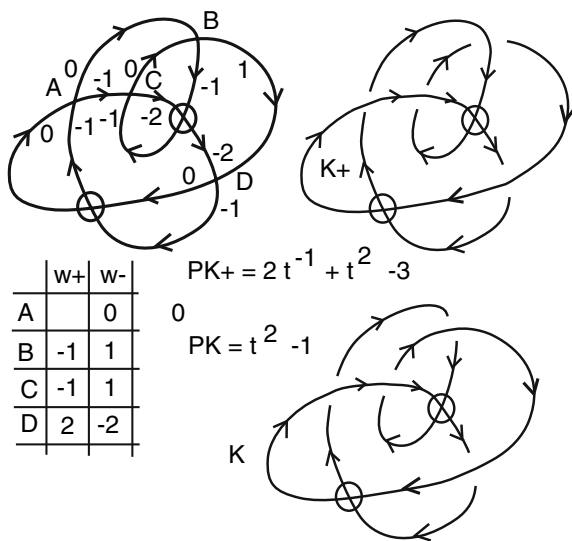
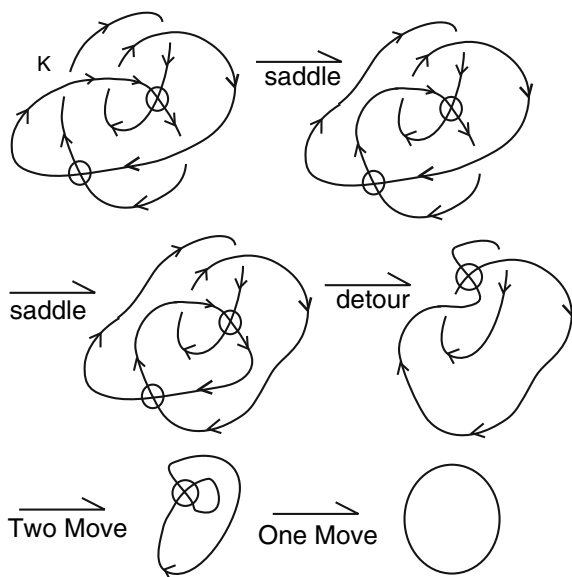


Fig. 55 The knot K has virtual genus one



K bounds a virtual surface of genus one.

making a cobordism that does not change the polynomial is particularly interesting in many examples. The link K' in its way, contains the core of the invariant for K and the remaining obstruction to making a concordance. Here are descriptions of some examples of this phenomenon (Figs. 52, 53, 54, 55, 56, 57, 58).

Fig. 56 Two flats differing by virtual crossing placement

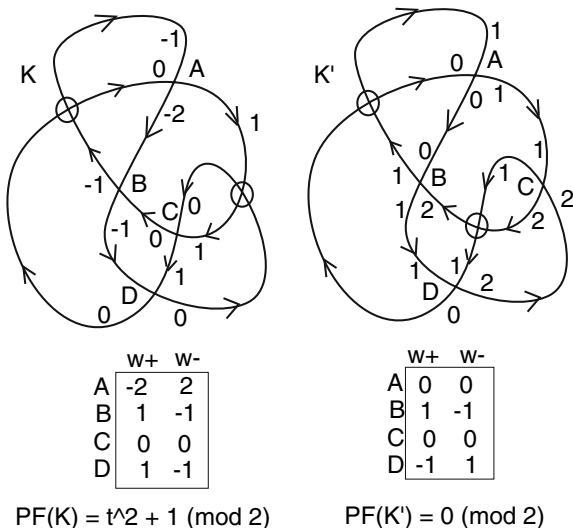
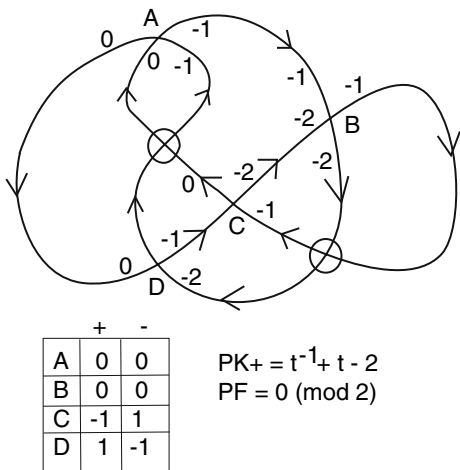
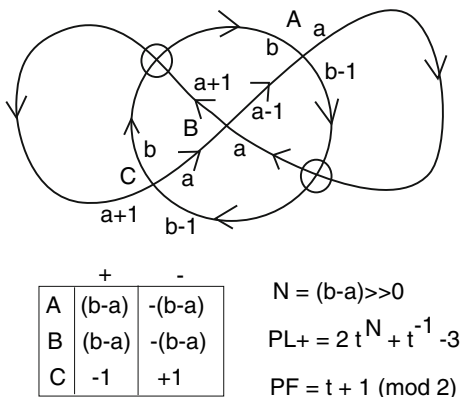


Fig. 57 A diagram with vanishing flat polynomial



In Figs. 52 and 53 we illustrate how the appearance of zeroes in the list of vertex weights for the polynomial can be used to produce labeled knots and links where the crossings with null weights have been smoothed. We will call the smoothing indicated in Fig. 52 a *basic labeled cobordism*. Thus if a knot has crossings with null weights, then it is labeled cobordant to a link with only non-zero weights (or an empty set of weights). While not all links can be labeled, this form of cobordism does produce labeled links, and the affine Index Invariant can be extended to such links as indicated in Fig. 44. Here we write down the most general labeling for the link, and then deduce a set of variable integer exponents for the polynomial invariant.

Fig. 58 A flat ink diagram that is not concordant to the unlink



In Fig. 54 we illustrate the calculation of the affine index polynomial for two knots K_+ and K . The knot K_+ is positive and by our theorem on the genus of positive virtual knots, it has genus two. The knot K is obtained from K_+ by switching one crossing. The affine index polynomial shows that it is not slice, and Fig. 55 shows that K bounds a genus one virtual surface. Thus we know, using the affine index polynomial, that K has genus equal to one.

Note that in this same Fig. 54 we can consider the corresponding flat virtuals for K_+ and K . Since $P(K_+) = 2t^{-1} + t^2 - 3$ and $P(K) = t^2 - 1$ we conclude that the corresponding mod 2 flat polynomial is $PF(D) = t^2 + 1$ for the flat diagram that they both overlie. We conclude that this flat diagram is not concordant to the unknot.

In Fig. 56 we give an examples of two flat diagrams K and K' such that the mod-2 affine Index invariant $PF(K) = t^2 + 1 \pmod{2}$ but $PF(K') = 0 \pmod{2}$. Thus we know that K is not concordant to the unknot, but the affine Index invariant does not indicate that K' is non-trivial as a flat virtual. An independent calculation of the Arrow polynomial for the flat K' shows that it is a non trivial virtual flat knot with flat arrow polynomial $3 + 2K_2 - 2K_3^2$ (see Sect. 2.4 for a discussion of the arrow polynomial). We conjecture that K' is not concordant to the unknot as a flat virtual knot.

In Fig. 57 we give an example of a flat knot K that has vanishing index polynomial. The reader can verify that the virtual Seifert surface for this knot has genus two. It appears that this flat knot is not concordant to the unknot and may even have four-ball genus two. Our techniques allow some explorations, but we do not have an answer to this question yet. An example of an exploration is shown in Fig. 58. The flat link in this figure is obtained from the flat knot in the previous figure by one saddle point move (by smoothing crossing A of Fig. 57). However this flat link has a non-trivial affine invariant and hence is not concordant to the unlink. We conclude that this saddle move on the knot of Fig. 57 cannot be part of the production of a slice surface for K .

Acknowledgements This work was supported by the Laboratory of Topology and Dynamics, Novosibirsk State University (contract no. 14.Y26.31.0025 with the Ministry of Education and Science of the Russian Federation).

References

1. V.G. Bardakov, The virtual and universal braids. *Fund. Math.* **184**, 1–18 (2004)
2. V.G. Bardakov, Yu.A. Mikhailchishina, M.V. Neshchadim, Virtual link groups (Russian). *Sibirsk. Mat. Zh.* **58**(5), 989–1003 (2017); Translation in *Sib. Math. J.* **58**(5), 765–777 (2017)
3. V.G. Bardakov, Yu.A. Mikhailchishina, M.V. Neshchadim, Groups of virtual trefoil and Kishino knots (2018), [arXiv:1804.06240v1](https://arxiv.org/abs/1804.06240v1) [math.GT]. Accessed 17 Apr 2018
4. H. Boden, M. Chrisman, R. Gaudreau, Virtual knot cobordism and bounding the silce genus (2017), [arXiv:1708.05982v2](https://arxiv.org/abs/1708.05982v2). Accessed 26 Dec 2017
5. H. Boden, M. Nagel, Concordance group of virtual knots. *Proc. Am. Math. Soc.* **145**(12), 5451–5461 (2017)
6. Z. Cheng, A polynomial invariant of virtual knots. *Proc. Am. Math. Soc.* **142**(2), 713–725 (2014)
7. M. Chrisman, Band-passes and long virtual knot concordance. *J. Knot Theory Ramif.* **26**(10), 1750057, 11 pp. (2017)
8. Q. Deng, X. Jin, L.H. Kauffman, Graphical virtual links and a polynomial for signed cyclic graphs. *J. Knot Theory Ramif.* **27**(10), 1850054, 14 pp. (2018)
9. H.A. Dye, Vassiliev invariants from parity mappings. *J. Knot Theory Ramif.* **22**(4), 1340008, 21 pp. (2013)
10. H.A. Dye, L.H. Kauffman, Minimal surface representations of virtual knots and links. *Algebr. Geom. Topol.* **5**, 509–535 (2005)
11. H.A. Dye, L.H. Kauffman, Virtual crossing number and the arrow polynomial. *JKTR* **18**(10), 1335–1357 (2009)
12. H.A. Dye, A. Kaestner, L.H. Kauffman, Khovanov homology, Lee homology and a Rasmussen invariant for virtual knots. *J. Knot Theory Ramif.* **26**(3), 1741001, 57 pp. (2017)
13. S. Eliahou, L.H. Kauffman, M. Thistlethwaite, Infinite families of links with trivial Jones polynomial. *Topology* **42**, 155–169 (2003)
14. R.A. Fenn, L.H. Kauffman, V.O. Manturov, Virtual knots: unsolved problems. *Fundamenta Mathematicae*, in *Proceedings of the Conference “Knots in Poland-2003”*, vol. 188, pp. 293–323 (2005)
15. R. Fenn, D.P. Ilyutko, L.H. Kauffman, V.O. Manturov, Unsolved problems in virtual knot theory and combinatorial knot theory. *Knots in Poland III. Part III*, vol. 103 (Banach Center Publications, Institute of Mathematics, Polish Academy of Sciences, Warsaw, 2014), pp. 9–61
16. R.H. Fox, J.W. Milnor, Singularities of 2-spheres in 4-space and cobordism of knots. *Osaka J. Math.* **3**, 257–267 (1966)
17. M. Goussarov, M. Polyak, O. Viro, Finite-type invariants of classical and virtual knots. *Topology* **39**(5), 1045–1068 (2000)
18. N. Gügümcü, L.H. Kauffman, New invariants of knotoids. *Eur. J. Combin.* **65**, 186–229 (2017)
19. N. Gügümcü, L.H. Kauffman, On the height of knotoids, *Algebraic Modeling of Topological and Computational Structures and Applications*. Springer Proceedings in Mathematics & Statistics, vol. 219 (Springer, Cham, 2017), pp. 259–281
20. A. Henrich, A sequence of degree one Vassiliev invariants for virtual knots. *J. Knot Theory Ramif.* **19**(4), 461–487 (2010)
21. D.P. Ilyutko, V.O. Manturov, Cobordisms of free knots (Russian). *Dokl. Akad. Nauk* **429**(4), 439–441 (2009); Translation in *Dokl. Math.* **80**(3), 844–846 (2009)
22. V.F.R. Jones, A polynomial invariant for links via von Neumann algebras. *Bull. Am. Math. Soc.* **129**, 103–112 (1985)

23. V.F.R. Jones, Hecke algebra representations of braid groups and link polynomials. *Ann. Math.* **126**, 335–338 (1987)
24. V.F.R. Jones, On knot invariants related to some statistical mechanics models. *Pac. J. Math.* **137**(2), 311–334 (1989)
25. D.A. Joyce, A classifying invariant of knots, the knot quandle. *J. Pure Appl. Algebr.* **23**(1), 37–65 (1982)
26. N. Kamada, Y. Miyazawa, A 2-variable polynomial invariant for a virtual link derived from magnetic graphs. *Hiroshima Math. J.* **35**(2), 309–326 (2005)
27. L.H. Kauffman, *Formal Knot Theory*. Lecture Notes Series, vol. 30 (Princeton University Press, Princeton, 1983). Dover Publications (2011)
28. L.H. Kauffman, State models and the Jones polynomial. *Topology* **26**, 395–407 (1987)
29. L.H. Kauffman, *On Knots* (Princeton University Press, Princeton, 1987)
30. L.H. Kauffman, *Knots and Physics* (World Scientific Publishers, Singapore, 1991). Second Edition (1993), Third Edition (2002), Fourth Edition (2012)
31. L.H. Kauffman, Virtual knot theory. *Eur. J. Comb.* **20**, 663–690 (1999)
32. L.H. Kauffman, A survey of virtual knot theory, in *Proceedings of Knots in Hellas '98* (World Scientific Publishers, Singapore, 2000), pp. 143–202
33. L.H. Kauffman, Detecting virtual knots, *Atti. Sem. Mat. Fis. Univ. Modena Supplemento al*, vol. IL (2001), pp. 241–282
34. L.H. Kauffman, A self-linking invariant of virtual knots. *Fund. Math.* **184**, 135–158 (2004), [arXiv:math.GT/0405049](https://arxiv.org/abs/math/0405049)
35. L.H. Kauffman, Knot diagrammatics, in *Handbook of Knot Theory* ed. by W. Menasco, M. Thistlethwaite (Elsevier, Amsterdam, 2005), pp. 233–318
36. L.H. Kauffman, H.A. Dye, Minimal surface representations of virtual knots and links. *Algebr. Geom. Topol.* **5**(2005), 509–535 (2005)
37. L.H. Kauffman, Introduction to virtual knot theory. *J. Knot Theory Ramif.* **21**(13), 1240007, 37 pp. (2012)
38. L.H. Kauffman, An affine index polynomial invariant of virtual knots. *J. Knot Theory Ramif.* **22**(4), 1340007, 30 pp. (2013)
39. L.H. Kauffman, Virtual knot cobordism, in *New Ideas in Low Dimensional Topology*, ed. by L.H. Kauffman, V.O. Manturov. Series on Knots and Everything, vol. 56 (World Scientific Publishing, Hackensack, 2015), pp. 335–377
40. L.H. Kauffman, Virtual knot cobordism and the affine index polynomial. *J. Knot Theory Ramif.* 1843017, 29 pp. (2018)
41. L.H. Kauffman, S. Lambropoulou, Virtual braids. *Fund. Math.* **184**, 159–186 (2004)
42. L.H. Kauffman, S. Lambropoulou, Virtual braids and the L-move. *J. Knot Theory Ramif.* **15**(6), 773–811 (2006)
43. L.H. Kauffman, S. Lambropoulou, The L-move and virtual braids, *Intelligence of Low Dimensional Topology 2006*. Series on Knots and Everything, vol. 40 (World Scientific Publishing, Hackensack, 2007), pp. 133–142
44. L.H. Kauffman, S. Lambropoulou, A categorical structure for the virtual braid group. *Commun. Algebr.* **39**(12), 4679–4704 (2011)
45. L.H. Kauffman, S. Lambropoulou, A categorical model for the virtual braid group. *J. Knot Theory Ramif.* **21**(13), 1240008, 48 pp. (2012)
46. G. Kuperberg, What is a virtual link? *Algebr. Geom. Topol.* **3**, 587–591 (2003)
47. V.O. Manturov, On invariants of virtual links. *Acta Appl. Math.* **72**, 295–309 (2002)
48. V.O. Manturov, Parity in knot theory. *Math. sb.* **201**(5), 693–733 (2010). Original Russian Text in *Mathematical Sbornik* **201**(5), 65–110 (2010)
49. V.O. Manturov, *Virtual Knot Theory - The State of the Art* (World Scientific Publishing, Singapore, 2012)
50. V.O. Manturov, Parity and cobordisms of free knots (Russian). *Mat. Sb.* **203**(2), 45–76 (2012); Translation in *Sb. Math.* **203**(1–2), 196–223 (2012)
51. S.V. Matveev, Distributive groupoids in knot theory (Russian). *Mat. Sb. (N.S.)* **119**(161), 78–88 (1982). 160(1)

52. J.A. Rasmussen, Khovanov homology and the slice genus. *Invent. Math.* **182**(2), 419–447 (2010)
53. S. Satoh, Virtual knot presentation of ribbon torus-knots. *JKTR* **9**(4), 531–542 (2000)
54. J. Sawollek, An orientation-sensitive Vassiliev invariant for virtual knots. *J. Knot Theory Ramif.* **12**(6), 767–779 (2003)
55. J. Scott Carter, S. Kamada, M. Saito, Stable equivalence of knots on surfaces and virtual knot cobordisms. *Knots 2000 Korea, Vol. 1* (Yongpyong). *J. Knot Theory Ramif.* **11**(3), 311–322 (2002)
56. Y. Takeda, Introduction to virtual surface-knot theory. *JKTR* **21**(14), 1250131, 6 pp. (2012)
57. V. Turaev, Cobordisms of words. *Commun. Contemp. Math.* **10**(suppl. 1), 927–972 (2008)
58. E. Witten, Quantum field theory and the Jones polynomial. *Commun. Math. Phys.* **121**, 351–399 (1989)

Knot Theory: From Fox 3-Colorings of Links to Yang–Baxter Homology and Khovanov Homology



Józef H. Przytycki

Dedicated to Lou Kauffman for his 70th birthday.

Abstract This paper is an extended account of my “Introductory Plenary talk at Knots in Hellas 2016” conference. We start from the short introduction to Knot Theory from the historical perspective, starting from Heraclitus text (the first century AD), mentioning R. Lull (1232–1315), A. Kircher (1602–1680), Leibniz idea of Geometria Situs (1679), and J.B. Listing (student of Gauss) work of 1847. We spend some space on Ralph H. Fox (1913–1973) elementary introduction to diagram colorings (1956). In the second section we describe how Fox work was generalized to distributive colorings (racks and quandles) and eventually in the work of Jones and Turaev to link invariants via Yang–Baxter operators; here the importance of statistical mechanics to topology will be mentioned. Finally we describe recent developments which started with Mikhail Khovanov work on categorification of the Jones polynomial. By analogy to Khovanov homology we build homology of distributive structures (including homology of Fox colorings) and generalize it to homology of Yang–Baxter operators. We speculate, with supporting evidence, on co-cycle invariants of knots coming from Yang–Baxter homology. Here the work of Fenn–Rourke–Sanderson (geometric realization of pre-cubic sets of link diagrams) and Carter–Kamada–Saito (co-cycle invariants of links) will be discussed and expanded. No deep knowledge of Knot Theory, homological algebra, or statistical mechanics is assumed as we work from basic principles. Because of this, some topics will be only briefly described.

I decided to keep the original abstract of the talk omitting only the last sentence “But I believe in *Open Talks*, that is I hope to discuss and develop above topics in an after-talk discussion over coffee or tea with willing participants”, which applies to a talk but not a paper.

J. H. Przytycki (✉)
Department of Mathematics, The George Washington University, Washington,
DC 20052, USA
e-mail: przytyck@gwu.edu

University of Gdańsk, Gdańsk, Poland

© Springer Nature Switzerland AG 2019
C. C. Adams et al. (eds.), *Knots, Low-Dimensional Topology
and Applications*, Springer Proceedings in Mathematics & Statistics 284,
https://doi.org/10.1007/978-3-030-16031-9_5

Keywords Knot theory · History of knots · Fox colorings · Cocycle invariants · Yang–Baxter operator · Khovanov homology · Categorification

2010 Mathematics Subject Classification 57M25

1 Knot Theory Started in Peloponnese

As the popular saying goes “All science started in Ancient Greece”. Knot Theory is not an exception. We have no proof that ancient Greeks thought of Knot Theory as a part of Mathematics but surgeons for sure thought that knots are important: a Greek physician named Heraklas, who lived during the first century AD is our main example (see Sect. 1.2). Even before, in pre-Hellenic times, there is mysterious stamp from Lerna, the place famous in classical times as the scenes of Herakles’ encounter with the hydra [18, 72, 73].

1.1 Seal-Impressions from Lerna, About 2200 BC

Excavations at Lerna by the American School of Classical Studies under the direction of Professor J.L. Caskey (1952–1958) discovered two rich deposits of clay seal-impressions. The second deposit dated from about 2200 BC contains several impressions of knots and links¹ [18, 21, 72] (see Fig. 1).

I have chosen two more patterns from seals of Lerna; these are not knots or links but “pseudoknots” which I will mention later with respect to extreme Khovanov homology and RNA (Fig. 2).

1.2 Heraklas Slings, First Century AD

A Greek physician named Heraklas, who lived during the first century AD and who was likely a pupil or associate of Heliodorus,² wrote an essay on surgeon’s slings [19].

¹The early Bronze Age in Greece is divided, as in Crete and the Cyclades, into three phases. The second phase lasted from 2500 to 2200 BC, and was marked by a considerable increase in prosperity. There were palaces at Lerna, Tiryns, and probably elsewhere, in contact with the Second City of Troy. The end of this phase (in the Peloponnese) was brought about by invasion and mass burnings. The invaders are thought to be the first speakers of the Greek language to arrive in Greece.

²Heliodorus was a surgeon in the 1st century AD, probably from Egypt, and mentioned in the Satires of Juvenal. This Heliodorus wrote several books on medical technique which have survived in fragments and in the works of Oribasius [39]. It is worth to cite Miller: “In the ‘Iatrikon Synagogos,’ a medical treatise of Oribasius of Pergamum (...) Heliodorus, who lived at the time of Trajan (Roman Emperor 98–117 AD), also mentions in his work knots and loops” [39, 57].



Fig. 1 A seal-impression from the House of the Tiles in Lerna (c. 2200 BC)

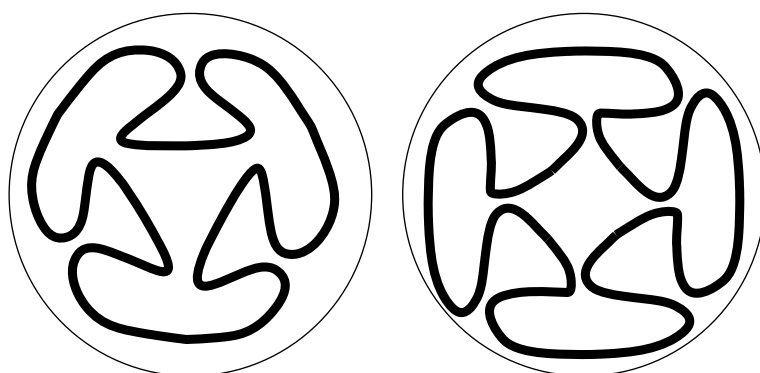


Fig. 2 Pseudoknots from Lerna

Heraklas explains, giving step-by-step instructions, eighteen ways to tie orthopedic slings. Here also Hippocrates “the father of western medicine” should be mentioned.³ Heraklas work survived because Oribasius of Pergamum (c. 325–400; physician of

³Hippocrates of Cos (c. 460–375 BC). A commentary on the Hippocratic treatise on *Joints* was written by Apollonios of Citon (in Cypros), who flourished in Alexandria in the first half of the first century BC. That commentary has obtained a great importance because of an accident in its transmission. A manuscript of it in Florence (Codex Laurentianus) is a Byzantine copy of the ninth century, including surgical illustrations (for example, with reference to reposition methods), which might go back to the time of Apollonios and even Hippocrates. Iconographic tradition of this kind are very rare, because the copying of figures was far more difficult than the writing of the text and

the emperor Julian the Apostate) included it toward the end of the fourth century in his “Medical Collections”.⁴ The oldest extant manuscript of “Medical Collections” was made in the tenth century by the Byzantine physician Nicetas. The Codex of Nicetas was brought to Italy in the fifteenth century by an eminent Greek scholar, J. Lascaris, a refugee from Constantinople. Heraklas’ part of the Codex of Nicetas has no illustrations⁵ and around 1500 an anonymous artist depicted Heraklas’ knots in one of the Greek manuscripts of Oribasius “Medical Collections” (in Fig. 3 we reproduce, after Day and with his comments the first page of drawings [11]). Vidus Vidius (1500–1569), a Florentine who became physician to Francis I (king of France, 1515–1547) and professor of medicine in the Collège de France, translated the Codex of Nicetas into Latin; it contains also drawings of Heraklas’ surgeon’s slings by the Italian painter, sculptor and architect Francesco Primaticcio (1504–1570); [11, 53].

Heraklas’ essay is the first surviving text on Knot Theory even if it is not proper Knot Theory but rather its application. The story of the survival of Heraklas’ work and efforts to reconstruct his knots in Renaissance is typical of all science disciplines and efforts to recover lost Greek books provided the important engine for development of modern science. This was true in Mathematics as well: the beginning of modern calculus in XVII century can be traced to efforts of reconstructing lost books of Archimedes and other ancient Greek mathematicians. It was only the work of Newton and Leibniz which went much farther than their Greek predecessors.

On a personal note: When I started to be interested in History of Knot Theory, the texts of Heraklas or Oribasius were unknown to Knot Theory community. It was by chance that when in 1992 I had a job interview at Memphis State University I had a meeting with a Dean, an English professor. Learning that I work on Knot Theory he mentioned that he had a friend C.L. Day⁶ who wrote a “humanistic” book about knots and their “classical” beginnings. Thus I learned about the book of Day [11] and Heraclas slings.

was often abandoned [57]. The story of the illustrations to Apollonios’ commentary is described in [58].

⁴From [59]: “The purpose of Oribasios *Medical Collection* is so well explained at the beginning of it that it is best to quote his own words”: *Autocrator Iulian, I have completed during our stay in Western Gaul the medical summary which your Divinity had commanded me to prepare and which I have drawn exclusively from the writings of Galen. After having praised it, you commanded me to search for and put together all that is most important in the best medical books and all that contributed to attain the medical purpose. I gladly undertook that work being convinced that such a collection would be very useful. (...) As it would be superfluous and even absurd to quote from the authors who have written in the best manner and then again from those who have not written as careful, I shall take my material exclusively from the best authors without omitting anything which I first obtained from Galen....*

⁵Otherwise the Codex of Nicetas is the earliest surviving illustrated surgical codex, containing 30 full page images illustrating the commentary of Apollonios of Kition and 63 smaller images scattered through the pages.

⁶Cyrus Lawrence Day (Dec. 2, 1900–July 5, 1968) was (in 1967) Professor Emeritus of English of the University of Delaware. A graduate of Harvard, he took an M.A. degree at Columbia and returned to Harvard for his PhD degree. (...) Mr. Day, a yachtsman since his boyhood, is the author, also, of a standard book on sailor’s knots [10–12].

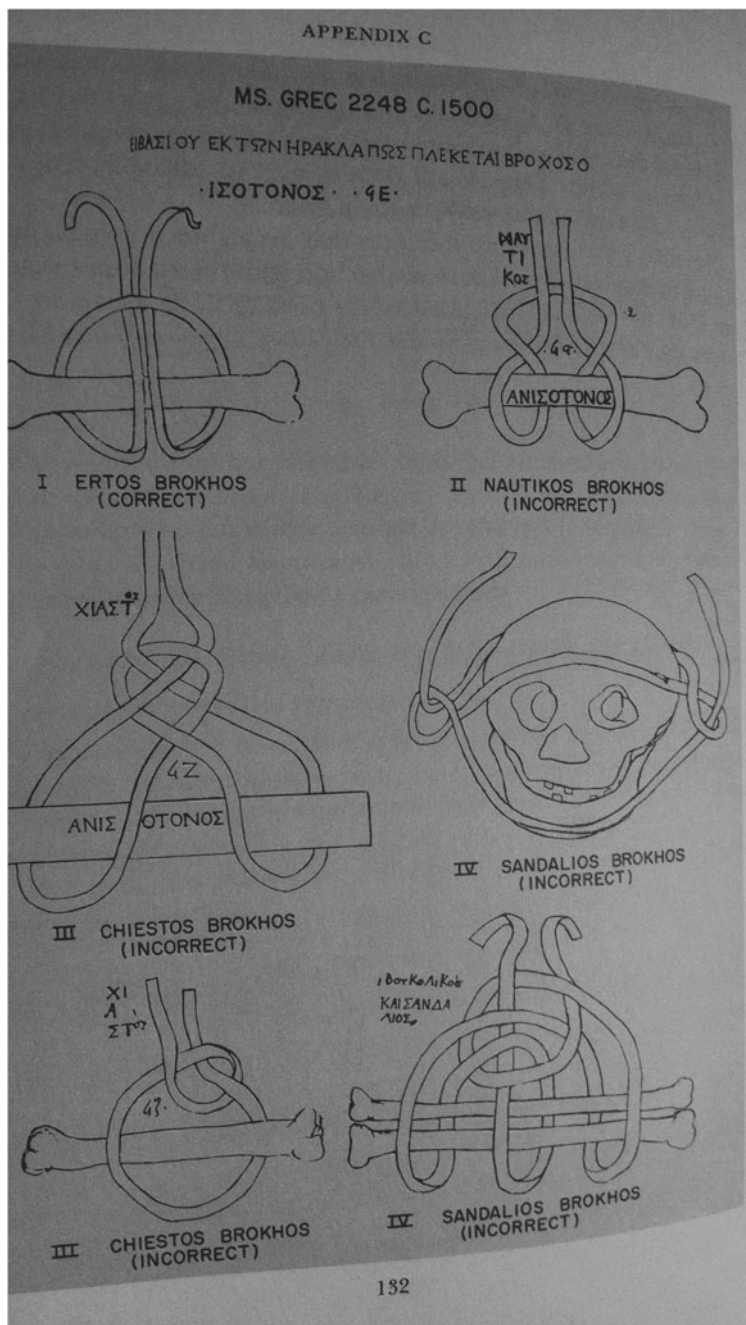
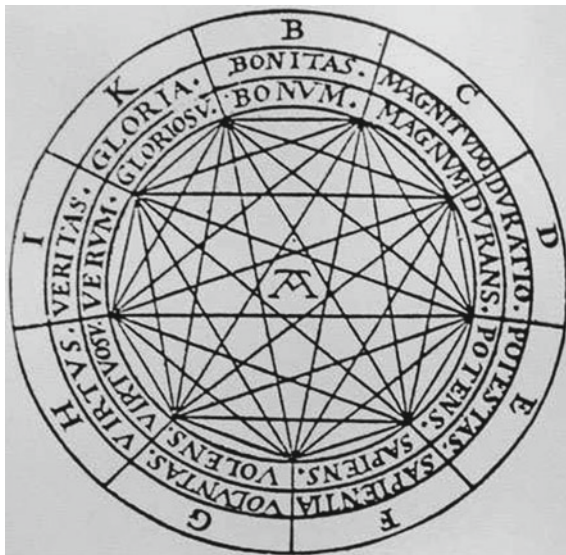


Fig. 3 Slings of Heraklas, c. 100 AD, [11]

Fig. 4 Combinatorial machine of Ramon Llull from his *Ars Generalis Ultima*



1.3 Ramon Llull, Leonardo da Vinci, and Albert Dürer

Let us mention in passing the work of Ramon Llull (1232–1315) and his combinatorial machines which greatly influenced Leibniz and his idea of *Geometria Situs* (Fig. 4).

The drawing of knots by Leonardo da Vinci and Albert Dürer should be also acknowledged (see Figs. 5 and 6).

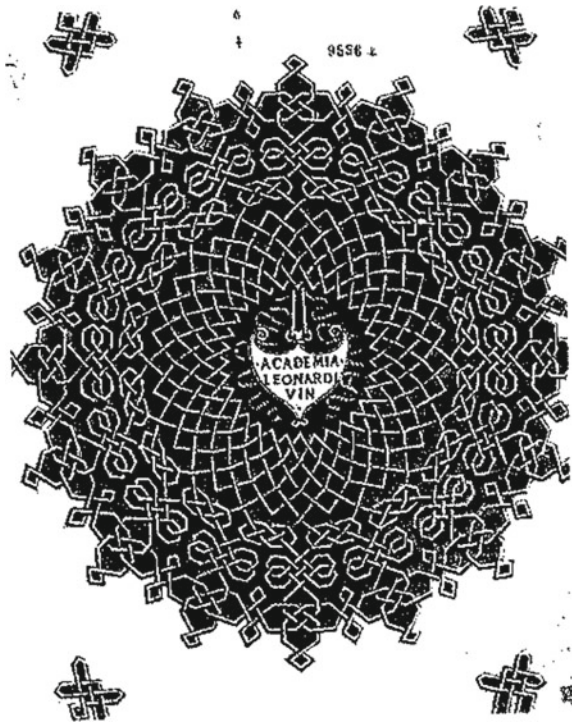
Here the anecdote: are this knots really knots or maybe links of more than one component? What is the structure of these links? The graph theorist of note, Frank Harary, took a task of checking it and made precise analysis of Leonardo and Dürer links⁷ [17] (compare also [20, 22]). This paper is based on my *Knots in Hellas* talks, taking place in ancient Olympia; such a venue is tempting me to write more of history, but I am already straying too far. I would refer to Chapter II of my Book [48] where I describe the early Knot Theory and the work of Kircher, Leibniz, Vandermonde, Gauss, and Listing; the Chapter is based on my papers [41, 42].

Engraving by Leonardo da Vinci⁸ (1452–1519) [37].

⁷Only after *Knots in Hellas* conference (July 2016) I learned about the paper by Hoy and Millett [22] with very detailed discussion of Leonardo and Dürer knots, see also [20].

⁸Giorgio Vasari writes in [66]: “[Leonardo da Vinci] spent much time in making a regular design of a series of knots so that the cord may be traced from one end to the other, the whole filling a round space. There is a fine engraving of this most difficult design, and in the middle are the words: *Leonardus Vinci Academia*.”

Fig. 5 Leonardo da Vinci,
Leonardus Vinci Academia



1.4 Fox and Fox-Trotter Colorings

My space is finite so let us jump to the second part of XX century, as I promised, to connect Fox colorings with Yang–Baxter invariants (and Khovanov homology).

Yes we all know about Fox colorings; in Fig. 7 we have iconic nontrivial Fox 3-coloring of the trefoil knot. The rule of 3-coloring is that we color arcs of a diagram using three colors, say red, blue, and yellow in such a way that at each crossing either all colors are used or only one color is used.

One also can play the coloring game with the link from Lerna, and yes it has nontrivial Fox 3-coloring as illustrated in Fig. 8. Indeed Fox 3-colorings motivated many popular, school level articles, notable of them is [67]. I also wrote about Fox colorings for middle school children [44, 45].

Still there is some controversy who really invented them.⁹ I think it was as follows (I describe likely story based on facts but also my experience with teaching in America). In 1956 Ralph Fox spent a sabbatical at Haveford College as it is explained in the Preface to his book [9]: “This book, which is an elaboration of a series of

⁹Reidemeister was considering homomorphisms of the fundamental group of the knot complement into n -dihedral groups. This easily leads to n th Fox coloring [54, 55].

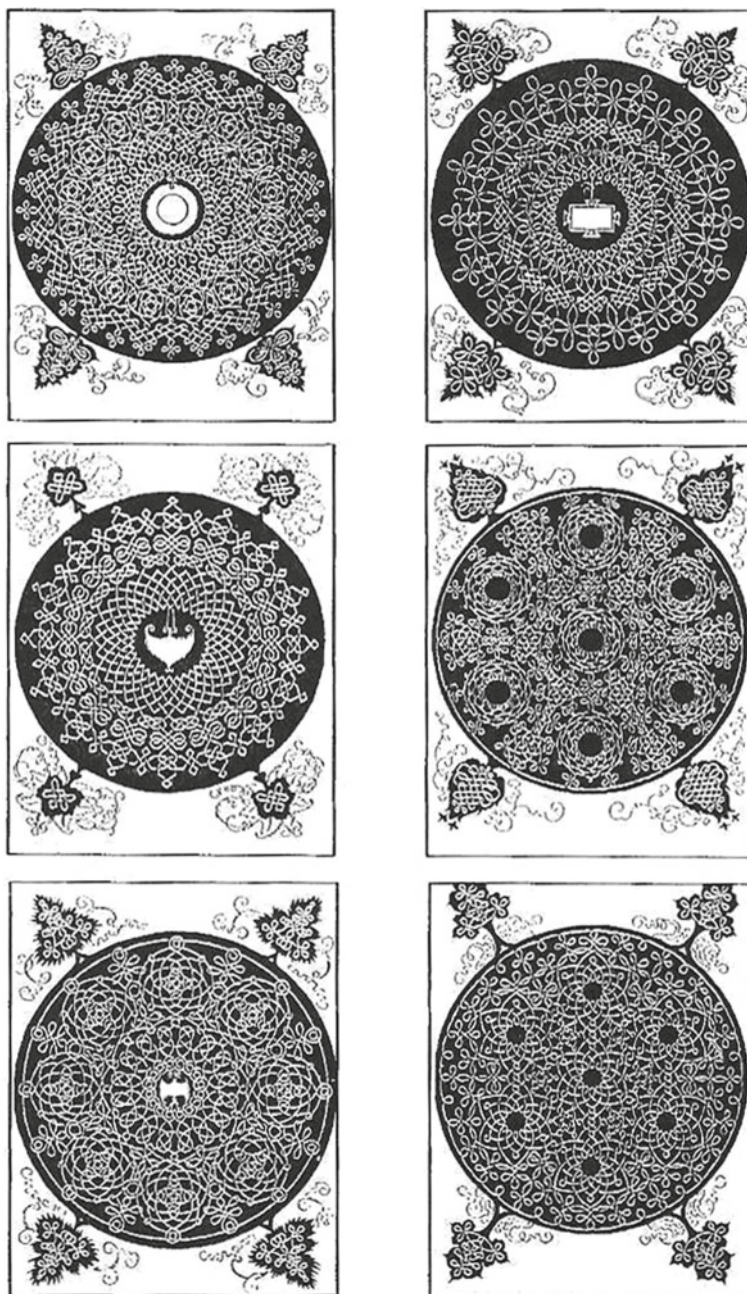


Fig. 6 Dürer's knots, 1505/6

Fig. 7 Nontrivial Fox 3-coloring of the trefoil knot

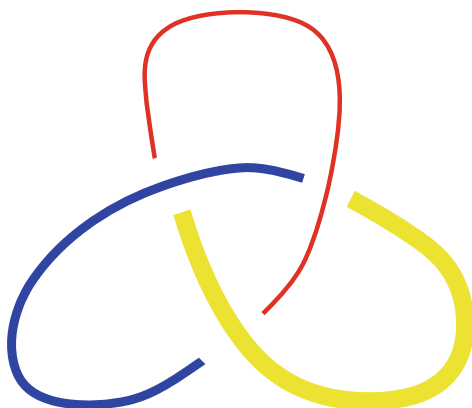
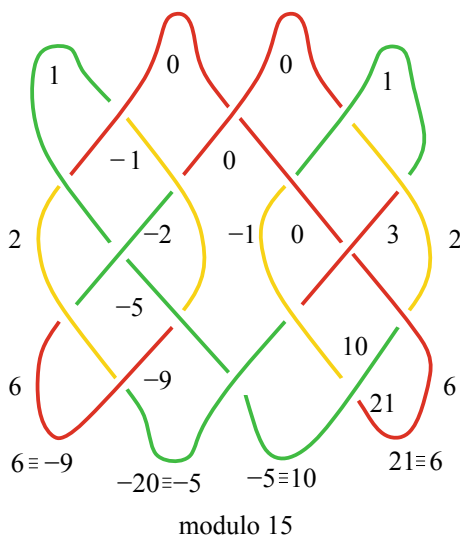


Fig. 8 Nontrivial Fox 3-coloring of the Lerna link. Numbers on the picture describe Fox 15-coloring. In fact the space of colorings of this link is $Col_{\mathbb{Z}}(L) = \mathbb{Z} \oplus \mathbb{Z}_2 \oplus \mathbb{Z}_3 \oplus \mathbb{Z}_5^2 \oplus \mathbb{Z}_7$ where \mathbb{Z} can be represented by trivial (monochromatic) colorings; compare [43]



lectures given by Fox at Haveford College while a Philips Visitor there in the spring of 1956, is an attempt to make the subject accessible to everyone. Primarily it is a textbook for a course at the junior-senior level”.

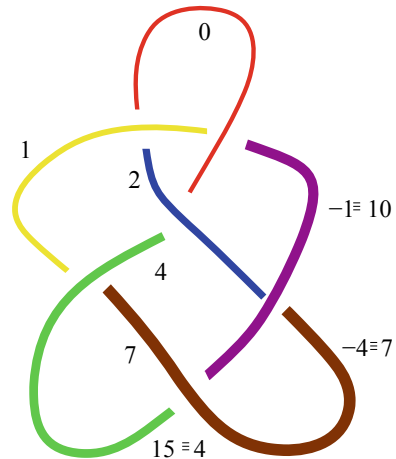
It is curious that 3-coloring and n -coloring are mentioned only in Exercises:

For instance Exercises 6 and 7 in Chapter VI are about Fox 3-colorings:

“Exercise 6. Let us say that a knot diagram has property ℓ if it is possible to color the projected overpasses in three colors, assigning a color to each edge in such a way that

- (a) the three overpasses that meet at a crossing are either all colored the same or are all colored differently;

Fig. 9 Nontrivial Fox 11-coloring of the knot 6_2



(b) all three colors are actually used.

Show that a diagram of a knot K has property ℓ if and only if K can be mapped homomorphically onto the symmetric group of degree 3.

Exercise 7. Show that property ℓ is equivalent to the following: It is possible to assign an integer to each edge in such a way that the sum of the three edges that meet at any crossing is divisible by 3.”

Fox 3-coloring can be naturally extended to n -coloring, again already hidden in Reidemeister work as homomorphisms of the fundamental group of link complement to the n th dihedral group D_{2n} , sending meridians to reflections. The diagrammatic definition is hidden in Exercises of Chap. VIII of [9], in particular Exercise 8 for $k = n - 1$ and then $-(b - a) = b - c \pmod n$ that is around a crossing Fox

n -coloring looks like $\frac{a}{b} \Big| \frac{c \equiv 2b - a}{\text{modulo } n}$.

Fox 11-coloring of the knot 6_2 of the Rolfsen tables [56] is shown in Fig. 9.

Interestingly when Richard Crowell, a student of Ralph Fox, was talking about Fox colorings to teachers in 1961, he referred to Fox as an inventor of 3-colorings but he said that he learned n -coloring from Halle Trotter [8]. I asked the question to Trotter and he remembers discussions with Crowell but not inventing n -colorings; he kindly answered my inquiry: “I am afraid my historical recollection is now very vague. Dick Crowell and I had many discussions of various things, and if he says so, I perhaps said something to suggest n -coloring before he did. He worked out all the details – I did not know even that he was writing the NCTM paper until he sent me a reprint.”

2 From Arc Colorings to Yang–Baxter Weighted Colorings

2.1 Magma Colorings

Fox n -coloring had to wait for its direct generalization (at least in print, discussion of the Conway-Wraith correspondence of 1959 would take another lecture [74]) for quarter of century. These, despite the fact that Wirtinger coloring, giving the fundamental group of a link complement or Alexander coloring, giving Alexander module and Alexander polynomial, were known from 1905 and 1928, respectively [1, 70].¹⁰

With Fox n -colorings, an orientation of a diagram is not needed. To save time I will move immediately to oriented diagrams but start naively from a fixed finite set X and coloring arcs of a diagram¹¹ by elements of X . Then we can ask under which conditions the set of such colorings is a link invariant. The simplest approach is now to think that at a crossing colorings change according to some operation. Because we can have positive and negative crossings, we need two operations $*$, $\bar{*} : X \times X \rightarrow X$. The convention for coloring by $(X, *, \bar{*})$ (called 2-magma) is given in Fig. 10.

The set of 2-magma colorings is denoted by $Col_X(D)$ and its cardinality by $col_X(D) = |Col_X(D)|$. Of course $col_X(D)$ is not necessary a link invariant and in next subsection we analyze when Reidemeister moves are preserving it.

2.2 Reidemeister Moves and Quandles

If we want $col_X(D)$ to be a link invariant, we check Reidemeister moves and obtain, after Joyce and Matveev [26, 38], the algebraic structure satisfying conditions (1), (2), (3) below, which Joyce in his 1979 PhD thesis named a *quandle* [25].

Definition 2.1

- (1) $a * a = a$, for any $a \in X$ (idempotence condition).
- (2) There is the inverse binary operation¹² $\bar{*}$, to $*$, that is for any pair $a, b \in X$ we have

¹⁰The year 1928 is the year of publication of the Alexander’s paper, however already in 1919 he discusses in a letter to Oswald Veblen, his former Ph.D. adviser, “a genuine and rather jolly invariant” which we call today the determinant of the knot. It is this construction which Alexander extends later to the Alexander polynomial $\Delta_D(t)$ (determinant is equal to $\Delta_D(t)$ for $t = -1$). In fact the Alexander letter contains more: Alexander constructs the space which we call often today the space of nontrivial Fox \mathbb{Z} -colorings or the first homology of the double branched cover of S^3 along the knot [2].

¹¹We consider arcs from undercrossing to undercrossing and semi-arcs from crossing to crossing.

¹²We can think of “inverse” formally: we introduce the monoid of binary operations on X , $Bin(X)$, with composition given by $a(*_1*_2)b = (a*_1 b) *_2 b$ and identity element $*_0$ given by $a*_0 b = a$, then the inverse means the inverse in the monoid, that is $*\bar{*} = *_0 = \bar{*}*$; see [46].

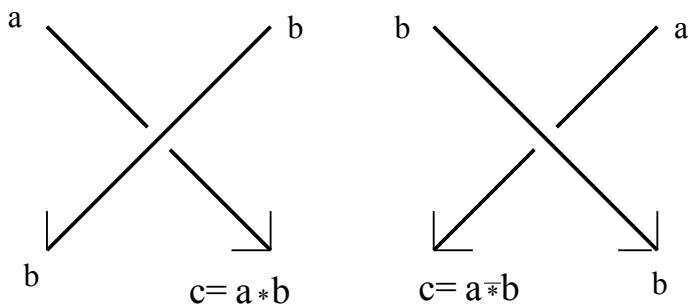


Fig. 10 Convention for a 2-magma coloring, $f: \text{Arcs}(D) \rightarrow X$, of a crossing

$$(a * b) \bar{*} b = a = (a \bar{*} b) * b \text{ (invertibility condition).}$$

Equivalently we define $*_b : X \rightarrow X$ by $*_b(a) = a * b$, and invertibility condition means that $*_b$ is invertible; we denote $*_b^{-1}$ by $\bar{*}_b$.

- (3) $(a * b) * c = (a * c) * (b * c)$ (distributivity), for any $a, b, c \in X$. Figure 14 illustrates how the third Reidemeister move leads to right selfdistributivity, and in fact can be taken as a “proof without words” that $col_X(D)$ is preserved by the positive third Reidemeister move if and only if $*$ is right self-distributive.

If only conditions (2) and (3) hold, then $(X; *, \bar{*})$ is called a rack (or wrack); the name coined by J.H. Conway in 1959.

If $* = \bar{*}$ in the condition (2), that is $(a * b) * b = a$ then the quandle is called an involutive quandle or kei $\begin{matrix} \pm \\ \pm \\ \pm \end{matrix}$ (the last term coined in 1942 by M. Takasaki [64]).

Before we show how quandle axioms are motivated by Reidemeister moves it is worth making metamathematical remark:

We have two equivalent approaches to quandle definition. The first approach starts from a magma $(X, *)$ and because the second condition says that $*$ is invertible we can introduce the inverse operation $\bar{*}$. The second approach uses only equations, thus we start from a set X with two binary operations $*$ and $\bar{*}$ and in the second axiom we assume that equations $(a * b) \bar{*} b = a$ and $(a \bar{*} b) * b = b$ hold. In both approaches axioms (1) and (3) are given by equations. The algebraic structure in which conditions are given by identities is called *variety* and G. Birkhoff proved that a class of algebras is a variety if and only if it is closed under homomorphic images, subalgebras, and arbitrary direct products [4]. On the other hand the first nonequational approach to a quandle allows that homomorphic image of a quandle is not a quandle (only spindle – the name used for magmas $(X, *)$ satisfying conditions (1) and (3)). See the discussion in Sect. 1.2 of [63] about combinatorial and equational definitions of quasigroup.

After this detour we go back to Reidemeister moves (Fig. 11).

First Reidemeister Move and Idempotence

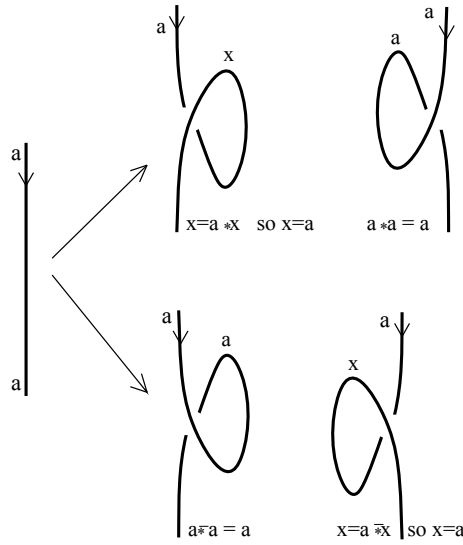


Fig. 11 First Reidemeister move leads to idempotent conditions $a * a = a$ and $\bar{a} * a = a$. It gives also the stronger condition that a is the only solution of the equation $a * x = x$ and $\bar{a} * x = x$; However this follows from the idempotent condition and the condition (2) (that $\bar{*}$ is the inverse of $*$)

First Reidemeister Move As Framing Change

For many considerations it is important to observe that the first Reidemeister move can be interpreted as a framing change of a framed diagram; Fig. 12.

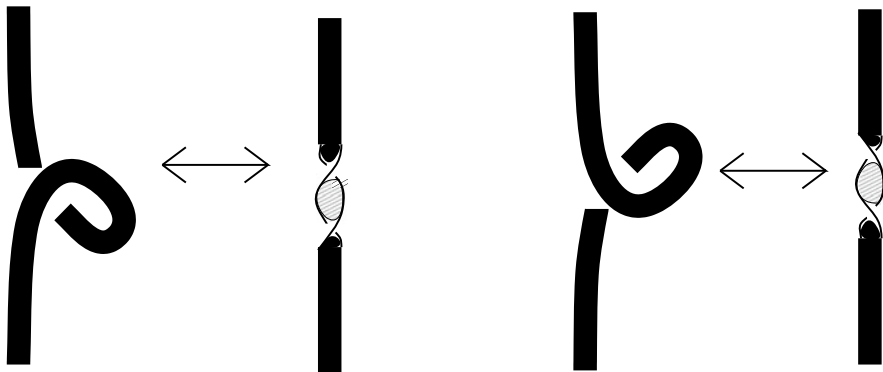
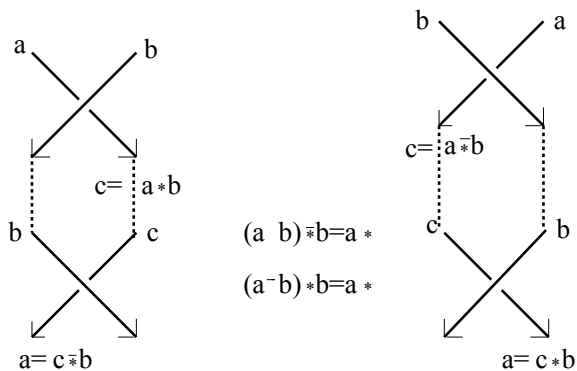


Fig. 12 First Reidemeister move can be interpreted as a framing change

Second Reidemeister Move and Invertibility

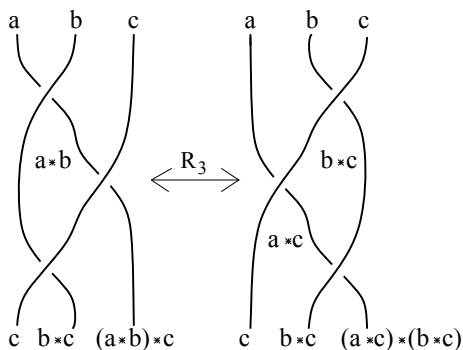
Fig. 13 Second Reidemeister move and magma coloring



The cardinality $col_X(D)$ is preserved by the second Reidemeister move if $*$ is invertible (Fig. 13).

Third Reidemeister Move and Distributivity

Fig. 14 Third Reidemeister move leads to right selfdistributivity. $(a * b) * c = (a * c) * (b * c)$

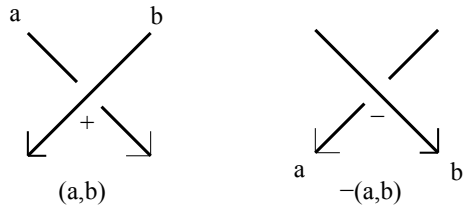


2.3 2-(Co)Cycle Invariants

Let X be a finite set and $*$ and $\bar{*}$ two binary operations. We define, after Carter–Kamada–Saito [7], 2-(co)cycle invariants of links:

- (1) A 2-chain, $\Psi(D, \phi)$ associated to the diagram D and coloring of its arcs by $\phi : arcs(D) \rightarrow X$ is an element of $\mathbb{Z}X^2$ defined as a sum over all crossings of D of the pair $\pm(a, b)$ according to conditions in figure below, that is $\Psi(D, \phi) = \sum_v sgn(v)(a, b)$, where the sum is taken over all crossings of D .

Fig. 15 Convention for the 2-chain



(2) A 2-cochain with coefficients in an abelian group A is a function $\alpha : X^2 \rightarrow A$ or equivalently an element of $Hom(\mathbb{Z}X^2, A)$. A 2-cochain associated to the diagram D and coloring of its arcs by $\phi : arcs(D) \rightarrow X$ is an element of $Hom(\mathbb{Z}X^2, A)$, defined by $\Psi(D, \phi, \alpha) = \sum_v sgn(v)\alpha(a, b)$ (Fig. 14).

In order to have Knot Theory applications one would like to have the chain $\Psi(D, \phi)$ (resp. cochain α) to be a 2-cycle (resp. cocycle) in some homology (resp. cohomology) theory. Further we would like to have Reidemeister moves preserving homology (resp. cohomology) class. This motivated initially authors of [6] and led to the discovery that what they need is essentially rack homology introduced around 1990 by Fenn, Rourke and Sanderson [14, 15] but taking into account the first Reidemeister move and degeneracy. We explain more in next subsections (Fig. 15).

2.4 Presimplicial Sets and Modules

Let $X_n, n \geq 0$ be a sequence of sets and $d_i = d_{i,n} : X_n \rightarrow X_{n-1}, 0 \leq i \leq n$ maps (called face maps) such that:

$$(1) d_i d_j = d_{j-1} d_i \text{ for any } i < j.$$

Then the system (X_n, d_i) satisfying the above equality is called a presimplicial set.¹³ Similarly if $C_n, n \geq 0$ is a sequence of k -modules, for fixed commutative ring k (e.g. $C_n = kX_n$) and $d_i = d_{i,n} : C_n \rightarrow C_{n-1}, 0 \leq i \leq n$ are homomorphisms satisfying

$$(1) d_i d_j = d_{j-1} d_i \text{ for any } i < j,$$

then (C_n, d_i) satisfying the above equality is called a presimplicial module. The important basic observation is that if (C_n, d_i) is a presimplicial module then (C_n, ∂_n) , for $\partial_n = \sum_{i=0}^n (-1)^i d_i$, is a chain complex.

¹³The concept was introduced in 1950 by Eilenberg and Zilber under the name *semi-simplicial complex* [13].

2.5 One-Term Distributive Homology

Definition 2.2 ([46]) We define a (one-term) distributive chain complex $C^{(*)}$ as follows: $C_n = \mathbb{Z}X^{n+1}$ and the boundary operation $\partial_n^{(*)} : C_n \rightarrow C_{n-1}$ is given by:

$$\partial_n^{(*)}(x_0, \dots, x_n) = (x_1, \dots, x_n) + \sum_{i=1}^n (-1)^i (x_0 * x_i, \dots, x_{i-1} * x_i, x_{i+1}, \dots, x_n).$$

The homology of this chain complex is called a one-term distributive homology of $(X; *)$ (denoted by $H_n^{(*)}(X)$).

We directly check that $\partial^{(*)}\partial^{(*)} = 0$, however it is useful to note that (X^{n+1}, d_i) is a presimplicial (semi-simplicial) set with $d_i(x_0, \dots, x_n) = (x_0 * x_i, \dots, x_{i-1} * x_i, x_{i+1}, \dots, x_n)$.

2.6 Two-Term Rack (Spindle) Homology

The trivial quandle $(X, *_0)$, is defined by $a *_0 b = a$. The 2-term rack homology of a spindle (right self-distributive system (RDS)) is defined by the presimplicial module (C_n, d_i^R) with $d_i^R = d_i^{(*)} - d_i^{(*_0)}$. One can recognize here a precubic set (X^n, d_i^c) (compare [47]). This precubic set and its geometric realization were important in the initial approach in [14, 15].

2.7 More General Colorings

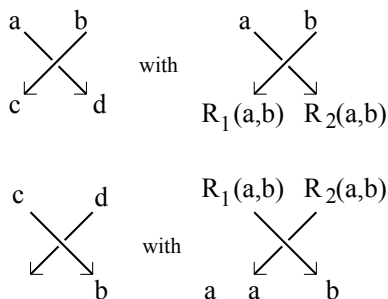
We can consider more general colorings when we allow two parts of an overcrossing to have different colors. Namely, we start from the set of colors X and consider a function $R : X \times X \rightarrow X \times X$ such that for any coloring of semi-arcs by colors from X at any crossing the convention given in Fig. 16 holds (here $R(a, b) = (R_1(a, b), R_2(a, b))$).

If R is invertible and the number of colorings (for finite X) is preserved by a braid like oriented third Reidemeister move, we call R a set theoretic Yang–Baxter operator which can be used to construct link invariants (e.g. 2-cocycle invariants) [5, 51].

Before we move to general Yang–Baxter operators and their invariants, I would suggest the reader the following simple but important exercise:

Exercise 2.3 Let D be an oriented link diagram, X a finite set of colors, and $R : X \times X$ a set theoretic Yang–Baxter operator. Let ϕ be a coloring of semi-arcs of D sat-

Fig. 16 General semi-arc colorings



isfying rules of Fig. 16. Following Sect. 2.3, we define $\Psi(D, \phi) = \sum_v \text{sgn}(v)(a, b)$. Let us consider $\partial_2(a, b) = a + b - R_1(a, b) - R_2(a, b)$. Show that $\Psi(D, \phi)$ is a cycle, that is $\partial_2(\Psi(D, \phi)) = 0$ for every diagram D and coloring ϕ .

3 Yang–Baxter Homology

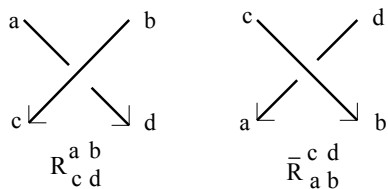
In quandle coloring and set-theoretic Yang–Baxter coloring of an oriented link diagram we are assuming that at every crossing a coloring of the input semi-arcs defines uniquely coloring of the output semi-arcs. We can however, in a natural way, relax this condition by allowing any coloring and then for a crossing to associate a weight from a fixed commutative ring (for set-theoretic Yang–Baxter operator this weight is 0 if coloring is not allowed and 1 if it is allowed). The details are as follows.

Fix a finite set X and color semi-arcs of an oriented diagram D by elements of X allowing different weights from a fixed ring k for every crossing. Following statistical mechanics terminology we call these weights Boltzmann weights. We allow also differentiating between a negative and a positive crossing; see Fig. 17.

We can now generalize the number of colorings to state sum (basic notion of statistical physics) by multiplying Boltzmann weight over all crossings and adding over all colorings [24, 65]:

$$\text{col}_{(X; BW)}(X) = \sum_{\phi \in \text{col}_X(D)} \prod_{p \in \{\text{crossings}\}} \hat{R}_{c,d}^{a,b}(p)$$

Fig. 17 Boltzmann weights $R_{c,d}^{a,b}$ and $\bar{R}_{a,b}^{c,d}$ for positive and negative crossings



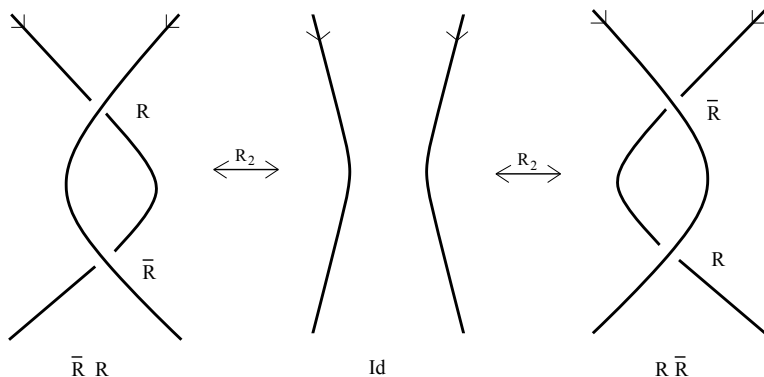


Fig. 18 Invertibility of R and the parallel second Reidemeister move

where $\hat{R}_{c,d}^{a,b}$ is $R_{c,d}^{a,b}$ or $\bar{R}_{c,d}^{a,b}$ depending on whether p is a positive or negative crossing. Our state sum is an invariant of a diagram but to get a link invariant we should test it on Reidemeister moves. To get analogue of a shelf invariant we start from the third Reidemeister move with all positive crossings. Recall that in the distributive case, passing through a positive crossing was coded by a map $R : X \times X \rightarrow X \times X$ with $R(a, b) = (b, a * b)$. Thus in the general case passing through a positive crossing is coded by a linear map $R : kX \otimes kX \rightarrow kX \otimes kX$ and in basis X the map R is given by the $|X|^2 \times |X|^2$ matrix with entries $(R_{c,d}^{a,b})$, that is $R(a, b) = \sum_{(c,d)} R_{c,d}^{a,b} \cdot (c, d)$. The third Reidemeister move leads to the equality of the following maps $V \otimes V \otimes V \rightarrow V \otimes V \otimes V$ where $V = kX$:

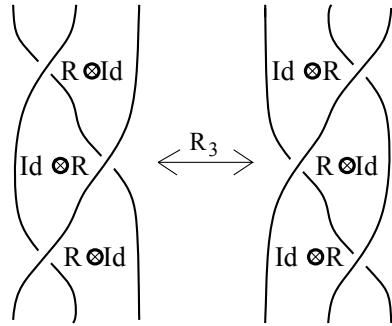
$$(R \otimes Id)(Id \otimes R)(R \otimes Id) = (Id \otimes R)(R \otimes Id)Id \otimes R,$$

as illustrated in Fig. 19. This is called the Yang–Baxter equation¹⁴ and R is called a pre–Yang–Baxter operator. If R is additionally invertible it is called a Yang–Baxter operator. If entries of R^{-1} are denoted by $\bar{R}_{c,d}^{a,b}$ then the state sum is invariant under “parallel” (directly oriented) second Reidemeister move, see Fig. 18.¹⁵

¹⁴Older names include: the star-triangle relation, the triangle equation, and the factorization equation [23].

¹⁵We should stress that to find link invariants it suffices to use directly oriented second and third Reidemeister moves in addition to both first Reidemeister moves, as we can restrict ourselves to braids and use the Markov theorem. This point of view was used in [65].

Fig. 19 Yang–Baxter equation. From the positive third Reidemeister move



Examples leading to the Jones polynomial [24, 65] start from a 2-dimensional set X and the free k -module over X , $V = kX^2$ and $R : V \otimes V \rightarrow V \otimes V$ is given by:

$$\begin{pmatrix} -q & 0 & 0 & 0 \\ 0 & q^{-1} - q & 1 & 0 \\ 0 & 1 & 0 & 0 \\ 0 & 0 & 0 & -q \end{pmatrix}$$

or using column unital (i.e. entries of each column adds to 1) matrix [52, 71]

$$\begin{pmatrix} 1 & 0 & 0 & 0 \\ 0 & 1 - y^2 & 1 & 0 \\ 0 & y^2 & 0 & 0 \\ 0 & 0 & 0 & 1 \end{pmatrix}$$

Graphical Visualization of Yang–Baxter Face Maps

The presimplicial set corresponding to a (two term) Yang–Baxter homology has the following visualization. In the case of a set-theoretic Yang–Baxter equation we recover the homology of J.S. Carter, M. Elhamdadi, M. Saito [5]; compare [31, 32, 47, 51] (Fig. 20).

In particular for a Yang–Baxter operator R given by

$$R(a, b) = \sum_{(c,d) \in X^2} R_{c,d}^{a,b} \cdot (c, d)$$

we have

$$\begin{aligned} \partial_2(a, b) &= (d_1^\ell(a, b) - d_1^r(a, b)) - (d_2^\ell(a, b) - d_2^r(a, b)) = \\ &((b) - \sum_{c,d} R_{c,d}^{a,b} \cdot (c)) - (\sum_{c,d} R_{c,d}^{a,b} \cdot ((d) - (a))) = \end{aligned}$$

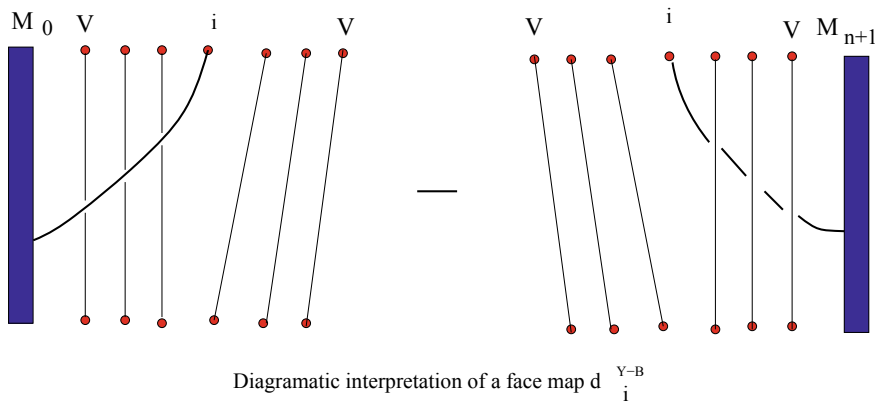


Fig. 20 Graphical interpretation of the face map d_i

$$(a) + (b) - \sum_{c,d} R_{c,d}^{a,b} \cdot ((c) + (d)).$$

Exercise 3.1 Consider a Yang–Baxter operator R and a coloring ϕ such that associated to a diagram elements $R_{c,d}^{a,b}$ are all different than zero. Find when the 2-chain $\Psi(D, \phi) = \sum_v sgn(v) \cdot (a, b)$ is a 2-cycle.

Decomposition of the Third Reidemeister Move into Cubic Face Maps

The main idea is illustrated by the following picture, we can contemplate a precubic structure of the third Reidemeister move (Fig. 21):

The idea leads to (co)cycle invariants of links, at least for stochastic (or more generally column unital) Yang–Baxter matrices. An example was given in the Knot in Hellas talk by Xiao Wang (compare [52] and Wang’s PhD thesis [71]).

4 Khovanov Homology After Oleg Viro

One of the biggest discovery (or construction) in Topology after the first Knots in Hellas conference¹⁶ was that of Khovanov homology [30].

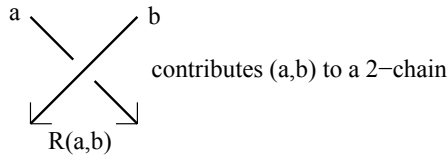
We start from the description of the Khovanov homology for framed links, after [68, 69].

Definition 4.1 ([27–29]) The unreduced Kauffman polynomial is defined by initial conditions

$$[U_n] = (-A^2 - A^{-2})^n,$$

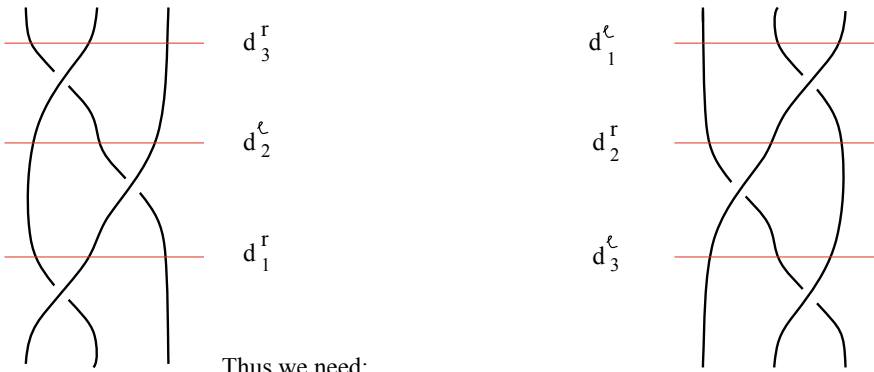
¹⁶The conference Knots in Hellas I took place in Delphi, Greece in August of 1998, while the e-print of Khovanov work was put on arXiv in August of 1999. However Mikhail Khovanov had already an idea of Khovanov homology in summer of 1997.

Yang–Baxter operator with $R=(R_{c,d}^{a,b})$ and fixed semi–arc coloring



$$\partial_3(a,b,c) = \sum_{i=1}^3 (-1)^i (d_i^{\ell} - d_i^r)(a,b,c)$$

We illustrate here the fact that the third Reidemeister move preserves homology classes, that is changes any chain by a boundary



Thus we need:

$$d_3^r + d_2^{\ell} + d_1^r = d_1^{\ell} + d_2^r + d_3^{\ell}$$

and this is given by $\partial_3(a,b,c)$

Fig. 21 Reidemeister third move and face maps d_i^{ε}

where U_n is the crossingless diagram of a trivial link of n components, and the skein relation:

$$[\text{crossing}] = A[\text{smoothing}] + A^{-1}[\text{other smoothing}]$$

A Kauffman state is a function from a set of crossings to the two element set $\{A, B\}$, that is $s : cr(D) \rightarrow \{A, B\}$, see Fig. 22. We denote by D_s the diagram (system of circles) obtained from D by smoothing all crossings of D according to s ; $|D_s|$ denotes the number of circles in D_s .

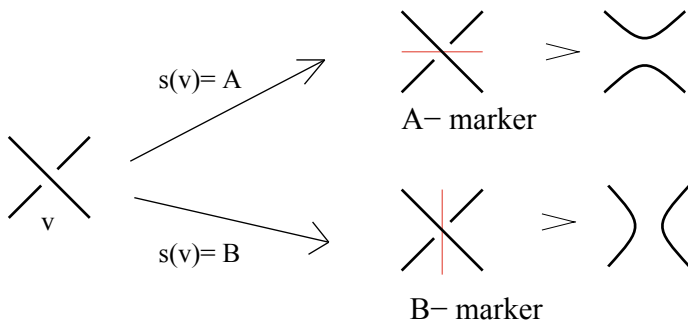


Fig. 22 Interpretation of Kauffman states

Proposition 4.2 (Kauffman) *The unreduced Kauffman bracket polynomial can be written as the state sum (over all Kauffman states):*

$$[D] = \sum_{s \in KS} A^{|s^{-1}(A)| - |s^{-1}(B)|} (-A^2 - A^{-2})^{|D_s|},$$

where KS is the set of all Kauffman states of the diagram D .

Notice that the Kauffman bracket associates to every trivial circle the polynomial $-(A^2 + A^{-2})$. In order to have state sum with monomial entries Viro considers two type of circles: positive with A^2 associated to it, and negative with A^{-2} associated to it. These lead to Enhanced Kauffman States (EKS).

Definition 4.3

- (i) An enhanced Kauffman state, S , is a Kauffman state s together with a function $h : D_s \rightarrow \{+1, -1\}$.
- (ii) The enhanced Kauffman state formula for the unreduced Kauffman bracket is the Kauffman state formula written using the set of enhanced Kauffman states EKS:

$$[D] = \sum_{S \in EKS} (-1)^{|D_s|} A^{\sigma(s) + 2\tau(S)},$$

where the signature of s is $\sigma(s) = |s^{-1}(A)| - |s^{-1}(B)|$ and $\tau(S) = |h^{-1}(+1)| - |h^{-1}(-1)|$ that is the number of positive circles minus the number of negative circles in D_s with enhanced Kauffman state function h of S .

With the above preparation we can define the Khovanov chain complex and Khovanov homology of a diagram.

Definition 4.4 Consider bidegree on the Enhanced Kauffman States as follows:

$$\mathcal{S}_{a,b} = \{S \in EKS \mid \sigma(s) = a, \sigma(s) + 2\tau(S) = b\}$$

- (a) The chain groups are free abelian groups with basis $\mathcal{S}_{a,b}$, that is $C_{a,b}(D) = \mathbb{Z}\mathcal{S}_{a,b}$.
- (b) Boundary maps are $\partial_{a,b} : C_{a,b}(D) \rightarrow C_{a-2,b}(D)$ given by the formula:

$$\partial_{a,b}(S) = \sum_{S' \in \mathcal{S}_{a-2,b}} (-1)^{t(S,S')} [S; S'] S'$$

where $[S, S']$ is 1 or 0 and it is 1 if and only if the following two conditions hold:

- (i) S and S' differ at exactly one crossings, say v , at which $s(v) = A$ and $s'(v) = B$. In particular $\sigma(s') = \sigma(s) - 2$.
- (ii) $\tau(S') = \tau(S) + 1$ and common circles to D_s and $D_{s'}$ have the same sign. The possible signs of circles around the crossing v is shown in Fig. 23.

To define the sign $(-1)^{t(S,S')}$ we need to order crossings of D . Then $t(S, S')$ is equal to the number of crossings with label A smaller than the crossing v in the chosen ordering.

- (c) The Khovanov homology is defined in the standard way as: $H_{a,b}(D) = \ker(\partial_{a,b}) / \text{im}(\partial_{a+2,b})$.

For every diagram D we check easily that $C_{a,b}(D) = 0$ for $a > cr(D)$ or $a < -cr(D)$, or $b > cr(D) + 2|D_{s_A}|$, or $b < -cr(D) - 2|D_{s_B}|$.

These justify notation $a_{max} = cr(D)$, $b_{max} = cr(D) + 2|D_{s_A}|$, $a_{min} = -cr(D)$, and $b_{min} = -cr(D) - 2|D_{s_B}|$.

We always have $C_{a_{max},b_{max}} = \mathbb{Z} = C_{a_{min},b_{min}}$ but it often happens that $H_{*,b_{max}} = 0$ or $H_{*,b_{min}} = 0$. To say more we recall, after Lickorish and Thistlethwaite [36], the concept of adequate diagrams.

Definition 4.5 ([3, 36]) We say, that a diagram D is s -adequate for a Kauffman state s if circles of D_s have no self-touchings. Equivalently, D is s -adequate if any diagram D'_s obtained from D by smoothing according to s all but one crossing has smaller number of components than D_s . In particular, D is said to be A -adequate if the state s_A having all marker A is adequate. Similarly, D is said to be B -adequate if s_B is adequate.

We have classical observation [30, 49]:

Proposition 4.6 For an A -adequate diagram D we have:

$$H_{*,cr(D)+2|D_{s_A}|} = H_{cr(D),cr(D)+2|D_{s_A}|} = \mathbb{Z}$$

Similarly for a B -adequate diagram D we have:

$$H_{*,-cr(D)-2|D_{s_B}|} = H_{-cr(D),-cr(D)-2|D_{s_B}|} = \mathbb{Z}$$

In the case of any diagram D the groups $H_{*,cr(D)+2|D_{s_A}|}$ and $H_{*,-cr(D)-2|D_{s_B}|}$ were studied in the PhD thesis of Marithania Silvero [62]. In particular she conjectures that

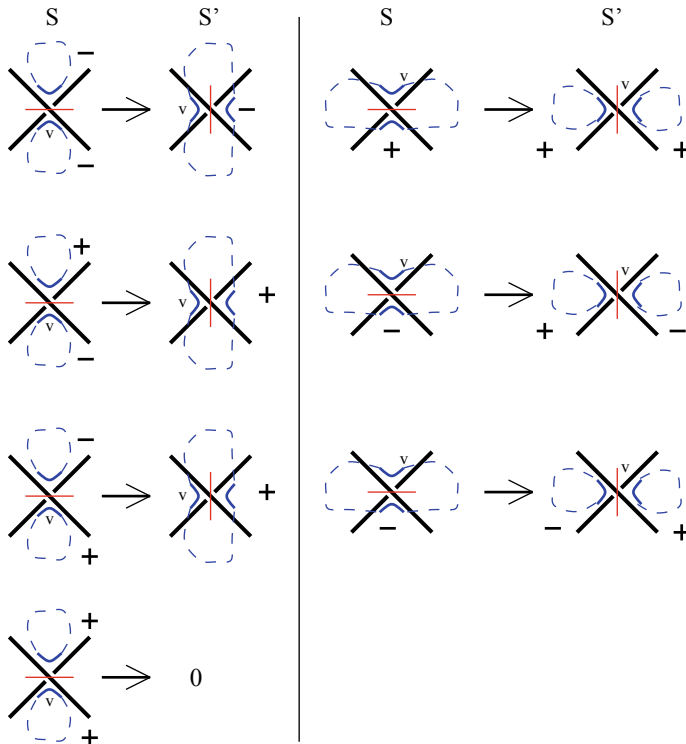


Fig. 23 List of neighboring states with $[S, S'] = 1$

these groups have no torsion. More on these groups and their geometric realization (conjectured to be of homotopy type of wedge of spheres) can be read in [16, 50]. We propose to call diagrams with nonzero Khovanov homology at $H_{*, cr(D)+2|D_{s_A}|}$ Khovanov A -adequate. Similarly Khovanov B -adequate diagram has to have nonzero groups $H_{-cr(D), -cr(D)-2|D_{s_B}|}$. We proved, playing odd Khovanov homology versus even Khovanov homology that there are links without A -Khovanov adequate diagrams. The simplest such example, we were able to find is the torus knot of type $T(4, -5)$.

Being in Greece let us look at some properties of Khovanov homology for the link of Lerna. Below is the table of its Khovanov homology computed by Sujoy Mukherjee using KhoHo program [60]. Since in tables one uses original oriented version of Khovanov (co)homology recall that if \vec{D} is any oriented diagram of D and $w(\vec{D})$ its writhe or Tait number then $H^{i,j}(\vec{D}) = H_{a,b}(D)$ for $i = \frac{w-a}{2}$ and $j = \frac{3w-b}{2}$.

The Lerna link has two components, and we can orient it so it has either $w(\vec{D}) = 16$ and all crossings positive (as in Fig. 25) or $w(\vec{D}) = -4$. We use the second case in

table calculation (Fig. 24). With this convention we get the following unreduced Jones polynomial of the Lerna link¹⁷:

$$\begin{aligned}
 & q^8 - 5q^6 + 12q^4 - 20q^2 + 27 - 29q^{-2} + 26q^{-4} - 18q^{-6} + 4q^{-8} + 11q^{-10} - 21q^{-12} + \\
 & 29q^{-14} - 27q^{-16} + 23q^{-18} - 16q^{-20} + 10q^{-22} - 4q^{-24} + q^{-26}) = \\
 & (q + q^{-1}) \left(q^7 - 6q^5 + 18q^3 - 38q + 65q^{-1} - 94q^{-3} + 120q^{-5} - 138q^{-7} + \right. \\
 & \left. 142q^{-9} - 131q^{-11} + 110q^{-13} - 81q^{-15} + 54q^{-17} - 31q^{-19} + 15q^{-21} - 5q^{-23} + q^{-25} \right).
 \end{aligned}$$

The second factor of the product is the reduced Jones polynomial of the Lerna link. Thus we notice that the coefficients alternate in signs, as the Lerna link is alternating. Furthermore the absolute values of the coefficients form a strictly unimodal sequence

$$\begin{aligned}
 & 1 < 6 < 18 < 38 < 65 < 94 < 120 < 138 < 142 \\
 & 142 > 131 > 110 > 81 > 54 > 31 > 15 > 5 > 1
 \end{aligned}$$

which is also strictly logarithmically concave (i.e. $c_i^2 > c_{i-1}c_{i+1}$).

As the Lerna link is a non-split alternating link the nontrivial entries of Khovanov Homology are on two diagonals of slope 2 and torsion is on the lower one (Eun Soo Lee [33–35]). Furthermore we observed that there is only \mathbb{Z}_2 torsion. It agrees with a general, but yet not published, result of Alexander Shumakovitch that alternating links can have only \mathbb{Z}_2 -torsion [61]. The adequacy of Lerna link is reflected in extreme coefficients $H^{-10,-26} = \mathbb{Z} = H^{6,8}$ if $w(\bar{D}) = -4$. Furthermore by results of [3, 40, 49] and the fact that $D(Lerna)$ is strongly A -adequate we know that $H^{-10,-24} = \mathbb{Z}$ and $H^{-9,-24} = \mathbb{Z}^5$ (the Tait diagrams of the Lerna link are shown in Fig. 25; notice that the A -smoothing diagram has no odd cycles).

$H^{-8,-22} = \mathbb{Z}^{10} \oplus \mathbb{Z}_2^5$ and $tor H^{5,4} = \mathbb{Z}_2^5$. To compute torsion here we use the following result from [49]. To formulate Theorem 4.8 we need to recall the notion of a state graph (Definition 2.1 of [3]):

Definition 4.7 ([3, 40]) Given a diagram D and a Kauffman state s , we define an associated state graph G_s with vertices in bijection with circles of D_s and edges in bijection with crossings of D . An edge connects given vertices if the corresponding crossing connects circles of D_s corresponding to the vertices.

Theorem 4.8 ([49]) For a given loopless graph G let G' denote the simple graph obtained from G by replacing a multiple edge by a single one (see Fig. 25).

(A) Let D be an A -adequate diagram of n crossings and G_{s_A} associated graph. Assume that G_{s_A} is connected then:

¹⁷To get the classical Jones notation we put $q = -t^{1/2}$.

$\begin{matrix} i \\ j \end{matrix}$	-10	-9	-8	-7	-6	-5	-4	-3	-2	-1	0	1	2	3	4	5	6
8																	1
6																5	1_2
4															13	$1,5_2$	
2														25	$5,13_2$		
0												40	$13,25_2$				
-2											54	$25,40_2$					
-4										66	$40,54_2$						
-6									73	$55,65_2$							
-8								69	$65,73_2$								
-10							62	$73,69_2$									
-12					48	$69,62_2$											
-14				33	$62,48_2$												
-16			21	$48,33_2$													
-18		10	$33,21_2$														
-20		5	$21,10_2$														
-22		$10,5_2$															
-24	1	5															
-26	1																

Fig. 24 Table of Khovanov homology for the Lerna link

$$tor H_{n-4, n+2 | D_{s_A} | -8} = \begin{cases} \mathbb{Z}_2^{p_1(G'_{s_A}(D)) - 1} & \text{if } G'_{s_A}(D) \text{ has an odd cycle} \\ \mathbb{Z}_2^{p_1(G'_{s_A}(D))} & \text{if } G'_{s_A}(D) \text{ is a bipartite graph} \end{cases}$$

(B) Let D be an B -adequate diagram of n crossings and G_{s_B} associated graph, then:

$$tor H_{-n+2, -n-2 | D_{s_B} | +8} = \begin{cases} \mathbb{Z}_2^{p_1(G'_{s_B}(D)) - 1} & \text{if } G'_{s_B}(D) \text{ has an odd cycle} \\ \mathbb{Z}_2^{p_1(G'_{s_B}(D))} & \text{if } G'_{s_B}(D) \text{ is a bipartite graph} \end{cases}$$

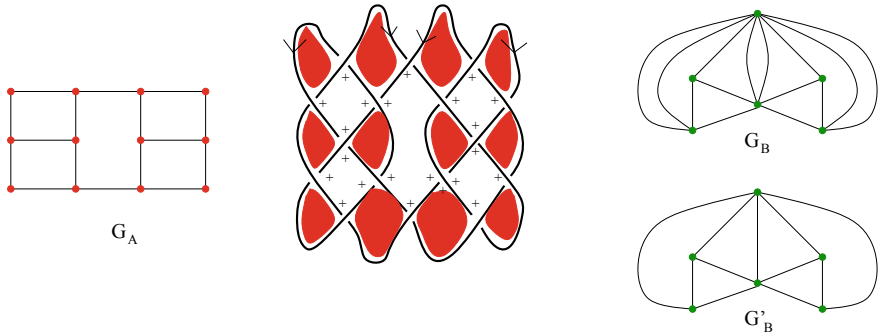


Fig. 25 Checkerboard coloring of Lerna diagram and Tait's graphs G_{s_A} and G_{s_B}

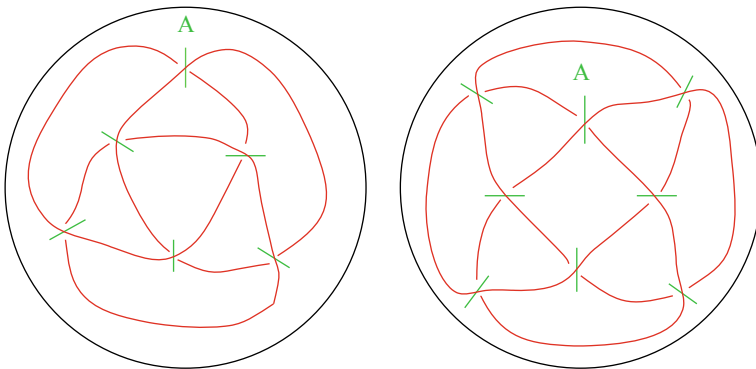


Fig. 26 Links whose A Kauffman states are Lerna pseudoknots

Proof Part (A) is Proposition 4.8(i) of [49] and part (B) follows from (A) by Khovanov duality and universal coefficient theory. That is if \bar{D} denotes the mirror image of D then $H_{-a,-b}(D) = H^{a,b}(\bar{D}) = free(H_{a,b}(\bar{D})) \oplus tor(H_{a-2,b}(\bar{D}))$.

Notice that these links, closed 3-braids $(\sigma_1\sigma_2)^{-3}$ and $(\sigma_1\sigma_2)^{-4}$, respectively, are very far from being A -adequate but they are Khovanov A -adequate (see [16, 50, 62]) (Fig. 26).

5 Summary

We discussed historical ramifications of the beginning of Knot Theory. For the paper based on talks in Greece it is a natural turn. The reader can ask however what is a relation between distributive and Yang–Baxter homology on one hand and Khovanov homology on the other. The answer is simple: a connection is not yet found but my feeling is that we are only a step away. Maybe by the next Knots in Hellas III

conference a link will be established and use of Khovanov homology in statistical physics will be demonstrated.

Acknowledgements I would like to thank Sofia Lambropoulou for organizing for the second time the great Knots in Hellas conference.

I was partially supported by the Simons Collaboration Grant-316446 and CCAS Dean's Research Chair award.

References

1. J.W. Alexander, Topological invariants of knots and links. *Trans. Am. Math. Soc.* **30**, 275–306 (1928)
2. J.W. Alexander, Letter to Oswald Veblen, 1919, *Papers of Oswald Veblen, 1881–1960* (bulk 1920–1960), in *Archival Manuscript Material (Collection), Library of Congress*
3. M.M. Asaeda, J.H. Przytycki, Khovanov homology: torsion and thickness, in *Proceedings of the Workshop, “New Techniques in Topological Quantum Field Theory” Calgary/Kananaskis, Canada, August 2001*, ed. by J. Bryden, <http://front.math.ucdavis.edu/math.GT/0402402>
4. G. Birkhoff, On the structure of abstract algebras. *Proc. Camb. Philos. Soc.* **31**, 433–454 (1935)
5. J.S. Carter, M. Elhamdadi, M. Saito, Homology theory for the set-theoretic Yang-Baxter equation and knot invariants from generalizations of quandles. *Fund. Math.* **184**, 31–54 (2004), <http://front.math.ucdavis.edu/0206.5255>
6. J.S. Carter, D. Jelsovsky, S. Kamada, L. Langford, M. Saito, State-sum invariants of knotted curves and surfaces from quandle cohomology. *Electron. Res. Announc. Am. Math. Soc.* **5**, 146–156 (1999)
7. J.S. Carter, S. Kamada, M. Saito, Surfaces in 4-space, in *Encyclopaedia of Mathematical Sciences. Low-Dimensional Topology III*, ed. by R.V. Gamkrelidze, V.A. Vassiliev (Springer, Berlin, 2004), p. 213
8. R.H. Crowell, *Knots and Wheels, National Council of Teachers of Mathematics (N.C.T.M.) Yearbook* (1961), (published in 1963)
9. R.H. Crowell, R.H. Fox, *An Introduction to Knot Theory* (Ginn and Co., Cambridge, 1963), pp. 10+182; (2nd edn., Springer, New York, 1977); (3rd edn., Dover Publications, Inc., New York, 2008)
10. C.L. Day, *The Art of Knotting and Splicing*, 4th edn. (Naval Institute Press, 1986); (1st edn., 1947; which in turn has its beginning in 1935 book *Sailor's Knots*)
11. C.L. Day, *Quipus and Witches' Knots, With a Translation and Analysis of “Oribasius De Laqueis”* (The University of Kansas Press, Lawrence, 1967)
12. Cyrus Lawrence Day Papers; they contain Day's research, notes, correspondence on topics of interest, and a draft of his book, in *Quipus and Witches' Knots: the Role of the Knot in Primitive and Ancient Cultures* (The Phillips Library at the Peabody Essex Museum 132 Essex Street Salem, MA)
13. S. Eilenberg, J. Zilber, Semi-simplicial complexes and singular homology. *Ann. Math.* **51**(2), 499–513 (1950)
14. R. Fenn, C. Rourke, B. Sanderson, An introduction to species and the rack space, in *Topics in Knot Theory (Proceedings of the Topology Conference, Erzurum)*. NATO Adv. Sci. Inst. Ser. C. Math. Phys. Sci., vol. 399, ed. by M.E. Bozhuyuk (Kluwer Academic Publishers, Dordrecht, 1993), pp. 33–35
15. R. Fenn, C. Rourke, B. Sanderson, Trunks and classifying spaces. *Appl. Categ. Struct.* **3**, 321–356 (1995)
16. J. González-Meneses, P.M.G. Manchón, M. Silvero, A geometric description of the extreme Khovanov cohomology. *Proc. R. Soc. Edinb.: Sect. Math.* **148**(3), 541–557 (2018), [arXiv:1511.05845](https://arxiv.org/abs/1511.05845) [math.GT]

17. F. Harary, The knots and links of Albrecht Dürer. *Atti Accad. Pontaniana (N.S.)* **34**, 97–106 (1985)
18. M.C. Heath, Early Helladic Clay Sealings from the House of the Tiles at Lerna. *Hesperia* **XXVII**(2), 81–120 (1958). (Based on PhD thesis of Martha C. Heath, Yale 1957)
19. Heraklas, first century AD, included in Oribasius “Medical collections”, fourth century AD
20. B. Herrera, A. Samper, Generating infinite links as periodic tilings of the da Vinci-Dürer Knots, in *The Mathematical Intelligencer*, First Online: 13 July, 2017, pp. 1–6
21. R. Higgins, *Minoan and Mycean Art* (Thames and Hudson, London, 1997). (Revised edition)
22. J. Hoy, K.C. Millett, *A Mathematical Analysis of Knotting and Linking in Leonardo da Vinci’s Cartelle of the Accademia Vinciana* (To appear in the *J. Math, Arts* submitted, 2014)
23. M. Jimbo (ed.), *Yang-Baxter Equation in Integrable Systems*. Advanced Series in Mathematical Physics, vol. 10 (World Scientific, Singapore, 1990)
24. V.F.R. Jones, On knot invariants related to some statistical mechanical models. *Pac. J. Math.* **137**(2), 311–334 (1989)
25. D. Joyce, An algebraic approach to symmetry with applications to knot theory, Ph.D. thesis, University of Pennsylvania (1979). (Adviser D.Freyd)
26. D. Joyce, A classifying invariant of knots: the knot quandle. *J. Pure Appl. Algebra* **23**, 37–65 (1982)
27. L.H. Kauffman, State models and the Jones polynomial. *Topology* **26**, 395–407 (1987)
28. L.H. Kauffman, *On Knots* (Princeton University Press, Princeton, 1987)
29. L.H. Kauffman, An invariant of regular isotopy. *Trans. Am. Math. Soc.* **318**(2), 417–471 (1990)
30. M. Khovanov, A categorification of the Jones polynomial. *Duke Math. J.* **101**(3), 359–426 (2000), [arXiv:math/9908171](https://arxiv.org/abs/math/9908171) [math.QA]
31. V. Lebed, Braided objects: unifying algebraic structures and categorifying virtual braids December 2012, Thesis (Ph.D.), Université Paris 7
32. V. Lebed, Homologies of algebraic structures via braidings and quantum shuffles. *J. Algebra* **391**, 152–192 (2013)
33. E.S. Lee, The support of the Khovanov’s invariants for alternating knots (2002), <http://arxiv.org/abs/math.GT/0201105>
34. E.S. Lee, On Khovanov invariant for alternating links (2002), <http://arxiv.org/abs/math.GT/0210213>
35. E.S. Lee, An endomorphism of the Khovanov invariant. *Adv. Math.* **197**, 554–586 (2005)
36. W.B.R. Lickorish, M.B. Thistlethwaite, Some links with non-trivial polynomials and their crossing-numbers. *Comment. Math. Helv.* **63**, 527–539 (1988)
37. E. MacCurdy, *The Notebooks of Leonardo*, vol. 2 (Reynal and Hitchcock, New York, 1938), p. 588
38. S. Matveev, Distributive groupoids in knot theory, (in Russian). *Math. USSR-Sbornik* **47**, 73–83 (1982)
39. G. Lawrence, Miller, The earliest (?) description of a string figure. *Am. Anthropol.* **47**(3), 461–462 (1945). <https://doi.org/10.1525/aa.1945.47.3.02a00190>
40. M.D. Pabiniak, J.H. Przytycki, R. Sazdanovic, On the first group of the chromatic cohomology of graphs. *Geom. Dedicata* **140**(1), 19–48 (2009), <http://arxiv.org/abs/math.GT/0607326>
41. J.H. Przytycki, History of the knot theory from Vandermonde to Jones. *Aport. Matemáticas Comun.* **11**, 173–185 (1992)
42. J.H. Przytycki, Classical roots of knot theory. *Chaos, Solitons Fractals* **9**(4–5), 531–545 (1998)
43. J.H. Przytycki, 3-coloring and other elementary invariants of knots, in *Knot Theory, Banach Center Publications*, vol. 42 (1998), pp. 275–295, <http://arxiv.org/abs/math.GT/0608172>
44. J.H. Przytycki, Jak odróżnić węzły; in Polish (How to distinguish knots). *Delta* **4**, 8–9 (2002)
45. J.H. Przytycki, Kolorowanie splotów; in Polish (Coloring of knots). *Delta* **7**, 8–10 (2003)
46. J.H. Przytycki, Distributivity versus associativity in the homology theory of algebraic structures. *Demonst. Math.* **44**(4), 821–867 (2011), <http://front.math.ucdavis.edu/1109.4850>
47. J.H. Przytycki, Knots and distributive homology: from arc colorings to Yang-Baxter homology, chapter in *New Ideas in Low Dimensional Topology*, vol. 56 (World Scientific, Singapore, 2015), pp. 413–488, [arXiv:1409.7044](https://arxiv.org/abs/1409.7044) [math.GT]

48. J.H. Przytycki, **Knots: From Combinatorics of knot Diagrams to the Combinatorial Topology Based on Knots** (Cambridge University Press, accepted for publication, to appear 2021), p. 650. Chapter II <http://arxiv.org/abs/math/0703096>, Chapter III, [arXiv:1209.1592v1](http://arxiv.org/abs/math/1209.1592v1) [math.GT], Chapter IV, [arXiv:0909.1118v1](http://arxiv.org/abs/math/1118v1) [math.GT], Chapter V, <http://arxiv.org/abs/math.GT/0601227>, Chapter VI, <http://front.math.ucdavis.edu/1105.2238>, Chapter IX, <http://arxiv.org/abs/math.GT/0602264>, Chapter X, <http://arxiv.org/abs/math.GT/0512630>
49. J.H. Przytycki, R. Sazdanovic, Torsion in Khovanov homology of semi-adequate links. *Fund. Math.* **225**, 277–303 (2014), [arXiv:1210.5254](http://arxiv.org/abs/1210.5254) [math.QA]
50. J.H. Przytycki, M. Silvero, Homotopy type of circle graphs complexes motivated by extreme Khovanov homology. *J. Algebraic Combin.* **48**(1), 119–156 (2018), [arXiv:1608.03002](http://arxiv.org/abs/1608.03002) [math.GT]
51. J.H. Przytycki, X. Wang, Equivalence of two definitions of set-theoretic Yang-Baxter homology. *J. Knot Theory Ramific.* **27**(7), 1841013 (15 pages) (2018), [arXiv:1611.01178](http://arxiv.org/abs/1611.01178) [math.GT]
52. J.H. Przytycki, X. Wang, in preparation
53. J. Raeder, *Oribassi Collectioinum Medicarum Reliquiae*, 4 volumes (Leipzig and Berlin, 1928–1933)
54. K. Reidemeister, *Knoten und Gruppen*. Hamburg Abhandlungen MSHU **5**, 7–23 (1926)
55. K. Reidemeister, *Knotentheorie*. *Ergebn. Math. Grenzgeb.*, Bd.1. Springer, Berlin (*English translation: Knot Theory* (BSC Associates, Moscow, Idaho, USA, 1932), p. 1983)
56. D. Rolfsen, *Knots and Links* (Publish or Perish, 1976) (2nd edn., 1990; 3rd edn., AMS Chelsea Publishing, 2003)
57. G. Sarton, *Ancient Science through the Golden Age of Greece* (Dover Publication, New York, 1993). (1st edn.: Harvard University Press, Harvard, 1952)
58. G. Sarton, *A History of Science; Hellenistic Science and Culture in the Last Three Centuries* (Harvard University Press, Cambridge, 1959). (see page 402 with History of Apollonios of Citon Illustrations)
59. G. Sarton, *Ancient Science and Modern Civilization* (University of Nebraska Press, Lincoln, 1954). (This book Reproduces the Full Text of the Three Montgomery Lectures (...) Delivered at the University of Nebraska, in Lincoln, on April 19, 21, 23, 1954)
60. A. Shumakovitch, KhoHo – a program for computing and studying Khovanov homology, <https://github.com/AShumakovitch/KhoHo>
61. A. Shumakovitch, Torsion in Khovanov homology of homologically thin knots. *J. Knot Theory Ramific.* recommended; [arXiv:1806.05168](http://arxiv.org/abs/1806.05168) [math.GT]
62. M. Silvero Casanova, Chapter: Geometric realization of extreme part of Khovanov homology, Ph.D thesis, March, 2016, University of Seville, Spain
63. J.D.H. Smith, *An Introduction to Quasigroups and Their Representations* (Chapman & Hall/CRC, Boca Raton, 2007)
64. M. Takasaki, Abstraction of symmetric transformation, (in Japanese). *Tohoku Math. J.* **49**, 145–207 (1942/3); Translation to English is being prepared by S. Kamada
65. V.G. Turaev, The Yang-Baxter equation and invariants of links. *Invent. Math.* **92**, 527–553 (1988)
66. G. Vasari, *Lives of the Most Excellent Italian Painters, Sculptors, and Architects, from Cimabue to Our Times, Florence 1550*, Modern edition: *The Lives of the Artists* (Oxford World's Classics) (Oxford University Press, 1998); Chapter: Life of Leonardo Da Vinci: Painter and Sculptor of Florence
67. O.Ya. Viro, Raskrasiennyje uzly, in Russian (Colored knots), *Kvant* **3**, 1981, 8–14 (Russian). English translation: Tied into Knot Theory: unraveling the basics of mathematical knots, *Quantum* **8**(5), 16–20 (1998)
68. O. Viro, *Remarks on Definition of Khovanov Homology*, (extended version in [Vi-3]), <http://arxiv.org/abs/math.GT/0202199>
69. O. Viro, Khovanov homology, its definitions and ramifications. *Fund. Math.* **184**, 317–342 (2004)
70. W. Wirtinger, Über die Verzweigungen bei Funktionen von zwei Veränderlichen. *ahresbericht d. Deutschen Mathematiker Vereinigung*, **14**, 517 (1905). (The title of the talk supposedly given at September 26 1905 at the annual meeting of the German Mathematical Society in Meran)

71. X. Wang, Knot theory and algebraic structures motivated by and applied to knots. Ph.D. thesis at George Washington University (2018)
72. M.H. Wiencke, Further Seals and Sealings from Lerna. *Hesperia* **38**, 500–521 (1969)
73. Martha Heath Wiencke The Architecture, *Stratification, and Pottery of Lerna III*; Princeton (American School of Classical Studies at Athens, N.J., 2000)
74. G. Wraith, in *A Personal Story About Knots* (1959). <http://www.wraith.plus.com/gcw/rants/math/Rack.html>

Algebraic and Computational Aspects of Quandle 2-Cocycle Invariant



W. Edwin Clark and Masahico Saito

Abstract Quandle homology theories have been developed and cocycles have been used to construct invariants in state-sum form for knots using colorings of knot diagrams by quandles. Quandle 2-cocycles can be also used to define extensions as in the case of groups. There are relations among algebraic properties of quandles, their homology theories, and cocycle invariants; certain algebraic properties of quandles affect the values of the cocycle invariants, and identities satisfied by quandles induce subcomplexes of homology theory. Recent developments in these matters, as well as computational aspects of the invariant, are reviewed. Problems and conjectures pertinent to the subject are also listed.

Keywords Quandles · Quandle homology · Cocycle extensions · Cocycle knot invariants

2010 Mathematics Subject Classification 57M25

1 Introduction

Quandle homology theories have been developed and cocycles have been used to construct invariants of knots in state-sum form using colorings of knot diagrams by quandles (see [4], for example). It is known [18, 20] that the fundamental quandles of K and K' are isomorphic if and only if $K = K'$ or $K = rm(K')$, the reversed mirror of K' . This implies that colorings alone do not distinguish all oriented knots. On the other hand, it is known that the cocycle invariant can distinguish K from $rm(K)$ for some knots K . In fact, the following fundamental conjecture on the quandle cocycle invariant was stated in [6] (notation and definitions will be presented in Sect. 2):

W. E. Clark · M. Saito (✉)
University of South Florida, Tampa, FL 33620, USA
e-mail: saito@usf.edu

W. E. Clark
e-mail: wclark@mail.usf.edu

© Springer Nature Switzerland AG 2019
C. C. Adams et al. (eds.), *Knots, Low-Dimensional Topology and Applications*, Springer Proceedings in Mathematics & Statistics 284,
https://doi.org/10.1007/978-3-030-16031-9_6

Conjecture 1 *The 2-cocycle invariant Φ_ϕ is a complete invariant for oriented knots, that is, if K_1 and K_2 are non-isotopic oriented knots, then there exists a finite quandle Q and a 2-cocycle ϕ such that $\Phi_\phi(K_1) \neq \Phi_\phi(K_2)$.*

This conjecture could have been stated, of course, at the time when the invariant was defined [3], since it is one of the most fundamental questions for any knot invariant. At that time, however, computing the invariant was difficult. It took a while to get better algorithms for computing the invariant. Extensive studies of the invariant over the years, both theoretical and computational, have made the conjecture plausible (see Remarks 1, 2 in Sect. 4).

Recent studies also have revealed relations among algebraic properties of quandles, their homology theories, and cocycle invariants; certain algebraic properties of quandles affect the values of the cocycle invariants, and identities satisfied by quandles induce subcomplexes of homology theory. In this paper, recent developments in these matters, as well as computational aspects of the invariant, are reviewed, mostly from the results in [6, 8–10].

After a brief review of definitions and examples in Sect. 2, a few algebraic aspects are discussed in Sect. 3. How certain sequences of quandles affect the values of the cocycle invariant, and how quandle properties persist in cocycle extensions, are described in Sects. 3.1 and 3.2, respectively. Certain quandle identities and their relations to homology are presented in Sect. 3.3. The current status of computer calculations using the invariant $\Psi_Q^c(K)$, a generalization of the cocycle invariant, is discussed in Sect. 4.

2 Preliminary

In this section, we provide preliminary material, definitions and notation. More details can be found, for example, in [4, 14].

2.1 Definitions and Examples of Quandles

A rack X is a set with a binary operation $(a, b) \mapsto a * b$ satisfying the following conditions.

- (1) For all $b \in X$, the map $R_b : X \rightarrow X$ defined by $R_b(a) = a * b$ for $a \in X$ is a bijection.
- (2) For all $a, b, c \in X$, we have $(a * b) * c = (a * c) * (b * c)$.

The map R_b in the first axiom is called the *right translation by b* . By the axioms R_b is a rack isomorphism. A quandle X is a rack with idempotency: $a * a = a$ for all $a \in X$. A quandle homomorphism between two quandles X, Y is a map $f : X \rightarrow Y$ such that $f(x *_X y) = f(x) *_Y f(y)$, where $*_X$ and $*_Y$ denote the quandle operations of X and Y , respectively. A few definitions and conventions follow.

- The subgroup of $\text{Sym}(X)$ generated by the permutations $R_a, a \in X$, is called the *inner automorphism group* of X , and is denoted by $\text{Inn}(X)$. The map $\text{inn} : X \rightarrow \text{Inn}(X), \text{inn}(a) = R_a$, is a quandle homomorphism, with the conjugation quandle structure on $\text{Inn}(X)$.

- A quandle is *connected* if $\text{Inn}(X)$ acts transitively on X .

- A quandle is *faithful* if inn is injective.

- An epimorphism $p : E \rightarrow X$ of quandles is called a *covering* [12] if $p(x) = p(y)$ implies $R_x = R_y$ for all $x, y \in E$.

- A *generalized Alexander quandle*, denoted by $\text{GAlex}(G, f)$, is defined by a pair (G, f) where G is a group, $f \in \text{Aut}(G)$, and the quandle operation is defined by $x * y = f(xy^{-1})y$. If G is abelian, this is called an *Alexander quandle*.

- Let X be a rack. For brevity we sometimes omit $*$ and parentheses, so that for $x_i \in X, x_1x_2 = x_1 * x_2, x_1x_2x_3 = (x_1x_2)x_3$, and inductively, $x_1 \dots x_{k-1}x_k = (x_1 \dots x_{k-1})x_k$.

- We also use the notation $x *^n y = x * y * \dots * y$ where y is repeated n times. A rack X is said to be of *type n* (cf. [17]) if n is the least positive integer such that $x *^n y = x$ holds for all $x, y \in X$, and we write $\text{type}(X) = n$. A type 1 quandle is said to be *trivial*, and a type 2 quandle is called a *kei* or an *involutory* quandle.

Computations using GAP [25] significantly expanded the list of small connected quandles. These quandles, called *Rig* quandles, may be found in the GAP package Rig [24]. Rig includes all connected quandles of order less than 48, at this time. Properties of some of Rig quandles, such as homology groups and cocycle invariants, are also found in [24]. We use the notation $Q(n, i)$ for the i -th quandle of order n in the list of Rig quandles, denoted in [24] by $\text{SmallQuandle}(n, i)$. Note, however, that in [24] quandles are left distributive, so that as a matrix, $Q(n, i)$ is the transpose of the quandle matrix $\text{SmallQuandle}(n, i)$ in [24]. Determination of the quandles order less than 48 is also accomplished in [16].

2.2 Quandle Homology Theory and 2-Cocycle Extensions

The rack chain group $C_n(X) = C_n^R(X)$ for a rack X is defined [15] to be the free abelian group generated by n -tuples $(x_1, \dots, x_n), x_i \in X$ for $i = 1, \dots, n$. Let $d_h^{(n)}, \delta_h^{(n)} : C_n(X) \rightarrow C_{n-1}$ be defined by

$$d_h^{(n)}(x_1, \dots, x_h, \dots, x_n) = (x_1, \dots, \widehat{x}_h, \dots, x_n),$$

$$\delta_h^{(n)}(x_1, \dots, x_h, \dots, x_n) = (x_1 * x_h, \dots, x_{h-1} * x_h, \widehat{x}_h, \dots, x_n),$$

respectively, where $\widehat{}$ denotes deleting the entry. Then the boundary map is defined by $\partial_n = \sum_{h=2}^n (-1)^h [d_h^{(n)} - \delta_h^{(n)}]$. The subcomplex $C^D(X)$ was defined [3] for a quandle X with generating terms $(x_1, \dots, x_n) \in C_n(X)$ with $x_j = x_{j+1}$ for some $j = 1, \dots, n - 1$, and the quotient complex $\{C_n^Q(X) = C_n^R(X)/C_n^D(X), \partial_n\}$ was defined [3] as the quandle homology.

The corresponding 2-cocycle is formulated as follows. A quandle 2-cocycle is regarded as a function $\phi : X \times X \rightarrow A$ for an abelian group A , written multiplicatively, that satisfies

$$\phi(x, y)\phi(x * y, z) = \phi(x, z)\phi(x * z, y * z)$$

for all $x, y, z \in X$ and $\phi(x, x) = 1$ for all $x \in X$. For a quandle 2-cocycle ϕ , $E = A \times X$ becomes a quandle under the binary operation

$$(a, x) * (b, y) = (a\phi(x, y), x * y)$$

for $x, y \in X, a, b \in A$, denoted by $E(X, A, \phi)$ or simply $E(X, A)$, and it is called an *abelian extension* of X by A . Two epimorphisms $p_i : E_i \rightarrow X_i, i = 0, 1$, are *equivalent* if there exist isomorphisms $g : E_0 \rightarrow E_1$ and $f : X_0 \rightarrow X_1$ such that $p_1g = fp_0$. The epimorphism given by the projection to the second factor $p : E(X, A, \phi) \rightarrow X$, or an epimorphism equivalent to p , is also called an abelian extension. See [2, 4] for more details. Any abelian extension p is a covering. This construction also works when A is not necessarily abelian, see [6].

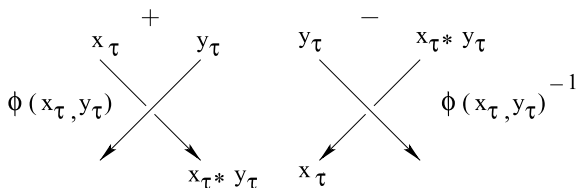
In [1], a different type of *non-abelian extension by a constant cocycle* was defined as follows: It was proved in [1] Proposition 2.11 that if Y is a connected quandle and $X = \text{inn}(Y) \subset \text{Inn}(Y)$, then each fiber has the same cardinality, and if S is a set with the same cardinality as a fiber, then there is a *constant cocycle* $\beta : X \times X \rightarrow \text{Sym}(S)$ such that Y is isomorphic to $X \times_{\beta} S$, defined by $(x, a) * (y, b) = (x * y, \beta(x, y)(a))$.

2.3 Quandle Colorings and the Cocycle Invariant

Let D be a diagram of a knot K , and $\mathcal{A}(D)$ be the set of arcs of D . A *coloring* of a knot diagram D by a quandle Q is a map $C : \mathcal{A}(D) \rightarrow Q$ satisfying the condition depicted in Fig. 1 at every positive (left) and negative (right) crossing τ , respectively. The pair (x_{τ}, y_{τ}) of colors assigned to a pair of nearby arcs of a crossing τ is called the *source colors*, and the third arc is required to receive the color $x_{\tau} * y_{\tau}$.

We recall the definition from [3] of the 2-cocycle invariant $\Phi_{\phi}(K)$ of a knot K . Let X be a quandle, and ϕ be a 2-cocycle with finite abelian coefficient group A . The

Fig. 1 Colored crossings and cocycle weights



2-cocycle invariant (or state-sum invariant) is the element of the group ring $\mathbb{Z}[A]$ defined by

$$\Phi_\phi(K) = \sum_C \prod_\tau \phi(x_\tau, y_\tau)^{\epsilon(\tau)},$$

where the product ranges over all crossings τ , the sum ranges over all colorings of a given knot diagram, (x_τ, y_τ) are source colors at the crossing τ , and $\epsilon(\tau)$ is the sign of τ as specified in Fig. 1. For a given coloring C , we write $B_\phi(K, C) = \prod_\tau \phi(x_\tau, y_\tau)^{\epsilon(\tau)} \in A$. Thus we may write

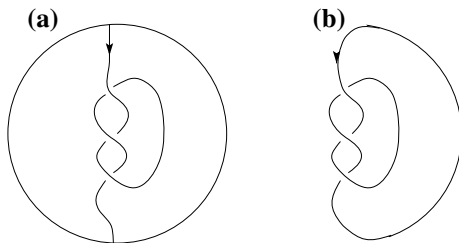
$$\Phi_\phi(K) = \sum_{a \in A} n_a a$$

where n_a is the number of colorings of K by X such that $B_\phi(K, C) = a$. We say that $\Phi_\phi(K)$ is *constant* if $n_a = 0$ when a is not the identity.

A *1-tangle* (also called a long knot) is a properly embedded arc in a 3-ball, and the equivalence of 1-tangles is defined by ambient isotopies of the 3-ball fixing the boundary (cf. [11]). A diagram of a 1-tangle is defined in a manner similar to a knot diagram, from a regular projection to a disk by specifying crossing information. We assume that the 1-tangles are oriented from top to bottom. See Fig. 2a. A knot diagram is obtained from a 1-tangle diagram by closing the end points by a trivial arc outside of a disk. This procedure is called the *closure* of a 1-tangle. If a 1-tangle is oriented, then the closure inherits the orientation. See Fig. 2b. Two diagrams of the same 1-tangle are related by Reidemeister moves. As indicated, for example in [12], there is a bijection from isotopy classes of knots to those of the 1-tangles, corresponding to the closure. Thus an invariant of a 1-tangle T corresponding to a knot K is an invariant of K .

For simplicity we often identify a 1-tangle T with a diagram of T and similarly for knots. A quandle coloring of an oriented 1-tangle diagram is defined in a manner similar to those for knots. We do not require that the end points receive the same color for a quandle coloring of 1-tangle diagrams. As in [10] we say that a quandle Q is *end monochromatic* for a tangle diagram T if any coloring of T by Q assigns the same color on the two end arcs.

Fig. 2 A 1-tangle and its closure



3 Algebraic Aspects

In this section we review relations between algebraic properties of quandles and quandle cocycle invariants.

3.1 Sequences of Quandles and Values of Cocycle Invariants

Let G be a finite group. For $a, b \in G$ we write $a^b = b^{-1}ab$ and denote the conjugacy class of G containing x by x^G . The conjugacy class x^G under conjugation, $a * b = a^b$, is a quandle. Here we call such a quandle a *conjugation quandle*. We note that such a quandle need not be connected. In general, a subquandle of a group G under conjugation need not be a conjugacy class. But it is easy to see that if X is a subset of a group G closed under conjugation and if X under conjugation is a connected quandle then X is a conjugacy class of the group $\langle X \rangle$ generated by X . Let $p : E = E(X, A, \phi) \rightarrow X$ be an abelian extension of quandles. Then we have the following.

Proposition 1 ([9]) *If there is a quandle Y with the quandle epimorphism $\text{inn} : Y \rightarrow E$, or E is a conjugation quandle, then $\Phi_\phi(K)$ is constant for all classical knots K .*

For all examples we computed for Rig quandles Q such that $E(Q, A, \phi)$ is a conjugation quandle, the coefficient group was $A = \mathbb{Z}_2$. Thus we raised the following question.

Problem ([9]) *Is there a connected quandle Q and a 2-cocycle $\phi : Q \times Q \rightarrow A$ with $|A| > 2$ such that $\text{Image}(\phi)$ generates A that is not null-cohomologous, such that $E(Q, A, \phi)$ is a connected conjugation quandle?*

David Stanovsky [23] has shown us how to find a connected quandle Q such that $E(Q, A, \phi)$ is a conjugation quandle, where ϕ is a trivial cocycle and $|A| > 2$. Note that $E(Q, A, \phi)$ is isomorphic to the product quandle $Q \times T$ where T is the trivial quandle of order $|A|$ if and only if ϕ is trivial. Note also that if Q is a conjugation quandle x^G for some group G and $x \in G$ and T is a conjugation quandle y^H for some group H and $y \in H$ then the quandle $Q \times T$ is the conjugation quandle in the group $G \times H$ on the conjugacy class of (x, y) . We note that it is possible to find for any positive integer n , a group H and $y \in H$ so that y^H is a trivial quandle of order n . For a specific example take $G = S_3$, $x = (1, 2)$ and $H = S_4$, $y = (1, 2)(3, 4)$. In this case x^G is the dihedral quandle R_3 and y^H is the trivial quandle of order 3.

Let $X = Q(12, 5)$ or $Q(12, 6)$. Then the second quandle cohomology group $H^2_Q(X, \mathbb{Z}_4)$ is known [24] to be isomorphic to \mathbb{Z}_4 . See [3, 4], for example, for details on quandle cohomology. Let $\psi : X \times X \rightarrow \mathbb{Z}_4$ be a 2-cocycle which represents a generator of $H^2_Q(X, \mathbb{Z}_4) \cong \mathbb{Z}_4$. Let u denote a multiplicative generator of $A = \mathbb{Z}_4$. The cocycle invariants $\Phi_\psi(K)$ for $X = Q(12, 5)$ or $Q(12, 6)$ with respect to ψ , computed for some knots in the table in [24] up to 9 crossing knots, contain non-constant values, while for $A = \mathbb{Z}_2$ the invariant is constant by Proposition 1 (computations

showed [9] that there are epimorphisms $Y \xrightarrow{\text{inn}} E \rightarrow X$). In addition, it was proved that the values of the invariant with ψ take the following restricted form.

Corollary 1 ([9]) *Let $X = Q(12, 5)$ or $Q(12, 6)$, and $\psi : X \times X \rightarrow A = \mathbb{Z}_4$ be a 2-cocycle which represents a generator of $H_Q^2(X, \mathbb{Z}_4) \cong \mathbb{Z}_4$. Let*

$$\Phi_\psi(K) = \sum_{j=0}^3 a_j(K) u^j \in \mathbb{Z}[A]$$

be the cocycle invariant. Then $a_1(K) = a_3(K) = 0$ for all classical knots K .

This is a corollary to the following theorem, which formulates a general case of this phenomenon.

Theorem 1 ([9]) *Let X be a quandle and $n, m, d > 1$ be positive integers such that $n = md$. Let ψ be a 2-cocycle of X with values in \mathbb{Z}_n , and $\Phi_\psi(K) = \sum_{j=0}^{n-1} a_j(K) u^j$ be the cocycle invariant of a knot K with respect to ψ .*

Let $E = E(X, \mathbb{Z}_m, \phi) \xrightarrow{\alpha} X$ be the abelian extension corresponding to $\phi = \psi^d$, and suppose that there is a sequence of quandles $Y \xrightarrow{\text{inn}} E \xrightarrow{\alpha} X$. Then $a_k(K) = 0$ for all k that are not divisible by m , for all classical knots K .

This situation is also found for $X = Q(18, 1)$ or $Q(18, 8)$, where $H_Q^2(X, \mathbb{Z}_6) \cong \mathbb{Z}_6$. Let u be a multiplicative generator of $A = \mathbb{Z}_6$. Then the invariant values are restricted to the following form.

Corollary 2 ([10]) *Let $X = Q(18, 1)$ or $Q(18, 8)$, and $\psi : X \times X \rightarrow \mathbb{Z}_6$ be a 2-cocycle which represents a generator of $H_Q^2(X, \mathbb{Z}_6) \cong \mathbb{Z}_6$. Let $\Phi_\psi(K) = \sum_{j=0}^5 a_j(K) u^j$ be the cocycle invariant. Then $a_k(K) = 0$ for $k = 1, 3, 5$ for all classical knots K .*

The cocycle invariants for connected quandles of order 18 are computed in [24] for up to 7 crossing knots at the time of writing. The invariant values for $Q(18, 8)$ do contain non-constant values of the above form. For $Q(18, 1)$, the invariant is constant, and we do not know whether this is an artifact of limited number of knots or it is constant for all classical knots. Other questions/conjectures for specific quandles can be found in [10], and we include unsolved cases:

Problem 1 Determine possible values of the cocycle invariants. In particular, the following specific questions remain unsolved, and we state them as conjectures.

- The invariant with $Q(18, 1)$ with a generating cocycle is constant for all classical knots.
- Let $X = Q(12, 10)$ and ϕ be the 2-cocycle chosen in Example 5.11 in [10]. For each knot K write $\Phi_\phi(K) = a + bu + cu^2 + du^3 + eu^4 + fu^5$, where $a, b, c, d, e, f \in \mathbb{Z}$. Then $b = f = 0$ for all K .

We note that the condition that K is a classical knot is critical. Indeed, this theorem can be used as obstruction for virtual knots being classical [9].

Theorem 1 can be applied contrapositively to derive the following result:

Corollary 3 ([9]) *For the following Rig quandles E , there is no finite quandle Y such that $\text{inn}(Y) = E$:*

$$Q(8, 1), Q(12, 2), Q(24, 1), Q(24, 7), Q(32, 1), Q(32, 9).$$

The quandle $Q(36, 1)$ listed in [9], Corollary 3.9 and its proof, is a typographic error and should be $Q(32, 1)$, which is already listed.

3.2 Sequences of Abelian Extensions

We have seen that certain sequences of quandles imply restricted forms in the quandle cocycle invariant. In addition, abelian extensions can be used in the following manner: (1) non-triviality of the second cohomology group can be confirmed, (2) knots and their reversed mirrors may be distinguished by colorings of composite knots [10], and (3) they are useful in computing cocycle knot invariants via colorings of 1-tangles [6].

We summarize findings on extensions of Rig quandles in this section. There are 35 non-faithful connected quandles of order less than 48. All but 5 are extensions by \mathbb{Z}_2 . In [10], the following facts were found.

- Among the non-faithful Rig quandles (of order less than 48), $Q(30, 4)$, $Q(36, 58)$, and $Q(45, 29)$ are the only quandles that are not abelian extensions.
- The quandles $Q(30, 4)$, $Q(36, 58)$, and $Q(45, 29)$ are non-abelian extensions by constant 2-cocycles of the quandles $Q(10, 1)$, $Q(12, 10)$ and $Q(15, 7)$, respectively.

Some sequences of quandles correspond to sequences of coefficient groups as follows.

Proposition 2 *Let X be a finite quandle, and $0 \rightarrow C \xrightarrow{\iota} A \xrightarrow{p_B} B \rightarrow 0$ be an exact sequence of finite abelian groups. Let $\phi : X \times X \rightarrow A$ be a quandle 2-cocycle. Then $E(X, A, \phi)$ is an abelian extension of $E(X, B, p_B\phi)$ with coefficient group C .*

The proof utilizes projections and their sections. If we suppress the 2-cocycle in the notation $E(X, A, \phi)$ and write merely $E(X, A)$ then the above Proposition 2 may be stated more simply.

Corollary 4 (i) *If $E(X, B)$ and $E(X, C)$ are abelian extensions, then so is $E(X, B \times C)$, and*

$$E(X, B \times C) = E(E(X, B), C).$$

(ii) If $E(X, A)$ is a finite abelian extension of a quandle X and C is a subgroup of the finite abelian group A then

$$E(X, A) = E(E(X, A/C), C).$$

We note that if $E(X, A)$ is connected, then $E(X, A/C)$ is connected since the epimorphic image of a connected quandle is connected.

Connected abelian extensions of Rig quandles of order up to 12 were examined in [10]. In the following, we use the notation $E \xrightarrow{n} X$ if $E = E(X, \mathbb{Z}_n, \phi)$ for some 2-cocycle ϕ such that E is connected. $E_2 \xrightarrow{m} E_1 \xrightarrow{d} X$ if there is a short exact sequence $0 \rightarrow \mathbb{Z}_m \rightarrow \mathbb{Z}_n \rightarrow \mathbb{Z}_d \rightarrow 0$ such that $\mathbb{Z}_n \subset H_Q^2(X, \mathbb{Z}_n)$ and E_1, E_2 are corresponding extensions as in Proposition 2. In this case $E_2 \xrightarrow{n} X$ where $n = md$. The notation $\emptyset \xrightarrow{1} X$ indicates that $H_Q^2(X, A) = 0$ for any coefficient group A , and hence there is no non-trivial abelian extension. It is noted to the left when all quandles in question are keis.

$$\begin{aligned} & \emptyset \xrightarrow{1} Q(8, 1) \xrightarrow{2} Q(4, 1) \\ \text{(Kei)} \quad & \emptyset \xrightarrow{1} Q(24, 1) \xrightarrow{2} Q(12, 1) \xrightarrow{2} Q(6, 1) \\ & \emptyset \xrightarrow{1} Q(24, 2) \xrightarrow{2} Q(12, 2) \xrightarrow{2} Q(6, 2) \\ \text{(Kei)} \quad & \emptyset \xrightarrow{1} Q(27, 1) \xrightarrow{3} Q(9, 2) = Q(3, 1) \times Q(3, 1) \\ & \emptyset \xrightarrow{1} Q(27, 6) \xrightarrow{3} Q(9, 3) = \mathbb{Z}_3[t]/(t^2 + 1) \\ & \emptyset \xrightarrow{1} Q(27, 14) \xrightarrow{3} Q(9, 6) = \mathbb{Z}_3[t]/(t^2 + 2t + 1) \\ & \emptyset \xrightarrow{1} Q(24, 8) = Q(3, 1) \times Q(8, 1) \xrightarrow{2} Q(12, 4) = Q(3, 1) \times Q(4, 1) \end{aligned}$$

In the following, we list abelian extensions of Rig quandles that contain quandles of order higher than 35. The notation $Q(n, -)$ indicates that it is a quandle of order $n > 35$ and is not a Rig quandle. The notation $? \rightarrow Q(n, -)$ indicates that we do not know if non-trivial abelian extension exists for the quandle $Q(n, -)$ in question. Except for the quandle $Q(120, -)$ in the third line, we have explicit quandle operation tables for the quandles appearing in the list and hence we can prove by computer that such quandles are connected.

$$\begin{aligned} ? & \rightarrow Q(120, -) \xrightarrow{6} Q(20, 3) \xrightarrow{2} Q(10, 1) \\ ? & \rightarrow Q(120, -) \xrightarrow{5} Q(24, 7) \xrightarrow{2} Q(12, 3) \\ ? & \rightarrow Q(120, -) \xrightarrow{2} Q(60, -) \xrightarrow{5} Q(12, 3) \\ ? & \rightarrow Q(48, -) \xrightarrow{2} Q(24, 4) \xrightarrow{2} Q(12, 5) \\ ? & \rightarrow Q(48, -) \xrightarrow{2} Q(24, 3) \xrightarrow{2} Q(12, 6) \end{aligned}$$

It is interesting to remark that all quandles appearing in the first and the last lines are keis. These observations raised the following questions.

Problem 2 What is a condition on cocycles for abelian, or non-abelian extensions to be connected?

In [1], a condition for an extension to be connected was given in terms of elements of the inner automorphism group.

More generally, one could ask for properties of quandles that persist in extensions. In this context, the following was conjectured in [10], and proved by David Stanovský [23]: If Q is connected then $\text{type}(Q) = \text{type}(\text{inn}(Q))$.

In the following an arrow $Y \rightarrow X$ represents an abelian extension.

Problem 3 Is there an infinite sequence of abelian extensions of connected quandles $\cdots \rightarrow Q_n \rightarrow \cdots \rightarrow Q_1$?

We note that sequences of abelian extensions of connected quandles terminate as much as we were able to compute.

We noticed [10] that some non-cohomologous cocycles give isomorphic extensions, as summarized below.

• Let $X = Q(12, 8)$. Then $H_Q^2(X, \mathbb{Z}_2) \cong (\mathbb{Z}_2)^3$. There are three epimorphisms from Rig quandles of order less than 36:

$$Q(24, 5) \rightarrow X, \quad Q(24, 16) \rightarrow X, \quad Q(24, 17) \rightarrow X$$

and their cohomology groups with $A = \mathbb{Z}_2$ are $(\mathbb{Z}_2)^3$, $(\mathbb{Z}_2)^2$, and $(\mathbb{Z}_2)^2$, respectively. We note that there are 7 cocycles that are not cohomologous to each other, yet there are only 3 extensions.

• Let $X = Q(12, 9)$. Then $H_Q^2(X, \mathbb{Z}_4) \cong \mathbb{Z}_4 \times \mathbb{Z}_4$. There are two extensions in Rig quandles of order less than 36:

$$Q(24, 6) \rightarrow Q(12, 9), \quad Q(24, 19) \rightarrow Q(12, 9)$$

and with $A = \mathbb{Z}_4$ their cohomology groups are $\mathbb{Z}_2 \times \mathbb{Z}_2 \times \mathbb{Z}_4$ and $\mathbb{Z}_2 \times \mathbb{Z}_4$, respectively. There are 3 cocycles that give order 2 extensions, yet there are two extensions.

• Let $X = Q(12, 10)$. Then $H_Q^2(X, \mathbb{Z}_6) \cong \mathbb{Z}_6$. There is one extension among Rig quandles of order less than 36, $Q(24, 20) \rightarrow Q(12, 10)$ and we have

$$H_Q^2(Q(24, 20), \mathbb{Z}_3) \cong \mathbb{Z}_3 \times \mathbb{Z}_3.$$

One of the order 3 cocycle corresponds to an extension of X of order 6.

• Let $X = Q(15, 2)$, which has cohomology group $H_Q^2(X, \mathbb{Z}_2) \cong \mathbb{Z}_2 \times \mathbb{Z}_2$. Hence there are three 2-cocycles that are non-trivial and pairwise non-cohomologous. There are, however, only two non-isomorphic abelian extensions of X by \mathbb{Z}_2 , $Q(30, 1)$ and $Q(30, 5)$. Then calculations show that two non-cohomologous cocycles define the extension $Q(30, 5)$.

3.3 Identities and Homology

It is observed in [10] by a straightforward calculation that if X is a kei, ϕ is a 2-cocycle with coefficient group A , and E is the abelian extension of X with respect to ϕ , then E is a kei if and only if $\phi(x, y) + \phi(x * y, y) = 0 \in A$ for all $x, y \in X$. This can be written as $\phi(c) = 0$, for a 2-chain $c = (x, y) + (x * y, y)$. By direct calculation we find that $\partial(c) = 0$, so that c is a 2-cycle. This suggests a relation between the identity $x * y * y = x$ and a 2-cycle c . Such a relation was studied in [8], and also in [26]. We summarize this phenomenon in this section through the example of type 3 quandles. We note that a subcomplex for type 2 quandles, or keis, is defined in [19] as a special case of their subcomplex. Recall that a rack X is of type 3 if it satisfies the identity $S: x * y * y * y = x$ for all $x, y \in X$. We observe the following three properties.

(i) From this identity S we form a 2-chain

$$L = L_S = (x, y) + (x * y, y) + (x * y * y, y).$$

We check that L is a 2-cycle:

$$\begin{aligned} \partial(L) &= [(x) - (x * y)] + [(x * y) - (x * y * y)] \\ &\quad + [(x * y * y) - (x * y * y * y)] \\ &= 0, \end{aligned}$$

using the identity S .

(ii) Let $\phi \in Z_R^2(X, A)$ be a rack 2-cocycle with the coefficient abelian group A such that $\phi(L) = 0$. Then for $E(X, A, \phi) = X \times A$, one computes

$$\begin{aligned} &(x, a) * (y, b) * (y, b) * (y, b) \\ &= (x * y, a + \phi(x, y)) * (y, b) * (y, b) \\ &= (x * y * y * y, a + \phi(x, y) + \phi(x * y, y) + \phi(x * y * y, y)) \\ &= (x, a). \end{aligned}$$

Hence $E(X, A, \phi)$ is of type 3.

(iii) Define, for each n , a subgroup $C_n^S(X) \subset C_n(X)$ generated by

$$\begin{aligned} &\bigcup_{j=1}^{n-1} \{ (x_1, \dots, x_j, y, x_{j+2}, \dots, x_n) \\ &\quad + (x_1 * y, \dots, x_j * y, y, x_{j+2}, \dots, x_n) \\ &\quad + (x_1 * y * y, \dots, x_j * y * y, y, x_{j+2}, \dots, x_n) \\ &\quad | x_i, y \in X, i = 1, \dots, \widehat{j+1}, \dots, n \}. \end{aligned}$$

For a fixed j, y is positioned at $(j + 1)$ -th entry. Then $\{C_n^S, \partial_n\}$ is a subcomplex.

This phenomenon was generalized in [8] to the identities satisfied in quandles of the following type. For brevity we sometimes omit $*$ and parentheses, so that for $x_i \in X$, $x_1x_2 = x_1 * x_2$, $x_1x_2x_3 = (x_1x_2)x_3$, and inductively, $x_1 \dots x_{k-1}x_k = (x_1 \dots x_{k-1})x_k$.

Definition 1 Fix a surjection $\tau : \{1, \dots, k\} \rightarrow \{1, \dots, m\}$, where $k \geq m$ are positive integers.

We call an identity S of the form $xy_{\tau(1)} \dots y_{\tau(k)} = x$ as described above a (τ, k, m) inner identity.

If an inner identity S above holds for all $x, y_j \in X$, $j = 1, \dots, m$, then we say that X satisfies the (τ, k, m) inner identity S .

For this type of identity, we obtained the following.

Theorem 2 Let X be a rack. Let S be a (τ, k, m) inner identity $xy_{\tau(1)} \dots y_{\tau(k)} = x$ that X satisfies. Then the following holds.

- (i) The 2-chain L_S is a 2-cycle, $L_S \in Z_2(X)$.
- (ii) For an abelian group A and a 2-cocycle ϕ , $E(X, A, \phi)$ satisfies S if and only if $\phi(L_S) = 0$.
- (iii) The sequence of subgroups $C_n^S(X) \subset C_n(X)$ forms a subcomplex $\{C_n^S(X), \partial_n\}$, $n \in \mathbb{Z}$.

Here, the groups $C_n^S(X)$ are defined for an inner identity $S: xy_{\tau(1)} \dots y_{\tau(k)} = x$ as follows. Set $\omega_i = y_{\tau(1)} \dots y_{\tau(i)}$, when $i > 0$. Then $C_n^S(X) \subset C_n(X)$, $n \in \mathbb{Z}$, are subgroups generated by

$$\begin{aligned} & \bigcup_{j=1}^{k-1} \{ (x_1, \dots, x_j, y_{\tau(1)}, x_{j+2}, \dots, x_n) \\ & + \sum_{i=1}^{k-1} (x_1\omega_i, \dots, x_j\omega_i, y_{\tau(i+1)}, x_{j+2}, \dots, x_n) \\ & | x_h, y_{\tau(i)} \in X, h = 1, \dots, \widehat{j+1}, \dots, n, i = 1, \dots, k-1 \}. \end{aligned}$$

We also observed the following.

Proposition 3 For all $m, n \in \mathbb{Z}$ such that $m > 0$ and $n > 1$, there exist infinitely many connected quandles that satisfy the identity $xw = x$ for

$$w = \underbrace{y_1 * \dots * y_m * y_1 \dots * y_m * \dots * y_1 \dots * y_m}_{n \text{ repetitions}}$$

where y_1, \dots, y_m are distinct letters.

In computing whether various identities are satisfied among Rig quandles, we found some identities that are not satisfied by any. The following conjecture was made in [8]:

Conjecture 2 *No connected quandle satisfies an identity of the form $xw = x$ where w is one of the following words:*

$$abaab, ababa, abbaa, ababb, abbab.$$

A few similar conjectures were made in [8] for identities of lengths 6.

4 Computational Aspects

In this section we review developments in computational methods of quandle cocycle invariants.

In [6] Conjecture 1 was examined computationally for prime knots with at most 12 crossings using colorings of 1-tangles to compute 2-cocycle invariants without explicitly finding 2-cocycles. Let $\mathcal{G} = \{1, m, r, rm\}$ be the group of symmetries of knots, where m and r denote taking the mirror image and the reversed orientation, respectively. Since $\text{Col}_Q(K)$ is equal to the 2-cocycle invariant for a coefficient group of order 1, it follows from the results of [7] that the conjecture holds when K_1 and K_2 are prime knots with crossing number at most 12 that lie in distinct \mathcal{G} -orbits. Thus we need only consider the cases where K_1 and K_2 lie in the same \mathcal{G} -orbit. For this purpose, effective ways of constructing abelian extensions by generalized Alexander quandles were found, and a set of 60 quandles is presented in [6] that distinguishes all distinct K_1 and K_2 in the same \mathcal{G} -orbit for all except 13 prime knots with up to 12 crossings.

For knots K and K' , we write $K = K'$ to denote that there is an orientation preserving homeomorphism of \mathbb{S}^3 that takes K to K' preserving the orientations of K and K' . We say that a knot has *symmetry* $s \in \{m, r, rm\}$ if $K = s(K)$. As in the definition of *symmetry type* in [5] we say that a knot K is

1. *reversible* if the only symmetry it has is r ,
2. *negative amphicheiral* if the only symmetry it has is rm ,
3. *positive amphicheiral* if the only symmetry it has is m ,
4. *chiral* if it has none of these symmetries,
5. *fully amphicheiral* if has all three symmetries m, r, rm .

The symmetry type of each prime oriented knot on at most 12 crossings is given at [5]. Thus each of the 2977 knots K given there represents 1, 2 or 4 knots depending on the symmetry type. Among the 2977 knots, there are 1580 reversible, 47 negative amphicheiral, 1 positive amphicheiral, 1319 chiral, and 30 fully amphicheiral knots.

For $s \in \mathcal{G}$ let \mathcal{K}_s denote the set of prime oriented knots K with at most 12 crossings such that $K \neq s(K)$. From the above we have

1. $|\mathcal{K}_m| = 1319 + 47 + 1580 = 2946$,
2. $|\mathcal{K}_r| = 1319 + 1 + 47 = 1367$,
3. $|\mathcal{K}_{rm}| = 1319 + 1 + 1580 = 2900$.

We have been able to find 60 connected quandles which will distinguish via the cocycle invariant the following.

1. K from $m(K)$ for all K in \mathcal{K}_m ,
2. K from $rm(K)$ for all K in \mathcal{K}_{rm} except $12a_{0427}$, the single positive amphicheiral prime knot with at most 12 crossings. Note that for this knot $rm(K) = r(K)$.
3. K from $r(K)$ for all K in \mathcal{K}_r , except the following 13 prime knots:

$$12a_{0059}, 12a_{0067}, 12a_{0292}, 12a_{0427}, 12a_{0700}, 12a_{0779}, 12a_{0926}, \\ 12a_{0995}, 12a_{1012}, 12a_{1049}, 12a_{1055}, 12n_{0180}, 12n_{0761}$$

all of which are chiral except for the positive amphicheiral knot $12a_{0427}$.

For these computations, we used colorings of 1-tangles by abelian extensions: Let T be a 1-tangle of a knot K . Let Q be a connected quandle. For arbitrary fixed $e \in Q$ denote the set of colorings $C : \mathcal{A}(T) \rightarrow Q$ such that $C(b_0) = e$ by $\text{Col}_Q^e(T)$. It is known (see for example [6, 21, 22]), for $C \in \text{Col}_Q^e(T)$, $b = C(b_1)$ satisfies $R_b = R_e$, where b_0 and b_1 denote the top and bottom arc of T , respectively. That is, b lies the the fiber $F_e = \text{inn}^{-1}(R_e)$. Thus we define the following invariant.

Definition 2 ([6, 13]) For arbitrary fixed $e \in Q$ denote the set of colorings $C : \mathcal{A}(T) \rightarrow Q$ by quandle Q such that $C(b_0) = e$ by $\text{Col}_Q^e(T)$. Define

$$\Psi_Q^e(K) = \sum_{C \in \text{Col}_Q^e(T)} C(b_1).$$

We think of $\Psi_Q^e(K)$ as lying in the free \mathbb{Z} -module $\mathbb{Z}[F_e]$ with basis F_e .

The relation to the cocycle invariant is stated as follows.

Theorem 3 ([6]) *Let $Q = E(X, A, \phi)$ be a connected abelian extension of quandle X corresponding to the 2-cocycle ϕ . If the projection $\pi : Q \rightarrow X$, $(a, x) \mapsto x$, is equivalent to $\text{inn} : Q \rightarrow \text{inn}(Q)$, then for $e = (1, x_0)$ we have for all knots K :*

$$\Psi_Q^e(K) = \frac{1}{|X|} \Phi_\phi(K)$$

if one identifies the fiber F_e with A via $a \mapsto (a, x_0)$.

To find more non-faithful connected quandles we constructed using GAP several thousand connected generalized Alexander quandles. As shown in [6], it suffices to run through the small groups G in GAP, for each group G compute representatives f of the conjugacy classes in $\text{Aut}(G)$, and construct $\text{GAlex}(G, f)$. When $\text{GAlex}(G, f)$ is connected then as shown in [6], it is an abelian extension of $\text{inn}(\text{GAlex}(G, f))$ if and only if the subgroup $\text{Fix}(G, f) = \{x \in G \mid f(x) = x\}$ is abelian.

Theorem 4 ([6]) *If $Q = \text{GAlex}(G, f)$ and $A = \text{Fix}(G, f)$ is abelian, where $f \in \text{Aut}(G)$ then*

$$Q = \text{GAlex}(G, f) \cong E(\text{inn}(Q), A, \phi)$$

for some 2-cocycle ϕ .

This allows us to compute many cocycle invariants $\Phi_\phi(K) = \Psi_{\text{GAlex}(G, f)}^e(K)$ $\text{inn}(\text{GAlex}(G, f))$ without finding explicit cocycles.

We recall the following.

Conjecture 3 ([7]) *If K and K' are any two knots such that $K' \neq K$ and $K' \neq \text{rm}(K)$ then there is a finite quandle Q such that $\text{Col}_Q(K) \neq \text{Col}_Q(K')$.*

In [10] the conjecture was proved when K' is the unknot.

Remark 1 It was shown in [10] that given two oriented knots K_1 and K_2 such that $K_1 \neq K_2$, there is a knot P such that $K_2 \# P \neq \text{rm}(K_1 \# P)$, where $\#$ denotes the connected sum. If Conjecture 3 is true then $\text{Col}_Q(K_1 \# P) \neq \text{Col}_Q(K_2 \# P)$ for some finite quandle Q . It was proved in [6] that if for knots K_1 and K_2 there is a quandle Q and a knot P such that $\text{Col}_Q(K_1 \# P) \neq \text{Col}_Q(K_2 \# P)$, then $\Psi_Q^e(K_1) \neq \Psi_Q^e(K_2)$. This leads to some hope that Ψ_Q^e may be a complete invariant.

Remark 2 The knot coloring polynomial P_G^x was defined in [13], and shown to generalize Φ_ϕ . The invariant Ψ_Q^e is closely related to P_G^x . In particular, if Q is a connected generalized Alexander quandle, $e \in Q$, $G = \text{Inn}(Q)$ and $x = R_e$ then P_G^x and Ψ_Q^e distinguish the same pairs of knots. As noted by Eisermann [13], since knot groups are residually finite, and the peripheral system characterizes a knot, that his knot coloring polynomial distinguishes all knots “is not completely hopeless”.

Acknowledgements MS was partially supported by NIH R01GM109459.

References

1. N. Andruskiewitsch, M. Graña, From racks to pointed Hopf algebras. *Adv. Math.* **178**, 177–243 (2003)
2. J.S. Carter, M. Elhamdadi, M.A. Nikiforou, M. Saito, Extensions of quandles and cocycle knot invariants. *J. Knot Theory Ramif.* **12**(6), 725–738 (2003)
3. J.S. Carter, D. Jelsovsky, S. Kamada, L. Langford, M. Saito, Quandle cohomology and state-sum invariants of knotted curves and surfaces. *Trans. Am. Math. Soc.* **355**, 3947–3989 (2003)
4. J.S. Carter, S. Kamada, M. Saito, *Surfaces in 4-Space*. Encyclopaedia of Mathematical Sciences, vol. 142 (Springer, Berlin, 2004)
5. J.C. Cha, C. Livingston, KnotInfo: table of knot invariants, 26 May 2011, <http://www.indiana.edu/~knotinfo>
6. W.E. Clark, L.A. Dunning, M. Saito, Computations of quandle 2-cocycle knot invariants without explicit 2-cocycles. *J. Knot Theory Ramif.* **26**, 1750035, 22pp (2017)

7. W.E. Clark, M. Elhamdadi, M. Saito, T. Yeatman, Quandle colorings of knots and applications. *J. Knot Theory Ramif.* **23**, 1450035, 29 pp (2014)
8. W.E. Clark, M. Saito, Quandle identities and homology, to appear in *Contemporary Mathematics* (AMS, Providence)
9. W.E. Clark, M. Saito, Algebraic properties of quandle extensions and values of cocycle knot invariants. *J. Knot Theory Ramif.* **25**, 1650080, 17pp (2016)
10. W.E. Clark, M. Saito, L. Vendramin, Quandle coloring and cocycle invariants of composite knots and Abelian extensions. *J. Knot Theory Ramif.* **25**, 1650024, 34pp (2016)
11. J.H. Conway, An enumeration of knots and links, and some of their algebraic properties, in *Computational Problems in Abstract Algebra*, ed. by J. Leech (Pergamon Press, Oxford, 1970), pp. 329–358
12. M. Eisermann, Homological characterization of the unknot. *J. Pure Appl. Algebra* **177**, 131–157 (2003)
13. M. Eisermann, Knot colouring polynomials. *Pac. J. Math.* **231**, 305–336 (2007)
14. R. Fenn, C. Rourke, Racks and links in codimension two. *J. Knot Theory Ramif.* **1**, 343–406 (1992)
15. R. Fenn, C. Rourke, B. Sanderson, Trunks and classifying spaces. *Appl. Categ. Struct.* **3**, 321–356 (1995)
16. A. Hulpke, D. Stanovsky, D. Vojtechovsky, Connected quandles and transitive groups. *J. Pure Appl. Algebr.* **220**, 735–758 (2016)
17. D. Joyce, Simple quandles. *J. Algebra* **79**, 307–318 (1982)
18. D. Joyce, A classifying invariant of knots, the knot quandle. *J. Pure Appl. Algebra* **23**, 37–65 (1983)
19. S. Kamada, K. Oshiro, Homology groups of symmetric quandles and cocycle invariants of links and surface-links. *Trans. Am. Math. Soc.* **362**, 5501–5527 (2010)
20. S. Matveev, Distributive groupoids in knot theory. *Mat. Sb. (N.S.) (Russian)* **119**(161), 78–88 (160) (1982)
21. T. Nosaka, On homotopy groups of quandle spaces and the quandle homotopy invariant of links. *Topol. Appl.* **158**, 996–1011 (2011)
22. J.H. Przytycki, 3-colorings and other elementary invariants of knots, *Knot Theory (Warsaw, 1995)*. Polish Academy of Science, vol. 42 (Banach Center Publications, Warsaw, 1998), pp. 275–295
23. D. Stanovsky, Personal communication
24. L. Vendramin, Rig – A GAP package for racks and quandles, <http://github.com/vendramin/rig/>
25. L. Vendramin, On the classification of quandles of low order. *J. Knot Theory Ramif.* **21**(9), 1250088 (2012)
26. J. Zablow, On relations and homology of the Dehn quandle. *Algebr. Geom. Topol.* **8**, 19–51 (2008)

A Survey of Quantum Enhancements



Sam Nelson

Abstract In this short survey article we collect the current state of the art in the nascent field of *quantum enhancements*, a type of knot invariant defined by collecting values of quantum invariants of knots with colorings by various algebraic objects over the set of such colorings. This class of invariants includes classical skein invariants and quandle and biquandle cocycle invariants as well as new invariants.

Keywords Biquandle brackets · Quantum invariants · Quantum enhancements of counting invariants

2010 Mathematics Subject Classification 57M25 · 57M27

1 Introduction

Counting invariants, also called *coloring invariants* or *coloring-counting invariants*, are a type of integer-valued invariant of knots or other knotted objects (links, braids, tangles, spatial graphs, surface-links etc.). They are defined by attaching elements of some algebraic structure, envisioned as “colors”, to portions of diagrams according to rules, typically stated in the form of algebraic axioms, which ensure that the number of such colorings is unchanged by the relevant diagrammatic moves. Underlying this simplistic combinatorial picture of diagrams and colorings lurks a more sophisticated algebraic structure, a set of morphisms from a categorical object associated to the knotted object to a (generally finite) coloring object. Perhaps the simplest nontrivial example is Fox tricoloring, where the simple rule of making all three colors match or all three differ at each crossing secretly encodes group homomorphisms from the fundamental group of the knot complement to the group of integers modulo 3. Examples of coloring structures include groups, kei, quandles, biquandles and many more.

S. Nelson (✉)

Claremont McKenna College, 850 Columbia Ave., Claremont, CA 91711, USA
e-mail: Sam.Nelson@cmc.edu

© Springer Nature Switzerland AG 2019

C. C. Adams et al. (eds.), *Knots, Low-Dimensional Topology and Applications*, Springer Proceedings in Mathematics & Statistics 284,
https://doi.org/10.1007/978-3-030-16031-9_7

An *enhancement* of a counting invariant is a stronger invariant from which the counting invariant can be recovered [3]. One strategy which has proven successful for defining enhancements is to seek invariants ϕ of colored knots; then for a given ϕ , the multiset of ϕ values over the set of colorings of our knot is a new invariant of knots whose cardinality is the original counting invariant but which carries more information about the original knot. One of the first such examples was the *quandle cocycle invariant* introduced in [2], in which integer-valued invariants of quandle-colored knots known as *Boltzmann weights* are defined using a cohomology theory for quandles. The multiset of such Boltzmann weights is then an invariant of the original uncolored knot; it is stronger than the quandle counting invariant in question since different multisets of Boltzmann weights can have the same cardinality.

A *quantum enhancement*, then, is a quantum invariant of X -colored knots for some knot coloring structure X . In [9] these are conceptualized as X -colored tangle functors, i.e. assignments of matrices of appropriate sizes to the various X -colored basic tangles (positive and negative crossings, maximum, minimum and vertical strand) which make up tangles via sideways stacking interpreted as tensor product and vertical stacking as matrix composition. In [6] some examples are found via structures known as *biquandle brackets*, skein invariants modeled after the Kauffman bracket but with coefficients which depend on biquandle colorings at crossings. In [7] biquandle brackets are generalized to include a virtual crossing as a type of smoothing. A special case of biquandle brackets was described independently in [1]. In [4] a type of biquandle bracket whose skein relation includes a vertex is considered. In [8] biquandle brackets are defined using *trace diagrams* in order to allow for recursive expansion as opposed to the state-sum definition in [6].

This paper is organized as follows. In Sect. 2 we survey some knot coloring structures and look in detail at one such structure, biquandles. In Sect. 3 we see the definition and examples of biquandle brackets as an example of a quantum enhancement. In Sect. 4 we summarize a few other examples of quantum enhancements, and we end in Sect. 5 with some questions for future research.

2 Biquandles and Other Coloring Structures

A *knot coloring structure* is a set X whose elements we can think of as colors or labels to be attached to portions of a knot or link diagram, together with coloring rules chosen so that the number of valid colorings of a knot diagram is not changed by Reidemeister moves and hence defines an invariant. In this section we will look in detail at one such structure, known as *biquandles*, and then briefly consider some other examples. For more about these topics, see [3].

Definition 1 Let X be a set. A *biquandle structure* on X is a pair of binary operations $\triangleright, \triangleright : X \times X \rightarrow X$ satisfying the following axioms:

- (i) For all $x \in X$, we have $x \triangleright x = x \triangleright x$,

- (ii) The maps $S : X \times X \rightarrow X \times X$ and $\alpha_x, \beta_x : X \rightarrow X$ for each $x \in X$ defined by

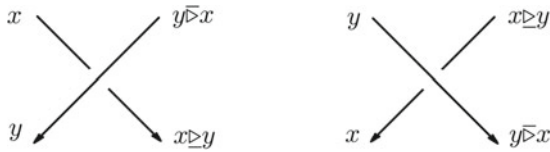
$$\alpha_x(y) = y\bar{\triangleright}x, \beta_x(y) = x\triangleright y \text{ and } S(x, y) = (y\bar{\triangleright}x, x\triangleright y)$$

are invertible, and

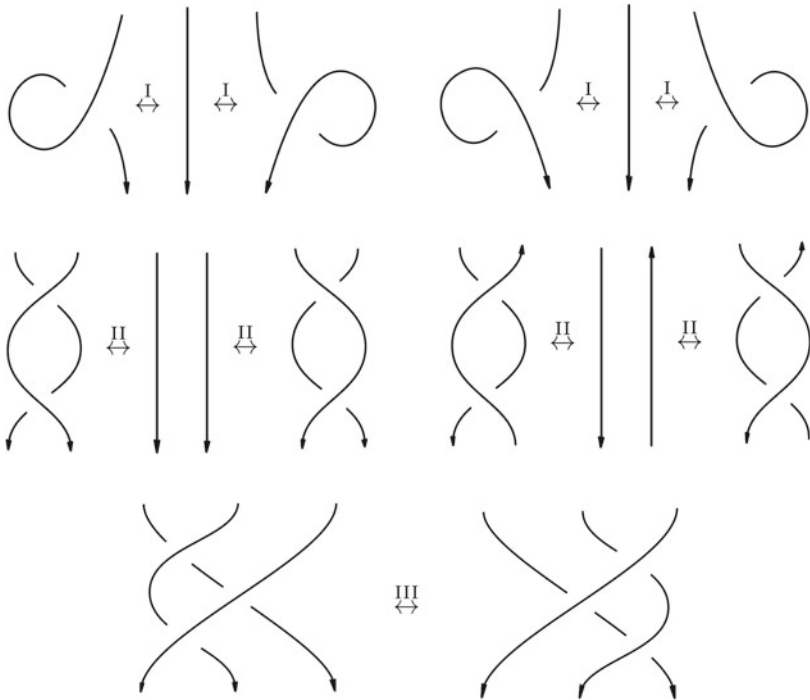
- (iii) For all $x, y, z \in X$, we have the *exchange laws*:

$$\begin{aligned} (x\triangleright y)\triangleright(z\triangleright y) &= (x\triangleright y)\triangleright(z\bar{\triangleright}y) \text{ (iii.i)} \\ (x\triangleright y)\bar{\triangleright}(z\triangleright y) &= (x\bar{\triangleright}y)\triangleright(z\bar{\triangleright}y) \text{ (iii.ii)} \\ (x\bar{\triangleright}y)\bar{\triangleright}(z\bar{\triangleright}y) &= (x\bar{\triangleright}y)\bar{\triangleright}(z\triangleright y) \text{ (iii.iii)}. \end{aligned}$$

The biquandle axioms encode the Reidemeister moves using a coloring scheme with elements of X coloring semiarcs in an oriented link diagram with the pictured coloring rules at crossings:



Then using the following generating set of oriented Reidemeister moves,



the following theorem is then easily verified:

Theorem 1 *Given an oriented link diagram D with a coloring by a biquandle X , for any diagram D' obtained from D by a single Reidemeister move, there is a unique coloring of D' by X which agrees with the coloring on D outside the neighborhood of the move.*

Hence we obtain:

Corollary 1 *The number of colorings of a knot or link diagram D by a biquandle X is an integer-valued invariant of the knot or link K represented by D , called the biquandle counting invariant and denoted by $\Phi_X^{\mathbb{Z}}(K)$.*

Example 1

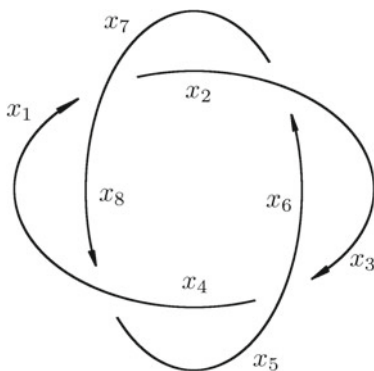
(Alexander biquandles) A straightforward example of a biquandle structure is to let X be any commutative ring with identity R with choice of units s, t and define binary operations

$$\begin{aligned} x \underset{\rhd}{\rhd} y &= tx + (s - t)y \\ x \underset{\lhd}{\lhd} y &= sx. \end{aligned}$$

For instance, setting $X = \mathbb{Z}_5$ with $t = 3$ and $s = 2$, we obtain biquandle operations

$$\begin{aligned} x \underset{\rhd}{\rhd} y &= 3x + (2 - 3)y = 3x + 4y \\ x \underset{\lhd}{\lhd} y &= 2x. \end{aligned}$$

To compute the biquandle counting invariant $\Phi_X^{\mathbb{Z}}(K)$ for an oriented knot or link K represented by a diagram D , we can then solve the system of the linear equations obtained from the crossings of D using the coloring rule above. For example, the $(4, 2)$ -torus link has system of coloring equations below.



$$\begin{aligned}
 3x_1 + 4x_8 &= x_2 \\
 2x_8 &= x_7 \\
 3x_8 + 4x_1 &= x_5 \\
 2x_1 &= x_4 \\
 3x_3 + 4x_6 &= x_4 \\
 2x_6 &= x_5 \\
 3x_6 + 4x_3 &= x_7 \\
 2x_3 &= x_2
 \end{aligned}$$

Then row-reducing over \mathbb{Z}_5 we have

$$\begin{bmatrix}
 3 & 4 & 0 & 0 & 0 & 0 & 0 & 4 \\
 0 & 0 & 0 & 0 & 0 & 0 & 4 & 2 \\
 4 & 0 & 0 & 0 & 4 & 0 & 0 & 3 \\
 2 & 0 & 0 & 4 & 0 & 0 & 0 & 0 \\
 0 & 0 & 3 & 4 & 0 & 4 & 0 & 0 \\
 0 & 0 & 0 & 0 & 4 & 2 & 0 & 0 \\
 0 & 0 & 4 & 0 & 0 & 3 & 4 & 0 \\
 0 & 4 & 2 & 0 & 0 & 0 & 0 & 0
 \end{bmatrix}
 \sim
 \begin{bmatrix}
 1 & 0 & 0 & 0 & 0 & 0 & 0 & 4 \\
 0 & 1 & 0 & 0 & 0 & 0 & 0 & 3 \\
 0 & 0 & 1 & 0 & 0 & 0 & 0 & 4 \\
 0 & 0 & 0 & 1 & 0 & 0 & 0 & 3 \\
 0 & 0 & 0 & 0 & 1 & 0 & 0 & 3 \\
 0 & 0 & 0 & 0 & 0 & 1 & 0 & 4 \\
 0 & 0 & 0 & 0 & 0 & 0 & 1 & 3 \\
 0 & 0 & 0 & 0 & 0 & 0 & 0 & 0
 \end{bmatrix}$$

and the space of colorings is one-dimensional, so $\Phi_X^{\mathbb{Z}}(K) = |\mathbb{Z}_5| = 5$. This distinguishes K from the unlink of two components, which has $\Phi_X^{\mathbb{Z}}(U_2) = |\mathbb{Z}_5|^2 = 25$ colorings by X .

A coloring of a diagram D representing an oriented knot or link K by biquandle X determines a unique homomorphism $f : \mathcal{B}(K) \rightarrow X$ from the *fundamental biquandle* of K , $\mathcal{B}(K)$, to X . Hence the set of colorings may be identified with the homset $\text{Hom}(\mathcal{B}(K), X)$. In particular, an X -labeled diagram D_f can be identified with an element of $\text{Hom}(\mathcal{B}(K), X)$, and we have

$$\Phi_X^{\mathbb{Z}}(K) = |\text{Hom}(\mathcal{B}(K), X)|.$$

See [3] for more about the fundamental biquandle of an oriented knot or link.

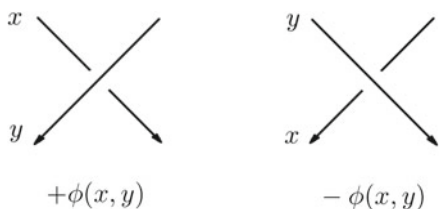
The key idea behind enhancements of counting invariants is the observation that it's not just the number of colorings of a diagram which is invariant, but the set of colored diagrams itself. More precisely, given a biquandle X and an oriented knot or link diagram D , the set of X -colorings of D is an invariant of K in the sense that changing D by a Reidemeister move yields a set of colorings of D' in one-to-one correspondence with the set of colorings of D . Then any invariant ϕ of X -colored oriented knot or link diagrams can give us a new invariant of the original knot or link, namely the multiset of ϕ -values over the set of colorings of D . We call such an invariant an *enhancement* of the counting invariant.

Example 2

Perhaps the simplest enhancement is the *image enhancement*, which sets ϕ for a coloring of a diagram to be the size of the image sub-biquandle of the coloring. For example, the trefoil knot has nine colorings by the Alexander biquandle $X = \mathbb{Z}_3$ with $t = 2$ and $s = 1$. Three of these colorings are monochromatic, while six are surjective colorings. Then the counting invariant value $\Phi_X^{\mathbb{Z}}(3_1) = 9$ is enhanced to the multiset $\Phi_X^{\text{Im},M}(3_1) = \{1, 1, 1, 3, 3, 3, 3, 3\}$. For convenience, we can convert the multiset to a polynomial by converting the multiplicities to coefficients and the elements to powers of a formal variable u , so the image enhanced invariant becomes $\Phi_X^{\text{Im},M}(3_1) = 3u + 6u^3$. This notation, adapted from [2], has the advantage that evaluation of the polynomial at $u = 1$ yields the original counting invariant. See [3] for more about enhancements.

Example 3

The earliest example of an enhancement of the counting invariant is the family of *quandle 2-cocycle invariants*, introduced in [2]. In this type of enhancement, we consider biquandles X with operation $x \bar{\triangleright} y = x$, known as *quandles*, and consider maps $\phi : X \times X \rightarrow A$ where A is an abelian group. For each X -coloring of an oriented knot or link diagram D , we obtain a contribution $+\phi(x, y)$ at positive crossings and $-\phi(x, y)$ at negative crossings as depicted:



The sum of such contributions over the all crossings in an X -colored diagram is called the *Boltzmann weight* of the colored diagram. The conditions on ϕ which make the Boltzmann weight unchanged by X -colored Reidemeister moves can be expressed in terms of a cohomology theory for quandles: the Boltzmann weight is preserved by Reidemeister III moves if ϕ is a *rack 2-cocycle* and preserved by Reidemeister I moves if ϕ evaluates to zero on *degenerate* cochains, which form a subcomplex; invariance under Reidemeister II moves is automatic from the way the Boltzmann weights are defined. The quotient of rack cohomology by the degenerate subcomplex yields *quandle cohomology*. In particular, 2-coboundaries always yield a Boltzmann weight of zero, so cohomologous cocycles define the same enhancement. See [2, 3] for more.

Other examples of knot coloring structures include but are not limited to the following:

- *Groups*. Any finite group G defines a counting invariant consisting of the set of group homomorphisms from the *knot group*, i.e., the fundamental group of the knot complement, to G .
- *Quandles*. Quandles are biquandles whose over-action operation is trivial, i.e. for all $x, y \in X$ we have $x \bar{\triangleright} y = x$. Introduced in [5], the *fundamental quandle* of a knot determines both the knot group and the peripheral structure, and hence determines the knot up to ambient homeomorphism.
- *Biracks*. Biracks are biquandles for framed knots and links, with the Reidemeister I move replaced with the framed version. To get invariants of unframed knots and links using biracks, we observe that the lattice of framings of a link is an invariant of the original link; then the lattice of, say, birack colorings of the framings of an unframed link L forms an invariant of L .

For each of these and other coloring structures, enhancements can be defined, resulting in new invariants.

3 Biquandle Brackets

A *biquandle bracket* is a skein invariant for biquandle-colored knots and links. The definition was introduced in [6] (and independently, a special case was introduced in [1]) and has only started to be explored in other recent work such as [4, 7, 8].

Definition 2 Let X be a biquandle and R a commutative ring with identity. A *biquandle bracket* β over X and R is a pair of maps $A, B : X \times X \rightarrow R^\times$ assigning units $A_{x,y}$ and $B_{x,y}$ to each pair of elements of X such that the following conditions hold:

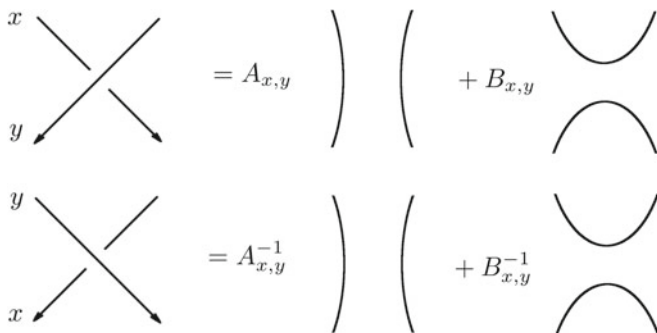
- For all $x \in X$, the elements $-A_{x,x}^2 B_{x,x}^{-1}$ are all equal, with their common value denoted by w ,
- For all $x, y \in X$, the elements $-A_{x,y} B_{x,y}^{-1} - A_{x,y}^{-1} B_{x,y}$ are all equal, with their common value denoted by δ , and
- For all $x, y, z \in X$ we have

$$\begin{aligned}
 A_{x,y} A_{y,z} A_{x \bar{\triangleright} y, z \bar{\triangleright} y} &= A_{x,z} A_{y \bar{\triangleright} x, z \bar{\triangleright} x} A_{x \bar{\triangleright} z, y \bar{\triangleright} z} \\
 A_{x,y} B_{y,z} B_{x \bar{\triangleright} y, z \bar{\triangleright} y} &= B_{x,z} B_{y \bar{\triangleright} x, z \bar{\triangleright} x} A_{x \bar{\triangleright} z, y \bar{\triangleright} z} \\
 B_{x,y} A_{y,z} B_{x \bar{\triangleright} y, z \bar{\triangleright} y} &= B_{x,z} A_{y \bar{\triangleright} x, z \bar{\triangleright} x} B_{x \bar{\triangleright} z, y \bar{\triangleright} z} \\
 A_{x,y} A_{y,z} B_{x \bar{\triangleright} y, z \bar{\triangleright} y} &= A_{x,z} B_{y \bar{\triangleright} x, z \bar{\triangleright} x} A_{x \bar{\triangleright} z, y \bar{\triangleright} z} \\
 &\quad + A_{x,z} A_{y \bar{\triangleright} x, z \bar{\triangleright} x} B_{x \bar{\triangleright} z, y \bar{\triangleright} z} \\
 &\quad + \delta A_{x,z} B_{y \bar{\triangleright} x, z \bar{\triangleright} x} B_{x \bar{\triangleright} z, y \bar{\triangleright} z} \\
 &\quad + B_{x,z} B_{y \bar{\triangleright} x, z \bar{\triangleright} x} B_{x \bar{\triangleright} z, y \bar{\triangleright} z} \\
 B_{x,y} A_{y,z} A_{x \bar{\triangleright} y, z \bar{\triangleright} y} & \\
 + A_{x,y} B_{y,z} A_{x \bar{\triangleright} y, z \bar{\triangleright} y} & \\
 + \delta B_{x,y} B_{y,z} A_{x \bar{\triangleright} y, z \bar{\triangleright} y} & \\
 + B_{x,y} B_{y,z} B_{x \bar{\triangleright} y, z \bar{\triangleright} y} &= B_{x,z} A_{y \bar{\triangleright} x, z \bar{\triangleright} x} A_{x \bar{\triangleright} z, y \bar{\triangleright} z}.
 \end{aligned}$$

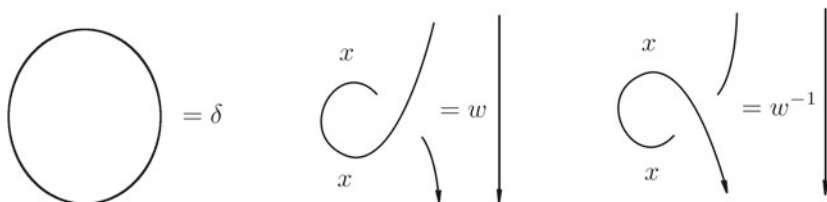
We can specify a biquandle bracket β over a ring R and finite biquandle $X = \{x_1, \dots, x_n\}$ by giving an $n \times 2n$ block matrix with entries in R whose left block lists the $A_{x,y}$ values and whose right block lists the $B_{x,y}$ values:

$$\beta = \left[\begin{array}{ccc|ccc} A_{x_1,x_1} & A_{x_1,x_2} & \dots & A_{x_1,x_n} & B_{x_1,x_1} & B_{x_1,x_2} & \dots & B_{x_1,x_n} \\ A_{x_2,x_1} & A_{x_2,x_2} & \dots & A_{x_2,x_n} & B_{x_2,x_1} & B_{x_2,x_2} & \dots & B_{x_2,x_n} \\ \vdots & \vdots & \ddots & \vdots & \vdots & \vdots & \ddots & \vdots \\ A_{x_n,x_1} & A_{x_n,x_2} & \dots & A_{x_n,x_n} & B_{x_n,x_1} & B_{x_n,x_2} & \dots & B_{x_n,x_n} \end{array} \right].$$

The biquandle bracket axioms are the conditions required for invariance of the *state-sum* value obtained by summing the products of smoothing coefficients and powers of δ and w for each Kauffman state of an X -colored diagram under X -colored Reidemeister moves. More precisely, we write skein relations



and assign δ to be the value of a component in a smoothed state, w the value of a positive kink and w^{-1} the value of a negative kink.



More formally, we have:

Definition 3 Let β be a biquandle bracket over a finite biquandle X and commutative ring with identity R and let D be an oriented knot or link diagram. Then for each X -coloring D_f of D , let $\beta(D_f)$ be the state-sum value obtained by summing over the set of Kauffman states the products of smoothing coefficients $\phi_{x,y} \in \{A_{x,y}^{\pm 1}, B_{x,y}^{\pm 1}\}$ at each crossing as determined by the colors and smoothing type times $\delta^k w^{n-p}$ where k is the number of components in the state, n is the number of negative crossings and p is the number of positive crossings. That is, for each X -coloring D_f of D , we have

$$\beta(D_f) = \sum_{\text{Kauffman States}} \left(\left(\prod_{\text{crossings}} \phi_{x,y} \right) \delta^k w^{n-p} \right).$$

Then the multiset of $\beta(D_f)$ -values over the set of X -colorings of D is denoted

$$\Phi_X^{\beta,M}(D) = \{\beta(D_f) \mid D_f \in \text{Hom}(\mathcal{B}(K), X)\}.$$

The same data may be expressed in “polynomial” form (scare quotes since the exponents are not necessarily integers but elements of R) as

$$\Phi_X^\beta(D) = \sum_{D_f \in \text{Hom}(\mathcal{B}(K), X)} u^{\beta(D_f)}.$$

Hence we have the following theorem (see [6]):

Theorem 2 *Let X be a finite biquandle, R a commutative ring with identity and β a biquandle bracket over X and R . Then for any oriented knot or link K represented by a diagram D , the multiset $\Phi_X^{\beta,M}(D)$ and the polynomial $\Phi_X^\beta(D)$ are unchanged by Reidemeister moves and hence are invariants of K .*

Example 4

A biquandle bracket in which $A_{x,y} = B_{x,y}$ for all $x, y \in X$ defines a biquandle 2-cocycle $\phi \in H_B^2(X)$. In this case the polynomial invariant $\Phi_X^\beta(D)$ is the product of the biquandle 2-cocycle enhancement $\Phi_X^\phi(K)$ with the Kauffman bracket polynomial of K evaluated at $A = -1$. See [6] for more details.

Example 5

A biquandle bracket β over the biquandle of one element $X = \{x_1\}$ is a classical skein invariant. For example, the biquandle bracket β over $R = \mathbb{Z}[A^{\pm 1}]$ with $A_{x_1,x_1} = A$ and $B_{x_1,x_1} = A^{-1}$ (and hence $\delta = -A^2 - A^{-2}$ and $w = -A^3$) is the Kauffman bracket polynomial.

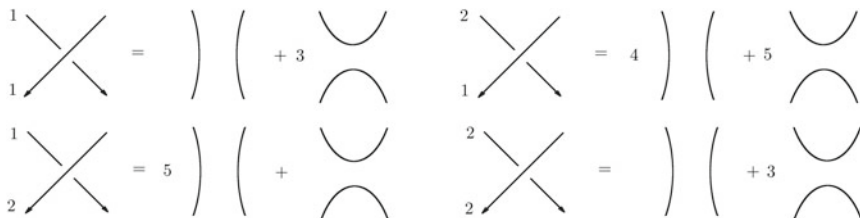
Thus, biquandle brackets provide an explicit unification of classical skein invariants and biquandle cocycle invariants. Even better though, there are biquandle brackets which are neither classical skein invariants nor cocycle invariants, but something new.

Example 6

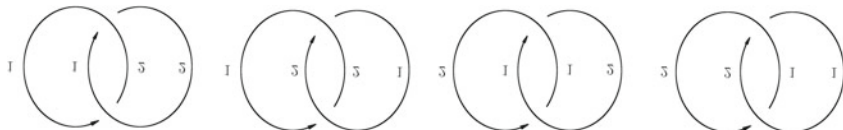
Let $R = \mathbb{Z}_7$ and $X = \mathbb{Z}_2 = \{1, 2\}$ with the biquandle operations $x \triangleright y = x \bar{\triangleright} y = x + 1$ (note that we are using the symbol 2 for the class of zero in \mathbb{Z}_2 so that our row and column numberings can start with 1 instead of 0). Then via a computer search, one can check that

$$\beta = \left[\begin{array}{cc|cc} 1 & 5 & 3 & 1 \\ 4 & 1 & 5 & 3 \end{array} \right]$$

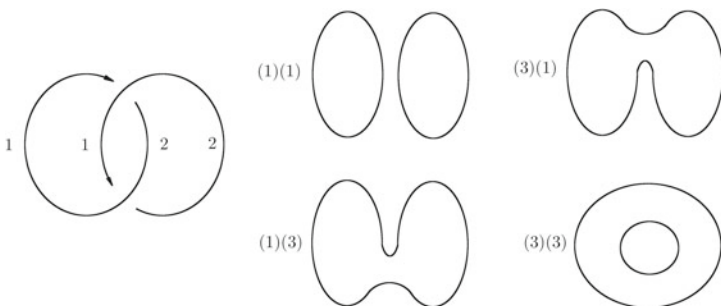
defines a biquandle bracket, with $\delta = -1(3)^{-1} - 1^{-1}3 = -5 - 3 = -1 = 6$ and $w = -(1)^2(3)^{-1} = -5 = 2$. The skein relations at positive crossings are as shown:



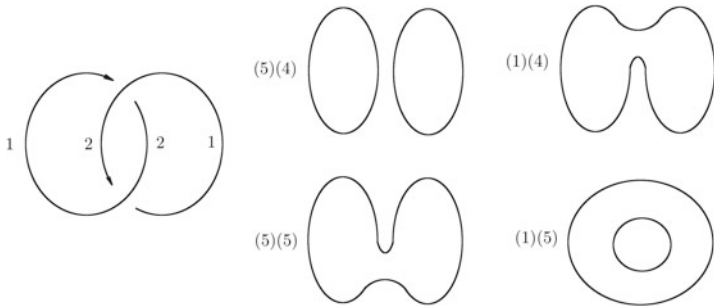
Let us illustrate in detail the computation of $\Phi_X^{\beta, M}(L)$ where L is the oriented Hopf link with two positive crossings. There are four X -colorings of the Hopf link and indeed of every classical link – the unenhanced counting invariant with this choice of coloring biquandle X can detect component number of classical links and nothing else.



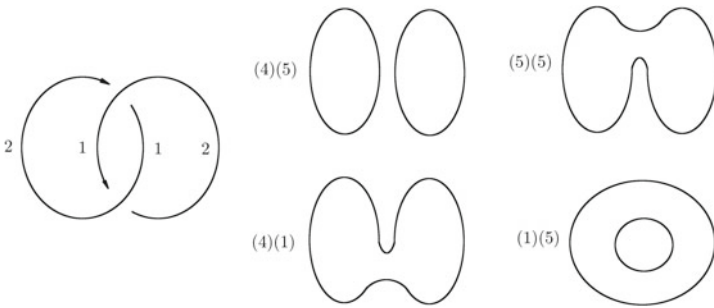
However, the biquandle bracket enhancement gives us more information. For each coloring, we compute the state-sum value:



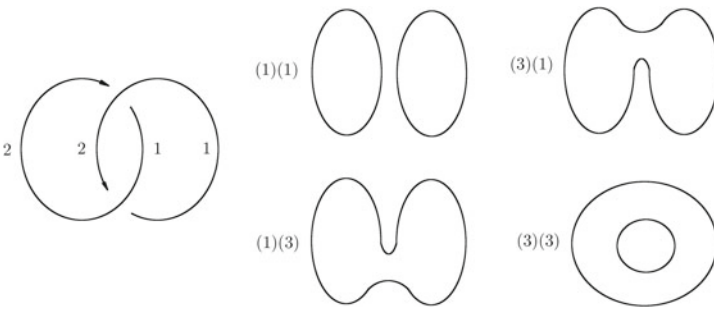
yields $[(1)(1)6^2 + (1)(3)6 + (3)(1)6 + (3)(3)6^2]2^{-2} = (1 + 4 + 4 + 2)2 = 1;$



yields $[(5)(4)6^2 + (1)(4)6 + (5)(5)6 + (1)(5)6^2]2^{-2} = (6 + 3 + 3 + 5)2 = 6;$



yields $[(4)(5)6^2 + (5)(5)6 + (4)(1)6 + (5)(1)6^2]2^{-2} = (6 + 3 + 3 + 5)2 = 6,$ and



yields $[(1)(1)6^2 + (3)(1)6 + (1)(3)6 + (3)(3)6^2]2^{-2} = (1 + 4 + 4 + 2)2 = 1.$ Then the multiset form of the invariant is $\Phi_X^{\beta, M}(L) = \{1, 1, 6, 6\}$, or in polynomial form we have $\Phi_X^{\beta}(L) = 2u + 2u^6$. Since the unlink of two components has invariant value $\Phi_X^{\beta, M}(U_2) = \{6, 6, 6, 6\}$, the enhanced invariant is stronger than the unenhanced counting invariant.

Example 6 is merely a small toy example meant to illustrate the computation of the invariant, of course. Biquandle brackets over larger biquandles and larger (finite or infinite) rings have already proved their utility as powerful knot and link invariants, with cocycle invariants at one extreme (information concentrated in the coloring) and skein invariants at the other (information concentrated in the skein relations). So far, the known examples of biquandle brackets which are neither classical skein invariants nor cocycle invariants have been largely found by computer search; it is our hope that other examples can be found by more subtle methods.

4 Other Quantum Enhancements

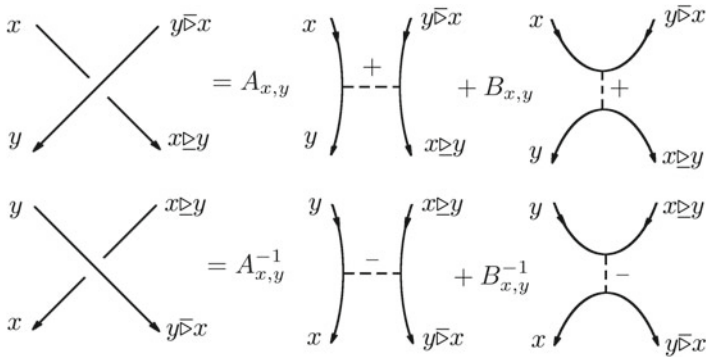
Biquandle brackets are one example of a more general phenomenon known as *quantum enhancements*, broadly defined as quantum invariants of X -colored knots or other knotted structures for an appropriate coloring structure X . In this section we collect a few other recent examples of quantum enhancements.

In [7], the author together with coauthors K. Oshiro, A. Shimizu and Y. Yaguchi defined *biquandle virtual brackets*, a generalization of biquandle brackets which includes a virtual crossing as a type of smoothing, i.e.,

$$\begin{array}{l}
 \begin{array}{c} x \\ \diagdown \\ \diagup \\ y \end{array} = A_{x,y} \left(\begin{array}{c} \diagdown \\ \diagup \end{array} \right) \left(\begin{array}{c} \diagup \\ \diagdown \end{array} \right) + B_{x,y} \left(\begin{array}{c} \cup \\ \cap \end{array} \right) + V_{x,y} \left(\begin{array}{c} \diagdown \\ \diagup \end{array} \right) \otimes \left(\begin{array}{c} \diagup \\ \diagdown \end{array} \right) \\
 \\
 \begin{array}{c} y \\ \diagdown \\ \diagup \\ x \end{array} = C_{x,y} \left(\begin{array}{c} \diagdown \\ \diagup \end{array} \right) \left(\begin{array}{c} \diagup \\ \diagdown \end{array} \right) + D_{x,y} \left(\begin{array}{c} \cup \\ \cap \end{array} \right) + U_{x,y} \left(\begin{array}{c} \diagdown \\ \diagup \end{array} \right) \otimes \left(\begin{array}{c} \diagup \\ \diagdown \end{array} \right)
 \end{array}$$

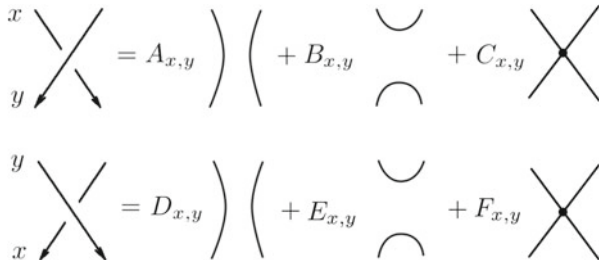
A biquandle bracket is then a biquandle virtual bracket in which the virtual coefficients are all zero. This framework gives another way of recovering the biquandle cocycle invariants, this time without the factor of the Kauffman bracket evaluated at -1 , by having classical smoothing coefficients all zero. Examples of these invariants are shown to be able to detect mirror image and orientation reversal. In particular, these are examples of invariants of classical knots and links which are defined in a way that fundamentally requires virtual knot theory; it is our hope that these invariants can provide a reason for classical knot theorists to care about virtual knot theory.

In [8], the author together with coauthor N. Oyamaguchi addressed the issue of how to compute biquandle brackets in a recursive term-by-term expansion as opposed to the state-sum approach described in Sect. 3. Our method uses *trace diagrams*, trivalent spatial graphs with decorations carrying information about smoothings which enable maintaining a biquandle coloring throughout the skein expansion.



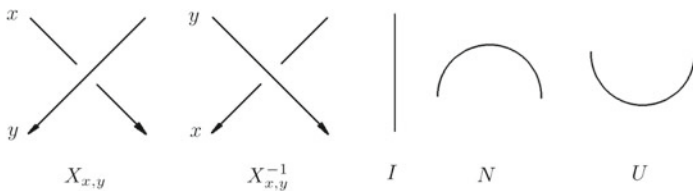
These are equivalent to the original state-sum biquandle brackets but can allow for faster hand computation as well as for allowing moves and diagram reduction during the course of the expansion. Technical conditions are identified for which trace moves (e.g., moving a strand over, under or through a trace) are permitted depending on certain algebraic conditions being satisfied by the bracket coefficients.

In [4], another skein relation is used in the biquandle bracket setting, superficially similar to the biquandle virtual brackets described above but with the virtual smoothing replaced with a 4-valent vertex.



This family of quantum enhancements includes Manturov’s parity bracket invariant as special case, as well as the biquandle brackets defined in Sect. 3.

In [9], the author together with coauthor V. Rivera (a high school student at the time) introduced the notion of quantum enhancements in the form of X -colored TQFTs or X -colored tangle functors for the case of involutory biracks X . These are given by matrices $X_{x,y}^{\pm 1}$, I , U and N over a commutative ring with identity R corresponding to the basic X -colored tangles

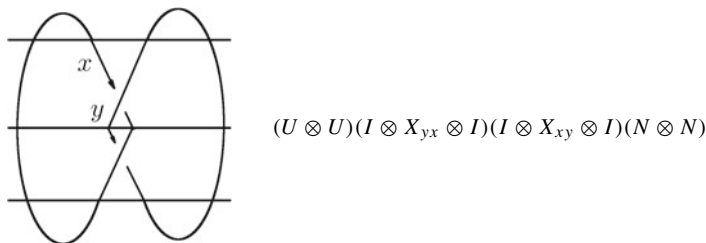


such that the tensor equations representing the X -colored Reidemeister moves and planar isotopy moves are satisfied, where we interpret vertical stacking as matrix product and horizontal stacking as tensor (Kronecker) product. Computer searches for solutions to these equations proved inefficient even for small rings, so we considered X -colored braid group representations as a first step. Indeed, biquandle brackets have so far been the best method for producing examples of this type of quantum enhancement. For example, the biquandle bracket in Example 6 defines the following quantum enhancement:

$$X_{11} = X_{22} = \begin{bmatrix} 1 & 0 & 0 & 0 \\ 0 & 0 & 3 & 0 \\ 0 & 3 & 6 & 0 \\ 0 & 0 & 0 & 1 \end{bmatrix}, \quad X_{12} = \begin{bmatrix} 5 & 0 & 0 & 0 \\ 0 & 0 & 1 & 0 \\ 0 & 1 & 2 & 0 \\ 0 & 0 & 0 & 5 \end{bmatrix}, \quad X_{21} = \begin{bmatrix} 4 & 0 & 0 & 0 \\ 0 & 0 & 5 & 0 \\ 0 & 5 & 3 & 0 \\ 0 & 0 & 0 & 4 \end{bmatrix},$$

$$I = \begin{bmatrix} 1 & 0 \\ 0 & 1 \end{bmatrix}, \quad N = [0 \ 1 \ 4 \ 0], \quad U = \begin{bmatrix} 0 \\ 5 \\ 1 \\ 0 \end{bmatrix}.$$

To compute a quantum enhancement in this format, our X -colored oriented diagrams D_f are decomposed into matrix products of tensor products of the five basic tangles which are then replaced with the appropriate matrices and multiplied to obtain 1×1 matrices, i.e., ring elements. These are then multiplied by the appropriate writhe correction factor w^{n-p} and collected into a multiset. For example, the Hopf link with pictured coloring decomposes as



The enhanced invariant for the Hopf link in Example 6 is then the multiset

$$\left\{ \begin{array}{l} (U \otimes U)(I \otimes X_{11} \otimes I)^2(N \otimes N)w^{-2}, \\ (U \otimes U)(I \otimes X_{22} \otimes I)^2(N \otimes N)w^{-2}, \\ (U \otimes U)(I \otimes X_{12} \otimes I)(I \otimes X_{21} \otimes I)(N \otimes N)w^{-2}, \\ (U \otimes U)(I \otimes X_{21} \otimes I)(I \otimes X_{12} \otimes I)(N \otimes N)w^{-2} \end{array} \right\}$$

$$= \{3(2), 3(2), 4(2), 4(2)\} = \{1, 1, 6, 6\}$$

as in Example 6.

5 Questions

We end this short survey with some questions and directions for future research.

- As mentioned in [6], biquandle 2-cocycles define biquandle brackets, and the operation of componentwise multiplication of the biquandle bracket matrix of a 2-cocycle with a bracket representing a 2-coboundary yields a biquandle bracket representing a cohomologous 2-cocycle. Weirdly, this also works with biquandle brackets which do not represent 2-cocycles, extending the equivalence relation of cohomology to the larger set of biquandle brackets. What exactly is going on here?
- So far, biquandle brackets over finite biquandles have been found primarily by computer search using finite coefficient rings. We would like to find examples of biquandle brackets over larger finite biquandles and over larger rings, especially infinite polynomial rings.
- The first approach for generalization, examples of which have been considered in [4, 7], is to apply the biquandle bracket idea to different skein relations. One may find that skein relations which do not yield anything new in the uncolored case can provide new invariants in various biquandle-colored cases.
- In addition to biquandle brackets, we would like to find other examples of quantum enhancements. Possible avenues of approach include representations of biquandle-colored braid groups, biquandle-colored Hecke algebras, biquandle-colored TQFTs and many more.
- Like the Jones, Homflypt and Alexander polynomials, every biquandle bracket should be susceptible to Khovanov-style categorification, providing another infinite source of new knot and link invariants.
- Since biquandle brackets contain both classical skein invariants and cocycle enhancements as special cases, we can ask which other known (families of) knot and link invariants are also describable in this way or recoverable from biquandle bracket invariants. For example, can every Vassiliev invariant be obtained as a coefficient in some biquandle bracket invariant over a polynomial ring, like the coefficients of the Jones polynomial?
- Finally, we can define quantum enhancements for coloring structures other than biquandles and for knotted objects other than classical knots. The possibilities are limitless!

Acknowledgements Partially supported by Simons Foundation collaboration grant 316709.

References

1. F. Aicardi, An invariant of colored links via skein relation. *Arnold Math. J.* **2**(2), 159–169 (2016)
2. J.S. Carter, D. Jelsovsky, S. Kamada, L. Langford, M. Saito, State-sum invariants of knotted curves and surfaces from quandle cohomology. *Electron. Res. Announc. Am. Math. Soc.* **5**, 146–156 (1999)

3. M. Elhamdadi, S. Nelson, *Quandles: An Introduction to the Algebra of Knots*, vol. 74, Student Mathematical Library (American Mathematical Society, Providence, 2015)
4. D.P. Ilyutko, V.O. Manturov, Picture-valued biquandle bracket. [arXiv:1701.06011](https://arxiv.org/abs/1701.06011)
5. D. Joyce, A classifying invariant of knots, the knot quandle. *J. Pure Appl. Algebr.* **23**, 37–65 (1982)
6. S. Nelson, M.E. Orrison, V. Rivera, Quantum enhancements and biquandle brackets. *J. Knot Theory Its Ramif.* **26**(24), 1750034 (2017)
7. S. Nelson, K. Oshiro, A. Shimizu, Y. Yaguchi, Biquandle virtual brackets. [arXiv:1701.03982](https://arxiv.org/abs/1701.03982)
8. S. Nelson, N. Oyamaguchi, Trace diagrams and biquandle brackets. *Int. J. Math.* **28**(24), 1750104 (2017)
9. S. Nelson, V. Rivera, Quantum enhancements of involutory birack counting invariants. *J. Knot Theory Its Ramif.* **23**(15), 1460006 (2014)

From Alternating to Quasi-Alternating Links



Nafaa Chbili

Abstract In this short survey, we introduce the class of quasi-alternating links and review some of their basic properties. In particular, we discuss the obstruction criteria for links to be quasi-alternating introduced recently in terms of quantum link invariants.

Keywords Alternating links · Quasi-alternating links · Quantum invariants · Link homology

2010 Mathematics Subject Classification 57M25 · 57M27

1 Introduction

Alternating links represent an important class of links in the three-sphere which admit a simple diagrammatic definition. They have been subject to extensive study. In particular, the study of their Jones polynomials led to the proof of old challenging conjectures in knot theory, see [15, 27, 38]. Their Khovanov homologies are quite simple and depend only on the Jones polynomial and the signature of the link [20]. Similarly, their link Floer homologies are determined by the Alexander polynomial and the signature of the link [31]. In addition, the Heegaard Floer homology of their branched double covers Σ_L depends only on the determinant of the link, $\det(L)$. In this context, an interesting generalization of alternating links has been obtained by Ozsváth and Szabó [31]. They proved that this homological property of Σ_L extends to a wider class of links, that they called quasi-alternating links. Unfortunately, unlike alternating links which admit a simple definition, quasi-alternating links are defined in a recursive way. The recursive nature of the definition makes it difficult to decide whether a given link is quasi-alternating by using only the definition. Over the

N. Chbili (✉)

Department of Mathematical Sciences, College of Sciences, United Arab Emirates University,
15551 Al Ain, United Arab Emirates
e-mail: nafaachbili@uaeu.ac.ae

© Springer Nature Switzerland AG 2019

C. C. Adams et al. (eds.), *Knots, Low-Dimensional Topology and Applications*, Springer Proceedings in Mathematics & Statistics 284,
https://doi.org/10.1007/978-3-030-16031-9_8

179

past decade, several obstruction criteria have been developed to characterize quasi-alternating links, see [23, 28, 31] for instance. The purpose of this paper is to give a short introduction to the subject, focusing on the obstruction criteria introduced recently in terms of quantum invariants of links.

This paper is organized as follows. In Sect. 2, we review some properties of alternating links relevant to our subject. In Sect. 3, we introduce the class of quasi-alternating links and review their basic properties. Finally, Sect. 4 will discuss some results on the polynomial invariants of quasi-alternating links.

2 Alternating Links

A link diagram is said to be alternating if the underpass and the overpass alternate when one travels along any component of the diagram. The alternating diagram is reduced if it contains no nugatory crossing, see Fig. 1. A link L is alternating if it admits an alternating diagram. Well-known examples of alternating links are two-bridge links. While the (p, q) -torus links with $p, q \geq 3$ are examples non-alternating links.

The class of alternating links has played an important role in the development of knot theory since its early age. This section is devoted to briefly review some results concerning the polynomial invariants of alternating links. In 1928, Alexander introduced an invariant of isotopy classes of oriented links [1]. This polynomial invariant $\Delta_L(t)$ which is related to the Seifert matrix can be defined in several equivalent ways. In [24, 25], Murasugi proved that $\Delta_L(t)$ for alternating knots satisfies interesting properties. Indeed, the degree of $\Delta_L(t)$ is equal to the genus of the knot. Moreover, if the knot is alternating then so is the polynomial $\Delta_L(t)$. More precisely,

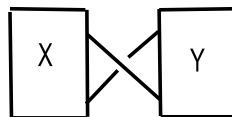
if for a knot K we write $\Delta_K(t) = \sum_{-m}^m \alpha_i t^i$ with $\alpha_{-m} \neq 0$ and $\alpha_m \neq 0$, then we have the following.

Theorem 1 ([24, 25]) *Suppose that K is an alternating knot, then:*

1. *The genus of the knot $g(K)$ is equal to the degree of $\Delta_K(t)$.*
2. *For all i , $\alpha_i \neq 0$ and $\alpha_i \alpha_{i+1} < 0$, for all $-m \leq i \leq m - 1$.*

In addition to the theorem above, the coefficients of the Alexander polynomial of an alternating knot are believed to satisfy Fox trapezoidal conjecture. We refer the

Fig. 1 A link diagram with a nugatory crossing



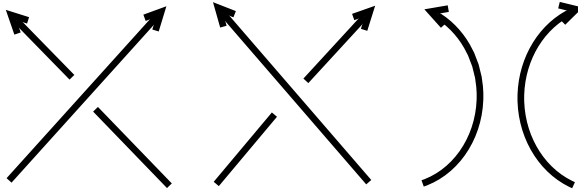


Fig. 2 L_+ , L_- and L_0 , respectively

reader to [11] for more details.

In 1984, Jones discovered a new polynomial invariant $V_L(t)$ of ambient isotopy of oriented links in the three-sphere. This invariant $V_L(t)$ admits several equivalent definitions. The simplest is the following recursive definition on link diagrams:

$$V_U(t) = 1,$$

$$tV_{L_+}(t) - t^{-1}V_{L_-}(t) = (\sqrt{t} + \frac{1}{\sqrt{t}})V_{L_0}(t),$$

where U is the unknot and L_+ , L_- and L_0 are three links which are identical except in a small ball where they are as pictured in Fig. 2. It is worth mentioning here that the Jones polynomial takes values in $\mathbb{Z}[t^{\pm 1/2}]$ and that for any link L , we can write

$$V_L(t) = t^s \sum_{i=0}^m a_i t^i, \text{ where } 2s \in \mathbb{Z}, m \geq 0, a_0 \neq 0 \text{ and } a_m \neq 0.$$

Kauffman [16] introduced a two-variable generalization of the Jones polynomial which can be defined as follows. Let $\Lambda(a, z)$ be the invariant of regular isotopy of un-oriented link diagrams defined by the following relations:

$$\Lambda_{\bigcirc}(a, z) = 1$$

$$\Lambda_{L_+}(z) + \Lambda_{L_-}(a, z) = z(\Lambda_{L_0}(a, z) + \Lambda_{L_\infty}(a, z))$$

$$\Lambda_{\text{cross}}(a, z) = a\Lambda_{\text{smooth}}(a, z)$$

$$\Lambda_{\text{cross}}(a, z) = a^{-1}\Lambda_{\text{smooth}}(a, z)$$

where L_+ , L_- , L_0 and L_∞ are four links which are identical except in a small ball where they are as displayed in Fig. 3.

Let D be an oriented link diagram of a link L and $w(D)$ its writhe. Then, the two-variable Kauffman polynomial of L is defined by $F_L(a, z) = a^{-w(D)}\Lambda_D(a, z)$, where Λ_D is obtained by forgetting the orientation of D . The polynomial F_L is an invariant of ambient isotopy of links which specializes to the Jones polynomial. Another interesting specialization of the Kauffman polynomial is the Brandt-Lickorish-Millet polynomial $Q(x)$, known also as the Q -polynomial [3]. This invariant was introduced shortly after the discovery of the Jones polynomial and it can be obtained from the

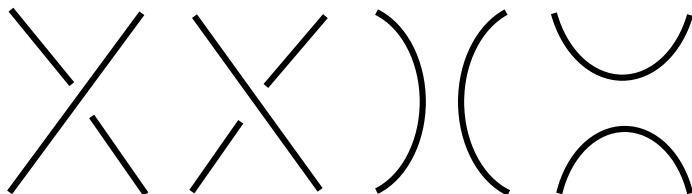


Fig. 3 L_+ , L_- , L_0 and L_∞ , respectively

Kauffman polynomial as $Q(x) = F(1, x)$.

The determinant is a numerical invariant of oriented links that was first defined from the Seifert matrix as $\det(L) = |\Delta_L(-1)|$. It is well known that $\det(L) = |V_L(-1)| = \sqrt{Q(2)}$ and that if Σ_L is the branched double cover of L , then $\det(L)$ is equal to the order of the first homology group of Σ_L . If a link L is alternating with an alternating connected diagram D , then $\det(L)$ is known to be equal to the number of spanning trees in the Tait graph associated with L .

Now, let us fix some notation needed in the sequel. The breadth of the Jones polynomial of an oriented link $\text{breadth} V_L(t)$ is defined to be the difference between the highest and the lowest power of t that appear in $V_L(t)$. We denote by $\text{deg} Q_L$ the highest power of x that appears in $Q_L(x)$ and by $\text{deg}_z F_L$ the highest power of the variable z that appears in $F_L(a, z)$. It is well known that we have always $0 \leq \text{deg} Q_L \leq \text{deg}_z F_L$. Finally, for any link L we denote by $\sigma(L)$ the signature of L . It was shown that the Jones polynomial of alternating links satisfies the following properties [38].

Theorem 2 ([38]) *If L is a non-split alternating link, then:*

1. $\text{breadth} V_L = c(L)$, where $c(L)$ is the crossing number of L .
2. $V_L(t) = t^s \sum_{i=0}^m a_i t^i$ is an alternating polynomial and if L is a prime link, other than $(2, n)$ -torus link, then $a_i a_{i+1} < 0$, for all $0 \leq i \leq m - 1$.
3. The coefficients of the highest and lowest degree in $V_L(t)$ are both ∓ 1 .

Inspired by this relationship between alternating diagrams and the Jones polynomial, Kidwell [19] studied the Q -polynomial of alternating links and showed that if L is a prime non-split alternating link, then $\text{deg} Q_L = c(L) - 1$. Yokota [43] studied the two-variable Kauffman polynomial of alternating links and proved that if L is a non-split alternating link, then the reduced degree of $F_L(a, z)$, with respect to the variable a , is equal to the crossing number of L .

The conditions on the Jones polynomials of alternating links mentioned above led to the solution of two intriguing questions in classical knot theory asked by Tait in the nineteenth century [39].

1. Does a reduced alternating link diagram has minimal number of crossings?
2. Is the writhe of a reduced alternating diagram of an alternating link L an isotopy invariant of L ?

Recently, Greene, Juhász and Lackenby gave new proofs to these results using geometric characterization of alternating links by definite spanning surfaces [9].

In 1999, Khovanov introduced a bi-graded link homology theory whose Euler characteristic is the Jones polynomial [17]. Let L be an l -component oriented link and $\widehat{KH}^{*,*}$ be its reduced Khovanov homology, then

$$V_L(t) = \sum_{i \in \mathbb{Z}, j \in \mathbb{Z} + \frac{l-1}{2}} (-1)^i t^j \text{rank}(\widehat{KH}^{i,j}(L)).$$

Few years later, another link homology theory $\widehat{HFK}^{*,*}$ called link Floer homology was introduced by Ozsváth and Szabó in [29] and independently by Rasmussen in [36]. For any link L , the graded Euler characteristic of $\widehat{HFK}^{*,*}(L)$ is, up to the multiplication by a factor, the Alexander-Conway polynomial of L . More precisely, we have

$$(t^{-1/2} - t^{1/2})^{l-1} \Delta_L(t) = \sum_{j \in \mathbb{Z}, i \in \mathbb{Z} + \frac{l-1}{2}} (-1)^{i+\frac{l-1}{2}} t^j \text{rank}(\widehat{HFK}^{i,j}(L)).$$

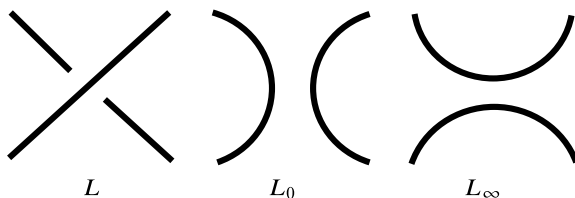
If L is an alternating link, then the Khovanov homology of L is determined by the Jones polynomial $V_L(t)$ and the signature of the link, $\sigma(L)$. Similarly, the link Floer homology of an alternating link depends only on the Alexander polynomial and the signature of the link. Indeed, these links are homologically thin in both Khovanov and link Floer homologies. In other words, both $\widehat{KH}^{i,j}(L)$ (over \mathbb{Z}) and $\widehat{HFK}^{i,j}(L)$ (over \mathbb{Z}_2) are trivial whenever $i - j \neq \frac{\sigma(L)}{2}$.

3 Quasi-Alternating Links

Ozsváth and Szabó studied the Heegaard Floer homology of the branched double cover Σ_L of S^3 branched over a link L [31]. They proved that if L is a non-split alternating link then the homology of Σ_L is determined by the determinant of the link, $\det(L)$. Rational homology spheres with such simple Heegaard Floer homology are called L-spaces. Examples of such 3-manifolds include lens spaces and Seifert fibered manifolds with finite fundamental group. In the same paper, it was proved that this homological property of Σ_L extends to a wider class of links, which the authors called quasi-alternating links. These links are defined recursively as follows.

Definition 1 The set Q of quasi-alternating links is the smallest set satisfying the following properties:

Fig. 4 The diagram of the link L at the crossing c and its smoothings L_0 and L_∞ , respectively



1. The unknot belongs to \mathcal{Q} .
2. If L is a link with a diagram D containing a crossing c such that
 - a. both smoothings of the diagram D at the crossing c , L_0 and L_∞ as in Fig. 4 belong to \mathcal{Q} ;
 - b. $\det(L_0), \det(L_\infty) \geq 1$;
 - c. $\det(L) = \det(L_0) + \det(L_\infty)$;
 then L is in \mathcal{Q} . In this case we say that L is quasi-alternating with quasi-alternating diagram D at the crossing c .

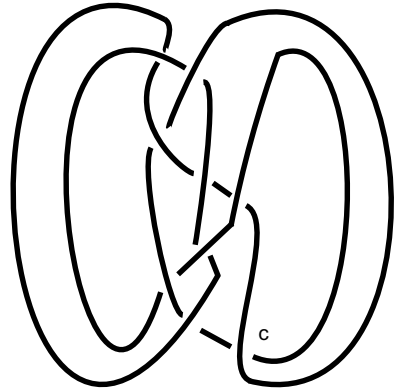
Here are some facts about this class of links. These facts can be obtained easily from the definition and an elementary induction on the determinant of the link.

- The determinant of a quasi-alternating link is always positive and it is equal to 1 if and only if L is the unknot.
- Any non-split alternating link is quasi-alternating at any crossing of any reduced alternating diagram [31].
- If K_1 and K_2 are two quasi-alternating knots, then so is their connected sum $K_1 \sharp K_2$, [4].
- If L is quasi-alternating, then so is its mirror image $L!$

In [31], the authors used the definition to show that the non-alternating knot 9_{47} is quasi-alternating by giving a quasi-alternating 11-crossing diagram of the knot. A minimal quasi-alternating diagram of the knot is given below. We present 9_{47} as the closure of the 4-braid $\sigma_1^{-1}\sigma_2\sigma_1^{-1}\sigma_2\sigma_3\sigma_2\sigma_1^{-1}\sigma_2\sigma_3$, see Fig. 5. If we smooth at the crossing c , then L_0 will be the closure of the 3-braid $\sigma_1^{-1}\sigma_2\sigma_1^{-1}\sigma_2^2\sigma_1^{-1}\sigma_2$. It is indeed the link $L7a1\{1\}$ which is alternating with determinant 24. However, L_∞ is the trefoil knot whose determinant is 3. Both L_0 and L_∞ are quasi-alternating and their determinants sum to $\det(9_{47}) = 27$.

A simple way to produce new examples of quasi-alternating links from old ones was introduced by Champanerkar and Kofman [4]. Given a link L with quasi-alternating diagram D at a crossing c , any link diagram obtained by replacing the crossing c by an alternating rational tangle of the same type is quasi-alternating at any of the new crossings. This construction was applied to prove that pretzel links of type $P(p_1, \dots, p_n, -q)$, where $n \geq 1$, $p_i \geq 1$ for all i , and $q \geq \min\{p_1, \dots, p_n\}$ are quasi-alternating.

Fig. 5 A minimal quasi-alternating diagram of the knot 9_{47}



Ozsváth and Szabó proved that if L is quasi-alternating, then Σ_L is an L-space which bounds a negative definite 4-manifold W with $H_1(W) = 0$. The Khovanov and link Floer homologies of quasi-alternating links have been computed in [23].

Theorem 3 ([23]) *If L is a quasi-alternating link, then:*

- (i) *The reduced Khovanov homology of L is σ -thin (over \mathbb{Z});*
- (ii) *The link Floer homology of L is σ -thin (over \mathbb{Z}_2);*

It is worth mentioning here that the previous theorem extends to odd Khovanov homology as well [28]. Among the 85 knots with up to 9 crossings only the two knots 8_{19} , which is indeed the $(3, 4)$ -torus knot, and 9_{42} don't satisfy the conditions of the previous theorem. So they are not quasi-alternating. The knot 9_{46} is odd Khovanov homology thick, hence not quasi-alternating. All the other 82 knots are quasi-alternating, see [2, 22, 31]. Among these 82 knots there are only 8 which are quasi-alternating non-alternating knots:

$$8_{20}, 8_{21}, 9_{43}, 9_{44}, 9_{45}, 9_{47}, 9_{48}, 9_{49}.$$

Note that quasi-alternating diagrams of all these knots except 8_{20} are given in [22]. In that paper, the diagram of 9_{46} seems to be included by mistake as it was pointed by the author in the Arxiv version of the same paper. A quasi-alternating diagram of 8_{20} can be given by presenting the knot as the closure of the 3-braid $\sigma_1^5 \sigma_2^2 \sigma_1^{-2} \sigma_2^{-2} \sigma_1^{-1} \sigma_2^{-3} \sigma_1^{-1}$.

For $p, q \geq 3$, the (p, q) -torus knot is Khovanov homology thick, so not quasi-alternating [37]. So are adequate non-alternating knots [18]. In general, these homological properties have been of great help in the characterization of quasi-alternating links. However, Greene proved the existence of homologically thin non quasi-alternating knots by showing that the knot 11_{n50} is homologically thin in reduced Khovanov, odd Khovanov and link Floer homology but not quasi-alternating [7].

Moreover, the knot 11_{n50} represents an example of a non-quasi-alternating knot whose double branched cover is an L -space. This example was generalized to an infinite family of homologically thin, hyperbolic non-quasi-alternating knots in [10]. Namely, the family of Kanenobu knots of type $K(-10n, 10n + 3)$, for $n \geq 0$. Different other techniques have been used to find obstructions for a link to be quasi-alternating and led to the complete characterization of certain classes of quasi-alternating links. In particular:

1. Quasi-alternating pretzel links have been determined, see [4, 7]. The classification of quasi-alternating Montesinos links has been first conjectured in [5, 33], see also [42]. Then, a complete classification has been obtained by Issa in [12]. Furthermore, Issa proved that a Montesinos link L is quasi-alternating if and only if its double branched cover Σ_L is an L -space and there exist a smooth negative definite 4-manifold W_1 and a smooth positive definite 4-manifold W_2 whose boundaries is Σ_L and $H_1(W_1) = H_1(W_2) = 0$.
2. Quasi-Alternating links of braid index at most 3 have been determined by Baldwin [2] based on Murasugi's classification of 3-braids [26].

Finally, we would like to mention that as a result of careful combination of all the above, the list of quasi-alternating knots with 10-crossings has been determined. In addition to alternating knots, the list includes the 31 non-alternating knots below.

- $10_{125}, 10_{126}, 10_{127}, 10_{141}, 10_{143}, 10_{148}, 10_{149}, 10_{155}, 10_{157}$ and 10_{159} which are closed 3-braids, see [2];
- $10_{150}, 10_{151}, 10_{156}, 10_{158}, 10_{162}, 10_{163}, 10_{164}$ and 10_{165} , see [8];
- $10_{129}, 10_{130}, 10_{131}, 10_{133}, 10_{134}, 10_{135}, 10_{137}, 10_{138}, 10_{142}, 10_{144}, 10_{146}, 10_{147}$ and 10_{160} , see [4].

More comprehensive tables of quasi-alternating knots are to be found in [13].

4 Polynomial Invariants of Quasi-alternating Links

The properties of the Alexander and the Jones polynomials of alternating links suggest that these polynomials might be a useful tool for the study of quasi-alternating links as well. Since the Jones polynomial is obtained as the Euler characteristic of the Khovanov homology, the σ -thinness of this homology implies that the Jones polynomial of a quasi-alternating link is alternating [18]. A similar conclusion can be made for the Alexander polynomial of quasi-alternating knots. Moreover, according to [30] the genus of any quasi-alternating knot is equal to the degree of its Alexander polynomial. This is indeed true for any knot whose Heegaard Floer homology is thin. We will postpone the discussion of the Jones polynomial of quasi-alternating links to the end of this section and start by looking at this simple obstruction defined in terms of the Q -polynomial. Actually, by studying the relationship between the degree of the Q -polynomials of the quadruplet L_+, L_-, L_0 and L_∞ , Qazaqzeh and the author [32] proved the following:

Theorem 4 ([32]) *If L is a quasi-alternating link, then: $\deg Q_L \leq \det(L) - 1$.*

A slightly more precise condition has been obtained by Teragaito [40] in the following theorem:

Theorem 5 ([40]). *Let L be a quasi-alternating link, then either:*

- (i) *L is the $(2, n)$ -torus link, or*
- (ii) *$\deg Q_L < \det(L) - 1$.*

These conditions are easy to test since they rely only on the computation of the Q -polynomials. They can be used to rule out the quasi-alternating property of several knots and links. By considering the figure eight knot, Teragaito showed that the condition given by Theorem 5 is sharp. A nice application of Theorem 4 shows that there are only finitely many Kanenobu knots which are quasi-alternating. The Kanenobu knot $K(p, q)$ is known to have determinant equal to 25 regardless of the values of the two integers p and q , see [14]. According to [34], the degree of $Q_{K(p,q)}$ is $|p| + |q| + 6$ if $pq \geq 0$ and $|p| + |q| + 5$ otherwise. Thus, if $K(p, q)$ is quasi-alternating then $|p| + |q| < 19$. This gives a simple proof that the interesting family of homologically thin knots introduced in [10] is non-quasi-alternating.

Teragaito proved a similar necessary condition for links to be quasi-alternating using the two-variable Kauffman polynomial:

Theorem 6 ([41]) *Let L be a quasi-alternating link, then either:*

- (i) *L is a $(2, n)$ -torus link for $n \neq 0$, and $\deg_z F_L = \det(L) - 1$;*
- (ii) *L is the figure-eight knot or the connected sum of two Hopf links, and $\deg_z F_L = \det(L) - 2$; or*
- (iii) *$\deg_z F_L \leq \det(L) - 3$.*

These results are stronger than the ones obtained in terms of the Q -polynomials. Teragaito gave an infinite family of links where the condition on $\deg Q_L$ fails to decide on the quasi-alternateness of the link, while the condition on $\deg_z F_L$ does. As a consequence of the results above, Teragaito determined all the quasi-alternating links with determinant 5 and conjectured results for those of determinant 4, [41]. Quasi-alternating links of determinant 2 and 3 have been classified earlier by Greene [7]. Table 1 summarizes the situation for quasi-alternating links with determinant at most 5. Note that for any integers p and q , $T(p, q)$ denotes the (p, q) -torus link.

More recently, these results about quasi-alternating links with small determinants have been extended by Lidman and Sivek, who characterized all quasi-alternating links with determinants less than 8, [21].

Theorem 7 ([21]) *Let L be a quasi-alternating link such that $\det(L) \leq 7$. Then L is either a two-bridge link or a connected sum of two-bridge links. Consequently, if L is a non-alternating quasi-alternating link then $\det(L) \geq 8$.*

We close this discussion with the following conjecture about the Jones polynomial of quasi-alternating links. This conjecture is obviously true for non-split alternating

Table 1 Quasi-alternating links with determinant less than or equal 5

n	quasi-alternating links with $\det(L) = n$
1	0_1
2	2_1
3	3_1 and $3_1!$
4	$2_1\#2_1$ and $T(2, \pm 4)$
5	4_1 and $T(2, \pm 5)$

links. It was also proved to be true in the case of links with braid index at most 3, see [32]. A more general conjecture has been stated in [35].

Conjecture *If L is a quasi-alternating link, then: $\text{breadth} V_L \leq \det(L)$.*

Partial results related to the conjecture above and more discussions about the Jones polynomial of quasi-alternating links can be found in [6].

Acknowledgements The author was supported by a research grant from United Arab Emirates University, UPAR grant #G00002650.

References

1. J.W. Alexander, Topological invariants of knots and links. *Trans. Amer. Math. Soc.* **30**, 275–306 (1928)
2. J. Baldwin, Heegaard Floer homology and genus one, one-boundary component open books. *J. Topol.* **1**, 963–992 (2008)
3. R.D. Brandt, W.B.R. Lickorish, K.C. Millett, A polynomial invariant for un-oriented knots and links. *Invent. Math.* **84**, 563–573 (1986)
4. A. Champanerkar, I. Kofman, Twisting quasi-alternating links. *Proc. Amer. Math. Soc.* **137**, 2451–2458 (2009)
5. A. Champanerkar, P. Ording, A note on quasi-alternating Montesinos links. *J. Knot Theor. Ramificat.* **24** 09, 1550048 (2015)
6. N. Chbili, K. Qazaqzeh, On the Jones polynomial of quasi-alternating links. [arXiv:1810.11773](https://arxiv.org/abs/1810.11773) [math.GT]
7. J. Greene, Homologically thin, non-quasi-alternating links. *Math. Res. Lett.* **17**, 39–49 (2009)
8. J. Greene, A spanning tree model for the Heegaard Floer homology of a branched double-cover. *J. Topol.* **6**, 525–567 (2013)
9. J. Greene, A. Juhász, M. Lackenby, Alternating links and definite surfaces. *Duke Math. J.* **166**, 2133–2151 (2017)
10. J. Greene, L. Watson, Turaev Torsion, definite 4-manifolds, and quasi-alternating knots. *Bull. Lond. Math. Soc.* **45**, 962–972 (2013)
11. R.H. Fox, Some problems in knot theory. In: *Topology of 3-manifolds and related topics*, in *Proceedings of the University of Georgia Institute*, 1961, pp. 168–176. Prentice-Hall, Englewood Cliffs, N.J. (1962)
12. A. Issa, The classification of quasi-alternating Montesinos links. *Proc. Amer. Math. Soc.* **146**(9), 4047–4057 (2018)

13. S. Jablan, Tables of quasi-alternating knots with at most 12 crossings. [arXiv:1404.4965](https://arxiv.org/abs/1404.4965) [math.GT]
14. T. Kanenobu, Infinitely many knots with the same polynomial invariant. Proc. Amer. Math. Soc. **97**(1986), 158–162 (1986)
15. L. Kauffman, State models and the Jones polynomial. Topology **26**(3), 395–407 (1987)
16. L. Kauffman, An invariant of regular isotopy. Trans. Amer. Math. Soc. **318**, 417–471 (1990)
17. M. Khovanov, Categorification of the Jones polynomial. Duke Math. J. **87**, 409–480 (1999)
18. M. Khovanov, Patterns in knot cohomology I. Experiment. Math. **12**, 365–374 (2003)
19. M. Kidwell, On the Degree of the Brandt-Lickorish-Millett-Ho Polynomial of a Link. Proc. Amer. Math. Soc. **100**(4), 755–762 (1987)
20. E.S. Lee, An endomorphism of the Khovanov Invariant. Adv. Math. **197**, 554–586 (2005)
21. T. Lidman, S. Sivek, Quasi-alternating links with small determinant. Math. Proc. Camb. Phil. Soc. **162**, 319–336 (2017)
22. C. Manolescu, An unoriented skein exact triangle for knot Floer homology. Math. Res. Lett. **14**, 839–852 (2007)
23. C. Manolescu, P. Ozsváth, On the Khovanov and knot Floer homologies of quasi-alternating links, in *Proceedings of Gökova Geometry-Topology Conference 2007*, pp. 60–81. Gökova Geometry-Topology Conference (GGT), Gökova (2008)
24. K. Murasugi, On the genus of the alternating knots I. J. Math. Soc. Japan **10**, 94–105 (1958)
25. K. Murasugi, On the Alexander polynomial of the alternating knot. Osaka Math. J. **10**, 181–189 (1958)
26. K. Murasugi, On closed 3-braids. Memoirs of the American Mathematical Society, No. 151. American Mathematical Society, Providence, R.I., 1974. vi+114 pp
27. K. Murasugi, Jones polynomials and classical conjectures in knot theory. Topology **26**(2), 187–194 (1987)
28. P. Ozsváth, J. Rasmussen, Z. Szabó, Odd Khovanov homology, . Algebr. Geom. Topol. **13**, 1465–1488 (2013)
29. P. Ozsváth, Z. Szabó, Holomorphic disks and knot invariants, Adv. Math. **186**, 58–116 (2004)
30. P. Ozsváth, Z. Szabó, Holomorphic disks and genus bounds, Geom. Topol. **8**, 311–334 (2004)
31. Ozsváth P., Szabó Z., On the Heegaard Floer homology of branched double-covers. Adv. Math. **194**, 1–33 (2005)
32. K. Qazaqzeh, N. Chbili, A new obstruction of quasi-alternating links. Algebr. Geom. Topol. **15**, 1847–1862 (2015)
33. K. Qazaqzeh, N. Chbili, B. Qublan, Characterization of quasi-alternating Montesinos links. J. Knot Theor. Ramificat. **24** 01, 1550002 (2015)
34. K. Qazaqzeh, I. Mansour, On Kanenobu Knots. Kobe J. Math. **33**, 31–52 (2016)
35. K. Qazaqzeh, B. Qublan, A. Jaradat, A remark on the determinant of quasi-alternating links. J. Knot Theor. Ramificat. **22** 6, 1350031 (2013)
36. J. Rasmussen, Floer homology and knot complements. Ph.D. Thesis, Harvard University (2003)
37. M. Stoic, Homological thickness and stability of torus knots. Algebr. Geom. Topol. **7**, 261–284 (2007)
38. M.B. Thistlethwaite, A spanning tree expansion of the Jones polynomial. Topology **26**(3), 297–309 (1987)
39. M.B. Thistlethwaite, Kauffman’s polynomial and alternating links. Topology **27**(3), 311–318 (1988)
40. M. Teragaito, Quasi-alternating links and Q -polynomials. J. Knot Theor. Ramificat. **23** 12, 1450068 (2014)
41. M. Teragaito, Quasi-alternating links and Kauffman polynomials. J. Knot Theor. Ramificat. **24** 07, 1550038 (2015)
42. L. Watson, A surgical perspective on quasi-alternating links. Low dimensional and Symplectic Topology, 2009 Georgia International Topology Conference (Michael Usher, ed.), Proceedings of Symposia in Pure Mathematics, vol. 82, pp. 39-51 American Mathematical Society, (2011)
43. Y. Yokota, The Kauffman polynomial of alternating links. Topol. Appl. **65**, 229–236 (1995)

Hoste's Conjecture and Roots of the Alexander Polynomial



Alexander Stoimenov

Abstract The Alexander polynomial remains one of the most fundamental invariants of knots and links in 3-space. Its topological understanding has led a long time ago to the insight of what (Laurent) polynomials occur as Alexander polynomials of arbitrary knots. Ironically, the question to characterize the Alexander polynomials of alternating knots turns out to be far more difficult, even although in general alternating knots are much better understood. J. Hoste, based on computer verification, made the following conjecture about 15 years ago: If z is a complex root of the Alexander polynomial of an alternating knot, then $\Re z > -1$. We discuss some results toward this conjecture, about 2-bridge (rational) knots or links, 3-braid alternating links, and Montesinos knots.

Keywords Alternating knot · Alexander polynomial · Skein polynomial · Rational link · 3-braid link · Polynomial root

2010 Mathematics Subject Classification Primary 57M25 · 13F20 · 11C08; Secondary 12D10

1 Links and Alexander Polynomial

We consider a *knot* $S^1 \hookrightarrow S^3$ or (more generally) *link* $S^1 \cup \dots \cup S^1 \hookrightarrow S^3$. The *Alexander polynomial*

$$\Delta : \{ \text{knots and links} \} \rightarrow \mathbb{Z}[t^{\pm 1/2}]$$

A. Stoimenov (✉)

Gwangju Institute of Science and Technology, GIST College, 123 Cheomdan-gwagiro, Gwangju 61005, Korea

e-mail: stoimeno@stoimenov.net

URL: <http://www.stoimenov.net/stoimeno/homepage>

© Springer Nature Switzerland AG 2019

C. C. Adams et al. (eds.), *Knots, Low-Dimensional Topology and Applications*, Springer Proceedings in Mathematics & Statistics 284, https://doi.org/10.1007/978-3-030-16031-9_9

is one of the most fundamental invariants of knots and links in 3-space. It is determined by (and studied below using) the *skein relation*

$$\Delta\left(\begin{array}{c} \nearrow \\ \searrow \end{array}\right) - \Delta\left(\begin{array}{c} \searrow \\ \nearrow \end{array}\right) = (t^{1/2} - t^{-1/2}) \Delta\left(\begin{array}{c} \nearrow \\ \nearrow \end{array}\right), \tag{1}$$

and here with the common normalization

$$\Delta\left(\bigcirc\right) = 1.$$

(There is an alternative approach using Seifert matrices, Fox calculus, etc.)

Remark 1 We have $\Delta(L) \in \mathbb{Z}[t^{\pm 1}]$ for links L of odd (number of) components (in particular, for *knots*), and $\Delta(L) \in t^{1/2}\mathbb{Z}[t^{\pm 1}]$ for even components.

Due to its profound importance, many features of the polynomial have been studied over the years in a variety of contexts. *Roots* of the polynomial are related, among others, to

- the monodromy and dynamics of surface homeomorphisms [27, 30],
- divisibility [23] and orderability [26] of knot groups, and
- statistical mechanical models of the Alexander polynomial [18].
- They are also studied in connection to Lehmer’s question on the existence of a Mahler measure minimizing polynomial [4, 6, 29].

Remark 2 The Alexander polynomial is *a priori* an *oriented* link invariant. It is invariant when the orientation of *all components* is reversed, and so for *knots* orientation does not matter, but is *does* a lot for *links*.

There is a Conway version of Δ , the *Conway polynomial* $\nabla(z) \in \mathbb{Z}[z]$:

$$\nabla(L)(t^{1/2} - t^{-1/2}) = \Delta(L)(t).$$

For an n -component link,

$$\nabla(L) \in z^{n-1}\mathbb{Z}[z^2]. \tag{2}$$

The topological understanding of the Alexander polynomial has led long ago—some time in the late 60s—to the insight of what (Laurent) polynomials occur for an arbitrary knot.

Theorem 1 (Levine [15], Kondo [10], ...) *A polynomial $\Delta \in \mathbb{Z}[t^{\pm 1}]$ is the Alexander polynomial of a knot if and only if Δ satisfies*

- (1) $\Delta(t) = \Delta(1/t)$ (reciprocity), and
- (2) $\Delta(1) = 1$ (unimodularity).

There is also a corresponding theorem for n -component links, which is an easy consequence of Kondo’s proof for knots [10]. The conditions are *superreciprocity*

$$\Delta(t) = (-1)^{n-1} \Delta(1/t),$$

and a divisibility property, following from (2).

Our attention will turn now to *alternating* knots and links. Hoste, based on computer verification, made a conjecture about 15 years ago. (I learned about it from personal communication with Murasugi.)

Conjecture 1 (Hoste's conjecture) *If $z \in \mathbb{C}$ is a root of the Alexander polynomial Δ of an alternating knot, then $\Re z > -1$.*

The main goal of this note is to present, and somewhat substantiate, the content of the author's talk at *Knots in Hellas*, with strong emphasis on this conjecture. This paper differs from the talk by leaving out the discussion of positive knots, but includes instead a treatise of the skein polynomial. The author's results are mostly included in the papers [39, 40]. See also the paper by M. Hirasawa in these same *Proceedings*.

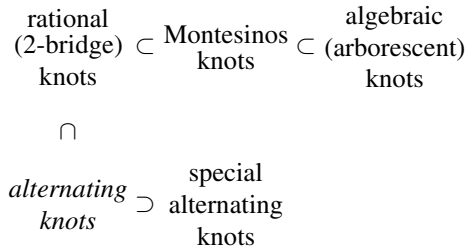
2 Alexander Polynomial of Alternating Links

Hoste's conjecture fits into the more general

Problem 1 Characterize the Alexander polynomials of *alternating* knots (or links).

Even though in many aspects alternating knots are much better understood than general knots, this problem seems very difficult. A complete solution is likely impossible. Here is a summary of what is known.

Below are some classes of knots in relation to alternating knots (similarly links).



Positive knots are knots with diagrams in which all crossings are positive (that is, like the leftmost diagram in (1)). Special alternating knots are knots which are simultaneously positive and alternating. (There are other descriptions, like saying that in an alternating diagram, one of the checkerboard surfaces is orientable, etc.)

Let $[\Delta]_k$ for $k \in \mathbb{Z} \cdot \frac{1}{2}$ be the coefficient of t^k in Δ . Define further

$$\text{maximal degree } \max \deg \Delta = \max \{ k \in \mathbb{Z} \cdot \frac{1}{2} : [\Delta]_k \neq 0 \},$$

$$\text{minimal degree } \min \deg \Delta = \min \{ k \in \mathbb{Z} \cdot \frac{1}{2} : [\Delta]_k \neq 0 \}.$$

Remark 3 Degrees make sense if $\Delta \neq 0$. Unimodularity implies that $\Delta \neq 0$ for all knots ($\Delta(-1) \neq 0$, because it is odd). But there are links with $\Delta = 0$. However, for an *alternating link* L ,

$$\Delta(L) \neq 0 \iff L \text{ non-split(table)}.$$

(Split means that there is a sphere in S^3 which separates the components of L non-trivially.) We thus assume alternating *links are non-split*.

Note that (super)reciprocity implies that $\min \deg \Delta = -\max \deg \Delta$.

Definition 1 • We call a coefficient $[\Delta]_k$ *admissible* if $\min \deg \Delta \leq k \leq \max \deg \Delta$ and $k - \min \deg \Delta$ (or $\max \deg \Delta - k$) is an integer.

- We call Δ *positive/negative* if all its admissible coefficients are positive/negative (and in particular non-zero).
- We call $\Delta(t)$ *alternating* if $\Delta(-t)$ is positive or negative.

Remark 1 implies that $[\Delta]_k \neq 0$ only if $[\Delta]_k$ is admissible.

Theorem 2 (Crowell-Murasugi [2, 21]) *If L is an alternating knot or (non-split) alternating link, then $\Delta_L(t)$ is alternating.*

Crowell-Murasugi prove also that if K is an alternating knot, then $\max \deg \Delta = g(K)$, the *genus* of K . (For a link L , it is $\frac{1 - \chi(L)}{2}$.)

Fox conjectured more:

Conjecture 2 (Fox’s Trapezoidal conjecture) *If K is an alternating knot, then there is a number $0 \leq n \leq g(K)$ such that for $\Delta_{[k]} := \lfloor [\Delta_K]_k \rfloor$ we have*

$$\begin{aligned} \Delta_{[k]} &= \Delta_{[k-1]} \quad \text{for } 0 < |k| \leq n, \\ \Delta_{[k]} &< \Delta_{[k-1]} \quad \text{for } n < |k| \leq g(K). \end{aligned} \tag{3}$$

(The number n can be regarded as the half-length of the ‘upper base of the trapezoid’. In particular, $n = 0$ if the ‘trapezoid’ is a ‘triangle’.)

The Trapezoidal conjecture was verified for

- rational (2-bridge) knots [7] (and later [1]), and
- some more algebraic knots [24].

The *signature* of a knot $\sigma(K)$ is even and satisfies

$$|\sigma(K)| \leq 2g(K). \tag{4}$$

There are two extensions of the Trapezoidal conjecture. The first (made by the author in [32]) states that for n in (3),

$$n \leq |\sigma(K)|/2.$$

We call this the *Extended Trapezoidal conjecture*.

(In particular $\sigma(K) = 0$ implies that $n = 0$, i.e., Δ is a ‘triangle’; Murasugi independently conjectured this special case.)

There are some recent partial results toward the (Extended) Trapezoidal conjecture:

- The paper [37] proves the Extended form for knots of genus $g(K) \leq 4$, using a combinatorial method developed from Stoimenov-Vdovina [41] (and Jong [12, 13] in the ordinary form for genus $g \leq 2$ using [33] and the same method);
- Ozsváth-Szabó prove the (Extended) Trapezoidal conjecture for $g(K) \leq 2$, and $|k| = g(K)$ in (3) for the general case. (Using knot Floer homology [25], they obtain more generally certain inequalities on the coefficients of Δ for an alternating knot. The Extended form follows easily in the stated special cases, even if not explicitly treated there.)

For the second extension of the Trapezoidal conjecture [32], call a polynomial X *log-concave*, if $[X]_k$ are log-concave, i.e.

$$[X]_k^2 \geq [X]_{k+1}[X]_{k-1} \geq 0 \tag{5}$$

for all $k \in \mathbb{Z}$. (We wrote ‘ ≥ 0 ’, because we want to regard only positive and alternating polynomials as log-concave.)

Conjecture 3 (Log-concavity conjecture, [32]) *If K is an alternating knot, then $\Delta_K(t)$ is log-concave.*

It can be easily seen that the Log-concavity conjecture implies the Trapezoidal conjecture. Again there is a slight refinement.

Conjecture 4 (Refined log-concavity conjecture) *Equality in the left inequality of (5) occurs for admissible $[\Delta]_k$ only if*

$$[\Delta]_k = [\Delta]_{k-1} = [\Delta]_{k+1}.$$

Using a method related to Stoimenov-Vdovina, I verified the (refined) log-concavity conjecture for genus $g(K) \leq 4$ (and $\chi(L) \geq -7$ for links L) in [37].

3 Hoste’s Conjecture

We return to Hoste’s Conjecture 1. Still not too much is known.

1. Crowell-Murasugi: Since Δ is alternating, a *real* negative number is never a root. Thus Hoste’s conjecture is true if all roots of Δ are real.

2. Let

$$S^1 := \{t \in \mathbb{C} : |t| = 1\}.$$

There is the following ‘folklore’ inequality:

$$\#\{\text{zeros } t \text{ of } \Delta \text{ on } S^1 \text{ with } \Im m t > 0\} \geq \frac{|\sigma(K)|}{2}. \tag{6}$$

Using this inequality, and work of Murasugi [22], we have that when K is alternating,

- K special alternating \iff (4) is an equality
- \implies all roots of Δ are on S^1
- \implies Hoste’s conjecture holds for special alternating knots.

3. Using (6), Stoimenov–Vdovina, and a test based on Rouché’s theorem, the author verified Hoste’s conjecture for $g(K) \leq 4$ [37].

Remark 4 ‘Folklore’ is a synonym of something everyone *believes* to be true, but no one properly writes down. The history of (6) is long and confusing, but here is not the place to get into it. See [36] for some account on this history, and ultimately the appendix (joint with Feller) of L. Liehti’s paper [16], and Gilmer-Livingston [5] for a (finally) written proof.

Example 1 (Mizuma, as orally quoted by Murasugi; see [35]) The (unimodular reciprocal) polynomial

$$t^{-6} - 2t^{-5} + 4t^{-4} - 8t^{-3} + 16t^{-2} - 32t^{-1} + 43 - 32t + 16t^2 - 8t^3 + 4t^4 - 2t^5 + t^6$$

is trapezoidal (and log-concave), but has the zero $t \approx -1.17597 + 1.4979i$ with $\Re t < -1$.

Thus trapezoidality (or log-concavity) of Δ does not imply Hoste’s conjecture. In fact, they are *almost unrelated*:

Theorem 3 ([35]) *Zeros of log-concave (even monic) alternating Alexander knot polynomials are dense in \mathbb{C} .*

Monic means that the leading coefficient is ± 1 ; such polynomials can be realized by a *fibred* (hyperbolic) knot [34].

Remark 5 There are minor relations, e.g.,

- An alternating polynomial cannot have a real negative root.
- There are conditions when restricting the degree. For example, when $\max \deg \Delta = 2$, then Δ alternating implies Hoste’s conjecture (Murasugi).

4 Results for 2-Bridge Links

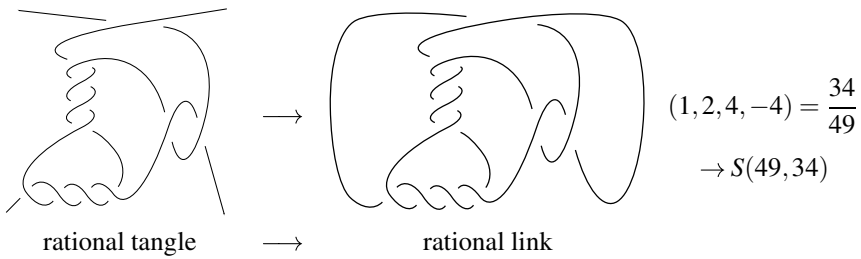
Rational (2-bridge) links are one important class of alternating links. *Schubert's form* [28] $L = S(q, p)$, for p and q coprime integers with $0 < p < q$, determines L up to mirror image up to the ambiguity

$$\pm p^{\pm 1} \in \mathbb{Z}_q^*. \tag{7}$$

There is a *continued fraction expansion* of $p/q \in \mathbb{Q}$:

$$\frac{p}{q} = (b_1, \dots, b_n) = \frac{1}{b_1 + \frac{1}{b_2 + \dots \frac{1}{b_n}}} \tag{8}$$

Here is how to join twists into a rational tangle and close up. (Twists are composed in a non-alternating way when the sign of b_i changes.)



The ambiguity (7) allows for special types of continued fractions (8): a positive fraction expansion (all $b_i > 0$, giving an alternating diagram), or an even fraction expansion (all $b_i \neq 0$ even, as used below).

Lyubich-Murasugi [19] examine the roots of Δ of a 2-bridge (rational) knot or link, by studying the stability of the Seifert matrix. One of their results is:

Theorem 4 (Lyubich-Murasugi) *If L is a 2-bridge knot or link, and t a root of $\Delta(L)$, then $-3 < \Re t < 6$.*

One of the first results in [39] improves this as follows.

Theorem 5 ([39]) *If L is 2-bridge, and $\Delta(L)(t) = 0$, then*

$$|t^{1/2} - t^{-1/2}| < 2, \tag{9}$$

or:

$$\nabla(L)(z) = 0 \Rightarrow |z| < 2. \tag{10}$$

The author subsequently found that Theorem 5 was independently obtained by Koseleff and Pecker [14].

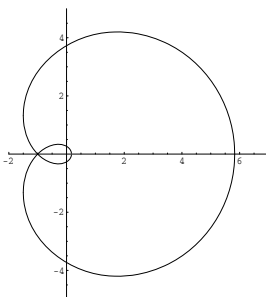
Let

$$\begin{aligned}
 t \in \mathbb{C} \setminus \{0\} \text{ internal} &: \iff t \text{ satisfies (9),} \\
 \text{external} & \text{ otherwise.} \\
 \mathcal{D} &:= \{t \in \mathbb{C} \setminus \{0\} : t \text{ internal}\}.
 \end{aligned}$$

The domain \mathcal{D} (see [17]) is bounded by the graphs of the four functions

$$\pm f_{\pm}(x) = \pm \sqrt{-x^2 + 2x + 7 \pm 4\sqrt{2x + 3}}.$$

f_{\pm} is defined on $\left[-\frac{3}{2}, 3 \pm 2\sqrt{2}\right]$.



A few special values are

$$f_{\pm}\left(-\frac{3}{2}\right) = \frac{\sqrt{7}}{2}, \quad f_{-}(-1) = 0, \quad f_{+}(-1) = \sqrt{8}, \quad f_{\pm}(3 \pm 2\sqrt{2}) = 0. \tag{11}$$

Thus (9) implies

- $$-\frac{3}{2} < \Re t. \tag{12}$$

(improves lower bound in Lyubich-Murasugi);

- $$(\Re t \leq) |t| < 3 + 2\sqrt{2} \approx 5.8284 \tag{13}$$

(improves upper bound in Lyubich-Murasugi).

Lyubich-Murasugi prove Hoste’s conjecture for certain 2-bridge links:

Theorem 6 (Lyubich-Murasugi) *Consider the even expansion (8), with*

$$b_i = 2a_i \quad (a_i \in \mathbb{Z} \setminus \{0\}). \tag{14}$$

- If no two consecutive $a_i = \pm 1$, then Hoste’s conjecture holds.
- If no $a_i = \pm 1$, then $-1 < \Re t < 3$.

One of the advantages of the skein relation is that such a result can be improved quite easily (proof is 1 page).

Proposition 1 ([39]) *Under the previous assumption,*

- if no three consecutive $a_i = \pm 1$, then Hoste’s conjecture holds;
- if no $a_i = \pm 1$, then $|z| < 1$ in (10). In particular,

$$\frac{3}{8} < \Re t \quad \text{and} \quad |t| < \frac{3 + \sqrt{5}}{2}.$$

Interestingly, the two approaches—Seifert matrix (Lyubich-Murasugi) and skein relation (the author)—meet similar difficulties.

Here the skein relation does better, but Lyubich-Murasugi have further results, not skein theoretically recovered. For example:

Proposition 2 (Lyubich-Murasugi) *If all $a_i > 0$ in (14), then all zeros of Δ are real (and in particular, Hoste’s conjecture holds).*

Many related statements and special cases of the conjecture were treated by similar methods in Hirasawa-Murasugi’s long monograph [8] (which Hirasawa discussed in his talk at the conference).

On the other hand, the skein approach does more. With (embarrassingly, see last section) no reasonable class of alternating knots fully resolved, the author was pushed to finally get at least one major piece done.

Theorem 7 ([40]) *Hoste’s conjecture is true for rational knots (and links).*

Another (purely algebraic) way of saying it is: for every sequence of polynomials

$$P_0 = 0, \quad P_1 = 1, \quad P_n(z) = a_n z P_{n-1}(z) + P_{n-2}(z)$$

for integers a_n , the roots of $P_n(t^{1/2} - t^{-1/2})$ satisfy $\Re t > -1$.

The proof is a numero-trigonometric marathon (40–60 pages; contrast with above Proposition 1). One (if not the) central reason is overcoming the singular behaviour in the limiting process $t \rightarrow -1$. One has to separate between t close to and far from -1 , which roughly results in doubling the length of the proof.

The skein approach does a few other things:

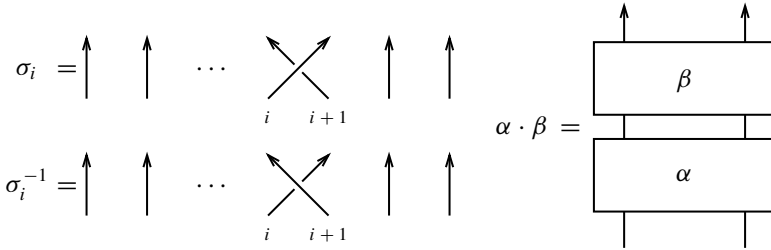
- it gives a condition on the zeros of the *skein (HOMFLY-PT)* polynomial of a 2-bridge link (see Sect. 7), and
- for Δ of more general links (below).

5 3-Braid Alternating Links

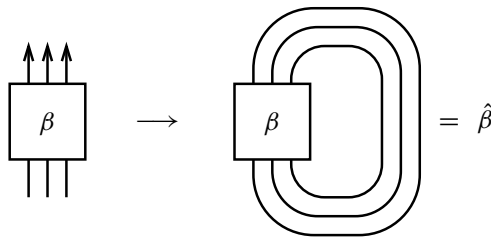
Definition 2 The braid group B_n on n strands is given by

$$\left\langle \sigma_1, \dots, \sigma_{n-1} \mid \begin{array}{l} [\sigma_i, \sigma_j] = 1 \quad |i - j| > 1 \\ \sigma_j \sigma_i \sigma_j = \sigma_i \sigma_j \sigma_i \quad |i - j| = 1 \end{array} \right\rangle,$$

with σ_i being the Artin standard generators. An element $\beta \in B_n$ is an n -braid.



The braid closure $\hat{\beta}$



is a knot or link. (Alexander’s theorem states that all links arise this way.)

We say that a braid (word)

$$\beta = \prod_{i=1}^n \sigma_{p_i}^{q_i} \tag{15}$$

(with $q_i \neq 0$) is *alternating* if $q_i q_j \cdot (-1)^{p_i - p_j} > 0$ whenever $i \neq j$.

We consider here $\beta \in B_3$.

Theorem 8 ([31]) *If an alternating link L is a closed 3-braid, then L is either*
 (a) *a closed alternating 3-braid, or*
 (b) *a (special alternating) pretzel link $P(1, p, q, r)$ ($p, q, r > 0$; see (17) below).*

For special alternating links, Hoste’s conjecture is true, so let us consider alternating 3-braids. (We stipulate that all decimal constants are rounded.)

Theorem 9 ([39]) *If L is a closed alternating 3-braid, and $\Delta(L)(t) = 0$, then*

$$|t^{1/2} - t^{-1/2}| < 2.45317,$$

i.e., $|z| < 2.45317$ in (10).

The proof (like the constant) is more technical than for Theorem 5, and is somewhat tricky, but manageable.

A discourse on *non-alternating* braids (and links) is:

Proposition 3 *If L is a closed positive 3-braid (in (15) all $q_i > 0$), then*

$$|t^{1/2} - t^{-1/2}| < 3.274601.$$

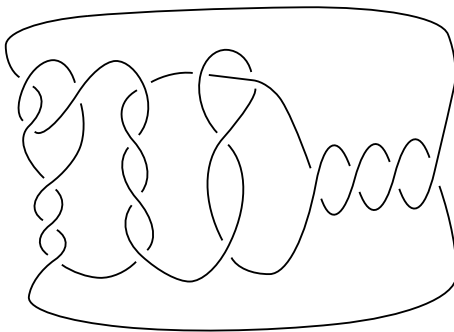
Remark 6 It was shown in [38] that if L is a closed positive braid and closed 3-braid, then L is a closed positive 3-braid. This is *not* true for 4-braids (there are counterexamples).

Example 2 (Hirasawa) The knot 10_{152} is a closed positive 3-braid, but Δ has the (real) root $t \approx -1.85$, and therefore Hoste's conjecture (and (9)) fails for positive 3-braid links.

6 Montesinos Links

A Montesinos link has the presentation

$$L = M(e, p_1/q_1, \dots, p_n/q_n). \tag{16}$$



$M(4, 3/11, -1/4, 2/5)$

In our terminology, e is the *integer part*, and p_i/q_i the *fractional parts*. Their number n is called the *length*.

Special cases:

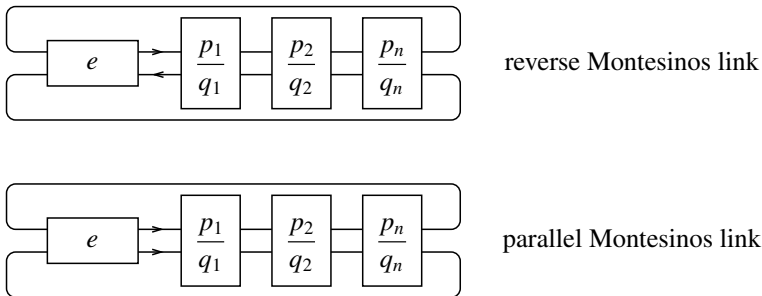
- If $n \leq 2$, the Montesinos link is rational.
- When $e = 0$ and all $p_i = \pm 1$, we can sign q_i so that $p_i = 1$, and have a *pretzel link*

$$L = M(1/q_1, \dots, 1/q_n) = P(q_1, \dots, q_n). \tag{17}$$

We accordingly call a fractional part with $p_i = \pm 1$ a *pretzel part*.

The defining convention is that all $q_i > 0$ and if $p_i < 0$, then the tangle is composed so as to give a non-alternating sum with a tangle with $p_{i\pm 1} > 0$. This defines the diagram up to mirroring. Thus one can find an alternating diagram from the presentation (16) if and only if e (when non-zero) and all p_i/q_i have the same sign, which we call accordingly an *alternating presentation*. We call an alternating Montesinos link to be *simply alternating*, if it has an alternating presentation with all fractional parts being pretzel parts except at most one.

Here orientation issues become essential, and we distinguish:



The author’s result regarding Montesinos links is:

Theorem 10 *Let L be a simply alternating Montesinos link, $\Delta(L)(t) = 0$ and $t \notin \mathcal{D}$ (i.e., t external). Then:*

- If L is reverse, then $\Re t > 0$.
- If L is parallel, then $\Re t > -1$ and t satisfies (13).

Corollary 1 *If L is a simply alternating Montesinos link, Hoste’s conjecture holds for external zeros; in particular $\Delta(L)(t) = 0$ implies (12).*

One more specific statement is possible for reverse links (works also for many non-alternating ones):

$$\text{if } t \notin \mathcal{D}, \text{ then } |\Re(z^2)| < |z| \quad (\text{with } z = t^{1/2} - t^{-1/2}),$$

i.e., (roughly) when $|t|$ is large, $|\Im t|$ or $|\Re t|$ is small.

But there is no bound on $|t|$. (Murasugi has non-simply alternating examples, where $t \in \mathbb{R}, t \rightarrow \infty$.)

The proof is 20+ pages: still not deep, but very painful. I went into the proof for simply alternating Montesinos links originally motivated to prove it for all alternating Montesinos links, until at a very late stage I realized that the proof works only in this restricted class...

7 Extensions to the Skein Polynomial

An advantage of using the skein relation (1), in contrast to the Seifert matrix, is that, to a limited extent, it offers some information beyond the Alexander polynomial. One goal is to address the *skein (HOMFLY-PT) polynomial* P . I report on partial progress, although much work remains ahead.

We use the convention of P with the variables v, w , the unknot having polynomial $P = 1$, and the skein relation

$$v^{-1} P \left(\begin{array}{c} \nearrow \searrow \\ \searrow \nearrow \end{array} \right) - v P \left(\begin{array}{c} \searrow \nearrow \\ \nearrow \searrow \end{array} \right) = w P \left(\begin{array}{c} \nearrow \\ \searrow \end{array} \right) \left(\begin{array}{c} \searrow \\ \nearrow \end{array} \right).$$

Theorem 11 *Let L be a 2-bridge link, and $(v, w) \in \mathbb{C}^2$, $v, w \neq 0$ be a root of $P_L(v, w)$ with $|v| \neq 1$. Then*

$$|w| < \max_{k>0} \frac{(|v|^{2k} + 1) |v - v^{-1}|}{|1 - v^{2k}|}. \tag{18}$$

Remark 7 One can restrict the maximum in (18) further to those k being a divisor of the leading coefficient μ of the Alexander-Conway polynomial $\nabla(w) = P(1, w)$. This is because in the presentation (8) for even $b_i = 2a_i \neq 0$, the coefficient expresses as $\mu = \pm \prod_{i=1}^n a_i$. In such a way, we can make sense of (18) also when $|v| = 1$, except for the 2μ -th roots of unity. (Note that when $v = \pm 1$, we have the Alexander-Conway polynomial, for which the recursion works in a slightly different way.) In particular, for a fibered 2-bridge link ($\mu = \pm 1$) one needs to take only $k = \pm 1$, and obtains

$$|w| < |v| + \frac{1}{|v|}$$

instead of (18) (which is then valid except if $v = \pm 1$).

Example 3 We tested the condition (18) for several values of v on the alternating Rolfsen [27, appendix] knots. It can identify as non-rational at least the following ones: 8₁₅, 9₃₅, 9₃₈, 9₃₉, 9₄₁, 10₄₉, 10₅₃, 10₆₃, 10₆₉, 10₇₈, 10₉₆, 10₉₇, 10₁₀₁, and 10₁₂₀. The improvement explained in Remark 7 rules further out from being rational 9₂₅, 10₅₅, 10₅₈, 10₆₆, and 10₈₀.

The complexity of (18), compared to (9), already suggests that statements about the skein polynomial become increasingly technical. We have one (technical) result about 3-braids.

Proposition 4 *Let L be an alternating 3-braid link, and $(v, w) \in \mathbb{C}^2$, $v, w \neq 0$ be a root of $P_L(v, w)$. Let $l = \max_{\pm} |1 - v^{\pm 2}|$.*

(a) *If $l \leq 1$, then $|w| < 3.15393$.*

(b) *If $1 < l \leq 1.40819$, then $|w| < 3.44984$.*

Proposition 4 has a far more limited scope, and the author does not know if it can be of much practical use. The proof is a tedious reworking of the proof for Theorem 9. There are other strong restrictions on the skein polynomial of (even general) 3-braids, most obviously from the Morton-Franks-Williams (MFW) inequality [3, 20], with some refinements found in [31]. Experiments with knots in the tables of KnotScape [9] whose skein polynomial passes the 3-braid test of the MFW inequality have not turned up any examples interesting with regard to Proposition 4.

I have not attempted a refinement of the Montesinos link calculation, which appears too technical.

Moreover, the recursive skein approach is difficult to use for another important special case of P , the Jones polynomial V . This expresses as $V(z) = P(z, w)$, with w related to z by

$$w = z^{1/2} - z^{-1/2}.$$

(Note, for example, that under this relation, the restriction (18) is always satisfied, and so Theorem 11 is useless.) There is indeed a denseness result in [11] about Jones polynomial roots of alternating pretzel links. Thus caution is needed among what classes of links the question about location of roots makes sense.

8 Further Open Questions

Apart from the classical problems mentioned earlier, several questions are related to use of the skein method with regard to Hoste's conjecture, and link polynomial properties more broadly.

- A problem for Montesinos links, formulated in [34]: Is there a condition (and what is it?) on the Alexander polynomial of an arbitrary Montesinos link? Whatever zero location technique is used, it must naturally bypass, at least, Montesinos links with vanishing polynomial (which—unlike among 3-braid links, for example—are not completely described).
- Finally, Hoste's conjecture remains also open for 3-braids. A computer test of alternating 3-braids of even length up to 18 determined the maximum of the left hand-side of (9) to be ≈ 1.94 , which suggests that (9) may still be true. However, as in the remark below Theorem 7, again there are serious problems in (and close to) $t = -1$. See also Example 2.

> **Important**

As this material went to press, the author has learned that an alternative proof of Theorem 7 was given by K. Ishikawa, who also announced counterexamples to Hoste's conjecture.

Acknowledgements The author thanks the referee and the *Knots in Hellas* organizers. It was a pleasure to attend the conference.

References

1. G. Burde, Das Alexanderpolynom der Knoten mit zwei Brücken. Arch. Math. (Basel) **44**(2), 180–189 (1985)
2. R. Crowell, Genus of alternating link types. Ann. Math. **69**(2), 258–275 (1959)
3. J. Franks, R.F. Williams, Braids and the Jones-Conway polynomial. Trans. Am. Math. Soc. **303**, 97–108 (1987)
4. E. Ghate, E. Hironaka, The arithmetic and geometry of Salem numbers. Bull. Am. Math. Soc. (N.S.) **38**(3), 293–314 (2001)
5. P.M. Gilmer, C. Livingston, Signature jumps and Alexander polynomials for links. Proc. Am. Math. Soc. **144**(12), 5407–5417 (2016)
6. E. Hironaka, The Lehmer polynomial and pretzel links. Canad. Math. Bull. **44**(4), 440–451 (2001); Erratum, Canad. Math. Bull. **45**(2), 231 (2002)
7. R.I. Hartley, On two-bridged knot polynomials. J. Austral. Math. Soc. Ser. A **28**(2), 241–249 (1979)
8. M. Hirasawa, K. Murasugi, Various stabilities of the Alexander polynomials of knots and links. [arXiv:1307.1578](https://arxiv.org/abs/1307.1578)
9. J. Hoste, M. Thistlethwaite, KnotScape, a knot polynomial calculation and table access program. <http://www.math.utk.edu/~morwen>
10. H. Kondo, Knots of unknotting number 1 and their Alexander polynomials. Osaka J. Math. **16**(2), 551–559 (1979)
11. X. Jin, F. Zhang, F. Dong, E.G. Tay, Zeros of the Jones polynomial are dense in the complex plane. Electron. J. Comb. **17**, #R94, 1–10 (2010)
12. I.D. Jong, Alexander polynomials of alternating knots of genus two. Osaka J. Math. **46**(2), 353–371 (2009)
13. I.D. Jong, Alexander polynomials of alternating knots of genus two II. J. Knot Theory Ramif. **19**(8), 1075–1092 (2010)
14. P.-V. Koseleff, D. Pecker, On Alexander-Conway polynomials of two-bridge links. J. Symbolic Comput. **68**(2), 215–229 (2015)
15. J. Levine, A characterization of knot polynomials. Topology **4**, 135–141 (1965)
16. L. Liechti, Signature, positive hopf plumbing and the coxeter transformation. Osaka J. Math. **53**(1), 251–267 (2016)
17. Limaçon of Pascal. <http://www-groups.dcs.st-and.ac.uk/~history/Curves/Limacon.html>
18. X.-S. Lin, Z. Wang, Braid representation and random walk on string links. [arXiv:q-alg/9605023](https://arxiv.org/abs/q-alg/9605023)
19. L. Lyubich, K. Murasugi, On zeros of the Alexander polynomial of an alternating knot. Topology Appl. **159**(1), 290–303 (2012). [arXiv:1102.0701v1](https://arxiv.org/abs/1102.0701v1)
20. H.R. Morton, Seifert circles and knot polynomials. Proc. Camb. Phil. Soc. **99**, 107–109 (1986)
21. K. Murasugi, On the genus of the alternating knot. J. Math. Soc. Jpn. **10**, 94–105, 235–248 (1958)
22. K. Murasugi, On a certain numerical invariant of link types. Trans. Am. Math. Soc. **117**, 387–422 (1965)

23. K. Murasugi, On the divisibility of knot groups. *Pac. J. Math.* **52**, 491–503 (1974)
24. K. Murasugi, On the Alexander polynomial of alternating algebraic knots. *J. Austral. Math. Soc. Ser. A* **39**(3), 317–333 (1985)
25. P.S. Ozsváth, Z. Szabó, Holomorphic disks and knot invariants. *Adv. Math.* **186**(1), 58–116 (2004)
26. B. Perron, D. Rolfsen, On orderability of fibered knot groups. *Proc. Camb. Phil. Soc.* **135**, 147–153 (2003)
27. D. Rolfsen, *Knots, and Links*, Publish or Perish (1976)
28. H. Schubert, Knoten mit zwei Brücken. *Math. Z.* **65**, 133–170 (1956)
29. D.S. Silver, S.G. Williams, Mahler measure of Alexander polynomials. *J. Lond. Math. Soc.* **69**(3), 767–782 (2004)
30. D.S. Silver, S.G. Williams, Lehmer’s question, links and surface dynamics. *Math. Proc. Camb. Phil. Soc.* **143**, 649–661 (2007). [arXiv:math.GT/0509068](https://arxiv.org/abs/math/0509068)
31. A. Stoimenov, The skein polynomial of closed 3-braids. *J. Reine Angew. Math.* **564**, 167–180 (2003)
32. A. Stoimenov, Newton-like polynomials of links. *Enseign. Math. (2)* **51**(3–4), 211–230 (2005)
33. A. Stoimenov, Knots of (canonical) genus two. *Fund. Math.* **200**(1), 1–67 (2008). [arXiv:math.GT/0303012](https://arxiv.org/abs/math/0303012)
34. A. Stoimenov, Realizing Alexander polynomials by hyperbolic links. *Expos. Math.* **28**(2), 133–178 (2010)
35. A. Stoimenov, Log-Concavity and zeros of the Alexander polynomial. *Bull. Korean Math. Soc.* **51**(2), 539–545 (2014)
36. A. Stoimenov, Application of braiding sequences III: Concordance of Positive Knots. *Int. J. Math.* **26**(7), 1550050, 1–36 (2015)
37. A. Stoimenov, *Diagram Genus, Generators and Applications*. T&F/CRC Press, Monographs and Research Notes in Mathematics (2016). ISBN 9781498733809
38. A. Stoimenov, *Properties of Closed 3-Braids and Braid Representations of Links*. Springer Briefs in Mathematics (2017). [arXiv:math.GT/0606435](https://arxiv.org/abs/math/0606435), ISBN 978-3-319-68148-1
39. A. Stoimenov, Hoste’s conjecture and roots of Link polynomials. *Ann. Combin.* **22**(2), 393–431 (2018)
40. A. Stoimenov, Hoste’s conjecture for generalized Fibonacci polynomials. *Commun. Algebra* **47**(1), 362–406 (2019)
41. A. Stoimenov, A. Vdovina, Counting alternating knots by genus. *Math. Ann.* **333**, 1–27 (2005)

A Survey of Grid Diagrams and a Proof of Alexander's Theorem



Nancy C. Scherich

Abstract Grid diagrams are a representation of knot projections that are particularly useful as a format for algorithmic implementation on a computer. This paper gives an introduction to grid diagrams and demonstrates their programmable viability in an algorithmic proof of Alexander's Theorem. Throughout, there are detailed comments on how to program a computer to encode the diagrams and algorithms.

Keywords Knot theory · Braid groups · Grid diagrams · Alexander's theorem

2010 Mathematics Subject Classification: 57M25 · 57M27 · 20F36

1 Introduction

Grid diagrams were first introduced by Cromwell, Dynnikov and Brunn [2–4] and have gained popularity since the use of grids to give a combinatorial definition of knot Floer homology [13]. They have also proved useful in determining the mosaic number of knot mosaics [9] and understanding arc index [3]. Additionally, grid diagrams can further simplify knot invariance arguments as there are only two required grid moves in contrast to the three required Reidemeister moves [3, 4]. The purpose of this paper is to provide an introduction to grid diagrams and grid moves with a focus on computer implementation. The main result of this paper is a computer implemented, grid diagrammatic proof of the Alexander Theorem, based on the work of Lambropoulou [7, 8, 10] and its variations by Kauffman and Lambropoulou [6].

N. C. Scherich (✉)

University of California, 552 University Rd, Isla Vista, Santa Barbara,
CA 93117, USA

e-mail: nscherich@math.ucsb.edu

© Springer Nature Switzerland AG 2019

C. C. Adams et al. (eds.), *Knots, Low-Dimensional Topology
and Applications*, Springer Proceedings in Mathematics & Statistics 284,
https://doi.org/10.1007/978-3-030-16031-9_10

207

1.1 Grid Diagrams

A **grid diagram** is a square grid such that each square within the grid is decorated with an x , o or is left blank. This is done in a manner such that every column and every row has exactly one x and one o , see Fig. 1 for an example. The choice of x and o decorations is a convention to mirror a tic tac toe game; one can define a grid diagram using only a single x decoration if desired. However, using two decorations can be useful when considering the orientation of the grid. The **grid number** (or index) of a grid diagram is the number of columns (or rows) in the grid. This paper follows the grid notation used by [13] which uses matrix notation with the convention that the rows and columns are numbered top to bottom and left to right.

A grid diagram is associated with a knot by connecting the x and o decorations in each column and row by a straight line *with the convention that vertical lines cross over horizontal lines*. These lines form arcs of the knot, and removing the grid leaves a diagram of the knot. Figure 1 shows an example of this process. As a result, grid diagrams represent particular planar projections of knots. Note that grid diagrams are equivalent to arc presentations as representations of knots, which was originally discovered by Brunn [2].

Here we use the word *knot* synonymously for a knot or link. The *knot type of a grid* is the knot type of the knot associated with the grid. The *arc of the grid* or *arc of the knot* refers to a portion of the knot that is represented in a single column or row of the grid. There are some instances where the distinction between the x and o decorations is important. However, for the results in this paper, it is only the location of the decorations, and not the actual decoration that is needed.

1.1.1 Computer Implementation

Each x and o decoration has a location (row, column) which will be called a **node** of the grid. We can define an object *grid* as a set of $2n$ nodes.

$$grid = \{(r_1, c_1), \dots, (r_{2n}, c_{2n})\}$$

For the example grid in Fig. 1, we get the grid

$$\{(1,2), (1,7), (2,7), (2,6), (3,3), (3,7), (4,2), (4,4), (5,3), (5,5), (6,4), (6,6), (7,1), (7,5)\}.$$

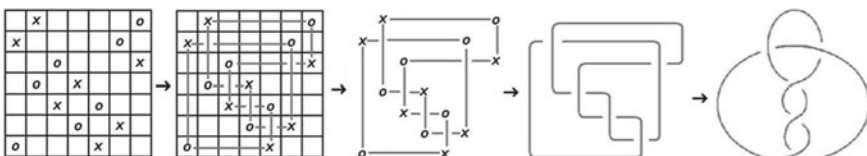


Fig. 1 An example of a grid diagram and the process to obtain the associated knot of the grid diagram

The notation *node.row* and *node.column* will be used to collect either the row or column number of the node. Here are some helper functions that can be defined on a grid diagram. To locate an arc of the knot in a row or column, one needs to find the corresponding nodes in the same row or same column; this is accomplished by the function *find-row-neighbor*, or analogously *find-column-neighbor*.

find-row-neighbor

```

Input: node
for node in grid do
  if node.row == input.row and node.column  $\neq$  input.column then
    return node
  end if
end for

```

Drawing a diagram of the knot represented by the grid is as easy as plotting lines between the nodes in each row and column. This will not encode the crossing information, but it is understood that vertical lines cross over horizontal lines. Be aware that the nodes in the grid are of the form (row, column) which is not in Euclidean (x, y) coordinates (i.e. columns are labeled top to bottom which is reversed from the standard Euclidean y -coordinate increasing bottom to top).

Euc

```

Input: node
return  $(n + \text{node.row} + 1, \text{node.column})$ 

```

graph

```

Input: grid
for node in grid do
  plot line from Euc(node) to Euc(find-row-neighbor(node))
  plot line from Euc(node) to Euc(find-column-neighbor(node))
end for

```

1.2 Grid Moves

Thanks to the work of Cromwell and Dynnikov [3, 4], there are two grid moves used to relate grid diagrams: (de-)stabilization and commutation. These play a role analogous to the Reidemeister moves for knot diagrams [14]. Following the notation from [13, 15], these grid moves are defined below.

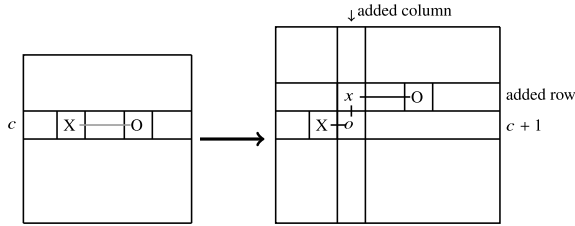


Fig. 2 (de-)stabilization, or kink addition

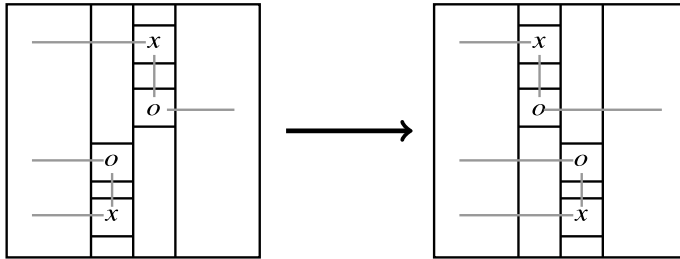


Fig. 3 An example of an admissible column commutation

(de-)Stabilization: Stabilization is the addition of a kink while destabilization is the removal of a kink. The term (de-)stabilization is used to describe this move without specifying whether a kink is being added or removed. It is important to note that (de-)stabilization does not preserve the grid number, but simply corresponds to an isotopy of the underlying knot. A kink may be added to the right or left of a column, above or below a row, and at any point along the arc of the knot in any row or column. For one example, Fig. 2 shows a kink addition to row c . To do this, insert an empty column between the x and o markers of row c . Then insert an empty row above or below row c . Move either the x or o decoration in row c into the adjacent grid square in the added row. Complete the added row and column with x and o decorations appropriately.

To add a kink to a column, switch the notions of column and row. To remove a kink, follow these instructions in reverse order. Stabilization increases the grid number by 1 while de-stabilization reduces the grid number by 1.

Commutation: Commutation interchanges two consecutive rows or columns of a grid diagram. This move preserves the grid number, but does not always preserve the knot type. See Fig. 3 for an example column commutation.

When a commutation preserves the knot type of the grid, it will be called an *admissible commutation*, which is explained in more detail in Sect. 1.3. The following theorem, due to Cromwell [3] and Dynnikov [4], see also [15], explains the relationship between grid diagrams, knots and the two grid moves.

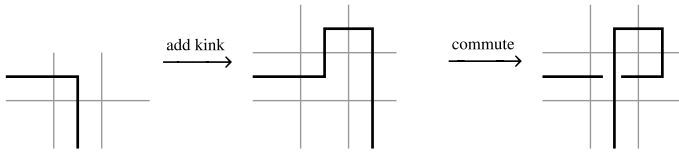


Fig. 4 Reidemeister I move via grid moves

Theorem 1 *Two grid diagrams have the same knot type if and only if there exists a finite sequence of admissible commutation and (de-)stabilization grid moves to relate one grid to the other.*

One way to see this theorem is to accomplish all of the Reidemeister moves using the two grid moves. For example, the Reidemeister I move can be done by adding a kink and then commuting the new column, shown in Fig. 4.

1.2.1 Computer Implementation

While the commutation grid move has subtleties when admissible, it is very straightforward to implement. Either two rows or two columns can be commuted.

column-commutation

```

Input: grid, column numbers  $i$  and  $i + 1$ 
for node in grid with node.column  $i$  or  $i + 1$  do
  if node.column ==  $i$  then
    increase node.column to  $i + 1$ 
  else if node.column ==  $i + 1$ 
    decrease node.column to  $i$ 
  end if
end for
return grid
    
```

On the other hand, (de-)stabilization is always admissible, but much more complicated to implement. There are many different ways a kink can be added or removed, each of which requires a separate implementation. The following algorithm will implement the specific kink addition depicted in Fig. 2 which adds a kink below an indicated row. This function can be gently altered to accomplish the other types of kink addition.

specific-kink-addition

```

Input: grid, nodes  $(i, j)$ ,  $(i, k)$  with  $j < k$ 
for node in grid do
  if node.column  $> j$  then
    
```

```

    increase node.column by 1
  end if
  if node.row > i then
    increase node.row by 1
  end if
end for
replace (i, j) by (i + 1, j)
add nodes to grid: (i, j + 1), (i + 1, j + 1)
return grid

```

1.3 Commutation; A Closer Look

The commutation grid move is defined to interchange *any* two consecutive rows or columns in a grid. Depending on the relative positions of the x and o decorations in the columns or rows to be commuted, a commutation could change the knot type of the grid. This section will establish some conditions under which commutation is admissible. The results of this section focus on column commutation, but conditions for row commutation are analogous. For a more detailed discussion, see [15].

Figure 5 shows the four possible relative positions of two consecutive columns, up to different x and o labeling and exact positioning. Denote these possibilities as *disjoint*, *nested*, *point-shared* and *interlocked*. The terminology is justified by observing the four instances of Fig. 5.

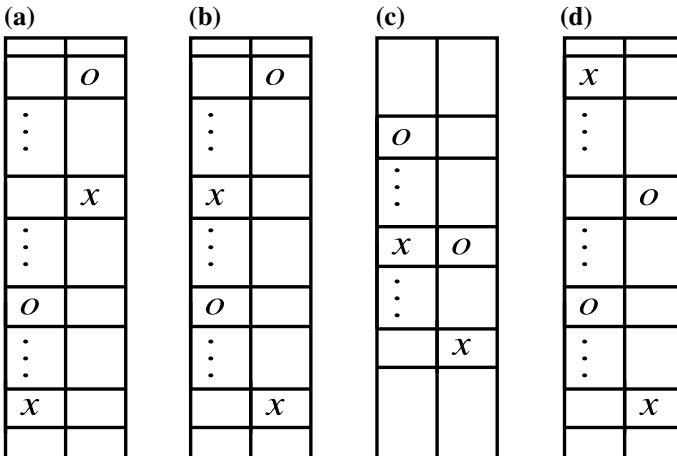


Fig. 5 Consecutive columns that are: **a** disjoint, **b** nested, **c** point-shared, **d** interlocked

Proposition 1 ([15]) *Commutation of columns that are disjoint, nested or point-shared are admissible commutations.*

Proof This can be quickly proven by considering the different arc configurations of the underlying knot diagrams, all of which commutations correspond to an isotopy and Reidemeister I or II move. □

Depending on the arc configuration of the underlying knot, commutation of interlocked columns can change the knot type of the grid. So as long as the two columns are not interlocked, then commutation is admissible.

Corollary 1 *A column that has the x and o in adjacent grid squares or in outermost grid squares can be admissibly commuted with any other column.*

Proof This column can never be interlocked with another column. □

2 From Knot Diagram to Grid Diagram; An Algorithm

Cromwell proved in [3] that every knot can be represented by a grid diagram. Shown below is a detailed algorithm of a process to create a grid diagram for a knot. This 6 step algorithm is easy to implement and an example is shown for the Trefoil knot in Fig. 7.

Step 1: Start with a projection of the knot in general position. Locally isotope each crossing by a rotation so that the vertical arcs crosses over the horizontal arcs, as show in Fig. 6.

Step 2: Rectilinearize or polygonalize the knot.

Step 3: Isotope the rectangular knot so that no two arcs are colinear.

Step 4: Superimpose a grid on top of the knot so that there is one column for every vertical arc and one row for every horizontal arc.

Step 5: Place an x or an o on the corners of the knot in an alternating fashion so that every row and every column of the grid has exactly one x and one o .

Step 6: Remove the arcs of the knot leaving only the grid diagram behind.

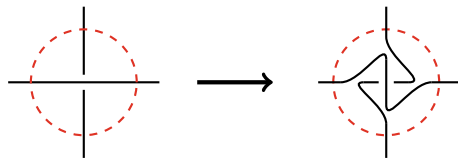


Fig. 6 Local isotopy of Step 1

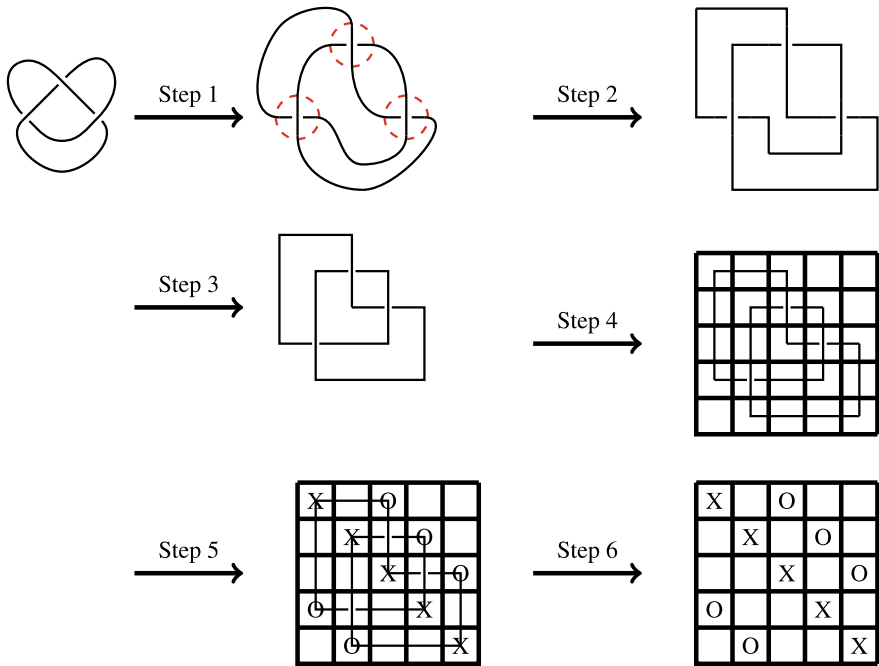


Fig. 7 An example of applying the 6 step algorithm to construct a grid diagram representing the Trefoil knot

3 Braids and Alexander’s Theorem; A Review

Geometrically, a **braid** on n strands is a vertical stack of pictures of the form σ_i and σ_i^{-1} as shown in Fig. 8.

Here, σ_i has the strand in the i th position cross downwards behind the strand in the $(i + 1)$ st position, and σ_i^{-1} has the strand in the i th position cross downwards in front of the strand in the $(i + 1)$ st position. A braid can be described by listing the σ_i ’s that occur in order from top to bottom. Conversely, given a word in σ_i ’s, one can recreate a braid by stacking the diagrams in order from top to bottom. Importantly, what distinguishes a braid from a more general tangle is the monotonicity of the strands and, by general position, the crossings occur at distinct heights in the braid. This is best seen by orienting the strands with a downward flow. Braids are only

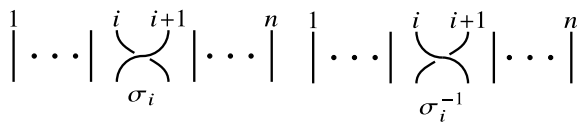


Fig. 8 A geometric visualization of the generating crossing diagrams within a braid

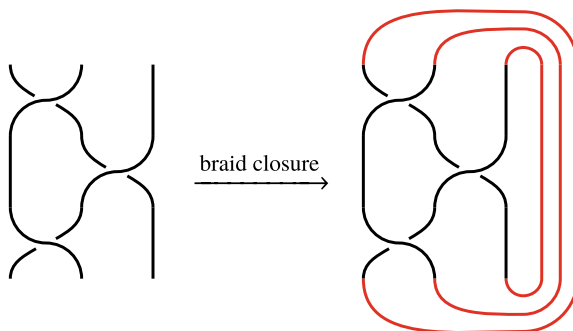


Fig. 9 An example braid closure

considered up to isotopy of the strands relative to the endpoints, which preserves the monotonicity of the strands. To get a knot from a braid, one takes the **braid closure** by connecting the top endpoints of the braids to the bottom endpoints of the braid without adding extra crossings. By convention, these new arcs wrap around the right side of the braid, as in Fig. 9.

It is important to understand exactly what a braid closure looks like. In Fig. 9, the knot on the right has all of its crossings on the left side, and the rest of the arcs wrap around on the right. The crossings on the left occur as a braid, namely the crossings occur at distinct heights and the arcs flow monotonically downward. It is clear that some knots can be represented as the closure of a braid, but Alexander’s Theorem gives the full result.

Alexander’s Theorem [1] *Every knot diagram is isotopic to a braid closure.*

There are many proofs of Alexander’s theorem, including Yamada and Vogel’s algorithm in [16], Morton’s algorithm by threading [12], Lambropoulou’s algorithm by eliminating upward arcs using braiding moves/*L*-moves [7, 8, 10] and Jones’ more casual algorithm in [5] by “throwing the bad parts over one’s shoulder”. At first glance, one might naively try to prove Alexander’s theorem by isotoping all the crossing of an oriented knot diagram into a bounded region, in a way that resembles a braid closure. It is easy to force the crossings to occur at distinct heights, but the problem that quickly arises is the arcs may not be monotone. Now Kauffman and Lambropoulou in [6] offer a solution to fix this monotonicity by using *L*-moves. The idea behind the *L*-move is to break an arc with the wrong orientation and replace it by two arcs with correct orientations, as shown in Fig. 10.

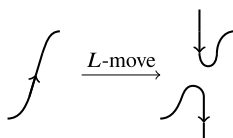


Fig. 10 An abstract illustration of the *L*-move

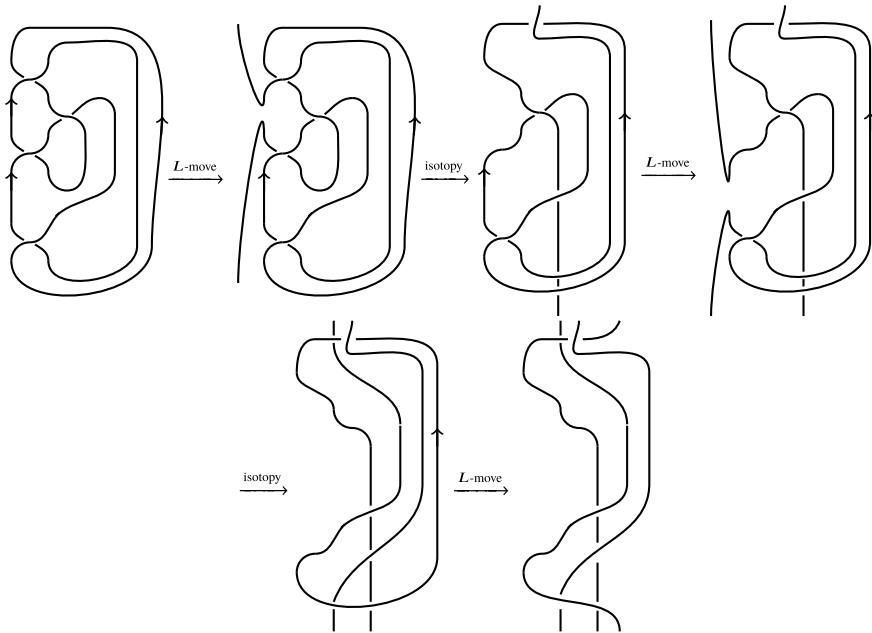


Fig. 11 An example using a sequence of L -moves to find a braid for the Fig. 8 knot

After applying an L -move, the two new vertical arcs either both lie above the entire knot diagram, or both below. This is determined visually by the crossings of the arc on either side of where the move is applied. The algorithm suggested by Kauffman and Lambropoulou is to choose an orientation of the knot diagram and apply L -moves to the upwards oriented arcs. This leaves a resulting diagram isotopic to a braid, and the closure of this braid is isotopic the original knot. One downfall of this procedure is the amount of visual decisions and isotopy to choose where to apply the L -moves, and then to finally adjust the diagram to look like a braid. Figure 11 shows an example of this algorithm to find a braid for the Fig. 8 knot.

4 Mid-Grid Moves and Main Result

In the closure of the braid, all of the arcs in the braid flow downward, while the arcs in the closure flow monotonically upward. These upward arcs lie on the outside righthand side of the braid. The idea of the mid-grid move is to move arcs of the knot represented in the middle of a grid to the outside of the grid. This move, when applied to an oriented knot will lead to a shape similar to the braid closure. If applied to an arc with an upwards orientation, this move changes the orientation of the arc to have two downwards oriented arcs in the middle of grid, and one upward oriented arc on the outside right of the grid.

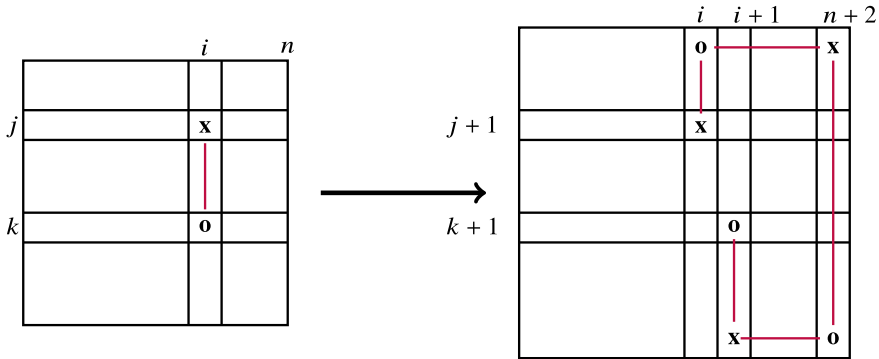


Fig. 12 Mid-grid move on column i

This move is the grid analogue of the L -move. There are several benefits of interpreting this move in the grid environment. The mid-grid move can be concretely described by a sequence of admissible commutation and (de)-stabilization grid moves giving a clear proof that the knot type is preserved. Additionally, there is no ambiguity on whether the new vertical arcs will lie above or below the entire knot. Since within the constraints of a grid, all vertical arcs cross over horizontal arcs, the new vertical arcs can be seen as lying entirely above without question or need of visual determination.

4.1 Mid-Grid Move on Column i

Starting with a grid diagram for the knot, keep the arcs of the knot pictured in the grid. The mid-grid move will increase the grid size by 2 and is shown in Fig. 12 (up to x and o labeling).

Proposition 2 *The mid-grid move preserves the knot type of the grid.*

Proof It suffices to show that the mid-grid move can be accomplished by a sequence of admissible commutation and (de)-stabilization grid moves. The following five steps accomplish the mid-grid move and are demonstrated in Fig. 13.

Let j be the row of the top decoration and k be the row of the bottom decoration of the arc in column i . In Fig. 13, the specific decorations have been omitted for clarity.

1. Add a kink above and to the left of row j . The new row and column are shaded in Fig. 13.
2. The horizontal portion lying in the new row j has its endpoints in adjacent grid squares. By Corollary 1 this row can be admissibly commuted with any other row. So commute row j upwards $j - 1$ times until it is the new top row. The vertical arc that was in column i has been shifted to column $i + 1$ and the bottom entry has been shifted to row $k + 1$.
3. Add a kink below and to the left of the bottom endpoint of the arc in column $i + 1$.

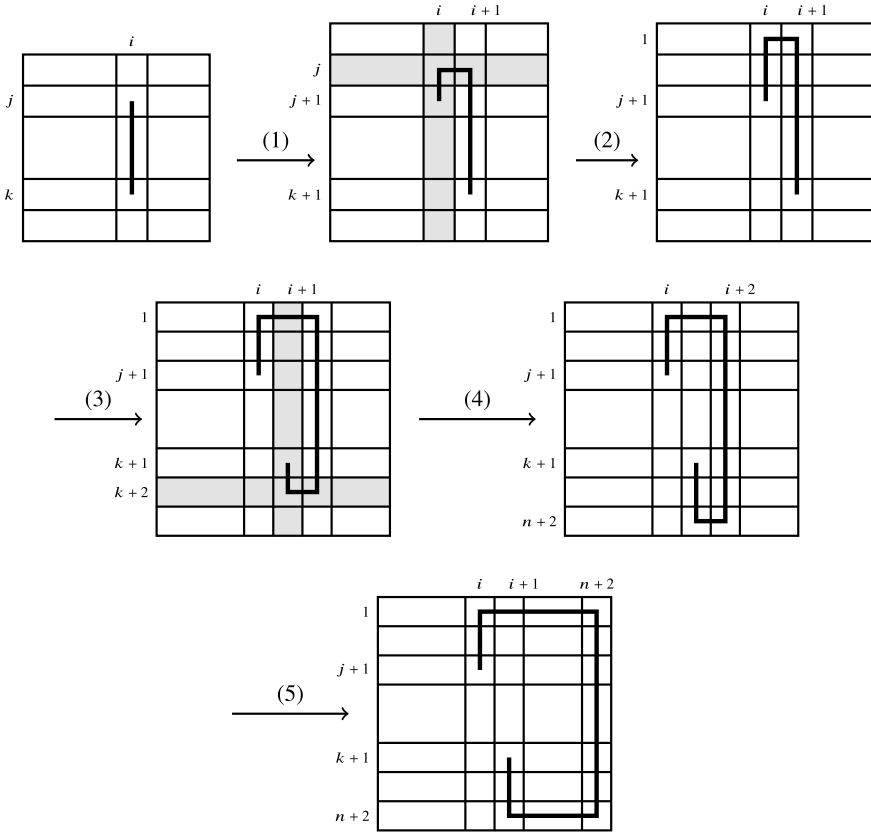


Fig. 13 Steps 1 through 5

4. The horizontal portion of the new row is now in row $k + 2$. Since the horizontal endpoints are in adjacent grid squares, again Corollary 1 gives that this row admissibly commutes with any other row. So commute row $k + 2$ downwards $n - k$ times until it is the new bottom row.
5. The vertical arc that was originally in column i is now in column $i + 2$ and extends the entire height of the grid. By Corollary 1 column $i + 2$ can be admissibly commuted to the right $n - i$ until it is the right-most column. □

4.1.1 Computer Implementation

The midgrid move, while a complicated list of commutation and (de)-stabilizations, can be described very succinctly.

midgrid

```

Input: grid, column number  $i$ 
for node in grid do
  increase node.row by 1
  if node.column >  $i$  then
    increase node.column by 1
  else
    if node.column =  $i$  and node.row > (find-column-neighbor(node)).row then
      increase node.column by 1
    end if
  end if
end for
add nodes to grid:  $(1, i), (1, n + 2), (n + 2, i + 1), (n + 2, n + 2)$ 
increase  $n$  by 2
return grid
  
```

4.2 A Proof of Alexander’s Theorem

Proof Start with the an oriented diagram of the knot. Follow the algorithm in Sect. 2 to get a grid diagram for the knot, but leave the arcs of the knot on the grid. Locate the columns where the orientation is upwards. Perform mid-grid moves on those columns in successive order starting with the furthest right column and work one by one to the left. This will leave a grid diagram so that all the crossings are on the left side with orientations flowing downwards, pictured in Fig. 14.

Now that all of the crossings have been grouped together with the appropriate downward orientation, the last hurdle is to create monotonicity of the crossings; each row needs to have only one crossing. To achieve this, working from top to bottom, identify the first row that has more than one crossing. Because of the downward orientation, there are only two possibilities for how the horizontal arc in the row enters and exists the row.

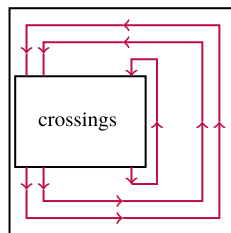


Fig. 14 Resulting grid format after performing all necessary mid-grid moves

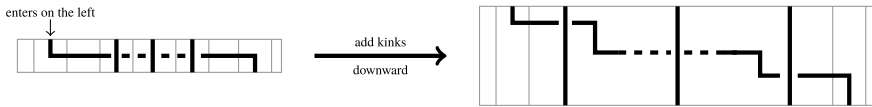


Fig. 15 Adding downward kinks

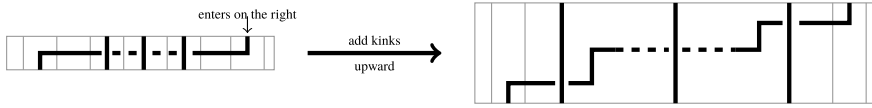


Fig. 16 Adding upward kinks

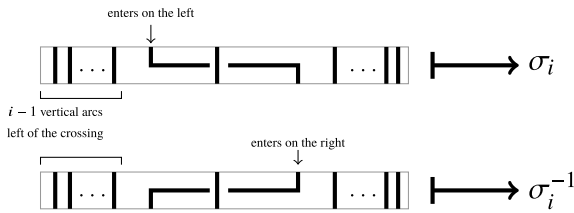


Fig. 17 Assignment rules for σ_i and σ_i^{-1}

One possibility is that the arc enters the row on the left of the crossings and exists on the right. Working from left to right, add a kink downward in between each vertical arc passing through the row, shown in Fig. 15. This forces each crossing to happen in a separate row.

The other possibility is that the horizontal portion of the arcs enters the row on the right and exists on the left. Working from left to right, add a kink upwards between each vertical stand, as in Fig. 16, again forcing each crossing to happen in a separate row.

At this point, you can read off the desired braid word by assigning a braid element to each row and listing the elements from top to bottom. Rows with out a crossing get assigned the identity braid element. Each row with a crossing gets assigned either a σ_i or σ_i^{-1} using the rules in Fig. 17.

The index i depends only on the number of vertical arcs passing through the row *to the left of the crossing*. Notice that it is not enough to just consider the column number of the crossing. There may be many columns to the left of the crossing without a vertical arc and these columns do not count towards the index of the σ_i . Whether you assign a generator σ_i or its inverse depends only on where (to the left or right of the crossing) the end of the horizontal arc enters the row. \square

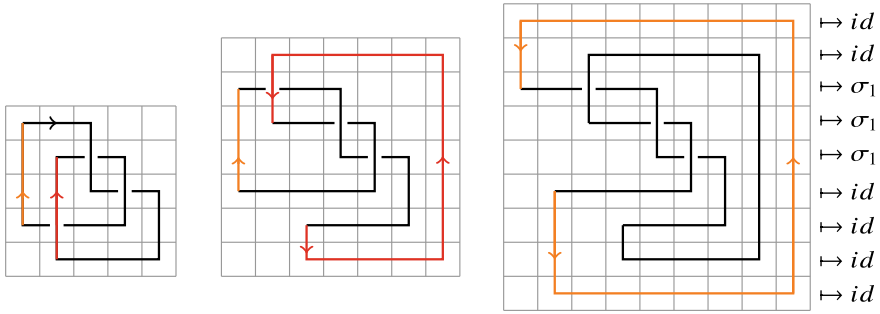


Fig. 18 Algorithm result for the Trefoil knot

Example: Starting with the grid diagram of a trefoil knot described earlier, this algorithm finds the braid σ_1^3 , shown in Fig. 18.

4.2.1 Computer Implementation

A working implementation in Python can be found in [11].

The first step in this algorithm is to fix an orientation of the knot within the grid. Because this implementation utilizes object oriented design, we define a new object type `OrientedGrid` which adds two attributes to the nodes:

(row, column, in-orientation, out-orientation).

Here the in/out-orientations are *above*, *below*, *left* or *right*. These correspond to the in-orientation flowing in from left, in from above, or the out-orientation is flowing to the left, to the box above etc.

For example, the oriented node (1, 2, *below*, *right*) shows:

Every grid has many different associated `OrientedGrids`. However, there are only two `OrientedGrids` that give rise to an orientation of the associated knot. The in and out orientations must agree on every row, column and node. The following algorithm systematically traverses the grid to produce an `OrientedGrid` that does gives rise to one choice of orientation for the associated knot.

orient

```

Input: grid, start= first node in grid
if find-row-neighbor(start).column > start.column then
    set out-orientation of start to “right”
else
    set out-orientation of start to “left”
end if
    
```



```

previous-node = start
current-node = find-row-neighbor(start)
while True do
  if previous-node.row == current-node.row then
    if previous-node.column > current-node.column then
      set in-orientation of current-node to “left”
    else:
      set in-orientation of current-node to “right”
    end if
    next = find-col-neighbor(current-node)
    if next.row > current-node.row then
      set out-orientation of current-node to “below”
    else
      set out-orientation of current-node to “above”
    end if
  else
    if previous-node.col == current-node.col then
      if previous-node.row > current-node.row then
        set in-orientation of current-node to “above”
      else
        set in-orientation of current-node to “below”
      end if
      next = find-row-neighbor(current-node)
      if next.column > current-node.column then
        set out-orientation of current-node to “right”
      else
        set out-orientation of current-node to “left”
      end if
      break if current-node=start
    end if
  end if
end while
return OrientedGrid

```

Now, all of the machinery is in place to implement the algorithm described in the proof of Alexander’s Theorem, which we will call grid-to-braid. As written, the grid-to-braid algorithm will not output a braid word, but will output a diagram of the knot represented by the grid after the appropriate midgrid moves are applied. The user then would have to manually make the crossings monotone and assign braid elements to each row, which is a simple visual process.

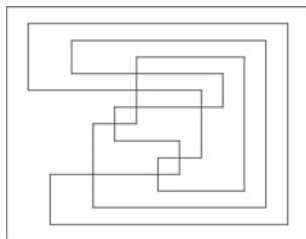


Fig. 19 Computer generated output grid diagram

grid-to-braid

```

Input: grid
OrientedGrid = orient(grid)
for node in OrientedGrid do
    mark node if out-orientation is "above"
end for
for marked nodes in OrientedGrid do
    if node.column is largest column of marked nodes then
        OrientedGrid = midgrid(node, node.column)
    end if
end for
return graph(OrientedGrid)

```

Example: The code in [11] when applied to the grid in Fig. 1 outputs the diagram in Fig. 19.

This diagram requires two adjustments because rows 6 and 10 each have two crossings. After adjusting, this diagram gives the braid word $\sigma_2\sigma_1\sigma_2^{-1}\sigma_1^{-1}\sigma_1^{-1}\sigma_2^{-1}\sigma_2^{-1}\sigma_1^{-1}$.

Acknowledgements Many of the results in this paper were written by the author in an unpublished VIGRE funded REU paper advised by Liam Watson in 2010. After attending Lambropoulou's talk at the Knots in Hellas 2016 conference, the author was inspired to re-write this paper to give a rounded perspective of the results. The author would like to especially thank Andrew Malta and Kevin Malta for their great help with the computer implementation.

References

1. J. Alexander, A lemma on a system of knotted curves. Proc. Natl. Acad. Sci. USA **9**, 93 (1923)
2. H. Brunn, Über verknötete kurven, in *Verhandlungen des Internationalen Mathematiker Kongresses (Zurich 1897)* (1898), pp. 256–259
3. P.R. Cromwell, Embedding knots and links in an open book. I. basic properties. Topol. Appl. **64**(1), 37–58 (1995)

4. I.A. Dynnikov, Arc-presentations of links: monotonic simplification. *Fundam. Math.* **190**, 29–76 (2006)
5. V.F.R. Jones, *The Jones Polynomial for Dummies*. Lecture Notes (2014)
6. L.H. Kauffman, S. Lambropoulou, Virtual braids. *Fundam. Math.* **184**, 159–186 (2004)
7. S. Lambropoulou, Short proofs of Alexander’s and Markov’s theorems. *Warwick University Preprint* (1990)
8. S. Lambropoulou, *A Study of Braids in 3-Manifolds*. Ph.D. Thesis, University of Warwick, Coventry, UK (1993)
9. H.J. Lee, K. Hong, H. Lee, and S. Oh, Mosaic number of knots
10. S. Lambropoulou, C.P. Rourke, Markov’s theorem in 3-manifolds. *Topol. Appl.* **78**(1-2), 95–122 (1997). Special issue on braid groups and related topics (Jerusalem, 1995)
11. A. Malta, K. Malta, N. Scherich. <https://github.com/nscherich/grid-algorithm>
12. H.R. Morton, Threading knot diagrams. *Math. Proc. Camb. Philos. Soc.* **99**, 247–260 (1986)
13. C. Manolescu, P. Ozsváth, Z. Szabó, D. Thurston, On combinatorial link Floer homology. *Geom. Topol.* **11**, 2339–2412 (2007)
14. K. Reidemeister, *Knotentheorie*, (Springer, Berlin, 1974), Reprint
15. N. Scherich, A simplification of grid equivalence. *Involve* **8**(25), 721–734 (2015)
16. P. Vogel, Representation of links by braids: a new algorithm. *Comment. Math. Helv.* **65**(1), 104–113 (1990)

Extending the Classical Skein



Louis H. Kauffman and Sofia Lambropoulou

Abstract We summarize the theory of a new skein invariant of classical links $H[H]$ that generalizes the regular isotopy version of the Homflypt polynomial, H . The invariant $H[H]$ is based on a procedure where we apply the skein relation only to crossings of distinct components, so as to produce collections of unlinked knots and then we evaluate the resulting knots using the invariant H and inserting at the same time a new parameter. This procedure, remarkably, leads to a generalization of H but also to generalizations of other known skein invariants, such as the Kauffman polynomial. We discuss the different approaches to the link invariant $H[H]$, the algebraic one related to its ambient isotopy equivalent invariant Θ , the skein-theoretic one and its reformulation into a summation of the generating invariant H on sublinks of a given link. We finally give examples illustrating the behaviour of the invariant $H[H]$ and we discuss further research directions and possible application areas.

Keywords Classical links · Yokonuma–Hecke algebras · Mixed crossings · Reidemeister moves · Stacks of knots · Homflypt polynomial · Kauffman polynomial · Dubrovnik polynomial · Skein relations · Skein invariants · 3-variable link invariant · Closed combinatorial formulae

2010 Mathematics Subject Classification 57M27 · 57M25

L. H. Kauffman

Department of Mathematics, Statistics, and Computer Science,
University of Illinois at Chicago, 851 South Morgan St., Chicago, IL 60607-7045, USA
e-mail: kauffman@uic.edu
URL: <http://homepages.math.uic.edu/~kauffman/>

Department of Mechanics and Mathematics, Novosibirsk State University,
Novosibirsk, Russia

S. Lambropoulou (✉)

School of Applied Mathematical and Physical Sciences, National Technical
University of Athens, Zografou Campus, GR-157 80 Athens, Greece
e-mail: sofia@math.ntua.gr
URL: <http://www.math.ntua.gr/~sofia>

© Springer Nature Switzerland AG 2019

C. C. Adams et al. (eds.), *Knots, Low-Dimensional Topology
and Applications*, Springer Proceedings in Mathematics & Statistics 284,
https://doi.org/10.1007/978-3-030-16031-9_11

225

Introduction

In this expository paper we summarize the theory of the new generalized skein invariant of links $H[H]$ based on the regular isotopy version H of the 2-variable Jones or Homflypt polynomial P . Recall that regular isotopy refers to invariance under the second and the third Reidemeister moves, while ambient isotopy refers to invariance under all three Reidemeister moves. We assume that the reader is familiar with the Reidemeister moves. Recall also that a *skein invariant* can be computed on each link diagram solely by the use of skein relations and a set of initial conditions.

The invariant $H[H]$ in its ambient isotopy version was originally discovered in [9] via Yokonuma–Hecke algebra traces and was named Θ . As shown in [9], the invariant Θ depends on three variables, and it is stronger than the Homflypt polynomial on links and different from the Kauffman polynomial. It was shown in [9] that Θ satisfies the skein relation of P , but only if it is applied on *mixed crossings*, that is, crossings formed by distinct components, or else if it is applied on a single knot. Then Θ is evaluated via a two-level procedure: for a given link we first untangle its compound knots using the skein relation of P and only then we evaluate on unions of unlinked knots by applying a new rule which is based on the evaluation of P on each knot, introducing at the same time a new variable, E . On knots the invariant Θ has the same evaluation as P . In [9] a list of six 3-component links are given, which are Homflypt equivalent but are distinguished by the invariant Θ and thus also by $H[H]$. See Table 1 in Sect. 1.

It was further discovered by W. B. R. Lickorish [9, Appendix] that the invariant Θ on a given link can be expressed by the closed combinatorial formula (1) given in Sect. 1, which is a summation over products of linking numbers and Homflypt evaluations of sublinks. The Lickorish formula can, thus, serve as a definition for Θ .

In [46] we give for the first time a self-contained skein theoretic proof for the invariant Θ .

A succinct exposition of the above can be found in [40]. These constructions opened the way to new research directions, cf. [1–3, 8–15, 19, 22–26, 28, 32–37, 45, 46, 53].

More precisely, let \mathcal{L} denote the set of classical oriented link diagrams. Let also L_+ be an oriented diagram with a positive crossing specified and let L_- be the same diagram but with that crossing switched. Let also L_0 indicate the same diagram but with the smoothing which is compatible with the orientations of the emanating arcs in place of the crossing, see (1). The diagrams L_+, L_-, L_0 comprise a so-called *oriented Conway triple*.

$$\begin{array}{ccc}
 \begin{array}{c} \nearrow \\ \nwarrow \end{array} & \begin{array}{c} \nwarrow \\ \nearrow \end{array} & \begin{array}{c} \text{---} \\ \text{---} \end{array} & (1) \\
 L_+ & L_- & L_0 &
 \end{array}$$

We then have the following:

Theorem 1 (cf. [46]) *Let $H(z, a)$ denote the regular isotopy version of the Homflypt polynomial. Then there exists a unique regular isotopy invariant of classical oriented links $H[H] : \mathcal{L} \rightarrow \mathbb{Z}[z, a^{\pm 1}, E^{\pm 1}]$, where z, a and E are indeterminates, defined by the following rules:*

1. On mixed crossings the following mixed skein relation holds:

$$H[H](\text{crossing}) - H[H](\text{crossing}) = z H[H](\text{triple}),$$

where crossing and triple denote an oriented Conway triple,

2. For a union of r unlinked knots, $\mathcal{K}^r := \sqcup_{i=1}^r K_i$, with $r \geq 1$, it holds that:

$$H[H](\mathcal{K}^r) = E^{1-r} H(\mathcal{K}^r).$$

We recall that the invariant $H(z, a)$ is determined by the following rules:

- (H1) For L_+, L_-, L_0 an oriented Conway triple, the following skein relation holds for mixed or self-crossings:

$$H(L_+) - H(L_-) = z H(L_0),$$

- (H2) The indeterminate a is the positive curl value for H :

$$H(\text{curl}) = a H(\text{crossing}) \quad \text{and} \quad H(\text{crossing}) = a^{-1} H(\text{curl}),$$

- (H3) On the standard unknot:

$$H(\bigcirc) = 1.$$

We also recall that the above defining rules imply the following:

- (H4) For a diagram of the unknot, U , H is evaluated by taking:

$$H(U) = a^{wr(U)},$$

where $wr(U)$ denotes the writhe of U –instead of 1 that is the case in the ambient isotopy category.

- (H5) H being the Homflypt polynomial, it is multiplicative on a union of unlinked knots, $\mathcal{K}^r := \sqcup_{i=1}^r K_i$. Namely, for $\eta := \frac{a-a^{-1}}{z}$ we have:

$$H(\mathcal{K}^r) = \eta^{r-1} \prod_{i=1}^r H(K_i).$$

Consequently, the evaluation of $H[H]$ on the standard unknot is $H[H](\bigcirc) = H(\bigcirc) = 1$.

In [46], we give for the first time a self-contained skein theoretic proof of the existence of Θ (in the form of $H[H]$), which was missing in the literature. We work out the skein theory from first principles, in order to investigate how it applies to this new invariant.

Recall further that one can obtain the classical Homflypt polynomial P from its regular isotopy counterpart H via the formula:

$$P(L) := a^{-wr(L)} H(L),$$

where $wr(L)$ is the total writhe of the oriented diagram L . Analogously, from our generalized regular isotopy invariant $H[H]$ one can derive an ambient isotopy invariant $P[P]$, which is precisely the invariant Θ mentioned earlier, via the formula [45, 46]:

$$\Theta = P[P](L) := a^{-wr(L)} H[H](L). \tag{2}$$

Furthermore, for an oriented link L on n components, we have the Lickorish-type combinatorial formula for $H[H]$:

Theorem 2 (cf. [45, 46]) *Let L be an oriented link with n components. Then*

$$H[H](L) = \sum_{k=1}^n \eta^{k-1} E_k \sum_{\pi} H(\pi L) \tag{3}$$

where the second summation is over all partitions π of the components of L into k (unordered) subsets and $H(\pi L)$ denotes the product of the Homflypt polynomials of the k sublinks of L defined by π . Furthermore, $E_k = (E^{-1} - 1)(E^{-1} - 2) \dots (E^{-1} - k + 1)$ and $\eta = \frac{a-a^{-1}}{z}$.

The reader should note that the formula above (the right hand side) is, by its very definition, a regular isotopy invariant of the link L . This follows from the regular isotopy invariance of H and the well-definedness of summing over all partitions of the link L into k parts. In fact the summations $I_k(L) = \sum_{\pi} H(\pi L)$, where π runs over all partitions of L into k parts, are each regular isotopy invariants of L . What is remarkable here is that these all assemble into the new invariant $H[H](L)$ with its striking two-level skein relation. We see from this combinatorial formula how the extra strength of $H[H](L)$ comes from its ability to detect certain sublinks of Homflypt-equivalent links. It further becomes clear from (3) that the linking numbers of sublinks, appearing in formula (1), do not play an intrinsic role in the theory.

In Sect. 3 of this paper we give the proof of Theorem 2 by proving by induction that it satisfies the two-tiered skein relations. Hence, formula (3) can be used as a mathematical basis for $H[H]$ and one could understand the skein relations on that basis.

In [46] we develop the skein theory for $H[H]$ in its full generality, namely by considering a 4-variable invariant $H[R]$, where we separate the two types of skein operations and which allows for R to be either H or any specialization of H . Yet, as it was observed by Karvounis [39], the full invariant $H[R]$ is topologically equivalent to the 3-variable invariant $H[H]$. The 4-variable formulation is, nevertheless, useful for clarifying the logic of the skein theoretic proofs of invariance. It could also be useful in some specific applications.

In [45] we use the 3-variable formulation exclusively and we proceed with defining associated state sum models for the new invariants. These state sums have a double

level due to the combination in our invariants of a skein calculation combined with the evaluation of a specific invariant on the knots that are at the bottom of the skein process. In [45] we discuss the context of statistical mechanics models and partition functions in relation to multiple level state summations and we speculate about possible applications for these ideas.

The skein-theoretic method generalizes also the Kauffman (Dubrovnik) polynomial to a new invariant of links in a completely analogous manner. The same is true for the Lickorish formula [45, 46] and the two-tiered state sum model construction [45]. This paper concentrates only on the Homflypt polynomial.

We note that there are only a few known skein invariants in the literature for classical knots and links. Skein invariants include: the Alexander–Conway polynomial [4, 5], the Jones polynomial [29], and the Homflypt polynomial [20, 30, 50, 52, 54], which specializes to both the Alexander–Conway and the Jones polynomial; there is also the bracket polynomial [41], the Brandt–Lickorish–Millett–Ho polynomial [6], the Dubrovnik polynomial, and the Kauffman polynomial [42], which specializes to both the bracket and the Brandt–Lickorish–Millett–Ho polynomial. More recently, we have the Juyumaya–Lambropoulou family of invariants $\Delta_{d,D}$ [34] and the analogous Chlouveraki–Juyumaya–Karvounis–Lambropoulou family of invariants $\Theta_d(q, \lambda_d)$ and their generalization $\Theta(q, \lambda, E)$ [9], which specializes to the Homflypt polynomial. Finally, we have the regular isotopy analogue $H[H]$ of $\Theta(q, \lambda, E)$ and the Kauffman–Lambropoulou generalizations $K[K]$ and $D[D]$ of the Kauffman and the Dubrovnik polynomials [45, 46]. These recent constructions alter the philosophy of classical skein-theoretic techniques, whereby mixed as well as self-crossings in a link diagram would get indiscriminately switched. In the skein approach to the invariants Θ_d , Θ , $H[H]$, $K[K]$ and $D[D]$ one first unlinks all components using the skein relation of a known skein invariant and then one evaluates that skein invariant on unions of unlinked knots, introducing at the same time a new variable.

The paper is organized as follows: In Sect. 1 we detail on the initial algebraic construction of the recently discovered skein invariants Θ_d and Θ . In Sect. 2 we present the main ideas for the skein-theoretic proof of the existence of the invariant $H[H]$ (Theorem 1). In Sect. 3 we prove the Lickorish-type closed combinatorial formula for $H[H]$ (Theorem 2). In Sect. 4 we give two key examples illustrating the behaviour of the invariant $H[H]$. In the first example we show by direct calculation how $H[H]$, specialized to directly generalize the Jones polynomial, detects a link (the Thistlethwaite Link) whose linking is invisible to the Jones polynomial. In the second example we detail how to specialize $H[H]$ so that it generalizes and strengthens the Kauffman bracket polynomial. Finally, in Sect. 5 we discuss further theoretical research directions emanating from the results presented in this paper, as well as possible relationships with two-tiered physical processes, such as strand switching and replication of DNA, particularly the possible relations with the replication of Kinetoplast DNA.

1 The Discovery of the Invariant Θ

Our motivation for the above generalization $H[H]$ of the invariant H as well as of the Kauffman polynomial [45, 46] is the following: In [34] 2-variable framed link invariants $\Gamma_{d,D}$ were constructed for each $d \in \mathbb{N}$ via the Yokonuma–Hecke algebras $Y_{d,n}(u)$, the Juyumaya trace and specializations imposed on the framing parameters of the trace, where D is any non-empty subset of $\mathbb{Z}/d\mathbb{Z}$. When restricted to classical links, seen as links with zero framings on all components, these invariants give rise to ambient isotopy invariants for classical links $\Delta_{d,D}$. We note that for $d = 1$ the algebra $Y_{1,n}$ coincides with the Iwahori–Hecke algebra of type A , the trace coincides with the Ocneanu trace and the invariant $\Delta_{1,\{1\}}$ coincides with the Homflypt polynomial, P . The invariants $\Delta_{d,D}$ were studied in [10, 35], especially their relation to P , but topological comparison had not been possible due to algebraic and diagrammatic difficulties.

Eventually, in [9, 15] another presentation using a different quadratic relation for the Yokonuma–Hecke algebra was adopted from [13] and the classical link invariants related to the new presentation of the Yokonuma–Hecke algebras were now denoted $\Theta_{d,D}$. For $d = 1$, $\Theta_{1,\{1\}}$ also coincides with P with variables related to the corresponding different presentation of the Iwahori–Hecke algebra. Consequently, in [9] a series of results were proved, which led to the topological identification of the invariants $\Theta_{d,D}$ and to their generalization to a new 3-variable ambient isotopy invariant Θ . Firstly, it was shown that the invariants $\Theta_{d,D}$ can be enumerated only by d and so they were denoted as Θ_d . It was also shown that on *knots* the invariants Θ_d are topologically equivalent to the Homflypt polynomial. Namely, if K is a *knot*, then

$$\Theta_d(q, z)(K) = P(q, dz)(K).$$

The above result was generalized to unions of unlinked knots. Namely, if $\mathcal{K}^r := \sqcup_{i=1}^r K_i$ is a union of r unlinked knots, we have

$$\Theta_d(q, z)(\mathcal{K}^r) = 1/d^{1-r} P(q, dz)(\mathcal{K}^r).$$

It was further shown in [9] that the invariants Θ_d satisfy on any oriented link diagram L a *mixed skein relation* on mixed crossings of L :

$$\frac{1}{\sqrt{\lambda_d}} \Theta_d(\text{crossing}) - \sqrt{\lambda_d} \Theta_d(\text{crossing}) = (q - q^{-1}) \Theta_d(\text{two parallel strands}),$$

where L_+, L_-, L_0 is an oriented Conway triple and $\lambda_d := \frac{dz - (q - q^{-1})}{dz}$. The above skein relation is identical to the skein relation of the Homflypt polynomial P considered at variables (q, λ_d) . As a consequence, the invariants Θ_d can be computed directly from the diagram L by applying the mixed skein relation between pairs of different components and gradually decomposing L into unions of unlinked knots that result as mergings of components of L via the smoothings in the mixed skein relation. Then, one has to evaluate the Homflypt polynomials of the unions of unlinked knots. Namely:

$$\Theta_d(L) = \sum_{k=1}^c \frac{1}{d^{1-k}} \sum_{\ell \in \mathcal{K}^k} p(\ell) P(\ell),$$

where c is the number of components of the link L , \mathcal{K}^k denotes the set of all split links ℓ with k split components, obtained from L by applying the mixed skein relation, for $k = 1, \dots, c$, and $p(\ell)$ are the coefficients coming from the application of the mixed skein relation. Finally, the above enabled in [9] the topological distinction of the invariants Θ_d from the Homflypt polynomial on Homflypt-equivalent pairs of links. Indeed, we present below data from [9]. Out of 4188 links (with up to 11 crossings), there are 89 pairs of P -equivalent links that do not differ just by orientation, that is, they are different links if considered as unoriented links. Using the data from *LinkInfo* [7], the invariants Θ_d were computed in [9] on all of them. Out of these 89 P -equivalent pairs of links, 83 are still Θ_d -equivalent for generic d , yet we found that the following six pairs of 3-component P -equivalent links are not Θ_d -equivalent for every $d \geq 2$:

The reader is referred to [9] or <http://www.math.ntua.gr/~sofia/yokonuma> for details of the computations.

To summarize, the family of invariants $\{\Theta_d(q, \lambda_d)\}_{d \in \mathbb{N}}$ is a family of relatively new skein invariants for links that includes the Homflypt polynomial P for $d = 1$ and are distinct from P for each $d > 1$. The invariants Θ_d are also *distinct from the Kauffman polynomial*, since they are topologically equivalent to P on knots [9, 15].

In [9] it is further proved that the family of invariants $\{\Theta_d(q, \lambda_d)\}_{d \in \mathbb{N}}$ generalizes to a new 3-variable skein link invariant $\Theta(q, \lambda, E)$, which is defined skein-theoretically on link diagrams by the following inductive rules:

1. On mixed crossings the following skein relation holds:

$$\frac{1}{\sqrt{\lambda}} \Theta(\text{crossing}) - \sqrt{\lambda} \Theta(\text{crossing}) = (q - q^{-1}) \Theta(\text{crossing}),$$

2. For $\mathcal{K}^r := \sqcup_{i=1}^r K_i$, a union of r unlinked knots, with $r \geq 1$, it holds that:

$$\Theta(\mathcal{K}^r) = E^{1-r} P(\mathcal{K}^r).$$

The invariant Θ specializes to P for $E = 1$ and to Θ_d for $E = 1/d$, and thus is stronger than P . Further, Θ satisfies the same properties as the invariants Θ_d and P , namely: multiplicative behaviour on connected sums, inversion of certain variables on mirror images, non-distinction of mutants. For details see [15]. The well-definedness of Θ is proved in [9] by comparing it to an invariant $\bar{\Theta}$ for tied links, constructed

Table 1 Six P -equivalent pairs of 3-component links that are not Θ -equivalent

$L11n358\{0, 1\}$	$L11n418\{0, 0\}$	$L10n79\{1, 1\}$	$L10n95\{1, 0\}$
$L11a467\{0, 1\}$	$L11a527\{0, 0\}$	$L11a404\{1, 1\}$	$L11a428\{0, 1\}$
$L11n325\{1, 1\}$	$L11n424\{0, 0\}$	$L10n76\{1, 1\}$	$L11n425\{1, 0\}$

from the algebra of braids and ties [1], but using now the new quadratic relation for it. The invariant $\overline{\Theta}$ is analogous but, as computational evidence indicates, not the same as the invariant $\overline{\Delta}$ for tied links of Aicardi and Juyumaya [2]. In Sect. 2 below we sketch an independent purely skein-theoretic proof for the well-definedness of Θ .

Finally, in [9, Appendix B] W.B.R. Lickorish proved the following closed combinatorial formula for the invariant Θ on an oriented link L with n components (proved also in [53] with different methods), showing that it is a mixture of Homflypt polynomials and linking numbers of sublinks of a given link:

$$\Theta(L) = \sum_{k=1}^n \mu^{k-1} E_k \sum_{\pi} \lambda^{\nu(\pi)} P(\pi L), \tag{1}$$

where the second summation is over all partitions π of the components of L into k (unordered) subsets and $P(\pi L)$ denotes the product of the Homflypt polynomials of the k sublinks of L defined by π . Furthermore, $\nu(\pi)$ is the sum of all linking numbers of pairs of components of L that are in distinct sets of π , $E_k = (E^{-1} - 1)(E^{-1} - 2) \dots (E^{-1} - k + 1)$, with $E_1 = 1$, and $\mu = \frac{\lambda^{-1/2} - \lambda^{1/2}}{q - q^{-1}}$. We see from this combinatorial formula that the extra strength of Θ_d and Θ comes from its ability to detect linking numbers and non-triviality of certain sublinks of the link L . In our regular isotopy formulation [45, 46], see Sect. 3 below, the linking numbers are eventually irrelevant.

2 Sketch of the Proof of Theorem 1

In this section we present the main ideas for proving Theorem 1 by skein-theoretic methods applied on link diagrams. The full details can be found in [46].

Assuming Theorem 1, one can compute $H[H]$ on any given oriented link diagram L by applying the following two-level procedure: skein rule (1) of Theorem 1 can be used to give an evaluation of $H[H](L_+)$ in terms of $H[H](L_-)$ and $H[H](L_0)$ or of $H[H](L_-)$ in terms of $H[H](L_+)$ and $H[H](L_0)$. We choose to switch mixed crossings so that the switched diagram is more unlinked than before. Applying this principle recursively we obtain a sum with polynomial coefficients and evaluations of $H[H]$ on unions of unlinked knots. These knots are formed by the mergings of components caused by the smoothings in the skein relation (1). To evaluate $H[H]$ on a given union of unlinked knots we then use the invariant H according to rule (2) of the Theorem. Note that the appearance of the indeterminate E in rule (2) for $H[H]$ is the critical difference between $H[H]$ and H . Finally, formula (H5) after Theorem 1 allows evaluations of the invariant H on individual knotted components and knowledge of H provides the basis for this.

More precisely, we apply the following algorithm for computing $H[H](L)$:

- Step 1: Order the components of L and choose a basepoint on each component. Then L becomes a *generic diagram*.
- Step 2: Start from the chosen point of component no. 1 and go along it in the direction of its orientation. When arriving at a mixed crossing for the first time along an under-arc switch it by rule (1), so that we pass by the mixed crossing along the over-arc. At the same time smooth the mixed crossing, obtaining a new diagram in which the two components of the crossing merge into one. Repeat for all mixed crossings of the first component. In the end, among all resulting diagrams there is only one with the same number of crossings as the initial diagram and in this one this component gets unlinked from the rest and lies above all of them. The other resulting diagrams have one less crossing and have the first component fused together with some other component. All resulting diagrams become generic by inheriting the choices made on L .
- Step 3: Proceed similarly with the second component of the maximal crossing diagram of Step 1, switching all its mixed crossings except for crossings involving the first component. In the end the second component gets unlinked from all the rest and lies below the first one and above all others in the maximal crossing diagram, while we also obtain diagrams containing mergings of the second component with others (except component one). Again all resulting diagrams inherit the generic choices from the starting one.
- Step 4: Continue in the same manner with all components in order, starting each time from the maximal crossing diagram of the previous step.
- Step 5: Apply the same procedure to all product diagrams coming from smoothings of mixed crossings. In the end we obtain a maximal crossing diagram which is a descending stack of knots, dL , the unlinked version of L , plus a linear sum of generic link diagrams ℓ with unlinked components resulting from the mergings of different components.
- Step 6: After all applications of rule (1) of Theorem 1 we have a linear sum of evaluations on split links ℓ . The evaluation of $H[H]$ on each ℓ reduces to the evaluation $H(\ell)$ by rule (2), where r is the number of knotted components of ℓ . In the end we obtain a linear sum of the values of the $H[H]$ on all resulting split links ℓ :

$$H[H](L) = \sum_{k=1}^c E^{1-k} \sum_{\ell \in \mathcal{K}^k} p(\ell) H(\ell),$$

where $p(\ell)$ are the coefficients coming from the applications of the mixed skein relation. Then, on each $H(\ell)$ rule (H5) applies and then rules (H1)–(H5) are employed.

The evaluation $H[H](L)$ is an element in the ring of finite Laurent polynomials $\mathbb{Z}[z, a^{\pm 1}, E^{\pm 1}]$ in three variables z, a, E .

For proving Theorem 1 one has to show that for any generic link diagram L the evaluation of $H[H](L)$ is independent of the choices made and invariant under regular isotopy moves, that is, Reidemeister moves II and III.

Our proof [46] follows in principle the logic of Lickorish–Millett of the well-definedness of the Homflypt polynomial [50] but with the necessary adaptations and modifications, taking for granted the well-definedness of H . The fact that the

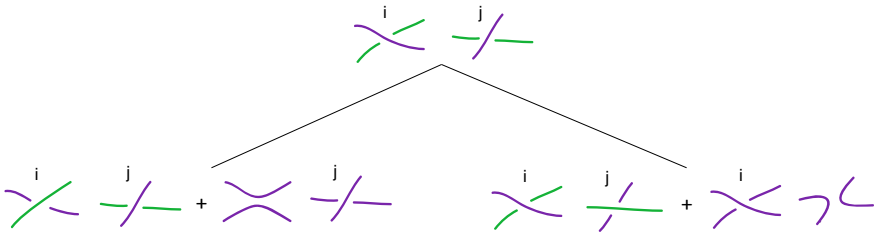


Fig. 1 Changing the sequence of switching mixed crossings

process treats self-crossings and mixed crossings differently is the main difference from [50] and it causes the need of special arguments. The main difficulty lies in proving independence of the computations under the sequence of mixed crossing switches.

Take for example the case where two mixed crossings need to be switched, which are shared between the same components, as abstracted in Fig. 1. Then, switching the first one causes the second one to become a self-crossing in the smoothed diagram, so we cannot operate on it. Changing now the order of switches results in different diagrams, which are not comparable in an obvious way, as is the case in [50]. In order to compare the polynomials before and after one needs first to reach down to the unlinked components of the diagrams and then apply the skein relation of the invariant H on the self-crossings in question. The complexity of the argument depends on the number of mixed crossings shared by the same components that need to be switched. So, our proof is done by induction on the distance of a generic diagram from its associated descending stack and not on the total number of crossings as in the classical argument [50].

A generic diagram on r components is said to be a *descending stack* if, when walking along the components of \mathcal{K}^r in their given order following the orientations and starting from their basepoints, every mixed crossing is first traversed along its over-arc. Clearly, the structure of a descending stack no longer depends on the choice of basepoints; it is entirely determined by the order of its components. Note also that a descending stack is isotopic to the corresponding split link \mathcal{K}^r comprising the r knotted components of the initial diagram. The descending stack of knots associated to a given generic link diagram L by applying the computing algorithm on L is denoted dL .

The *distance* of L from dL is the number of mixed crossing switches needed to arrive at dL by applying the computing algorithm. Clearly, the distance of a generic diagram is well-defined. We note that, if the generic diagram L has distance n from dL and rule (1) is applied on L within the computing algorithm, then the other two resulting diagrams have distances less than n from their associated descending stacks, if we assume that they are generic and their generic choices are inherited from L . Note finally that the distance of a descending stack is zero. The same is true for knots, on which we assume the well-definedness of H . Clearly, the basis of the induction is the set of all descending stacks, and rule (2) of Theorem 1 applies.

Namely, for a descending stack of knots \mathcal{K}^r we define $H[H](\mathcal{K}^r) := E^{1-r} R(\mathcal{K}^r)$. We then assume that the statement is valid for all generic link diagrams of distance less than n . Our aim is to prove that the statement is valid for all diagrams of distance n , independently of choices and Reidemeister II and III moves. More precisely, we prove for a generic diagram L of distance n :

- If the mixed crossings of L that differ from those of dL are switched in any sequence to achieve dL , then the corresponding polynomial $H[H](L)$ does not change.
- The polynomial $H[H](L)$ does not depend on the choice of basepoints (which is an immediate consequence of the above).
- The polynomial $H[H](L)$ satisfies the skein relation (1) of Theorem 1 on mixed crossings not increasing the distance.
- The polynomial $H[H](L)$ is invariant under Reidemeister II and Reidemeister III moves.
- The polynomial $H[H](L)$ is independent of the order of the components of L .

The proof of Theorem 1 then follows from the above. Once this Theorem is in place and by normalizing $H[H]$ to obtain its ambient isotopy counterpart (recall (2)), we have a direct skein-theoretic proof of the well-definedness of the invariant Θ , without the need of algebraic tools or the theory of tied links.

3 The Proof of Theorem 2

In this section we prove the closed combinatorial formula (3) for our regular isotopy invariant $H[H]$. See also [45, 46]. As we mentioned in the Introduction, in [9, Appendix B] W. B. R. Lickorish provides an analogous closed combinatorial formula for the definition of the invariant $\Theta = P[P]$, that uses the Homflypt polynomials and linking numbers of sublinks of a given link.

Proof of Theorem 2 We present the proof in full detail, as we believe it is instructive and it proves the existence of $H[H]$. Before proving the result, note the following equalities:

$$\begin{aligned}
 H(L_1 \sqcup L_2) &= \eta H(L_1) H(L_2), \\
 H[H](L_1 \sqcup L_2) &= \frac{\eta}{E} H[H](L_1) H[H](L_2).
 \end{aligned}$$

In the case where both L_1 and L_2 are knots the above formulæ follow directly from rule (H5) and rule (2) of Theorem 1. If at least one of L_1 and L_2 is a true link, then the formulæ follow by doing independent skein processes on L_1 and L_2 for bringing them down to unlinked components, and then using the defining rules above.

Suppose now that a diagram of L is given. The proof is by induction on the number n of the components of L and on the number u of crossing changes between distinct components required to change L to n unlinked knots. If $n = 1$ there is nothing to

prove. So assume the result true for $n - 1$ components and $u - 1$ crossing changes and prove it true for n and u .

The induction starts when $u = 0$. Then L is the union of n unlinked components L_1, \dots, L_n . A classic elementary result concerning the Homflypt polynomial shows that $H(L) = \eta^{n-1} H(L_1) \dots H(L_n)$. Furthermore, in this situation, for any k and π , $H(\pi L) = \eta^{n-k} H(L_1) \dots H(L_n)$. Note that $H[H](L) = E^{1-n} H(L) = \eta^{n-1} E^{1-n} H(L_1) \dots H(L_n)$. So, it is required to prove that:

$$\eta^{n-1} E^{1-n} = \eta^{n-1} \sum_{k=1}^n S(n, k)(E^{-1} - 1)(E^{-1} - 2) \dots (E^{-1} - k + 1), \quad (1)$$

where $S(n, k)$ is the number of partitions of a set of n elements into k subsets. Now it remains to prove that:

$$E^{1-n} = \sum_{k=1}^n S(n, k)(E^{-1} - 1)(E^{-1} - 2) \dots (E^{-1} - k + 1). \quad (2)$$

However, in the theory of combinatorics, $S(n, k)$ is known as a Stirling number of the second kind and this required formula is a well-known result about such numbers.

Now let $u > 0$. Suppose that in a sequence of u crossing changes that changes L into unlinked knots, the first change is to a crossing c of sign ϵ between components L_1 and L_2 . Let L' be L with the crossing changed and L^0 be L with the crossing annulled. Now, from the definition of $H[H]$,

$$H[H](L) = H[H](L') + \epsilon z H[H](L^0).$$

The induction hypotheses imply that the result is already proved for L' and L^0 so:

$$H[H](L) = \sum_{k=1}^n \eta^{k-1} E_k \sum_{\pi'} H(\pi' L') + \epsilon z \sum_{k=1}^{n-1} \eta^{k-1} E_k \sum_{\pi^0} H(\pi^0 L^0), \quad (3)$$

where π' runs through the partitions of the components of L' and π^0 through those of L^0 .

A sublink X^0 of L^0 can be regarded as a sublink X of L containing L_1 and L_2 but with L_1 and L_2 fused together by annulling the crossing at c . Let X' be the sublink of L' obtained from X by changing the crossing at c . Then

$$H(X) = H(X') + \epsilon z H(X^0).$$

This means that the second (big) term in (3) is

$$\sum_{k=1}^{n-1} \eta^{k-1} E_k \sum_{\rho} (H(\rho L) - H(\rho' L')), \tag{4}$$

where the summation is over all partitions ρ of the components of L for which L_1 and L_2 are in the same subset and ρ' is the corresponding partition of the components of L' .

Note that, for any partition π of the components of L inducing partition π' of L' , if L_1 and L_2 are in the same subset then we can have a difference between $H(\pi L)$ and $H(\pi' L')$, but when L_1 and L_2 are in different subsets then

$$H(\pi' L') = H(\pi L). \tag{5}$$

Thus, substituting (4) in (3) we obtain:

$$H[H](L) = \sum_{k=1}^n \eta^{k-1} E_k \left(\sum_{\pi'} H(\pi' L') + \sum_{\rho} (H(\rho L) - H(\rho' L')) \right), \tag{6}$$

where π' runs through all partitions of L' and ρ through partitions of L for which L_1 and L_2 are in the same subset. Note that, for $k = n$ the second sum is zero. Therefore:

$$H[H](L) = \sum_{k=1}^n \eta^{k-1} E_k \left(\sum_{\pi'} H(\pi' L') + \sum_{\rho} H(\rho L) \right), \tag{7}$$

where π' runs through only partitions of L' for which L_1 and L_2 are in different subsets and ρ through all partitions of L for which L_1 and L_2 are in the same subset. Note that in the transition from (6) to (7) the partition set π' changes from all partitions of L' to only partitions of L' for which L_1 and L_2 are in different subsets. The equality in (7) follows from the equality in (6) once this difference in partitions is appreciated. Hence, using (7) and also (5), we obtain:

$$H[H](L) = \sum_{k=1}^n \eta^{k-1} E_k \sum_{\pi} H(\pi L)$$

and the induction is complete. □

The combinatorial formula (3) shows that the strength of $H[H]$ against H comes from its ability to distinguish certain sublinks of Homflypt-equivalent links. Note that in the formula no linking numbers of sublinks are involved.

The formula (3) can be regarded by itself as a definition of the invariant $H[H]$, in the same way that the original Lickorish formula (1) can be regarded as a definition for the invariant $\Theta = P[P]$. Clearly, the two formulae, for $H[H]$ and for Θ , are interchangeable by writhe normalization, recall (2).

4 Examples

As pointed out in the Introduction, in Theorem 1 we could specialize the z , the a and the E in any way we wish. For example, if $a = 1$ then $H(z, 1)$ becomes the Alexander–Conway polynomial, while if $z = \sqrt{a} - 1/\sqrt{a}$ then $H(\sqrt{a} - 1/\sqrt{a}, a)$ becomes the unnormalized Jones polynomial V' . Furthermore, for the ambient isotopy version $P[P]$ of $H[H]$, which coincides with the invariant Θ [9], we have for $E = 1/d$ that $P[P]$ coincides with the invariant Θ_d (for $E = 1$ it coincides with P), recall Sect. 1. For $z = \sqrt{a} - 1/\sqrt{a}$ the invariant $P[P]$ is renamed to $V[V]$, V denoting the ambient isotopy version of the Jones polynomial, and it coincides with the 2-variable specialization of Θ , $\theta(a, E)$ [26]. The invariant θ generalizes V and is stronger than V .

We shall now present two examples illustrating the behaviour and strength of the invariant $H[H]$, also presented in [26, 45, 46].

Example 1

Here is an example, worked by L. Kauffman and D. Goundaroulis, showing how $H[H]$ and the combinatorial formula give extra information in the case of a 2-component link. We will use the ambient isotopy version of the Jones polynomial V and so first work with a skein calculation of V and then with a calculation of the generalized invariant $V[V]$. We use the link *ThLink* first found by Morwen Thistlethwaite [58] and generalized by Eliahou, Kauffman and Thistlethwaite [17]. This link of two components is not detectable by the Jones polynomial, but it is detectable by our extension of the Jones polynomial. In doing this calculation, Louis Kauffman and Dimos Goundaroulis used Dror Bar Natan’s Knot Theory package for Mathematica. In this package the Jones polynomial is a function of q and satisfies the skein relation:

$$q^{-1}V_{K_+}(q) - qV_{K_-}(q) = (q^{1/2} - q^{-1/2})V_{K_0}(q)$$

where K_+, K_-, K_0 is a usual skein triple. Let

$$a = q^2, z = (q^{1/2} - q^{-1/2}), b = qz, c = q^{-1}z.$$

Then we have the skein expansion formulae:

$$V_{K_+} = aV_{K_-} + bV_{K_0} \quad \text{and} \quad V_{K_-} = a^{-1}V_{K_+} - cV_{K_0}.$$

In Fig. 2 we show the Thistlethwaite link that is invisible to the Jones polynomial. In the same figure we show an unlink of two components obtained from the Thistlethwaite link by switching four crossings. In Fig. 3 we show the links K_1, K_2, K_3, K_4 that are intermediate to the skein process for calculating the invariants of L by first switching only crossings between different components. From this it follows that the knots and links in the figures indicated here satisfy the formula

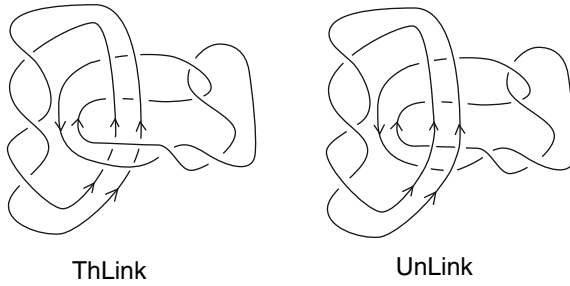


Fig. 2 The Thistlethwaite Link and Unlink

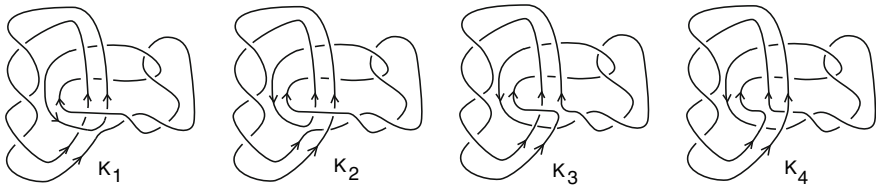


Fig. 3 The links K_1, K_2, K_3, K_4

$$V_{ThLink} = bV_{K_1} + abV_{K_2} - ca^2V_{K_3} - acV_{K_4} + V_{Unlinked}.$$

This can be easily verified by the specific values computed in Mathematica:

$$V_{ThLink} = -q^{-1/2} - q^{1/2}$$

$$V_{K_1} = -1 + \frac{1}{q^7} - \frac{2}{q^6} + \frac{3}{q^5} - \frac{4}{q^4} + \frac{4}{q^3} - \frac{4}{q^2} + \frac{3}{q} + q$$

$$V_{K_2} = 1 - \frac{1}{q^9} + \frac{3}{q^8} - \frac{4}{q^7} + \frac{5}{q^6} - \frac{6}{q^5} + \frac{5}{q^4} - \frac{4}{q^3} + \frac{3}{q^2} - \frac{1}{q}$$

$$V_{K_3} = 1 - \frac{1}{q^9} + \frac{2}{q^8} - \frac{3}{q^7} + \frac{4}{q^6} - \frac{4}{q^5} + \frac{4}{q^4} - \frac{3}{q^3} + \frac{2}{q^2} - \frac{1}{q}$$

$$V_{K_4} = -1 - \frac{1}{q^6} + \frac{2}{q^5} - \frac{2}{q^4} + \frac{3}{q^3} - \frac{3}{q^2} + \frac{2}{q} + q$$

$$V_{Unlinked} = \frac{1}{q^{13/2}} - \frac{1}{q^{11/2}} - \frac{1}{q^{7/2}} + \frac{1}{q^{3/2}} - \frac{1}{\sqrt{q}} - q^{3/2}$$

This is a computational proof that the Thistlethwaite link is not detectable by the Jones polynomial. If we compute $V[V]_{ThLink}$ then we modify the computation to:

$$V[V]_{ThLink} = bV_{K_1} + abV_{K_2} - ca^2V_{K_3} - acV_{K_4} + E^{-1}V_{Unlinked}.$$

and it is quite clear that this is non-trivial when the new variable E is not equal to 1.

On the other hand, the Lickorish formula for this case tells us that, for the regular isotopy version of the Jones polynomial $V'[V']_{ThLink}$,

$$V'[V']_{ThLink} = \eta(E^{-1} - 1)V'_{K_1} V'_{K_2} + V'_{ThLink}(q)$$

whenever we evaluate a 2-component link. Note that $\eta(E^{-1} - 1)$ is non-zero whenever $E \neq 1$. Thus it is quite clear that the Lickorish formula detects the Thistlethwaite link since the Jones polynomials of the components of that link are non-trivial. We have, in this example, given two ways to see how the extended invariant detects the link $ThLink$. The first way shows how the detection works in the extended skein theory. The second way shows how it works using the Lickorish formula.

Example 2

In this example, we point out how to see a generalization of the Jones polynomial (in Kauffman bracket form) as a specialization of our invariant $H[H]$. We begin with an expansion formula for the bracket polynomial that is adapted to our situation. View Fig. 4. At the top of the figure we show the standard oriented expansion of the bracket. If the reader is familiar with the usual unoriented expansion [43], then this oriented expansion can be read by forgetting the orientations. The oriented states in this state summation contain smoothings of the type illustrated in the far right hand terms of the two formulas at the top of the figure. We call these *disoriented smoothings* since two arrowheads point to each other at these sites. Then by multiplying the two equations by A and A^{-1} respectively, we obtain a difference formula of the type: $A \langle K_+ \rangle - A^{-1} \langle K_- \rangle = (A^2 - A^{-2}) \langle K_0 \rangle$, where K_+ denotes the local appearance of a positive crossing, K_- denotes the local appearance of a negative crossing and K_0 denotes the local appearance of standard oriented smoothing. The difference equation

Fig. 4 Oriented bracket with Homflypt skein relation

$$\begin{aligned} \langle \text{crossing} \rangle &= A \langle \text{smoothing} \rangle + A^{-1} \langle \text{disoriented smoothing} \rangle \\ \langle \text{crossing} \rangle &= A^{-1} \langle \text{smoothing} \rangle + A \langle \text{disoriented smoothing} \rangle \\ A \langle \text{crossing} \rangle - A^{-1} \langle \text{crossing} \rangle &= (A^2 - A^{-2}) \langle \text{smoothing} \rangle \end{aligned}$$

Define $\{K\} = A^{wr(K)} \langle K \rangle$.

$$\{ \text{crossing} \} - \{ \text{crossing} \} = (A^2 - A^{-2}) \{ \text{smoothing} \}$$

eliminates the disoriented terms. It then follows easily from this difference equation that if we define a *curly bracket* by the equation

$$\{K\} = A^{wr(K)} \langle K \rangle$$

where $wr(K)$ is the diagram writhe, then we have a Homflypt type relation for $\{K\}$ as follows:

$$\{K_+\} - \{K_-\} = (A^2 - A^{-2})\{K_0\}. \tag{1}$$

This means that we can regard $\{K\}$ as a specialization of the Homflypt polynomial and so we can use it as the invariant H for $H[H]$.

From Fig. 4 it is not difficult to see that

$$\{K_+\} = A^2\{K_0\} + \{K_\infty\} \tag{2}$$

and

$$\{K_-\} = A^{-2}\{K_0\} + \{K_\infty\}. \tag{3}$$

Here K_∞ denotes the disoriented smoothing shown in the figure. These formulas then define the skein expansion for the curly bracket. The reader should note that the difference of these two expansion Eqs. (2) and (3) is the skein relation (1) for the curly bracket in Homflypt form.

5 Discussing Mathematical Directions and Applications

We shall now discuss some possible research directions emanating from the results presented in the paper. We further contemplate how these new ideas can be applied to physical situations. For more discussion and new research problems the interested reader is directed to [46].

1. The categorification of the new skein invariants is another interesting problem. For the invariant $\theta(q, E)$, which generalizes the Jones polynomial and is a specialization of $\Theta(q, z, E)$ this is accomplished in [8].
2. While the Homflypt polynomial is linked with the knot algebras discussed in Sect. 1, it is an open and interesting question to have a similar full connection to an appropriate knot algebra for the generalization of the Kauffman polynomial [45, 46], such as the framization of the BMW algebra proposed in [36, 37]. See also [3].
3. Another direction for further research is to extend the results in [9, 45, 46] to the area of skein modules and invariants of links in three-manifolds, and invariants of three-manifolds (see for example [14, 16, 19, 21, 27, 48, 49, 55, 59]).

4. In [45] we give state summation models for the new invariants, based on the skein process for computing them. That is, we use the skein process that first unlinks links and then computes invariants on stacks of knots. We systematize this process and write it as a state summation that is a version of the skein template algorithm explained in [44]. The interest in rewriting as a state summation is that we can then interface our work with ideas from both statistical mechanics and from state models for knot invariants. We also can examine how this state summation process with its multiple levels may be analogous to the way certain physical systems have structural levels. These matters are discussed in detail in [45]. We will return to these themes in subsequent papers on the subject.
5. In DNA, strand switching using topoisomerases of types I and II is vital for the structure of DNA recombination and DNA replication [18]. The mixed interaction of topological change and physical evolution of the molecules in vitro may benefit from a mixed state summation that averages quantities respecting the hierarchy of interactions.
6. Remarkably, the process of separation and evaluation described in [9, 45, 46] and also here is analogous to proposed processing of Kinetoplast DNA [51] where there are huge links of DNA circles and these must undergo processes that both unlink them from one another and produce new copies for each circle of DNA. The double-tiered structure of DNA replication for the Kinetoplast appears to be related to the mathematical patterns of our double state summations. For chainmail DNA, if the reader examines the Wiki on Kinetoplast DNA, he/she will note that Topoisomerase II figures crucially in the self-replication [47].

Acknowledgements Louis H. Kauffman’s work was supported by the Laboratory of Topology and Dynamics, Novosibirsk State University (contract no. 14.Y26.31.0025 with the Ministry of Education and Science of the Russian Federation). Sofia Lambropoulou’s work has been co-financed by the European Union (European Social Fund—ESF) and Greek national funds through the Operational Program “Education and Lifelong Learning” of the National Strategic Reference Framework (NSRF)—Research Funding Program: THALES: Reinforcement of the interdisciplinary and/or inter-institutional research and innovation, MIS: 380154.

References

1. F. Aicardi, J. Juyumaya, Markov trace on the algebra of braids and ties. *Moscow Math. J.* **16**(3), 397–431 (2016)
2. F. Aicardi, J. Juyumaya, Tied Links. *J. Knot Theory Ramif.* **25**(9), 1641001 (2016)
3. F. Aicardi, J. Juyumaya, Kauffman type invariants for tied links. *J. Mathematische Zeitschrift* (2017). <https://doi.org/10.1007/s00209-017-1966-0>
4. J.W. Alexander, Topological invariants of knots and links. *Trans. Am. Math. Soc.* **30**(2), 275–306 (1928)
5. J.H. Conway, An enumeration of knots and links and some of their algebraic properties, in *Computational Problems in Abstract Algebra (Proc. Conf. Oxford, 1967)* (Pergamon, Oxford, 1970), pp. 329–358
6. R. Brandt, W.B.R. Lickorish, K.C. Millett, A polynomial invariant for unoriented knots and links. *Invent. Math.* **84**, 563–573 (1986)

7. J.C. Cha, C. Livingston, LinkInfo: Table of Knot Invariants (2015). <http://www.indiana.edu/~linkinfo>
8. M. Chlouveraki, D. Goundaroulis, A. Kontogeorgis, S. Lambropoulou, A skein relation for Khovanov homology and a categorification of the θ -invariant. Submitted for publication
9. M. Chlouveraki, J. Juyumaya, K. Karvounis, S. Lambropoulou, Identifying the invariants for classical knots and links from the Yokonuma–Hecke algebra. *Int. Math. Res. Notices* 74 (2018). <https://doi.org/10.1093/imrn/my013>.
10. M. Chlouveraki, S. Lambropoulou, The Yokonuma–Hecke algebras and the Homflypt polynomial. *J. Knot Theory Ramif.* 22(14), 1350080 (2013)
11. M. Chlouveraki, G. Pouchin, Determination of the representations and a basis for the Yokonuma–Temperley–Lieb algebra. *Algebras Representation Theory* 18 (2015)
12. M. Chlouveraki, G. Pouchin, Representation theory and an isomorphism theorem for the Framization of the Temperley–Lieb algebra. *Mathematische Zeitschrift* 285(3), 1357–1380 (2017)
13. M. Chlouveraki, L. Poulain d’Andecy, Representation theory of the Yokonuma–Hecke algebra. *Adv. Math.* 259, 134–172 (2014)
14. M. Chlouveraki, L. Poulain D’ Andecy, Markov trace on affine and cyclotomic Yokonuma–Hecke algebras. *Int. Math. Res. Notices* (14), 4167–4228 (2016). <https://doi.org/10.1093/imrn/mv257>.
15. S. Chmutov, S. Jablan, K. Karvounis, S. Lambropoulou, On the knot invariants from the Yokonuma–Hecke algebras. *J. Knot Theory Ramif.* 25(9) (2016). <https://doi.org/10.1142/S0218216516410042>
16. I. Diamantis, S. Lambropoulou, The Braid Approach to the HOMFLYPT Skein Module of the Lens Spaces $L(p, 1)$, in *Algebraic Modeling of Topological and Computational Structures and Applications, Athens, Greece, July 1–3, 2015*, vol. 219, Springer Proceedings in Mathematics and Statistics (PROMS), ed. by S. Lambropoulou, P. Stefanias, D. Theodorou, L.H. Kauffman, 2017. <https://doi.org/10.1007/978-3-319-68103-0>
17. S. Eliahou, L.H. Kauffman, M.B. Thistlethwaite, Infinite families of links with trivial Jones polynomial. *Topology* 42, 155–169 (2003)
18. C. Ernst, D.W. Sumners, Solving tangle equations arising in a DNA recombination model. *Math. Proc. Camb. Philos. Soc.* 126(1), 23–36 (1999)
19. M. Flores, J. Juyumaya, S. Lambropoulou, A Framization of the Hecke algebra of Type B. *J. Pure Appl. Algebra* (2017). <https://doi.org/10.1016/j.jpaa.2017.05.006>
20. P. Freyd, D. Yetter, J. Hoste, W.B.R. Lickorish, K.C. Millett, A. Ocneanu, A new polynomial invariant of knots and links. *Bull. AMS* 12, 239–246 (1985)
21. B. Gabrovšek, M. Mroczkowski, The Homlypt skein module of the lens spaces $L(p, 1)$. *Topol. Appl.* 175, 72–80 (2014)
22. D. Goundaroulis, Framization of the Temperley–Lieb algebra and related link invariants, Ph.D. thesis, Department of Mathematics, National Technical University of Athens (2014)
23. D. Goundaroulis, J. Juyumaya, A. Kontogeorgis, S. Lambropoulou, The Yokonuma–Temperley–Lieb algebra. *Banach Center Pub.* 103, 73–95 (2014)
24. D. Goundaroulis, J. Juyumaya, A. Kontogeorgis, S. Lambropoulou, Framization of the Temperley–Lieb algebra. *Math. Res. Lett.* 24(2), 299–345 (2017). <http://dx.doi.org/10.4310/MRL.2017.v24.n2.a3>
25. D. Goundaroulis, S. Lambropoulou, Classical link invariants from the framizations of the Iwahori–Hecke algebra and the Temperley–Lieb algebra of type A. *J. Knot Theory Ramif.* 26(9) (2017). <https://doi.org/10.1142/S0218216517430052>
26. D. Goundaroulis, S. Lambropoulou, A new two-variable generalization of the Jones polynomial. *J. Knot Theory Ramif.* (2016). To appear. Special issue dedicated to the Proceedings of the International Conference on Knots, Low-dimensional Topology and Applications—Knots in Hellas 2016. [arXiv:1608.01812](https://arxiv.org/abs/1608.01812) [math.GT]
27. J. Hoste, M. Kidwell, Dichromatic link invariants. *Trans. Am. Math. Soc.* 321(1), 197–229 (1990)
28. N. Jacon, L. Poulain d’Andecy, An isomorphism theorem for Yokonuma–Hecke algebras and applications to link invariants. *Mathematische Zeitschrift* 283, 301–338 (2016)

29. V.F.R. Jones, A polynomial invariant for knots via von Neumann algebras. *Bull. Am. Math. Soc. (N.S.)* **12**(1), 103–111 (1985)
30. V.F.R. Jones, Hecke algebra representations of braid groups and link polynomials. *Ann. Math.* **126**(2), 335–388 (1987)
31. J. Juyumaya, Markov trace on the Yokonuma-Hecke algebra. *J. Knot Theory Ramif.* **13**, 25–39 (2004)
32. J. Juyumaya, A partition temperley–Lieb algebra (2013). [arXiv:1304.5158](https://arxiv.org/abs/1304.5158) [math.QA]
33. J. Juyumaya, S. Lambropoulou, An invariant for singular knots. *J. Knot Theory Ramif.* **18**(6), 825–840 (2009)
34. J. Juyumaya, S. Lambropoulou, p -adic framed braids II. *Adv. Math.* **234**, 149–191 (2013)
35. J. Juyumaya, S. Lambropoulou, An adelic extension of the Jones polynomial, in *The mathematics of knots*, vol. 1, Contributions in the Mathematical and Computational Sciences, ed. by M. Banagl, D. Vogel (Springer, Berlin, 2009), pp. 825–840
36. J. Juyumaya, S. Lambropoulou, Modular framization of the BMW algebra (2010). [arXiv:1007.0092v1](https://arxiv.org/abs/1007.0092v1) [math.GT]
37. J. Juyumaya, S. Lambropoulou, On the framization of knot algebras, in *New Ideas in Low-dimensional Topology*, Series on Knots and Everything, ed. by L.H. Kauffman, V. Manturov (World Scientific, Singapore, 2014). [arXiv:1406.6849v1](https://arxiv.org/abs/1406.6849v1) [math.GT]
38. K. Karvounis, Enabling computations for link invariants coming from the Yokonuma-Hecke algebras. *J. Knot Theory Ramif.* **25**(9) (2016). <https://doi.org/10.1142/S0218216516410042>
39. Private communication with K. Karvounis, April 2017
40. K. Karvounis, S. Lambropoulou, Link invariants from the Yokonuma-Hecke algebras, in *Algebraic Modeling of Topological and Computational Structures and Applications, THALES, Athens, Greece, July 1–3, 2015*, vol. 219, Springer Proceedings in Mathematics and Statistics (PROMS), ed. by S. Lambropoulou, P. Stefanias, D. Theodorou, L.H. Kauffman, 2017. <https://doi.org/10.1007/978-3-319-68103-0>
41. L.H. Kauffman, State models and the Jones polynomial. *Topology* **26**(3), 395–407 (1987)
42. L.H. Kauffman, An invariant of regular isotopy. *Trans. Am. Math. Soc.* **318**, 417–471 (1990)
43. L.H. Kauffman, State models for link polynomials. *Enseignement Math.* **36**(2), 1–37 (1990)
44. L.H. Kauffman, *Knots and Physics*, vol. 53, 4th edn., Series on Knots and Everything (World Scientific Publishing Co. Pte. Ltd., NJ, 2013)
45. L.H. Kauffman, S. Lambropoulou, Skein invariants of links and their state sum models. *Symmetry* **9**, 226 (2017). <https://doi.org/10.3390/sym9100226>.
46. L.H. Kauffman, S. Lambropoulou, New skein invariants of links. Submitted for publication. [arXiv:1703.03655](https://arxiv.org/abs/1703.03655)
47. <https://en.wikipedia.org/wiki/Kinetoplast>
48. S. Lambropoulou, Solid torus links and Hecke algebras of B-type, in *Quantum Topology*, ed. by D.N. Yetter (World Scientific Press, Singapore, 1994), pp. 225–245
49. S. Lambropoulou, Knot theory related to generalized and cyclotomic Hecke algebras of Type B. *J. Knot Theory Ramif.* **8**(5), 621–658 (1999)
50. W.B.R. Lickorish, K.C. Millett, A polynomial invariant of oriented links. *Topology* **26**(1), 107–141 (1987)
51. D. Michieletto, D. Marenduzzo, M.S. Turner, Topology Regulation during Replication of the Kinetoplast DNA. [arXiv:1408.4237](https://arxiv.org/abs/1408.4237) [cond-mat.soft]
52. A. Ocneanu, A polynomial invariant for knots—A combinatorial and algebraic approach (1984). Preprint MSRI, Berkeley
53. L. Poulain d’Andecy, E. Wagner, The HOMFLYPT polynomials of sublinks and the Yokonuma–Hecke algebras. *Proc. R. Soc. Edinburgh A*. To appear
54. J.H. Przytycki, P. Traczyk, Invariants of links of Conway type. *Kobe J. Math.* **4**, 115–139 (1987)
55. J.H. Przytycki, Skein modules of 3-manifolds. *Bull. Pol. Acad. Sci.: Math.* **39**(1–2), 91–100 (1991)
56. R.L. Ricca, X. Liu, HOMFLYPT polynomial is the best quantifier for topological cascades of vortex knots. *Fluid Dyn. Res.* **50**, 011404 (2018)

57. M.W. Scheeler, D. Kleckner, D. Proment, G.L. Kindlmann, W.T.M. Irvine, Helicity conservation by flow across scales in reconnecting vortex links and knots. [arXiv:1404.6513](https://arxiv.org/abs/1404.6513) [physics.flu-dyn]
58. M. Thistlethwaite, Links with trivial Jones polynomial. *J. Knot Theory Ramif.* **10**, 641–643 (2001)
59. V.G. Turaev, The Conway and Kauffman modules of the solid torus. *Zap. Nauchn. Sem. Lomi* **167**, 79–89. English translation: *J. Soviet Math.* **1990**, 2799–2805 (1988)

From the Framisation of the Temperley–Lieb Algebra to the Jones Polynomial: An Algebraic Approach



Maria Chlouveraki

Abstract We prove that the Framisation of the Temperley–Lieb algebra is isomorphic to a direct sum of matrix algebras over tensor products of classical Temperley–Lieb algebras. We use this result to obtain a closed combinatorial formula for the invariants for classical links obtained from a Markov trace on the Framisation of the Temperley–Lieb algebra. For a given link L , this formula involves the Jones polynomials of all sublinks of L , as well as linking numbers.

Keywords Temperley–Lieb algebra · Yokonuma–Hecke algebra · Framisation of the Temperley–Lieb algebra · Markov trace · Jones polynomial · θ -Invariant

2010 Mathematics Subject Classification 20C08 · 05E10 · 16S80 · 57M27 · 57M25

1 Introduction

The Temperley–Lieb algebra was introduced by Temperley and Lieb [33] for its applications in statistical mechanics. Jones later showed that the Temperley–Lieb algebra can be seen as a quotient of the Iwahori–Hecke algebra of type A [15, 16]. He defined a Markov trace on it, now known as the Jones–Ocneanu trace, and used it to construct his famous polynomial link invariant, the Jones polynomial. This trace is also obtained as a specialisation of a trace defined directly on the Iwahori–Hecke algebra of type A , which in turn yields another famous polynomial link invariant, the HOMFLYPT polynomial (also known as the 2-variable Jones polynomial) [13, 30].

Yokonuma–Hecke algebras were introduced by Yokonuma [34] as generalisations of Iwahori–Hecke algebras. In particular, the Yokonuma–Hecke algebra of type A

M. Chlouveraki (✉)

Laboratoire de Mathématiques de Versailles, UVSQ, Université Paris-Saclay,
Bâtiment Fermat, 45 Avenue des Etats-Unis, 78035 Versailles Cedex, France
e-mail: maria.chlouveraki@uvsq.fr

© Springer Nature Switzerland AG 2019

C. C. Adams et al. (eds.), *Knots, Low-Dimensional Topology
and Applications*, Springer Proceedings in Mathematics & Statistics 284,
https://doi.org/10.1007/978-3-030-16031-9_12

247

is the centraliser algebra associated to the permutation representation with respect to a maximal unipotent subgroup of the general linear group over a finite field. In later years, Juyumaya transformed its presentation to “almost” the one we use in this paper and defined a Markov trace on it [17–19]. Following Jones’s method, Juyumaya and Lambropoulou used this trace to construct invariants for framed [20, 21], classical [22] and singular [23] links. The exact presentation for the Yokonuma–Hecke algebra used in this paper is due to the author and Poulain d’Andecy, who modified Juyumaya’s generators in [6]. Although the construction of the Markov trace with the new generators remains similar, the invariants for framed and classical links obtained from it are not topologically equivalent to the Juyumaya–Lambropoulou ones. This was shown in [1], where the new invariants were constructed and studied. From then on, these are the “standard” link invariants obtained from the Yokonuma–Hecke algebra of type A . As was shown in [1], they are not topologically equivalent to the HOMFLYPT polynomial and they can be generalised to a 3-variable skein link invariant which is stronger than the HOMFLYPT. In the Appendix of [1], Lickorish gave a closed combinatorial formula for the value of these invariants on a link L which involves the HOMFLYPT polynomials of all sublinks of L and linking numbers. The same formula was obtained independently by Poulain d’Andecy and Wagner [29] with a method that we will discuss at the end of the introduction.

However, even prior to these recent results, there has been algebraic and topological interest in finding the analogue of the Temperley–Lieb algebra in the Yokonuma–Hecke algebra context. On the one hand, it would be a quotient of the Yokonuma–Hecke algebra of type A such that the Markov trace on it would yield a link invariant more general (and now known to be stronger) than the Jones polynomial. On the other hand, it would be an example of the “framisation technique” proposed in [24], according to which known algebras producing invariants for classical links can be enhanced with extra generators to produce invariants for framed links; the foremost example is the Yokonuma–Hecke algebra of type A which can be seen as the “framisation” of the Iwahori–Hecke algebra of type A .

Goundaroulis, Juyumaya, Kontogeorgis and Lambropoulou defined and studied three quotients of the Yokonuma–Hecke algebra of type A as potential candidates [10, 11]. The one with the biggest topological interest was named “Framisation of the Temperley–Lieb algebra” and it is the one that produces the suitable generalisation of the Jones polynomial. The claim that this algebra is the natural analogue of the Temperley–Lieb algebra in this context is backed up algebraically by our findings in [4, 5], where we studied the representation theory of this algebra and we proved the isomorphism theorem that we present in the current article (we also studied similarly the other two candidates in [3, 5]). This isomorphism theorem states that the Framisation of the Temperley–Lieb algebra is isomorphic to a direct sum of matrix algebras over tensor products of Temperley–Lieb algebras. This result makes the Framisation of the Temperley–Lieb algebra the ideal analogue of the Temperley–Lieb algebra in view of Lusztig’s isomorphism theorem [27], later reproved by Jacon and Poulain d’Andecy [14], Espinoza and Ryom–Hansen [8] and Rostam [31], that states that the Yokonuma–Hecke algebra of type A is isomorphic to a direct sum of matrix algebras over tensor products of Iwahori–Hecke algebras of type A . To

prove our result we use the exposition by Jacon and Poulain d’Andecy, where the presentation of the Yokonuma–Hecke algebra of [6] is used. In fact, in the current article we do not use the modified presentation that we used in [4, 5], but we reprove the results with the presentation of [6] in order to be with agreement with the most recent topologically oriented papers on the subject (for example, [1, 12, 28], etc.). Finally, our isomorphism theorem allows us to determine a basis for the Framisation of the Temperley–Lieb algebra.

In the second part of the paper, we discuss the Markov traces on the Temperley–Lieb algebra and its Framisation, and explain how we can use them to define invariants for classical links from the former and for framed and classical links from the latter. We give several definitions of the traces. First, for the Jones–Ocneanu trace, we give the original definition of [16] of a trace that needs to be normalised and re-scaled to produce a link invariant, and another one which is already invariant under positive and negative stabilisation. As far as the Juyumaya trace is concerned, the original definition of [18] is also of a trace that needs to be normalised and re-scaled to produce a link invariant (under certain conditions discussed in detail in Sect. 4.3), and its stabilised version appears as a particular case of the Markov traces defined and classified by Jacon and Poulain d’Andecy in [14]. Using these stabilised traces and the isomorphism theorem for the Yokonuma–Hecke algebra, Poulain d’Andecy and Wagner in [29] obtained closed formulas that connect the values of these traces on a link L with the values of the HOMFLYPT polynomials of all sublinks of L , as well as their linking numbers. For a certain choice of parameters (see [28, Remarks 5.4] for details), they obtain Lickorish’s formula. Here, we consider stabilised Markov traces on the Framisation of the Temperley–Lieb algebra, and thanks to our isomorphism theorem, we obtain an analogue of this formula for the link invariants obtained in this case; for a given link L , this formula involves the Jones polynomials of all sublinks of L and linking numbers. This formula has been obtained independently in [12] as a specialisation of Lickorish’s formula.

2 The Temperley–Lieb Algebra and Its Framisation

In this section, we give the definition of the Temperley–Lieb algebra as a quotient of the Iwahori–Hecke algebra of type A given by Jones [16], as well as the definition of the Framisation of the Temperley–Lieb algebra as a quotient of the Yokonuma–Hecke algebra of type A given by Goundaroulis–Juyumaya–Kontogeorgis–Lambropoulou [11]. From now on, let $n \in \mathbb{N}$, $d \in \mathbb{N}^*$, and let q be an indeterminate. Set $R := \mathbb{C}[q, q^{-1}]$.

2.1 The Iwahori–Hecke Algebra $\mathcal{H}_n(q)$

The Iwahori–Hecke algebra of type A, denoted by $\mathcal{H}_n(q)$, is an R -associative algebra generated by the elements

$$G_1, \dots, G_{n-1}$$

subject to the following braid relations:

$$\begin{aligned} G_i G_j &= G_j G_i && \text{for all } i, j = 1, \dots, n - 1 \text{ with } |i - j| > 1, \\ G_i G_{i+1} G_i &= G_{i+1} G_i G_{i+1} && \text{for all } i = 1, \dots, n - 2, \end{aligned} \tag{1}$$

together with the quadratic relations:

$$G_i^2 = 1 + (q - q^{-1})G_i \quad \text{for all } i = 1, \dots, n - 1. \tag{2}$$

Remark 1 If we specialise q to 1, the defining relations (1)–(2) become the defining relations for the symmetric group \mathfrak{S}_n . Thus, the algebra $\mathcal{H}_n(q)$ is a deformation of $\mathbb{C}[\mathfrak{S}_n]$, the group algebra of \mathfrak{S}_n over \mathbb{C} .

Remark 2 The relations (1) are defining relations for the classical braid group B_n on n strands. Thus, the algebra $\mathcal{H}_n(q)$ arises naturally as a quotient of the braid group algebra $R[B_n]$ over the quadratic relations (2).

Let $w \in \mathfrak{S}_n$ and let $w = s_{i_1} s_{i_2} \dots s_{i_r}$ be a reduced expression for w , where s_i denotes the transposition $(i, i + 1)$. We define $\ell(w) := r$ to be the length of w . By Matsumoto’s lemma, the element $G_w := G_{i_1} G_{i_2} \dots G_{i_r}$ is well defined. It is well-known that the set $\mathcal{B}_{\mathcal{H}_n(q)} := \{G_w\}_{w \in \mathfrak{S}_n}$ forms a basis of $\mathcal{H}_n(q)$ over R , which is called the standard basis. One presentation of the standard basis $\mathcal{B}_{\mathcal{H}_n(q)}$ is the following:

$$\left\{ (G_{i_1} G_{i_1-1} \dots G_{i_1-k_1}) \dots (G_{i_p} G_{i_p-1} \dots G_{i_p-k_p}) \mid \begin{array}{l} 1 \leq i_1 < \dots < i_p < n \\ i_j - k_j \geq 1 \quad \forall j = 1, \dots, p \end{array} \right\}$$

In particular, $\mathcal{H}_n(q)$ is a free R -module of rank $n!$.

2.2 The Temperley–Lieb Algebra $TL_n(q)$

Let $i = 1, \dots, n - 2$. We set

$$G_{i,i+1} := 1 + qG_i + qG_{i+1} + q^2G_iG_{i+1} + q^2G_{i+1}G_i + q^3G_iG_{i+1}G_i = \sum_{w \in (s_i, s_{i+1})} q^{\ell(w)} G_w.$$

We define the Temperley–Lieb algebra $TL_n(q)$ to be the quotient $\mathcal{H}_n(q)/I_n$, where I_n is the ideal generated by the element $G_{1,2}$ (if $n \leq 2$, we take $I_n = \{0\}$). We have $G_{i,i+1} \in I_n$ for all $i = 1, \dots, n - 2$, since

$$G_{i,i+1} = (G_1 G_2 \dots G_{n-1})^{i-1} G_{1,2} (G_1 G_2 \dots G_{n-1})^{-(i-1)}.$$

Jones [15] has shown that the set $\mathcal{B}_{\text{TL}_n(q)}$ defined as:

$$\left\{ (G_{i_1} G_{i_1-1} \dots G_{i_1-k_1}) \dots (G_{i_p} G_{i_p-1} \dots G_{i_p-k_p}) \mid \begin{array}{l} 1 \leq i_1 < \dots < i_p < n \\ 1 \leq i_1 - k_1 < \dots < i_p - k_p < n \end{array} \right\}$$

is a basis of $\text{TL}_n(q)$ as an R -module. In particular, $\text{TL}_n(q)$ is a free R -module of rank C_n , where C_n denotes the n -th Catalan number, that is,

$$C_n = \frac{1}{n+1} \binom{2n}{n} = \frac{1}{n+1} \sum_{k=0}^n \binom{n}{k}^2.$$

2.3 The Yokonuma–Hecke Algebra $Y_{d,n}(q)$

The Yokonuma–Hecke algebra of type A , denoted by $Y_{d,n}(q)$, is an R -associative algebra generated by the elements

$$g_1, \dots, g_{n-1}, t_1, \dots, t_n$$

subject to the following relations:

$$\begin{aligned} (b_1) \quad & g_i g_j = g_j g_i && \text{for all } i, j = 1, \dots, n-1 \text{ with } |i-j| > 1, \\ (b_2) \quad & g_i g_{i+1} g_i = g_{i+1} g_i g_{i+1} && \text{for all } i = 1, \dots, n-2, \\ (f_1) \quad & t_i t_j = t_j t_i && \text{for all } i, j = 1, \dots, n, \\ (f_2) \quad & t_j g_i = g_i t_{s_i(j)} && \text{for all } i = 1, \dots, n-1 \text{ and } j = 1, \dots, n, \\ (f_3) \quad & t_j^d = 1 && \text{for all } j = 1, \dots, n, \end{aligned} \tag{3}$$

where s_i denotes the transposition $(i, i+1)$, together with the quadratic relations:

$$g_i^2 = 1 + (q - q^{-1}) e_i g_i \quad \text{for all } i = 1, \dots, n-1, \tag{4}$$

where

$$e_i := \frac{1}{d} \sum_{s=0}^{d-1} t_i^s t_{i+1}^{d-s}. \tag{5}$$

Note that we have $e_i^2 = e_i$ and $e_i g_i = g_i e_i$ for all $i = 1, \dots, n-1$. Moreover, we have

$$t_i e_i = t_{i+1} e_i \quad \text{for all } i = 1, \dots, n-1. \tag{6}$$

Remark 3 If we specialise q to 1, the defining relations (3)–(4) become the defining relations for the complex reflection group $G(d, 1, n) \cong (\mathbb{Z}/d\mathbb{Z}) \wr \mathfrak{S}_n$. Thus, the alge-

bra $Y_{d,n}(q)$ is a deformation of $\mathbb{C}[G(d, 1, n)]$. Moreover, for $d = 1$, the Yokonuma–Hecke algebra $Y_{1,n}(q)$ coincides with the Iwahori–Hecke algebra $\mathcal{H}_n(q)$ of type A .

Remark 4 The relations (b_1) , (b_2) , (f_1) and (f_2) are defining relations for the classical framed braid group $\mathcal{F}_n \cong \mathbb{Z} \wr B_n$, where B_n is the classical braid group on n strands, with the t_j ’s being interpreted as the “elementary framings” (framing 1 on the j th strand). The relations $t_j^d = 1$ mean that the framing of each braid strand is regarded modulo d . Thus, the algebra $Y_{d,n}(q)$ arises naturally as a quotient of the framed braid group algebra $R[\mathcal{F}_n]$ over the modular relations (f_3) and the quadratic relations (4). Moreover, relations (3) are defining relations for the modular framed braid group $\mathcal{F}_{d,n} \cong (\mathbb{Z}/d\mathbb{Z}) \wr B_n$, so the algebra $Y_{d,n}(q)$ can be also seen as a quotient of the modular framed braid group algebra $R[\mathcal{F}_{d,n}]$ over the quadratic relations (4).

Remark 5 The generators g_i satisfying the quadratic relation (4) were introduced in [6]. In all the papers [2, 10, 11, 18, 21–23] prior to [6], the authors consider the braid generators $\bar{g}_i := g_i + (q - 1) e_i g_i$ (and thus, $g_i = \bar{g}_i + (q^{-1} - 1) e_i \bar{g}_i$), which satisfy the quadratic relation

$$\bar{g}_i^2 = 1 + (q^2 - 1) e_i + (q^2 - 1) e_i \bar{g}_i, \tag{7}$$

and the Yokonuma–Hecke algebra is defined over the ring $\mathbb{C}[q^2, q^{-2}]$. Note that

$$e_i \bar{g}_i = q e_i g_i \quad \text{for all } i = 1, \dots, n - 1. \tag{8}$$

Remark 6 In [4, 5], we consider the braid generators $\tilde{g}_i := q g_i$, which satisfy the quadratic relation

$$\tilde{g}_i^2 = q^2 + (q^2 - 1) e_i \tilde{g}_i, \tag{9}$$

and the Yokonuma–Hecke algebra is defined over the ring $\mathbb{C}[q^2, q^{-2}]$. Note that

$$e_i \tilde{g}_i = q e_i g_i \quad \text{for all } i = 1, \dots, n - 1. \tag{10}$$

Let $w \in \mathfrak{S}_n$ and let $w = s_{i_1} s_{i_2} \dots s_{i_r}$ be a reduced expression for w . By Matsumoto’s lemma, the element $g_w := g_{i_1} g_{i_2} \dots g_{i_r}$ is well defined. Juyumaya [18] has shown that the set

$$\mathcal{B}_{Y_{d,n}(q)} := \{t_1^{a_1} t_2^{a_2} \dots t_n^{a_n} g_w \mid 0 \leq a_1, a_2, \dots, a_n \leq d - 1, w \in \mathfrak{S}_n\}$$

forms a basis of $Y_{d,n}(q)$ over R , which is called the *standard basis*. In particular, $Y_{d,n}(q)$ is a free R -module of rank $d^n n!$.

2.4 The Framisation of the Temperley–Lieb Algebra $\text{FTL}_{d,n}(q)$

Let $i = 1, \dots, n - 2$. We set

$$g_{i,i+1} := 1 + qg_i + qg_{i+1} + q^2g_i g_{i+1} + q^2g_{i+1}g_i + q^3g_i g_{i+1}g_i = \sum_{w \in \langle s_i, s_{i+1} \rangle} q^{\ell(w)} g_w.$$

We define the *Framisation of the Temperley–Lieb algebra* to be the quotient $Y_{d,n}(q)/I_{d,n}$, where $I_{d,n}$ is the ideal generated by the element $e_1e_2g_{1,2}$ (if $n \leq 2$, we take $I_{d,n} = \{0\}$). Note that, due to (6), the product e_1e_2 commutes with g_1 and with g_2 , so it commutes with $g_{1,2}$. Further, we have $e_i e_{i+1} g_{i,i+1} \in I_{d,n}$ for all $i = 1, \dots, n - 2$, since

$$e_i e_{i+1} g_{i,i+1} = (g_1 g_2 \dots g_{n-1})^{i-1} e_1 e_2 g_{1,2} (g_1 g_2 \dots g_{n-1})^{-(i-1)}.$$

Remark 7 The ideal $I_{d,n}$ is also generated by the element $\sum_{0 \leq a, b \leq d-1} t_1^a t_2^b t_3^{-a-b} g_{1,2}$.

Remark 8 For $d = 1$, the Framisation of the Temperley–Lieb algebra $\text{FTL}_{1,n}(q)$ coincides with the classical Temperley–Lieb algebra $\text{TL}_n(q)$.

Remark 9 In [11], the Framisation of the Temperley–Lieb algebra is defined to be the quotient $Y_{d,n}(q)/\bar{I}_{d,n}$, where $\bar{I}_{d,n}$ is the ideal generated by the element $e_1e_2\bar{g}_{1,2}$, where

$$\bar{g}_{1,2} = 1 + \bar{g}_1 + \bar{g}_2 + \bar{g}_1\bar{g}_2 + \bar{g}_2\bar{g}_1 + \bar{g}_1\bar{g}_2\bar{g}_1.$$

Due to (8) and the fact that the e_i 's are idempotents, we have $e_1e_2\bar{g}_{1,2} = e_1e_2g_{1,2}$, and so $I_{d,n} = \bar{I}_{d,n}$.

Remark 10 In [4, 5], we define the Framisation of the Temperley–Lieb algebra to be the quotient $Y_{d,n}(q)/\tilde{I}_{d,n}$, where $\tilde{I}_{d,n}$ is the ideal generated by the element $e_1e_2\tilde{g}_{1,2}$, where

$$\tilde{g}_{1,2} = 1 + \tilde{g}_1 + \tilde{g}_2 + \tilde{g}_1\tilde{g}_2 + \tilde{g}_2\tilde{g}_1 + \tilde{g}_1\tilde{g}_2\tilde{g}_1.$$

Due to (10) and the fact that the e_i 's are idempotents, we have $e_1e_2\tilde{g}_{1,2} = e_1e_2g_{1,2}$, and so $I_{d,n} = \tilde{I}_{d,n}$.

3 An Isomorphism Theorem for the Framisation of the Temperley–Lieb Algebra

Lusztig has proved that Yokonuma–Hecke algebras are isomorphic to direct sums of matrix algebras over certain subalgebras of classical Iwahori–Hecke algebras [27, §34]. For the Yokonuma–Hecke algebras $Y_{d,n}(q)$, these are all tensor products of Iwahori–Hecke algebras of type A . This result was reproved in [14] using the

presentation of $Y_{d,n}(q)$ given by Juyumaya. Since we use the same presentation, we will use the latter exposition of the result in order to prove an analogous statement for $\text{FTL}_{d,n}(q)$.

3.1 Compositions and Young Subgroups

Let $\mu \in \text{Comp}_d(n)$, where

$$\text{Comp}_d(n) = \{\mu = (\mu_1, \mu_2, \dots, \mu_d) \in \mathbb{N}^d \mid \mu_1 + \mu_2 + \dots + \mu_d = n\}.$$

We say that μ is a *composition of n with d parts*. The Young subgroup \mathfrak{S}_μ of \mathfrak{S}_n is the subgroup $\mathfrak{S}_{\mu_1} \times \mathfrak{S}_{\mu_2} \times \dots \times \mathfrak{S}_{\mu_d}$, where \mathfrak{S}_{μ_1} acts on the letters $\{1, \dots, \mu_1\}$, \mathfrak{S}_{μ_2} acts on the letters $\{\mu_1 + 1, \dots, \mu_1 + \mu_2\}$, and so on. Thus, \mathfrak{S}_μ is a parabolic subgroup of \mathfrak{S}_n generated by the transpositions $s_j = (j, j + 1)$ with $j \in J^\mu := \{1, \dots, n - 1\} \setminus \{\mu_1, \mu_1 + \mu_2, \dots, \mu_1 + \mu_2 + \dots + \mu_{d-1}\}$.

We have an Iwahori–Hecke algebra $\mathcal{H}^\mu(q)$ associated with \mathfrak{S}_μ , which is the subalgebra of $\mathcal{H}_n(q)$ generated by $\{G_j \mid j \in J^\mu\}$. The algebra $\mathcal{H}^\mu(q)$ is a free R -module with basis $\{G_w \mid w \in \mathfrak{S}_\mu\}$, and it is isomorphic to the tensor product (over R) of Iwahori–Hecke algebras $\mathcal{H}_{\mu_1}(q) \otimes \mathcal{H}_{\mu_2}(q) \otimes \dots \otimes \mathcal{H}_{\mu_d}(q)$ (with $\mathcal{H}_{\mu_i}(q) \cong R$ if $\mu_i \leq 1$).

For $i = 1, \dots, d$, we denote by ρ_{μ_i} the natural surjection $\mathcal{H}_{\mu_i}(q) \twoheadrightarrow \mathcal{H}_{\mu_i}(q)/I_{\mu_i} \cong \text{TL}_{\mu_i}(q)$, where I_{μ_i} is the ideal generated by $G_{\mu_1 + \dots + \mu_{i-1} + 1, \mu_1 + \dots + \mu_{i-1} + 2}$ if $\mu_i > 2$ and $I_{\mu_i} = \{0\}$ if $\mu_i \leq 2$. We obtain that $\rho^\mu := \rho_{\mu_1} \otimes \rho_{\mu_2} \otimes \dots \otimes \rho_{\mu_d}$ is a surjective R -algebra homomorphism $\mathcal{H}^\mu(q) \twoheadrightarrow \text{TL}^\mu(q)$, where $\text{TL}^\mu(q)$ denotes the tensor product of Temperley–Lieb algebras $\text{TL}_{\mu_1}(q) \otimes \text{TL}_{\mu_2}(q) \otimes \dots \otimes \text{TL}_{\mu_d}(q)$.

3.2 An Isomorphism Theorem for the Yokonuma–Hecke Algebra $Y_{d,n}(q)$

Let $\{\xi_1, \dots, \xi_d\}$ be the set of all d -th roots of unity (ordered arbitrarily). Let χ be an irreducible character of the abelian group $\mathcal{A}_{d,n} \cong (\mathbb{Z}/d\mathbb{Z})^n$ generated by the elements t_1, t_2, \dots, t_n . There exists a primitive idempotent of $\mathbb{C}[\mathcal{A}_{d,n}]$ associated with χ defined as

$$E_\chi := \prod_{j=1}^n \left(\frac{1}{d} \sum_{s=0}^{d-1} \chi(t_j^s) t_j^{d-s} \right) = \prod_{j=1}^n \left(\frac{1}{d} \sum_{s=0}^{d-1} \chi(t_j)^s t_j^{d-s} \right).$$

Moreover, we can define a composition $\mu^\chi \in \text{Comp}_d(n)$ by setting

$$\mu_i^\chi := \#\{j \in \{1, \dots, n\} \mid \chi(t_j) = \xi_i\} \quad \text{for all } i = 1, \dots, d.$$

Conversely, given a composition $\mu \in \text{Comp}_d(n)$, we can consider the subset $\text{Irr}^\mu(\mathcal{A}_{d,n})$ of $\text{Irr}(\mathcal{A}_{d,n})$ defined as

$$\text{Irr}^\mu(\mathcal{A}_{d,n}) := \{\chi \in \text{Irr}(\mathcal{A}_{d,n}) \mid \mu^\chi = \mu\}.$$

There is an action of \mathfrak{S}_n on $\text{Irr}^\mu(\mathcal{A}_{d,n})$ given by

$$w(\chi)(t_j) := \chi(t_{w^{-1}(j)}) \quad \text{for all } w \in \mathfrak{S}_n, j = 1, \dots, n.$$

Let $\chi_1^\mu \in \text{Irr}^\mu(\mathcal{A}_{d,n})$ be the character given by

$$\left\{ \begin{array}{llll} \chi_1^\mu(t_1) & = \cdots = & \chi_1^\mu(t_{\mu_1}) & = \xi_1 \\ \chi_1^\mu(t_{\mu_1+1}) & = \cdots = & \chi_1^\mu(t_{\mu_1+\mu_2}) & = \xi_2 \\ \chi_1^\mu(t_{\mu_1+\mu_2+1}) & = \cdots = & \chi_1^\mu(t_{\mu_1+\mu_2+\mu_3}) & = \xi_3 \\ \vdots & \vdots \vdots \vdots & \vdots & \vdots \vdots \\ \chi_1^\mu(t_{\mu_1+\dots+\mu_{d-1}+1}) & = \cdots = & \chi_1^\mu(t_n) & = \xi_d \end{array} \right.$$

The stabiliser of χ_1^μ under the action of \mathfrak{S}_n is the Young subgroup \mathfrak{S}_μ . In each left coset in $\mathfrak{S}_n/\mathfrak{S}_\mu$, we can take a representative of minimal length; such a representative is unique (see, for example, [9, §2.1]). Let

$$\{\pi_{\mu,1}, \pi_{\mu,2}, \dots, \pi_{\mu,m_\mu}\}$$

be this set of distinguished left coset representatives of $\mathfrak{S}_n/\mathfrak{S}_\mu$, with

$$m_\mu = \frac{n!}{\mu_1! \mu_2! \dots \mu_d!}$$

and the convention that $\pi_{\mu,1} = 1$. Then, if we set

$$\chi_k^\mu := \pi_{\mu,k}(\chi_1^\mu) \quad \text{for all } k = 1, \dots, m_\mu,$$

we have

$$\text{Irr}^\mu(\mathcal{A}_{d,n}) = \{\chi_1^\mu, \chi_2^\mu, \dots, \chi_{m_\mu}^\mu\}.$$

We now set

$$E_\mu := \sum_{\chi \in \text{Irr}^\mu(\mathcal{A}_{d,n})} E_\chi = \sum_{k=1}^{m_\mu} E_{\chi_k^\mu}.$$

Since the set $\{E_\chi \mid \chi \in \text{Irr}(\mathcal{A}_{d,n})\}$ forms a complete set of orthogonal idempotents in $Y_{d,n}(q)$, and

$$t_j E_\chi = E_\chi t_j = \chi(t_j) E_\chi \quad \text{and} \quad g_w E_\chi = E_{w(\chi)} g_w \tag{11}$$

for all $\chi \in \text{Irr}(\mathcal{A}_{d,n})$, $j = 1, \dots, n$ and $w \in \mathfrak{S}_n$, we have that the set $\{E_\mu \mid \mu \in \text{Comp}_d(n)\}$ forms a complete set of central orthogonal idempotents in $Y_{d,n}(q)$ (cf. [14, §2.4]). In particular, we have the following decomposition of $Y_{d,n}(q)$ into a direct sum of two-sided ideals:

$$Y_{d,n}(q) = \bigoplus_{\mu \in \text{Comp}_d(n)} E_\mu Y_{d,n}(q).$$

We can now define an R -linear map

$$\Psi_\mu : E_\mu Y_{d,n}(q) \rightarrow \text{Mat}_{m_\mu}(\mathcal{H}^\mu(q))$$

as follows: for all $k \in \{1, \dots, m_\mu\}$ and $w \in \mathfrak{S}_n$, we set

$$\Psi_\mu(E_{\chi_k^\mu} g_w) := G_{\pi_{\mu,k}^{-1} w \pi_{\mu,l}} M_{k,l},$$

where $l \in \{1, \dots, m_\mu\}$ is uniquely defined by the relation $w(\chi_l^\mu) = \chi_k^\mu$ and $M_{k,l}$ is the elementary $m_\mu \times m_\mu$ matrix with 1 in position (k, l) . Note that $\pi_{\mu,k}^{-1} w \pi_{\mu,l} \in \mathfrak{S}_\mu$. We also define an R -linear map

$$\Phi_\mu : \text{Mat}_{m_\mu}(\mathcal{H}^\mu(q)) \rightarrow E_\mu Y_{d,n}(q)$$

as follows: for all $k, l \in \{1, \dots, m_\mu\}$ and $w \in \mathfrak{S}_\mu$, we set

$$\Phi_\mu(G_w M_{k,l}) := E_{\chi_k^\mu} g_{\pi_{\mu,k} w \pi_{\mu,l}^{-1}} E_{\chi_l^\mu}.$$

Then we have the following [14, Theorem 3.1]:

Theorem 1 *Let $\mu \in \text{Comp}_d(n)$. The linear map Ψ_μ is an isomorphism of R -algebras with inverse map Φ_μ . As a consequence, the map*

$$\Psi_{d,n} := \bigoplus_{\mu \in \text{Comp}_d(n)} \Psi_\mu : Y_{d,n}(q) \rightarrow \bigoplus_{\mu \in \text{Comp}_d(n)} \text{Mat}_{m_\mu}(\mathcal{H}^\mu(q))$$

is also an isomorphism of R -algebras, with inverse map

$$\Phi_{d,n} := \bigoplus_{\mu \in \text{Comp}_d(n)} \Phi_\mu : \bigoplus_{\mu \in \text{Comp}_d(n)} \text{Mat}_{m_\mu}(\mathcal{H}^\mu(q)) \rightarrow Y_{d,n}(q).$$

Remark 11 In [5], we show that we can construct similar isomorphisms over the smaller ring $\mathbb{C}[q^2, q^{-2}]$ when we consider the generators $\tilde{g}_i := qg_i$ and $\tilde{G}_i := qG_i$. Note that

$$\Psi_\mu(E_{\chi_k^\mu} \tilde{g}_w) := q^{\ell(w) - \ell(\pi_{\mu,k}^{-1} w \pi_{\mu,l})} \tilde{G}_{\pi_{\mu,k}^{-1} w \pi_{\mu,l}} M_{k,l}$$

and

$$\Phi_\mu(\widetilde{G}_w M_{k,l}) := q^{\ell(w) - \ell(\pi_{\mu,k}^{-1} w \pi_{\mu,l})} E_{\chi_k^\mu} \widetilde{g}_{\pi_{\mu,k} w \pi_{\mu,l}^{-1}} E_{\chi_l^\mu}.$$

In order to do this, we make use of Deodhar’s lemma (see, for example, [9, Lemma 2.1.2]) about the distinguished left coset representatives of $\mathfrak{S}_n/\mathfrak{S}_\mu$:

Lemma 1 (Deodhar’s lemma) *Let $\mu \in \text{Comp}_d(n)$. For all $k \in \{1, \dots, m_\mu\}$ and $i = 1, \dots, n - 1$, let $l \in \{1, \dots, m_\mu\}$ be uniquely defined by the relation $s_i(\chi_l^\mu) = \chi_k^\mu$. We have*

$$\pi_{\mu,k}^{-1} s_i \pi_{\mu,l} = \begin{cases} 1 & \text{if } k \neq l; \\ s_j & \text{if } k = l, \end{cases}$$

for some $j \in J^\mu$.

Deodhar’s lemma implies that, for all $i = 1, \dots, n - 1$, $\Psi_\mu(E_\mu \widetilde{g}_i)$ is a symmetric matrix whose diagonal non-zero coefficients are of the form \widetilde{G}_j with $j \in J^\mu$, while all non-diagonal non-zero coefficients are equal to q . Thus, if consider the diagonal matrix

$$U_\mu := \sum_{k=1}^{m_\mu} q^{\ell(\pi_{\mu,k})} M_{k,k},$$

the coefficients of the matrix $U_\mu \Psi_\mu(E_\mu \widetilde{g}_i) U_\mu^{-1}$ satisfy:

$$(U_\mu \Psi_\mu(E_\mu \widetilde{g}_i) U_\mu^{-1})_{k,l} = q^{(\ell(\pi_{\mu,k}) - \ell(\pi_{\mu,l}))} (\Psi_\mu(E_\mu \widetilde{g}_i))_{k,l},$$

for all $k, l \in \{1, \dots, m_\mu\}$. Therefore, following the definition of Ψ_μ and Deodhar’s lemma, the matrix $U_\mu \Psi_\mu(E_\mu \widetilde{g}_i) U_\mu^{-1}$ is a matrix whose diagonal coefficients are the same as the diagonal coefficients of $\Psi_\mu(E_\mu \widetilde{g}_i)$ (and thus of the form \widetilde{G}_j with $j \in J^\mu$), while all non-diagonal non-zero coefficients are equal to either 1 or q^2 . Moreover, since, for all $j = 1, \dots, n$,

$$\Psi_\mu(E_\mu t_j) = \sum_{k=1}^{m_\mu} \chi_k^\mu(t_j) M_{k,k}$$

is a diagonal matrix, we have $U_\mu \Psi_\mu(E_\mu t_j) U_\mu^{-1} = \Psi_\mu(E_\mu t_j)$. We conclude that the map

$$\widetilde{\Psi}_\mu : E_\mu Y_{d,n}(q) \rightarrow \text{Mat}_{m_\mu}(\mathcal{H}^\mu(q))$$

defined by

$$\widetilde{\Psi}_\mu(E_\mu a) := U_\mu \Psi_\mu(E_\mu a) U_\mu^{-1},$$

for all $a \in Y_{d,n}(q)$, is an isomorphism of $\mathbb{C}[q^2, q^{-2}]$ -algebras. Its inverse is the map

$$\widetilde{\Phi}_\mu : \text{Mat}_{m_\mu}(\mathcal{H}^\mu(q)) \rightarrow E_\mu Y_{d,n}(q)$$

defined by

$$\tilde{\Phi}_\mu(A) := \Phi_\mu(U_\mu^{-1}AU_\mu),$$

for all $A \in \text{Mat}_{m_\mu}(\mathcal{H}^\mu(q))$. As a consequence, the map

$$\tilde{\Psi}_{d,n} := \bigoplus_{\mu \in \text{Comp}_d(n)} \tilde{\Psi}_\mu : Y_{d,n}(q) \rightarrow \bigoplus_{\mu \in \text{Comp}_d(n)} \text{Mat}_{m_\mu}(\mathcal{H}^\mu(q))$$

is also an isomorphism of $\mathbb{C}[q^2, q^{-2}]$ -algebras, with inverse map

$$\tilde{\Phi}_{d,n} := \bigoplus_{\mu \in \text{Comp}_d(n)} \tilde{\Phi}_\mu : \bigoplus_{\mu \in \text{Comp}_d(n)} \text{Mat}_{m_\mu}(\mathcal{H}^\mu(q)) \rightarrow Y_{d,n}(q).$$

3.3 From $\text{FTL}_{d,n}(q)$ to Temperley–Lieb

Recall that $\text{FTL}_{d,n}(q)$ is the quotient $Y_{d,n}(q)/I_{d,n}$, where $I_{d,n}$ is the ideal generated by the element $e_1e_2g_{1,2}$ (with $I_{d,n} = \{0\}$ if $n \leq 2$). Let $\mu \in \text{Comp}_d(n)$. We will study the image of $e_1e_2g_{1,2}$ under the isomorphism Ψ_μ .

By (11), for all $i = 1, \dots, n - 1$ and $\chi \in \text{Irr}(\mathcal{A}_{d,n})$, we have

$$e_iE_\chi = E_\chi e_i = \frac{1}{d} \sum_{s=0}^{d-1} \chi(t_i)^s \chi(t_{i+1})^{d-s} E_\chi = \begin{cases} E_\chi & \text{if } \chi(t_i) = \chi(t_{i+1}); \\ 0 & \text{if } \chi(t_i) \neq \chi(t_{i+1}). \end{cases} \tag{12}$$

We deduce that, for all $k = 1, \dots, m_\mu$,

$$E_{\chi_k^\mu} e_1 e_2 g_{1,2} = \begin{cases} E_{\chi_k^\mu} g_{1,2} & \text{if } \chi_k^\mu(t_1) = \chi_k^\mu(t_2) = \chi_k^\mu(t_3); \\ 0 & \text{otherwise.} \end{cases} \tag{13}$$

Proposition 1 *Let $\mu \in \text{Comp}_d(n)$ and $k \in \{1, \dots, m_\mu\}$. We have*

$$\Psi_\mu(E_{\chi_k^\mu} e_1 e_2 g_{1,2}) = \begin{cases} G_{i,i+1} M_{k,k} & \text{for some } i \in \{1, \dots, n - 2\} \text{ if } \chi_k^\mu(t_1) = \chi_k^\mu(t_2) = \chi_k^\mu(t_3); \\ 0 & \text{otherwise.} \end{cases}$$

Thus, $\Psi_\mu(E_{\chi_k^\mu} e_1 e_2 g_{1,2})$ is a diagonal matrix in $\text{Mat}_{m_\mu}(\mathcal{H}^\mu(q))$ with all non-zero coefficients being of the form $G_{i,i+1}$ for some $i \in \{1, \dots, n - 2\}$.

Proof If $\chi_k^\mu(t_1) = \chi_k^\mu(t_2) = \chi_k^\mu(t_3)$, then $w(\chi_k^\mu) = \chi_k^\mu$ for all $w \in \langle s_1, s_2 \rangle \subseteq \mathfrak{S}_n$, and so

$$\Psi_\mu(E_{\chi_k^\mu} g_{1,2}) = \sum_{w \in \langle s_1, s_2 \rangle} \Psi_\mu(E_{\chi_k^\mu} g_w) = \sum_{w \in \langle s_1, s_2 \rangle} G_{\pi_{\mu,k}^{-1} w \pi_{\mu,k}} M_{k,k}. \tag{14}$$

We will show that there exists $i \in \{1, \dots, n - 2\}$ such that

$$\sum_{w \in \langle s_1, s_2 \rangle} G_{\pi_{\mu,k}^{-1} w \pi_{\mu,k}} = G_{i,i+1}.$$

By Lemma 1, there exist $i, j \in J^\mu$ such that

$$\pi_{\mu,k}^{-1} s_1 \pi_{\mu,k} = s_i \quad \text{and} \quad \pi_{\mu,k}^{-1} s_2 \pi_{\mu,k} = s_j.$$

Consequently, $\pi_{\mu,k}^{-1} s_1 s_2 \pi_{\mu,k} = s_i s_j$, $\pi_{\mu,k}^{-1} s_2 s_1 \pi_{\mu,k} = s_j s_i$ and $\pi_{\mu,k}^{-1} s_1 s_2 s_1 \pi_{\mu,k} = s_i s_j s_i$. Moreover, since s_1 and s_2 do not commute, s_i and s_j do not commute either, so we must have $j \in \{i - 1, i + 1\}$. Hence, if $j = i - 1$, then

$$\sum_{w \in \langle s_1, s_2 \rangle} G_{\pi_{\mu,k}^{-1} w \pi_{\mu,k}} = G_{i-1,i},$$

while if $j = i + 1$, then

$$\sum_{w \in \langle s_1, s_2 \rangle} G_{\pi_{\mu,k}^{-1} w \pi_{\mu,k}} = G_{i,i+1}.$$

We conclude that there exists $i \in \{1, \dots, n - 2\}$ such that

$$\sum_{w \in \langle s_1, s_2 \rangle} G_{\pi_{\mu,k}^{-1} w \pi_{\mu,k}} = G_{i,i+1},$$

whence we deduce that

$$\Psi_\mu(E_{\chi_k^\mu} g_{1,2}) = G_{i,i+1} M_{k,k}.$$

Combining this with (13) yields the desired result. □

Example 1

Let us consider the case $d = 2$ and $n = 4$. We have

$$(\mu, m_\mu) \in \{((4, 0), 1), ((3, 1), 4), ((2, 2), 6), ((1, 3), 4), ((0, 4), 1)\}.$$

Then

$$\Psi_\mu(E_{\chi_k^\mu} e_1 e_2 g_{1,2}) = \begin{cases} G_{1,2} & \text{if } \mu = (4, 0) \text{ or } \mu = (0, 4), \\ G_{1,2} M_{1,1} & \text{if } \mu = (3, 1) \text{ and } k = 1, \\ G_{2,3} M_{4,4} & \text{if } \mu = (1, 3) \text{ and } k = 4, \\ 0 & \text{otherwise,} \end{cases}$$

where we take $\pi_{(1,3),4} = s_3 s_2 s_1$.

Now, recall the surjective R -algebra homomorphism $\rho^\mu : \mathcal{H}^\mu(q) \rightarrow \text{TL}^\mu(q)$ defined in Sect. 3.1. The map ρ^μ induces a surjective R -algebra homomorphism $\text{Mat}_{m_\mu}(\mathcal{H}^\mu(q)) \rightarrow \text{Mat}_{m_\mu}(\text{TL}^\mu(q))$, which we also denote by ρ^μ . We obtain that

$$\rho^\mu \circ \Psi_\mu : E_\mu Y_{d,n}(q) \rightarrow \text{Mat}_{m_\mu}(\text{TL}^\mu(q))$$

is a surjective R -algebra homomorphism.

In order for $\rho^\mu \circ \Psi_\mu$ to factor through $E_\mu Y_{d,n}(q)/E_\mu I_{d,n} \cong E_\mu \text{FTL}_{d,n}(q)$, all elements of $E_\mu I_{d,n}$ have to belong to the kernel of $\rho^\mu \circ \Psi_\mu$. Since $I_{d,n}$ is the ideal generated by the element $e_1 e_2 g_{1,2}$, it is enough to show that $(\rho^\mu \circ \Psi_\mu)(e_1 e_2 g_{1,2}) = 0$. This is immediate by Proposition 1. Hence, if we denote by ϱ^μ the natural surjection $E_\mu Y_{d,n}(q) \rightarrow E_\mu Y_{d,n}(q)/E_\mu I_{d,n} \cong E_\mu \text{FTL}_{d,n}(q)$, there exists a unique R -algebra homomorphism

$$\psi_\mu : E_\mu \text{FTL}_{d,n}(q) \rightarrow \text{Mat}_{m_\mu}(\text{TL}^\mu(q))$$

such that the following diagram is commutative:

$$\begin{array}{ccc} E_\mu Y_{d,n}(q) & \xrightarrow{\Psi_\mu} & \text{Mat}_{m_\mu}(\mathcal{H}^\mu(q)) \\ \downarrow \varrho^\mu & & \downarrow \rho^\mu \\ E_\mu \text{FTL}_{d,n}(q) & \xrightarrow{\psi_\mu} & \text{Mat}_{m_\mu}(\text{TL}^\mu(q)) \end{array} \tag{15}$$

Since $\rho^\mu \circ \Psi_\mu$ is surjective, ψ_μ is also surjective.

3.4 From Temperley–Lieb to $\text{FTL}_{d,n}(q)$

We now consider the surjective R -algebra homomorphism:

$$\varrho^\mu \circ \Phi_\mu : \text{Mat}_{m_\mu}(\mathcal{H}^\mu(q)) \rightarrow E_\mu \text{FTL}_{d,n}(q),$$

where Φ_μ is the inverse of Ψ_μ . In order for $\varrho^\mu \circ \Phi_\mu$ to factor through $\text{Mat}_{m_\mu}(\text{TL}^\mu(q))$, we have to show that $G_{i,i+1}M_{k,l}$ belongs to the kernel of $\varrho^\mu \circ \Phi_\mu$ for all $i = 1, \dots, n - 2$ such that $G_{i,i+1} \in \mathcal{H}^\mu(q)$ (that is, $\{i, i + 1\} \subseteq J^\mu$) and for all $k, l \in \{1, \dots, m_\mu\}$. Since

$$G_{i,i+1}M_{k,l} = M_{k,1}G_{i,i+1}M_{1,1}M_{1,l}$$

and $\varrho^\mu \circ \Phi_\mu$ is an homomorphism of R -algebras, it is enough to show that $(\varrho^\mu \circ \Phi_\mu)(G_{i,i+1}M_{1,1}) = 0$.

Let $i = 1, \dots, n - 2$ such that $G_{i,i+1} \in \mathcal{H}^\mu(q)$. By definition of Φ_μ , and since $\pi_{\mu,1} = 1$, we have

$$\Phi_\mu(G_{i,i+1}M_{1,1}) = E_{\chi_1^\mu} g_{i,i+1} E_{\chi_1^\mu}. \tag{16}$$

Now, since $G_{i,i+1} \in \mathcal{H}^\mu(q)$, there exists $j \in \{1, \dots, d\}$ such that $\mu_j > 2$ and $G_{i,i+1} \in \mathcal{H}_{\mu_j}(q)$, that is, $i \in \{\mu_1 + \dots + \mu_{j-1} + 1, \dots, \mu_1 + \dots + \mu_{j-1} + \mu_j - 2\}$. By definition of χ_1^μ , we have

$$\chi_1^\mu(t_{\mu_1+\dots+\mu_{j-1}+1}) = \dots = \chi_1^\mu(t_{\mu_1+\dots+\mu_{j-1}+\mu_j}) = \xi_j,$$

whence

$$\chi_1^\mu(t_i) = \chi_1^\mu(t_{i+1}) = \chi_1^\mu(t_{i+2}) = \xi_j.$$

Following (12), we obtain

$$\Phi_\mu(G_{i,i+1}M_{1,1}) = E_{\chi_1^\mu} g_{i,i+1} E_{\chi_1^\mu} = E_{\chi_1^\mu} e_i e_{i+1} g_{i,i+1} E_{\chi_1^\mu}.$$

Since $e_i e_{i+1} g_{i,i+1} \in I_{d,n}$, we deduce that $(\varrho^\mu \circ \Phi_\mu)(G_{i,i+1}M_{1,1}) = 0$, as desired.

We conclude that there exists a unique R -algebra homomorphism

$$\phi_\mu : \text{Mat}_{m_\mu}(\text{TL}^\mu(q)) \rightarrow E_\mu \text{FTL}_{d,n}(q)$$

such that the following diagram is commutative:

$$\begin{array}{ccc} E_\mu Y_{d,n}(q) & \xleftarrow{\Phi_\mu} & \text{Mat}_{m_\mu}(\mathcal{H}^\mu(q)) \\ \downarrow \varrho^\mu & & \downarrow \rho^\mu \\ E_\mu \text{FTL}_{d,n}(q) & \xleftarrow{\phi_\mu} & \text{Mat}_{m_\mu}(\text{TL}^\mu(q)) \end{array} \tag{17}$$

Since $\varrho^\mu \circ \Phi_\mu$ is surjective, ϕ_μ is also surjective.

3.5 An Isomorphism Theorem for the Framisation of the Temperley–Lieb Algebra $\text{FTL}_{d,n}(q)$

We are now ready to prove the main result of this section.

Theorem 2 *Let $\mu \in \text{Comp}_d(n)$. The linear map ψ_μ is an isomorphism of R -algebras with inverse map ϕ_μ . As a consequence, the map*

$$\psi_{d,n} := \bigoplus_{\mu \in \text{Comp}_d(n)} \psi_\mu : \text{FTL}_{d,n}(q) \rightarrow \bigoplus_{\mu \in \text{Comp}_d(n)} \text{Mat}_{m_\mu}(\text{TL}^\mu(q))$$

is also an isomorphism of R -algebras, with inverse map

$$\phi_{d,n} := \bigoplus_{\mu \in \text{Comp}_d(n)} \phi_\mu : \bigoplus_{\mu \in \text{Comp}_d(n)} \text{Mat}_{m_\mu}(\text{TL}^\mu(q)) \rightarrow \text{FTL}_{d,n}(q).$$

Proof Since the diagrams (15) and (17) are commutative, we have

$$\rho^\mu \circ \Psi_\mu = \psi_\mu \circ \varrho^\mu \quad \text{and} \quad \varrho^\mu \circ \Phi_\mu = \phi_\mu \circ \rho^\mu.$$

This implies that

$$\rho^\mu \circ \Psi_\mu \circ \Phi_\mu = \psi_\mu \circ \phi_\mu \circ \rho^\mu \quad \text{and} \quad \varrho^\mu \circ \Phi_\mu \circ \Psi_\mu = \phi_\mu \circ \psi_\mu \circ \varrho^\mu.$$

By Theorem 1, $\Psi_\mu \circ \Phi_\mu = \text{id}_{\text{Mat}_{m_\mu}(\mathcal{H}^\mu(q))}$ and $\Phi_\mu \circ \Psi_\mu = \text{id}_{E_\mu Y_{d,n}(q)}$, whence

$$\rho^\mu = \psi_\mu \circ \phi_\mu \circ \rho^\mu \quad \text{and} \quad \varrho^\mu = \phi_\mu \circ \psi_\mu \circ \varrho^\mu.$$

Since the maps ρ^μ and ϱ^μ are surjective, we obtain

$$\psi_\mu \circ \phi_\mu = \text{id}_{\text{Mat}_{m_\mu}(\text{TL}^\mu(q))} \quad \text{and} \quad \phi_\mu \circ \psi_\mu = \text{id}_{E_\mu \text{FTL}_{d,n}(q)},$$

as desired. □

Remark 12 In [5], we show that we can construct similar isomorphisms over the smaller ring $\mathbb{C}[q^2, q^{-2}]$ when we consider the generators $\tilde{g}_i = qg_i$ and $\tilde{G}_i = qG_i$. For this, we use the presentation of $\text{FTL}_{d,n}(q)$ given in Remark 10 and the isomorphisms $\tilde{\Psi}_\mu$ and $\tilde{\Phi}_\mu$ defined in Remark 11.

3.6 A Basis for the Framisation of the Temperley–Lieb Algebra $\text{FTL}_{d,n}(q)$

We recall that in Sect. 2.2 we defined a basis $\mathcal{B}_{\text{TL}_n(q)}$ for the Temperley–Lieb algebra $\text{TL}_n(q)$. Thanks to Theorem 2, we obtain the following basis for $\text{FTL}_{d,n}(q)$ as an R -module:

Proposition 2 *The set*

$$\left\{ \phi_\mu(b_1 b_2 \dots b_d M_{k,l}) \mid \mu \in \text{Comp}_d(n), b_i \in \mathcal{B}_{\text{TL}_{\mu_i}(q)} \forall i = 1, \dots, d, 1 \leq k, l \leq m_\mu \right\}$$

is a basis of $\text{FTL}_{d,n}(q)$ as an R -module. In particular, $\text{FTL}_{d,n}(q)$ is a free R -module of rank

$$\sum_{\mu \in \text{Comp}_d(n)} m_\mu^2 C_{\mu_1} C_{\mu_2} \dots C_{\mu_d}.$$

4 Markov Traces and Link Invariants

The presentation for the Temperley–Lieb algebra given in Sect. 2.2 is due to Jones, who used a Markov trace defined on it, the *Jones–Ocneanu trace*, to construct his famous polynomial invariant for classical links, the *Jones polynomial* [16]. A similar construction on the Framisation of the Temperley–Lieb algebra yields invariants for framed and classical links [11]. In this section, we will relate the latter to the Jones polynomial using the isomorphism of Theorem 2.

4.1 The Inductive Jones–Ocneanu Trace

Using the natural algebra inclusions $\mathcal{H}_n(q) \subset \mathcal{H}_{n+1}(q)$ for $n \in \mathbb{N}$ (setting $\mathcal{H}_n(q) := R$ for $n \leq 1$), we can define the Jones–Ocneanu trace on $\bigcup_{n \geq 0} \mathcal{H}_n(q)$ as follows [16, Theorem 5.1]:

Theorem 3 *Let z be an indeterminate over \mathbb{C} . There exists a unique linear Markov trace*

$$\tau_z : \bigcup_{n \geq 0} \mathcal{H}_n(q) \longrightarrow R[z]$$

defined inductively on $\mathcal{H}_n(q)$, for all $n \geq 0$, by the following rules:

$$\begin{aligned} \tau_z(1) &= 1 & 1 &\in \mathcal{H}_n(q) \\ \tau_z(ab) &= \tau_z(ba) & a, b &\in \mathcal{H}_n(q) \\ \tau_z(aG_n) &= z \tau_z(a) & a &\in \mathcal{H}_n(q). \end{aligned}$$

It is easy to check (by solving the equation $\tau_z(G_{1,2}) = 0$) that the trace τ_z passes to the quotient Temperley–Lieb algebra $\text{TL}_n(q)$ if and only if

$$z = -\frac{1}{q^2(q + q^{-1})} = -\frac{1}{q^3 + 1} \quad \text{or} \quad z = -q^{-1}.$$

The second value is discarded as not being topologically interesting. For $z = -(q^3 + 1)^{-1}$, we will simply denote τ_z by τ .

Recall that we denote by ρ_n the natural surjection $\mathcal{H}_n(q) \twoheadrightarrow \mathcal{H}_n(q)/I_n \cong \text{TL}_n(q)$. Let us denote by $\sigma_1, \dots, \sigma_{n-1}$ the generators of the classical braid group B_n , such that the natural epimorphism $\delta_n : RB_n \twoheadrightarrow \mathcal{H}_n(q)$ is given by $\delta_n(\sigma_i) = G_i$. Then $\rho_n \circ \delta_n : RB_n \twoheadrightarrow \text{TL}_n(q)$ is also an epimorphism.

Let now \mathcal{L} denote the set of oriented links. For any $\alpha \in B_n$, we denote by $\widehat{\alpha}$ the link obtained as the closure of α . By the Alexander Theorem, we have $\mathcal{L} = \bigcup_n \{\widehat{\alpha} \mid \alpha \in B_n\}$. Further, by the Markov Theorem, isotopy of links is generated by conjugation in B_n ($\alpha\beta \sim \beta\alpha$) and by positive and negative stabilisation ($\alpha \sim \alpha\sigma_n^{\pm 1}$). Jones’s method for constructing polynomial link invariants consists of normalising and re-scaling τ

Fig. 1 The Hopf link with two positive crossings



with respect to the latter: For any $\alpha \in B_n$, let

$$V_q(\widehat{\alpha}) := (-q - q^{-1})^{n-1} q^{2\epsilon(\alpha)} (\tau \circ \rho_n \circ \delta_n)(\alpha) ,$$

where $\epsilon(\alpha)$ is the sum of the exponents of the braiding generators σ_i in the word α . Then the map

$$V_q : \mathcal{L} \rightarrow R, \widehat{\alpha} \mapsto V_q(\widehat{\alpha})$$

is an 1-variable ambient isotopy invariant of oriented links, known as the *Jones polynomial* (cf. [16]).

Example 2

We consider the Hopf link with two positive crossings (Fig. 1), which is the closure of the braid $\sigma_1^2 \in B_2$. We have

$$V_q(\widehat{\sigma_1^2}) = (-q - q^{-1})q^4 \tau(G_1^2) = -(q + q^{-1})q^4 \left(1 - \frac{q - q^{-1}}{q^2(q + q^{-1})}\right) = -(q + q^{-1})q^4 + (q - q^{-1})q^2 = -q^5 - q.$$

Remark 13 More generally, for any value of z , the trace τ_z can be normalised and re-scaled with respect to positive and negative stabilisation as follows: For any $\alpha \in B_n$, let

$$P_{q,z}(\widehat{\alpha}) := \Lambda_H^{n-1} (\sqrt{\lambda_H})^{\epsilon(\alpha)} (\tau_z \circ \delta_n)(\alpha) ,$$

where

$$\lambda_H := \frac{z - (q - q^{-1})}{z} \quad \text{and} \quad \Lambda_H := \frac{1}{z\sqrt{\lambda_H}}.$$

Then the map

$$P_{q,z} : \mathcal{L} \rightarrow R[z^{\pm 1}, \sqrt{\lambda_H^{\pm 1}}], \widehat{\alpha} \mapsto P_{q,z}(\widehat{\alpha})$$

is a 2-variable invariant of oriented links, known as the *HOMFLYPT polynomial* (cf. [13, 30]). For $z = -(q^3 + 1)^{-1}$, we get $\lambda_H = q^4$ and $\Lambda_H = -q - q^{-1}$, whence $P_{q,z} = V_q$.

4.2 The Stabilised Jones–Ocneanu Traces

Instead of normalising and re-scaling the Jones–Ocneanu trace τ , we can consider a family of traces $\tau^n : \mathcal{H}_n(q) \rightarrow R$ for $n \in \mathbb{N}$ that are stabilised by definition. However, for any $a \in \mathcal{H}_n(q)$, we have $\tau^n(a) \neq \tau^{n+1}(a)$.

More specifically, let us consider the Iwahori–Hecke algebra $\mathcal{H}_n(q)$ with braid generators $G'_i := q^2 G_i$. These satisfy the quadratic relation

$$G_i^2 = q^4 + q^2(q - q^{-1})G'_i. \tag{18}$$

We then have the following (see, for example, [9, Theorem 4.5.2]):

Theorem 4 *There exists a unique family of R -linear Markov traces $\tau^n : \mathcal{H}_n(q) \rightarrow R$ such that*

$$\begin{aligned} \tau^1(1) &= 1 \\ \tau^n(ab) &= \tau^n(ba) && a, b \in \mathcal{H}_n(q) \\ \tau^{n+1}(aG'_n) &= \tau^{n+1}(aG_n^{-1}) = \tau^n(a) && a \in \mathcal{H}_n(q). \end{aligned}$$

Moreover, we have $\tau^{n+1}(a) = (-q - q^{-1})\tau^n(a)$ for all $a \in \mathcal{H}_n(q)$.

We observe that

$$G_{1,2} = 1 + q^{-1}G'_1 + q^{-1}G'_2 + q^{-2}G'_1G'_2 + q^{-2}G'_2G'_1 + q^{-3}G'_1G'_2G'_1.$$

We have

$$\begin{aligned} \tau^3(1) &= (-q - q^{-1})^2 \tau^1(1) = q^2 + 2 + q^{-2} \\ \tau^3(G'_1) &= (-q - q^{-1})\tau^2(G'_1) = (-q - q^{-1})\tau^1(1) = -q - q^{-1} \\ \tau^3(G'_2) &= \tau^2(1) = (-q - q^{-1})\tau^1(1) = -q - q^{-1} \\ \tau^3(G'_1G'_2) &= \tau^2(G'_1) = \tau^1(1) = 1 \\ \tau^3(G'_2G'_1) &= \tau^2(G'_1) = \tau^1(1) = 1 \\ \tau^3(G'_1G'_2G'_1) &= \tau^2(G_1^2) = q^4\tau^2(1) + q^2(q - q^{-1})\tau^2(G'_1) = -q^5 - q \end{aligned}$$

whence

$$\tau^3(G_{1,2}) = q^2 + 2 + q^{-2} - 2 - 2q^{-2} + 2q^{-2} - q^2 - q^{-2} = 0.$$

Since we have

$$\tau^n(G_{1,2}) = (-q - q^{-1})^{n-3} \tau^3(G_{1,2}),$$

the trace τ^n factors through the Temperley–Lieb algebra $TL_n(q)$ for all $n \in \mathbb{N}$. Further, if we consider the natural epimorphism $\delta'_n : RB_n \twoheadrightarrow \mathcal{H}_n(q)$ given by $\delta'(\sigma_i) = G'_i$, we have [16, §11]:

$$(\tau^n \circ \rho_n \circ \delta'_n)(\alpha) = V_q(\widehat{\alpha}) \quad \text{for all } \alpha \in B_n. \tag{19}$$

Example 3

We have

$$(\tau^2 \circ \rho_2 \circ \delta'_2)(\sigma_1^2) = \tau^2(G_1'^2) = -q^5 - q.$$

Remark 14 More generally, for any value of z , if we consider the braid generators $G'_i := \sqrt{\lambda_H} G_i$, where $\lambda_H = \frac{z-(q-q^{-1})}{z}$, and we define a family of stabilised Jones–Ocneanu traces $(\tau_z^n)_{n \in \mathbb{N}}$ as in Theorem 4, with $\tau_z^{n+1}(a) = (\sqrt{z\lambda_H})^{-1} \tau_z^n(a)$ and with values in $R[z^{\pm 1}, \sqrt{\lambda_H^{\pm 1}}]$, then we have [16, (6.2)]:

$$(\tau_z^n \circ \delta'_n)(\alpha) = P_{q,z}(\widehat{\alpha}) \quad \text{for all } \alpha \in B_n.$$

4.3 The Inductive Juyumaya Trace

An important property of the Yokonuma–Hecke algebra is that it also supports a Markov trace defined for all values of n . More precisely, due to the inclusions $Y_{d,n}(q) \subset Y_{d,n+1}(q)$ (setting $Y_{d,0}(q) := R$), we obtain (cf. [17, Theorem 12]):

Theorem 5 *Let z, x_1, \dots, x_{d-1} be indeterminates over \mathbb{C} . There exists a unique linear Markov trace*

$$\text{tr}_{d,z} : \bigcup_{n \geq 0} Y_{d,n}(q) \longrightarrow \mathbb{C}[z, x_1, \dots, x_{d-1}]$$

defined inductively on $Y_{d,n}(q)$, for all $n \geq 0$, by the following rules:

$$\begin{aligned} \text{tr}_{d,z}(1) &= 1 & 1 &\in Y_{d,n}(q) \\ \text{tr}_{d,z}(ab) &= \text{tr}_{d,z}(ba) & a, b &\in Y_{d,n}(q) \\ \text{tr}_{d,z}(ag_n) &= z \text{tr}_{d,z}(a) & a &\in Y_{d,n}(q) \\ \text{tr}_{d,z}(at_{n+1}^k) &= x_k \text{tr}_{d,z}(a) & a &\in Y_{d,n}(q) \quad (1 \leq k \leq d-1). \end{aligned}$$

Remark 15 Note that, for $d = 1$, the trace $\text{tr}_{1,z}$ is defined by only the first three rules. Thus, tr_1 coincides with the Jones–Ocneanu trace τ_z on the Iwahori–Hecke algebra $\mathcal{H}_n(q) \cong Y_{1,n}(q)$.

The values of the parameters for which the trace $\text{tr}_{d,z}$ passes to the quotient algebra $\text{FTL}_{d,n}(q)$ are given in [11, Theorem 6]; their determination is not straightforward as in the classical case. However, not all of them are topologically interesting.

First, let us denote by $\varrho_{d,n}$ the natural surjection $Y_{d,n}(q) \twoheadrightarrow Y_{d,n}(q)/I_{d,n} \cong \text{FTL}_{d,n}(q)$. Recall that we denote by \mathcal{F}_n the classical framed braid group. We have $\mathcal{F}_n \cong \mathbb{Z} \wr B_n$, and there exists a natural epimorphism $\gamma_{d,n} : R\mathcal{F}_n \twoheadrightarrow Y_{d,n}(q)$ given

by $\gamma_{d,n}(\sigma_i) = g_i$ and $\gamma_{d,n}(t_j^k) = t_j^{k \pmod d}$ for all $k \in \mathbb{Z}$. The map $Q_{d,n} \circ \gamma_{d,n} : R\mathcal{F}_n \rightarrow \text{FTL}_{d,n}(q)$ is also an algebra epimorphism.

Let now \mathcal{L}_f denote the set of oriented framed links. By the Alexander Theorem, we have $\mathcal{L}_f = \cup_n \{\widehat{\alpha} \mid \alpha \in \mathcal{F}_n\}$. Further, by the Markov Theorem for framed links [26, Lemma 1], isotopy of framed links is generated by conjugation in \mathcal{F}_n ($\alpha\beta \sim \beta\alpha$) and by positive and negative stabilisation ($\alpha \sim \alpha\sigma_n^{\pm 1}$), for any n . In view of all this, Juyumaya and Lambropoulou [21] attempted to normalise and re-scale the trace $\text{tr}_{d,z}$ in order to obtain invariants for framed knots and links following Jones’s method; they discovered that this is the only Markov trace known in literature that cannot be re-scaled directly. They showed that $\text{tr}_{d,z}$ re-scales when the parameters $(x_k)_{1 \leq k \leq d-1}$ satisfy the following system of equations, known as the *E-system*:

$$\sum_{s=0}^{d-1} x_{k+s}x_{d-s} = x_k \sum_{s=0}^{d-1} x_sx_{d-s} \quad (1 \leq k \leq d-1), \tag{20}$$

with $x_0 = x_d = 1$. The solutions of the E-system were computed by Gérardin in the Appendix of [11] and they are parametrised by the non-empty subsets of $\mathbb{Z}/d\mathbb{Z}$: If D is such a subset, then

$$x_k = \frac{1}{|D|} \sum_{j \in D} \exp\left(\frac{2\pi ijk}{d}\right) \quad (1 \leq k \leq d-1).$$

For the rest of the paper, D will denote a non-empty subset of $\mathbb{Z}/d\mathbb{Z}$ and (x_1, \dots, x_{d-1}) will be the corresponding solution of the E-system. We will denote by $\text{tr}_{d,D,z}$ the Juyumaya trace with these parameters and we will call it the *specialised Juyumaya trace*. We have $\text{tr}_{d,D,z}(e_i) = 1/|D| =: E_D$ for all i . According to [11, (7.7)], the trace $\text{tr}_{d,D,z}$ passes to the quotient algebra $\text{FTL}_{d,n}(q)$ if and only if

$$z = -\frac{E_D}{q^2(q+q^{-1})} = -\frac{E_D}{q^3+1} \quad \text{or} \quad z = -\frac{E_D}{q}.$$

The second value is discarded as not being topologically interesting. For $z = -E_D(q^3+1)^{-1}$, we will simply denote $\text{tr}_{d,D,z}$ by $\text{tr}_{d,D}$. Normalising and re-scaling $\text{tr}_{d,D}$ with respect to positive and negative stabilisation yields the following: For any $\alpha \in \mathcal{F}_n$, let

$$\phi_{d,D,q}(\widehat{\alpha}) := \left(-\frac{q+q^{-1}}{E_D}\right)^{n-1} q^{2\epsilon(\alpha)} (\text{tr}_{d,D} \circ Q_{d,n} \circ \gamma_{d,n})(\alpha),$$

where $\epsilon(\alpha)$ is the sum of the exponents of the braiding generators σ_i in the word α . Then the map

$$\phi_{d,D,q} : \mathcal{L}_f \rightarrow R, \quad \widehat{\alpha} \mapsto \phi_{d,D,q}(\widehat{\alpha})$$

is an 1-variable ambient isotopy invariant of oriented framed links [11, (7.8)].

We denote by $\theta_{d,D,q}$ the restriction of $\phi_{d,D,q}$ to the set \mathcal{L} of classical links; the map $\theta_{d,D,q}$ is an 1-variable ambient isotopy invariant of oriented classical links.

Example 4

We consider the classical Hopf link with two positive crossings. We have

$$\theta_{d,D,q}(\widehat{\sigma_1^2}) = \left(-\frac{q+q^{-1}}{E_D}\right) q^4 \text{tr}_{d,D}(g_1^2) = \left(-\frac{q+q^{-1}}{E_D}\right) q^4 \left(1 - \frac{(q-q^{-1})E_D}{q^2(q+q^{-1})}\right) = -\frac{q^5+q^3}{E_D} + q^3 - q.$$

We now consider the framed Hopf link with framings 0 and 1. This is the closure of the framed braid $t_2\sigma_1^2$. Note that $(\text{tr}_{d,D} \circ \mathcal{Q}_{d,n} \circ \gamma_{d,n})(t_2\sigma_1^2) = \text{tr}_{d,D}(t_2g_1^2) = \text{tr}_{d,D}(g_1 t_1 g_1) = \text{tr}_{d,D}(t_1 g_1^2) = (\text{tr}_{d,D} \circ \mathcal{Q}_{d,n} \circ \gamma_{d,n})(t_1\sigma_1^2)$. We have

$$\text{tr}_{d,D}(t_1 g_1^2) = \text{tr}_{d,D}(t_1) + (q - q^{-1})\text{tr}_{d,D}(t_1 e_1 g_1) = \text{tr}_{d,D}(t_1) \left(1 - \frac{(q - q^{-1})E_D}{q^2(q + q^{-1})}\right) = x_1 \text{tr}_{d,D}(g_1^2).$$

We deduce that

$$\phi_{d,D,q}(\widehat{t_2\sigma_1^2}) = \left(-\frac{q+q^{-1}}{E_D}\right) q^4 \text{tr}_{d,D}(t_2 g_1^2) = x_1 \theta_{d,D,q}(\sigma_1^2) = x_1 \left(-\frac{q^5+q^3}{E_D} + q^3 - q\right).$$

Remark 16 More generally, for any value of z , the trace $\text{tr}_{d,D,z}$ can be normalised and re-scaled with respect to positive and negative stabilisation as follows: For any $\alpha \in \mathcal{F}_n$, let

$$\Phi_{d,D,q,z}(\widehat{\alpha}) := \Lambda_D^{n-1} (\sqrt{\lambda_D})^{\epsilon(\alpha)} (\text{tr}_{d,D,z} \circ \gamma_{d,n})(\alpha),$$

where

$$\lambda_D := \frac{z - (q - q^{-1})E_D}{z} \quad \text{and} \quad \Lambda_D := \frac{1}{z\sqrt{\lambda_D}}.$$

Then the map

$$\Phi_{d,D,q,z} : \mathcal{L}_f \rightarrow R[z^{\pm 1}, \sqrt{\lambda_D^{\pm 1}}], \quad \widehat{\alpha} \mapsto \Phi_{d,D,q,z}(\widehat{\alpha})$$

is a 2-variable invariant of oriented framed links [1, Theorem 3.1]. For $z = -E_D(q^3 + 1)^{-1}$, we get $\lambda_D = q^4$ and $\Lambda_D = -(q + q^{-1})/E_D$, whence $\Phi_{d,D,q,z} = \phi_{d,D,q}$.

We denote by $\Theta_{d,D,q,z}$ the restriction of $\Phi_{d,D,q,z}$ to the set \mathcal{L} of classical links; the map $\Theta_{d,D,q,z}$ is a 2-variable invariant of oriented classical links. For $z = -E_D(q^3 + 1)^{-1}$, we have $\Theta_{d,D,q,z} = \theta_{d,D,q}$.

Remark 17 Using the same construction, but replacing the generators g_i with the generators $\bar{g}_i := g_i + (q - 1) e_i g_i$, Juyumaya and Lambropoulou defined 2-variable invariants for framed [21] and classical [22] links from the specialised Juyumaya

trace on the Yokonuma–Hecke algebra $Y_{d,n}(q)$. Considering the specialised Juyumaya trace on $FTL_{d,n}(q)$, but replacing again g_i with \bar{g}_i , Goundaroulis, Juyumaya, Kontogeorgis and Lambropoulou defined 1-variable invariants for framed and classical links in [11]. As shown in [1, Sect. 8], these invariants are not topologically equivalent to the ones we define in this paper. There is no such issue when replacing g_i with $\tilde{g}_i := qg_i$ or with $g'_i := q^2g_i$.

Remark 18 For $d = 1$, we have $\theta_{1,\{0\},q} = V_q$ and $\Theta_{1,\{0\},q,z} = P_{q,z}$. More generally, when $|D| = 1$, it was shown in [2] that the invariants $\theta_{d,D,q}$ and $\Theta_{d,D,q,z}$ are equivalent to the Jones and HOMFLYPT polynomials respectively.

4.4 The Stabilised Jacon–Poulain d’Andecy Traces

Similarly to the Jones–Ocneanu trace, instead of normalising and re-scaling $\text{tr}_{d,D}$, we can consider a family of traces $\text{tr}_{d,D}^n : Y_{d,n}(q) \rightarrow R$ for $n \in \mathbb{N}$ that are stabilised by definition. However, for any $a \in Y_{d,n}(q)$, we have $\text{tr}_{d,D}^n(a) \neq \text{tr}_{d,D}^{n+1}(a)$.

More specifically, let us consider the Yokonuma–Hecke algebra $Y_{d,n}(q)$ with braid generators $g'_i := q^2g_i$. These satisfy the quadratic relation

$$g_i'^2 = q^4 + q^2(q - q^{-1})e_i g'_i. \tag{21}$$

We then have the following (see also [14, §5.2], [28, §5.2]):

Theorem 6 *There exists a unique family of R -linear Markov traces $\text{tr}_{d,D}^n : Y_{d,n}(q) \rightarrow R$ such that*

$$\begin{aligned} \text{tr}_{d,D}^1(1) &= 1 \\ \text{tr}_{d,D}^n(ab) &= \text{tr}_{d,D}^n(ba) && a, b \in Y_{d,n}(q) \\ \text{tr}_{d,D}^{n+1}(ag'_n) &= \text{tr}_{d,D}^{n+1}(ag_n'^{-1}) = \text{tr}_{d,D}^n(a) && a \in Y_{d,n}(q) \\ \text{tr}_{d,D}^{n+1}(a_i^k) &= x_k \text{tr}_{d,D}^{n+1}(a) && a \in Y_{d,n}(q) \quad (1 \leq k \leq d - 1). \end{aligned}$$

Moreover, we have $\text{tr}_{d,D}^{n+1}(a) = (-q - q^{-1})E_D^{-1}\text{tr}_{d,D}^n(a)$ for all $a \in Y_{d,n}(q)$.

First of all, note that

$$q^4g_n'^{-1} = g'_n - q^2(q - q^{-1})e_n.$$

Therefore, for all $a \in Y_{d,n}(q)$, we have

$$q^2(q - q^{-1})\text{tr}_{d,D}^{n+1}(ae_n) = \text{tr}_{d,D}^{n+1}(ag'_n) - q^4\text{tr}_{d,D}^{n+1}(ag_n'^{-1}) = (1 - q^4)\text{tr}_{d,D}^n(a),$$

whence

$$\text{tr}_{d,D}^{n+1}(ae_n) = (-q - q^{-1})\text{tr}_{d,D}^n(a) = E_D\text{tr}_{d,D}^{n+1}(a). \tag{22}$$

Moreover,

$$\text{tr}_{d,D}^{n+1}(ae_n g'_n) = \frac{1}{d} \sum_{s=0}^{d-1} \text{tr}_{d,D}^{n+1}(at_n^s g'_n t_n^{d-s}) = \frac{1}{d} \sum_{s=0}^{d-1} \text{tr}_{d,D}^n(at_n^s t_n^{d-s}) = \text{tr}_{d,D}^n(a). \quad (23)$$

Now, we observe that

$$g_{1,2} = 1 + q^{-1}g'_1 + q^{-1}g'_2 + q^{-2}g'_1g'_2 + q^{-2}g'_2g'_1 + q^{-3}g'_1g'_2g'_1.$$

We have

$$\begin{aligned} \text{tr}_{d,D}^3(e_1e_2) &= (-q - q^{-1})\text{tr}_{d,D}^2(e_1) = (-q - q^{-1})^2\text{tr}_{d,D}^1(1) = q^2 + 2 + q^{-2} \\ \text{tr}_{d,D}^3(e_1e_2g'_1) &= (-q - q^{-1})\text{tr}_{d,D}^2(e_1g'_1) = (-q - q^{-1})\text{tr}_{d,D}^1(1) = -q - q^{-1} \\ \text{tr}_{d,D}^3(e_1e_2g'_2) &= \text{tr}_{d,D}^2(e_1) = (-q - q^{-1})\text{tr}_{d,D}^1(1) = -q - q^{-1} \\ \text{tr}_{d,D}^3(e_1e_2g'_1g'_2) &= \text{tr}_{d,D}^2(e_1g'_1) = \text{tr}_{d,D}^1(1) = 1 \\ \text{tr}_{d,D}^3(e_1e_2g'_2g'_1) &= \text{tr}_{d,D}^2(e_1g'_1) = \text{tr}_{d,D}^1(1) = 1 \\ \text{tr}_{d,D}^3(e_1e_2g'_1g'_2g'_1) &= \text{tr}_{d,D}^2(e_1g_1'^2) = q^4\text{tr}_{d,D}^2(e_1) + q^2(q - q^{-1})\text{tr}_{d,D}^2(e_1g'_1) = -q^5 - q \end{aligned}$$

whence

$$\text{tr}_{d,D}^3(e_1e_2g_{1,2}) = q^2 + 2 + q^{-2} - 2 - 2q^{-2} + 2q^{-2} - q^2 - q^{-2} = 0.$$

Since we have

$$\text{tr}_{d,D}^n(e_1e_2g_{1,2}) = \left(-\frac{q + q^{-1}}{E_D}\right)^{n-3} \text{tr}_{d,D}^3(e_1e_2g_{1,2}),$$

the trace $\text{tr}_{d,D}^n$ factors through the Framisation of the Temperley–Lieb algebra $\text{FTL}_{d,n}(q)$ for all $n \in \mathbb{N}$. Further, if we consider the natural epimorphism $\gamma'_{d,n} : R\mathcal{F}_n \twoheadrightarrow Y_{d,n}(q)$ given by $\gamma'_{d,n}(\sigma_i) = g'_i$ and $\gamma'_{d,n}(t_j^k) = t_j^{k(\text{mod } d)}$ for all $k \in \mathbb{Z}$, we have [28, Remarks 5.4]:

$$(\text{tr}_{d,D}^n \circ \varrho_{d,n} \circ \gamma'_{d,n})(\alpha) = \phi_{d,D,q}(\widehat{\alpha}) \quad \text{for all } \alpha \in \mathcal{F}_n. \quad (24)$$

Example 5

We have

$$(\text{tr}_{d,D}^2 \circ \varrho_{d,2} \circ \gamma'_{d,2})(\sigma_1^2) = \text{tr}_{d,D}^2(g_1'^2) = \text{tr}_{d,D}^2(q^4 + q^2(q - q^{-1})e_1g'_1) = -\frac{q^5 + q^3}{E_D} + q^3 - q.$$

and

$$(\text{tr}_{d,D}^2 \circ \varrho_{d,2} \circ \gamma'_{d,2})(t_2 \sigma_1^2) = \text{tr}_{d,D}^2(t_1 g_1'^2) = q^4 \text{tr}_{d,D}^2(t_1) + q^2(q - q^{-1}) \text{tr}_{d,D}^1(t_1) = x_1 \left(-\frac{q^5 + q^3}{E_D} + q^3 - q \right).$$

Remark 19 More generally, for any value of z , if we consider the braid generators $g'_i := \sqrt{\lambda_D} g_i$, where $\lambda_D = \frac{z - (q - q^{-1})E_D}{z}$, and we define a family of stabilised Jones–Ocneanu traces $(\text{tr}_{d,D,z}^n)_{n \in \mathbb{N}}$ as in Theorem 6, with $\text{tr}_{d,D,z}^{n+1}(a) = (\sqrt{z\lambda_D})^{-1} \text{tr}_{d,D,z}^n(a)$ and with values in $R[z^{\pm 1}, \sqrt{\lambda_D}^{\pm 1}]$, then we have [28, Remarks 5.4]:

$$(\text{tr}_{d,D,z}^n \circ \gamma'_{d,n})(\alpha) = \Phi_{d,D,q,z}(\widehat{\alpha}) \quad \text{for all } \alpha \in \mathcal{F}_n.$$

4.5 Connecting the Invariants with the Use of the Isomorphism Theorem

In this last subsection, we will only be interested in invariants of classical links. The invariants $\Theta_{d,D,q,z}$ and $\theta_{d,D,q}$ of Sect. 4.3 have been further studied in [1, 12] respectively. where their following properties have been proved:

- (P1) They do not depend on d and D , but only on the cardinality of D (and equivalently on E_D).
- (P2) They can be generalised to skein link invariants where E_D is taken to be an indeterminate.
- (P3) They are not topologically equivalent to the HOMFLYPT polynomial and the Jones polynomial respectively.

We will illustrate point (P3) for the invariant $\theta_{d,D,q}$ with the following example.

Example 6

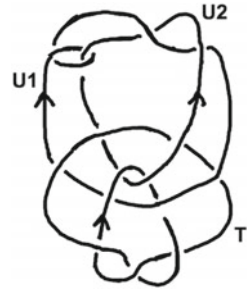
We consider the link $L := LLL(0)$ of [7] with the orientation of Fig. 2. This is a 3-component link, whose components are one left-handed trefoil (T) and 2 unknots (U1 and U2). The link L has the same Jones polynomial as the disjoint union of 3 unknots, even though it is not topologically equivalent to it. We have:

$$V_q(L) = (q + q^{-1})^2 = V_q(\widehat{1_{B_3}})$$

Now, the link L is the closure of the following braid:

$$\sigma_1^{-1} \sigma_2^2 \sigma_3^{-1} \sigma_2^{-1} \sigma_4^{-1} \sigma_3^{-2} \sigma_2^{-1} \sigma_1^{-1} \sigma_2 \sigma_3 \sigma_2^{-3} \sigma_3 \sigma_2 \sigma_4 \sigma_3 \sigma_2 \in B_5.$$

Fig. 2 The link $LLL(0)$



In order to compute $\theta_{d,D,q}$ on the closure of this braid, we used the program designed for this reason by Karvounis [25], which is available at <http://www.math.ntua.gr/~sofia/yokonuma>. We have that $\theta_{d,D,q}(L)$ is equal to:

$$V_q(L) + (E_D - 1) \frac{q + q^{-1}}{E_D^2 q^{11}} (E_D (q^{16} - 3q^{14} + 2q^{12} - 5q^{10} + 6q^8 - 4q^6 + 4q^4 - 5q^2 + 2) - q^{10} - q^8 - q^6 + q^2).$$

We observe that for $E_D = 1$, $\theta_{d,D,q}(L) = V_q(L)$. Moreover,

$$\theta_{d,D,q}(\widehat{1}_{B_3}) = \left(-\frac{q + q^{-1}}{E_D} \right)^2 = E_D^{-2} V_q(\widehat{1}_{B_3}),$$

and so $\theta_{d,D,q}$ distinguishes two links that the Jones polynomial cannot distinguish.

In the Appendix of [1], Lickorish gave a closed combinatorial formula for computing the value of $\Theta_{d,D,q,z}$ on a link L which involves the HOMFLYPT polynomials of all sublinks of L and linking numbers [1, Theorem B.1]. A specialisation of the above formula for $z = -E_D(q^3 + 1)^{-1}$ yields a similar result for the invariant $\theta_{d,D,q}$ [12, Corollary 2]. Lickorish’s formula for $\Theta_{d,D,q,z}$ was independently obtained by Poulain d’Andecy and Wagner [29] with the use of Theorem 1. In this section, we will obtain the corresponding formula for $\theta_{d,D,q}$ with the use of our Theorem 2.

First of all, due to property (P1), we can restrict our study to $\theta_{d,q} := \theta_{d,\mathbb{Z}/d\mathbb{Z},q}$. In this case, $E_D = 1/d$. We have already seen that the stabilised Jones–Ocneanu traces defined in Theorem 4 factor through the Temperley–Lieb algebra. Thus, one can define on

$$\bigoplus_{\mu \in \text{Comp}_d(n)} \text{Mat}_{m_\mu}(\text{TL}^\mu(q)) = \bigoplus_{\mu \in \text{Comp}_d(n)} \text{Mat}_{m_\mu}(\text{TL}_{\mu_1}(q) \otimes \text{TL}_{\mu_2}(q) \otimes \dots \otimes \text{TL}_{\mu_d}(q))$$

the trace

$$\sum_{\mu \in \text{Comp}_d(n)} (\tau^{\mu_1} \otimes \tau^{\mu_2} \otimes \dots \otimes \tau^{\mu_d}) \circ \text{Tr}_{\text{Mat}_{m_\mu}}$$

where $\text{Tr}_{\text{Mat}_{m\mu}}$ denotes the usual trace of a matrix. By [14, §6], the map

$$T_{d,q} : \mathcal{L} \rightarrow R, \quad \widehat{\alpha} \mapsto \sum_{\mu \in \text{Comp}_d(n)} (\tau^{\mu_1} \otimes \tau^{\mu_2} \otimes \dots \otimes \tau^{\mu_d}) \circ \text{Tr}_{\text{Mat}_{m\mu}} \circ (\psi_{d,n} \circ \varrho_{d,n} \circ \gamma'_{d,n})(\alpha)$$

is an 1-variable invariant of oriented classical links. This in turn implies that, for a given oriented link L , we have [29, Corollary 4.2]:

$$T_{d,q}(L) = d! \sum_{\pi} q^{4\nu(\pi)} V_q(\pi L) \tag{25}$$

where the sum is over all partitions π of the components of L into d (unordered) subsets, $V_q(\pi L)$ is the product of the Jones polynomials of the d sublinks of L defined by π and $\nu(\pi)$ is the sum of all linking numbers of pairs of components that are in distinct sets of π .

Remark 20 Note that the sum of linking numbers appearing in [29, Corollary 4.2] is twice the sum of linking numbers $\nu(\pi)$, as defined in [1, Theorem B.1] and here.

We then obtain the following closed combinatorial formula for $\theta_{d,q}$.

Proposition 3 *Let L be an oriented link with m components. Then*

$$\theta_{d,q}(L) = \sum_{k=1}^m \frac{(d-1)(d-2)\dots(d-k+1)}{k!} (-q - q^{-1})^{k-1} T_{k,q}(L) \tag{26}$$

Proof Recall that $\theta_{d,q}(L) = (\text{tr}_{d, \mathbb{Z}/d\mathbb{Z}} \circ \varrho_{d,n} \circ \gamma'_{d,n})(\alpha)$, where $\alpha \in B_n$ is such that $\widehat{\alpha} = L$. Then, by [28, Proposition 5.5], we have

$$\theta_{d,q}(L) = \frac{1}{d} \sum_{k=1}^m \binom{d}{k} (-q - q^{-1})^{k-1} T_{k,q}(L) = \sum_{k=1}^m \frac{(d-1)!}{k!(d-k)!} (-q - q^{-1})^{k-1} T_{k,q}(L),$$

and so (26) holds. □

Remark 21 Because of property (P2), Formula (26) is still valid if we replace the integer d by an indeterminate (corresponding to E_D^{-1}). The standard notation used for this generalised invariant is θ (cf. [12]).

Example 7

We will use Formula (26) to compute the value of $\theta_{d,q}$ on the Hopf link with two positive crossings. The Hopf link has two components, each of them being an unknot, and linking number $ln(\text{Hopf}) = 1$. Formula (26) in combination with Eq. (25) reads:

$$\begin{aligned} \theta_{d,q}(\text{Hopf}) &= V_q(\text{Hopf}) + (d-1)(-q - q^{-1})q^{4ln(\text{Hopf})} V_q(\text{Unknot})^2 \\ &= -q^5 - q + d(-q^5 - q^3) + q^5 + q^3 = q^3 - q - d(q^5 + q^3) \end{aligned}$$

since $V_q(\text{Unknot}) = 1$. This coincides with the value that we found in Example 4 for $E_D = 1/d$.

Example 8

We will now use Formula (26) to compute the value of $\theta_{d,q}$ on $L := LLL(0)$ of Fig. 2. We will denote by TU1 (respectively TU2) the 2-component link obtained when removing the component U2 (respectively U1) from L , and by $U^{1,2}$ the 2-component link obtained when removing the component T from L . We have used the programming language SAGE [32] to compute the Jones polynomials of these three 2-component links, while it is easy to determine their linking numbers by hand. We have:

$$\begin{aligned} V_q(\text{TU1}) &= -q^{-3}(q^{10} + q^6 + q^2 - 1) & \text{and } \ln(\text{TU1}) &= 2 \\ V_q(\text{TU2}) &= -q^{-15}(q^{10} + q^6 + q^2 - 1) & \text{and } \ln(\text{TU2}) &= -2 \\ V_q(U^{1,2}) &= q^{-3}(q^{10} + q^6 + q^2 - 1) - 2(q^5 + q) & \text{and } \ln(U^{1,2}) &= 0. \end{aligned} \tag{27}$$

Formula (26) in combination with Eq. (25) reads:

$$\begin{aligned} \theta_{d,q}(L) &= V_q(L) + \\ &+ (d-1)(-q-q^{-1})q^{4(\ln(\text{TU2})+\ln(U^{1,2}))} V_q(\text{TU1})V_q(\text{U2}) + \\ &+ (d-1)(-q-q^{-1})q^{4(\ln(\text{TU1})+\ln(U^{1,2}))} V_q(\text{TU2})V_q(\text{U1}) + \\ &+ (d-1)(-q-q^{-1})q^{4(\ln(\text{TU1})+\ln(\text{TU2}))} V_q(U^{1,2})V_q(\text{T}) + \\ &+ (d-1)(d-2)(-q-q^{-1})^2 q^{4(\ln(\text{TU1})+\ln(\text{TU2})+\ln(U^{1,2}))} V_q(\text{T})V_q(\text{U1})V_q(\text{U2}) \end{aligned}$$

Using the fact that $V_q(\text{U1}) = V_q(\text{U2}) = 1$, since U1 and U2 are unknots, and replacing the linking numbers with their values from (27), we obtain that $\theta_{d,q}(L)$ is equal to:

$$V_q(L) - (d-1)(q+q^{-1})(q^{-8}V_q(\text{TU1}) + q^8V_q(\text{TU2}) + V_q(U^{1,2})V_q(\text{T})) + (d-1)(d-2)(q+q^{-1})^2V_q(\text{T}).$$

Moreover, since T is a left-handed trefoil knot, we have $V_q(\text{T}) = q^{-2} + q^{-6} - q^{-8}$. Using also the values for $V_q(\text{TU1})$, $V_q(\text{TU2})$ and $V_q(U^{1,2})$ from (27), we calculate:

$$\begin{aligned} \theta_{d,q}(L) &= V_q(L) - (d-1)(q+q^{-1})(q^5 - 3q^3 + 2q - 7q^{-1} + 4q^{-3} - 6q^{-5} + 4q^{-7} - 3q^{-9} + 2q^{-11}) \\ &+ (d-1)(d-2)(q+q^{-1})(q^{-1} + q^{-3} + q^{-5} - q^{-9}) \end{aligned}$$

which in turn is equal to:

$$V_q(L) - (d-1)(q+q^{-1})q^{-11} (q^{16} - 3q^{14} + 2q^{12} - 5q^{10} + 6q^8 - 4q^6 + 4q^4 - 5q^2 + 2 - d(q^{10} + q^8 + q^6 - q^2)).$$

This coincides with the value that we found in Example 6 for $E_D = 1/d$.

Remark 22 It is obvious from the examples that, as the number of components becomes larger, the algebraic definition of $\theta_{d,q}$ directly from the Markov trace (or traces) on $\text{FTL}_{d,n}(q)$ is more efficient computationally than its combinatorial definition with the use of Formula (26).

Acknowledgements The author would like to thank the organisers of the conference “Knots in Hellas” for the wonderful organisation and for allowing her to contribute the the volume of the Proceedings of this conference with the current article. She would also like to thank the referees for their useful comments (especially about looking at the example of $LLL(0)$), and Dimos Goundaroulis and Konstantinos Karvounis for their advice on the programming part.

References

1. M. Chlouveraki, J. Juyumaya, K. Karvounis, S. Lambropoulou, Identifying the invariants for classical knots and links from the Yokonuma–Hecke algebras. *Int. Math. Res. Not.* **74**, (2018). <https://doi.org/10.1093/imrn/rny013>
2. M. Chlouveraki, S. Lambropoulou, The Yokonuma–Hecke algebras and the HOMFLYPT polynomial. *J. Knot Theory Ramif.* **22**(14), 1350080 (2013)
3. M. Chlouveraki, G. Pouchin, Determination of the representations and a basis for the Yokonuma–Temperley–Lieb algebra. *Algebr. Represent. Theory* **18**(2), 421–447 (2015)
4. M. Chlouveraki, G. Pouchin, Representations of the framisation of the Temperley–Lieb algebra, *Perspectives in Lie Theory*. Springer INdAM Series (Springer, Berlin, 2017), pp. 253–265
5. M. Chlouveraki, G. Pouchin, Representation theory and an isomorphism theorem for the framisation of the Temperley–Lieb algebra. *Math. Z.* **285**(3), 1357–1380 (2017)
6. M. Chlouveraki, L. Poulain d’Andecy, Representation theory of the Yokonuma–Hecke algebra. *Adv. Math.* **259**, 134–172 (2014)
7. S. Eliahou, L.H. Kauffman, M.B. Thistlethwaite, Infinite families of links with trivial Jones polynomial. *Topology* **42**, 155–169 (2003)
8. J. Espinoza, S. Ryom-Hansen, Cell structures for the Yokonuma–Hecke algebra and the algebra of braids and ties. *J. Pure Appl. Algebr.* **222**(11), 3675–3720 (2018)
9. M. Geck, G. Pfeiffer, *Characters of Finite Coxeter Groups and Iwahori–Hecke Algebras*. London Mathematical Society Monographs, New Series, vol. 21 (Oxford University Press, New York, 2000)
10. D. Goundaroulis, J. Juyumaya, A. Kontogeorgis, S. Lambropoulou, The Yokonuma–Temperley–Lieb algebra. *Banach Cent. Publ.* **103**, 73–95 (2014)
11. D. Goundaroulis, J. Juyumaya, A. Kontogeorgis, S. Lambropoulou, Framization of the Temperley–Lieb algebra. *Math. Res. Lett.* **24**(7), 299–345 (2017)
12. D. Goundaroulis, S. Lambropoulou, A new two-variable generalization of the Jones polynomial, [arXiv:1608.01812](https://arxiv.org/abs/1608.01812)
13. J. Hoste, A. Ocneanu, K. Millett, P. Freyd, W.B.R. Lickorish, D. Yetter, A new polynomial invariant of knots and links. *Bull. Am. Math. Soc.* **12**(2), 239–246 (1985)
14. N. Jacon, L. Poulain d’Andecy, An isomorphism theorem for Yokonuma–Hecke algebras and applications to link invariants. *Math. Z.* **283**(1), 301–338 (2016)
15. V.F.R. Jones, Index for subfactors. *Invent. Math.* **72**, 1–25 (1983)
16. V.F.R. Jones, Hecke algebra representations of braid groups and link polynomials. *Ann. Math.* **126**(2), 335–388 (1987)
17. J. Juyumaya, Sur les nouveaux générateurs de l’algèbre de Hecke $H(G, U, 1)$. *J. Algebr.* **204**, 49–68 (1998)
18. J. Juyumaya, Markov trace on the Yokonuma–Hecke algebra. *J. Knot Theory Ramif.* **13**, 25–39 (2004)

19. J. Juyumaya, S. Kannan, Braid relations in the Yokonuma-Hecke algebra. *J. Algebr.* **239**, 272–297 (2001)
20. J. Juyumaya, S. Lambropoulou, p -Adic framed braids. *Topol. Appl.* **154**, 1804–1826 (2007)
21. J. Juyumaya, S. Lambropoulou, p -Adic framed braids II. *Adv. Math.* **234**, 149–191 (2013)
22. J. Juyumaya, S. Lambropoulou, An adelic extension of the Jones polynomial, *The Mathematics of Knots. Contributions in the Mathematical and Computational Sciences*, vol. 1 (Springer, Berlin, 2011)
23. J. Juyumaya, S. Lambropoulou, An invariant for singular knots. *J. Knot Theory Ramif.* **18**(6), 825–840 (2009)
24. J. Juyumaya, S. Lambropoulou, On the framization of knot algebras, in *New Ideas in Low-Dimensional Topology*, ed. by L. Kauffman, V. Manturov. Series of Knots and Everything (World Scientific, Singapore, 2014)
25. K. Karvounis, Enabling computations for link invariants coming from the Yokonuma–Hecke algebras. *J. Knot Theory Ramif.* **25**(9), 1641012 (2016) (15 pages)
26. K.H. Ko, L. Smolinsky, The framed braid group and 3-manifolds. *Proc. Am. Math. Soc.* **115**(2), 541–551 (1992)
27. G. Lusztig, Character sheaves on disconnected groups VII. *Represent. Theory* **9**, 209–266 (2005)
28. L. Poulain d’Andecy, Invariants for links from classical and affine Yokonuma–Hecke algebras, in *Algebraic Modeling of Topological and Computational Structures and Applications*, ed. by S. Lambropoulou, D. Theodorou, P. Stefanias, L.H. Kauffman. Springer Proceedings in Mathematics and Statistics, vol. 219 (Springer, Berlin, 2017), pp. 77–95
29. L. Poulain d’Andecy, E. Wagner, The HOMFLYPT polynomials of sublinks and the Yokonuma–Hecke algebras, to appear in *Proceedings of the Royal Society of Edinburgh A* See also [Arxiv: 1606.00237](https://arxiv.org/abs/1606.00237)
30. J. Przytycki, P. Traczyk, Conway algebras and skein equivalence of links. *Proc. Am. Math. Soc.* **100**, 744–748 (1987)
31. S. Rostam, Cyclotomic Yokonuma-Hecke algebras are cyclotomic quiver Hecke algebras. *Adv. Math.* **311**, 662–729 (2017)
32. SageMath, The Sage mathematics software system (Version 8.1), The Sage developers (2017), <http://www.sagemath.org>
33. N. Temperley, E. Lieb, Relations between the percolation and colouring problem and other graph-theoretical problems associated with regular planar lattices: some exact results for the percolation problem. *Proc. R. Soc. Ser. A* **322**, 251–280 (1971)
34. T. Yokonuma, Sur la structure des anneaux de Hecke d’un groupe de Chevalley fini. *C.R. Acad. Sci. Paris* **264**, 344–347 (1967)

A Note on $\mathfrak{gl}_{m|n}$ Link Invariants and the HOMFLY–PT Polynomial



Hoel Queffelec and Antonio Sartori

Abstract We present a short and unified representation-theoretical treatment of type A link invariants (that is, the HOMFLY–PT polynomials, the Jones polynomial, the Alexander polynomial and, more generally, the quantum $\mathfrak{gl}_{m|n}$ invariants) as link invariants with values in the quantized oriented Brauer category.

Keywords Reshetikhin–Turaev link invariants · Alexander polynomial · HOMFLY–PT polynomial · Brauer category

2010 Mathematics Subject Classification 57M25 · 57M27 · 81R50

1 Introduction

The HOMFLY–PT polynomial [6, 14] is a 2-variable polynomial link invariant generalizing the Jones polynomial [10], the Alexander polynomial [2] and the \mathfrak{sl}_k Reshetikhin–Turaev link invariant [16]. These polynomials can be even further generalized to invariants of colored links, i.e. links whose components are labeled by integer partitions. All these link invariants arise from the representation theory of the Lie superalgebra $\mathfrak{gl}_{m|n}$, and because of this we call them *invariants of type A*. To elaborate, link invariants of type A can be constructed as equivariant homomorphisms under the action of the quantum enveloping algebra of $\mathfrak{gl}_{m|n}$.

In this short note we present a unified approach to such link invariants by seeing them as invariants with values in the quantized oriented Brauer category,

H. Queffelec (✉)
IMAG, Univ Montpellier, CNRS, Montpellier, France
e-mail: hoel.queffelec@umontpellier.fr

A. Sartori
Mathematisches Institut, Albert-Ludwigs-Universität Freiburg, Eckerstrasse 1,
79104 Freiburg in Breisgau, Germany
e-mail: antoniosartorimath@gmail.com

© Springer Nature Switzerland AG 2019
C. C. Adams et al. (eds.), *Knots, Low-Dimensional Topology and Applications*, Springer Proceedings in Mathematics & Statistics 284,
https://doi.org/10.1007/978-3-030-16031-9_13

a universal category describing intertwiners of $U_q(\mathfrak{gl}_{m|n})$ -representations. We also define reduced link invariants by the usual trick of cutting open one of the strands.

This approach enables us to give an easy construction of link invariants of type A, which does not directly require the knowledge of R-matrices. Moreover, our approach allows for short and self-contained proofs of some well-known properties, which are interesting for categorification problems (see [8]). In particular, we prove that colored $\mathfrak{gl}_{m|n}$ polynomials of links only depend on the difference $d = m - n$ (see Theorem 1 and, in the reduced case, Proposition 2), and we use an automorphism of the Brauer category to prove the symmetry property of the HOMFLY-PT polynomial (Theorem 2).

2 Notation and Conventions

We will work over a field \mathbb{k} containing the complex numbers \mathbb{C} and two elements q and q^t which are not roots of the unity. The first main case we are interested in is $\mathbb{k} = \mathbb{C}(q, q^\beta)$, i.e. a transcendental extension of $\mathbb{C}(q)$ by a formal variable q^β . In this case we say that β is *generic*. The second main example is when t is some integer d and $\mathbb{k} = \mathbb{C}(q)$. As a convention, we use the letter t for encompassing both cases above, while we will use β when we will assume that we are in the first case and we will use d when we will assume that we are in the second case.

For $x \in \mathbb{Z}t + \mathbb{Z}$ we define

$$[x] = \frac{q^x - q^{-x}}{q - q^{-1}} \in \mathbb{k}. \tag{1}$$

2.1 Tangles

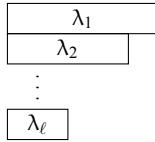
Let **Tangles** be the monoidal category of oriented, framed tangles. Its objects are generated by $\{\uparrow, \downarrow\}$, and its morphisms are (diagrams of) oriented, framed tangles modulo isotopy [11, Sect. XII]. Let also **Tangles** $_{\mathbb{k}}$ be its \mathbb{k} -linear version, with the same objects but with morphisms being \mathbb{k} -vector spaces

$$\mathbf{Tangles}_{\mathbb{k}}(\eta, \eta') = \text{span}_{\mathbb{k}} \mathbf{Tangles}(\eta, \eta'). \tag{2}$$

2.2 Partitions

We denote by $\lambda \vdash N$ a partition λ of $N \geq 0$, which is a non-increasing sequence $\lambda = (\lambda_1, \lambda_2, \dots)$ of non-negative integers such that $|\lambda| = \sum \lambda_i = N$. The transposed partition λ^\top is defined by $\lambda_i^\top = \#\{h \mid \lambda_h \geq i\}$. Partitions can be identified with Young diagrams, as exemplified in the picture below. The only partition of 0 is the empty

partition \emptyset , and the only partition of 1 is the one-box partition \square . Transposition of partitions corresponds to transposition of diagrams.



2.3 Labeled Tangles

We let $\mathbf{Tangles}^{lab}$ be the monoidal category of oriented, framed tangles whose connected components are labeled by partitions. We will regard a morphism in $\mathbf{Tangles}^{lab}$ as a pair consisting of a tangle T and a labeling ℓ of its strands. Given a tangle T and a partition λ , we denote by (T, λ) the labeled tangle T such that all strands are labeled by λ . There is an obvious inclusion $\mathbf{Tangles} \hookrightarrow \mathbf{Tangles}^{lab}$, given by $T \mapsto (T, \square)$. We will use *color* and *label* interchangeably.

3 The Quantized Oriented Brauer Category

We define the quantized oriented Brauer algebra/category, following [5].¹

Definition 1 The *quantized oriented Brauer category* $\mathbf{Br}(t)$ is the quotient of $\mathbf{Tangles}_{\mathbb{k}}$ modulo the following relations

$$\left(\begin{array}{c} \text{crossing} \\ \text{crossing} \end{array} \right) - \left(\text{crossing} \right) = (q^{-1} - q) \left(\begin{array}{c} \text{cup} \\ \text{cup} \end{array} \right), \quad \left(\text{circle} \right) = \left(\text{circle} \right) = [t], \quad (3a)$$

$$\left(\text{cup} \right) = \left(\text{cup} \right) = q^{-t} \left(\begin{array}{c} \text{cup} \\ \text{cup} \end{array} \right), \quad \left(\text{cup} \right) = \left(\text{cup} \right) = q^{+t} \left(\begin{array}{c} \text{cup} \\ \text{cup} \end{array} \right). \quad (3b)$$

Being a quotient of the ribbon category $\mathbf{Tangles}_{\mathbb{k}}$ (see [11, Chap. XIV.5.1] for more details on the ribbon structure), the category $\mathbf{Br}(t)$ inherits a ribbon structure. We denote by $\mathcal{Q}_t : \mathbf{Tangles} \rightarrow \mathbf{Br}(t)$ the composition of the inclusion $\mathbf{Tangles} \hookrightarrow \mathbf{Tangles}_{\mathbb{k}}$ with the quotient functor $\mathbf{Tangles}_{\mathbb{k}} \rightarrow \mathbf{Br}(t)$. Note that $\text{End}_{\mathbf{Br}(t)}(\uparrow^{\otimes r} \downarrow^{\otimes s})$ is free of rank $(r + s)!$, cf. [5, Lemma 2.4]. In particular, for the monoidal unit \emptyset we have $\text{End}_{\mathbf{Br}(t)}(\emptyset) \cong \mathbb{k}$.

¹Note that to precisely match the definitions, one should replace q by q^{-1} and q^β by $q^{-\beta}$.

3.1 The Hecke Algebra

There is a clear algebra morphism $\mathcal{H}_N \rightarrow \text{End}_{\text{Br}(t)}(\uparrow^{\otimes N})$, where \mathcal{H}_N is the Hecke algebra over \mathbb{k} , sending crossings to crossings. This is easily shown to be onto. One way to prove it to be an isomorphism is to introduce a functor $\mathcal{G}_{m|n}$ between $\text{Br}(d)$ and $\text{Rep}_{m|n}$, the category of representations of $U_q(\mathfrak{g}_{m|n})$. Since we will use this as a tool, we refer to [15, Sect. 3] for references and details. By all means, restricting to the $n = 0$ case, this yields the following commuting triangle:

$$\begin{array}{ccc}
 & & \text{End}_{\text{Br}(d)}(\uparrow^{\otimes N}) \\
 & \nearrow & \downarrow \mathcal{G}_{d|0} \\
 \mathcal{H}_N & \longrightarrow & \text{End}_{\text{Rep}_{d|0}}((\mathbb{C}(q)^d)^{\otimes N})
 \end{array}$$

where the bottom arrow is the usual map involved in generic quantum Schur–Weyl duality (see for example [3, Theorem 10.2.5]). In particular, it is faithful for $d \geq N$, proving that $\mathcal{H}_N \simeq \text{End}_{\text{Br}(t)}(\uparrow^{\otimes N})$.

The algebra \mathcal{H}_N is a finite-dimensional semisimple algebra. Its finite-dimensional simple representations up to isomorphism are parametrized by partitions λ of N , and we denote them by $S(\lambda)$ for $\lambda \vdash N$ (we refer to [12, Chap. 3] for details). In particular, \mathcal{H}_N decomposes as

$$\mathcal{H}_N = \bigoplus_{\lambda \vdash N} e_\lambda \mathcal{H}_N e_\lambda, \tag{4}$$

where the e_λ 's are central idempotents, $\mathcal{H}_N e_\lambda \cong S(\lambda)^{\oplus \dim_{\mathbb{k}} S(\lambda)}$ as a left module and $e_\lambda \mathcal{H}_N e_\lambda$ is isomorphic to a matrix algebra. We note that one can write explicit formulas for the idempotents e_λ , similarly as for the symmetric group, see [9].

For each $\lambda \vdash N$, we choose a primitive idempotent p_λ in $e_\lambda \mathcal{H}_N e_\lambda$. Unless e_λ itself is primitive (and this happens if and only if λ is a row or a column partition, see for example [9, Theorem 3.10]), the element p_λ is not uniquely determined. But any two choices are conjugated in $e_\lambda \mathcal{H}_N e_\lambda$, and hence also in \mathcal{H}_N .

3.2 Cabling

We adopt the following graphical convention for picturing morphisms in the Brauer category: when we draw a thick strand labeled by λ , then this stands for $|\lambda|$ parallel strands, next to each other and intertwined by the idempotent p_λ as illustrated by the following picture:

$$\uparrow^\lambda = \boxed{\begin{array}{c} \uparrow \dots \uparrow \\ p_\lambda \\ \dots \\ \uparrow \dots \uparrow \end{array}} \tag{5}$$

Since the Brauer category is a ribbon category, all morphisms obtained from a given diagram by placing the same idempotent at different positions on the same strand are equal (p_λ can be “slid around”). Furthermore, it might be easier in some computations to make use of the idempotent property and put more than one copy of p_λ along the strands.

This procedure allows us to define a monoidal functor $\mathcal{Q}_t^{lab} : \text{Tangles}^{lab} \rightarrow \text{Br}(t)$.

Remark 1 One can also make sense of this cabling procedure more formally in the category-theoretical setting. Namely, one can construct the Karoubi envelope of the additive closure of $\text{Br}(t)$, as explained for example in [4, Sect.2]. This enlarged category is monoidally generated by primitive idempotents in $\text{Br}(t)$. In fact, for our purposes it would be sufficient to consider a partial Karoubi envelope $\tilde{\text{Br}}(t)$ which is the smallest additive monoidal category containing all images of the primitive idempotents p_λ . The ribbon structure of $\text{Br}(t)$ induces a ribbon structure on $\tilde{\text{Br}}(t)$, and one obtains immediately a functor $\mathcal{Q}_t^{lab} : \text{Tangles}^{lab} \rightarrow \tilde{\text{Br}}(t)$.

4 Link Invariants of Type A

Definition 2 Let L be an oriented, framed link.

- The **HOMFLY-PT polynomial** of L , denoted by $P_\beta(L)$, is the image of L under the functor \mathcal{Q}_β , i.e. $\mathcal{Q}_\beta(L) \in \text{End}_{\text{Br}(\beta)}(\mathcal{O}) = \mathbb{k}$.
- Let $d \in \mathbb{Z}$. The **d -polynomial** of L , denoted by $P_d(L)$, is the image of L under the functor \mathcal{Q}_d , i.e. $\mathcal{Q}_d(L) \in \text{End}_{\text{Br}(d)}(\mathcal{O}) = \mathbb{k}$.

Remark 2 It follows from the fact that $\text{Br}(d)$ is defined over \mathbb{k} that $P_d(L)$ is actually a Laurent polynomial in the variable q . Similarly, one sees that $P_\beta(L)$ is an element of $\mathbb{C}[q, q^{-1}, q^\beta, q^{-\beta}, [\beta]]$.

Definition 3 Let L be an oriented, framed link and ℓ be a labeling of its strands.

- The **ℓ -labeled HOMFLY-PT polynomial** of L , denoted by $P_\beta^\ell(L)$, is the image of (L, ℓ) under the functor \mathcal{Q}_β^{lab} , i.e. $\mathcal{Q}_\beta^{lab}(L, \ell) \in \text{End}_{\text{Br}(\beta)}(\mathcal{O}) = \mathbb{k}$.
- Let $d \in \mathbb{Z}$. The **ℓ -labeled d -polynomial** of L , denoted by $P_d^\ell(L)$, is the image of (L, ℓ) under the functor \mathcal{Q}_d^{lab} , i.e. $\mathcal{Q}_d^{lab}(L, \ell) \in \text{End}_{\text{Br}(d)}(\mathcal{O}) = \mathbb{k}$.

Lemma 1 *The definition above does not depend on the choice of the elements p_λ .*

Proof Suppose $\lambda \vdash N$, and let p'_λ another choice for a primitive idempotent in $e_\lambda \mathcal{H}_N e_\lambda$. Then there is an invertible element $x \in \mathcal{H}_N$ such that $x p'_\lambda x^{-1} = p_\lambda$. Since we can slide x around on the cabled strands and cancel it with x^{-1} , the independence on the particular choice for p_λ follows. □

Remark 3 In the general case, it is not clear to us how one can deduce from this definition that $P_d^\ell(L)$ is a Laurent polynomial. If ℓ labels every strand by a one-column partition, then this can be deduced using the category $\text{Sp}(\beta)$, introduced by

the two authors in [15], which is defined over $\mathbb{C}[q, q^{-1}]$. One can argue analogously if ℓ labels every strand by a one-row partition.

Note that it follows immediately that the $\beta = d$ specialization of the (labeled) HOMFLY–PT polynomial yields the (labeled) d –polynomial. We stress that Definition 3 is just a reformulation of Reshetikhin–Turaev’s construction [16]:

Proposition 1 *Let $m, n \in \mathbb{Z}_{\geq 0}$ and let $d = m - n$. Then $P_d^\ell(L)$ is the labeled $\mathfrak{gl}_{m|n}$ link invariant (given by the Reshetikhin–Turaev construction).*

Proof In this proof, we assume familiarity with the Reshetikhin–Turaev construction, for which we refer to [16] or [13].

Let $\text{Rep}_{m|n}$ denote the category of finite-dimensional representations of the quantum group $U_q(\mathfrak{gl}_{m|n})$ (we refer to [15] for detailed definitions and references). Note that one can make sense of this also for $m = n = 0$: in this case, $\mathfrak{gl}_{0|0}$ is the trivial (zero-dimensional) Lie algebra, and $\text{Rep}_{0|0}$ is equivalent to the category of finite-dimensional $\mathbb{C}(q)$ –vector spaces. The Reshetikhin–Turaev functor $\mathcal{RT}_{m|n} : \text{Tangles}^{\text{lab}} \rightarrow \text{Rep}_{m|n}$ factors as

$$\begin{array}{ccc}
 & \mathcal{Q}_d^{\text{lab}} & \text{Br}(d) \\
 & \nearrow & \downarrow \mathcal{G}_{m|n} \\
 \text{Tangles}^{\text{lab}} & \xrightarrow{\mathcal{RT}_{m|n}} & \text{Rep}_{m|n}
 \end{array} \tag{6}$$

For this, one only has to check that the relations (3) are satisfied in $\text{Rep}_{m|n}$, and this is well-known, see for example [15, Sect. 3] and references therein. Moreover, after extension of scalars from \mathbb{k} to $\mathbb{C}(q)$, it is easy to see that $\mathcal{G}_{m|n}$ induces an isomorphism between $\text{End}_{\text{Br}(d)}(\emptyset)$ and $\text{End}_{U_q(\mathfrak{gl}_{m|n})}(\mathbb{C}(q))$, which are both naturally identified with \mathbb{k} . Hence, we have $\mathcal{G}_{m|n} \circ \mathcal{Q}_d^{\text{lab}}(L, \ell) = \mathcal{RT}_{m|n}(L, \ell)$. \square

As an immediate consequence, we obtain the following well-known important result:

Theorem 1 *The $\mathfrak{gl}_{m|n}$ Reshetikhin–Turaev invariant of links colored by partitions only depends on the difference $m - n$.*

In particular, since the $d = 2$ case of [16] is the Jones polynomial, $P_2(L)$ is the Jones polynomial of L .

5 Symmetry for the HOMFLY–PT Polynomial

In this section, we give an easy proof of a classical symmetry of the HOMFLY–PT polynomial, which follows immediately from the existence of an automorphism of the quantized oriented Brauer category. Another proof of this symmetry (although in

a slightly different formulation) has been given using web categories in [18, Proposition 4.4] (see also references therein for previous discussions).

Theorem 2 *Let (L, ℓ) be a labeled link, and let ℓ^\top denote the transpose labeling (which labels each strands by the transpose partition). We have*

$$P_\beta^\ell(L)(q, q^\beta) = P_\beta^{\ell^\top}(L)(-q^{-1}, q^\beta). \tag{7}$$

Proof In the case β generic, we can define a \mathbb{C} -linear involution τ of the quantized walled Brauer category. On objects, τ is simply the identity functor. On each morphism space, τ is the unique \mathbb{C} -linear involution which fixes **Tangles** and acts on \mathbb{k} via $\tau(q) = -q^{-1}$ and $\tau(q^\beta) = q^\beta$. It is immediate to check that the defining relations are satisfied. By applying τ to the Hecke algebra \mathcal{H}_N one interchanges the simple representations $S(\lambda)$ and $S(\lambda^\top)$ (this is easily checked on exterior and symmetric powers and then extends for example using Gyoja-Aiston idempotents [1, 9]). In particular, $\tau(p_\lambda)$ is conjugated to p_{λ^\top} . Hence $P_\beta^{\ell^\top}(L)(q, q^\beta) = \tau(P_\beta^\ell(L)(q, q^\beta)) = P_\beta^\ell(L)(-q^{-1}, q^\beta)$. \square

For the usual (uncolored) HOMFLY-PT polynomial we get the following property:

Corollary 1 *We have $P_\beta(L)(q, q^\beta) = P_\beta(L)(-q^{-1}, q^\beta)$.*

Remark 4 From the proof above it is also clear why this symmetry holds for the HOMFLY-PT polynomial but fails for the d -polynomial.

6 Reduced Link Invariants of Type A

In this section we discuss reduced link invariants, following ideas from [7] and related works. The main goal is to get non-trivial invariants also in the case $d = 0$, and in particular to define the Alexander polynomial. Indeed, we have:

Lemma 2 *If $d = 0$, then $P_0^\ell(L) = 0$ for all links L and non-trivial labelings ℓ .*

Proof This follows immediately from Theorem 1, since the $\mathfrak{gl}_{0|0}$ link invariant is zero if at least one strand is labeled by a non-empty partition. \square

Given a link L with a labeling ℓ of its strands and a chosen strand labeled by λ , we can cut open this strand and obtain a tangle $T \in \text{End}_{\text{Tangles}^{\text{wb}}}(\uparrow)$. The link L is obtained as closure of the tangle T :

$$\boxed{L} = \boxed{T} \begin{array}{c} \curvearrowright \\ \curvearrowleft \end{array} \lambda \tag{8}$$

Note that, since the Hecke algebra is semisimple and p_λ is a primitive idempotent, we have $p_\lambda \text{End}_{\text{Br}(t)}(\uparrow^{|\lambda|})p_\lambda \cong \mathbb{k}p_\lambda$. This allows us to give the following definition:

Definition 4 Let L be an oriented, framed link and ℓ be a labeling of its strands. Regard L as closure of a tangle T obtained by cutting open a strand labeled by λ , as in (8).

- The ℓ -labeled λ -reduced HOMFLY-PT polynomial of L , denoted by $P_\beta^{\ell,\lambda}(L)$, is the scalar α such that $\mathcal{Q}_\beta^{ab}(T, \ell) = \alpha p_\lambda \in p_\lambda \text{End}_{\text{Br}(\beta)}(\uparrow^{\otimes|\lambda|})p_\lambda$.
- Let $d \in \mathbb{Z}$. The ℓ -labeled λ -reduced d -polynomial of L , denoted by $P_d^{\ell,\lambda}(L)$, is the scalar α such that $\mathcal{Q}_d^{ab}(T, \ell) = \alpha p_\lambda \in p_\lambda \text{End}_{\text{Br}(d)}(\uparrow^{\otimes|\lambda|})p_\lambda$.

Of course, we have to check that the definition does not depend on the chosen strand labeled by λ (and on the particular point where we cut the strand). This is implied by Lemma 3 below. First, notice that by applying \mathcal{Q}_t^{ab} to both sides of (8) we get

$$P_t^\ell(L) = \text{tr}_{\text{Br}(t)} p_\lambda \cdot P_t^{\ell,\lambda}(L), \tag{9}$$

where

$$\text{tr}_{\text{Br}(t)} p_\lambda = \text{tr}_{\text{Br}(t)} \left(\text{circle with } \lambda \text{ on top} \right) = P_t^\lambda(\bigcirc) \in \text{End}_{\text{Br}(t)}(\mathbb{C}). \tag{10}$$

In particular, if $\text{tr}_{\text{Br}(t)} p_\lambda$ is non-zero then $P_t^{\ell,\lambda}(L)$ is well-defined and can be obtained by division by $P_t^\ell(L)$, whence the name ‘‘reduced’’.

Lemma 3 *The invariants $P_\beta^{\ell,\lambda}(L)$ and $P_d^{\ell,\lambda}(L)$ are well-defined.*

Proof Note first that, if $d > 0$ and λ is a partition with at most d rows, then $\text{tr}_{\text{Br}(d)} p_\lambda$ is the quantum dimension of the irreducible $U_q(\mathfrak{gl}_d)$ -module with highest weight corresponding to λ , hence it is nonzero. (This can be seen for example by application of the functor $\mathcal{G}_{d|0}$, after which this is a consequence of quantum Schur–Weyl duality.)

Now, for β generic, $\text{tr}_{\text{Br}(\beta)} p_\lambda$ is always non-zero (since it has to specialize for $\beta = d$ to $\text{tr}_{\text{Br}(d)}(p_\lambda)$, which for $d \gg 0$ is non-zero). Hence, $P_\beta^{\ell,\lambda}(L)$ is equal to $P_\beta^\ell(L)$ divided by $\text{tr}_{\text{Br}(\beta)} p_\lambda$, and so it is well-defined.

In the case $t = d \in \mathbb{Z}$, by construction, $P_d^{\ell,\lambda}(L)$ is the specialization of $P_\beta^{\ell,\lambda}(L)$ at $\beta = d$, hence also $P_d^{\ell,\lambda}(L)$ is well-defined. \square

Note that, as follows from the proof of the previous lemma, for β generic the reduced invariants do not give any more information, since we always have

$$P_\beta^{\ell,\lambda}(L) = \frac{P_\beta^\ell(L)}{\text{tr}_{\text{Br}(\beta)} p_\lambda}. \tag{11}$$

On the other hand, in the specialized case $t = d$ it often happens that $\text{tr}_{\text{Br}(d)} p_\lambda = 0$, and hence the invariant $P_d^\ell(L)$ is zero as long as one of the strands is labeled by such a λ , while the reduced invariant $P_d^{\ell,\lambda}(L)$ may be non-zero (cf. also Remark 5 below).

Let us denote by $Hook_{m|n}$ the set of hook partitions of type $m|n$ (i.e. the partitions λ with $\lambda_{m+1} \leq n$). Then we have the following analog of Proposition 1:

Proposition 2 *Let $m, n \in \mathbb{Z}_{\geq 0}$ and let $d = m - n$. Suppose $\lambda \in Hook_{m|n}$. Then $P_d^{\ell, \lambda}(L)$ is the λ -reduced ℓ -labeled $\mathfrak{gl}_{m|n}$ link invariant (given by the Reshetikhin–Turaev construction). In particular, this link invariant only depends on $m - n$.*

Proof The proof is analogous to the proof of Proposition 1. Since $\lambda \in Hook_{m|n}$, the image of p_λ in $\text{Rep}_{m|n}$ is non-zero (it projects onto one copy of the simple $U_q(\mathfrak{gl}_{m|n})$ -module $L(\lambda)$ labeled by λ). In particular, $\mathcal{G}_{m|n}$ induces an isomorphism between the idempotent truncation $p_\lambda \text{End}_{\text{Br}(d)}(\uparrow^{\otimes |\lambda|}) p_\lambda$ and $\text{End}_{U_q(\mathfrak{gl}_{m|n})}(L(\lambda))$, which are both naturally identified with $\mathbb{C}(q)$. Hence, the claim follows from the commutativity of (6). □

Corollary 2 *The link invariant $P_0^{\square, \square}(L)$ is (up to rescaling) the Alexander polynomial of L .*

Proof This follows from Proposition 2 above together with [17, Theorem 4.10]. Alternatively, one can argue that, up to rescaling, $P_0^{\square, \square}$ satisfies the skein relations of the Alexander polynomial. □

Remark 5 In Proposition 2 it is crucial to assume that m, n are big enough so that $\lambda \in Hook_{m|n}$. This makes a big difference with the situation of Proposition 1. Indeed, Proposition 1 implies that the labeled $\mathfrak{gl}_{m|n}$ link invariant vanishes as long as one strand is labeled by a partition λ such that $\lambda \notin H_{m-k|n-k}$ for some $k \geq \min\{m, n\}$. For example, the $\mathfrak{gl}_{2|1}$ link invariant always vanishes if one strand is labeled by a partition with more than one row. On the other hand, Proposition 2 does not imply that the λ -reduced $\mathfrak{gl}_{m|n}$ link invariant vanishes if the $\mathfrak{gl}_{m-1|n-1}$ does.

Acknowledgements H.Q. was funded by the ARC DP 140103821.

References

1. A.K. Aiston, H.R. Morton, Idempotents of Hecke algebras of type A. *J. Knot Theory Ramif.* **7**(4), 463–487 (1998). <https://doi.org/10.1142/S0218216598000243>
2. J.W. Alexander, Topological invariants of knots and links. *Trans. Am. Math. Soc.* **30**(2), 275–306 (1928). <https://doi.org/10.2307/1989123>
3. V. Chari, A. Pressley, *A Guide to Quantum Groups* (Cambridge University Press, Cambridge, 1994)
4. J. Comes, B. Wilson, Deligne’s category $\text{REP}(GL_\delta)$ and representations of general linear supergroups. *Represent. Theory* **16**, 568–609 (2012). <https://doi.org/10.1090/S1088-4165-2012-00425-3>
5. R. Dipper, S. Doty, F. Stoll, The quantized walled Brauer algebra and mixed tensor space. *Algebras Represent. Theory* **17**(2), 675–701 (2014). <https://doi.org/10.1007/s10468-013-9414-2>
6. P. Freyd, D. Yetter, J. Hoste, W.B.R. Lickorish, K. Millett, A. Ocneanu, A new polynomial invariant of knots and links. *Bull. Am. Math. Soc. (N.S.)* **12**(2), 239–246 (1985). <https://doi.org/10.1090/S0273-0979-1985-15361-3>

7. N. Geer, B. Patureau-Mirand, V. Turaev, Modified quantum dimensions and re-normalized link invariants. *Compos. Math.* **145**(1), 196–212 (2009). <https://doi.org/10.1112/S0010437X08003795>
8. E. Gorsky, S. Gukov, M. Stosic, Quadruply-graded colored homology of knots (2013), [arXiv:1304.3481](https://arxiv.org/abs/1304.3481)
9. A. Gyoja, A q-analogue of Young symmetrizer. *Osaka J. Math.* **23**(4), 841–852 (1986), <http://projecteuclid.org/euclid.ojm/1200779724>
10. V.F.R. Jones, A polynomial invariant for knots via von Neumann algebras. *Bull. Am. Math. Soc. (N.S.)* **12**(1), 103–111 (1985). <https://doi.org/10.1090/S0273-0979-1985-15304-2>
11. C. Kassel, *Quantum Groups*. Graduate Texts in Mathematics, vol. 155 (Springer, New York, 1995)
12. A. Mathas, *Iwahori-Hecke Algebra and Schur Algebras of the Symmetric Group*. University Lecture Series, vol. 15 (American Mathematical Society, Providence, 1999)
13. T. Ohtsuki, *Quantum Invariants*. Series on Knots and Everything, vol. 29 (World Scientific, Singapore, 2002)
14. J.H. Przytycki, P. Traczyk, Conway algebras and skein equivalence of links. *Proc. Am. Math. Soc.* **100**(4), 744–748 (1987). <https://doi.org/10.2307/2046716>
15. H. Queffelec, A. Sartori, Mixed quantum skew Howe duality and link invariants of type A. *J. Pure Appl. Algebra.* **223**(7), 2733–2779 (2019) . <https://doi.org/10.1016/j.jpaa.2018.09.014>
16. N.Y. Reshetikhin, V.G. Turaev, Ribbon graphs and their invariants derived from quantum groups. *Commun. Math. Phys.* **127**(1), 1–26 (1990), <http://projecteuclid.org/euclid.cmp/1104180037>
17. A. Sartori, The Alexander polynomial as quantum invariant of links. *Ark. Mat.* **53**(1), 177–202 (2015). <https://doi.org/10.1007/s11512-014-0196-5>
18. D. Tubbenhauer, P. Vaz, P. Wedrich, Super q-howe duality and web categories. *Algebr. Geom. Topol.* **17**(6), 3703–3749 (2017). <https://doi.org/10.2140/agt.2017.17.3703>

On the Geometry of Some Braid Group Representations



Mauro Spera

Abstract In this note we report on recent differential geometric constructions aimed at devising representations of braid groups in various contexts, together with some applications in different domains of mathematical physics. First, the classical Kohno construction for the 3- and 4-strand pure braid groups P_3 and P_4 is explicitly implemented by resorting to the Chen-Hain-Tavares nilpotent connections and to hyperlogarithmic calculus, yielding unipotent representations able to detect Brunnian and nested Brunnian phenomena. Physically motivated unitary representations of Riemann surface braid groups are then described, relying on Bellingeri's presentation and on the geometry of Hermitian–Einstein holomorphic vector bundles on Jacobians, via representations of Weyl-Heisenberg groups.

Keywords Braid groups · Chen iterated integrals · Hermitian–Einstein bundles · Weyl-Heisenberg groups

2010 Mathematics Subject Classification 53D50 · 81S10 · 20F36 · 55R50 · 58B34

1 Introduction

Braid groups, with their multifaceted incarnations, play a prominent role throughout mathematics and enter in an essential way in the formulation of various physical theories [17, 18, 30, 40, 41, 80]. The present note is devoted to surveying some recent geometric approaches for constructing braid group representations, building on [10, 70]. We first discuss low-dimensional matrix representations of pure braid groups (on three and four strands) obtained via holonomy of suitable nilpotent flat connections [10]. Flatness is directly enforced by means of the Arnol'd relations,

M. Spera (✉)

Dipartimento di Matematica e Fisica “Niccolò Tartaglia”,
Università Cattolica del Sacro Cuore, Via dei Musei 41, 25121 Brescia, Italy
e-mail: mauro.spera@unicatt.it

© Springer Nature Switzerland AG 2019

C. C. Adams et al. (eds.), *Knots, Low-Dimensional Topology and Applications*, Springer Proceedings in Mathematics & Statistics 284,
https://doi.org/10.1007/978-3-030-16031-9_14

287

and computations heavily rely on hyperlogarithmic calculus [79]. These explicit representations were used in [10] for the investigation of Brunnian and “nested” Brunnian phenomena.

Subsequently we review the construction of unitary representations of Riemann surface braid groups of [70], obtained by resorting to Bellingeri’s presentation [8] and to the geometry of Hermitian–Einstein holomorphic vector bundles on Jacobians (à la Matsushima [51]), also commenting on the noncommutative geometric route outlined in [70] and concisely portraying the motivating physical background.

2 Braid and Pure Braid Groups

2.1 Standard Braid and Pure Braid Groups

This subsection is meant to provide a minimal background on standard braid and pure braid groups and to establish notation. For a full account see e.g. [3, 10, 17, 18, 40, 47, 53] as well.

The Artin braid group B_n is the group generated by $n - 1$ generators b_1, b_2, \dots, b_{n-1} subject to the *braid relations*

$$b_i b_j = b_j b_i$$

for all $i, j = 1, 2, \dots, n - 1$ with $|i - j| \geq 2$, and

$$b_i b_{i+1} b_i = b_{i+1} b_i b_{i+1}$$

for $i = 1, 2, \dots, n - 2$.

The *pure* (or *coloured*) *braid group* P_n is the kernel of the natural projection $\pi : B_n \rightarrow S_n$ where S_n is the symmetric group:

$$P_n = \text{Ker}(\pi : B_n \rightarrow S_n)$$

(the symmetric group itself being obtained from B_n by adding the extra relations $\sigma_i^2 = 1$). The n -strand pure braid group on P_n is the fundamental group of the configuration space $\text{Conf}(n, \mathbb{C})$ of n distinct points on the complex plane \mathbb{C} . We take its base point at $(1, 2, \dots, n) \in \text{Conf}(n, \mathbb{C})$.

The pure braid group P_n is generated by the $n(n - 1)/2$ elements $\{A_{ij}\}_{1 \leq i < j \leq n}$ subject to the so-called Artin relations, which will be written down explicitly only for $n = 3$ below. One sets, $A_{ij} = A_{ji}$, for $i \neq j$. The generators A_{ij} can be represented (up to isotopy) by downward directed *geometric braids* such that strand i (starting from and ending at $z = i$) winds *clockwise* around strand j or conversely. We do not need their expression in terms of the b ’s. In what follows we shall blur the distinction between a geometric braid and the element of the braid group it represents. Concretely

(and with an abuse of language) the product $b_1 \cdot b_2$ is given by juxtaposition, drawing b_2 below b_1 .

The Artin relations for P_3 read

$$\begin{aligned} A_{12}^{-1} A_{23} A_{12} &= A_{13} A_{23} A_{13}^{-1} \\ A_{12}^{-1} A_{13} A_{12} &= A_{13} A_{23} A_{13} A_{23}^{-1} A_{13}^{-1} \end{aligned}$$

whereas the centre of P_3 is generated by $\Delta_3^2 = A_{12} A_{13} A_{23}$.

The (co)homology ring of the coloured braid group (namely, that of $Conf(n, \mathbb{C})$) is isomorphic to the exterior graded ring generated by one-dimensional elements $\omega_{ij} = \omega_{ji}$, $1 \leq i \neq j \leq n$ satisfying the Arnol'd relations [2] (i, j, k distinct)

$$I_{ijk} := \omega_{ij} \wedge \omega_{jk} + \omega_{jk} \wedge \omega_{ki} + \omega_{ki} \wedge \omega_{ij} = 0$$

Concretely, one takes the logarithmic 1-forms

$$\omega_{ij} := \frac{1}{2\pi\sqrt{-1}} d \log(z_i - z_j) = \frac{1}{2\pi\sqrt{-1}} \frac{d(z_i - z_j)}{z_i - z_j}$$

(for $z_i \neq z_j$, $\sqrt{-1} = +i$). Thus there are $\binom{n}{3}$ independent Arnol'd relations.

Specifically, the Arnol'd identity for P_3 reads

$$\mathbb{I}_1 := \omega_{12} \wedge \omega_{23} + \omega_{23} \wedge \omega_{31} + \omega_{31} \wedge \omega_{12} = 0$$

whereas one gets three additional Arnol'd identities for P_4 .

Let us also recall for completeness the definition of the *holonomy algebra* \mathcal{P}_n (see e.g. [58]), generated (over \mathbb{C}), by elements t_{ij} , $i, j = 1, 2, \dots, n$, $i < j$, fulfilling the so-called *infinitesimal pure braid relations*:

$$t_{ij} = t_{ji}$$

$$[t_{ik}, t_{ij} + t_{jk}] = [t_{ij}, t_{ik} + t_{jk}] = 0, \quad i, j, k \text{ all distinct}$$

$$[t_{ij}, t_{hk}] = 0 \text{ if } i, j, k, h \text{ all distinct}$$

It is actually the universal enveloping algebra of the Lie algebra generated by the t 's subject to the infinitesimal braid relations. It is well known that t_{ij} can be depicted as a set of n parallel vertical strings together with a horizontal string connecting string i with string j (with the product defined by juxtaposition).

2.2 Riemann Surface Braid Groups

The braid group on n strands $B(X, n)$ pertaining to a topological space X is by definition the fundamental group of the associated configuration space $C_n(X)$ consisting of all n -ples of distinct points, *up to order* or, equivalently, of all n -point subsets of X . Here we take $X = \Sigma_g$, a closed orientable surface (actually, a Riemann surface) of genus $g \geq 1$. Its associated braid group $B(\Sigma_g, n)$ admits, among others, the following presentation due to Bellingeri [8]. The generators are $\sigma_1, \dots, \sigma_{n-1}; a_1, \dots, a_g, b_1, \dots, b_g$ (the former are the standard braid group generators previously generically denoted by b , the latter have a simple geometric interpretation, in terms of the natural dissection of the surface by means of a $4g$ -gon, see [8]). The presence of the extra generators is natural: if, say, two points loop around each other, their trajectories can at the same time wind around the handles of the surface.

In the presentation, in addition to the ordinary braid relations

$$(B1) : \sigma_j \sigma_{j+1} \sigma_j = \sigma_{j+1} \sigma_j \sigma_{j+1} \quad j = 1, 2, \dots, n - 2$$

$$(B2) : \sigma_i \sigma_j = \sigma_j \sigma_i, \quad |i - j| > 1$$

one has “mixed” relations

$$(R1) : \quad a_r \sigma_i = \sigma_i a_r, \quad 1 \leq r \leq g, \quad i \neq 1$$

$$\quad b_r \sigma_i = \sigma_i b_r, \quad 1 \leq r \leq g, \quad i \neq 1$$

$$(R2) : \quad \sigma_1^{-1} a_r \sigma_1^{-1} a_r = a_r \sigma_1^{-1} a_r \sigma_1^{-1}, \quad 1 \leq r \leq g,$$

$$\quad \sigma_1^{-1} b_r \sigma_1^{-1} b_r = b_r \sigma_1^{-1} b_r \sigma_1^{-1}, \quad 1 \leq r \leq g,$$

$$(R3) : \quad \sigma_1^{-1} a_s \sigma_1 a_r = a_r \sigma_1^{-1} a_s \sigma_1, \quad s < r$$

$$\quad \sigma_1^{-1} b_s \sigma_1 b_r = b_r \sigma_1^{-1} b_s \sigma_1, \quad s < r$$

$$\quad \sigma_1^{-1} a_s \sigma_1 b_r = b_r \sigma_1^{-1} a_s \sigma_1, \quad s < r$$

$$\quad \sigma_1^{-1} b_s \sigma_1 a_r = a_r \sigma_1^{-1} b_s \sigma_1, \quad s < r$$

$$(R4) : \quad \sigma_1^{-1} a_r \sigma_1^{-1} b_r = b_r \sigma_1^{-1} a_r \sigma_1, \quad 1 \leq r \leq g$$

$$(TR) : \quad [a_1, b_1^{-1}] \cdots [a_g, b_g^{-1}] = \sigma_1 \sigma_2 \cdots \sigma_{n-1}^2 \cdots \sigma_2 \sigma_1$$

with the usual group theoretical convention $[a, b] = aba^{-1}b^{-1}$.

3 Unipotent Representations of the Pure Braid Group via Differential Geometry

3.1 Overview

This section summarises the content of the (purely mathematical) paper [10], devoted to elaboration of quite concrete instances of the abstract general framework developed

in [44–47] (see also [1, 6, 48, 50, 58]). We eventually obtain fully explicit *families* of pure braid invariants by a systematic approach resting on a vivid differential geometric principle. These topological invariants turn out to be able to distinguish, at least partially, pure braids with three or four strands, especially those exhibiting a *Brunnian-like* character, namely, those which become trivial after removing some strands therefrom in an arbitrary way (see below for precise definitions).

First notice that the general theory already tells us that the Kohno monodromy representations exhaust all unipotent representations on P_n , ([46], Theorem 1.2.6, see also [1], Théorème 1); nevertheless explicit calculations are unavoidable if one aims at getting more detailed information.

Thus, specifically, the procedure expounded in [10] is the following: recall, in general, the abstract Kniznik–Zamolodchikov–Kohno (KZK) connection [44–47]

$$\mathbf{v} = \sum_{i < j} t_{ij} \omega_{ij}$$

defined on $Conf(n, \mathbb{C})$, with the t 's fulfilling the infinitesimal braid relations and the ω 's fulfilling, in turn, Arnol'd's relations. The KZK connection is flat, namely

$$d\mathbf{v} + \mathbf{v} \wedge \mathbf{v} = \mathbf{v} \wedge \mathbf{v} = \mathbf{0}$$

Then, its *parallel transport*, defined by a time-ordered exponential involving *Chen iterated path integrals* [22, 23]

$$\rho(\gamma) = T \exp \int_{\gamma} \mathbf{v}$$

(γ being a path in $Conf(n, \mathbb{C})$), gives rise to a representation (call again it ρ) of P_n via the holonomy algebra \mathcal{P}_n discussed above. This is the crucial ingredient in Kontsevich's universal knot invariant construction [6, 48, 58]. In what follows we aim at finding concrete *nilpotent matrix* valued Hain–Tavares connections [32, 71], enforcing flatness via the Arnol'd relations (in this manner, the infinitesimal braid relations for the ensuing t 's will then be automatically fulfilled). The Chen series then becomes a finite sum. It is then clearly enough to calculate holonomies around the (Artin) generators, a non trivial task, which can be achieved in principle by resorting to hyperlogarithms and their monodromy [79]; in our setting, it will be enough to compute suitable *double* iterated integrals. In the following subsections we shall outline such a programme for P_3 and P_4 . It should be noticed from the outset that the specific method illustrated here does not produce non trivial representations for $P_n, n > 4$ [10].

3.2 Representations of P_3

We are going to discuss P_3 -representations manufactured through the method described above. For the sake of clarity, we shall give a few details, which, on the contrary, will be omitted when dealing with P_4 .

In this specific case we look for 1-forms v_k

$$v_k := t_k^{12} \omega_{12} + t_k^{13} \omega_{13} + t_k^{23} \omega_{23} \quad k = 1, 2, 3 \quad t_k^{ij} (= t_k^{ji}) \in \mathbb{C}$$

such that $v_1 \wedge v_2 = \lambda(\omega_{12} \wedge \omega_{23} + \omega_{23} \wedge \omega_{31} + \omega_{31} \wedge \omega_{12})$ with $\lambda \in \mathbb{C}$. We take the following connection 1-form

$$\mathbf{v} = \begin{pmatrix} 0 & v_1 & v_3 \\ 0 & 0 & v_2 \\ 0 & 0 & 0 \end{pmatrix}$$

with curvature

$$\Omega = d\mathbf{v} + \mathbf{v} \wedge \mathbf{v} = \begin{pmatrix} 0 & 0 & v_1 \wedge v_2 \\ 0 & 0 & 0 \\ 0 & 0 & 0 \end{pmatrix}$$

to be set equal to zero, this leading to the conditions:

$$t_1^{12} t_2^{23} - t_2^{12} t_1^{23} = t_1^{23} t_2^{31} - t_2^{23} t_1^{31} = t_1^{31} t_2^{12} - t_2^{31} t_1^{12}$$

Upon interpreting 1-forms as geometric vectors (so long as their coefficients are real), together with their wedge products (which, in turn, become ordinary vector products), the above condition tells us that the two vectors $(t_k^{12}, t_k^{13}, t_k^{23}), k = 1, 2$ lie on the plane $x + y + z = 0$:

$$t_k^{12} + t_k^{23} + t_k^{31} = 0 \quad k = 1, 2$$

(slight abuses of language and obvious notation), so long as they are real, that is, *linear* conditions. The geometric picture persists algebraically for complex t 's as well. So we get parametric solutions (with $\alpha, \beta, \gamma, \delta, x_{12}, x_{23}, x_{31}$ complex; we also set $x_{ij} = x_{ji}$ throughout):

$$\begin{aligned} v_1 &= \alpha (\omega_{12} - \omega_{13}) + \beta (\omega_{12} - \omega_{23}) \\ v_2 &= \gamma (\omega_{12} - \omega_{13}) + \delta (\omega_{12} - \omega_{23}) \\ v_3 &= x_{12} \omega_{12} + x_{23} \omega_{23} + x_{31} \omega_{31} \end{aligned}$$

or

$$\begin{aligned} v_1 &= (\alpha + \beta) \omega_{12} - \alpha \omega_{13} - \beta \omega_{23} \\ v_2 &= (\gamma + \delta) \omega_{12} - \gamma \omega_{13} - \delta \omega_{23} \\ v_3 &= x_{12} \omega_{12} + x_{23} \omega_{23} + x_{31} \omega_{31} \end{aligned}$$

with the only condition $\alpha\delta \neq \beta\gamma$ in order to avoid trivialities in

$$v_1 \wedge v_2 = -(\alpha\delta - \beta\gamma) \cdot \mathbb{I}_1$$

In order to calculate the *holonomy* (parallel transport)

$$\rho(b) = \begin{pmatrix} 1 & \int_b v_1 & \int_b v_1 v_2 + v_3 \\ 0 & 1 & \int_b v_2 \\ 0 & 0 & 1 \end{pmatrix}$$

for a generic pure braid b written as a word in the Artin generators A_{ij} , we must use the following easily established results involving hyperlogarithms ($\int_{A_{ij}}$ meaning Chen integration along the geometric pure braid A_{ij} , see [10]):

$$\int_{A_{ij}} \omega_{kh} = -\delta_{(ij),(kh)},$$

$$\int_{A_{ij}} (\omega_{ij})^n = \frac{(-1)^n}{n!}$$

Also, upon moving “1” around “2” *clockwise*:

$$\int_{A_{12}} \omega_{12} = -1 \qquad \int_{A_{12}} \omega_{12}\omega_{12} = +\frac{1}{2}$$

$$\int_{A_{12}} \omega_{12}\omega_{13} = +\frac{\sqrt{-1}}{2\pi} \log 2 \qquad \int_{A_{12}} \omega_{13}\omega_{12} = -\frac{\sqrt{-1}}{2\pi} \log 2$$

and similar results for the other generators (see [10] for complete details).

Thus we eventually find

$$\rho_3(A_{12}) = \begin{pmatrix} 1 - \alpha - \beta & \frac{1}{2}(\alpha + \beta)(\gamma + \delta) + (\alpha\delta - \beta\gamma) \frac{\sqrt{-1}}{2\pi} \log 2 + x_{12} \\ 0 & 1 & -\gamma - \delta \\ 0 & 0 & 1 \end{pmatrix}$$

$$\rho_3(A_{13}) = \begin{pmatrix} 1 + \alpha & \frac{1}{2}\alpha\gamma + \frac{1}{2}(\alpha\delta - \beta\gamma) + x_{13} \\ 0 & 1 & +\gamma \\ 0 & 0 & 1 \end{pmatrix}$$

$$\rho_3(A_{23}) = \begin{pmatrix} 1 + \beta & \frac{1}{2}\beta\delta + (\alpha\delta - \beta\gamma) \frac{\sqrt{-1}}{2\pi} \log 2 + x_{23} \\ 0 & 1 & +\delta \\ 0 & 0 & 1 \end{pmatrix}$$

The central element reads,

$$\rho_3(\Delta_3^2) = \begin{pmatrix} 1 & 0 & x_{12} + x_{13} + x_{23} \\ 0 & 1 & 0 \\ 0 & 0 & 1 \end{pmatrix}$$

Now, if we observe that the x_{ij} 's are arbitrary, one gets the following

Theorem 1 (i) *There exists a 7-complex parameter family of 3×3 nilpotent representations ρ_3 of P_3 reading, on Artin's generators:*

$$\rho_3(A_{12}) = \begin{pmatrix} 1 & -\alpha - \beta & X_{12} \\ 0 & 1 & -\gamma - \delta \\ 0 & 0 & 1 \end{pmatrix}$$

$$\rho_3(A_{13}) = \begin{pmatrix} 1 & +\alpha & X_{13} \\ 0 & 1 & +\gamma \\ 0 & 0 & 1 \end{pmatrix}$$

$$\rho_3(A_{23}) = \begin{pmatrix} 1 & +\beta & X_{23} \\ 0 & 1 & +\delta \\ 0 & 0 & 1 \end{pmatrix}$$

(ii) *The central element reads, in turn, with respect to the new parameters:*

$$\rho_3(\Delta_3^2) = \begin{pmatrix} 1 & 0 & -\alpha\delta - \beta\delta - \alpha\gamma + X_{12} + X_{13} + X_{23} \\ 0 & 1 & 0 \\ 0 & 0 & 1 \end{pmatrix}$$

Remarks 1. It is important to notice that when computing the holonomy of a generic braid b , the representation matrices for the generators entering the word giving b must be written in the *reverse* order: in a product $b_1 \cdot b_2$, b_1 comes first, so $\rho(b_1)$ must accordingly act first. It is readily checked, retrospectively (by hand or by a computer algebra system, e.g. Mathematica®) that the Artin relations are fulfilled with the above convention.

2. Strictly speaking, in view of the arbitrary character of x_{ij} , the computation of double iterated integrals turns out to be unnecessary in this case, however we carried it out since it was actually needed for further calculations in [10].

3. The above representation is actually a Heisenberg group one.

3.3 Representations of P_4

More refined arguments along the lines of those previously given and computation of further double iterated integrals (there is no need to calculate an a priori present triple integral) lead in [10] to the following result:

Theorem 2 ([10]) (i) *There exists a 16-complex parameter family of 4×4 nilpotent representations ϱ_4 of P_4 reading, on Artin's generators:*

$$\varrho_4(A_{12}) = \begin{pmatrix} 1 - \alpha - \beta \frac{1}{2}(\alpha + \beta)(\gamma + \delta) + (\alpha\delta - \beta\gamma)\left(\frac{\sqrt{-1}}{2\pi} \log \frac{4}{3}\right) - (\sigma + \tau) & X_{12} \\ 0 & 1 \\ 0 & 0 \\ 0 & 0 \end{pmatrix} \begin{pmatrix} -\gamma - \delta & \frac{1}{2}(\gamma + \delta)(\eta + \xi) + (\gamma\eta - \delta\xi)\left(\frac{\sqrt{-1}}{2\pi} \log \frac{4}{3}\right) - (\zeta + \lambda) \\ 1 & -\eta - \xi \\ 0 & 1 \end{pmatrix}$$

$$\varrho_4(A_{13}) = \begin{pmatrix} 1 & \alpha \frac{\alpha\gamma}{2} + (\alpha\delta - \beta\gamma)\left(\frac{1}{2} + \frac{\sqrt{-1}}{2\pi} \log 3\right) + \sigma & X_{13} \\ 0 & 1 & \gamma \\ 0 & 0 & 1 \\ 0 & 0 & 0 \end{pmatrix} \begin{pmatrix} \frac{\zeta}{2} + (\gamma\eta - \delta\xi)\left(\frac{1}{2} + \frac{\sqrt{-1}}{2\pi} \log 3\right) + \zeta \\ \xi \\ 1 \end{pmatrix}$$

$$\varrho_4(A_{14}) = \begin{pmatrix} 1 & \beta \frac{\beta\delta}{2} + (\alpha\delta - \beta\gamma)\left(-\frac{\sqrt{-1}}{\pi} \log 2\right) + \tau & X_{14} \\ 0 & 1 & \delta \\ 0 & 0 & 1 \\ 0 & 0 & 0 \end{pmatrix} \begin{pmatrix} \frac{\delta\eta}{2} + (\gamma\eta - \delta\xi)\left(-\frac{\sqrt{-1}}{\pi} \log 2\right) + \lambda \\ \eta \\ 1 \end{pmatrix}$$

$$\varrho_4(A_{23}) = \begin{pmatrix} 1 & \beta \frac{\beta\delta}{2} + (\alpha\delta - \beta\gamma)\left(-\frac{\sqrt{-1}}{\pi} \log 2\right) + \tau & X_{23} \\ 0 & 1 & \delta \\ 0 & 0 & 1 \\ 0 & 0 & 0 \end{pmatrix} \begin{pmatrix} \frac{\delta\eta}{2} + (\gamma\eta - \delta\xi)\left(-\frac{\sqrt{-1}}{\pi} \log 2\right) + \lambda \\ \eta \\ 1 \end{pmatrix}$$

$$\varrho_4(A_{24}) = \begin{pmatrix} 1 & \alpha \frac{\alpha\gamma}{2} + (\alpha\delta - \beta\gamma)\left(-\frac{1}{2} + \frac{\sqrt{-1}}{2\pi} \log 3\right) + \sigma & X_{24} \\ 0 & 1 & \gamma \\ 0 & 0 & 1 \\ 0 & 0 & 0 \end{pmatrix} \begin{pmatrix} \frac{\zeta}{2} + (\gamma\eta - \delta\xi)\left(-\frac{1}{2} + \frac{\sqrt{-1}}{2\pi} \log 3\right) + \zeta \\ \xi \\ 1 \end{pmatrix}$$

$$\varrho_4(A_{34}) = \begin{pmatrix} 1 - \alpha - \beta \frac{1}{2}(\alpha + \beta)(\gamma + \delta) + (\alpha\delta - \beta\gamma)\left(\frac{\sqrt{-1}}{2\pi} \log \frac{4}{3}\right) - (\sigma + \tau) & X_{34} \\ 0 & 1 \\ 0 & 0 \\ 0 & 0 \end{pmatrix} \begin{pmatrix} -\gamma - \delta & \frac{1}{2}(\gamma + \delta)(\eta + \xi) + (\gamma\eta - \delta\xi)\left(\frac{\sqrt{-1}}{2\pi} \log \frac{4}{3}\right) - (\zeta + \lambda) \\ 1 & -\eta - \xi \\ 0 & 1 \end{pmatrix}$$

(ii) *The central element reads, in turn*

$$\varrho_4(\Delta_4^2) = \begin{pmatrix} 1 & 0 & 0 & W \\ 0 & 1 & 0 & 0 \\ 0 & 0 & 1 & 0 \\ 0 & 0 & 0 & 1 \end{pmatrix}$$

where

$$W = -(\alpha\lambda + \beta\zeta + \xi\tau + \eta\sigma) - 2(\alpha\zeta + \beta\lambda + \xi\sigma + \eta\tau) + \frac{1}{2}\gamma\eta(\alpha + \beta) + \frac{1}{2}\beta\gamma(\eta + \xi) - \frac{\sqrt{-1}}{2\pi}(\alpha\eta - \beta\xi)\left(\gamma \log \frac{9}{4} - \delta \log \frac{16}{3}\right) + X_{12} + X_{13} + X_{14} + X_{23} + X_{24} + X_{34}$$

Remarks 1. Matrices are again written in the reverse order; fulfilment of the Artin relations can be again readily checked.

2. Notice that, upon restriction to $P_3 \hookrightarrow P_4$ (obvious inclusion) one has

$$\rho_4|_{P_3} \neq \rho_3$$

3. Also observe that, whereas the P_3 case could be dealt with completely algebraically, in the P_4 case the geometric interpretation seems to be unavoidable.

4. (Important). The above 7-parameter and 13-parameter families of representations exhaust the unipotent representations of P_3 in view of Kohno’s general theory [44–46] (see also [1]). The fundamental theorem of Kohno [46], Theorem 1.2.6—see also Aomoto’s Théorème 1 in [1]—shows in particular that every unipotent representation of the pure braid group can be realised as a monodromy representation. A simple general argument for constructing unipotent representations of P_3 can be outlined as follows. One looks for $n \times n$ -nilpotent matrices t_{12}, t_{13}, t_{23} fulfilling the infinitesimal braid relations: therefore, two of them can be chosen arbitrarily, the third one can be chosen to be central. In total we have $2 \times n(n - 1)/2 + 1 = n(n - 1) + 1$ parameters, yielding 7 and 13 for $n = 3, 4$, respectively (adhering to [10]). Of course one has to explicitly solve the iterated integrals involving the Artin generators if one looks for concrete formulae.

3.4 Braids of Brunnian Type

In this subsection we wish to compute our representations on Brunnian type pure braids, showing that they are indeed able to detect this phenomenon, in the sense that, in general, evaluating the monodromy (parallel transport) matrix on such braids yields a non trivial result whereby they can be (partially) distinguished. We do not attempt to give a systematic classification but provide specific significant examples. See the remarks in [10] (and [16, 50] as well).

In analogy to the link case, a pure braid is called Brunnian if upon removing any strand therefrom, it becomes trivial (cf. [59, 60] for the analogous notion for knots). One may also think of stratified Brunnian braids $B_k^n, k = 0, 1, \dots, n - 2$, i.e. those n -strand braids which become trivial after (and only after) arbitrarily removing k strands therefrom (so Brunnian braids yield B_1^n , and the trivial braid is the only element of B_0^n). Removal of a strand, the j -th, say, of a braid b , is obtained by erasing the generators containing the index j in any word representing b .

An immediate example of Brunnian braid is the following:

$$b = [A_{12}, [A_{13}, [\dots, [A_{1,n-1}, A_{1n}] \dots]]]$$

generalizing the *pigtail braid* $b = [A_{12}, A_{13}] = A_{12}A_{13}A_{12}^{-1}A_{13}^{-1}$ which, upon closure, provides a realization of the *Borromean rings*. More generally, the Brunnian braid $[A_{12}^n, A_{13}^m], n, m \in \mathbb{Z}$ can be represented, via ρ_3 , as follows:

$$\rho_3 ([A_{12}^n, A_{13}^m]) = \begin{pmatrix} 1 & 0 & mn(\alpha\delta - \beta\gamma) \\ 0 & 1 & 0 \\ 0 & 0 & 1 \end{pmatrix}$$

The “mirror-inverse” $abcd \dots (\dots dcba)^{-1}$ words, using the six generators of P_4 (and any permutation thereof) give rise to braids of type B_2^4 : indeed, upon deleting a strand, we easily see that the remaining braid is of type B_1^3 . For instance, take

$$b'' = A_{12}A_{13}A_{14}A_{23}A_{24}A_{34}A_{12}^{-1}A_{13}^{-1}A_{14}^{-1}A_{23}^{-1}A_{24}^{-1}A_{34}^{-1}$$

with ϱ_4 -representation

$$\varrho_4(b'') = \begin{pmatrix} 1 & 0 & 0 & -(\alpha\delta - \beta\gamma)(2\eta + \xi) + (\alpha + 2\beta)(\gamma\eta - \delta\xi) \\ 0 & 1 & 0 & 0 \\ 0 & 0 & 1 & 0 \\ 0 & 0 & 0 & 1 \end{pmatrix}$$

This does not exhaust all possibilities since, for instance, the “shorter” braid $b''' = A_{12}A_{24}A_{13}A_{34}A_{12}^{-1}A_{24}^{-1}A_{13}^{-1}A_{34}^{-1}$ is also of type B_2^4 , and differs from b'' :

$$\varrho_4(b''') = \begin{pmatrix} 1 & 0 & 0 & \xi(\alpha\delta - \beta\gamma) + \alpha(\delta\xi - \gamma\eta) \\ 0 & 1 & 0 & 0 \\ 0 & 0 & 1 & 0 \\ 0 & 0 & 0 & 1 \end{pmatrix}$$

Notice that, in dealing with Brunnian phenomena, the parameters $\sigma, \tau, \zeta, \lambda$ and X_{ij} play no role.

Additional representations are extensively studied in [10]. For related approaches see e.g. [13–15, 27].

4 Geometric Representations of Riemann Surface Braid Groups

4.1 Overview

In the paper [70], which we closely follow from now on, we studied the simplest unitary representations of the braid group associated to a general Riemann surface from a geometrical standpoint. Besides being interesting in itself, such an investigation could prove useful in topological quantum computing [56, 78], where unitary braid group representations are employed for constructing quantum gates (topology would then automatically enforce robustness and fault tolerance), with the Fractional

Quantum Hall Effect (FQHE) possibly yielding the physical clue to its practical implementation [56].

Recall that the FQHE arises for a (Coulomb) interacting spin-polarised 2d-electron gas, at low temperature and in the presence of a strong magnetic field. It is usually observed in semiconductor structures, such as electrons trapped in a thin layer of GaAs surrounded by AlGaAs, Si-MOSFETs (see e.g. [21]) and it has been recently detected in graphene [20] as well. The ground state of such a system can be approximately (but most effectively) described by a *Laughlin wave function* of the form (in a plane geometry, [21, 49]):

$$\prod_{i < j} (z_i - z_j)^m e^{-\sum_{i=1}^N |z_i|^2} \quad (L)$$

Here N is the number of electrons in the sample, m is an odd integer (this ensuring Fermi statistics). One notes the appearance of the ground state of a quantum harmonic oscillator (also cf. [12, 69]). The quantity $\nu = \frac{1}{m}$ is the *filling factor* intervening in the fractional quantization of the *Hall conductance*:

$$\sigma_H = \nu \frac{e^2}{h}$$

and, in the limit $N \rightarrow \infty$, equals the electron density per state: $\nu = \frac{N}{N_S}$ with N_S the number of magnetic flux quanta: $N_S = B \cdot \mathcal{A} / \Phi_0$ (B is the modulus of the constant magnetic field, acting perpendicularly to the layer, \mathcal{A} is the area of the given sample, whereas $\Phi_0 := hc/e$ is the flux quantum). The number N_S also gives the degeneracy of the lowest Landau level (for the free system), which appears as a degenerate ground state of a quantum harmonic oscillator.

On the mathematical side, Landau levels admit elegant algebraic-geometric descriptions along the lines of geometric quantization (see e.g. [28, 42, 74, 81]): for instance, if the layer is a (closed) Riemann surface of genus g , the lowest Landau level is the space of holomorphic sections of a suitable holomorphic line bundle [37, 72]; on a torus ($g = 1$) it can be realised as a space of theta functions, see e.g. [31, 57], and also [65] and below.

Now, *on the one hand*, it turns out that the elementary excitations around the Laughlin ground state are *quasiparticles/holes* having *fractional charge* $\pm \nu$ [21, 49] and *anyon statistics* $(-1)^\nu$ [21, 34], and this leads to considering the *braid group* associated to the N -point configuration space of the given layer (N now being the number of quasiparticles/holes). Wave functions for quasiparticles/holes can be cast in the form (L), with ν replacing m (see [21, 34]).

On the other hand, the filling factor $\nu = 1/m$ (together with others) for a *torus* sample has been interpreted as the *slope* (that is, degree over rank) of a *stable* holomorphic vector bundle over the corresponding “spectral”, or “Brillouin manifold” (which is again a torus, parametrising all admissible boundary conditions, see [31, 33, 76]); therefore, the filling factor has a *topological* meaning. (For ν integral

one recovers the interpretation of the integral Quantum Hall Effect via the first Chern class of a line bundle over the Brillouin manifold, see e.g. [21, 52, 73].)

It turns out [70] that the above coincidence has an abstract braid group theoretical origin: we consider a general closed Riemann surface—so that the role of the Brillouin manifold is played by the *Jacobian* of the surface (cf. [72])—and its associated braid group, with the Bellingeri presentation [8]; then the equalities, in the genus one case (cf. [76])

$$\nu := \text{filling factor} = \text{statistical parameter} = \text{slope of a stable vector bundle}$$

can be derived from a group theoretical perspective, and can be suitably generalised.

In brief, this runs as follows: first of all, braiding can be approached via representations of the Weyl-Heisenberg group corresponding to the (rational) statistical parameter ν , both infinite dimensional and finite dimensional (see [9] for an abstract manifestation of this phenomenon).

Then, generalising [65], we observe that the infinite dimensional representations can be constructed geometrically on L^2 -sections of holomorphic Hermitian stable bundles over the Jacobian of the Riemann surface under consideration. Stable bundles are irreducible holomorphic vector bundles over Kähler manifolds admitting a Hermitian-Einstein structure (HE)—namely a (unique) Hermitian connection with central constant curvature—in view of the Donaldson-Uhlenbeck-Yau theorem [26, 43, 55, 75]. Specifically, the representation of the Weyl-Heisenberg group we look for stems from suitable parallel transport operators associated to the HE-connection (which will have constant curvature, essentially given by the statistical parameter ν). The solution is actually reduced to finding suitable *projectively flat HE-bundles over Jacobians*, which can be obtained via a classical construction devised by Matsushima [35, 43, 51]. In particular, we get a “slope-statistics” formula $\mu = \nu g!$ (with μ denoting the slope of a holomorphic vector bundle). The other important geometrical ingredient needed to describe the statistical behaviour governing “particle” exchange is the Klein prime form on a Riemann surface, manufactured via theta function theoretic tools. The problem of extracting general roots of a line bundle then arises and it is circumvented by exploiting a universal property of the prime form. Then we define, following Halperin [21, 34, 49], (Laughlin type) vector valued wave functions obeying, in general, *fractional* statistics and having their “centre of mass” part represented by holomorphic sections of the above bundles (see also [12, 33, 37, 76]). In the following sections we shall develop the programme outlined above.

4.2 *The Simplest Unitary Representations of the Riemann Surface Braid Group*

We shall restrict ourselves to *unitary* representations

$$\rho : B(\Sigma_g, n) \rightarrow U(\mathcal{H})$$

($U(\mathcal{H})$ being the unitary group on a complex separable Hilbert space \mathcal{H}) with $\rho(\sigma_j) = \sigma I, j = 1, \dots, n - 1$ (I being the identity operator on \mathcal{H}). One writes

$$\sigma = e^{2\pi\sqrt{-1}\theta} \equiv e^{\pi\sqrt{-1}v} = (-1)^v$$

and calls θ (a priori defined up to integers) the *statistics parameter* (same for $v = 2\theta$, with abuse of language). Referring to Sect. 2.2, we see that the relations B1, B2, R1 and R2 are automatically fulfilled, the relations R3 become:

$$[\rho(a_s), \rho(a_r)] = [\rho(b_s), \rho(b_r)] = I, \quad r, s = 1, \dots, g \quad (\diamond)$$

whereas R4 yields:

$$[\rho(a_r), \rho(b_r)] = \sigma^2 I, \quad r = 1, \dots, g$$

Condition TR gives, in turn, after checking that

$$[\rho(a_r), \rho(b_r^{-1})] = \sigma^{-2} I \quad (\diamond \diamond)$$

the constraint

$$\sigma^{2(n-1+g)} = 1$$

furnishing (for $n - 1 + g \neq 0$)

$$\theta = \frac{q}{2(n - 1 + g)}, \quad q \in \mathbb{Z} \quad \text{or, equivalently} \quad v = \frac{q}{n - 1 + g},$$

that is, *fractional statistics*, in general. Notice that if $\sigma^2 = 1$, that is $\theta \in 1/2 \cdot \mathbb{Z}$ (slight abuse of notation) we recover ordinary Fermi-Bose statistics (see also below).

Next we introduce the following tensor product Hilbert space:

$$\mathcal{H} := H_1 \otimes H_2$$

with H_1 carrying a representation of the *Weyl-Heisenberg Canonical Commutation Relations (CCR)* ([77], see also e.g. [61]) up to obvious inessential notational changes:

$$V(\boldsymbol{\beta}) U(\boldsymbol{\alpha}) = e^{2\pi\sqrt{-1}\cdot v \boldsymbol{\alpha}\cdot\boldsymbol{\beta}} U(\boldsymbol{\alpha}) V(\boldsymbol{\beta})$$

with $\boldsymbol{\alpha}, \boldsymbol{\beta} \in \mathbb{R}^g$, and where H_2 is one-dimensional. Clearly $H_1 \otimes H_2 \cong H_1$, but we keep the distinction in view of our subsequent physical applications. Now take, after denoting by (e_1, e_2, \dots, e_g) the canonical basis of \mathbb{R}^g :

$$\rho_1(a_r) = U(e_r), \quad \rho_1(b_r^{-1}) = V(e_r), \quad r = 1, 2, \dots, g$$

Upon setting

$$\begin{aligned} \rho(a_r) &= \rho_1(a_r) \otimes I_{H_2}, & \rho(b_r^{-1}) &= \rho_1(b_r^{-1}) \otimes I_{H_2}, & r &= 1, \dots, g \\ \rho(\sigma_j) &= I_{H_1} \otimes \sigma I_{H_2} \equiv I_{H_2} \otimes \rho_2(\sigma_j), & j &= 1, \dots, n-1 \end{aligned}$$

and in view of (\diamond) and $(\diamond \diamond)$, we have:

Theorem 3 ([70]) (i) *Any representation of the Weyl-Heisenberg Commutation relations yields, via the map*

$$\rho : B(\Sigma_g, n) \rightarrow U(\mathcal{H})$$

defined above, an infinite dimensional unitary representation of the Riemann surface braid group $B(\Sigma_g, n)$ on the Hilbert space \mathcal{H} .

(ii) *Irreducible finite dimensional unitary RS-braid group representations $\hat{\rho}$ also exist, stemming from the finite version of Weyl-Heisenberg commutation relations.*

The representations in (ii) correspond in fact to particular rational *noncommutative tori* (see also below).

4.3 The Matsushima Construction

We shall now outline a geometric construction of the Hilbert spaces H_j , $j = 1, 2$ and of the representation ρ . See e.g. [54] for the relevant background on Riemann surface theory.

Concerning the space H_1 , in [70], taking inspiration from [65], we were naturally led to look for a Hermitian holomorphic vector bundle $\mathcal{E} \rightarrow J(\Sigma_g)$ over the Jacobian $J(\Sigma_g)$ of the Riemann surface in question, equipped with a HE-connection ∇ having constant curvature equal (up to a $2\pi\sqrt{-1}$ factor) to $2\theta = \nu$, and this will give rise to a holomorphic stable bundle with slope $\mu(\mathcal{E}) \propto \nu$.

The construction of such bundles over a generic Abelian variety is classical (cf. in particular [35, 43, 51, 70] as well). It turns out that the space of holomorphic sections $H^0(\mathcal{E}_\nu)$ is q -dimensional and, in the case $r = 1$, we retrieve the so-called q -level theta functions. Therefore, the conclusion is that *a projectively flat HE-bundle on the Jacobian $J(\Sigma_g)$ with HE-connection with curvature $-2\pi\sqrt{-1}\nu \omega$ can be manufactured via the Matsushima construction*, and, by a result of Hano [35], this is essentially the only way to achieve this (one uses the Riemann-Roch-Hirzebruch (RRH) theorem, together with a cohomology vanishing theorem, plus the fact that the Todd class is trivial for tori. We refer to [11, 36] for background and full details). The precise statement is the following:

Theorem 4 ([70]) (i) *Let \mathcal{E} be a projectively flat holomorphic vector bundle over $J(\Sigma_g)$ (or, more generally, over an Abelian variety) carrying a HE-connection ∇*

with constant curvature $\Omega_\nabla = -2\pi\sqrt{-1} v \cdot \omega := -2\pi\sqrt{-1} q/r \cdot \omega$, (with $r > 0$, $q > 0$ and $g.c.d(r, q) = 1$). Then one has,

$$R := \text{rk}(\mathcal{E}) = k r^g, \quad h^0(\mathcal{E}) = k q^g$$

with k a positive integer.

(ii) The following slope-statistics formula holds:

$$\mu(\mathcal{E}) = v g!$$

Remark Varnhagen’s result [76] is recovered for $g = 1$. The general factor $g!$ comes from the application of the RHH formula with a specific connection (the result is independent of the latter, since it is topological in nature). So, in a nutshell, the thread of the argument is the following: statistical parameter \rightarrow CCR \rightarrow curvature of the Chern–Bott connection on a HE-vector bundle (more details below) \rightarrow slope.

4.4 Construction of ρ_1

Now consider the projectively flat HE-vector bundles \mathcal{E} of the preceding Subsection and take $H_1 := L^2(\mathcal{E})$, namely the L^2 -sections of \mathcal{E} obtained by completing its smooth sections with respect to the inner product

$$\langle \cdot, \cdot \rangle := \int_{J(\Sigma_g)} h(\cdot, \cdot) \frac{\omega^g}{g!}$$

(h being the HE-metric). The braid generators a_i and b_i , $i = 1, 2, \dots, g$, can be realised as *parallel transport* operators pertaining to the Hermitian connection with constant curvature ∇ , and actually will yield a representation of the Weyl-Heisenberg Commutation Relations as above. (Indeed, there exists a family of such connections parametrized by the Jacobian itself.) Specifically, with respect to the standard (Darboux) symplectic coordinates $(q_1, p_1, q_2, p_2, \dots, q_g, p_g)$ of $J(\Sigma_g)$, we have

$$[\nabla_{\frac{\partial}{\partial q_j}}, \nabla_{\frac{\partial}{\partial q_k}}] = [\nabla_{\frac{\partial}{\partial p_j}}, \nabla_{\frac{\partial}{\partial p_k}}] = 0; \quad [\nabla_{\frac{\partial}{\partial q_j}}, \nabla_{\frac{\partial}{\partial p_k}}] = -2\pi\sqrt{-1} v \delta_{jk} \cdot I$$

for $j, k = 1, 2 \dots, g$ (we tacitly switched to operator commutators).

Notice in fact that, by periodicity and the compatibility of ∇ with h , one has

$$0 = \int_{J(\Sigma_g)} X h(\cdot, \cdot) \frac{\omega^g}{g!} = \int_{J(\Sigma_g)} [h(\nabla_X \cdot, \cdot) + h(\cdot, \nabla_X \cdot)] \frac{\omega^g}{g!}$$

with $X = \partial/\partial q_j, \partial/\partial p_j$, thus the operators $\nabla_{\frac{\partial}{\partial q_j}}, \nabla_{\frac{\partial}{\partial p_j}}$ are formally skew-hermitian. By classical functional analytic arguments they are skew-adjoint (cf. [63]).

Thus, under the above assumptions, taking the von Neumann uniqueness theorem [77] into due account, we get an infinite dimensional representation of the Weyl-Heisenberg Commutation relations (generalising [65]) with multiplicity q^g .

The braid group generators a_i and $b_i, i = 1, \dots, g$ are then represented as

$$\rho_1(a_r) := \exp(\nabla_{\frac{\partial}{\partial q_r}}), \quad \rho_1(b_r^{-1}) := \exp(\nabla_{\frac{\partial}{\partial p_r}}), \quad r = 1, 2, \dots, g$$

Remark The holomorphic hermitian stable bundle $(\mathcal{E}, h, \nabla) \rightarrow J(\Sigma_g)$ can be pulled-back to Σ_g via the Abel map to

$$(\mathcal{A}^*\mathcal{E}, \mathcal{A}^*h, \mathcal{A}^*\nabla) \rightarrow C_n(\Sigma_g)$$

equipped with the pulled-back metric \mathcal{A}^*h and connection $\mathcal{A}^*\nabla$. The corresponding pulled-back representation is well defined on pulled-back sections. The Hilbert space H_1 will be the receptacle, because of the Abel map, of “centre of mass” wave functions, cf. [31, 33, 76], and below.

4.5 Construction of H_2 and Generalised Laughlin Wave Functions

A natural ingredient of the construction would be Klein’s prime form on the Riemann surface in question (see e.g. [54]). The analysis carried out in [70] showed that if one wished to implement fractional statistics then one would face the problem of extracting *roots* of suitable line bundles and this cannot be achieved in general for non trivial one. Thus, in order to circumvent this difficulty, we adopted a “minimalistic” approach and resorted to a local description, which however retains an intrinsic character with respect to braiding: define the Hilbert space

$$H_2 = \langle \psi_\nu = \prod_{i < j} (\zeta_i - \zeta_j)^\nu \rangle$$

with ζ being a local coordinate (the behaviour of the prime form near the diagonal is however independent of the choice of the local coordinate). Branching is then produced. Actually, ψ_ν is the “topological” part of the Laughlin wave function discussed in [12], upon regarding the coordinates ζ_i as global coordinates on the configuration space $C_n(\mathbb{C})$.

A scalar product can be introduced in H_2 in an obvious manner. The function ψ_ν then manifestly enjoys the correct transformation law under the exchange of two points $x_i \leftrightarrow x_j$:

$$\psi_\nu \mapsto (-1)^\nu \psi_\nu = \sigma \psi_\nu$$

The upshot is that we may devise generalised “ground state” *Laughlin wave functions* [33, 34, 37, 49] in $\mathcal{H} = H_1 \otimes H_2$, possessing, in general “anyon statistics” as follows:

$$\Psi(x_1, \dots, x_n) := \psi_\nu \cdot \xi$$

where x_1, \dots, x_n are distinct points in Σ_g , and ξ is a *holomorphic section*—when existing—of the stable bundle entering the construction (depending on a centre of mass coordinate). These holomorphic sections play the role of the ground states, or fundamental Landau levels, see also Sect. 5. Notice that they are not invariant under the action of the “full” braid group, since parallel transport does not preserve the holomorphic structure, in general.

In this way we have also generalised the geometric treatment given for the standard braid group by A. Besana and the author [12] as well.

We summarise the above developments through the following:

Theorem 5 ([70]) *Let $\mathcal{E} \rightarrow J(\Sigma_g)$ be a Matsushima HE-holomorphic vector bundle with slope $\mu(\mathcal{E}) = \nu g! = q/r \cdot g!$. The representation ρ_1 of the CCR on the Hilbert space $H_1 = L^2(\mathcal{E})$ —built up as above via parallel transport operators associated with the canonical HE-connection ∇ —together with the position*

$$\rho_2(\sigma_j)\psi := (-1)^\nu \psi, \quad \psi \in H_2$$

gives rise to a unitary representation

$$\rho : B(\Sigma_g, n) \rightarrow U(\mathcal{H})$$

where $n=r+1-g$, $\mathcal{H}=H_1 \otimes H_2$. The representation ρ_1 has multiplicity $h^0(\mathcal{E}) = q^g$. The vectors $\psi = \psi_\nu \xi$, $\xi \in H^0(\mathcal{E})$ (ξ is then a Matsushima theta vector) are called Laughlin generalised wave functions.

Remarks 1. Notice that, in general, one indeed deals with genuine vector-valued sections. In fact the case $\nu = 2\theta = 1$ gives back Fermi-Dirac statistics, and one can safely employ the prime form bundle (actually $\mathcal{L} \rightarrow C_n(\Sigma_g)$) as it stands. Of course one may take tensor powers thereof as well. As for the centre of mass part, one retrieves the ordinary theta line bundle, having first Chern class (and slope) equal to one, together with the geometric theory of Landau levels discussed in [31, 57], see also [65]. This matches the analysis carried out in [38].

2. The problem of root extraction deserves further scrutiny: an important step would be the determination of the second cohomology group $H^2(C_n(\Sigma_g), \mathbb{Z})$. The rational cohomology groups of configuration spaces of surfaces have been studied in [19].

5 Final Remarks and Outlook

The successive developments in [70] portray a possibly interesting “braid duality”. Specifically, focussing in particular on the $g = 1$ case, we demonstrated how everything can be made even more explicit by resorting to A. Connes’ noncommutative geometric setting [24, 25] for noncommutative tori (see also [4, 62, 66–68]) and to the notion of noncommutative theta vector introduced by A. Schwarz [64], encompassing the classical notions. The upshot is that the “centre of mass” parts of Laughlin wave functions are precisely the Schwarz theta vectors. A notable feature is now the following: the space of theta vectors naturally determines a finite dimensional braid group representation corresponding to the reciprocal parameter $\nu' = 1/\nu$, which, via Matsushima, gives rise to a projectively flat HE-bundle with the corresponding slope. Therefore a (Matsushima-Connes (MC)) “duality” emerges and it is essentially the one provided by the so-called Fourier-Mukai-Nahm (FMN) transform (see e.g. [7]). In particular, the noncommutative theta vector approach can be effortlessly used to calculate the Nahm-transformed connection explicitly ([70], see also [28] for an application to Landau levels).

More precisely, and as a sort of recap, the “ ν -anyon/ ν' -anyon duality” presented in [70] runs as follows: starting from a ν -anyon representation, we found that the q -dimensional ground state space $H^0(\mathcal{E}_\nu)$ has a dual braid symmetry which gives rise to a ν' -anyon representation, via Matsushima-Connes/Fourier-Mukai-Nahm. The crucial physical issue is that the change in the holomorphic structure of the Matsushima bundle \mathcal{E}_ν and the ensuing variation of the ground state spaces $H^0(\mathcal{E}_\nu)$ involved in the FMN transform can be interpreted as an *adiabatic motion* of the ν' -anyons, encoded in the centre of mass coordinate. The FMN-transform (plus dualization) ultimately creates an *effective* ν' -anyon wave function. See [70] for further discussion and physical examples.

Among the possible future research directions, it would be interesting to find a connection with the work [29], also unveiling an interesting connection (different from ours) between theta function theory and knots, via Przytycki skein modules. A recent intriguing geometrically flavoured approach to anyons has been proposed in [5]. See also [39] for further interesting applications of particular braid groups (cyclotronic braid groups) to 2d Hall systems.

Acknowledgements The author is grateful to the Organizers of the Workshop “Knots in Hellas 2016”, held at International Olympic Academy, Ancient Olympia, Greece, 17th–23rd July 2016, and to the staff of IOA, for the opportunity given to him to present a talk therein and for the excellent scientific level, atmosphere and hospitality in a marvellous historical and natural landscape. He also acknowledges financial support from D1-funds (Catholic University) (ex 60% Italian MIUR funds). This work has been carried out within the activities of INDAM (GNSAGA).

References

1. K. Aomoto, Fonctions hyperlogarithmiques et groupes de monodromie unipotents. *J. Fac. Sci. Tokio* **25**, 149–156 (1978)
2. V.I. Arnol'd, The cohomology ring of colored braids. *Mat. Zametki* **5**(2), 227–231 (1969). (Russian) English transl. in *Trans. Moscow Math. Soc.* **21**, 30–52 (1970)
3. E. Artin, Theorie der Zöpfe. *Abh. Math. Sem. Hamburg Univ.* **4**, 42–72 (1925). Theory of braids. *Ann. Math.* **48**, 101–126 (1947)
4. A. Astashkevich, A. Schwarz, Projective modules over non-commutative tori: classification of modules with constant curvature connection. *J. Oper. Theory* **46**, 619–634 (2001)
5. M.F. Atiyah, M. Marcolli, Anyons in geometric models of matter. *J. High Energy Phys.* **07**, 076 (2017)
6. D. Bar-Natan, On the Vassiliev knot invariants. *Topology* **34**, 423–472 (1995)
7. C. Bartocci, U. Bruzzo, D. Hernandez Ruiperez, *Fourier-Mukai and Nahm Transforms and Applications in Mathematical Physics*. Progress in Mathematics, vol. 276 (Birkäuser, Basel, 2009)
8. P. Bellingeri, On presentation of surface Braid groups. *J. Algebra* **274**, 543–563 (2004)
9. P. Bellingeri, E. Godelle, J. Guaschi, Abelian and metabelian quotients of surface braid groups. *Glas. Math. J.* **59**, 119–142 (2017)
10. A. Benvegnù, M. Spera, Low-dimensional pure braid group representations via nilpotent flat connections. *Boll. Un. Mat. Ital.* **VI**(9), 643–672 (2013)
11. N. Berline, E. Getzler, M. Vergne, *Heat Kernels and Dirac Operators* (Springer, Berlin, 1992)
12. A. Besana, M. Spera, On some symplectic aspects of knots framings. *J. Knot Theory Ram.* **15**, 883–912 (2006)
13. M. Berger, Third order link invariants. *J. Phys. A: Math. Gen.* **23**, 2787–2793 (1990)
14. M. Berger, Third order braid invariants. *J. Phys. A: Math. Gen.* **24**, 4027–4036 (1991)
15. M. Berger, Topological Invariants in braid theory *Lett. Math. Phys.* **55**, 181–192 (2001)
16. S. Bigelow, The Burau representation is not faithful for $n = 5$. *Geom. Topol.* **3**, 397–404 (1999)
17. J. Birman, *Braids, Links and Mapping Class Groups*. Annals of Mathematics Studies, vol. 82 (Princeton, New Jersey, 1974)
18. J.S. Birman, T.E. Brendle, Braids: A Survey, Chap. 2, in *Handbook of Knot Theory*, ed. by W. Menasco, M. Thistlethwaite (Elsevier B.V., Amsterdam, 2005), pp 19–103
19. M. Bökigheimer, F. Cohen, *Rational Cohomology of Configuration Spaces of Surfaces, Algebraic Topology and Transformation Groups (Göttingen 1987)*, Lecture Notes in Mathematics, vol. 1361 (Springer, Berlin, 1988), pp. 7–13
20. K.I. Bolotin, F. Ghahari, M.D. Shulman, H.L. Stormer, P. Kim, Observation of the fractional quantum Hall effect in graphene. *Nature* **462**, 196–199 (2009); corrigendum: *Nature* **475**, 122 (2011)
21. T. Chakraborty, P. Pietiläinen, *The Quantum Hall Effects - Fractional and Integral* (Springer, Berlin, 1995)
22. K.-T. Chen, Iterated path integrals. *Bull. Am. Math. Soc.* **83**, 831–879 (1977)
23. K.-T. Chen, *Collected Papers of K.-T. Chen*. Contemporary Mathematicians, ed. by P. Tondeur, R. Hain (Birkäuser, Boston, 2001)
24. A. Connes, C^* algèbres et géométrie différentielle. *C.R. Acad. Sc. Paris* **290**, 599–604 (1980)
25. A. Connes, *Noncommutative Geometry* (Academic, London, 1994)
26. S.K. Donaldson, A new proof of a theorem of Narasimhan and Seshadri. *J. Diff. Geom.* **18**, 269–277 (1983)
27. N.W. Evans, M.A. Berger, A hierarchy of linking integrals, in *Topological Aspects of the Dynamics of Fluids and Plasmas*, ed. by H.K. Moffatt, et al. (Kluwer, Dordrecht, 1992), pp. 237–248
28. A. Galasso, M. Spera, Remarks on the geometric quantization of Landau levels. *Int. J. Geom. Meth. Mod. Phys.* **18**, 1650122 (2016)
29. R. Gelca, *Theta Functions and Knots* (World Scientific Publishing Co. Pte. Ltd., Singapore, 2014)

30. G. Goldin, Parastatistics, θ -statistics, and topological quantum mechanics from unitary representations of diffeomorphism groups, in *Proceedings of the XV International Conference on Differential Geometric Methods in Physics*, ed. by H.D. Doebner, J.D. Henning (World Scientific, Singapore, 1987), pp. 197–207
31. J.M. Guilarte, J.M. Muñoz Porras, M. de la Torre Mayado, Elliptic theta functions and the fractional quantum Hall effects. *J. Geom. Phys.* **27**, 297–332 (1998)
32. R. Hain, The geometry of the mixed hodge structure on the fundamental group. *Proc. Symp. Pure Math.* **46**, 247–282 (1987)
33. F.D.M. Haldane, E.H. Rezayi, Periodic Laughlin-Jastrow wave functions for the fractional quantized Hall effect. *Phys. Rev. B* **31**, 2529 (1985)
34. B.I. Halperin, Statistics of quasiparticles and the hierarchy of fractional quantized hall states. *Phys. Rev. Lett.* **52**, 1583–1586 (1984). Erratum (1984), 2390
35. J. Hano, A geometrical characterization of a class of holomorphic vector bundles over a complex torus. *Nagoya Math. J.* **61**, 197–201 (1976)
36. F. Hirzebruch, *Topological Methods in Algebraic Geometry*, vol. 1966 (Springer, New York, 1978)
37. R. Iengo, D. Li, Quantum mechanics and quantum Hall effect on Riemann surfaces *Nucl. Phys. B* **413**, 735–753 (1994)
38. T.D. Imbo, C. Shah Imbo, E.C.G. Sudarshan, Identical particles, exotic statistics and braid groups. *Phys. Lett. B* **234**(1–2), 103–107 (1990)
39. J. Jacak, R. Gonczarek, L. Jacak, I. Jóźwiak, *Composite Fermion Structure - Application of Braid Groups in 2D Hall System Physics* (World Scientific Publishing Co. Pte. Ltd., Singapore, 2012)
40. C. Kassel, V. Turaev, *Braid Groups* (Springer, Berlin, 2008)
41. L.H. Kauffman, *Knots and Physics*, 3rd edn. (World Scientific, Singapore, 2001)
42. J. Klauder, E. Onofri, Landau levels and geometric quantization. *Int. J. Mod. Phys.* **4**, 3939–3949 (1989)
43. S. Kobayashi, *Differential geometry of complex vector bundles* (Iwanami Shoten Publishers, Tokyo - Princeton University Press, Princeton, 1987)
44. T. Kohno, Série de Poincaré-Koszul associé aux groupes de tresses pures. *Inv. Math.* **82**, 57–75 (1985)
45. T. Kohno, Monodromy representations of braid groups and Yang-Baxter equations. *Ann. Inst. Fourier, Grenoble* **37**, 139–160 (1987)
46. T. Kohno, Linear representations of braid groups and classical Yang-Baxter equations. *Cont. Math.* **78**, 339–363 (1988)
47. T. Kohno, *Conformal Field Theory and Topology* (AMS, Providence, 2002)
48. M. Kontsevich, *Vassiliev's Knot Invariants*. *Advances in Soviet Mathematics*, Part 2, vol. 16 (AMS, Providence, 1993), pp. 137–150
49. R.B. Laughlin, Anomalous quantum hall effect: an incompressible quantum fluid with fractionally charged excitations. *Phys. Rev. Lett.* **50**, 1395–1402 (1983)
50. R.E. Lawrence, Homological representations of the Hecke algebra. *Commun. Math. Phys.* **135**, 141–191 (1990)
51. Y. Matsushima, Heisenberg groups and holomorphic vector bundles over a complex torus. *Nagoya Math. J.* **61**, 161–195 (1976)
52. G. Morandi, *Quantum Hall Effect* (Bibliopolis, Naples, 1988)
53. G.D. Mostow, Braids, hypergeometric functions, and lattices. *Bull. Am. Math. Soc.* **16**, 225–246 (1987)
54. D. Mumford, *Tata Lectures on Theta I-III* (Birkhäuser, Basel, 1983, 1984, 1991)
55. D. Mumford, J. Fogarty, F. Kirwan, *Geometric Invariant Theory* (Springer, Berlin, 1994)
56. C. Nayak, S.H. Simon, A. Stern, M. Freedman, S.D. Sarma, Non-Abelian anyons and topological quantum computation. *Rev. Modern Phys.* **80**(3), 1083 (2008)
57. E. Onofri, Landau levels on a torus. *Int. J. Theor. Phys.* **40**(2), 537–549 (2001)
58. P. Papi, C. Procesi, *Invarianti di nodi* Quaderno U.M.I. 45, (Pitagora, Bologna, 1998) (in Italian)
59. D. Rolfsen, *Knots and Links* (Publish or Perish, Berkeley, 1976)

60. V. Penna, M. Spera, Higher order linking numbers, curvature and holonomy. *J. Knot Theory Ram.* **11**, 701–723 (2002)
61. A. Perelomov, *Generalized Coherent States and Their Applications* (Springer, Berlin, 1986)
62. A. Polishchuk, A. Schwarz, Categories of holomorphic vector bundles on noncommutative two-tori. *Commun. Math. Phys.* **236**, 135–159 (2003)
63. M. Reed, B. Simon, *Methods of Modern Mathematical Physics I, II, III* (Academic, New York, 1972-5; 1980; 1979)
64. A. Schwarz, Theta functions on noncommutative tori. *Lett. Math. Phys.* **58**, 81–90 (2001)
65. M. Spera, Quantization on Abelian varieties. *Rend. Sem. Mat. Univers. Politecn. Torino* **44**, 383–392 (1986)
66. M. Spera, Yang Mills theory in non commutative differential geometry. *Rend Sem. Fac. Scienze Univ. Cagliari Suppl.* **58**, 409–421 (1988)
67. M. Spera, A symplectic approach to Yang Mills theory for non commutative tori. *Can. J. Math.* **44**, 368–387 (1992)
68. M. Spera, A note on Yang-Mills minima on riemann modules ove higher dimensional non commutative Tori. *Boll. Un. Mat. Ital.* **8-A**, 365–375 (1994)
69. M. Spera, A survey on the differential and symplectic geometry of linking numbers. *Milan J. Math.* **74**, 139–197 (2006)
70. M. Spera, On the geometry of some unitary Riemann surface braid group representations and Laughlin-type wave functions. *J. Geom. Phys.* **94**, 120–140 (2015)
71. J.N. Tavares, Chen integrals, generalized loops and loop calculus. *Intl. J. Mod. Phys. A* **9**, 4511–4548 (1994)
72. C. Tejero Prieto, Fourier-Mukai Transform and Adiabatic Curvature of Spectral Bundles for Landau Hamiltonians on Riemann Surfaces. *Commun. Math. Phys.* **265**, 373–396 (2006)
73. D.J. Thouless, Topological interpretations of quantum Hall conductance. *J. Math. Phys.* **35**, 5362–5372 (1994)
74. A. Tyurin, *Quantization, Classical and Quantum Field Theory and Theta Functions*, vol. 21, CRM Monograph Series (AMS, Providence, RI, 2003)
75. K. Uhlenbeck, S.T. Yau, On the existence of Hermitian-Yang-Mills connections in stable vector bundles. *Commun. Pure Appl. Math.* **XXXIX**(Suppl.), 257–293 (1986); A note on our previous paper : on the existence of Hermitian-Yang-Mills connections in stable vector bundles. *Commun. Pure Appl. Math.* **XLII**, 703–707 (1989)
76. R. Varnhagen, Topology and fractional quantum hall effect. *Nucl. Phys. B* **443**, 501–515 (1995)
77. J. von Neumann, Die Eindeutigkeit der Schrödingerschen Operatoren. *Math. Ann.* **104**, 570–578 (1931)
78. Z. Wang, *Topological Quantum Computation* (American Mathematical Society, Providence, 2010)
79. G. Wechsung, Functional equations of hyperlogarithms, in *Structural Properties of Polylogarithms*, ed. by L. Lewin, Chap. 8 (AMS, Providence, 1991), pp. 171–184
80. F. Wilczek, Quantum mechanics of fractional-spin particles. *Phys. Rev. Lett.* **49**, 957–959 (1982)
81. N. Woodhouse, *Geometric Quantization* (Oxford University Press, Oxford, 1992)

Towards a Version of Markov's Theorem for Ribbon Torus-Links in \mathbb{R}^4



Celeste Damiani

Abstract In classical knot theory, Markov's theorem gives a way of describing all braids with isotopic closures as links in \mathbb{R}^3 . We present a version of Markov's theorem for extended loop braids with closure in $B^3 \times S^1$, as a first step towards a Markov's theorem for extended loop braids and ribbon torus-links in \mathbb{R}^4 .

Keywords Braid groups · Links · Welded braid groups · Loop braids · Welded links · Ribbon torus-links · Markov

Mathematics Subject Classification (2010) 57Q45

1 Introduction

In the classical theory of braids and links, Alexander's theorem allows us to represent every link as the closure of a braid. Moreover, Markov's theorem states that two braids (possibly with different numbers of strings) have isotopic closures in a 3-dimensional space if and only if one can be obtained from the other after a finite number of Markov moves, called *conjugation* and *stabilization*. This theorem is a tool to describe all braids with isotopic closures as links in a 3-dimensional space. Moreover, these two theorems allow us to recover certain link invariants as Markov traces.

When considering *extended loop braids* as braided annuli in a 4-dimensional space on one hand, and *ribbon torus-links* on the other hand, we have that a version of Alexander's theorem is a direct consequence of three facts. First of all, every ribbon torus-link can be represented by a welded braid [22]. Then, a version of Markov's theorem is known for welded braids and welded links [14, 17]. Finally, welded braid groups and loop braid groups are isomorphic [8], and loop braids are a particular class of extended loop braids.

C. Damiani (✉)

Department of Pure Mathematics, School of Mathematics, University of Leeds,
Leeds LS29QJ, UK

e-mail: c.damiani@leeds.ac.uk

© Springer Nature Switzerland AG 2019

C. C. Adams et al. (eds.), *Knots, Low-Dimensional Topology*

and Applications, Springer Proceedings in Mathematics & Statistics 284,

https://doi.org/10.1007/978-3-030-16031-9_15

In this paper we take a first steps in formulating a version of Markov's theorem for extended loop braids with closure in the space $B^3 \times S^1$. We show that two extended loop braids have closures that are isotopic in $B^3 \times S^1$ if and only if they are conjugate in the extended loop braid groups. The reason for considering *extended* loop braid groups instead of loop braid groups is because this allows to prove a result that is exactly the analogous of the result that we have for 1-dimensional braids and knots in a 3-dimensional space. In fact, if we consider two loop braids in the first place, we have that their closures are isotopic as ribbon torus-knots in $B^3 \times S^1$ if and only if the pair of loop braids are conjugate in the extended loop braid group. This is due to the fact that isotopies of ribbon torus-links can introduce a phenomenon called *wen*, which we discuss in Sect. 2.4, on the components of the closed braided objects. Wens are natural phenomena in the context of ribbon torus-links in \mathbb{R}^4 , but they are not encoded in the theory of loop braids. Then, extended loop braids, who encode wens, seem to be the most natural analogue of classical braids, and the most appropriate notion that we need to consider.

1.1 Structure of the Paper

In Sect. 2 we give an overview of the many equivalent interpretations of extended loop braid groups, which are the braided objects coming to play in our main result. An expanded version of this overview can be found in [8].¹ A particular focus will be placed on the definition of extended loop braids as braided annuli in a 4-dimensional space. When we want to make clear that we are using this interpretation for extended loop braids, we use the terminology *ribbon braids*. We recall several results on these objects, and we use them to prove that every ribbon braid can be parametrized by a normal isotopy (Proposition 1).

In Sect. 3 we introduce the knotted counterpart of ribbon braids, which are ribbon torus-links.

In Sect. 4 we present the main result of this paper. This is a version of Markov's theorem for ribbon torus-links living in the space $B^3 \times S^1$ (Theorem 8).

Finally, in Sect. 5 we discuss possible ideas to complete the main result of this paper to a complete Markov's theorem for ribbon torus-links in \mathbb{R}^4 .

2 Extended Loop Braid Groups and Their Equivalent Definitions

Loop braid groups were introduced under this name for the first time by Xiao-Song Lin in 2007 [21], although they had been considered before in other contexts and with other terminologies, for instance *groups of conjugating automorphisms* in [23] and *welded braid groups* in [9].

¹Notations are slightly changed: differences will be pointed out along this text.

The groups we call *extended loop braid groups* appeared sooner in the literature, in [6, 11], who called them *motion groups of a trivial link of unknotted circles in \mathbb{R}^3* , but since then have been less treated.

In terms of configuration spaces, both groups appear in [5], loop braid groups as *untwisted ring groups*, and extended loop braid groups as *ring groups*. In this paper we focus on extended loop braid groups, for which we choose to adapt Lin's notation because it gives a good visual idea of the considered objects, while being more compact. In fact, the elements of both these groups can be seen as trajectories travelled by loops as they move in a 3-dimensional space to exchange their positions under some admissible motions. The "extended" attribute highlights the fact that in extended loop braid groups we admit an extra motion that can be described as a 180° -flip of a loop. For a detailed survey on loop braid groups, extended loop braid groups and the explicit equivalences among the different definitions, we refer to [8].

We dedicate this section to recall several definitions of extended loop braid groups, and give the terminology used in the different contexts. The diversity of points of view will be useful in the proof of the main result of this paper (Theorem 8), since it provides many approaches and tools to tackle problems involving extended loop braid groups and other knotted objects in the 4-dimensional space.

2.1 Extended Loop Braids as Mapping Classes

We present here a first definition for extended loop braid groups in terms of mapping classes of a 3-ball with n circles that are left setwise invariant in its interior.

Let us fix $n \in \mathbb{N}$, and let $C = C_1 \sqcup \dots \sqcup C_n$ be a collection of n disjoint, unknotted, oriented circles, that form a trivial link of n components in the interior of the 3-ball B^3 . A self-homeomorphism of the pair (B^3, C) is an homeomorphism $f: B^3 \rightarrow B^3$ that fixes ∂B^3 pointwise, preserves orientation on B^3 , and globally fixes C . Every self-homeomorphism of (B^3, C) induces a permutation on the connected components of C in the natural way. We consider the mapping class group of B^3 with respect to C to be the group of isotopy classes of self-homeomorphisms of (B^3, C) , with multiplication determined by composition. We denote it by $\text{MCG}(B^3, C^*)$.

Remark 1 The "*" on the submanifold C is to indicate that homeomorphisms do not preserve the orientation of the connected components of C . This is the difference between extended loop braid groups and loop braid groups in this context. In fact, in the latter, the homeomorphisms preserve orientation on C .

Remark 2 A map f from a topological space X to $\text{Homeo}(B^3; C^*)$ is continuous if and only if the map $X \times B^3 \rightarrow B^3$ sending $(x, y) \mapsto f(x)(y)$ is continuous [20]. Taking X equal to the unit interval I , we have that two self-homeomorphisms are isotopic if and only if they are connected by a path in $\text{Homeo}(B^3; C^*)$.

Therefore $\text{MCG}(B^3, C^*) = \pi_0(\text{Homeo}(B^3; C^*))$. The same can be said for the pure groups, $\text{PMCG}(B^3, C^*) = \pi_0(\text{PHomeo}(B^3; C^*))$.

Definition 1 For $n \geq 1$, the *extended loop braid group*, denoted by LB_n^{ext} , is the mapping class group $\text{MCG}(B^3, C^*)$.

2.2 Extended Loop Braids as Loops in a Configuration Space

The second interpretation of extended loop braid groups LB_n^{ext} that we give is in terms of configuration spaces, and has been introduced in [5]. Let $n \geq 1$, and consider the space of configurations of n Euclidean, unordered, disjoint, unlinked circles in B^3 , denoted by \mathcal{R}_n . The *ring group* R_n is its fundamental group.

Remark that in Sect. 2.1 we were not considering Euclidean circles as moving objects, but the components of a trivial link. We shall see now that these two families of objects are deeply related. Let \mathcal{L}_n be the space of configurations of smooth trivial links with n components in \mathbb{R}^3 : the following result allows us to consider the fundamental group of \mathcal{L}_n as being isomorphic to R_n .

Theorem 1 ([5, Theorem 1]) *For $n \geq 1$, the inclusion of \mathcal{R}_n into \mathcal{L}_n is a homotopy equivalence.*

As anticipated, the groups R_n are isomorphic to the groups LB_n^{ext} , as stated in the next theorem. Its proof heavily relies on Wattenberg’s results [25, Lemma 1.4 and Lemma 2.4] implying that the topological mapping class groups of the 3-ball with respect to an n -components trivial link are isomorphic to the C^∞ -mapping class groups of the same pair. In other terms, we have that $\pi_0(\text{Homeo}(B^3; C^*)) \cong \pi_0(\text{Diffeo}(B^3; C^*))$. We can define an evaluation map from $\text{Diffeo}(B^3)$ to the space of configurations of a smooth trivial link with n *ordered* components in \mathbb{R}^3 , that we denote by $\mathcal{P}\mathcal{L}_n$. We can refer to $\mathcal{P}\mathcal{L}_n$ as to the *pure* configuration space of a smooth trivial link. Fixed the n components of a trivial link in the interior of the 3-ball, this evaluation map sends self-diffeomorphisms of B^3 to the image of the n components through the considered self-diffeomorphism:

$$\varepsilon: \text{Diffeo}(B^3) \longrightarrow \mathcal{P}\mathcal{L}_n. \tag{1}$$

This map can be proved to be a locally trivial fibration [8, Lemma 3.8]. This fibration is then used as the main ingredient to prove the following, through the construction of exact sequences and a commutative diagram.

Theorem 2 ([8, Theorem 3.10]) *For $n \geq 1$, there is a natural isomorphism between ring group R_n and the extended loop braid group LB_n^{ext} .*

Brendle and Hatcher, in [5, Proposition 3.7], give a presentation for the ring groups R_n , and so, for LB_n^{ext} .

Proposition 1 For $n \geq 1$, the group LB_n^{ext} admits the presentation given by generators $\{\sigma_i, \rho_i \mid i = 1, \dots, n - 1\}$ and $\{\tau_i \mid i = 1, \dots, n\}$, subject to relations:

$$\left\{ \begin{array}{ll} \sigma_i \sigma_j = \sigma_j \sigma_i & \text{for } |i - j| > 1 \\ \sigma_i \sigma_{i+1} \sigma_i = \sigma_{i+1} \sigma_i \sigma_{i+1} & \text{for } i = 1, \dots, n - 2 \\ \rho_i \rho_j = \rho_j \rho_i & \text{for } |i - j| > 1 \\ \rho_i \rho_{i+1} \rho_i = \rho_{i+1} \rho_i \rho_{i+1} & \text{for } i = 1, \dots, n - 2 \\ \rho_i^2 = 1 & \text{for } i = 1, \dots, n - 1 \\ \rho_i \sigma_j = \sigma_j \rho_i & \text{for } |i - j| > 1 \\ \rho_{i+1} \rho_i \sigma_{i+1} = \sigma_i \rho_{i+1} \rho_i & \text{for } i = 1, \dots, n - 2 \\ \sigma_{i+1} \sigma_i \rho_{i+1} = \rho_i \sigma_{i+1} \sigma_i & \text{for } i = 1, \dots, n - 2 \\ \tau_i \tau_j = \tau_j \tau_i & \text{for } i \neq j \\ \tau_i^2 = 1 & \text{for } i = 1, \dots, n \\ \sigma_i \tau_j = \tau_j \sigma_i & \text{for } |i - j| > 1 \\ \rho_i \tau_j = \tau_j \rho_i & \text{for } |i - j| > 1 \\ \tau_i \rho_i = \rho_i \tau_{i+1} & \text{for } i = 1, \dots, n - 1 \\ \tau_i \sigma_i = \sigma_i \tau_{i+1} & \text{for } i = 1, \dots, n - 1 \\ \tau_{i+1} \sigma_i = \rho_i \sigma_i^{-1} \rho_i \tau_i & \text{for } i = 1, \dots, n - 1. \end{array} \right. \quad (2)$$

The elements σ_i , ρ_i , and τ_i of the presentation represent the following loops in R_n : if we place the n rings in a standard position in the yz -plane with centers along the y -axis, then σ_i is the loop that permutes the i th and the $(i + 1)$ st circles by passing the i th circle through the $(i + 1)$ st; ρ_i permutes them passing the i th around the $(i + 1)$ st, and τ_i is the loop that flips by 180° the i th circle, see Fig. 1.

2.3 Extended Loop Braids as Automorphisms of the Free Groups

We now give an interpretation of extended loop braids in terms of automorphisms of F_n , the free groups of rank n . Fixing $n \geq 1$, we consider the automorphisms that

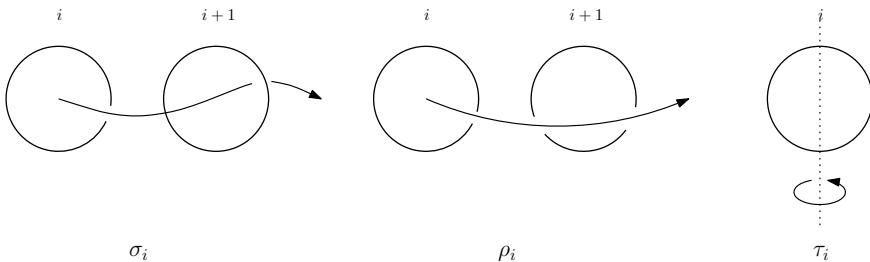


Fig. 1 Elements σ_i , ρ_i and τ_i

send each generator of F_n to a conjugate of some generator, or its inverse: these are in bijection with elements of LB_n^{ext} . We start recalling a result of Dahm’s unpublished thesis [6], that appears in the last section of Goldsmith’s paper [11].

Theorem 3 ([11, Theorem 5.3]) *For $n \geq 1$, there is an injective map from the extended loop braid group LB_n^{ext} into $\text{Aut}(F_n)$, where F_n is the free group on n generators $\{x_1, \dots, x_n\}$, and its image is the subgroup PC_n , consisting of all automorphisms of the form $\alpha: x_i \mapsto w_i^{-1}x_{\pi(i)}^{\pm 1}w_i$ where π is a permutation and w_i is a word in F_n . Moreover, the group PC_n is generated by the automorphisms $\{\sigma_1, \dots, \sigma_{n-1}, \rho_1, \dots, \rho_{n-1}, \tau_1, \dots, \tau_n\}$ defined as:*

$$\sigma_i : \begin{cases} x_i \mapsto x_{i+1}; \\ x_{i+1} \mapsto x_{i+1}^{-1}x_i x_{i+1}; \\ x_j \mapsto x_j, & \text{for } j \neq i, i + 1. \end{cases} \tag{3}$$

$$\rho_i : \begin{cases} x_i \mapsto x_{i+1}; \\ x_{i+1} \mapsto x_i; \\ x_j \mapsto x_j, & \text{for } j \neq i, i + 1. \end{cases} \tag{4}$$

$$\tau_i : \begin{cases} x_i \mapsto x_i^{-1}; \\ x_j \mapsto x_j, & \text{for } j \neq i. \end{cases} \tag{5}$$

This result is the analogue of Artin’s characterization of usual braids as automorphisms of the free group. In an intuitive way, we use for the automorphisms of PC_n the notations of the corresponding elements of the mapping class group.²

In [9] Fenn, Rimányi and Rourke consider the subgroups of $\text{Aut}(F_n)$ generated only by the sets of elements $\{\sigma_i \mid i = 1, \dots, n - 1\}$ and $\{\rho_i \mid i = 1, \dots, n - 1\}$. They call these groups by the name *braid-permutation groups*, and they prove independently from Dahm and Goldsmith that they are isomorphic to the groups of all automorphisms of $\text{Aut}(F_n)$ of the form $\alpha: x_i \mapsto w_i^{-1}x_{\pi(i)}w_i$ where π is a permutation and w_i is a word in F_n .

2.4 Extended Loop Braids as Ribbon Braids

The next interpretation of extended loop braids will be the one that we will focus on in the main result of this paper. This is an approach in terms of braided objects in a 4-dimensional space. Extended loop braids in this context are called *ribbon braids*, when we want to specify the used interpretation.³

²In [8] these groups are denote by PC_n^* , while PC_n is used for the groups of automorphisms of the form $\alpha: x_i \mapsto w_i^{-1}x_{\pi(i)}w_i$.

³In the survey [8] the terminology *ribbon braids* refers to loop braids seen as braided objects in the 4-dimensional braid, while the terminology *extended ribbon braids* refers to extended loop braids. We chose to simplify.

We need some notation before giving the definition of ribbon braids and their equivalence to extended loop braids. Let $n \geq 1$, and let D_1, \dots, D_n be a collection of disks in the 2-ball B^2 . Let $C_i = \partial D_i$ be the oriented boundary of D_i . Let us consider the 4-ball $B^4 \cong B^3 \times I$, where I is the unit interval. For any submanifold $X \subset B^m \cong B^{m-1} \times I$, with $m = 3, 4$, we use the following dictionary. To keep the notation readable, here we denote the interior of a topological space by “ $\text{int}(\)$ ”, whereas anywhere else it is denoted by “ \circ ”.

- $\partial_\varepsilon X = X \cap (B^{m-1} \times \{\varepsilon\})$, with $\varepsilon \in \{0, 1\}$;
- $\partial_* X = \partial X \setminus \left(\text{int}(\partial_0 X) \sqcup \text{int}(\partial_1 X) \right)$;
- $\overset{*}{X} = X \setminus \partial_* X$.

The image of an immersion $Y \subset X$ is said to be *locally flat* if and only if it is locally homeomorphic to a linear subspace \mathbb{R}^k in \mathbb{R}^m for some $k \leq m$, except on ∂X and/or ∂Y , where one of the \mathbb{R} summands should be replaced by \mathbb{R}_+ . Let Y_1, Y_2 be two submanifolds of B^m . The intersection $Y_1 \cap Y_2 \subset X$ is called *flatly transverse* if and only if it is locally homeomorphic to the transverse intersection of two linear subspaces \mathbb{R}^{k_1} and \mathbb{R}^{k_2} in \mathbb{R}^m for some positive integers $k_1, k_2 \leq m$ except on ∂X , ∂Y_1 and/or ∂Y_2 , where one of the \mathbb{R} summands should be replaced by \mathbb{R}_+ . In the next definition we introduce the kind of singularities we consider.

Definition 2 Let Y_1, Y_2 be two submanifolds of B^4 . *Ribbon disks* are intersections $D = Y_1 \cap Y_2$ that are isomorphic to the 2-dimensional disk, such that $D \subset \overset{\circ}{Y}_1, \overset{\circ}{D} \subset \overset{\circ}{Y}_2$ and ∂D is an essential curve in ∂Y_2 .

These singularities are the 4-dimensional analogues of the classical notion of ribbon singularities introduced by Fox in [10].

Definition 3 Let A_1, \dots, A_n be locally flat embeddings in $\overset{*}{B}^4$ of n disjoint copies of the oriented annulus $S^1 \times I$. We say that

$$b = \bigsqcup_{i \in \{1, \dots, n\}} A_i$$

is a *geometric ribbon braid* if:

1. the boundary of each annulus ∂A_i is a disjoint union $C_i \sqcup C_j$, for $C_i \in \partial_0 B^4$ and for some $C_j \in \partial_1 B^4$. The orientation induced by A_i on ∂A_i coincides with the one of the two boundary circles C_i and C_j ;
2. the annuli A_i are fillable, in the sense that they bound immersed 3-balls $\subset \mathbb{R}^4$ whose singular points consist in a finite number of ribbon disks;
3. it is transverse to the lamination $\bigcup_{t \in I} B^3 \times \{t\}$ of B^4 , that is: at each parameter t , the intersection between b and $B^3 \times t$ is a collection of exactly n circles;

The group of *ribbon braids*, denoted by rB_n , is the group of equivalence classes of geometric ribbon braids up to continuous deformations through the class of geometric

ribbon braids fixing the boundary circles, equipped with the natural product given by stacking and reparametrizing. The unit element for this product is the *trivial ribbon braid* $U = \bigsqcup_{i \in \{1, \dots, n\}} C_i \times [0, 1]$.

The monotony condition allows us to consider the interval I in $B^4 = B^3 \times I$ as a time parameter, and to think of a ribbon braid as a trajectory $\beta = (C_1(t), \dots, C_n(t))$ of circles in $B^3 \times I$. This trajectory corresponds to a parametrization of the ribbon braid. This interpretation is also referred to in terms of *flying rings* in [3]. When one of the n circles that we have at each time t makes a half-turn, we have what is called a *wen* on the corresponding component. One can think of a wen as an embedding in \mathbb{R}^4 of a Klein bottle cut along a meridional circle. A detailed treatment of wens can be found in Kanenobu and Shima’s paper [15].

The following result states the equivalence of the interpretations of LB_n^{ext} as mapping class groups and as ribbon braid groups. Its proof consists in explicitly defining an isomorphism between rB_n and R_n , and composing it with the isomorphism from Theorem 2.

Theorem 4 ([8, Theorem 5.17]) *For $n \geq 1$, there is an isomorphism between the ribbon braid group rB_n and the extended loop braid group LB_n^{ext} .*

We can show that when two ribbon braids are equivalent in the sense of Definition 3, there is an ambient isotopy of \mathbb{R}^4 bringing one to the other.

Theorem 5 ([8, Theorem 5.5]) *Every relative isotopy of a geometric ribbon braid in $B^3 \times I$ extends to an isotopy of $B^3 \times I$ in itself constant on the boundary.*

This result is true also for *surface links*, which are closed surfaces locally flatly embedded in \mathbb{R}^4 [13, Theorem 6.7].

With the results we recalled, we prove now that given a geometric ribbon braid b and its set of starting set of circles, we can find a normal isotopy parametrizing it. We take $C = (C_1, \dots, C_n)$ to be an ordered tuple of n disjoint, unlinked, unknotted circles living in B^3 . We consider the space of configurations of ordered smooth trivial links of n components $\mathcal{P}\mathcal{L}_n$ introduced in Sect. 2.2. As mentioned above, we have an evaluation map

$$\varepsilon: \text{Diffeo}(B^3) \longrightarrow \mathcal{P}\mathcal{L}_n$$

sending a self-diffeomorphism f to $f(C)$. We remark that $f(C)$ is an ordered tuple of n disjoint, unlinked, trivial, smooth knots living in B^3 , which is a locally trivial fibration with fibre the group of self-diffeomorphisms of the pair (B^3, C) that send each connected component of C to itself. Composing ε with the covering map $\mathcal{P}\mathcal{L}_n \rightarrow \mathcal{L}_n$, seeing \mathcal{L}_n as the orbit space with of the action of the symmetric group of $\mathcal{P}\mathcal{L}_n$, we define a locally trivial fibration

$$\tilde{\varepsilon}: \text{Diffeo}(D^3) \longrightarrow \mathcal{L}_n$$

sending f to $f(C)$. More details on this construction can be found in [8].

Lemma 1 *Let $n \geq 1$. For every geometric ribbon braid $b \subset B^4$ on n components, there is a normal isotopy parametrizing b .*

Proof Let us consider a geometric ribbon braid b , through the isomorphism between rB_n and R_n (Theorem 4). This gives rise to a loop $f^b: I \rightarrow \mathcal{P}\mathcal{L}_n \subset \mathcal{L}_n$ sending $t \in I$ into the unique n -circles set b_t such that

$$b \cap (B^3 \times I) = b_t \times \{t\}.$$

This loop begins and ends at the point $\tilde{\varepsilon}(\text{id}_{B^3}) \in \mathcal{L}_n$ represented by C . Being $\tilde{\varepsilon}$ a fibration, we apply the homotopy lifting property, and lift f^b to a path $\hat{f}^b: I \rightarrow \text{Diffeo}(B^3)$ beginning at $\tilde{\varepsilon}^{-1}(C) = \text{Diffeo}(B^3; C^*)$ and ending at id_{B^3} . The path \hat{f}^b is a normal isotopy. The commutativity $\tilde{\varepsilon} \circ \hat{f}^b = f^b$ means that this isotopy parametrizes b . □

2.5 Extended Loop Braids as Extended Welded Braids

In this part we discuss 1-dimensional diagrams immersed in a 2-dimensional space for extended loop braids. An *extended welded braid diagram* on n strings is a planar diagram composed by a set of n oriented and monotone 1-manifolds immersed in \mathbb{R}^2 starting from n points on a horizontal line at the top of the diagram down to a similar set of n points at the bottom of the diagram. The 1-manifolds are allowed to cross in transverse double points, which will be decorated in three kinds of ways, as shown in Fig. 2. Depending on the decoration, double points will be called: *classical positive crossings*, *classical negative crossings* and *welded crossings*. On each 1-manifold there can possibly be marks as in Fig. 3, which we will call *wen marks*.

Fig. 2 **a** Classical positive crossing, **b** classical negative crossing, **c** welded crossing

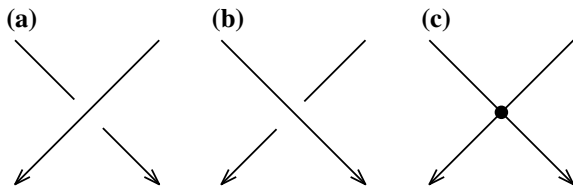


Fig. 3 A wen mark on a strand



Remark 3 The inclination of the wen mark on the strand is not fixed, and does not carry any information.

Let us assume that the double points occur at different y -coordinates. Then an extended welded braid diagram determines a word in the elementary diagrams illustrated in Fig. 4. We call σ_i the elementary diagram representing the $(i + 1)$ th strand passing over the i th strand, ρ_i the welded crossing of the strands i and $(i + 1)$, and τ_i the wen mark diagram.

Definition 4 An *extended welded braid* is an equivalence class of extended welded braid diagrams under the equivalence relation given by isotopy of \mathbb{R}^2 and the following moves:

- classical Reidemeister moves (Fig. 5);
- virtual Reidemeister moves (Fig. 6);
- mixed Reidemeister moves (Fig. 7);

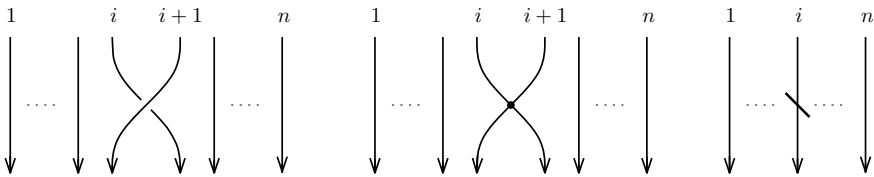


Fig. 4 Elementary diagrams σ_i , ρ_i , and τ_i

Fig. 5 Classical Reidemeister moves for braid-like objects

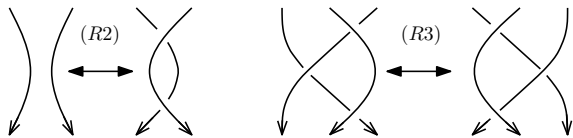


Fig. 6 Virtual Reidemeister moves for braid-like objects

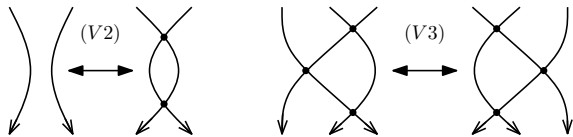


Fig. 7 Mixed Reidemeister moves

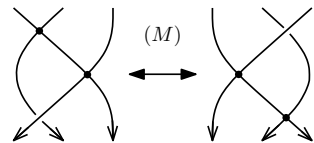
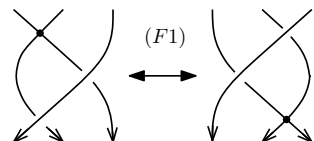


Fig. 8 Welded Reidemeister moves



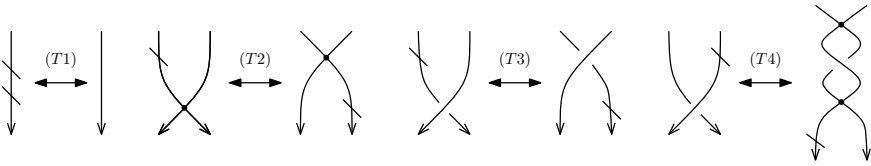


Fig. 9 Extended Reidemeister moves

- welded Reidemeister moves (Fig. 8);
- extended Reidemeister moves (Fig. 9).

This equivalence relation is called *(braid) generalized Reidemeister equivalence*. For $n \geq 1$, the *extended welded braid group* on n strands WB_n^{ext} is the group of equivalence classes of extended welded braid diagrams by generalized Reidemeister equivalence. The group structure on these objects is given by: stacking and rescaling as product, braid mirror image as inverse, and the trivial diagram as identity.

Remark 4 If wren marks were not allowed, the group defined would be the group of *welded braids* WB_n , introduced by Fenn, Rimányi and Rourke in [9]. This group is isomorphic to *loop braid groups* LB_n .

In [22] the author defines a surjective map *Tube* from welded knotted objects to ribbon knotted objects in dimension 4. This map *Tube* can be easily defined on extended welded braids and extended loop braids, in their interpretation as ribbon braids. Its definition uses as a stepping stone a projection of ribbon braids onto a certain class of 3-dimensional surfaces, called *broken surface diagrams*. We do not treat them in this paper since they are not relevant to the main result. However they are an interesting way of representing ribbon braids, and more detail can be found in [2]. In the framework of extended welded braids and ribbon braids, it can be proved that the *Tube* map is an isomorphism [8, Theorem 6.12]. Hence, we have the last isomorphism that we recall in this overview on extended loop braids.

Theorem 6 *For $n \geq 1$, there is an isomorphism between the extended welded braid group WB_n^{ext} and the extended loop braid group LB_n^{ext} .*

2.6 Pure Subgroups

As in the case of classical braid groups B_n , we have a notion of pure subgroups for the extended loop braid groups LB_n^{ext} . Let us consider the first definition we gave for extended loop braids, as elements of $MCG(B^3, C^*)$, where $C = C_1 \sqcup \dots \sqcup C_n$ is a collection of n disjoint, unknotted, oriented circles, that form a trivial link of n components. Let $p: LB_n^{ext} \rightarrow S_n$ be the homomorphism that forgets the details of the braiding, remembering only the permutation of the circles. Then the *pure*

extended loop braid group PLB_n^{ext} is the kernel of p . In each one of the approaches to extended loop braid groups that we exposed, such subgroups can be defined with tools inherent to the particular context. We will not dwell on these groups here, but they are discussed in all the references we gave on extended loop braid groups throughout this section.

3 Ribbon Torus-Links

In this part we introduce the knotted counterpart of extended loop braid groups: ribbon torus-links. Classical references for these objects are [13, 18, 27].

Definition 5 A *geometric ribbon torus-knot* is an embedded oriented torus $S^1 \times S^1 \subset \mathbb{R}^4$ which is *fillable*, in the sense that it bounds a *ribbon torus*. A ribbon torus is an oriented immersed solid torus $D^2 \times S^1 \subset \mathbb{R}^4$ whose singular points consist in a finite number of ribbon disks (see Definition 2, and compare with point 2 of Definition 3). *Ribbon torus-knots* are equivalence classes of geometric ribbon torus-knots defined up to ambient isotopy.

Remark 5 Wens can appear on portions of a ribbon knot, but for an argument of coherence of the co-orientation, there are an even number of them on each component, and they cancel pairwise, as remarked in [1, proof of Proposition 2.4].

Definition 6 A *geometric ribbon torus-link* with n components is the embedding of a disjoint union of n oriented fillable tori. The set of *ribbon torus-links* is the set of equivalence classes of geometric ribbon torus-knots defined up to ambient isotopy.

3.1 Extended Welded Diagrams for Ribbon Torus-Links

An *extended welded link diagram* is the immersion in \mathbb{R}^2 of a collection of disjoint, closed, oriented 1-manifolds such that all multiple points are transverse double points. Double points are decorated with classical positive, classical negative, or welded information as in Fig. 2. On each 1-manifold there can possibly be an even number of wen marks as in Fig. 3, the motivation for this lying in Remark 5. We assume that extended welded link diagrams are the same if they are isotopic in \mathbb{R}^2 . Taken an extended welded link diagram K , we call *real crossings* its set of classical positive and classical negative crossings.

Definition 7 An *extended welded link* is an equivalence class of extended welded link diagrams under the equivalence relation given by isotopies of \mathbb{R}^2 , moves from Definition 4, and classical and virtual Reidemeister moves (R1) and (V1) as in Fig. 10. This equivalence relation is called *generalized Reidemeister equivalence*.

Fig. 10 Reidemeister moves of type I

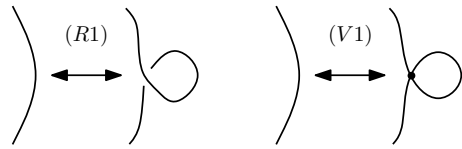
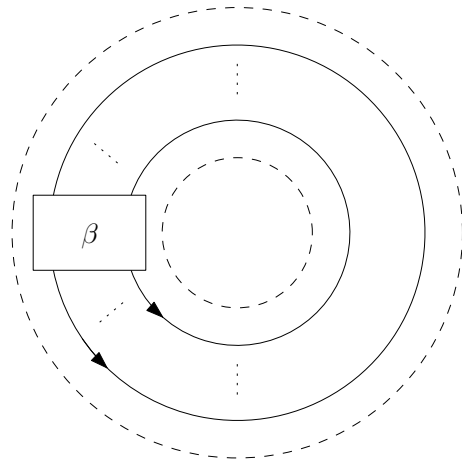


Fig. 11 Closure of an extended welded braid diagram



The *closure* of an extended welded braid diagram is obtained as for usual braid diagrams (see Fig. 11), with the condition that extended welded braids can be closed only when they have an even number of wens marks on each component.

For completeness we recall that for extended welded diagrams we have two results that are analogous to Alexander's and Markov's theorems, that we state here in the following.

Proposition 2 ([7, Proposition 3.3]) *Any extended welded link can be described as the closure of an extended welded braid diagram which is generalized Reidemeister equivalent to a welded braid diagram.*

Theorem 7 ([7, Theorem 4.1]) *Two extended welded braid diagrams that admit closure have equivalent closures as extended welded link diagrams if and only if they are related by a finite sequence on the following moves:*

- (M0) *isotopy of \mathbb{R}^2 and generalized Reidemeister moves;*
- (M1) *conjugation in the extended welded braid group WB_n^{ext} ;*
- (M2) *a right stabilization of positive, negative or welded type, and its inverse operation.*

The *Tube* map we briefly discussed in Sect. 2.5 can be defined also from extended welded links to ribbon torus-links, thanks to the intermediate passage through broken surfaces, and to the fact that the map is defined locally, for details see [8, Sect. 6.3]. On link-like objects there is no result stating that the map is an isomorphism, however we have the following result, which is a direct consequence of [1, Proposition 2.5].

Proposition 3 *The map Tube, defined on extended welded links, with values in the set of ribbon torus-links, is a well-defined surjective map.*

We will not linger on this construction, but we remark that the importance of this result is that it allows us to associate an extended welded link to every ribbon torus-link.

3.2 Closed Ribbon Braids in $V = B^3 \times S^1$

We introduce a particular kind of ribbon torus-links in the space $V = B^3 \times S^1$.

Definition 8 A torus-link L in V is called a *closed n -ribbon braid* with $n \geq 1$ if L meets each ball $B^3 \times \{t\}$, for $t \in S^1$, transversely in n circles.

Remark 6 Two closed ribbon braids in V are isotopic if they are isotopic as oriented torus-links. This implies that the tubes don't necessarily stay transverse to the lamination during the isotopy.

Remark 7 In general a torus-link in V is not isotopic to a closed ribbon braid in V . For instance a torus link lying inside a small 4-ball in V is never isotopic to a closed braid.

Definition 9 Given an n -ribbon braid β , its *tube closure* is the ribbon torus-knot $\widehat{\beta}$ obtained by gluing a copy of the trivial ribbon braid U along β , identifying the pair $(B^3 \times \{0\}, \partial_0\beta)$ with $(B^3 \times \{1\}, \partial_1U)$ and $(B^3 \times \{1\}, \partial_1\beta)$ with $(B^3 \times \{0\}, \partial_0U)$.

On the diagrammatical side: an extended welded link diagram for $\widehat{\beta}$ in $S^1 \times I$ is obtained by closing a diagram for β .

4 A Version of Markov's Theorem in $B^3 \times S^1$

In classical braid theory, closed braids in the solid torus are classified up to isotopy by the conjugacy classes of braids in B_n . We give here a classification of this kind for closed ribbon braids: their closures will be classified, up to isotopy in $B^3 \times S^1$, by conjugacy classes of ribbon braids. The proof is inspired by the one given for the classical case in [16, Chap. 2]. In the following statement we will consider extended loop braids in their interpretation as braided annuli in the 4-dimensional space, so we will use the terminology "ribbon braids" which is inherent to this approach.

Theorem 8 *Let $n \geq 1$ and $\beta, \beta' \in rB_n$ a pair of ribbon braids. The closed ribbon braids $\widehat{\beta}, \widehat{\beta}'$ are isotopic in $B^3 \times S^1$ if and only if β and β' are conjugate in rB_n .*

Proof We begin with the “if” part. Suppose first the case that β and β' are conjugate in rB_n . We recall that rB_n is isomorphic to the group of extended welded braids WB_n^{ext} . We call with the same name an element in rB_n and a diagram for it as a representative of the corresponding class in WB_n^{ext} . Conjugate elements of WB_n^{ext} give rise to isotopic closed welded braid, which correspond to isotopic closed ribbon braids. This means that, since β and β' are conjugate in WB_n^{ext} , $\beta' = \alpha\beta\alpha^{-1}$ with $\alpha \in WB_n^{ext}$, and we have that $\widehat{\alpha\beta\alpha^{-1}} = \widehat{\beta}$. To see this, it is enough to stack the diagrams of α , β and α^{-1} , close the composed welded braid diagram, and push the upper diagram representing α along the parallel strands until α and α^{-1} are stacked one next to the other at the bottom of the diagram.

Let us now prove the converse, which is: any pair of ribbon braids with isotopic closures in $V = B^3 \times S^1$ are conjugate in rB_n . Passing through the isomorphism between rB_n and PC_n , it will be enough to prove the following: any pair of ribbon braids with isotopic closures in $V = B^3 \times S^1$ have associated automorphisms of PC_n that are conjugate. Set $\overline{V} = B^3 \times \mathbb{R}$. Considering the cartesian product of (B^3, id_{B^3}) and the universal covering (\mathbb{R}, p) of S^1 given by

$$p: \mathbb{R} \longrightarrow S^1$$

$$t \longmapsto \exp(2\pi it)$$

we obtain a universal covering $(\overline{V}, \text{id}_{B^3} \times p)$ of V . Denote by T the covering transformation

$$T: \overline{V} \longrightarrow \overline{V}$$

$$(x, t) \longmapsto (x, t + 1)$$

for all $x \in B^3$ and $t \in \mathbb{R}$. If L is a closed n -ribbon braid in V , then its preimage $\overline{L} \subset \overline{V}$ is a 2-dimensional manifold meeting each 3-ball $B^3 \times \{t\}$, for $t \in \mathbb{R}$, transversely in n disjoint pairwise unlinked circles. This implies that \overline{L} consists of n fillable components homeomorphic to $S^1 \times \mathbb{R}$.

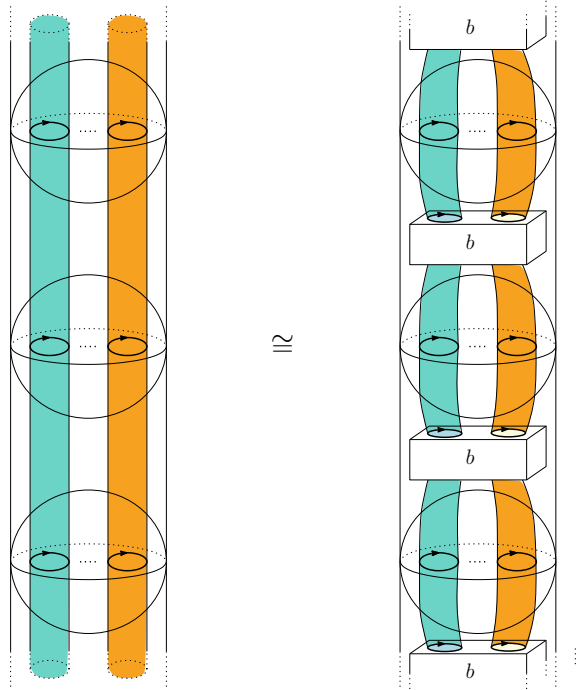
Being L a closed ribbon braid, we can present it as a closure of a geometric ribbon braid $b \subset B^4 = B^3 \times I$ where we identify $\partial_0 B^4$ with $\partial_1 B^4$. Then $\overline{L} = \bigcup_{m \in \mathbb{Z}} T^m(b)$, i.e., we can see \overline{L} as a tiling of an infinite number of copies of b .

For $n \geq 1$, let $C = (C_1, \dots, C_n)$ be a family of n disjoint, pairwise unlinked, euclidean circles in \mathring{B}^3 , lying on parallel planes. We consider a parametrization for b , i.e., a family $\{\alpha_t: B^3 \rightarrow B^3\}_{t \in I}$ such that $\alpha_0(C) = C$, $\alpha_1 = \text{id}_{B^3}$, all α_t fix ∂B^3 pointwise, and $b = \bigcup_{t \in I} (\alpha_t(C), t)$ (see Lemma 1).

We take the self-homeomorphism of $\overline{V} = B^3 \times \mathbb{R}$ given by

$$(x, t) \longmapsto (\alpha_{t-[t]}\alpha_0^{-[t]}(x), t)$$

Fig. 12 A homeomorphism between $(B^3 \times \mathbb{R}, C \times \mathbb{R})$ and $(B^3 \times \mathbb{R}, \bar{L})$



where $x \in B^3$, $t \in \mathbb{R}$, and $\lfloor t \rfloor$ is the greatest integer less than or equal to t . This homeomorphism fixes $\partial \bar{V} = S^2 \times \mathbb{R}$ pointwise and sends $C \times \mathbb{R}$ onto \bar{L} , see Fig. 12 for an intuitive (although necessarily imprecise) idea.

The induced homeomorphism $(B^3 \setminus C) \times \mathbb{R} \cong \bar{V} \setminus \bar{L}$ shows that $B^3 \setminus C = (B^3 \setminus C) \times \{0\} \subset \bar{V} \setminus \bar{L}$ is a deformation retract of $\bar{V} \setminus \bar{L}$. Pick a point $d \in \partial B^4 = B^3$ and set $\vec{d} = (d, 0) \in \bar{V}$; then the inclusion homomorphism

$$i: \pi_1(B^3 \setminus C, d) \longrightarrow \pi_1(\bar{V} \setminus \bar{L}, \vec{d})$$

is an isomorphism.

By definition the image of d by the covering transformation T is $T(d) = (d, 1)$; the covering transformation T restricted to $\bar{V} \setminus \bar{L}$ induces an isomorphism $\pi_1(\bar{V} \setminus \bar{L}, \vec{d}) \rightarrow \pi_1(\bar{V} \setminus \bar{L}, T(\vec{d}))$. Let T_* be the composition of this isomorphism with the isomorphism $\pi_1(\bar{V} \setminus \bar{L}, T(\vec{d})) \rightarrow \pi_1(\bar{V} \setminus \bar{L}, \vec{d})$ obtained by conjugating the loops by the path $d \times [0, 1] \subset \partial B^3 \times \mathbb{R} \subset \bar{V} \setminus \bar{L}$. Then T_* is an automorphism of $\pi_1(\bar{V} \setminus \bar{L}, \vec{d})$. Therefore the following diagram commutes:

$$\begin{array}{ccc}
 \pi_1(B^3 \setminus C, d) & \xrightarrow{i} & \pi_1(\overline{V} \setminus \overline{L}, \overline{d}) \\
 \tilde{\beta} \downarrow & & \downarrow T_* \\
 \pi_1(B^3 \setminus C, d) & \xrightarrow{i} & \pi_1(\overline{V} \setminus \overline{L}, \overline{d})
 \end{array}$$

where $\tilde{\beta}$ is the automorphism induced by the restriction of α_0 to $B^3 \setminus C$. The isomorphism between rB_n and $MCG(B^3, C^*)$ allows us to send the ribbon braid β , represented by b , to the isotopy class of α_0 .

Identifying $\pi_1(B^3 \setminus C, d)$ with the free group F_n with generators x_1, x_2, \dots, x_n , we conclude that the automorphism $\tilde{\beta}$ is equal to $\nu(b)$, where $\nu: rB_n \rightarrow PC_n$ is the isomorphism between the group of ribbon braids rB_n and PC_n , the subgroup of $\text{Aut}(F_n)$ generated by the automorphisms of the form $\alpha: x_i \mapsto w_i^{-1} x_{\pi(i)}^{\pm 1} w_i$ where π is a permutation and w_i is a word in F_n . Then it is the automorphism of F_n corresponding to β , the ribbon braid represented by b . Thus $i^{-1}T_*i = \tilde{\beta}$.

Suppose now that $\beta, \beta' \in rB_n$ are two ribbon braids with isotopic closures in V , and that b and $b' \subset B^4 = B^3 \times I$ are two geometric ribbon braids that represent them. Let L and $L' \subset V = B^3 \times S^1$ be their respective closures.

Then there is a homeomorphism $g: V \rightarrow V$ such that g maps L onto L' , preserving their canonical orientation along the annuli, but possibly reversing the orientation of the circles at some instant (for example when Reidemeister moves of type I occur). Note that a Reidemeister move of type I is isotopic to the composition of two wens [1, Corollary 3.3], so globally the orientation of the circles at the starting and ending time parameter is preserved. In fact the orientation of the ambient V is preserved by g , but when considering a section $B^3 \times \{t\}$ the orientation of the circles can be concordant or not concordant with the one induced by V . In addition the restriction of g to ∂V is isotopic to the identity id_V . This fact, plus the isomorphism of the map induced by the inclusion $\pi_1(\partial V) = \pi_1(S^2 \times S^1) \rightarrow \pi_1(V) = \pi_1(B^3 \times S^1) \cong \mathbb{Z}$ implies that g induces an identity automorphism of $\pi_1(V)$. Therefore g lifts to a homeomorphism $\bar{g}: \overline{V} \rightarrow \overline{V}$ such that \bar{g} is isotopic to the identity on $\partial \overline{V}$, $\bar{g}T = T\bar{g}$, and $\bar{g}(\overline{L}) = \overline{L}'$.

Hence \bar{g} induces an isomorphism

$$\bar{g}_*: \pi_1(\overline{V} \setminus \overline{L}, \overline{d}) \longrightarrow \pi_1(\overline{V} \setminus \overline{L}', \overline{d})$$

commuting with T_* . The following diagram commutes:

$$\begin{array}{ccc}
 \pi_1(B^3 \setminus C, d) & \xrightarrow{i} & \pi_1(\overline{V} \setminus \overline{L}, \overline{d}) \\
 \varphi \downarrow & & \downarrow \bar{g}_* \\
 \pi_1(B^3 \setminus C, d) & \xrightarrow{i'} & \pi_1(\overline{V} \setminus \overline{L}', \overline{d}).
 \end{array}$$

Consider the automorphism $\varphi = (i')^{-1}\bar{g}_*i$ of $F_n = \pi_1(B^3 \setminus C, d)$, where:

$$i : \pi_1(B^3 \setminus C, d) \longrightarrow \pi_1(\overline{V} \setminus \overline{L}, \overline{d}) \text{ and}$$

$$i' : \pi_1(B^3 \setminus C, d) \longrightarrow \pi_1(\overline{V} \setminus \overline{L}', \overline{d})$$

are the inclusion isomorphisms.

Applying the same arguments to β' , we have $\tilde{\beta}' = (i')^{-1}T_*i'$, and from the preceding commutative diagram we have:

$$\varphi\tilde{\beta}\varphi^{-1} = ((i')^{-1}\overline{g}_*i) (i^{-1}T_*i) (i^{-1}\overline{g}_*^{-1}i') = (i')^{-1}T_*i' = \tilde{\beta}'$$

We claim that φ is an element of the subgroup of $\text{Aut}(F_n)$ consisting of all automorphisms of the form $x_i \mapsto q_i x_{j(i)}^{\pm 1} q_i^{-1}$, where $i = 1, \dots, n$, $j(i)$ is some permutation of the numbers $1, \dots, n$, and q_i a word in x_1, \dots, x_n . Then the isomorphism between this subgroup and rB_n implies that β and β' are conjugate in rB_n .

We prove this claim. The conjugacy classes of the generators x_1, x_2, \dots, x_n in $F_n = \pi_1(B^3 \setminus C, d)$ are represented by loops encircling the circles C_i . The inclusion $B^3 \setminus C = (B^3 \setminus C) \times \{0\} \subset \overline{V} \setminus \overline{L}$ maps these loops to some loops in $\overline{V} \setminus \overline{L}$ encircling at each parameter t the rings that form the components of \overline{L} . The homeomorphism $\overline{g}: \overline{V} \rightarrow \overline{V}$ transforms these loops into loops in $\overline{V} \setminus \overline{L}'$ encircling the components of \overline{L}' . The latter represent the conjugacy classes of the images of x_1, \dots, x_n under the inclusion $B^3 \setminus C = (B^3 \setminus C) \times \{0\} \subset \overline{V} \setminus \overline{L}'$.

The automorphism φ transforms the conjugacy classes of x_1, \dots, x_n into themselves, up to permutation and orientation changes. This verifies the condition. The possible orientation changes are due to the fact that the isotopy of closed braid is not monotone with respect to the time parameter as ribbon braid isotopy is, thus Reidemeister moves of type I can occur. □

When one ribbon braid is a conjugate of another ribbon braid, we can describe the form of the conjugating element.

Lemma 2 *Let $n \geq 1$ and $\beta, \beta' \in rB_n$ a pair of ribbon braids. They are conjugates in rB_n if and only if $\beta' = \pi_\tau \alpha \beta \alpha^{-1} \pi_\tau^{-1}$, where π_τ is composed only by wens and α does not contain any wen. Speaking in terms of presented group, π_τ is represented by a word in the τ_i generators of presentation (2).*

Proof Take β and β' in rB_n conjugate by another element in rB_n . Then there exists an element γ in rB_n such that $\beta = \gamma\beta'\gamma^{-1}$. Consider γ as an element of the configuration space of n circles R_n . We can use relations from presentation (2) to push to the right of the word the generators τ_i , to obtain an equivalent element $\gamma' = \pi_\tau \alpha$, where π_τ is a word in the τ_i s and α only contains generators σ_i and ρ_i . This means that α is in fact an element that can be written without τ generators. Finally, when considering γ^{-1} for the conjugacy, we remark that π_τ^{-1} is just the mirror image word of π_τ . □

5 Ideas for Further Developments

To extend the result in \mathbb{R}^4 we shall prove the invariance of isotopy classes of closed ribbon braids under the operation known as stabilisation. The approaches used for usual knotted objects, for instance those of [4, 24], rely on the bijection given by Reidemeister theorem between knots and knot diagrams up to Reidemeister moves. We do not have such a result for ribbon torus-links. In fact, as Proposition 3 points out, the injectivity of the map *Tube* between extended welded links and ribbon torus-links is an open question. When applied to welded links (not extended), we know that the *Tube* map is not injective: for instance, it is invariant under the *horizontal mirror image* on welded diagrams ([12, Proposition 3.3], see also [22, 26]), while welded links in general are not equivalent to their horizontal mirror images. However, extended welded links *are* equivalent to their horizontal mirror image ([7, Proposition 5.1]). This fact suggest they could be good candidates to be in bijection with ribbon torus-links. Of course, other obstructions to injectivity may exist, so the relation between extended welded links and ribbon torus-links shall be investigated. It is worth noticing that an alternative approach to solve the problem of establishing a bijection between welded diagrams and ribbon torus-links has been suggested by Kawauchi in [19, Problem, Sect. 2].

Acknowledgements During the writing of this paper, the author was supported by a JSPS Post-doctoral Fellowship For Foreign Researchers and by JSPS KAKENHI Grant Number 16F16793. The author thanks Emmanuel Wagner for valuable conversations.

References

1. B. Audoux, On the welded tube map, *Knot Theory and Its Applications*. Contemporary Mathematics, vol. 670 (American Mathematical Society, Providence, 2016), pp. 261–284
2. J.C. Baez, D.K. Wise, A.S. Crans, Exotic statistics for strings in 4D *BF* theory. *Adv. Theor. Math. Phys.* **11**(5), 707–749 (2007)
3. D. Bar-Natan, Z. Dancso, Finite-type invariants of w-knotted objects, I: w-knots and the Alexander polynomial. *Algebr. Geom. Topol.* **16**(2), 1063–1133 (2016)
4. J.S. Birman, *Braids, Links, and Mapping Class Groups*. Annals of Mathematics Studies, vol. 82 (Princeton University Press, Princeton; University of Tokyo Press, Tokyo, 1974)
5. T.E. Brendle, A. Hatcher, Configuration spaces of rings and wickets. *Comment. Math. Helv.* **88**(1), 131–162 (2013)
6. D.M. Dahm, A generalisation of braid theory. Ph.D. thesis, Princeton University (1962)
7. C. Damiani, A Markov's theorem for extended welded braids and links (2017). [arXiv:1705.05580](https://arxiv.org/abs/1705.05580). To appear in *Osaka J. Math*
8. C. Damiani, A journey through loop braid groups. *Expo. Math.* **35**(3), 252–285 (2017)
9. R. Fenn, R. Rimányi, C. Rourke, The braid-permutation group. *Topology* **36**(1), 123–135 (1997)
10. R.H. Fox, Characterizations of slices and ribbons. *Osaka J. Math.* **10**, 69–76 (1973)
11. D.L. Goldsmith, The theory of motion groups. *Mich. Math. J.* **28**(1), 3–17 (1981)
12. A. Ichimori, T. Kanenobu, Ribbon torus knots presented by virtual knots with up to four crossings. *J. Knot Theory Ramif.* **21**(13), 1240005, 30 (2012)

13. S. Kamada, *Braid and Knot Theory in Dimension Four*. Mathematical Surveys and Monographs, vol. 95 (American Mathematical Society, Providence, 2002)
14. S. Kamada, Braid presentation of virtual knots and welded knots. *Osaka J. Math.* **44**(2), 441–458 (2007)
15. T. Kanenobu, A. Shima, Two filtrations of ribbon 2-knots, in *Proceedings of the First Joint Japan-Mexico Meeting in Topology (Morelia, 1999)*, vol. 121 (2002), pp. 143–168
16. C. Kassel, V. Turaev, *Braid Groups*. Graduate Texts in Mathematics, vol. 247 (Springer, New York, 2008). With the graphical assistance of O. Dodane
17. L.H. Kauffman, S. Lambropoulou, Virtual braids and the L -move. *J. Knot Theory Ramif.* **15**(6), 773–811 (2006)
18. A. Kawauchi, *A Survey of Knot Theory* (Birkhäuser Verlag, Basel, 1996). Translated and revised from the 1990 Japanese original by the author
19. A. Kawauchi, A chord graph constructed from a ribbon surface-link, *Knots, Links, Spatial Graphs, and Algebraic Invariants*. Contemporary Mathematics, vol. 689 (American Mathematical Society, Providence, 2017), pp. 125–136
20. J.L. Kelley, *General Topology*. Graduate Texts in Mathematics, vol. 27 (Springer, New York, 1975). Reprint of the 1955 edition [Van Nostrand, Toronto]
21. X.-S. Lin, The motion group of the unlink and its representations, in *Topology and Physics: Proceedings of the Nankai International Conference in Memory of Xiao-Song Lin, Tianjin, China, 27–31 July 2007*. Nankai Tracts in Mathematics, vol. 12 (World Scientific Publishing, Hackensack, 2008), pp. 359–417
22. S. Satoh, Virtual knot presentation of ribbon torus-knots. *J. Knot Theory Ramif.* **9**(4), 531–542 (2000)
23. A.G. Savushkina, On the group of conjugating automorphisms of a free group. *Math. Notes* **60**(1), 68–80 (1996)
24. P. Traczyk, A new proof of Markov’s braid theorem, *Knot Theory (Warsaw, 1995)*, vol. 42 (Banach Center Publications, Polish Academy of Sciences, Warsaw, 1998)
25. F. Wattenberg, Differentiable motions of unknotted, unlinked circles in 3-space. *Math. Scand.* **30**, 107–135 (1972)
26. B. Winter, The classification of spun torus knots. *J. Knot Theory Ramif.* **18**(9), 1287–1298 (2009)
27. T. Yajima, On the fundamental groups of knotted 2-manifolds in the 4-space. *J. Math. Osaka City Univ.* **13**, 63–71 (1962)

An Alternative Basis for the Kauffman Bracket Skein Module of the Solid Torus via Braids



Ioannis Diamantis

Abstract In this paper we give an alternative basis, \mathcal{B}_{ST} , for the Kauffman bracket skein module of the solid torus, KBSM (ST). The basis \mathcal{B}_{ST} is obtained with the use of the Temperley–Lieb algebra of type B and it is appropriate for computing the Kauffman bracket skein module of the lens spaces $L(p, q)$ via braids.

Keywords Kauffman bracket polynomial · Skein modules · Solid torus · Temperley–Lieb algebra of type B · Mixed links · Mixed braids · Lens spaces

2010 Mathematics Subject Classification 57M27 · 57M25 · 20F36 · 20F38 · 20C08

1 Introduction and Overview

Skein modules were independently introduced by Przytycki [15] and Turaev [16] as generalizations of knot polynomials in S^3 to knot polynomials in arbitrary 3-manifolds. The essence is that skein modules are quotients of free modules over ambient isotopy classes of links in 3-manifolds by properly chosen local (skein) relations.

Definition 1 Let M be an oriented 3-manifold and \mathcal{L}_{fr} be the set of isotopy classes of unoriented framed links in M . Let $R = \mathbb{Z}[A^{\pm 1}]$ be the Laurent polynomials in A and let $R\mathcal{L}_{fr}$ be the free R -module generated by \mathcal{L}_{fr} . Let \mathcal{S} be the ideal generated by the skein expressions $L - AL_{\infty} - A^{-1}L_0$ and $L \sqcup \bigcirc - (-A^2 - A^{-2})L$, where L_{∞} and L_0 are represented schematically by the illustrations in Fig. 1. Note that blackboard framing is assumed.

I. Diamantis (✉)

International College Beijing, China Agricultural University,
No.17 Qinghua East Road, Haidian District, Beijing 100083,
People's Republic of China
e-mail: ioannis.diamantis@hotmail.com

© Springer Nature Switzerland AG 2019

C. C. Adams et al. (eds.), *Knots, Low-Dimensional Topology and Applications*, Springer Proceedings in Mathematics & Statistics 284, https://doi.org/10.1007/978-3-030-16031-9_16

329

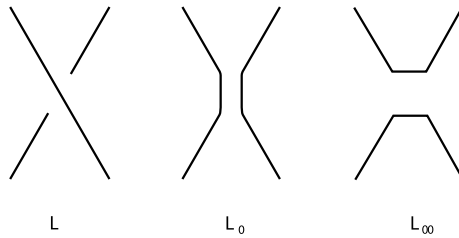


Fig. 1 The links L , L_0 and L_{∞} locally

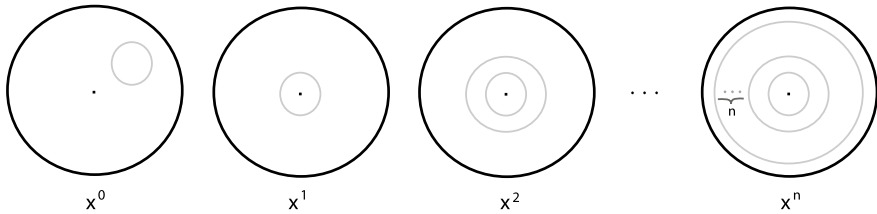


Fig. 2 The Turaev basis of $\text{KBSM}(ST)$

Then the *Kauffman bracket skein module* of M , $\text{KBSM}(M)$, is defined to be:

$$\text{KBSM}(M) = R\mathcal{L}/S.$$

□

In [16] the Kauffman bracket skein module of the solid torus, ST , is computed using diagrammatic methods by means of the following theorem:

Theorem 1 ([16]) *The Kauffman bracket skein module of ST , $\text{KBSM}(ST)$, is freely generated by an infinite set of generators $\{x^n\}_{n=0}^{\infty}$, where x^n denotes a parallel copy of n longitudes of ST and x^0 is the affine unknot (see Fig. 2).* □

In [11] the most generic analogue of the HOMFLYPT polynomial, X , for links in the solid torus ST has been derived from the generalized Hecke algebras of type B , $H_{1,n}$, which is related to the knot theory of the solid torus and the Artin group of Coxeter group of type B , $B_{1,n}$, via a unique Markov trace constructed on them. As explained in [3, 12], the Lambropoulou invariant X recovers the HOMFLYPT skein module of ST , $\mathcal{S}(ST)$, and is appropriate for extending the results to the lens spaces $L(p, q)$, since the combinatorial setting is the same as for ST , only the braid equivalence includes the braid band moves (abbreviated to *bbm*), which reflect the surgery description of $L(p, q)$. In [8] the same procedure is applied for the case of Temperley–Lieb algebras of type B and an invariant V^B for knots and links in ST is constructed, via a unique Markov trace constructed on them, and which is the analogue of the Kauffman bracket polynomial for knots and links in ST .

In this paper the Kauffman bracket skein module of ST, $KBSM(ST)$, is computed using braids and algebraic techniques developed in [2, 3, 5–8, 11–14]. The motivation of this work is the computation of $KBSM(L(p, q))$ via algebraic means. The new basic set is described in Eq. 1 in terms of mixed braids (that is, classical braids with the first strand identically fixed). For an illustration see bottom part of Fig. 5.

Our main result is the following:

Theorem 2 *The following set forms a basis for $KBSM(ST)$:*

$$\mathcal{B}_{ST} = \{t^n, n \in \mathbb{N}\}. \tag{1}$$

The method for obtaining the basis \mathcal{B}_{ST} , is the following:

- We start from elements in the standard basis of $KBSM(ST)$, \mathcal{B}'_{ST} , presented in [16]. Then, following the technique in [3], we express these elements into sums of elements in Λ , using conjugation and stabilization moves. As shown in [3], the set Λ (see Remark 3) forms a basis for the HOMFLYPT skein module of the solid torus.
- We then express elements in Λ as sums of elements in \mathcal{B}_{ST} , using conjugation, stabilization moves and the Kauffman bracket skein relation.
- We relate the two sets \mathcal{B}'_{ST} and \mathcal{B}_{ST} via an infinite lower triangular matrix and conclude that the set \mathcal{B}_{ST} forms a basis for $KBSM(ST)$.

It is worth mentioning that in [9], Theorem 2 was obtained via diagrammatic methods.

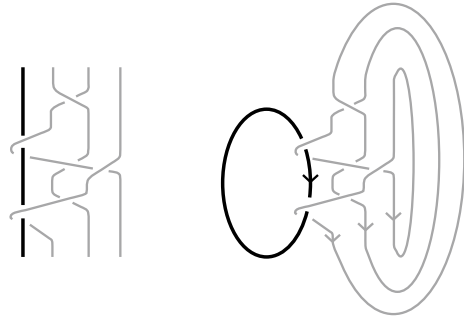
The paper is organized as follows: In Sect. 2 we recall the setting and the essential techniques and results from [2, 11–14]. More precisely, we present isotopy moves for knots and links in ST and we then describe braid equivalence for knots and links in ST. We also present results from [8, 12] and in particular we present the basis of the Kauffman bracket skein module of ST in terms of braids and braid groups of type B. In Sect. 3 we present results from [3] that are crucial for this paper, and using these results, in Sect. 3.4 we present a new basis for the Kauffman bracket skein module of the solid torus ST, \mathcal{B}_{ST} . As explained in the beginning of Sect. 3, the importance of the basis \mathcal{B}_{ST} lies in the fact that the *braid band moves* or *slide moves* (that reflect isotopy in the lens spaces $L(p, q)$) are naturally described via \mathcal{B}_{ST} . Finally in [1] and starting from \mathcal{B}_{ST} , the computation of the Kauffman bracket skein module of the lens spaces is presented.

2 Preliminaries

2.1 Mixed Links and Isotopy in ST

We consider ST to be the complement of a solid torus in S^3 . As explained in [2, 13, 14], an oriented link L in ST can be represented by an oriented *mixed link* in S^3 , that is a link in S^3 consisting of the unknotted fixed part \widehat{T} representing the complementary

Fig. 3 The closure of a mixed braid to a mixed link



solid torus in S^3 and the moving part L that links with \widehat{T} . A *mixed link diagram* is a diagram $\widehat{T} \cup \widetilde{L}$ of $\widehat{T} \cup L$ on the plane of \widehat{T} , where this plane is equipped with the top-to-bottom direction of I (see right hand side of Fig. 3).

Consider now an isotopy of an oriented link L in ST. As the link moves in ST, its corresponding mixed link will change in S^3 by a sequence of moves that keep the oriented \widehat{T} point-wise fixed. This sequence of moves consists in isotopy in the S^3 and the *mixed Reidemeister moves*. In terms of diagrams we have the following result for isotopy in ST:

The mixed link equivalence in S^3 includes the classical Reidemeister moves and the mixed Reidemeister moves, which involve the fixed and the standard part of the mixed link, keeping \widehat{T} pointwise fixed.

2.2 Mixed Braids and Braid Equivalence for Knots and Links in ST

By the Alexander theorem for knots and links in the solid torus (cf. Thm. 1 [11]), a mixed link diagram $\widehat{T} \cup \widetilde{L}$ of $\widehat{T} \cup L$ may be turned into a *mixed braid* $I \cup \beta$ with isotopic closure. This is a braid in S^3 where, without loss of generality, its first strand represents \widehat{T} , the fixed part, and the other strands, β , represent the moving part L . The subbraid β is called the *moving part* of $I \cup \beta$ (see left hand side of Fig. 3).

The sets of braids related to ST form groups, which are in fact the Artin braid groups of type B, denoted $B_{1,n}$, with presentation:

$$B_{1,n} = \left\langle t, \sigma_1, \dots, \sigma_{n-1} \left| \begin{array}{l} \sigma_1 t \sigma_1 t = t \sigma_1 t \sigma_1 \\ t \sigma_i = \sigma_i t, \quad i > 1 \\ \sigma_i \sigma_{i+1} \sigma_i = \sigma_{i+1} \sigma_i \sigma_{i+1}, \quad 1 \leq i \leq n - 2 \\ \sigma_i \sigma_j = \sigma_j \sigma_i, \quad |i - j| > 1 \end{array} \right. \right\rangle,$$

where the generators σ_i and t are illustrated in Fig. 4i (see also [11] and references therein).

Let now \mathcal{L} denote the set of oriented knots and links in ST. Then, isotopy in ST is translated on the level of mixed braids by means of the following theorem:

Theorem 3 (Theorem 3, [11]) *Let L_1, L_2 be two oriented links in ST and let $I \cup \beta_1, I \cup \beta_2$ be two corresponding mixed braids in S^3 . Then L_1 is isotopic to L_2 in ST if and only if $I \cup \beta_1$ is equivalent to $I \cup \beta_2$ in \mathcal{B} by the following moves:*

- (i) *Conjugation* : $\alpha \sim \beta^{-1}\alpha\beta, \quad \text{if } \alpha, \beta \in B_{1,n}.$
- (ii) *Stabilization moves* : $\alpha \sim \alpha\sigma_n^{\pm 1} \in B_{1,n+1}, \text{ if } \alpha \in B_{1,n}.$

2.3 The Kauffman Bracket Skein Module of ST via Braids

In [12] the most generic analogue of the HOMFLYPT polynomial, X , for links in the solid torus ST has been derived from the generalized Iwahori–Hecke algebras of type B, $H_{1,n}$, via a unique Markov trace constructed on them. This algebra was defined by Lambropoulou as the quotient of $\mathbb{C}[q^{\pm 1}]B_{1,n}$ over the quadratic relations $g_i^2 = (q - 1)g_i + q$. Namely:

$$H_{1,n}(q) = \frac{\mathbb{C}[q^{\pm 1}]B_{1,n}}{\langle \sigma_i^2 - (q - 1)\sigma_i - q \rangle}.$$

It is also shown that the following sets form linear bases for $H_{1,n}(q)$ ([12, Proposition 1 & Theorem 1]):

- (i) $\Sigma_n = \{t_{i_1}^{k_1} \dots t_{i_r}^{k_r} \cdot \sigma\}$, where $0 \leq i_1 < \dots < i_r \leq n - 1$,
- (ii) $\Sigma'_n = \{t'_{i_1}{}^{k_1} \dots t'_{i_r}{}^{k_r} \cdot \sigma\}$, where $0 \leq i_1 < \dots < i_r \leq n - 1$,

where $k_1, \dots, k_r \in \mathbb{Z}, t'_0 = t_0 := t, t'_i = g_i \dots g_1 t g_1^{-1} \dots g_i^{-1}$ and $t_i = g_i \dots g_1 t g_1 \dots g_i$ are the ‘looping elements’ in $H_{1,n}(q)$ (see Fig. 4ii) and σ a basic element in the Iwahori–Hecke algebra of type A, $H_n(q)$, for example in the form of the elements in the set [10]:

$$S_n = \{(g_{i_1} g_{i_1-1} \dots g_{i_1-k_1})(g_{i_2} g_{i_2-1} \dots g_{i_2-k_2}) \dots (g_{i_p} g_{i_p-1} \dots g_{i_p-k_p})\},$$

for $1 \leq i_1 < \dots < i_p \leq n - 1$. In [12] the bases Σ'_n are used for constructing a Markov trace on $\mathcal{H} := \bigcup_{n=1}^{\infty} H_{1,n}$, and using this trace, a universal HOMFLYPT-type invariant for oriented links in ST is constructed.

Theorem 4 ([12, Theorem 6 and Definition 1]) *Given z, s_k with $k \in \mathbb{Z}$ specified elements in $R = \mathbb{C}[q^{\pm 1}]$, there exists a unique linear Markov trace function on \mathcal{H} :*

$$\text{tr} : \mathcal{H} \rightarrow R(z, s_k), \quad k \in \mathbb{Z}$$

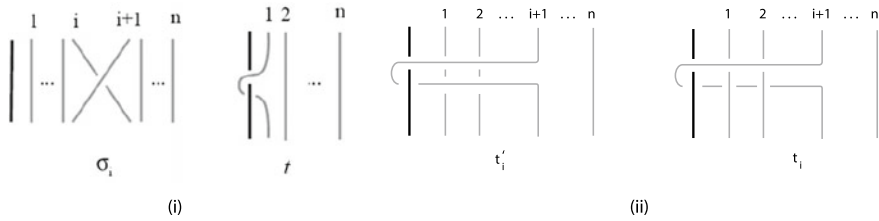


Fig. 4 The generators of $B_{1,n}$ and the ‘looping’ elements t_i' and t_i

determined by the rules:

- (1) $\text{tr}(ab) = \text{tr}(ba)$ for $a, b \in H_{1,n}(q)$
- (2) $\text{tr}(1) = 1$ for all $H_{1,n}(q)$
- (3) $\text{tr}(ag_n) = z\text{tr}(a)$ for $a \in H_{1,n}(q)$
- (4) $\text{tr}(at_n^k) = s_k\text{tr}(a)$ for $a \in H_{1,n}(q), k \in \mathbb{Z}$

Then, the function $X : \mathcal{L} \rightarrow R(z, s_k)$

$$X_{\widehat{\alpha}} = \Delta^{n-1} \cdot (\sqrt{\lambda})^e \text{tr}(\pi(\alpha)),$$

is an invariant of oriented links in ST, where $\Delta := -\frac{1-\lambda q}{\sqrt{\lambda}(1-q)}, \lambda := \frac{z+1-q}{qz}, \alpha \in B_{1,n}$ is a word in the σ_i 's and t_i' 's, $\widehat{\alpha}$ is the closure of α, e is the exponent sum of the σ_i 's in α, π the canonical map of $B_{1,n}$ to $H_{1,n}(q),$ such that $t \mapsto t$ and $\sigma_i \mapsto g_i.$ \square

Remark 1 As shown in [3, 12] the invariant X recovers the HOMFLYPT skein module of ST. For a survey on the HOMFLYPT skein module of the lens spaces $L(p, 1)$ via braids, the reader is referred to [4].

Following the same idea as in [12], in [8] the analogue of the normalized Kauffman bracket polynomial, $V,$ for links in the solid torus ST has been derived from the Temperley–Lieb algebra of type B, $TL_n^B.$ This algebra is defined as a quotient of the generalized Iwahori–Hecke algebra of type B, $H_{1,n}(q),$ over the ideal generated by the elements:

$$h_{1,2} := 1 + u(\sigma_1 + \sigma_2) + u^2(\sigma_1\sigma_2 + \sigma_2\sigma_1) + u^3\sigma_1\sigma_2\sigma_1,$$

$$h_B := 1 + u\sigma_1 + v t + uv(\sigma_1 t + t\sigma_1) + u^2 v\sigma_1 t\sigma_1 + uv^2 t\sigma_1 t + (uv)^2\sigma_1 t\sigma_1 t \tag{3}$$

Note that in [8] a different presentation for $H_{1,n}$ is used, that involves the parameters u, v and the quadratic equations

$$\sigma_i^2 = (u - u^{-1})\sigma_i + 1. \tag{4}$$

One can switch from one presentation to the other by a taking $\sigma_i = u\sigma_i, t = vt$ and $q = u^2$.

Since the Temperley–Lieb algebra of type B is a quotient of the Iwahori–Hecke algebra of type B, in [8] the authors present the necessary and sufficient conditions so that the Markov trace factors through to TL_n^B . Indeed:

Theorem 5 ([8, Theorem 4]) *The trace defined in $H_n(1, q)$ factors through to TL_n^B if and only if the trace parameters take the following values:*

$$z = -\frac{1}{u(1 + u^2)}, \quad s_1 = \frac{-1 + v^2}{(1 + u^2)v}. \tag{5}$$

It is worth mentioning that in [8] more values of the trace parameters that allow the trace to factor through to TL_n^B are presented, but as explained in [8], only the values in (5) are of topological interest. Moreover, for those values of the parameters one deduces $\lambda = u^4$. We have the following:

Theorem 6 ([8]) *The following is an invariant for knots and links in ST:*

$$V_{\widehat{\alpha}}^B(u, v) := \left(-\frac{1 + u^2}{u}\right)^{n-1} (u)^{2e} \text{tr}(\overline{\pi}(\alpha)),$$

where $\alpha \in B_{1,n}$ is a word in the σ_i 's and t_i 's, $\widehat{\alpha}$ is the closure of α , e is the exponent sum of the σ_i 's in α , $\overline{\pi}$ the canonical map of $B_{1,n}$ to TL_n^B , such that $t \mapsto t$ and $\sigma_i \mapsto g_i$. □

In the braid setting of [12], the elements of $KBSM(ST)$ correspond bijectively to the elements of the following set:

$$\mathcal{B}'_{ST} = \{tt'_1 \dots t'_n, n \in \mathbb{N}\}. \tag{6}$$

The set \mathcal{B}'_{ST} forms a basis of $KBSM(ST)$ in terms of braids (see also [16]) (Fig. 5). Note that \mathcal{B}'_{ST} is a subset of \mathcal{H} and, in particular, \mathcal{B}'_{ST} is a subset of $\Sigma' = \bigcup_n \Sigma'_n$. Note also that in contrast to elements in Σ' , the elements in \mathcal{B}'_{ST} have no gaps in the indices, the exponents are all equal to one and there are no ‘braiding tails’.

Remark 2 The invariant V^B recovers $KBSM(ST)$. Indeed, it gives distinct values to distinct elements of \mathcal{B}'_{ST} , since $\text{tr}(tt'_1 \dots t'_n) = s_1^n$.

3 The Basis \mathcal{B}_{ST} of $KBSM(ST)$

In this section we prove the main result of this paper, Theorem 2. Before proceeding with the proof we present the motivation that lead to the new basis \mathcal{B}_{ST} of $KBSM(ST)$:

The relation between $\text{KBSM}(L(p, 1))$ and $\text{KBSM}(\text{ST})$ is presented in [15] and it is shown that:

$$\text{KBSM}(L(p, 1)) = \frac{\text{KBSM}(\text{ST})}{\langle a - \text{bbm}(a) \rangle}, \quad a \text{ in the basis of } \text{KBSM}(\text{ST}).$$

In order to extend V^B to an invariant of links in $L(p, q)$ we need to solve an infinite system of equations resulting from the braid band moves. Namely we force:

$$V_{\alpha}^B = V_{\widehat{\text{bbm}(\alpha)}}^B, \tag{7}$$

for all α in the basis of $\text{KBSM}(\text{ST})$.

The above equations have particularly simple formulations with the use of the new basis, \mathcal{B}_{ST} , for the Kauffman bracket skein module of ST . This is a very technical and difficult task and is the subject of a sequel paper.

We now recall results from [3] that we will use throughout the paper.

3.1 An Ordering in the Bases of $\mathcal{S}(\text{ST})$

In [3] an ordering relation is defined on the sets Σ and Σ' which plays a crucial role in this paper. Before presenting this ordering relation, we first introduce the sets Λ' and Λ and the notion of the *index* of a word w , denoted $\text{ind}(w)$, in any of these sets.

Definition 2 We define the following subsets of Σ_n and Σ' respectively:

$$\begin{aligned} \Lambda_{(k)} &:= \{t_0^{k_0} t_1^{k_1} \dots t_m^{k_m} \mid k_i \geq k_{i+1}, \sum_{i=0}^m k_i = k, k_i \in \mathbb{Z} \setminus \{0\}, \forall i\}, \\ \Lambda'_{(k)} &:= \{t_0'^{k_0} t_1'^{k_1} \dots t_m'^{k_m} \mid k_i \geq k_{i+1}, \sum_{i=0}^m k_i = k, k_i \in \mathbb{Z} \setminus \{0\}, \forall i\}, \\ \Lambda_{(k)}^{aug} &:= \{t_0^{k_0} t_1^{k_1} \dots t_m^{k_m} \mid \sum_{i=0}^m k_i = k, k_i \in \mathbb{Z} \setminus \{0\}, \forall i\}, \\ \Lambda'_{(k)}{}^{aug} &:= \{t_0'^{k_0} t_1'^{k_1} \dots t_m'^{k_m} \mid \sum_{i=0}^m k_i = k, k_i \in \mathbb{Z} \setminus \{0\}, \forall i\}. \end{aligned} \tag{8}$$

Note that elements in the set $\Lambda_{(k)}$ have ordered exponents, while elements in $\Lambda_{(k)}^{aug}$ have arbitrary exponents. Obviously, $\Lambda_{(k)} \subset \Lambda_{(k)}^{aug} \subset \Sigma_n$.

Remark 3 In [3] the set $\Lambda := \bigcup_k \Lambda_{(k)}$ is showed to be a basis for the HOMFLYPT skein module of ST .

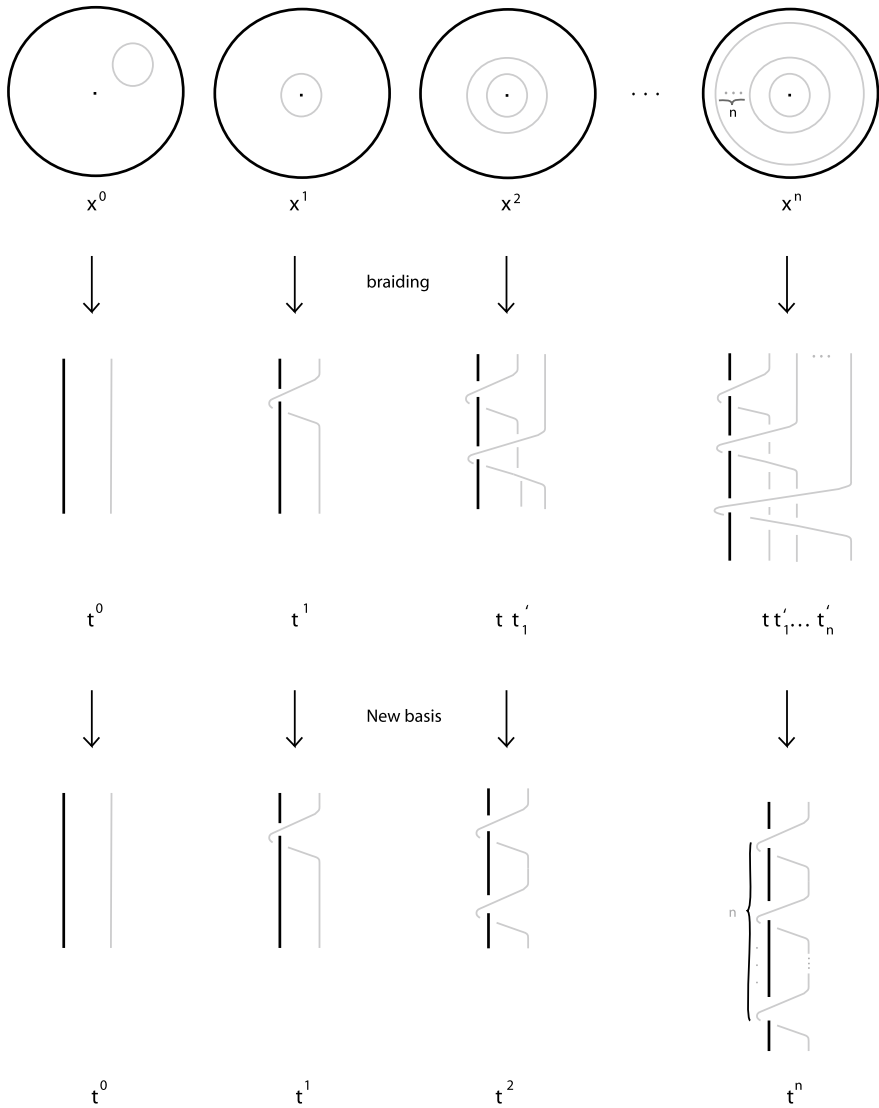


Fig. 5 Elements in the different bases of KBSM(ST)

Definition 3 ([3, Definition 1]) Let w be a word in Λ . Then, the index of w , $ind(w)$, is defined to be the highest index of the t_i 's in w . Similarly, in Σ' or Σ , $ind(w)$ is defined as above by ignoring possible gaps in the indices of the looping generators and by ignoring the braiding parts in the algebras $H_n(q)$. Moreover, the index of a monomial in $H_n(q)$ is equal to 0. \square

We now proceed with presenting an ordering relation in the sets Σ and Σ' , which passes to their respective subsets \mathcal{B}_{ST} and \mathcal{B}'_{ST} .

Definition 4 ([3, Definition 2]) Let $w = t'_{i_1}{}^{k_1} \dots t'_{i_\mu}{}^{k_\mu} \cdot \beta_1$ and $u = t'_{j_1}{}^{\lambda_1} \dots t'_{j_\nu}{}^{\lambda_\nu} \cdot \beta_2$ in Σ' , where $k_t, \lambda_s \in \mathbb{Z}$ for all t, s and $\beta_1, \beta_2 \in H_n(q)$. Then, we define the following ordering in Σ' :

- (a) If $\sum_{i=0}^\mu k_i < \sum_{i=0}^\nu \lambda_i$, then $w < u$.
- (b) If $\sum_{i=0}^\mu k_i = \sum_{i=0}^\nu \lambda_i$, then:
 - (i) if $ind(w) < ind(u)$, then $w < u$,
 - (ii) if $ind(w) = ind(u)$, then:
 - (α) if $i_1 = j_1, \dots, i_{s-1} = j_{s-1}, i_s < j_s$, then $w > u$,
 - (β) if $i_t = j_t$ for all t and $k_\mu = \lambda_\mu, k_{\mu-1} = \lambda_{\mu-1}, \dots, k_{i+1} = \lambda_{i+1}, |k_i| < |\lambda_i|$, then $w < u$,
 - (γ) if $i_t = j_t$ for all t and $k_\mu = \lambda_\mu, k_{\mu-1} = \lambda_{\mu-1}, \dots, k_{i+1} = \lambda_{i+1}, |k_i| = |\lambda_i|$ and $k_i > \lambda_i$, then $w < u$,
 - (δ) if $i_t = j_t \forall t$ and $k_i = \lambda_i, \forall i$, then $w = u$.

The ordering in the set Σ is defined as in Σ' , where t'_i 's are replaced by t_i 's. \square

3.2 From \mathcal{B}'_{ST} to Λ

In this subsection we recall a series of results from [3] in order to convert elements in \mathcal{B}'_{ST} to elements in Λ . In order to simplify the algebraic expressions obtained throughout this procedure and throughout the paper in general, we first introduce the following notation:

Notation 1 We set $\tau_{i,i+m}^{k_i, i+m} := t_i^{k_i} \dots t_{i+m}^{k_{i+m}} \in \Sigma$ and $\tau'_{i,i+m}{}^{k_i, i+m} := t'_i{}^{k_i} \dots t'_{i+m}{}^{k_{i+m}} \in \Sigma'$, for $m \in \mathbb{N}, k_j \neq 0$ for all j . \square

Remark 4 Using Notation 1, elements in \mathcal{B}'_{ST} are of the form $\tau'_{0,n} := tt'_1 \dots t'_n$, for $n \in \mathbb{N}$, that is $\mathcal{B}'_{ST} = \{\tau'_{0,n}\}_{n=0}^\infty$. Moreover, we set $\mathcal{K}_{ST} = \{\tau_{0,n}\}_{n=0}^\infty$, and so elements in \mathcal{K}_{ST} are of the form $\tau_{0,n} := tt_1 \dots t_n$, for $n \in \mathbb{N}$.

Moreover,

$$\Lambda'_{(k)} = \left\{ \tau'_{0,n}{}^{k_{0,n}} \mid k_i \geq k_{i-1}, \sum_{i=0}^n k_i = k, k_i \in \mathbb{Z} \setminus \{0\} \right\}, \Lambda' = \bigoplus_{k \in \mathbb{Z}} \Lambda'_{(k)}$$

$$\Lambda_{(k)} = \left\{ \tau_{0,n}{}^{k_{0,n}} \mid k_i \geq k_{i-1}, \sum_{i=0}^n k_i = k, k_i \in \mathbb{Z} \setminus \{0\} \right\}, \Lambda = \bigoplus_{k \in \mathbb{Z}} \Lambda_{(k)}$$

We also introduce the notion of *homologous words*, which is crucial for relating the sets \mathcal{B}'_{ST} and \mathcal{K}_{ST} via a triangular matrix.

Definition 5 ([3, Definition 4]) We say that two words $w' \in \Sigma'$ and $w \in \Sigma$ are *homologous*, denoted $w' \sim w$, if w is obtained from w' by changing t'_i into t_i for all i and ignoring the braiding parts. □

We now recall a result from [3] in order to convert monomials in the t'_i 's in general to monomials in the t_i 's in Σ_n . More precisely:

Theorem 7 ([3, Theorem 7]) *The following relations hold:*

$$\tau'^{k_{0,n}}_{0,n} = \tau^{k_{0,n}}_{0,n} + A \cdot \tau_{0,n} \cdot w + \sum_j B_j \tau_j \cdot \beta_j,$$

where $w, \beta_j \in H_{n+1}(q), \forall j, \tau_j \in \Sigma_n$, such that $\tau_j < \tau_{0,n}, \forall j$ and A, B_j coefficients. □

Since now we are only interested in converting elements in the set \mathcal{B}'_{ST} to sums of monomials in the t_i 's, we have the following corollary:

Corollary 1 *The following relations hold:*

$$\tau'_{0,n} = \tau_{0,n} + A \cdot \tau_{0,n} \cdot w + \sum_j B_j \tau_j \cdot \beta_j, \tag{9}$$

where $w, \beta_j \in H_{n+1}(q), \forall j, \tau_j \in \Sigma_n$, such that $\tau_j < \tau_{0,n}, \forall j$ and A, B_j coefficients.

After expressing an element $\tau'_{0,n} \in \mathcal{B}'_{ST}$ as sums of elements in Σ_n , we obtain the homologous word $\tau_{0,n}$, the homologous word again followed by a ‘braiding tail’ $w \in TL_n$ and elements in Σ_n with possible ‘gaps’ in the indices. In [3], using conjugation, monomials in the t_i 's with ‘gaps’ in the indices are expressed as sums of monomials in Λ , followed by ‘braiding tails’. For the expressions that we obtain after appropriate conjugations we shall use the notation $\hat{=}$. We recall the following result from [3]:

Theorem 8 ([3, Theorem 8]) *Let T be a monomial in the t_i 's with ‘gaps’ in the indices. The following relations hold:*

$$T \hat{=} \sum_i A_i \cdot T_i \cdot w_i, \tag{10}$$

where $T_i \in \Lambda_{(n)}$, such that $T_i < T, \forall i, w_i \in TL_{n+1}, \forall i$, and A_i coefficients. □

As shown in [3], elements in the set Λ followed by ‘braiding tails’ can be expressed as sums of elements in Λ^{aug} by using conjugation and stabilization moves. For the expressions that we obtain after appropriate conjugations and stabilization moves we shall use the notation $\hat{=}$. Indeed, we have the following:

Theorem 9 ([3, Theorem 10]) *Let $\tau \in \Lambda$ and $w \in \text{TL}_n$. Then, applying conjugation and stabilization moves, we have that:*

$$\tau \cdot w \cong \sum_j A_j \cdot \tau_j, \tag{11}$$

where $\Lambda_{(n)} \ni \tau_j < \tau$, for all j . □

Combining now Theorems 7, 8 and 9 and Corollary 1 we have that an element $\tau' \in \mathcal{B}'_{\text{ST}}$ can be expressed as a sum of the homologous word $\tau \in \mathcal{K}_{\text{ST}}$ and lower order terms in $\Lambda_{(n)}$. More precisely, we have the following:

Corollary 2 *Let $\tau'_{0,n} \in \mathcal{B}'_{\text{ST}}$. The following relations hold:*

$$\tau'_{0,n} \cong \tau_{0,n} + \sum_i A_i \cdot \tau_i, \tag{12}$$

where $\tau_i \in \Lambda$ such that $\tau_i < \tau_{0,n} \sim \tau'_{0,n}$ for all i .

From Corollary 2 we have that monomials $\tau'_{0,n} \in \mathcal{B}'_{\text{ST}}$ can be expressed as sums of their corresponding homologous word $\tau_{0,n} \in \mathcal{K}_{\text{ST}}$ with invertible coefficients, and elements $\tau_i \in \Lambda$ of lower order than $\tau_{0,n}$. The point now is that the elements τ_i do not necessarily belong to \mathcal{B}_{ST} , but using conjugation and stabilization moves, we will show that these elements can be expressed as monomials in \mathcal{B}_{ST} of lower order than $\tau_{0,n}$, and thus, \mathcal{B}_{ST} spans $\text{KBSM}(\text{ST})$. We deal with these elements in the next subsection.

3.3 From Λ to \mathcal{B}_{ST}

As explained in the Introduction, our goal is to relate the sets \mathcal{B}'_{ST} and \mathcal{B}_{ST} via an infinite block diagonal, invertible matrix. From Corollary 2 we have that an element in \mathcal{B}'_{ST} can be expressed as a sum of the homologous word in $\mathcal{K}_{\text{ST}} \subset \Lambda$ and elements in Λ of lower order. In this subsection we convert elements in Λ to sums of elements in \mathcal{B}_{ST} . We first deal with the homologous word $\tau_{0,n} \in \Lambda$ of $\tau'_{0,n} \in \mathcal{B}'_{\text{ST}}$. We have the following:

Proposition 1 *Applying conjugation, stabilization moves and relations (3), the following relations hold:*

$$\Lambda \ni \tau_{0,n} \cong A \cdot t^{\text{ind}(\tau_{0,n})+1} + \sum_{i=0}^{\text{ind}(\tau_{0,n})} A_i \cdot t^i, \tag{13}$$

where A_i coefficients in the ground ring for all i . □

Proof We prove Proposition 1 by strong induction on the order of $\tau_{0,n}$.

The base of the induction is the monomial $tt_1 \in \Lambda$ of index 1. We have that:

$$\begin{aligned} tt_1 &= t\sigma_1t\sigma_1 = \sigma_1t\sigma_1t = \\ &= -\frac{1}{(uv)^2} (1 + u\sigma_1 + vt + uv(\sigma_1t + t\sigma_1) + u^2v\sigma_1t\sigma_1 + uv^2t\sigma_1t) \cong \\ &\cong -\frac{1}{(uv)^2} (1 + uz + vt + 2uvzt + u^2vt\sigma_1^2 + uv^2t^2\sigma_1) \cong \\ &\cong -\frac{1}{(uv)^2} (1 + uz + vt + 2uvzt + u^2vt + u^2vz(u - u^{-1})t + uv^2zt^2) = \\ &= (-u^{-1}z)t^2 + \sum_{i=0}^1 A_i \cdot t^i. \end{aligned}$$

So, Proposition 1 holds for tt_1 .

Assume now that Proposition 1 holds for all monomials τ_i of lower order than $\tau_{0,n}$. Then, we have:

$$\begin{aligned} \tau_{0,n} &:= tt_1(\tau_{2,n}) = (t\sigma_1t\sigma_1)(\tau_{2,n}) = (\sigma_1t\sigma_1t)(\tau_{2,n}) = \\ &= -\frac{1}{(uv)^2} [1 + u\sigma_1 + vt + uv(\sigma_1t + t\sigma_1) + u^2v\sigma_1t\sigma_1 + uv^2t\sigma_1t] (\tau_{2,n}) \cong \\ &\cong -\frac{1}{(uv)^2} [\tau_{2,n} + u\tau_{2,n}\sigma_1 + vt\tau_{2,n} + 2uvt\tau_{2,n}\sigma_1 + u^2vt\tau_{2,n}\sigma_1^2 + uv^2t^2\tau_{2,n}\sigma_1] \cong \\ &\cong -\frac{1}{u} t^2\tau_{2,n}\sigma_1 + \sum_i A_i \cdot \tau_i, \text{ where } \tau_i < \tau, \forall i. \end{aligned}$$

According to the ordering relation, on the right hand side of this equation we have the element $t^2\tau_{2,n}\sigma_1$ and a sum of elements of lower order than $\tau_{0,n}$, since the sums of the exponents in the t_i 's in these elements are less than $n + 1$. Moreover, the monomial $t^2\tau_{2,n}\sigma_1$ contains a gap in the indices, and thus it is of lower order than $\tau_{0,n}$ (recall Definition 4). Moreover, this monomial is followed by the 'braiding tail' σ_1 . According now to Theorems 8 and 9, this element can be expressed as a sum of elements in $\Lambda_{(n)}$ of lower order than $t^2\tau_{2,n}\sigma_1$ and hence, of lower order than $\tau_{0,n}$. By the induction hypothesis the proof is now concluded. \square

We now deal with arbitrary elements in Λ and convert them to sums of elements in $\mathcal{B}(\text{ST})$. We will need the following lemmas:

Lemma 1 *The following relations hold for all $n \in \mathbb{N}$:*

$$t^n t_1 \cong -\frac{1}{u} z t^{n+1} + \sum_{i=n-1}^n A_i t^i,$$

where A_i coefficients for all i .

Proof We prove Lemma 1 by induction on n . For $n = 1$ we have: $tt_1 = -\frac{1}{u}z t^{n+1} + \sum_{i=0}^1 A_i t^i$ (relations (3)). Assume now that the relation is true for n . Then for $n + 1$ we have:

$$t^{n+1}t_1 = t \cdot (t^n t_1) \stackrel{\text{ind.}}{\cong} -\frac{1}{u}z t^{n+2} + \sum_{i=n-1}^n A_i t^{i+1} = -\frac{1}{u}z t^{n+2} + \sum_{i=n}^{n+1} A_i t^i.$$

The following lemma will serve as a basis for the induction hypothesis applied in the proof of the main result of this section.

Lemma 2 *The following relations hold for $n, m \in \mathbb{N}$:*

$$t^n t_1^m \cong A \cdot t^{n+m} + \sum_{i=0}^{n+m-1} A_i t^i,$$

where A, A_i coefficients for all i .

Proof We prove Lemma 2 by strong induction on the order of $t^n t_1^m \in \Lambda^{aug}$. The base of the induction is Lemma 1 for $n = 1$. Assume that the relations are true for all elements in Λ^{aug} of lower order than $t^n t_1^m$. Then, for $t^n t_1^m$ we have:

$$\begin{aligned} t^n t_1^m &= t^{n-1}(\underline{tt_1})t_1^{m-1} = \\ &= -\frac{1}{u^2 v^2} t^{n-1} (1 + u\sigma_1 + vt + uv(\sigma_1 t + t\sigma_1) + u^2 v\sigma_1 t\sigma_1 + uv^2 t\sigma_1 t) t_1^{m-1} \cong \\ &\cong -\frac{1}{u^2 v^2} t^{n-1} t_1^{m-1} - \frac{1}{uv^2} t^{n-1} t_1^{m-1} \sigma_1 - \frac{1}{u^2 v} t^n t_1^{m-1} - \frac{2}{uv} t^n t_1^{m-1} \sigma_1 \\ &\quad - \frac{1}{v} t^{n-1} t_1^m - \frac{1}{u} t^{n+1} t_1^{m-1} \sigma_1. \end{aligned}$$

The sum of the exponents in the elements $t^{n-1} t_1^{m-1}$, $t^n t_1^{m-1}$ and $t^{n-1} t_1^m$ on the right hand side of the relation are less than $n + m$, and thus, these elements are of lower order than $t^n t_1^m$ (recall Definition 4). Applying now Theorem 9 on the elements $t^{n-1} t_1^{m-1} \sigma_1$, $t^n t_1^{m-1} \sigma_1$ and $t^{n+1} t_1^{m-1} \sigma_1$, we convert them to sums of elements in Λ^{aug} of lower order than $t^n t_1^m$. The proof is concluded by the induction hypothesis. \square

Theorem 10 *Let $\tau \in \Lambda_{(k)}^{aug}$. The following relations hold:*

$$\tau \cong \sum_{i=0}^k A_i t^i,$$

where A_i coefficients. \square

Proof Consider a monomial $\tau = t^{k_0} t_1^{k_1} \dots t_n^{k_n} \in \Lambda^{aug}$. We prove the relations by strong induction on the order of τ . The basis of the induction is Lemma 2, since it deals with the monomials of type $t^n t_1^m$, which are of minimal order among all non-trivial monomials in Λ^{aug} . We assume that the statement of Theorem 10 is true for all elements in Λ^{aug} of lower order than τ and we will show that it is true for τ . We have that:

$$\begin{aligned} \tau &= t^{k_0} t_1^{k_1} \dots t_n^{k_n} = t^{k_0-1} (\underline{t t_1}) t_1^{k_1-1} \dots t_n^{k_n} = \\ &= t^{k_0-1} \left[\frac{-1}{(uv)^2} (1 + u\sigma_1 + vt + uv(\sigma_1 t + t\sigma_1)) + u^2 v \sigma_1 t \sigma_1 + uv^2 t \sigma_1 t \right] t_1^{k_1-1} \dots t_n^{k_n} \cong \\ &\cong -\frac{1}{(uv)^2} t^{k_0-1} t_1^{k_1-1} \dots t_n^{k_n} - \frac{1}{uv^2} t^{k_0-1} t_1^{k_1-1} \dots t_n^{k_n} \sigma_1 - \frac{1}{u^2 v} t^{k_0} t_1^{k_1-1} \dots t_n^{k_n} - \\ &- \frac{1}{uv} t^{k_0} t_1^{k_1-1} \dots t_n^{k_n} \sigma_1 - \frac{1}{v} t^{k_0-1} t_1^{k_1} \dots t_n^{k_n} - \frac{1}{u} t^{k_0+1} t_1^{k_1-1} \dots t_n^{k_n} \sigma_1 = \\ &= -\frac{1}{(uv)^2} t^{k_0-1} t_1^{k_1-1} \tau_{2,n}^{k_2,n} - \frac{1}{uv^2} t^{k_0-1} t_1^{k_1-1} \tau_{2,n}^{k_2,n} \sigma_1 - \frac{1}{u^2 v} t^{k_0} t_1^{k_1-1} \tau_{2,n}^{k_2,n} - \\ &- \frac{1}{uv} t^{k_0} t_1^{k_1-1} \tau_{2,n}^{k_2,n} \sigma_1 - \frac{1}{v} t^{k_0-1} t_1^{k_1} \tau_{2,n}^{k_2,n} - \frac{1}{u} t^{k_0+1} t_1^{k_1-1} \tau_{2,n}^{k_2,n} \sigma_1. \end{aligned}$$

On the right-hand side of this relation we have the following monomials in Λ^{aug} :

$$t^{k_0-1} t_1^{k_1-1} \tau_{2,n}^{k_2,n} < t^{k_0} t_1^{k_1-1} \tau_{2,n}^{k_2,n} < t^{k_0-1} t_1^{k_1} \tau_{2,n}^{k_2,n} < \tau_{0,n}^{k_0,n} = \tau,$$

and the monomials $t^{k_0-1} t_1^{k_1-1} \tau_{2,n}^{k_2,n} \sigma_1$, $t^{k_0} t_1^{k_1-1} \tau_{2,n}^{k_2,n} \sigma_1$ and $t^{k_0+1} t_1^{k_1-1} \tau_{2,n}^{k_2,n} \sigma_1$ in the $H_n(q)$ -module Λ^{aug} . Applying Theorem 9 on these monomials we have that:

$$t^{k_0-1} t_1^{k_1-1} \tau_{2,n}^{k_2,n} \sigma_1 \cong \sum_i A_i \tau_i, \text{ such that } \tau_i < t^{k_0-1} t_1^{k_1-1} \tau_{2,n}^{k_2,n} < \tau_{0,n}^{k_0,n}, \text{ for all } i$$

$$t^{k_0} t_1^{k_1-1} \tau_{2,n}^{k_2,n} \sigma_1 \cong \sum_j B_j \tau_j, \text{ such that } \tau_j < t^{k_0} t_1^{k_1-1} \tau_{2,n}^{k_2,n} < \tau_{0,n}^{k_0,n}, \text{ for all } j$$

$$t^{k_0+1} t_1^{k_1-1} \tau_{2,n}^{k_2,n} \sigma_1 \cong \sum_i C_i \tau_m, \text{ such that } \tau_m < t^{k_0+1} t_1^{k_1-1} \tau_{2,n}^{k_2,n} < \tau_{0,n}^{k_0,n}, \text{ for all } m$$

and thus, from the induction hypothesis the relation hold.

3.4 Proof of Theorem 2

Let $\tau'_{0,n} \in \mathcal{B}'(\text{ST}) \subset \Lambda_{(k)} \subset \Lambda_{(k)}^{aug}$. Then:

$$\begin{aligned}
 \tau'_{0,n} &\stackrel{\text{Cor.2}}{\cong} \tau_{0,n} + \sum_{i=0} A_i \cdot \tau_i \stackrel{\text{Prop. 1}}{\cong} A \cdot t^{\text{index}(\tau+1)} + \sum_{i=0}^{\text{ind}(\tau)} A_i \cdot t^i + \sum_{i=0} A_i \cdot \tau_i \\
 &\stackrel{\text{Thm.10}}{\cong} A \cdot t^{\text{index}(\tau+1)} + \sum_{i=0}^{\text{ind}(\tau)} A_i \cdot t^i + \sum_{i=0}^k B_i \cdot t^i = \sum_i C_i \cdot t^i \Rightarrow \\
 \tau'_{0,n} &\cong \sum_{i=0}^{n+1} C_i \cdot t^i,
 \end{aligned}$$

where A_i, B_i, C_i coefficients. Thus, elements in $\mathcal{B}'(\text{ST})$ can be expressed as sums of elements in $\mathcal{B}(\text{ST})$, that is:

The set $\mathcal{B}(\text{ST})$ spans the Kauffman bracket skein module of the solid torus.

We now prove linear independence of the set $\mathcal{B}(\text{ST})$:

The t^n 's geometrically consist of closed loops in the fundamental group of ST. Since $\pi_1(\text{ST}) = \mathbb{Z}$, $t^n \neq t^m$ for $n \neq m$ on the level of $\pi_1(\text{ST})$. This fact factors through to the Kauffman bracket skein module of ST, since the t^n 's can not be simplified neither by applying braid relations, nor by conjugation and stabilization moves. Moreover, the Temperley-Lieb type crossing switches cannot be applied on the t^n 's, since they contain no classical crossings in our setting. Thus, the value of the KBSM(ST) on these elements remains the same as the value of the invariant V^B on these elements.

The proof of Theorem 2 is now concluded.

Acknowledgements The author would like to acknowledge several discussions with Professor Sofia Lambropoulou. Moreover, financial support by the China Agricultural University, International College Beijing is gratefully acknowledged.

References

1. I. Diamantis, The Kauffman bracket skein module of the lens spaces $L(p, q)$ via braids, in preparation
2. I. Diamantis, S. Lambropoulou, Braid equivalences in 3-manifolds with rational surgery description. *Topol. Its Appl.* **194**, 269–295 (2015)
3. I. Diamantis, S. Lambropoulou, A new basis for the HOMFLYPT skein module of the solid torus. *J. Pure Appl. Algebra* **220**(2), 577–605 (2016)
4. I. Diamantis, S. Lambropoulou, The braid approach to the HOMFLYPT skein module of the lens spaces $L(p, 1)$, *Algebraic Modeling of Topological and Computational Structures and Application*. Springer Proceedings in Mathematics and Statistics (PROMS) (2017), [arXiv:1702.06290v1](https://arxiv.org/abs/1702.06290v1) [math.GT]

5. I. Diamantis, S. Lambropoulou, An important step for the computation of the HOMFLYPT skein module of the lens spaces $L(p, 1)$ via braids, [arXiv:1802.09376v1](https://arxiv.org/abs/1802.09376v1) [math.GT], to appear
6. I. Diamantis, S. Lambropoulou, The HOMFLYPT skein module of the lens spaces $L(p, 1)$ via braids, in preparation
7. I. Diamantis, S. Lambropoulou, J.H. Przytycki, Topological steps on the HOMFLYPT skein module of the lens spaces $L(p, 1)$ via braids, *J. Knot Theory and Ramifications*, **25**, 14, (2016)
8. M. Flores, D. Goundaroulis, The Framization of a Temperley-Lieb algebra of type B, [arXiv:1708.02014](https://arxiv.org/abs/1708.02014) [math.GT]
9. B. Gabrovšek, M. Mroczkowski, Link diagrams and applications to skein modules, *Algebraic Modeling of Topological and Computational Structures and Applications*. Springer Proceedings in Mathematics and Statistics (2017)
10. V.F.R. Jones, A polynomial invariant for links via Neumann algebras. *Bull. Am. Math. Soc.* **129**, 103–112 (1985)
11. S. Lambropoulou, Solid torus links and hecke algebras of B-type, *Quantum Topology*, ed. by D.N. Yetter, World Scientific Press (1994) pp. 224–245
12. S. Lambropoulou, Knot theory related to generalized and cyclotomic Hecke algebras of type B. *J. Knot Theory Its Ramif.* **8**(5), 621–658 (1999)
13. S. Lambropoulou, C.P. Rourke, Markov's theorem in 3-manifolds. *Topology and its Applications* **78**, 95–122 (1997)
14. S. Lambropoulou, C.P. Rourke, Algebraic Markov equivalence for links in 3-manifolds. *Compos. Math.* **142**, 1039–1062 (2006)
15. J. Przytycki, Skein modules of 3-manifolds. *Bull. Pol. Acad. Sci. Math.* **39**(1–2), 91–100 (1991)
16. V.G. Turaev, The Conway and Kauffman modules of the solid torus. *Zap. Nauchn. Sem. Lomi* **167**, 79–89 (1988). English translation: *J. Sov. Math.* 2799–2805 (1990)

Knot Invariants in Lens Spaces



Boštjan Gabrovšek and Eva Horvat

Abstract In this survey we summarize results regarding the Kauffman bracket, HOMFLYPT, Kauffman 2-variable and Dubrovnik skein modules, and the Alexander polynomial of links in lens spaces, which we represent by mixed link diagrams. These invariants generalize the corresponding knot polynomials in the classical case. We compare the invariants by means of the ability to distinguish between some difficult cases of knots with certain symmetries.

Keywords Knot invariants · Skein modules · Alexander polynomial · Lens spaces

2010 Mathematics Subject Classification 57M25 (primary) · 57M05 (secondary)

1 Introduction

By the Lickorish-Wallace theorem, any closed, connected, orientable 3-manifold M can be obtained by performing Dehn surgeries on a framed link L_0 in S^3 , furthermore, each component of L_0 can be assumed to be unknotted. Fixing L_0 pointwise, we can present every link L in M by a *mixed link* $L_0 \cup L$, where we call L_0 the *fixed component* and L the *moving component*, see also [5, 20]. If we take the regular projection of $L_0 \cup L$ to the plane of L_0 , we obtain a *mixed link diagram*.

In particular, if we perform $-p/q$ surgery on the unknot U , we obtain the lens space $L(p, q)$. In more detail, remove the regular neighbourhood $\nu(U)$ of U from S^3 and attach to the solid torus $V_1 = S^3 \setminus \nu(U)$ the solid torus $V_2 = S^1 \times D^2$ by the boundary homeomorphism $h : \partial V_2 \rightarrow \partial V_1$ that maps the meridian m_2 of

B. Gabrovšek (✉)

Faculty of Mechanical Engineering and Faculty of Mathematics and Physics,
University of Ljubljana, Ljubljana, Slovenia
e-mail: bostjan.gabrovsek@fs.uni-lj.si

E. Horvat

Faculty of Education, University of Ljubljana, Kardeljeva ploščad 16,
1000 Ljubljana, Slovenia
e-mail: eva.horvat@pef.uni-lj.si

© Springer Nature Switzerland AG 2019

C. C. Adams et al. (eds.), *Knots, Low-Dimensional Topology
and Applications*, Springer Proceedings in Mathematics & Statistics 284,
https://doi.org/10.1007/978-3-030-16031-9_17

347

Fig. 1 The boundary homeomorphism h for $p = 3$ and $q = 1$

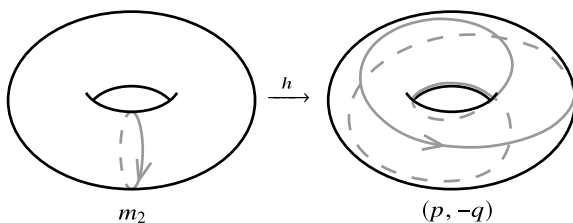


Fig. 2 The diagram of $L(p, q)$ and a mixed link, representing a knot in $L(p, q)$

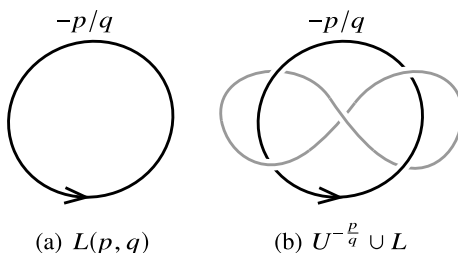
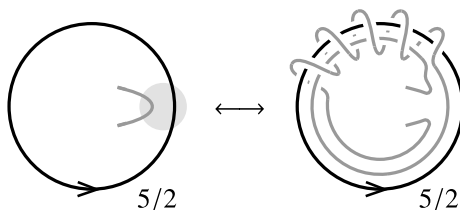


Fig. 3 The slide move $SL_{5,2}$ in $L(5, 2)$



$\partial V_2 \approx S^1 \times S^1$ to the $(p, -q)$ -curve on $\partial V_1 \approx S^1 \times S^1$, which is the curve that wraps p -times around the longitude and $-q$ -times around the meridian of ∂V_1 as illustrated in Fig. 1.

A link L in $L(p, q)$ can thus be represented by the mixed link diagram of $U \cup L$. When appropriate, we will emphasize that surgery has been performed on U by equipping the diagram with surgery coefficients as in Fig. 2 and we will denote such a link in $L(p, q)$ by $U^{-\frac{p}{q}} \cup L$. Note that even when dealing with unoriented links, the fixed component should be oriented, since the ambient manifold depends on this orientation.

If we approach the meridian disk of V_2 with an arc of L , we can slide the arc along the disk bounded by m_2 (the 2-handle in the CW decomposition of $L(p, q)$), which has the effect of making a connected sum with the $(p, -q)$ -curve representing ∂m_2 on ∂V_1 [5, 17, 21]. This isotopy move, called the *slide move* (or in some literature the *band move*), is illustrated in Fig. 3 and we denote it by $SL_{p,q}$. If we consider oriented links, we often differentiate between two variants of the slide move, one where the curve travels along the orientation of U and the other one where we travel in the opposite direction, depending on how the approaching arc is oriented with respect to the orientation of U . The two oriented flavours of $SL_{p,q}$ are illustrated in Fig. 4.

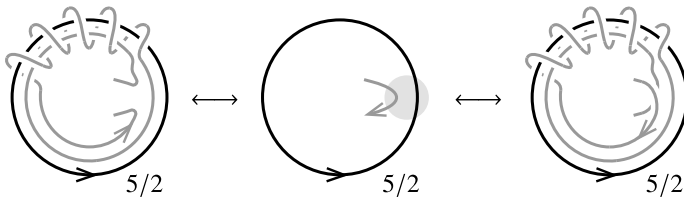


Fig. 4 Two oriented slide moves in $L(5, 2)$

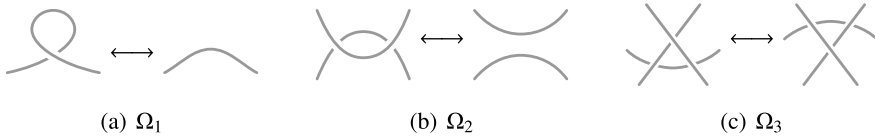


Fig. 5 Classical Reidemeister moves

The slide move, together with the planar Reidemeister moves in Fig. 5 are sufficient to describe isotopy in $L(p, q)$ as the following theorem states.

Theorem 1 ([17]) *Two mixed link diagrams represent the same link in $L(p, q)$ if and only if one can be transformed into the other by a finite sequence of Reidemeister moves $\Omega_1, \Omega_2, \Omega_3,$ and $SL_{p,q}$.*

Remark 1 Since U is fixed, the arcs involved in Ω_1 belong to the moving component, in Ω_2 at most one of the arcs can belong to the fixed component and in Ω_3 at most two arcs can belong to the fixed component.

2 The Kauffman Bracket Skein Module

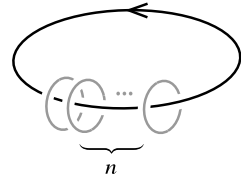
Let $\nearrow, \searrow, \updownarrow$ be the (oriented) skein triple and \times, \smile, \frown the (unoriented) Kauffman triple, i.e., links that are the same everywhere except inside a small 3-ball where they differ as the notation suggests.

Skein modules have their origin in the observation made by J. W. Alexander that the Alexander polynomials $\Delta(\nearrow, \searrow), \Delta(\searrow, \nearrow), \Delta(\updownarrow)$ are linearly related by the skein relation

$$\Delta(\nearrow, \searrow) - \Delta(\searrow, \nearrow) = (t^{1/2} - t^{-1/2})\Delta(\updownarrow).$$

J. H. Conway pursued this idea by taking $z = t^{1/2} - t^{-1/2}$ and considering the free $\mathbb{Z}[z]$ -module over the set of isotopy classes of links in S^3 modulo the $\mathbb{Z}[z]$ -module generated by the skein relation of the Alexander–Conway polynomial [19, 27, 29].

Fig. 6 The mixed link x^n



By formalizing such a construction and generalizing it for arbitrary 3-manifolds, J. H. Przytycki and V. G Turaev introduced the theory of skein modules in [28, 32].

The Kauffman bracket skein module generalizes the Kauffman bracket in the following sense.

Take a coefficient ring R with $A \in R$ being a unit (an element with a multiplicative inverse). Since, as in the case of the Kauffman bracket, we would like to study framed links, we set $\mathcal{L}_{\text{fr}}(M)$ to be the set of isotopy classes of framed links in M , including the empty link \emptyset . Let $R\mathcal{L}_{\text{fr}}(M)$ be the free R -module spanned by $\mathcal{L}_{\text{fr}}(M)$.

We would like to impose the Kauffman relation and the framing relation in $R\mathcal{L}_{\text{fr}}(M)$. We therefore take the submodule $S(M)$ of $R\mathcal{L}_{\text{fr}}(M)$ generated by

$$\begin{aligned} \begin{array}{c} \diagup \diagdown \\ \diagdown \diagup \end{array} &- A \begin{array}{c} \diagdown \diagup \\ \diagup \diagdown \end{array} - A^{-1} \begin{array}{c} \diagup \diagdown \\ \diagup \diagdown \end{array} \Big(, & \text{(Kauffman relator)} \\ L \sqcup \bigcirc &- (-A^2 - A^{-2})L. & \text{(framing relator)} \end{aligned}$$

The *Kauffman bracket skein module* $\mathcal{S}_{2,\infty}(M)$ is $R\mathcal{L}_{\text{fr}}(M)$ modulo these two relations:

$$\mathcal{S}_{2,\infty}(M) = R\mathcal{L}_{\text{fr}}(M)/S(M).$$

Let U be a fixed unknot in S^3 and let x^n be the mixed link where the moving components consist of n parallel copies of the unknot linked with U as in Fig. 6. Separately, we denote by x^0 the *affine* unknot (the unknot contained inside a 3-ball in M).

If we remove a tubular neighbourhood $\nu(U)$ of U , we can think of $U \cup L$ as a link in the solid torus $T = V_1$.

The Kauffman bracket skein module of the solid torus T has been calculated by Turaev:

Theorem 2 (Turaev [32]) $\mathcal{S}_{2,\infty}T$ is a free R -module generated by the set $\{x^n\}_{n=0}^\infty$.

If, instead of removing U , we perform $-p/q$ surgery on U , we can think of x^n as a link in $L(p, q)$.

Theorem 3 (Hoste, Przytycki [17]) $\mathcal{S}_{2,\infty}(L(p, q))$ is a free R -module generated by $\{x^n\}_{n=0}^{\lfloor p/2 \rfloor}$.

These generating sets are just natural choices, for alternative bases see [15]. The KBSM has been calculated for several other classes of manifolds, see for example [23–25].

3 The HOMFLYPT Skein Module

The HOMFLYPT skein module of a 3-manifold M generalizes the HOMFLYPT polynomial. Let the ring R this time have two units $v, z \in R$. Let $\mathcal{L}_{\text{or}}(M)$ be the set of isotopy classes of oriented links in M , including the empty link \emptyset and let $R\mathcal{L}_{\text{or}}(M)$ be the free R -module spanned by $\mathcal{L}_{\text{or}}(M)$.

We impose the HOMFLYPT skein relation in $R\mathcal{L}_{\text{or}}(M)$ by taking the submodule $\mathcal{S}(M)$ of $R\mathcal{L}_{\text{or}}(M)$ generated by the expressions

$$v^{-1} \begin{array}{c} \nearrow \\ \searrow \end{array} - v \begin{array}{c} \nwarrow \\ \swarrow \end{array} - z \begin{array}{c} \curvearrowright \\ \curvearrowleft \end{array}. \tag{HOMFLYPT relator}$$

We also add to $\mathcal{S}(M)$ the HOMFLYPT relation involving the empty knot,

$$v^{-1} \emptyset - v \emptyset - z \bigcirc. \tag{HOMFLYPT relator}$$

The HOMFLYPT skein module $\mathcal{S}_3(M)$ of M is $R\mathcal{L}_{\text{or}}(M)$ modulo the above relations:

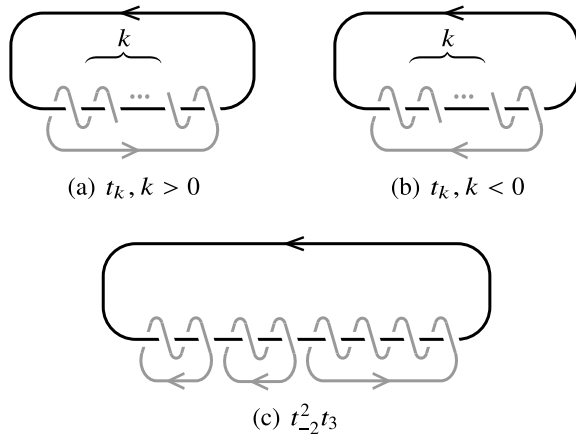
$$\mathcal{S}_3(M) = R\mathcal{L}_{\text{or}}(M) / \mathcal{S}(M).$$

Let U be a fixed unknot and let $t_k, k \in \mathbb{Z} \setminus \{0\}$, be the oriented link that wraps k times around U as in Fig. 7a, b (note that t_{-k} is t_k with reversed orientation). We define the product $t_{k_1} t_{k_2} \dots t_{k_s}, s \in \mathbb{N}$, as the links t_{k_i} placed consecutively along U as illustrated in Fig. 7c.

Theorem 4 (Turaev [32]) $\mathcal{S}_3(T)$ is a free R -module generated by

$$\{t_{k_1}^{i_1} \dots t_{k_s}^{i_s} \mid s \in \mathbb{N}, k_j \in \mathbb{Z} \setminus \{0\}, k_1 < \dots < k_s, i_j \in \mathbb{N}\} \cup \{\emptyset\}.$$

Fig. 7 Generators of $\mathcal{S}_3(T)$



Theorem 5 ([14]) $\mathcal{S}_3(L(p, 1))$ is a free R -module generated by

$$\{t_{k_1}^{i_1} \dots t_{k_s}^{i_s} \mid s \in \mathbb{N}, k_j \in \mathbb{Z} \setminus \{0\}, -\frac{p}{2} < k_1 < \dots < k_s \leq \frac{p}{2}, i_j \in \mathbb{N}\}.$$

For alternative bases see [15] and [6]. The proof of Theorem 5 in [14] is based on a diagrammatic approach, but the problem can be also attacked using a braid approach, see [7, 8].

The case of $\mathcal{S}_3(L(p, q))$, $q \geq 2$, is still an open question, but it is believed that the following conjecture holds.

Conjecture 1 $\mathcal{S}_3(L(p, q))$ is a free R -module generated by

$$\{t_{k_1}^{i_1} \dots t_{k_s}^{i_s} \mid s \in \mathbb{N}, k_j \in \mathbb{Z} \setminus \{0\}, -\frac{p}{2} < k_1 < \dots < k_s \leq \frac{p}{2}, i_j \in \mathbb{N}\}.$$

Related to this invariant, in [4] Cornwell constructed a 2-variable polynomial in $L(p, q)$ that satisfies the skein relation (but is in essence weaker than the HOMFLYPT skein module), see also [2], where this invariant has been studied.

4 The Kauffman and Dubrovnik Skein Modules

The Kauffman and Dubrovnik skein modules generalize the Kauffman 2-variable and Dubrovnik polynomials of unoriented links.

Let the ring R have two units $z, a \in R$. Take the submodule $\mathcal{S}(M)$ of $R\mathcal{L}_{fr}(M)$ generated by the expressions

$$\begin{aligned} \left(\begin{array}{c} \diagdown \diagup \\ \diagup \diagdown \end{array} + \epsilon \begin{array}{c} \diagup \diagdown \\ \diagdown \diagup \end{array} - z \right) \left(-\epsilon z \begin{array}{c} \diagdown \diagup \\ \diagdown \diagup \end{array}, \right. & \text{(Kauffman/Dubrovnik relator)} \\ \left. \begin{array}{c} \diagdown \diagup \\ \diagdown \diagup \end{array} - a \right). & \text{(framing relator)} \end{aligned}$$

We add to $\mathcal{S}(M)$ the relation involving the empty knot,

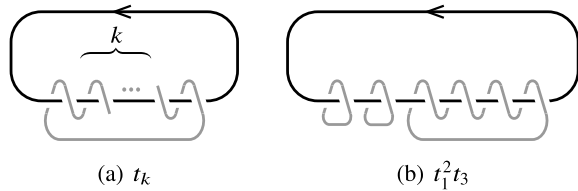
$$\bigcirc - \left(\frac{u + \epsilon u^{-1}}{z} - \epsilon \right) \emptyset.$$

We define the module

$$\mathcal{S}_{3,\infty}^\epsilon(M) = R\mathcal{L}(M)/\mathcal{S}(M).$$

Taking $\epsilon = +1$, we obtain the *Kauffman skein module* $\mathcal{S}_{3,\infty}(M)$ and for $\epsilon = -1$, we obtain the *Dubrovnik skein module* $\mathcal{S}_{3,\infty}^{-1}(M)$.

Fig. 8 Generators of $\mathcal{S}_{3,\infty}^{\pm 1}(T)$



Let $t_k, k \in \mathbb{N} \setminus \{0\}$, be the unoriented knot that wraps k times around U as in Fig. 8a. As in the previous section, the product $t_{k_1} t_{k_2} \dots t_{k_s}, s \in \mathbb{N}$ is the link consisting of t_{k_i} 's placed along U as illustrated in Fig. 8b.

For the solid torus, both modules have been calculated by Turaev:

Theorem 6 (Turaev [32]) $\mathcal{S}_{3,\infty}^{\pm 1}(T)$ are free R -modules generated by

$$\{t_{k_1}^{i_1} \dots t_{k_s}^{i_s} \mid s, k_j \in \mathbb{N}, 0 < k_1 < \dots < k_s, i_j \in \mathbb{N} \cup \{\emptyset\}\}.$$

For the lens spaces $L(p, 1)$, the modules have been calculated by Mroczkowski:

Theorem 7 (Mroczkowski [26]) $\mathcal{S}_{3,\infty}(L(p, 1))$ is generated by

$$\{t_{k_1}^{i_1} \dots t_{k_s}^{i_s} \mid s, k_j \in \mathbb{N}, 0 < k_1 < \dots < k_s \leq \lfloor \frac{p}{2} \rfloor, i_j \in \mathbb{N} \cup \{\emptyset\}\}.$$

The modules are free if p is odd and contain torsion if p is even.

Theorem 8 (Mroczkowski [26]) $\mathcal{S}_{3,\infty}^{-1}(L(p, 1))$ is a free R -module generated by

$$\{t_{k_1}^{i_1} \dots t_{k_s}^{i_s} \mid s, k_j \in \mathbb{N}, 0 < k_1 < \dots < k_s \leq \lfloor \frac{p}{2} \rfloor, i_j \in \mathbb{N} \cup \{\emptyset\}\}.$$

5 Alexander Polynomial

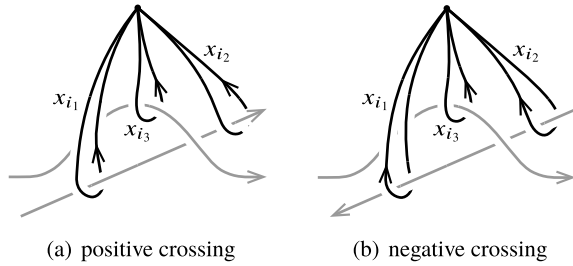
In this section we describe a Torres-type formula (see [31]), constructed in [16] for the Alexander polynomial of links in lens spaces defined by Fox's free differential calculus [9, 22, 33].

Recall that the fundamental group of a classical link admits a well-known Wirtinger presentation

$$\pi_1(S^3 \setminus L, *) = \langle x_1, \dots, x_n \mid r_1, \dots, r_n \rangle,$$

obtained from a link diagram. Generators x_i correspond to the simple closed loops based at $*$ and winding around the over-arcs of the diagram and r_i is the Wirtinger relation, $x_{i_1} x_{i_3} x_{i_2}^{-1} x_{i_3}^{-1}$ if the crossing is positive or $x_{i_1} x_{i_3}^{-1} x_{i_2}^{-1} x_{i_3}$ if the crossings is negative, corresponding to the i th crossing of the diagram, see Fig. 9.

Fig. 9 Wirtinger relations



Given a mixed link diagram of $U^{-p/q} \cup L$, the following proposition allows us to describe the fundamental group of $L(p, q) \setminus L$ (cf. [1, 12]).

Proposition 1 ([30]) *Let $\langle x_1, \dots, x_n \mid r_1, \dots, r_n \rangle$ be the Wirtinger presentation for $\pi_1(S^3 \setminus (U \cup L), *)$ obtained from a mixed link diagram. Denote by m_1 and l_1 the meridian and longitude of the regular neighbourhood of $S^3 \setminus U$, written in terms of the generators x_1, \dots, x_n . The presentation for the link group is given by*

$$\pi_1(L(p, q) \setminus L, *) = \langle x_1, \dots, x_n \mid w_1, \dots, w_n, m_1^p l_1^{-q} \rangle.$$

We briefly recall the construction of the Alexander polynomial using Fox calculus [16, 33]. Suppose

$$\mathcal{P} = \langle x_1, \dots, x_n \mid r_1, \dots, r_m \rangle$$

is a presentation of a group G . Denote by $H = G/G'$ its abelianization and by $F = \langle x_1, \dots, x_n \mid \rangle$ the corresponding free group. Apply the chain of maps

$$\mathbb{Z}F \xrightarrow{\frac{\partial}{\partial x}} \mathbb{Z}F \xrightarrow{\gamma} \mathbb{Z}G \xrightarrow{\alpha} \mathbb{Z}H,$$

where $\frac{\partial}{\partial x}$ denotes the Fox differential, γ is the quotient map by the relations r_1, \dots, r_m and α is the abelianization map.

The *Alexander-Fox matrix* of \mathcal{P} is the matrix $A = [a_{i,j}]$, where $a_{i,j} = \alpha(\gamma(\frac{\partial r_i}{\partial x_j}))$ for $i = 1, \dots, m$ and $j = 1, \dots, n$. The *first elementary ideal* $E_1(\mathcal{P})$ is the ideal of $\mathbb{Z}H$, generated by the determinants of all the $(n - 1)$ minors of A .

For a link L in S^3 , let $E_1(\mathcal{P})$ be the first elementary ideal obtained from a presentation \mathcal{P} of $\pi_1(S^3 \setminus L, *)$. The *Alexander polynomial* $\Delta(L)$ is the generator of the smallest principal ideal containing $E_1(\mathcal{P})$. The abelianization of $\pi_1(S^3 \setminus L, *)$ is a free abelian group, whose generators correspond to the components of L .

For a link in $L(p, q)$, the abelianization of its link group may also contain torsion, see [16, Corollary 2.10]. In this case, we need the notion of a twisted Alexander polynomial. We recall the following from [1].

Let G be a group with a finite presentation \mathcal{P} and abelianization $H = G/G'$ and denote $K = H/Tors(H)$. Then every homomorphism $\sigma : Tors(H) \rightarrow \mathbb{C}^* = \mathbb{C} \setminus \{0\}$ determines a twisted Alexander polynomial $\Delta^\sigma(\mathcal{P})$ as follows. Choosing a

splitting $H = Tors(H) \times K$, σ defines a ring homomorphism $\sigma : \mathbb{Z}[H] \rightarrow \mathbb{C}[K]$ sending $(f, g) \in Tors(H) \times K$ to $\sigma(f)g$. Thus we apply the chain of maps

$$\mathbb{Z}F \xrightarrow{\frac{\partial}{\partial x}} \mathbb{Z}F \xrightarrow{\gamma} \mathbb{Z}G \xrightarrow{\alpha} \mathbb{Z}H \xrightarrow{\sigma} \mathbb{C}[K]$$

and obtain the σ -twisted Alexander matrix $A^\sigma = \left[\sigma(\alpha(\gamma(\frac{\partial r_i}{\partial x_j}))) \right]$. The *twisted Alexander polynomial* is then defined by $\Delta^\sigma(\mathcal{P}) = \gcd(\sigma(E_1(\mathcal{P})))$.

The *Alexander polynomial* of $U^{-p/q} \cup L$, which we denote by $\Delta_{U^{-p/q} \cup L}$ or simply Δ_L if the context is clear, is defined to be the generator of the smallest principal ideal containing $E_1(\mathcal{P})$.

We continue by describing how to obtain the Alexander polynomial for $U^{-p/q} \cup L$ from the Alexander polynomial of $U \cup L \subset S^3$.

Let D be the disk bounded by U . We may assume that L intersects D transversely in k intersection points with algebraic intersection signs $\epsilon_1, \dots, \epsilon_k \in \{-1, 1\}$. We define $[L] = \sum_{i=1}^k \epsilon_i$, which corresponds to the integer representing the homology class of L in $H_1(S^3 \setminus U) \cong \mathbb{Z}$.

By Proposition 1, the presentation of $\pi_1(L(p, q) \setminus L, *)$ is obtained from the presentation of the link group $\pi_1(S^3 \setminus (U \cup L), *)$ by adding one relation. The Alexander-Fox matrices are thus closely related and consequently so are the Alexander polynomials, as the following theorem states.

Theorem 9 ([16]) *Let $p' = \frac{p}{\gcd\{p, [L]\}}$ and $[L]' = \begin{cases} 1, & \text{if } [L] = 0 \\ \frac{[L]}{\gcd\{p, [L]\}}, & \text{if } [L] \neq 0 \end{cases}$. The Alexander polynomial of $U^{-p/q} \cup L$ and the (classical) two-variable Alexander polynomial $\Delta_{U \cup L}(u, t)$, where variable u corresponds to the moving components and variable t corresponds to the fixed component, are related by*

$$\Delta_{U^{-p/q} \cup L}(t) = \frac{t - 1}{t^{[L]}' - 1} \Delta_{U \cup L}(t^{p'}, t^{q[L]'}) . \tag{1}$$

It is also shown in [16] that it is possible to normalize $\Delta_{U^{-p/q} \cup L}$ and obtain a normalized version of the Alexander polynomial in lens spaces, $\nabla(L)(t)$, which satisfies the skein relation

$$\nabla(\overrightarrow{\nearrow} \overrightarrow{\searrow}) - \nabla(\overleftarrow{\nearrow} \overleftarrow{\searrow}) = (t^{\frac{p'}{2}} - t^{-\frac{p'}{2}}) \nabla(\overrightarrow{\searrow} \overleftarrow{\searrow}) .$$

This result may be compared to the skein relation for links in the projective space $L(2, 1)$, obtained in [18]:

Theorem 10 (Huynh, Le [18]) *Let $\overrightarrow{\nearrow} \overrightarrow{\searrow}, \overleftarrow{\nearrow} \overleftarrow{\searrow}, \overrightarrow{\searrow} \overleftarrow{\searrow}$ be a skein triple in the projective space. If $\overrightarrow{\nearrow} \overrightarrow{\searrow}, \overleftarrow{\nearrow} \overleftarrow{\searrow}$, and $\overrightarrow{\nearrow} \overleftarrow{\searrow}$ belong to the same torsion class, then the normalized one variable twisted Alexander function satisfies the skein relation*

$$\nabla(\overrightarrow{\text{X}}) - \nabla(\overleftarrow{\text{X}}) = (t - t^{-1})\nabla(\overrightarrow{\text{C}}).$$

6 Examples

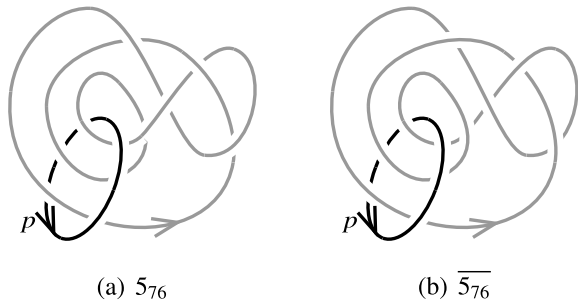
We finish by presenting some explicit calculations of difficult cases of links in $L(p, 1)$, where the mentioned invariants fail to detect inequivalent links. The knot notations are taken from the lens space knot table constructed in [11]. The Kauffman bracket skein modules and HOMFLY-PT skein modules (evaluated in the standard basis) were computed by the C++ program available in [10] (the algorithm itself is presented in [11]). The Alexander polynomials were computed using SnapPy and SageMath and applying equation (1). The Kauffman skein modules and Dubrovnik skein modules were computed by hand (for the solid torus and by linearity, substituting the solid torus generators by the lens space generators).

Example 1

Consider the knots 5_{76} and $\overline{5_{76}}$ in Fig. 10. The knot $\overline{5_{76}}$ differs from 5_{76} by exchanging the crossing on the moving component, which can be interpreted as $\overline{5_{76}}$ being the mirror image of 5_{76} under the self-homeomorphism of T that reverses the orientation of the meridian, but keeps the orientation of the longitude. Amphichirality of 5_{76} is not detected by the Kauffman bracket skein module for any value of p , but detected by the other skein modules and the Alexander polynomial.

p	$\mathcal{S}_{2,\infty}(5_{76}) = \mathcal{S}_{2,\infty}(\overline{5_{76}})$
2	x
3	$A^{13} + A + x(-A^8 + A^4)$
4	$x(-A^{11} + A^7 + A^5 - A^3 - A)$
≥ 5	$x(2A^7 - A^3 + 2A^{-1}) + x^3(-A^7 + A^3 - A^{-1})$

Fig. 10 The knot 5_{76} and its mirror image



p	$S_3(\overline{576})$
2	t_1
3	$-v^{-1}z_{-1} + v^{-3}z^{-1} - t_{-1}t_1 v^{-1}z$
4	$t_{-1}(-z^2 + v^{-2}) - t_1t_2 v z$
5	$-t_{-1}t_{-2} v z + t_2(-z^2 + v^{-2})$
≥ 6	$-t_1t_2 v z + t_3(-z^2 + v^{-2})$

p	$S_3(\overline{576})$
2	$t_1(2v^{-2}z^2 + 3v^{-2} - 2v^{-4}z^4 - 4v^{-4}z^2 - 3v^{-4} + 2v^{-6}z^2 + v^{-6}) + t_1^3(z^2 - v^{-2}z^4 - v^{-2}z^2)$
3	$-2v^{-1}z - v^{-1}z^{-1} + 2v^{-3}z^3 + 4v^{-3}z + v^{-3}z^{-1} - 2v^{-5}z^3 - 2v^{-5}z + t_1^3(z^2 - v^{-2}z^4 - v^{-2}z^2) + t_{-1}t_1(-2v^{-3}z + 2v^{-5}z^3 + v^{-5}z)$
4	$t_{-1}^3(z^2 - v^{-2}z^4 - v^{-2}z^2) + t_1(2v^{-2}z^2 + v^{-2} - 2v^{-4}z^4 - 2v^{-4}z^2) + t_{-1}t_2(-2v^{-3}z + 2v^{-5}z^3 + v^{-5}z)$
5	$t_{-2}t_{-1}(-2v^{-1}z + 2v^{-3}z^3 + v^{-3}z) + t_{-1}^3(z^2 - v^{-2}z^4 - v^{-2}z^2) + t_2(v^{-2} - v^{-4}z^2)$
≥ 6	$t_{-3}(v^{-2} - v^{-4}z^2) + t_{-2}t_{-1}(-2v^{-1}z + 2v^{-3}z^3 + v^{-3}z) + t_{-1}^3(z^2 - v^{-2}z^4 - v^{-2}z^2)$

p	$S_{3,\infty}(\overline{576})$
2	$t_1(-z + a^{-1} + za^2)$
3	$za^2 + a^3 + za^4 - a^2z^{-1} - a^4z^{-1} - a^3z^2 + t_1(-z - az^2 + a^{-1}z^2 + z^3 - a^2z^3) + t_1^2(za^2 + a^3z^2)$
4	$t_1(-z - a^5 + a^{-1}z^2 + a^3z^2 + a^5z^2 + z^3 + a^4z^3) + t_1t_2(-z - az^2)$
5	$t_1(-z + a^{-1}z^2 + z^3) + t_2(-a^7 + a^5z^2 + a^7z^2 + a^6z^3) + t_1t_2(-z - az^2)$
≥ 6	$t_1(-z + a^{-1}z^2 + z^3) + t_1t_2(-z - az^2) + t_3(-a^3 + az^2 + a^3z^2 + a^2z^3)$

p	$S_{3,\infty}(\overline{576})$
2	$t_1(-3 + 2az - 2za^{-1} - 2a^2 - 2za^2 - a^3 - a^5 + 8z^2 + 5a^2z^2 + 4a^3z^2 + 2a^4z^2 + 3az^3 + 2a^{-1}z^3 + 3a^2z^3 - 3z^4 - 7a^2z^4 - 5az^5) + t_1^2(-a^3z^2 - a^2z^3) + t_1^3(-z^2 - a^3z^2 - a^2z^3 + z^4 + a^2z^4 + az^5)$
3	$3az + a^2 + 4za^3 + za^4 + za^5 + za^6 - az^{-1} - a^3z^{-1} - 2a^2z^2 + a^3z^2 - 2az^3 - 5a^3z^3 - a^4z^3 - 2a^5z^3 + 2a^3z^5 + t_1(-2za^{-1} - za^2 + z^2 + 2a^2z^2 + a^3z^2 + a^5z^2 + 2az^3 + 2a^{-1}z^3 + a^2z^3 + a^4z^3 + z^4 - 3a^2z^4 - 2a^4z^4 - az^5 - 2a^3z^5) + t_1^2(-2za^3 - za^6 - a^3z^2 - a^5z^2 - a^2z^3 + 2a^3z^3 + 2a^5z^3 + 2a^4z^4) + t_1^3(-z^2 - a^3z^2 - a^2z^3 + z^4 + a^2z^4 + az^5)$
4	$t_1(-2za^{-1} - za^2 - a^4 + z^2 + a^3z^2 + a^4z^2 + a^6z^2 + 2az^3 + 2a^{-1}z^3 + a^2z^3 + a^5z^3 + z^4 - a^2z^4 - az^5) + t_1^2(-a^3z^2 - a^2z^3) + t_1t_2(2az + za^4 + a^3z^2 - 2az^3 - 2a^3z^3 - 2a^2z^4) + t_1^3(-z^2 - a^3z^2 - a^2z^3 + z^4 + a^2z^4 + az^5)$
5	$t_1(-2za^{-1} - za^2 + z^2 + a^3z^2 + 2az^3 + 2a^{-1}z^3 + a^2z^3 + z^4 - a^2z^4 - az^5) + t_1^2(-a^3z^2 - a^2z^3) + t_2(-a^6 + a^6z^2 + a^8z^2 + a^7z^3) + t_1t_2(2az + za^4 + a^3z^2 - 2az^3 - 2a^3z^3 - 2a^2z^4) + t_1^3(-z^2 - a^3z^2 - a^2z^3 + z^4 + a^2z^4 + az^5)$
≥ 6	$t_1(-2za^{-1} - za^2 + z^2 + a^3z^2 + 2az^3 + 2a^{-1}z^3 + a^2z^3 + z^4 - a^2z^4 - az^5) + t_1^2(-a^3z^2 - a^2z^3) + t_1^3(-z^2 - a^3z^2 - a^2z^3 + z^4 + a^2z^4 + az^5) + t_1t_2(2az + za^4 + a^3z^2 - 2az^3 - 2a^3z^3 - 2a^2z^4) + t_3(-a^2 + a^2z^2 + a^4z^2 + a^3z^3)$

p	$S_{3,\infty}^{-1}(576)$
2	$t_1(z + a^{-1} - za^2)$
3	$-za^2 + a^3 + za^4 - a^2z^{-1} + a^4z^{-1} + a^3z^2 + t_1(z - az^2 + a^{-1}z^2 + z^3 - a^2z^3) + t_1^2(-za^2 - a^3z^2)$
4	$t_1(z + a^5 + a^{-1}z^2 - a^3z^2 + a^5z^2 + z^3 - a^4z^3) + t_1t_2(-z - az^2)$
5	$t_1(z + a^{-1}z^2 + z^3) + t_2(a^7 - a^5z^2 + a^7z^2 - a^6z^3) + t_1t_2(-z - az^2)$
≥ 6	$t_1(z + a^{-1}z^2 + z^3) + t_1t_2(-z - az^2) + t_3(a^3 - az^2 + a^3z^2 - a^2z^3)$

p	$S_{3,\infty}^{-1}(\overline{576})$
2	$t_1(3 - 2az + 2za^{-1} - 2a^2 - a^3 + a^5 + 2z^2 - 5a^2z^2 + 2a^4z^2 - az^3 + 2a^{-1}z^3 - a^2z^3 + z^4 - a^2z^4 - az^5) + t_1^2(a^3z^2 - a^2z^3) + t_1^3(z^2 - a^3z^2 + a^2z^3 + z^4 - a^2z^4 + az^5)$
3	$-3az + a^2 + 4za^3 + za^4 - za^5 - za^6 - az^{-1} + a^3z^{-1} + 2a^2z^2 - a^3z^2 - 2az^3 + 5a^3z^3 + a^4z^3 - 2a^5z^3 + t_1(2za^{-1} - za^2 - z^2 - 2a^2z^2 + a^3z^2 + a^5z^2 - 2az^3 + 2a^{-1}z^3 - a^2z^3 - a^4z^3 + z^4 - a^2z^4 + 2a^4z^4 - az^5 - 2a^3z^5) + t_1^2(-2za^3 + za^6 + a^3z^2 - a^5z^2 - a^2z^3 - 2a^3z^3 + 2a^5z^3 - 2a^4z^4) + 2a^3z^5 + t_1^3(z^2 - a^3z^2 + a^2z^3 + z^4 - a^2z^4 + az^5)$
4	$t_1(2za^{-1} - za^2 + a^4 - z^2 + a^3z^2 + a^4z^2 - a^6z^2 - 2az^3 + 2a^{-1}z^3 - a^2z^3 + a^5z^3 + z^4 + a^2z^4 - az^5) + t_1^2(a^3z^2 - a^2z^3) + t_1t_2(-2az + za^4 - a^3z^2 - 2az^3 + 2a^3z^3 - 2a^2z^4) + t_1^3(z^2 - a^3z^2 + a^2z^3 + z^4 - a^2z^4 + az^5)$
5	$t_1(2za^{-1} - za^2 - z^2 + a^3z^2 - 2az^3 + 2a^{-1}z^3 - a^2z^3 + z^4 + a^2z^4 - az^5) + t_1^2(a^3z^2 - a^2z^3) + t_2(a^6 + a^6z^2 - a^8z^2 + a^7z^3) + t_1t_2(-2az + za^4 - a^3z^2 - 2az^3 + 2a^3z^3 - 2a^2z^4) + t_1^3(z^2 - a^3z^2 + a^2z^3 + z^4 - a^2z^4 + az^5)$
≥ 6	$t_1(2za^{-1} - za^2 - z^2 + a^3z^2 - 2az^3 + 2a^{-1}z^3 - a^2z^3 + z^4 + a^2z^4 - az^5) + t_1^2(a^3z^2 - a^2z^3) + t_1^3(z^2 - a^3z^2 + a^2z^3 + z^4 - a^2z^4 + az^5) + t_1t_2(-2az + za^4 - a^3z^2 - 2az^3 + 2a^3z^3 - 2a^2z^4) + t_3(a^2 + a^2z^2 - a^4z^2 + a^3z^3)$

$$\Delta(576) = -t^{2p-1} - 2t^{3p-2} + t^{4p-2} - 2t^p + 1.$$

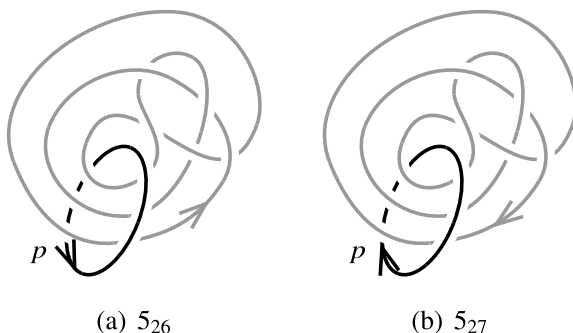
$$\Delta(\overline{576}) = -t^{2p+1} - 2t^{3p+2} + t^{4p+2} - 2t^p + 1.$$

Example 2

The knots 5_{26} and 5_{27} in Fig. 11 differ by exchanging both the orientation of the fixed and mixed sublinks, which can be interpreted as 5_{27} being the image of 5_{26} under the self-homeomorphism of the torus T that reverses both the meridian and the longitude (a so-called *flip* in the language of [13], see also [3]). The question whether $5_{26} \neq 5_{27}$ is equivalent to the question whether the links are non-invertible.

Non-invertible links were studied by Whitten [35] and are hard to detect, although in the case when the links are hyperbolic (most are), modern computational techniques using canonical triangulations of the link complements enable us to verifiably recognize them [34].

Fig. 11 The knots 5_{26} and its flip 5_{27}



It is shown in [11] that 5_{26} and 5_{27} are non-isotopic in any lens space $L(p, 1)$, but due to the symmetric nature of the two knots, none of our invariants are able to detect this.

p	$S_{2,\infty}(5_{26}) = S_{2,\infty}(5_{27})$
2	$x(-A^{24} + 3A^{20} - 2A^{16} + 3A^{12} - 3A^8 + 2A^4 - 1)$
3	$A^{17} - A^{13} + A^5 - A - xA^8(A^{16} - 3A^{12} + 2A^8 - 2A^4 + 1)$
4	$-x(A^{18} - 3A^{14} - A^{12} + 2A^{10} + 2A^8 - 2A^6 - 2A^4 + A^2 + 1)$
5	$A^{16} - A^{12} + A^4 - 1 + x(A^{21} - 3A^{17} + 2A^{13} - 2A^9 + A^5)$ $+ x^2(-A^{16} + 2A^{12} - 2A^8 + A^4)$
≥ 6	$x(A^{21} - A^{17} - A^{13} + A^5 - A) + x^3(-A^{17} + 2A^{13} - 2A^9 + A^5)$

p	$S_3(5_{26}) = S_3(5_{27})$
2	$t_1^3(-v^6z^4 - v^6z^2) + t_1(v^4z^6 + 3v^4z^4 + 2v^4z^2 - v^4 - v^2z^4 + 2v^2)$
3	$t_{-1}^2(v^3z^3 + v^3z) + t_{-1}t_1^2(-v^2z^4 - v^2z^2) + t_1(v^4z^2 + v^2z^4 + v^2z^2 + v^2)$
≥ 4	$t_{-1}t_1^2(-v^2z^4 - v^2z^2) + t_{-1}t_2(vz^3 + vz) + t_1(v^4z^2 + v^2)$

p	$S_{3,\infty}(5_{26}) = S_{3,\infty}(5_{27})$
2	$-az^2 - a^{-1}z^2 + 2z^3 + a^2z^3 - az^4 + t_1(-2a - z + 2az - za^{-2} + za^2 - a^3 + za^3$ $- 2az^2 - 2a^{-1}z^2 - 2a^2z^2 + z^3 - 2az^3 + 2a^{-2}z^3 - a^2z^3 + 2az^4 + 4a^{-1}z^4 + 2z^5)$ $+ t_1^2(-az^2 + a^2z^3 + az^4) - t_1^3az^2$
3	$-z + a^2 - za^2 - za^3 + a^4 - a^2z^2 - a^3z^2 - a^4z^2 + 2z^3 + 3a^2z^3 + a^3z^3 - az^4 + a^3z^4$ $- a^2z^5 + t_1(-a - az^2 - a^2z^2 + a^3z^2 + 2z^3 - a^3z^3 + 3az^4 + a^3z^4 + a^2z^5)$ $+ t_1^2(-za^4 - 2az^2 + a^4z^2 - a^2z^3 + az^4 - a^3z^4) - t_1^3az^2$
4	$-az^2 - a^{-1}z^2 + z^3 + t_1(-a + za^5 - az^2 - a^2z^2 - a^3z^2 - a^5z^2 + z^3 - a^4z^3 + az^4)$ $+ t_1^2(-az^2 + a^2z^3 + az^4) + t_2az^4 - t_1^3az^2 + t_1t_2(za^2 + a^{-1}z^2 - a^2z^2 + 2z^3 + az^4)$
5	$-az^2 - a^{-1}z^2 + z^3 + t_1(-a - az^2 - a^2z^2 + z^3 + az^4) + t_1^2a(-z^2 + az^3 + z^4) + t_2$ $(za^7 - a^5z^2 - a^7z^2 - a^6z^3 + az^4) - t_1^3az^2 + t_1t_2(za^2 + a^{-1}z^2 - a^2z^2 + 2z^3 + az^4)$
≥ 6	$-az^2 - z^2/a + z^3 + t_1(-a - az^2 - a^2z^2 + z^3 + az^4) + t_1^2a(-z^2 + az^3 + z^4) + t_2az^4$ $- t_1^3az^2 + t_1t_2(za^2 + a^{-1}z^2 - a^2z^2 + 2z^3 + az^4) + t_3(za^3 - az^2 - a^3z^2 - a^2z^3)$

p	$S_{3,\infty}^{-1}(5_{26}) = S_{3,\infty}^{-1}(5_{27})$
2	$-az^2 + a^{-1}z^2 - 2z^3 + a^2z^3 + az^4 + t_1(z + 2az - za^{-2} + za^2 + a^3 - za^3 + 2az^2 - 2a^{-1}z^2 - z^3 + a^2z^3) + t_1^2(a^2z^2 + a^2z^3 - az^4) - t_1^3az^2$
3	$z - a^2 - za^2 + za^3 + a^4 - 2az^2 + 2a^{-1}z^2 - a^2z^2 - a^3z^2 + a^4z^2 - 3a^2z^3 + a^3z^3 - az^4 - a^3z^4 - a^2z^5 + t_1(a - az^2 + a^2z^2 + a^3z^2 - a^3z^3 + az^4 + a^3z^4 + a^2z^5) + t_1^2(za^4 + 2az^2 - a^4z^2 + 3a^2z^3 - az^4 + a^3z^4) - t_1^3az^2$
4	$-az^2 + a^{-1}z^2 - z^3 + t_1(a + za^5 - az^2 + a^2z^2 - a^3z^2 + a^5z^2 - z^3 - a^4z^3 - az^4) + t_1^2(a^2z^2 + a^2z^3 - az^4) + t_2az^4 + t_1t_2(za^2 + a^{-1}z^2 - a^2z^2 + 2z^3 + az^4) - t_1^3az^2$
5	$-az^2 + a^{-1}z^2 - z^3 - t_1^3az^2 + t_1(a - az^2 + a^2z^2 - z^3 - az^4) + t_1^2a(z^2 + az^3 - z^4) + t_1t_2(za^2 + a^{-1}z^2 - a^2z^2 + 2z^3 + az^4) + t_2(za^7 - a^5z^2 + a^7z^2 - a^6z^3 + az^4)$
≥ 6	$-az^2 + a^{-1}z^2 - z^3 + t_1(a - az^2 + a^2z^2 - z^3 - az^4) + t_1^2a(z^2 + az^3 - z^4) + t_2az^4 - t_1^3az^2 + t_1t_2(za^2 + a^{-1}z^2 - a^2z^2 + 2z^3 + az^4) + t_3(za^3 - az^2 + a^3z^2 - a^2z^3)$

$$\Delta(5_{26}) = \Delta(5_{27}) = (t^2 - t + 1)(t^{p+1} - t + 1)(t^{p+1} - t^p + 1).$$

Acknowledgements The first author was supported by the Slovenian Research Agency grants J1-8131, J1-7025, and N1-0064. The second author was supported by the Slovenian Research Agency grant N1-0083.

References

1. A. Cattabriga, E. Manfredi, M. Mulazzani, On knots and links in lens spaces. *Topol. Appl.* **160**(2), 430–442 (2013)
2. A. Cattabriga, E. Manfredi, L. Rigolli, Equivalence of two diagram representations of links in lens spaces and essential invariants. *Acta Math. Hungar.* **146**(168), 168–201 (2015)
3. A. Cattabriga, E. Manfredi, Diffeomorphic vs isotopic links in lens spaces. *Mediterr. J. Math.* **15**, 172 (2018)
4. C. Cornwell, A polynomial invariant for links in lens spaces. *J. Knot Theory Ramif.* **21**, 6 (2012)
5. I. Diamantis, S. Lambropoulou, Braid equivalence in 3-manifolds with rational surgery description. *Topol. Appl.* **194**, 269–295 (2015)
6. I. Diamantis, S. Lambropoulou, A new basis for the Homflypt skein module of the solid torus. *Pure Appl. Algebr.* **220**(2), 577–605 (2016)
7. I. Diamantis, S. Lambropoulou, J. Przytycki, Topological steps toward the Homypt skein module of the lens spaces $L(p, 1)$ via braids. *J. Knot Theory Ramif.* **25**, 14 (2016)
8. I. Diamantis, S. Lambropoulou, An important step for the computation of the HOMFLYPT skein module of the lens spaces $L(p, 1)$ via braids (2018), [arXiv:1802.09376](https://arxiv.org/abs/1802.09376) [math.GT]
9. R.H. Fox, A quick trip through knot theory, in *Topology of 3-Manifolds*, ed. by M.K. Fort Jr. (Prentice-Hall, 1962)
10. B. Gabrovšek, Classification of knots in $L(p, q)$, C++ source code (2016), <https://github.com/bgabrovsek/lpq-classification>
11. B. Gabrovšek, Tabulation of prime knots in lens spaces. *Mediterr. J. Math.* **44**, 88 (2017)
12. B. Gabrovšek, E. Manfredi, On the Seifert fibered space link group. *Topol. Appl.* **206**, 255–275 (2016)
13. B. Gabrovšek, M. Mroczkowski, Knots in the solid torus up to 6 crossings. *J. Knot Theory Ramif.* **21**, 11 (2012)

14. B. Gabrovšek, M. Mroczkowski, The HOMFLYPT skein module of the lens spaces $L_{p,1}$. *Topology Appl.* **175**, 72–80 (2014)
15. B. Gabrovšek, M. Mroczkowski, Link diagrams in Seifert manifolds and applications to skein modules, in *Algebraic Modeling of Topological and Computational Structures and Applications*, ed. by S. Lambropoulou et al. Springer Proceedings in Mathematics & Statistics, vol. 219 (Springer, Berlin, 2015), pp. 117–141
16. E. Horvat, B. Gabrovšek, On the Alexander polynomial of links in lens spaces, to appear in *J. Knot Theory Ramif.* (2019), preprint available at [arXiv:1606.03224](https://arxiv.org/abs/1606.03224) [math.GT]
17. J. Hoste, J.H. Przytycki, The $(2, \infty)$ -skein module of lens spaces: a generalization of the Jones polynomial. *J. Knot Theory Ramif.* **2**(3), 321–333 (1993)
18. V.Q. Huynh, T.T.Q. Le, Twisted Alexander polynomial of links in the projective space. *J. Knot Theory Ramif.* **17**(4), 411–438 (2008)
19. L.H. Kauffman, The Conway polynomial. *Topology* **20**(1), 101–108 (1981)
20. S. Lambropoulou, C.P. Rourke, Markov’s theorem in 3-manifolds. *Topol. Appl.* **78**, 95–122 (1997)
21. S. Lambropoulou, C.P. Rourke, Algebraic Markov equivalence for links in 3-manifolds. *Compos. Math.* **142**, 1039–1062 (2006)
22. X.S. Lin, Representations of knot groups and twisted Alexander polynomials. *Acta Math. Sin. (Engl. Ser.)* **17**(3), 361–380 (2001)
23. M. Mroczkowski, M.K. Dabkowski, KBSM of the product of a disk with two holes and S^1 . *Topol. Appl.* **156**(10), 1831–1849 (2009)
24. M. Mroczkowski, Kauffman bracket skein module of the connected sum of two projective spaces. *J. Knot Theory Ramif.* **20**(5), 651–675 (2010)
25. M. Mroczkowski, Kauffman bracket skein module of a family of prism manifolds. *J. Knot Theory Ramif.* **20**(159), 159–170 (2011)
26. M. Mroczkowski, The Dubrovnik and Kauffman skein modules of the lens spaces $L_{p,1}$. *J. Knot Theory Ramif.* **20**, 159 (2018)
27. J.H. Przytycki, Algebraic topology based on knots: an introduction, in *Proceedings of Knots 96* (World Scientific, 1997), pp. 279–297
28. J.H. Przytycki, Skein modules of 3-manifolds. *Bull. Polish Acad. Sci.* **39**(1–2), 91–100 (1991)
29. J.H. Przytycki, KNOTS: from combinatorics of knot diagrams to combinatorial topology based on knots, draft book (2007), [arXiv:math/0703096](https://arxiv.org/abs/math/0703096) [math.GT] (Chapter II), [arXiv:math/0602264](https://arxiv.org/abs/math/0602264) [math.GT] (Chapter IX)
30. D. Rolfsen, *Knots and Links* (AMS Chelsea Publishing, Providence, RI, 2003)
31. G. Torres, On the Alexander polynomial. *Ann. Math.* **2**(57), 57–89 (1953)
32. V.G. Turaev, The Conway and Kauffman modules of the solid torus. *Zap. Nauchn. Sem. LOMI; English trans. in J. Soviet Math.* **167**, 79–89 (1998)
33. M. Wada, Twisted Alexander polynomial for finitely presentable groups. *Topology* **33**(2), 241–256 (1994)
34. J. Weeks, Convex hulls and isometries of cusped hyperbolic 3-manifolds. *Topol. Appl.* **52**, 127–149 (1993)
35. W.C. Whitten, A pair of non-invertible links. *Duke Math. J.* **36**, 695–698 (1969)

Identity Theorem for Pro- p -groups



Andrey M. Mikhovich

Abstract The concept of schematization consists in replacing simplicial groups by simplicial affine group schemes. In the case when the coefficient field has zero characteristic, there is a prominent theory of simplicial pronipotent groups, the origins of which lead to the rational homotopy theory of D. Quillen. It turns out that schematization reveals the profound properties of \mathbb{F}_p -pronipotent groups, especially in connection with pronipotent groups in zero characteristic and in the study of quasirationality. In this paper, using results on representations and cohomology of pronipotent groups in characteristic 0, we prove an analogue of Lyndon Identity theorem for one-relator pro- p -groups (question posed by J.P. Serre) and demonstrate the application to one more problem of J.-P. Serre concerning one-relator pro- p -groups of cohomological dimension 2. Schematic approach makes it possible to consider the problems of pro- p -groups theory through the prism of Tannaka duality, concentrating on the category of representations. In particular we attach special importance to the existence of identities in free pro- p -groups (“conjuring”).

Keywords Relation module · Cohomology groups · Identities in pronipotent groups

2010 Mathematics Subject Classification 20G05 · 20G10 · 16R10

1 Introduction

Part 1.1 of the introduction contains a brief review of a modern paradigm (as it seen by the author) of the pro- p -group theory and an explanation of the importance of one-relator pro- p -groups. In Sect. 1.2 we remind basic definitions of pronipotent group theory, those we need in the sequel. Section 1.3 provides condensed introduction to the results on quasirational presentations and their schematization. We also

A. M. Mikhovich (✉)
Lomonosov Moscow State University, Moscow, Russia
e-mail: mikhandr@mail.ru

© Springer Nature Switzerland AG 2019
C. C. Adams et al. (eds.), *Knots, Low-Dimensional Topology
and Applications*, Springer Proceedings in Mathematics & Statistics 284,
https://doi.org/10.1007/978-3-030-16031-9_18

363

include the proof of quasirationality for presentations of one-relator pro- p -groups. Section 1.4 will help to understand the motivations for our main result (Theorem 1), elucidating why one should consider it as an analog of Lyndon Identity theorem. We explain the importance of Tannakian philosophy in Sect. 1.5 presenting the construction of “conjurings”.

Let $p \geq 2$ be a prime. We use the standard notations: \mathbb{Z}_p for p -adic integers; \mathbb{Q}_p for rational p -adic numbers; \mathbb{F}_p for the prime field of positive characteristics.

1.1 Pro- p -groups with a Single Defining Relation

By a pro- p -group one calls a group isomorphic to an inverse limit of finite p -groups. This is a topological group (with the topology of inverse limit) which is compact and totally disconnected. For such groups one has a presentation theory similar in many aspects to the combinatorial theory of discrete groups [13, 31].

Let us say that a pro- p -group G is defined by a finite type pro- p -presentation if G is included into an exact sequence

$$1 \rightarrow R \rightarrow F \xrightarrow{\pi} G \rightarrow 1 \quad (1)$$

in which $F = F(X)$ is the free pro- p -group with a finite set X of generators, and R is a closed normal subgroup topologically generated by a finite set Y of elements in F , contained in the Frattini subgroup of F [13, 31].

Let $A = \varprojlim A_\alpha$, where A_α are finite rings, be a profinite ring (typically \mathbb{Z}_p or \mathbb{F}_p in the sequel), we denote by AG the completed group algebra of a (pro- p) group G . By the completed group algebra we understand the topological algebra $AG = \varprojlim A_\alpha[G_\mu]$ [31], where $G = \varprojlim G_\mu$ is a decomposition of the pro- p -group G into an inverse limit of finite p -groups G_μ .

The interest to pro- p -groups in the recent years is related, first of all, to problems which arose in a joint area of noncommutative geometry, topology, analysis, and group theory. They play an important role in papers on the problems of Kadison–Kaplansky [3], Atiyah [15], and Baum–Connes [33]. Let us mention the concept of *cohomological p -completeness* and a program (following from these problems) of studying pro- p -groups whose discrete and continuous cohomologies with coefficients in \mathbb{F}_p are isomorphic [2, Chap. 5], [6].

Complete group rings of pro- p -groups over the field \mathbb{F}_p are complete \mathbb{F}_p -Hopf algebras [30], and pro- p -groups themselves are analogs of Malcev groups in positive characteristics, hence the theory of presentations of pro- p -groups can be considered as two-dimensional p -adic homotopy theory. By p -adic homotopy theory we mean the analog of Quillen’s rational homotopy theory in positive characteristics. Despite the papers published already (for instance [18, 20]), such theory remains mostly conjectural, hence the potential of combinatorial pro- p -group theory is firstly in that we can check rightness of new concepts in application to solving open problems (in particular listed above).

The origins of cohomological and combinatorial theory of pro- p -groups lie in the early papers of J.-P. Serre and J. Tate, and they took the modern form in the monograph [35]. Some important results in discrete group theory arose as analogs of similar statements on pro- p -groups [16]. For example, the celebrated Stallings theorem, stating that a discrete group is free if and only if its cohomological dimension equals one, arose from the analogy, proposed by J.-P. Serre, with the known result from pro- p -group theory [35, Corollary 2, p. 30]. Nevertheless, after first bright successes of the theory such as the Shafarevich theorem on existence of infinite tower of class fields [35, I.4.4, Theorem 2] (proof uses the Golod–Shafarevich inequality [35, I.4.4, Theorem 1]) and the Demushkin–Labute classification of Galois groups of maximal p -extensions of p -adic fields in terms of generators and relations [35, II.5.6], [36], it became clear that the study of pro- p -groups given combinatorially sometimes leads to more complicated structures than in the case of similar discrete presentations. Thus, the first nontrivial question of J.-P. Serre on the structure of relation modules of pro- p -groups with one relation, stated at the Bourbaki seminar 1962/63 [36, 10.2], still waits for a final answer (we expect a counterexample).

Understanding pro- p -groups with one relation $r \in R \subseteq F^p[F, F]$ plays an important role since they potentially may provide examples of nontrivial zero divisors in complete group rings of torsion-free pro- p -groups. Actually, suppose there is $G_r = F/(r)_F$ a pro- p -group with one relation (in the notations (1)) which have no torsion but its cohomological dimension is greater than two. In this situation, $\frac{\partial r}{\partial x_i} \in \mathbb{Z}_p G$ the images of the Fox partial derivatives $\frac{\partial r}{\partial x_i} \in \mathbb{Z}_p F$ with respect to the homomorphism of completed group rings $\mathbb{Z}_p F \rightarrow \mathbb{Z}_p G$ (induced by the homomorphism π from (1)) are divisors of 0 in the completed group ring $\mathbb{Z}_p G$ of the torsion free pro- p -group. Indeed, the Crowell–Lyndon sequence [11, Theorem 2.2] of $\mathbb{Z}_p G$ -modules takes the form

$$0 \rightarrow \pi_2 \rightarrow \mathbb{Z}_p G \xrightarrow{\psi} \mathbb{Z}_p G^{|X|} \rightarrow IG \rightarrow 0,$$

where IG is the augmentation ideal in $\mathbb{Z}_p G$, and $\pi_2 = \ker \psi$. Here ψ is defined by the rule

$$\psi(\alpha) = \left(\alpha \frac{\partial r}{\partial x_1}, \dots, \alpha \frac{\partial r}{\partial x_i}, \dots \right), i = 1 \dots |X| = \dim_{\mathbb{F}_p} H^1(G, \mathbb{F}_p).$$

By the Koch theorem [13, Prop. 7.7], cohomological dimension of a pro- p -group G equals 2 if and only if $\pi_2 = 0$. Therefore the assumption that $cd(G) > 2$ for one-relator pro- p -group is equivalent to the statement that for all $i \in I$ the images of Fox partial derivatives $\frac{\partial r}{\partial x_i} \in \mathbb{Z}_p G$ are right zero divisors of some nontrivial elements of $\mathbb{Z}_p G$.

We can study discrete subgroups $\Gamma \subset G$ (for example, take $\Phi \subset F$ a free discrete subgroups of F and study its images under homomorphism π from (1)), we expect that ordinary group rings $\mathbb{Z}_p[\Gamma]$ of such subgroups could have zero divisors, providing counterexamples to the problems listed above.

1.2 Prounipotent Groups

By an affine group scheme over a field k one calls a representable functor G from the category Alg_k of commutative k -algebras with unit to the category of groups. If G is representable by the algebra $\mathcal{O}(G)$, then as a functor G is given, for any commutative k -algebra A , by the formula

$$G(A) = Hom_{Alg_k}(\mathcal{O}(G), A).$$

We assume that the considered homomorphisms Hom_{Alg_k} take the unit of the algebra $\mathcal{O}(G)$ to the unit of the k -algebra A . The algebra $\mathcal{O}(G)$ representing the functor G is usually called the *algebra of regular functions* of G . The Yoneda lemma implies the anti-equivalence of the categories of affine group schemes and commutative Hopf algebras [39, 1.3]. Let us say that an affine group scheme G is *algebraic* if its Hopf algebra of regular functions $\mathcal{O}(G)$ is finitely generated as the commutative k -algebra.

Definition 1 By a unipotent group over a field k one calls an affine algebraic group scheme G whose Hopf algebra of regular functions $\mathcal{O}(G)$ is conilpotent (or coconnected, for equivalent definitions see [39, 8.3], [38, Proposition 16]). An affine group scheme G is called a prounipotent group if there is a decomposition into inverse limit $G = \varprojlim G_\alpha$ of unipotent groups G_α over the field k .

There is also the well known correspondence between unipotent groups over a field k of characteristics 0 and nilpotent Lie algebras over k , which assigns to a unipotent group its Lie algebra. This correspondence is easily extended to the correspondence between prounipotent groups over k and pronilpotent Lie algebras over k [30, Appendix A.3]. Functoriality of the correspondence enables one, when it is convenient, to interpret problems on unipotent groups in the language of Lie algebras. For example, the image of a closed subgroup under a homomorphism of prounipotent groups will be always a closed subgroup. The main theorems on the structure of normal series, nontriviality of the center of a unipotent group [10, VII, 17] are transferred from the corresponding statements for Lie algebras [34, Part 1, Chap. V, §3]. By the Quillen theorem [30, A.3, Theorem 3.3], reconstruction of the algebra of regular functions $\mathcal{O}(G)$ of a prounipotent group G from the group of k -points $G(k)$ is made through the dual algebra by the formula $\mathcal{O}(G)^* \cong \widehat{k}G(k)$, where $\mathcal{O}(G)^* = Hom_k(\mathcal{O}(G), k)$ and $\widehat{k}G(k)$ is the group algebra completed with respect to the augmentation ideal. Recall also that $G(k) \cong \mathcal{G}\mathcal{O}(G)^*$ [38, Prop. 18], where \mathcal{G} is the functor of group-like elements in CHA. By the Campbell–Hausdorff formula [34, Part 1, Chap. IV, §7], [30, A.1] we have $G(k) = exp\mathcal{P}\mathcal{O}(G)^*$, $\mathcal{P}\mathcal{O}(G)^* = log\mathcal{G}\mathcal{O}(G)^*$, where \mathcal{P} is the functor of primitive elements, which gives the associated Lie algebra of G .

Let A be a Hopf algebra over a field k of characteristics 0, in which: (1) the product is commutative; (2) the coproduct is conilpotent. Then, as an algebra, A is isomorphic to a free commutative algebra [4, Theorem 3.9.1]. Thus, A is the algebra of functions on an affine space, and we can use results from the theory of linear algebraic groups in characteristics 0.

As in [9, 2], let us call by the Zariski closure of a subset $S \subseteq G(k)$ the least affine subgroup H in G such that $S \subseteq H(k)$ is the inverse limit $\varprojlim H_\alpha$, where we have denoted by H_α the closure of the image of S in $G_\alpha(k)$.

Pro- p -groups are \mathbb{F}_p -points of pronilpotent affine group schemes defined over the field \mathbb{F}_p . Indeed, consider the complete group algebra $\mathbb{F}_p G = \varprojlim \mathbb{F}_p[G_\alpha]$ of a pro- p -group $G = \varprojlim G_\alpha$, where G_α are finite p -groups. Each group algebra $\mathbb{F}_p[G_\alpha]$ is obviously a cocommutative Hopf algebra over the field \mathbb{F}_p . Then the dual Hopf algebra $\mathbb{F}_p[G_\alpha]^*$ [26, 3] is a finitely generated commutative Hopf algebra, and therefore it defines certain affine algebraic group scheme. Let \mathcal{G} be the functor of group like elements of a Hopf algebra. Note that [38, Proposition 18]

$$G_\alpha = \mathcal{G}\mathbb{F}_p[G_\alpha] \cong \text{Hom}_{\text{Alg}_{\mathbb{F}_p}}(\mathbb{F}_p[G_\alpha]^*, \mathbb{F}_p),$$

where $\text{Hom}_{\text{Alg}_{\mathbb{F}_p}}(\mathbb{F}_p[G_\alpha]^*, _)$ is the functor from the category of commutative \mathbb{F}_p -algebras with unit to the category of sets which assigns to each commutative \mathbb{F}_p -algebra A with unit the set $\text{Hom}_{\text{Alg}_{\mathbb{F}_p}}(\mathbb{F}_p[G_\alpha]^*, A)$ of homomorphisms $\phi : \mathbb{F}_p[G_\alpha]^* \rightarrow A$ of commutative \mathbb{F}_p -algebras with unit. But

$$G \cong \mathcal{G}\mathbb{F}_p G \cong \varprojlim \mathcal{G}\mathbb{F}_p[G_\alpha] \cong \varprojlim \text{Hom}_{\text{Alg}_{\mathbb{F}_p}}(\mathbb{F}_p[G_\alpha]^*, \mathbb{F}_p) \cong \text{Hom}_{\text{Alg}_{\mathbb{F}_p}}(\mathbb{F}_p G^\vee, \mathbb{F}_p),$$

where $\mathbb{F}_p G^\vee$ is the continuous dual of $\mathbb{F}_p G$ [38], [26, 3.1] (which is the commutative Hopf algebra representing the functor).

Since the action of a finite p -group G on a \mathbb{F}_p -vector space V of a finite dimension say n always has a fixed point, then there is a basis of V such that $G \hookrightarrow U(n)$ (see the proof of ‘‘Kolchin theorem’’ [39, Theorem 8.2]). It remains to note, that the corresponding affine algebraic group scheme represented by the commutative Hopf algebra $\mathbb{F}_p[G]^* = \mathbb{F}_p[G]^\vee$ is unipotent [39, Theorem 8.3] and therefore it is pronilpotent if G is a pro- p -group.

1.3 QR-Presentations and Their Schematization

For discrete groups, $p \geq 2$ will run over all primes, and for pro- p -groups p is fixed. Let G be a (pro- p)group with a finite type (pro- p)presentation (1), $\overline{R} = R/[R, R]$ be the corresponding relation module, where $[R, R]$ is the commutator, and the action of G is induced by conjugation of F on R . For each prime number $p \geq 2$ denote by Δ_p the augmentation ideal of the ring $\mathbb{F}_p G$. In the pro- p -case, by Δ^n we understand the closure of the module generated by n th powers of elements from $\Delta = \Delta_p$, and in the discrete case it is the n th power of the ideal Δ_p [28]. The properties of this filtration in the pro- p -case are exposed in [13, 7.4]; in the discrete case, the properties of the Zassenhaus filtration are similar [28, Chap. 11], the difference is in the use of the usual group ring instead of the complete one.

Denote by $\mathcal{M}_n, n \in \mathbb{N}$ its Zassenhaus p -filtration in F with coefficients in the field \mathbb{F}_p , defined by the rule $\mathcal{M}_{n,p} = \{f \in F \mid f - 1 \in \Delta_p^n\}$. We shall denote these filtrations simply by \mathcal{M}_n , omitting p , since its choice will be always clear from the context. Let us introduce the notation $\mathbb{Z}_{((p))}$ for \mathbb{Z} in the case of discrete groups and for \mathbb{Z}_p in the case of pro- p -groups.

Definition 2 We shall call presentation (1) quasirational (QR -presentation) if one of the following three equivalent conditions holds:

- (i) for each $n > 0$ and for each prime $p \geq 2$, the $F/R\mathcal{M}_n$ -module $R/[R, R\mathcal{M}_n]$ has no p -torsion (p is fixed for pro- p -groups and runs over all prime numbers $p \geq 2$ and the corresponding Zassenhaus p -filtrations in the discrete case).
- (ii) the quotient module of coinvariants $\bar{R}_G = \bar{R}_F = R/[R, F]$ is torsion free.
- (iii) $H_2(G, \mathbb{Z}_{((p))})$ is torsion free.

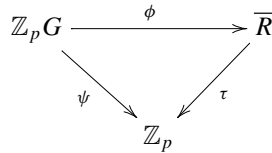
Proof of equivalence of conditions (i)–(iii) is contained in [24, Proposition 4] and [25, Proposition 1]. QR -presentations are curious in particular by the fact that they contain aspherical presentations of discrete groups and their subpresentations, and also pro- p -presentations of pro- p -groups with one relation. For the sake of completeness we present the proof of quasirationality for one-relator pro- p -groups.

Proposition 1 A pro- p -presentation (1) of a pro- p -group G with one relator is quasirational.

Proof First note, that $R = (r)_F$ has a basis I converging to 1, which consist of elements ${}^f r = f^{-1}rf, \{f\} \in F$ and also contain r . Indeed, since F is finitely generated pro- p -group it has a countable basis of neighbourhood of identity which consist of open normal subgroups [13, 7.4], say U_n and $F \cong \varprojlim_{n \in \mathbb{N}} F/U_n$. Since R is the closed subgroup of F , then subgroups $R \cap U_n \trianglelefteq R$ are the countable basis of neighborhood of identity of R and $R \cong \varprojlim_{n \in \mathbb{N}} R/R \cap U_n$. Since elements ${}^f r = f^{-1}rf, f \in F$ generate R , then their images will generate the quotient $R \twoheadrightarrow R/R \cap U_n$ and we can always choose minimal set of generators among such images (it is enough to take a basis in the quotient of $R/R \cap U_n$ by Frattini subgroup which is the \mathbb{F}_p -vector space containing the image of r and then lift it as in [31, Corollary 7.6.10]), we can always assume that the image of r is not identity in $R/R \cap U_n$ by taking $n \in \mathbb{N}$ sufficiently large (see also [31, 7.6–7.8] for details). We shall denote such minimal system of generators by I_n . It is straightforward to lift I_n to the system of generators I_{n+1} of $R/R \cap U_{n+1}$ with the same properties and therefore (I_n, ϕ_n^{n+1}) , where $\phi_n^{n+1} : I_{n+1} \twoheadrightarrow I_n$ are projections, is the inverse system. It turns out that $I = \varprojlim_{n \in \mathbb{N}} I_n$ is the convergent basis (since it is minimal by construction and convergent to 1 by construction as well).

Now we consider \bar{I} the image of I under the homomorphism of Abelianization $R \twoheadrightarrow \bar{R} = R/[R, R]$. \bar{I} is the basis of free Abelian pro- p -group \bar{R} (as a consequence of [31, 7.6.9]), \bar{I} is also convergent to 0 since I is convergent to 1. Since R acts trivially on \bar{R} we see that elements of \bar{I} could be written in the form ${}^g \bar{r}, g = \bar{f} = \pi(f) \in G$, where we denote \bar{r} the image of r in \bar{R} .

Now we shall prove that $R/[R, RF] \cong \mathbb{Z}_p$. Indeed, the map $\tau_{\bar{I}}$ of \bar{I} into \mathbb{Z}_p which sends \bar{I} into one point (the topological generator 1 of \mathbb{Z}_p) is continuous and convergent to identity in \mathbb{Z}_p [31, 3.3]. Therefore the universal property of free Abelian pro- p -group \bar{R} [31, Lemma 3.3.4] gives the extension of $\tau_{\bar{I}}$ to the epimorphism of pro- p -groups $\tau : \bar{R} \twoheadrightarrow \mathbb{Z}_p$, which sends the basis $\bar{I} = \langle {}^s\bar{r}, \{g\} \in G \rangle$ of \bar{R} into the element $\psi(1), 1 \in G$, where $\psi : \mathbb{Z}_p G \rightarrow \mathbb{Z}_p$ be the map of taking coinvariants.

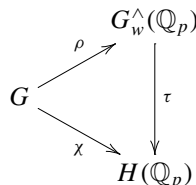


The composition of τ and ϕ ($\phi(1) = \bar{r}$) equals ψ as the homomorphism of free Abelian pro- p -groups (we regard $\mathbb{Z}_p G$ as free Abelian pro- p -group with G as the basis convergent to 0). Since ϕ is epi, then τ must be G -module homomorphism. Indeed, finite sums $a = \sum_{i \in I} a_i {}^{g_i}\bar{r}$ generate the dense subgroup of \bar{R} , and therefore the identities $\tau(g \cdot a) = g \cdot \tau(a)$ imply that τ is the module homomorphism (for profinite modules one should know the action on its finite factors):

$$\begin{aligned}
 g \cdot \tau(a) &= \tau(a) = \sum_{i \in I} a_i \\
 \tau(g \cdot a) &= \tau\left(g \cdot \sum_{i \in I} a_i \cdot {}^{g_i}\bar{r}\right) = \tau\left(\sum_{i \in I} a_i \cdot {}^{g \cdot g_i}\bar{r}\right) = \\
 & \text{(commutativity of the diagram)} = \psi\left(\sum_{i \in I} a_i (g \cdot g_i)\right) = \sum_{i \in I} a_i.
 \end{aligned}$$

We have proved that there is the $\mathbb{Z}_p G$ -module epimorphism $\tau : R/[R, F] \twoheadrightarrow \mathbb{Z}_p$. But since \bar{R} is generated as $\mathbb{Z}_p G$ -module by the single element \bar{r} , then $R/[R, F]$ is generated by the single element (the image of \bar{r}) as the \mathbb{Z}_p -module and therefore $R/[R, F] \cong \mathbb{Z}_p$.

Definition 3 ([9, A.2.]) Let us fix a group G (with the pro- p -topology). Define the (continuous) pronipotent completion of G as the following universal diagram, in which ρ is a (continuous) Zariski dense homomorphism from G to the group of \mathbb{Q}_p -points of a pronipotent affine group G_w^\wedge :



We require that for each continuous and Zariski dense homomorphism $\chi : G \rightarrow H(\mathbb{Q}_p)$, where H be a prounipotent affine group scheme, there exist a unique homomorphism τ of prounipotent groups, making the diagram commutative.

If we consider a finitely generated free group $F(X)$, then, as it is easy to see, its continuous prounipotent completion possesses the universal properties inherent to a free object [26, Sect. 2], and by analogy with the discrete or pro- p cases, we shall call such prounipotent group free and denote it by $F_u(X)$. Interesting relations between completions in positive and zero characteristics are obtained in [29].

In simplicial group theory, by analogy with gluing two-dimensional cells, it is convenient to identify presentation (1) with the second step of construction of free simplicial (pro- p) resolution F_\bullet of a (pro- p)group G by the “pas-à-pas” method going back to Andre [1]:

$$\begin{array}{c} \rightrightarrows \\ \rightrightarrows \end{array} F(X \cup Y) \begin{array}{c} \xleftarrow{s_0} \\ \xrightarrow{d_0} \\ \xrightarrow{d_1} \\ \longrightarrow \end{array} F(X) \longrightarrow G, \tag{2}$$

here d_0, d_1, s_0 for $x \in X, y \in Y, r_y \in R$ are defined by the identities $d_0(x) = x, d_0(y) = 1, d_1(x) = x, d_1(y) = r_y, s_0(x) = x$.

Recall [26] that (2) is a free finite type simplicial (pro- p) group, degenerate in dimensions greater than two. If the pro- p -presentation (1) is minimal, then

$$|Y| = \dim_{\mathbb{F}_p} H^2(G, \mathbb{F}_p), |X| = \dim_{\mathbb{F}_p} H^1(G, \mathbb{F}_p).$$

Let us assign to a finite type simplicial presentation (2) a presentation of prounipotent groups as follows (this construction will be called below by the schematization of a presentation). First, consider the corresponding diagram of group rings

$kF(X \cup Y) \begin{array}{c} \xleftarrow{s_0} \\ \xrightarrow{d_0} \\ \xrightarrow{d_1} \\ \longrightarrow \end{array} kF(X)$. Then we obtain from (2), taking into account finite generation of groups, using the I -adic completion, the following diagram of complete linearly compact Hopf algebras:

$$\widehat{kF(X \cup Y)} \begin{array}{c} \xleftarrow{s_0} \\ \xrightarrow{d_0} \\ \xrightarrow{d_1} \\ \longrightarrow \end{array} \widehat{kF(X)},$$

where $\widehat{kF(X)} = \varprojlim kF(X)/I^n$, I is the augmentation ideal in $kF(X)$. Applying continuous duality (we mention that some authors [38] also use the term “Pontryagin duality” for the duality between discrete and linearly compact vector spaces, this duality always assumes the discrete topology of the base field) and antiequivalence of the categories of commutative Hopf algebras and affine group schemes, we obtain the diagram of free prounipotent groups

$$F_u(X \cup Y) \begin{array}{c} \xleftarrow{s_0} \\ \xrightarrow{d_0} \\ \xrightarrow{d_1} \\ \longrightarrow \end{array} F_u(X).$$

Definition 4 Let us say that we are given a finite type presentation of a prounipotent group G_u if there exist finite sets X and Y such that G_u is included into the following diagram of free prounipotent groups:

$$F_u(X \cup Y) \begin{array}{c} \xleftarrow{s_0} \\ \xrightarrow{d_0} \\ \xrightarrow{d_1} \end{array} F_u(X) \longrightarrow G_u, \tag{3}$$

in which the identities similar to (2) and $G_u \cong F_u(X)/d_1(\ker d_0)$ hold.

Denote $R_u = d_1(\ker d_0)$, this is a normal subgroup in $F_u(X)$, and hence we obtain the analog of the notion of presentation (1) for a prounipotent group G_u , to which we shall refer also, for uniformity, as to a presentation of type (1).

By analogy with the discrete and pro- p cases, the set of rational points of the relation module $\overline{R}_u(\mathbb{Q}_p) = R_u/[R_u, R_u](\mathbb{Q}_p) \cong R_u(\mathbb{Q}_p)/[R_u(\mathbb{Q}_p), R_u(\mathbb{Q}_p)]$ of the prounipotent presentation (3) is endowed with a structure of topological $\mathcal{O}(G_u)^*$ -module [26, Prop. 3.13].

$\mathcal{O}R$ -presentations can be studied by passing to the rationalized completion $\overline{R} \widehat{\otimes}_{\mathbb{Q}_p} = \varprojlim_n R/[R, R\mathcal{M}_n] \otimes \mathbb{Q}_p$. It turns out [26, Lemma 3.14] that the topological \mathbb{Q}_p -vector space $\overline{R} \widehat{\otimes}_{\mathbb{Q}_p}$ is identified with $\overline{R}_w^\wedge(\mathbb{Q}_p)$ (where \overline{R}_w^\wedge is the Abelianization of R_w^\wedge which has been introduced in Definition 3) and one can define on it the structure of topological G -module (Definition 5 below), where G is the pro- p -group given by the pro- p -presentation (1). Moreover, these modules can be included into the exact sequence related with the prounipotent module of relations [26, Theorem 3.16].

1.4 Relation Modules of Prounipotent Groups

The celebrated Lyndon Identity theorem states that the relation modules of a discrete group with one defining relation is induced from a cyclic subgroup. That is, let (1) be a presentation of a group with one relation, then

$$\overline{R} = R/[R, R] \cong \mathbb{Z} \otimes_{\langle u \rangle} \mathbb{Z}G,$$

where $R = (u^m)_F$ and u is not a nontrivial power, $\langle u \rangle$ —the cyclic subgroup generated by u .

Presentations of pro- p -groups with one relation such that their $\text{mod}(p)$ modules of relations $\overline{R}/p\overline{R} = R/R^p[R, R]$ are induced, $R/R^p[R, R] \cong \mathbb{F}_p \otimes_{\langle u \rangle} \mathbb{F}_p G$, are (of course) permutational in the sense of the paper [22] (see also [25, Def. 4]), i.e. $\overline{R}/p\overline{R} = R/R^p[R, R] \cong \mathbb{F}_p(T, t_0)$, where (T, t_0) is a profinite G -space with a marked point. O.V. Melnikov shows [22, Theorem 3.2] that relation modules of aspherical pro- p -groups with one defining relation are induced from cyclic subgroups, as in the Lyndon Identity theorem.

In [36, 10.2] J.-P. Serre asks: “Let $r \in F^p[F, F]$, and let $G_r = F/(r)_F$. Can one extend to G_r the results proved by Lyndon in the discrete case?”

We see that this question (in the modern settings of [22]) is equivalent to the following one: “Is it true that relation modules of pro- p -groups with one defining relation are permutational?”

If the answer to this question were true, then each pro- p -group with one relator, such that in its presentation (1) the normal subgroup $R = (r)_F$ is not generated by a p -th power, would have, by [22, Theorem 3.2], cohomological dimension 2.

Shift of dimension enables one to calculate cohomology of a pro- p -group H as invariants of certain modules. From the viewpoint of the category of representations, in order to look similar to a group with elements of finite order, it suffices for the elements of the group H to act as elements of finite order, although these elements can be actually not of finite order. Using multiplication of the defining relator $r = y^p$ in the free pro- p -group by elements ζ^p of special kind, in the next subsection we shall obtain the defining relations $y^p \cdot \zeta^p$, which act on finite dimensional modules of arbitrarily high given dimension exactly as the initial relation r , but are not p th powers themselves. This observation is in favor of the assumption that pro- p -groups with one relator, which are not generated by a p -th power, in contrast to the discrete case, can have cohomological dimension greater than 2.

Nevertheless, we can construct, as in Sect. 1.3, schematization of a pro- p -presentation (3) (for details see [26, 3.1]). For such prounipotent presentation we shall prove the following prounipotent analog of Lyndon’s result, which can be interpreted as an answer to Serre’s question [36, 10.2]. We need the following definition [26, 3.12].

Definition 5 Let A be a complete linearly compact Hopf algebra over a field k (the field is considered with discrete topology). By a left (or equivalently right) complete topological A -module we shall call a linearly compact topological k -vector space M with a structure of A -module such that the corresponding k -linear action $A \widehat{\otimes} M \rightarrow M$ is continuous. We assume that the topology on M is given by a fundamental system of neighborhoods of zero $M = M^0 \supseteq M^1 \supseteq M^2 \supseteq \dots$, where M^j are topological A -submodules in M of finite codimension (finiteness of type) and $M \cong \varprojlim M/M^j$. By a homomorphism of topological A -modules one calls a continuous A -module homomorphism.

If the filtration M^j admits a compression such that for each j the compression quotients $M_i^{j_i} / M_{i+1}^{(j+1)_i}$ are trivial A -modules (i.e. the action of A is trivial), then we shall call such topological A -module prounipotent.

In what follows, prounipotent topological modules will take its origin from presentations of a prounipotent groups G acting by conjugations on its normal subgroup. And we use the I -adic filtration, that is $M^j = I^j \cdot M$, where by I^j we denote close of the powers of augmentation ideal of $A = \mathcal{O}(G)^*$ and M^j are topological (closed) submodules of M generated by elements of the form $a \cdot m$, where $a \in I^j, m \in M$ [26, Prop. 3.12].

Theorem 1 (Identity theorem for pro- p -groups) *Let G be a pro- p -group with one defining relation given by a finite presentation (1) in the category of pro- p -groups. Then one has the isomorphism of prounipotent left topological $\mathcal{O}(G_u)^*$ -modules $\overline{R_u}(\mathbb{Q}_p) \cong \mathcal{O}(G_u)^*$, where the prounipotent groups G_u and $\overline{R_u}$ are obtained from the schematization of the initial pro- p -presentation.*

The analogy with the celebrated Lyndon Identity theorem comes from the fact that if the natural homomorphism $G \rightarrow G_u(\mathbb{Q}_p)$ is embedding then G generates $\mathcal{O}(G_u)^*$ as the topological vector space and therefore should be considered as a permutational basis of $R_u(\mathbb{Q}_p)$ [26, Prop. 3]. We can always identify G_u with the continuous \mathbb{Q}_p -prounipotent completion of G [26, (3.3)]. Theorem 1 has been announced in [23, Cor. 12] and used in [26, Prop. 3, Cor. 3] for proof of the criterion of cohomological dimension equal to 2, providing a relation with the known group theory results (see [8, 14, 32, 37] and other papers cited there). Let us recall the results of [26, Prop. 3.19, Cor. 3.21], since they shed light on the following Serre’s question from [36].

Let $G_r = F/(r)_F$, where $(r)_F$ is the normal closure of $r \in F^p[F, F]$ in a free pro- p -group F of finite rank, then J.-P. Serre asks: “Can it be true that $cd(G_r) = 2$, if only G_r is torsion free (and $r \neq 1$)?”

By the well known Malcev theorem, a finitely generated discrete nilpotent group without torsion is embedded [38, 4] into its rational prounipotent completion. For \mathbb{F}_p -prounipotent groups, whose instances are pro- p -groups, it would be too optimistic to hope for a similar statement (there are counterexamples in [26]), however we have

Proposition 2 ([26, Prop. 3.19]) *Let G be a finitely generated pro- p -group given by presentation (1) with one defining relation $r \neq 1$, and assume that the natural homomorphism from G to the group of \mathbb{Q}_p -points $G_w^\wedge(\mathbb{Q}_p)$ of its prounipotent completion is an embedding, then $cd(G) = 2$.*

For given discrete or pro- p -groups G_1 and G_2 , where G_1 (typically G_1 is finitely generated) acts on G_2 . We shall call the action **prounipotent** [26] if there exists a chain $\{N_i\}_{i \in \mathbb{N}}$ of G_1 -invariant normal subgroups in G_2 with Abelian graded quotients, such that $\bigcap N_i = 1$, N_i/N_{i+1} have no torsion, finitely generated and the induced action of G_1 is trivial on graded quotients N_i/N_{i+1} .

We shall say that a finitely generated pro- p -group G is **p -regular** if the conjugation action of G on itself is prounipotent.

The following Corollary 3 generalizes and explains group theory results (see, for instance [14, 32]), where absence of zero divisors in graded algebras of special filtrations has been used. If finitely generated pro- p -group G has some central filtration G_i with torsion free factors, then G/G_i are nilpotent and therefore G is p -regular. It turns out, that p -regularity imply the required embedding $G \hookrightarrow G_w^\wedge(\mathbb{Q}_p)$ from Proposition 2.

Proposition 3 ([26, Cor. 3.21]) *Let G be a p -regular pro- p -group with one relation, then $cd(G) = 2$.*

1.5 Tannaka Duality and Conjurings

Let $\omega : Rep_k(G) \rightarrow Vec_k$ be the erasing functor from the category of representations of an affine group scheme G to the category of vector spaces. Then by definition elements of $Aut^{\otimes}(\omega)(A)$, for any k -algebra A , are families (λ_X) , $X \in ob(Rep_k(G))$, where (λ_X) are A -linear automorphisms of A -modules $X \otimes A$ such that

- (i) $\lambda_{X \otimes Y} = \lambda_X \otimes \lambda_Y$.
- (ii) $\lambda_1 = id_A$.
- (iii) $\lambda_Y \circ (\alpha \otimes 1) = (\alpha \otimes 1) \circ \lambda_X$ for any G -equivariant k -linear maps $\alpha : X \rightarrow Y$.

The Tannaka duality establishes [5, Prop. 2.8] the isomorphism of functors $G \rightarrow Aut^{\otimes}(\omega)$ on the category of k -algebras. Thus, an affine group scheme can be reconstructed from its category of representations, and hence the properties of an affine group scheme are determined by its representations.

Pro- p -groups are \mathbb{F}_p -points of prounipotent \mathbb{F}_p -group schemes Sect. 1.2. Our conjecture states that among pro- p -groups G with one relator, which are not embedded into their prounipotent completions, there are those which are torsion free but $cd(G) > 2$. It turns out that one can hide torsion of relations without changing the behavior of any unipotent representation $F \rightarrow GL_n(\mathbb{Q}_p)$ and $F \rightarrow GL_n(\mathbb{F}_p)$ for arbitrarily large fixed $n \in \mathbb{N}$. To be more precise, one has the following

Theorem 2 *Let $r = w^{p^l}$, $l \in \mathbb{N}$ be an element of the free pro- p -group $F = F_p(d)$ of rank $d \geq 2$ which is a p^l th power and fix $n \in \mathbb{N}$. Then there exist elements $z_n \in F$ (“conjurings”) with the following properties:*

- (a) *for any unipotent representations $\phi : F \rightarrow GL_n(\mathbb{Q}_p)$ and $\psi : F \rightarrow GL_n(\mathbb{F}_p)$, one has $\phi(z_n) = 1$, $\psi(z_n) = 1$.*
- (b) *$r \cdot z_n^p$ is not a p th power.*

In Sect. 4 we give, following the ideas of [19], a construction of Magid identities for free prounipotent groups over p -adic fields of zero characteristics and prove Theorem 2. In the presented article only the construction of conjurings is described, we plan to return to applications in subsequent works.

2 Cohomology and Presentations

Cohomology theory of prounipotent groups over the algebraically closed field k has been developed by Lubotzky and Magid [17], when k has zero characteristics. This theory closely parallels that of the cohomology of pro- p -groups [35, I, 4]: the free prounipotent groups turn out to be those of cohomological dimension ones, the dimension of the first and second cohomology groups give numbers of generators and defining relations. In addition, authors have proved that one-relator prounipotent groups turn out to have cohomological dimension two, similar to discrete one-relator

groups defined by relations r which are not powers $r \neq u^k$. Schematization leads to pronipotent groups over not algebraically closed fields ($k = \mathbb{Q}_p$ in our case) and hence we want to develop a similar theory. As was rigorously pointed out the author by Richard Hain, nothing new in this case can happen. Indeed, let k be a non algebraically closed field of zero characteristics with algebraic closure \bar{k} and consider unipotent group G_k over k . We already know that $G(k) \cong k^\alpha$ for some $\alpha \in \mathbb{N}$ and [39, 4.1] imply that the closure $G_{\bar{k}}$ of G_k in \bar{k}^α is just \bar{k}^α . It turns out that $\mathcal{O}(G_{\bar{k}}) \cong \mathcal{O}(G_k) \otimes_k \bar{k}$ and [12, Proposition 4.18] imply that $H^*(G_{\bar{k}}, \bar{k}) \cong H^*(G_k, k) \otimes_k \bar{k}$. Below we introduce necessary notions for defining Hochschild cohomology groups of affine group schemes in the modern setting [12]. In the case of algebraically closed field they coincide [12, p. 28] with the ones defined in [17].

2.1 Modules and Cohomology

Let G be an affine group scheme over a field k , and let $Rep(G)$ be the corresponding category of left G -modules [12, I, 2.7, 2.8], identified using the Yoneda lemma with the category of left $\mathcal{O}(G)$ -comodules [12, I, 2.8]. Each G -module M is representable as the inductive limit of its finite dimensional submodules [12, I, 2.13(1)].

Recall, following [12, I, 2.2], that a finite-dimensional module over k gives rise to the group-valued functor on commutative k -algebras. To this end, let us define for each finite dimensional k -vector space M certain k -group functor M_a by the rule $M_a(A) = (M \otimes A, +)$ for all k -algebras A . In our case, namely when k is a field, and dimension of M is finite, M_a is representable by the symmetric algebra of the dual k -module M^* , which we denote by $S(M^*)$, then $\mathcal{O}(M_a) = S(M^*)$ [27, 3.6], therefore M_a is an affine group scheme.

Denote by $Mor(G, M_a)$ the k -vector space of natural transformations of set valued functors. On $Mor(G, M_a)$ one has left regular action of G , given by the formula $(x \cdot f_R)(g) = f_R(gx)$, where $g \in G(R)$, $f_R \in Mor(G(R), M_a(R))$, $x \in G(R)$. Let us introduce also right regular action, given by the formula $f_R \cdot x = f_R(xg)$. If $M = k_a$ is the additive group of the field k [27, 3.1], then $Mor(G, k_a) \cong \mathcal{O}(G)$ is the coordinate ring of the affine group scheme G [27, 2.15]. For constructing injective envelopes we shall need the notion of induced module. Thus, let H be a subgroup of the affine group scheme G . For each H -module M define the induced module $M \uparrow_H^G$ as follows:

$$M \uparrow_H^G = \{f \in Mor(G, M_a) \mid f(gh) = h^{-1} f(g), \forall g \in G(A), h \in H(A), A \in Alg_k\},$$

where G acts regularly on the left. In [12, I, 3.3], using the identification $M \uparrow_H^G \cong (M \otimes \mathcal{O}(G))^H$, $M \otimes \mathcal{O}(G)$ is endowed with a structure of $(G \times H)$ -module, where the left action of H on M is given, and the action on $\mathcal{O}(G)$ is through the right regular representation; G acts on M_a trivially and on $\mathcal{O}(G)$ from the left through the left regular representation; one takes the tensor product of representations, and it is

shown that $M \uparrow_H^G$ is indeed the left G -module. From now and on we do not specify which G -module structure (left or right) is used since the theories are equivalent.

For arbitrary k -module M , let $\varepsilon_M : M \otimes \mathcal{O}(G) \rightarrow M$ be a linear map $\varepsilon_M = id_M \otimes \varepsilon_G$.

Proposition 4 (Frobenius Reciprocity) [12, I, 3.4] *Let H be a closed subgroup of an affine group scheme G and M be an H -module.*

- (a) $\varepsilon_M : M \uparrow_H^G \rightarrow M$ is a homomorphism of H -modules
- (b) For each G -module N the map $\varphi \mapsto \varepsilon_M \circ \varphi$ defines an isomorphism

$$Hom_G(N, M \uparrow_H^G) \cong Hom_H(N \downarrow_H^G, M).$$

Proposition 5 (The Tensor Identity) [12, I, 3.6] *Let H be a closed subgroup of an affine group scheme G and M be an H -module. If N is a G -module, then there is a canonical isomorphism of G -modules*

$$(M \otimes N \downarrow_H^G) \uparrow_H^G \cong M \uparrow_H^G \otimes N.$$

Following [12, I, 3.7], let us discuss some useful corollaries from the propositions given above. Assume that $H = 1$, then $M \uparrow_1^G = M \otimes \mathcal{O}(G)$, for any k -module M , and in particular $k \uparrow_1^G = \mathcal{O}(G)$.

Combining the latter identity with the Frobenius reciprocity (b) we obtain, for each G -module M ,

$$Hom_G(M, \mathcal{O}(G)) \cong M^*.$$

If we put $M = k_a$ in the tensor identity, then for each G -module N we obtain the remarkable isomorphism

$$N \otimes \mathcal{O}(G) \cong N \uparrow_1^G = N_{tr} \otimes \mathcal{O}(G),$$

given by the formula $x \otimes f \mapsto (1 \otimes f) \cdot (id_N \otimes \sigma_G) \circ \Delta_N(x)$, where we have denoted by N_{tr} the k -module N with the trivial action of G , and σ_G is the antipode in $\mathcal{O}(G)$.

We shall need M^G , the submodule of fixed points of a G -module M :

$$M^G = \{m \in M \mid g(m \otimes 1) = m \otimes 1, \forall g \in G(A), A \in Alg_k\}.$$

If in the definition we take $g = id_{\mathcal{O}(G)} \in G(\mathcal{O}(G))$, then we obtain

$$M^G = \{m \in M \mid \Delta_M(m) = m \otimes 1\}.$$

We remind also, that the regular representation of an affine group scheme G arise from comultiplication

$$\Delta : \mathcal{O}(G) \rightarrow \mathcal{O}(G) \otimes \mathcal{O}(G).$$

Let H is a closed subgroup of G , then $\mathcal{O}(H) = \mathcal{O}(G)/I_H$, where I_H is the Hopf ideal defining the subgroup H , and let M be a G -module, whence we obtain the k -linear map

$$\mu : M \rightarrow \mathcal{O}(G) \otimes M \rightarrow \mathcal{O}(H) \otimes M$$

which defines the H -module structure on M .

Since the category of G -modules is Abelian [12, I, 2.9] and since, due to [12, I, 3.9], it contains enough injective objects, one can define cohomology groups $H^n(G, M)$ of an affine group scheme G with coefficients in a G -module M as the n th derived functors of the fixed points functor $()^G$ computed for M . Note the possibility of computing $H^n(G, M)$ by means of the Hochschild complex $C^*(G, M)$ [12, I, 4.14].

Cohomology well behaves with respect to limits. Let us represent the affine group scheme G as $G \cong \varinjlim G_\alpha$, where G_α are affine algebraic group schemes. Since $\mathcal{O}(G) \cong \varinjlim \mathcal{O}(G_\alpha)$ and each G -module V can be represented as a direct limit of its finite-dimensional G -submodules $V = \varinjlim V_\beta$, we can construct (using V_β and $\mathcal{O}(G_\alpha)$) following [5, Prop. 2.3, 2.6] or [39, 3.3] a direct system V_γ of finite dimensional G_γ -submodules, where G_γ are also affine algebraic group schemes, such that $\mathcal{O}(G) \cong \varinjlim \mathcal{O}(G_\gamma)$, $V = \varinjlim V_\gamma$. Then $(V \otimes \mathcal{O}(G)^{\otimes n})^G \cong \varinjlim (V_\gamma \otimes \mathcal{O}(G_\gamma)^{\otimes n})^{G_\gamma}$. Homology commutes with direct limits, therefore

$$H^n(G, V) \cong \varinjlim H^n(G_\gamma, V_\gamma).$$

Note that pro- p -groups can be considered as \mathbb{F}_p -points of pronunipotent groups over the field \mathbb{F}_p (for constructing the \mathbb{F}_p -Hopf algebra it suffices to consider the decomposition of the \mathbb{F}_p -group ring of a pro- p -group into the inverse limit of the group rings of finite p -groups, consider the dual Hopf algebras, and take their direct limit), then cohomology groups of a pro- p -group in the sense of [31, 6.6] with coefficients in discrete module coincide with the cohomology of the corresponding affine group scheme (just explore the Hochschild complex).

Proposition 6 ([17, 1.10]) *Let $1 \rightarrow H \rightarrow K \rightarrow G \rightarrow 1$ be an exact sequence of affine group schemes, and let M be a G -module. Then there exists a spectral sequence with the initial term $E_2^{p,q} = H^p(G, H^q(H, N))$, converging to $H^{p+q}(K, M)$.*

In the case the affine group scheme G is pronunipotent, there is a more precise description of injective modules.

Proposition 7 ([17, 1.11]) *Let G be a pronunipotent group, and let V be a G -module. Then $V^G \otimes \mathcal{O}(G)$ is an injective G -module containing V . Each injective G -module containing V contains a copy of $V^G \otimes \mathcal{O}(G)$.*

Due to the previous statement we can define the injective envelope of a G -module V by the formula $\mathcal{E}_0(V) = V^G \otimes \mathcal{O}(G)$. Put $\mathcal{E}_{-1}(V) = V$, and let $d_{-1} : \mathcal{E}_{-1}(V) \rightarrow \mathcal{E}_0(V)$ be the corresponding inclusion.

Proposition 8 ([17, 1.12]) *Let G be a pronunipotent group and V be a G -module. Define the minimal resolution $\mathcal{E}_i(V)$ and $d_i : \mathcal{E}_i(V) \rightarrow \mathcal{E}_{i+1}(V)$ inductively,*

$$\mathcal{E}_{i+1}(V) = \mathcal{E}_0 \left(\frac{\mathcal{E}_i(V)}{d_{i-1}(V)} \right) \quad d_i = \mathcal{E}_i(V) \rightarrow \frac{\mathcal{E}_i(V)}{d_{i-1}(\mathcal{E}_{i-1}(V))} \rightarrow \mathcal{E}_{i+1}.$$

Then $\{\mathcal{E}_i(V), d_i\}$ is an injective resolution of V and $H^i(G, V) = \mathcal{E}_i(V)^G$.

We shall say that an affine group scheme G has cohomological dimension n and write $cd(G) = n$, if for any G -module V and for each $i > n$, $H^i(G, V) = 0$ and $H^n(G, V) \neq 0$. If G is prounipotent, then $cd(G) \leq n$ if and only if $H^{n+1}(G, k_a) = 0$, since k_a is the only simple G -module.

Proposition 9 ([17, 1.14]) *Let G be a prounipotent group and H be a subgroup. For any H -module V there is an isomorphism $H^n(G, V \uparrow_H^G) \cong H^n(H, V)$ for all $n \in \mathbb{N}$. In particular, $cd(H) \leq cd(G)$.*

Since the following statement is important for the succeeding exposition and for example of how to transfer arguments from [17] into our situation, let us give the following statement with a full proof. Denote by $Hom(G, k_a)$ the set of affine group scheme homomorphisms from G to k_a .

Proposition 10 ([17, 1.16]) *Let G be a prounipotent group, then:*

- (1) *there is an isomorphism of $\mathcal{O}(G)$ -comodules $H^1(G, k_a) \cong Hom(G, k_a)$;*
- (2) *if G is Abelian, then there is a natural identification of discrete k -vector spaces $G(k)^\vee = Hom_{cts}(G(k), k) \cong Hom(G, k_a)$.*

Proof (1) Proposition 7 shows that the beginning of the minimal injective resolution of the trivial G -module k_a (or equivalently of the trivial $\mathcal{O}(G)$ -comodule) has the form $k_a \rightarrow \mathcal{O}(G)$, and hence, due to triviality of differentials on the fixed points of the minimal resolution (Proposition 8), elements of $H^1(G, k_a)$ correspond to G -invariant modulo k_a elements of $\mathcal{O}(G)$. The Yoneda lemma arguments [27, 2.15] enables one to consider an element $\tilde{a} \in \mathcal{O}(G)$ as a natural transformation of underlying set-valued functors i.e. an element of $Mor(G, k_a)$, which of course could be factored through some morphism of Affine group schemes $\tau : G \rightarrow G_\tau$ and a morphism of Affine algebraic schemes $\kappa_\tau : G_\tau \rightarrow k_a$, where G_τ is a unipotent group scheme.

Recall that the regular action of $g \in G(k)$ on $a \in Mor(G(k), k)$ is the action defined by the formula $(g \cdot a)(x) = a(x \cdot g)$, $x \in G(k)$. Then $G(k)$ -invariance modulo k_a is written in the form $g \cdot a(x) - a(x) = const \in k$ for $\forall x \in G(k)$. Without loss of generality one can normalize a putting $a(1) = 0$. Now, since a is continuous in Zariski topology of $G_\tau(k)$ we can define a homomorphism of Affine algebraic groups $f : G_\tau(k) \rightarrow k_a$ for $g \in G(k)$ by the formula $f(g) = g \cdot a(x) - a(x)$ and therefore the homomorphism of Affine group schemes $G \rightarrow k_a$.

Conversely, if we are given a homomorphism of prounipotent groups $f : G \rightarrow k_a$ then we have some $a_f \in \mathcal{O}(G)$. Such a_f is the invariant modulo elements of the field. Indeed,

$$(g \cdot f)(x) = f(x \cdot g) = f(x) + f(g) = f(x) \pmod{k_a}.$$

(2) Since G is Abelian, the functorial correspondence between prounipotent groups and pronilpotent Lie algebras gives rise to the isomorphism

$$\text{Hom}(G, k_a) \cong \text{Hom}_{\text{Lie}}(\log(G(k)), k).$$

But commutative pro-finite dimensional Lie algebra $\log(G(k))$ and $G(k)$ are the same as linearly compact topological vector spaces, hence $\text{Hom}_{\text{Lie}}(\log(G(k)), k) \cong \text{Hom}_{\text{cts}}(G(k), k) = G(k)^\vee$.

2.2 Presentations of Prounipotent Groups

Below let $k = \mathbb{Q}_p$ and let us identify prounipotent groups with their groups of k -points (see Sect. 1.2). Let Z be a convergent basis in a free pro- p -group $F(Z)$. Denote by $F(Z)_w^\wedge$ its continuous k -prounipotent completion and $\rho : Z \rightarrow F(Z)_w^\wedge$ be the natural embedding (it is shown in [29] that the natural homomorphism $F(Z) \hookrightarrow F(Z)_w^\wedge$ is embedding). Let us construct a prounipotent group $F_u(Z)$ equipped with an inclusion $i : Z \rightarrow F_u(Z)$, which will be called the free prounipotent group on Z .

Let \mathcal{L} be the set of all normal subgroups $H \trianglelefteq F(Z)_w^\wedge$ of finite codimension and such that the set $\{x \in Z \mid \rho(x) \notin H\}$ is finite. If $H_1, H_2 \in \mathcal{L}$, then $H_1 \cap H_2 \in \mathcal{L}$. Let $K = \bigcap \{H \mid H \in \mathcal{L}\}$, then put $F_u(Z) = F(Z)_w^\wedge / K$. The definition shows that

$$F_u(Z) \cong \varprojlim \left\{ \frac{F(Z)_w^\wedge}{H} \mid H \in \mathcal{L} \right\}.$$

Put $i : Z \rightarrow F_u(Z)$; this is the composition of ρ with the canonical homomorphism $F(Z)_w^\wedge \rightarrow F_u(Z)$. It is not difficult to check [17, p. 83] that i is a monomorphism.

Definition 6 Let Z be a convergent basis, then the prounipotent group $F_u(Z)$ will be called the free prounipotent group on Z . Using i we identify Z with a subset of $F_u(Z)$.

Proposition 11 *Let Z be a convergent set, and G be a unipotent group. Then there is a bijection between the homomorphisms $f : F_u(Z) \rightarrow G$ and the sequences of elements $x_i \in G : \text{Card}(\{i \in Z \mid x_i \neq e\}) < \infty$, so that the homomorphisms correspond to the sequences of elements $\{f(i) \mid i \in Z\}$.*

Proposition 11 implies that the free prounipotent group $F_u(Z)$ has the following lifting property: let

$$1 \rightarrow k_a \rightarrow E \xrightarrow{g} U \rightarrow 1$$

be an exact sequence of unipotent groups and $f : F_u(Z) \rightarrow U$ be a homomorphism, then there exists a homomorphism $h : F_u(Z) \rightarrow E : gh = f$.

Proposition 12 ([17, Th. 2.4]) *Let G be a prounipotent group, then the following conditions are equivalent:*

(a) *If*

$$1 \rightarrow K \rightarrow E \xrightarrow{g} F \rightarrow 1$$

is an exact sequence of pronipotent groups and $f : G \rightarrow F$ is a homomorphism, then there exists a homomorphism $h : G \rightarrow E$ such that $gh = f$.

(b) If

$$1 \rightarrow k_a \rightarrow E \xrightarrow{g} F \rightarrow 1$$

is an exact sequence of pronipotent groups and $f : G \rightarrow F$ is a homomorphism, then there exists a homomorphism $h : G \rightarrow E$ such that $gh = f$.

If a group satisfies the conditions of the previous Proposition, then we shall say that such pronipotent group has the *lifting property*.

Lemma 1 ([17, Prop. 2.8]) *Let G be a pronipotent group, then there exists a free pronipotent group $F_u(Z)$ and an epimorphism $f : F_u(Z) \rightarrow G$. The data Z and f can be chosen so that $\text{Hom}_{cts}(G, k_a)$ has the dimension equal to the cardinality of Z . Assume that Y is a set and $g : F_u(Y) \rightarrow G$ is an epimorphism, then $\text{Card}(Y) \geq \text{Card}(Z) = \dim \text{Hom}_{cts}(G, k_a)$. If G has the lifting property then f is an isomorphism.*

The lifting property described above yields the following cohomological description of free pronipotent groups.

Lemma 2 ([17, Th. 2.9]) *A pronipotent group G is free if and only if $cd(G) \leq 1$.*

Now it is not difficult to obtain the statement used in [26, Corollary 3.18].

Proposition 13 ([17, Cor. 2.10]) *Let H be a subgroup of a free pronipotent group G , then H is free.*

Definition 7 A pronipotent group G is called finitely generated if there exists a set of elements $\{g_1, \dots, g_n\}$ in G such that the abstract subgroup in G generated by g_1, \dots, g_n is Zariski dense in G . In this case we say that $\{g_1, \dots, g_n\}$ is a set of generators in G . If G is finitely generated, then by the rank of G we mean the minimal cardinality of a set of generators.

Theorem 3 ([17, Theorem 3.2]) *A pronipotent group G is finitely generated if and only if $H^1(G, k_a)$ has finite dimension. If G is finitely generated then the rank of G equals the dimension of $H^1(G, k_a)$.*

Definition 8 Let G be a pronipotent group and N be its normal subgroup. Let us say that N is finitely related (as a normal subgroup) if there exists a set of elements $\{g_1, \dots, g_n\}$ in N such that the abstract subgroup of N generated by all G -conjugations of g_i is Zariski dense. If n is minimal then n is called the minimal number of relators of N .

Definition 9 Let us call by a *proper presentation* of a pronipotent group G an exact sequence (1) of pronipotent groups in which F is free, and the homomorphism $H^1(G, k_a) \rightarrow H^1(F, k_a)$ is an isomorphism. Let us say that G is given by a finite number of relations if there exists such a sequence in which R is finitely related as a normal subgroup of F .

Definition 10 We shall say that a pronipotent group G has n relations if in any proper presentation (1) the normal subgroup R is finitely related as the normal subgroup of F with the minimal number of relators equal to n .

Theorem 4 ([17, Th. 3.11]) *The pronipotent group G has a finite number of relations if and only if $H^2(G, k_a)$ is finite dimensional. If G has a finite number of relations and if (1) is any proper presentation of G , then R is finitely related as a normal subgroup of F , and its minimal number of relators is the dimension of $H^2(G, k_a)$.*

Proposition 14 ([17, Cor. 3.13]) *A pronipotent group G has n relations if and only if $H^2(G, k_a)$ has dimension n .*

Proposition 15 ([17, Theorem 3.14]) *Let G be a pronipotent group, and assume that for some $n > 1$, $H^n(G, k_a)$ has dimension one, then $cd(G) = n$.*

Proof Let $\mathcal{E}_i, i \in \mathbb{N}$ be a minimal injective G -module resolution of k_a , then Proposition 8 yields $H^1(G, k_a) \cong \mathcal{E}_1^G$ and by Proposition 7 $\mathcal{E}_i \cong H^1(G, k_a) \otimes \mathcal{O}(G)$. In particular, $\mathcal{E}_n = \mathcal{O}(G)$. Since $\mathcal{E}_n \neq 0$, then $d_{n-1} : \mathcal{E}_{n-1} \rightarrow \mathcal{E}_n$ is a nonzero map. Any nonzero G -endomorphism of $\mathcal{O}(G)$ is onto, since this is true for pronipotent groups obtained by extending scalars to the algebraic closure \bar{k} [17, Theorem 5.2] and $\mathcal{O}(G_{\bar{k}}) \cong \mathcal{O}(G_k) \otimes_k \bar{k}$. Therefore d_{n-1} is an epimorphism, and hence $\mathcal{E}_{n+1} = 0$ and $cd(G) = n$.

3 Proof of Theorem 1

Consider a proper ($dim_{\mathbb{F}_p} H^1(G, \mathbb{F}_p) = dim_{\mathbb{F}_p} H^1(F, \mathbb{F}_p)$) presentation (1) of a pro- p -group G with one defining relation. A proper presentation of G can give rise to a non-proper (Definition 9, $dim_{\mathbb{Q}_p} H^1(G_u, \mathbb{Q}_p) < dim_{\mathbb{Q}_p} H^1(F_u, \mathbb{Q}_p)$.) presentation of the pronipotent group $G_u = F_u(X)/R_u$, where $R_u = (r)_{F_u(X)}$ is the Zariski closure of the normal subgroup abstractly generated by the element r . Non-properness of the presentation is equivalent to the statement that the element r is a generator of the free pronipotent group $F_u = F_u(X)(\mathbb{Q}_p)$ (here we have identified the pronipotent group $F_u(X)$ with its group of \mathbb{Q}_p -points, which is correct by the arguments from Sect. 1.2). But Theorem 3 (see also [17, pp. 85–86]) implies that this is equivalent to non-triviality of the image $\phi(r)$ of the relation $r \in F_p \subset F_u$ under the homomorphism $\phi : F_u \rightarrow F_u/[F_u, F_u]$.

Proof (of Theorem 1)

(1) Consider the degenerate case. Without loss of generality we can assume that the pronipotent presentation Definition 4 has the following form:

$$1 \rightarrow R_u = (z)_{F_u(X \cup \{z\})} \rightarrow F_u(X \cup \{z\}) \xrightarrow{d_0} F_u(X) \rightarrow 1,$$

where X is the free basis of F_u . Consider the 2-reduced simplicial group

$$F_u(X \cup \{z\}) \begin{matrix} \xrightarrow{s_0} \\ \xrightarrow{d_0} \\ \xrightarrow{d_1} \\ \longrightarrow \end{matrix} F_u(X) \longrightarrow G_u \cong F_u(X),$$

here d_0, d_1, s_0 are defined on $x \in X, z$ by the identities: $d_0(x) = x, d_0(z) = 1, d_1(x) = x, d_1(z) = 1, s_0(x) = x$.

It is clear that $R_u \cong \ker d_0, F_u(X \cup \{z\}) \cong \ker d_0 \rtimes F_u(X)$. Finally, we can apply the arguments from [26, Prop. 3.9], showing that $(\ker d_0, F_u(X), d_1|_{\ker d_0} = 1)$ is a free pronipotent pre-crossed module. It remains to note that $\ker d_1 = \ker d_0$, and hence $\overline{C}_u = \ker d_0 / [\ker d_0, \ker d_0 \ker d_1] = \ker d_0 / [\ker d_0, \ker d_0] \cong \overline{R}_u$. It remains to use [26, Cor. 3.18], which implies the required isomorphism of topological $\mathcal{O}(G_u)^*$ -modules $\overline{C}_u(\mathbb{Q}_p) \cong \mathcal{O}(G_u)^*$.

(2) Now consider the case in which the pro- p -presentation (2) yields a proper pronipotent presentation (3) of the pronipotent group G_u . Now $r \in F_p \subset F_u := F_u(X)(\mathbb{Q}_p)$ is not a generator in F_u . Let us perform the proof by a series of reductions.

First, note that the proof of isomorphism of left topological $\mathcal{O}(G_u)^*$ -modules $\overline{R}_u(\mathbb{Q}_p) \cong \mathcal{O}(G_u)^*$, by continuous duality [26, 3.1], is equivalent to the proof of the isomorphism of $\mathcal{O}(G_u)$ -comodules $Hom_{cts}(\overline{R}_u(\mathbb{Q}_p), k) \cong \mathcal{O}(G_u)$.

Proposition 10 states that there is an isomorphism of $\mathcal{O}(G_u)$ -comodules

$$H^1(R_u, k_a) \cong Hom(\overline{R}_u, k_a) \cong Hom_{cts}(\log(\overline{R}_u(\mathbb{Q}_p)), k) \cong \overline{R}_u(\mathbb{Q}_p)^\vee.$$

Thus, we need to prove the isomorphism of $\mathcal{O}(G_u)$ -comodules $H^1(R_u, k_a) \cong \mathcal{O}(G_u)$.

Let us study the minimal injective $\mathcal{O}(G_u)$ -resolution of the trivial $\mathcal{O}(G_u)$ -comodule k_a . Proposition 8 implies that since the cohomological dimension of F_u equals one (Lemma 2), then the minimal $\mathcal{O}(F_u)$ -resolution of k_a will have the form

$$0 \rightarrow k_a \rightarrow \mathcal{O}(F_u) \rightarrow \mathcal{O}(F_u)^{dim_k H^1(F_u, k_a)} \rightarrow 0.$$

Reference [12, I, Proposition 4.12, Proposition 3.3] implies that we can consider this resolution as an injective resolution consisting of $\mathcal{O}(R_u)$ -comodules. Applying the functor of R_u -fixed points, we obtain an exact sequence (since R_u -fixed points of $\mathcal{O}(F_u)$ coincide with $\mathcal{O}(G_u)$ [39, 16.3])

$$0 \rightarrow k_a \rightarrow \mathcal{O}(G_u) \rightarrow \mathcal{O}(G_u)^{dim_k H^1(F_u, k_a)} \rightarrow H^1(R_u, k_a) \rightarrow 0.$$

Taking into account that the presentation is proper, in small dimensions the Grothendieck spectral sequence (Proposition 6) is written in the form

$$1 \rightarrow H^1(G_u, k_a) \rightarrow H^1(F_u, k_a) \rightarrow H^1(R_u, k_a)^F \rightarrow H^2(G_u, k_a) \rightarrow H^2(F_u, k_a) = 1,$$

which yields an isomorphism $H^1(R_u, k_a)^G \cong H^2(G_u, k_a)$. Hence, Proposition 7 shows that the injective envelope of $H^1(R_u, k_a)$ coincides with $\mathcal{O}(G_u)^{dim_k H^2(G_u, k_a)}$. Now, considering the composition of the map $\mathcal{O}(G_u)^{dim_k H^1(G_u, k_a)} \rightarrow H^1(R_u, k_a)$

with the inclusion of $H^1(R_u, k_a)$ into its injective envelope, we obtain the beginning of the minimal injective $\mathcal{O}(G_u)$ -resolution

$$0 \rightarrow k_a \rightarrow \mathcal{O}(G_u) \rightarrow \mathcal{O}(G_u)^{\dim_k H^1(G_u, k_a)} \rightarrow \mathcal{O}(G_u)^{H^2(G_u, k_a)}$$

of the trivial comodule k_a . In particular, one has an isomorphism of $\mathcal{O}(G_u)$ -comodules $H^1(R_u, k_a) \cong \text{im}\{\mathcal{O}(G_u)^{\dim_k H^1(G_u, k_a)} \rightarrow \mathcal{O}(G_u)^{H^2(G_u, k_a)}\}$. Therefore conditions (a) $H^1(R_u, k_a)$ is G -injective and (b) $cd(G_u) = 2$ are equivalent.

It remains to prove that a prounipotent group given by a proper presentation with one relation has cohomological dimension equal to two, but this is a particular case of Proposition 7, since Proposition 14 implies the equality $\dim_k H^2(G_u, k_a) = 1$.

4 Identities in Free Pro- p -groups

Definition 11 By an admissible ring of coefficients one calls a commutative complete local k -algebra R without divisors of zero and with the maximal ideal $m = m_R$ such that $R/m = k$ and $l = \dim_k(m/m^2) < \infty$.

Note that the decomposition $R = \varprojlim R/m^i$ enables one to consider $GL_n(R) \cong \varprojlim GL_n(R/m^i)$ as the inverse limit of linear algebraic groups $GL_n(R/m^i)$ and therefore it is the k -affine group scheme. One has the Levi decomposition into the semidirect product $GL_n(R/m^i) \cong (I + M_n(m/m^i)) \rtimes GL_n(k)$ of the linear algebraic (reductive) group $GL_n(k)$ and the unipotent group $I + M_n(m/m^i)$.

Let $K_i = \ker\{GL_n(R) \rightarrow GL_n(R/m^i)\}$, then $K_i \cong I + M_n(m^i)$ and

$$K_1/K_i \cong I + M_n(m/m^i) \cong \ker\{GL_n(R/m^i) \rightarrow GL_n(k)\}.$$

Since $I + M_n(m/m^i)$ are unipotent linear algebraic groups, then $K_1 \cong \varprojlim (K_1/K_i)$ is a prounipotent group, and in particular one has the Levi decomposition $\overleftarrow{GL}_n(R) = K_1 \rtimes GL_n(k)$.

Definition 12 Let R be an admissible ring of coefficients, then by an R -admissible representation of a prounipotent group U one calls a homomorphism of affine group schemes $\rho : U \rightarrow GL_n(R)$.

Let $\rho : U \rightarrow GL_n(R) \cong K_1 \rtimes GL_n(k)$ be an admissible representation. Then $\rho^{-1}K_1$ is a closed normal prounipotent subgroup of U of finite codimension, such that the quotient group $\tilde{U} = U/\rho^{-1}K_1$ has a faithful representation in $GL_n(k)$. Since U is unipotent, this means that its image is conjugate to a subgroup consisting of upper triangular matrices, hence U has the rank no more than n . Therefore, an $(n + 1)$ -multiple commutator from U belongs to $\rho^{-1}K_1$, and hence from the viewpoint of identities the study of representations into K_1 and into $GL_n(R)$ are equivalent. Hence below in the existence questions of identities we shall restrict ourselves by representations into K_1 .

Definition 13 By an identity of $d \geq 2$ variables with values in a pronipotent group G one calls an element u of the free pronipotent group $F = F(x_1, \dots, x_d)$ with d generators, which lies in the kernel of any homomorphism $f : F \rightarrow G$. The set of all identities of d variables with values in G forms a closed normal subgroup $I(d, G)$ in F . The set of identities of d variables with values in a set of pronipotent groups $\mathcal{G} = G_\alpha$ is the normal pronipotent subgroup $I(d, \mathcal{G}) = \bigcap_{\mathcal{G}} I(d, G_\alpha)$ in F . If $\mathcal{G} = \{GL_n(R) \mid R \text{ is admissible}\}$, then $I(d, \mathcal{G})$ is called the group of identities in $n \times n$ matrices, which is denoted $I(d, n)$. If $\mathcal{G} = \{I + M_n(m_R) \mid R \text{ is admissible}\}$, then we say that this is the group of restricted identities for $n \times n$ matrices, denoted by $I^r(d, n)$.

Definition 14 Let $d \geq 2$ and n be natural numbers. The pronipotent group $UG(n, d)$ of $d, n \times n$ general matrices is the closed subgroup in $I + M_n(m_S)$ generated by $X_p, 1 \leq p \leq d$, where $S = k[[x_{ij}^{(p)} \mid 1 \leq i, j \leq n, 1 \leq p \leq d]]$ is the ring of formal power series of dn^2 commuting variables, and $X_p = I + (x_{ij}^{(p)})$.

There is a natural homomorphism $F(x_1, \dots, x_d) \rightarrow UG(n, d)$ given on generators by the rule $x_i \mapsto X_i$, whose kernel contains $I^r(d, n)$. In [19] one proved the following proposition, which is an analog of earlier results of Amitsur (see for example [7, Prop. 19] and further references there).

Proposition 16 ([19, Theorem 2.5]) *The natural homomorphism $F(x_1, \dots, x_d) \rightarrow UG(n, d)$ induces the isomorphism of pronipotent groups $F(x_1, \dots, x_d)/I^r(d, n) \rightarrow UG(n, d)$.*

The following theorem on non-triviality of identities will be needed below for constructing conjurings. Recall that in free discrete groups there are no identities, they are linear.

Proposition 17 ([19, Theorem 2.6]) *If $d, n \geq 2$, then $I^r(d, n) \neq \{e\}$.*

4.1 Proof of Theorem 2

Proof Since $GL_n(\mathbb{F}_p)$ is a finite group, the set $M(n, d)$ of homomorphisms $\psi : F_p(d) \rightarrow GL_n(\mathbb{F}_p)$ is also finite. Then $\mathbb{M}(n, d) = \bigcap_{\psi \in M(n, d)} \ker \psi$ is a normal subgroup of finite index in the free pro- p -group $F_p(d)$, and any element $g \in \mathbb{M}(n, d)$ is an identity, in the sense that in any n -dimensional representation of the pro- p -group $F_p(d)$ over the field \mathbb{F}_p the action of g is trivial.

In free pronipotent groups there are identities (Proposition 17). Also $I^r(d, n) \triangleleft F_u(d) := F_u(d)(\mathbb{Q}_p)$ can be described (Proposition 16) as the kernel of the homomorphism γ_n onto $GU(n, d)$. Denote by $\tilde{\gamma}_n$ the restriction of γ_n to the Zariski dense free pro- p -subgroup $F_p(d) \subseteq F_u(d)$.

$$\begin{array}{ccccc}
 I^r(d, n) & \longrightarrow & F_u(d) & \xrightarrow{\gamma_n} & GU(n, d) \\
 \uparrow & & \uparrow & & \uparrow \\
 Z(d, n) & \longrightarrow & F_p(d) & \xrightarrow{\tilde{\gamma}_n} & GU^p(n, d)
 \end{array}$$

Assume the contrary, i.e. that $\ker(\tilde{\gamma}_n) = 1$, then $\tilde{\gamma}_n$ is an isomorphism. It is clear that any central filtration \tilde{W} in F_u induces a central filtration W on $F_p(d)$. On the other hand, by [9, Lemma 7.5] one has the isomorphism of graded quotients, where $\tilde{W} = \gamma_n(\tilde{W})$ is a central filtration in $GU(n, d)$:

$$Gr_m^{\tilde{W}} F_u(d) \cong Gr_m^W F_p(d) \otimes_{\mathbb{Z}_p} \mathbb{Q}_p \cong Gr_m^{\tilde{W}} GU^p(n, d) \otimes_{\mathbb{Z}_p} \mathbb{Q}_p \cong Gr_m^{\tilde{W}} GU(n, d).$$

Thus, γ_n provides an isomorphism of graded quotients $Gr_m^{\tilde{W}} F_u(d) \cong Gr_m^{\tilde{W}} GU(n, d)$, hence $\ker(\gamma_n) = 1$ ($\cap \tilde{W}_n = 1$). But this is not so by Proposition 17 ($I^r(d, n) \neq 1$). Therefore $Z(d, n) \neq 1$ and since $\mathbb{M}(n, d)$ has a finite index in $F_p(d)$, then $\mathcal{L}(d, n) = Z(d, n) \cap \mathbb{M}(n, d) \neq 1$. Let us call nontrivial elements of $\mathcal{L}(d, n)$ by *conjuring*s.

Assume that $r = w^{p^l}$. Since $d \geq 2$, for any r one can choose an conjuring $z_n \in \mathcal{L}(d, n)$, not lying in the centralizer of w^{p^l} (since $I^r(d, n) \triangleleft F_u(d)$ and since $d \geq 2$, it is not cyclic, hence non-Abelian, and therefore for any $r \in F_u$ there exists an conjuring $z_n \in Z(d, n)$, not lying in the centralizer of r ($z_n \notin Z(r)$). Now the ‘‘Fermat equality’’

$$w^{p^l} \cdot z_n^p = u^p$$

leads to a contradiction. Indeed, according to the pro- p -analog of the Lyndon–Schützenberger theorem [21, Theorem 1], the rank of the free pro- p -subgroup generated by $\langle w^{p^{l-1}}, z_n, u \rangle$ equals one, and hence z_n and w^{p^l} commute, which contradicts to the choice of z_n , and therefore $w^{p^l} \cdot z_n^p$ is not a p th power.

Property (b) follows by construction of z_n , since $z_n \in \mathcal{L}(d, n)$.

Acknowledgements The author expresses gratitude to A.S. Mishchenko and V.M. Manuilov for the constant interest and valuable discussions during the work on the article. He is also grateful to the referee for useful comments and corrections.

References

1. M. Andre, *Methodes simpliciales en algebre homologique et algebre commutative*. Lecture Notes in Mathematics, vol. 37 (Springer, Berlin, 1967)
2. M. Aschenbrenner, S. Friedl, 3-manifold groups are virtually residually p . *Mem. Am. Math. Soc.* **225**(1058) (2013)
3. M. Burger, A. Valette, Idempotents in complex group rings: theorems of Zalesskii and Bass revisited. *J. Lie Theory* **8**, 219–228 (1998)
4. P. Cartier, A primer of Hopf algebras, *Frontiers in Number Theory, Physics, and Geometry II* (Springer, Berlin, 2007), pp. 537–615

5. P. Deligne, J. Milne, Tannakian categories, *Hodge Cycles, Motives and Shimura Varieties* (1985), pp. 94–201
6. G.A. Fernández-Alcober, I.V. Kazatchkov, V.N. Remeslennikov, P. Symonds, Comparison of the discrete and continuous cohomology groups of a pro- p -group. *St. Petersburg. Math. J.* **19**(6), 126–142 (2007)
7. E. Formanek, *The Polynomial Identities and Invariants of $n \times n$ Matrices*. CBMS Regional Conference Series in Mathematics, vol. 78 (1991), 55 pp
8. D. Gildenhuis, S. Ivanov, O. Kharlampovich, On a family of one-relator pro- p -groups. *Proc. R. Soc. Edinb.: Sect. A Math.* **124**, 1199–1207 (1994)
9. R. Hain, M. Matsumoto, Weighted completion of Galois groups and Galois actions on the fundamental group of $\mathbb{P}^1 - \{0, 1, \infty\}$. *Compos. Math.* **139**(2), 119–167 (2003)
10. J.E. Humphreys, *Linear Algebraic Groups* (Springer, Berlin, 1981)
11. Y. Ihara, On Galois representations arising from towers of coverings of $\mathbb{P}^1 - \{0, 1, \infty\}$. *Invent. Math.* **86**(3), 427–459 (1986)
12. J.C. Jantzen, *Representations of Algebraic Groups*. AMS Mathematical Surveys and Monographs, vol. 107, 2nd edn. (American Mathematical Society, Rhode Island, 2003)
13. H. Koch, *Galois Theory of p -Extensions* (Springer, Berlin, 2002)
14. J. Labute, Algèbres de Lie et pro- p -groupes définis par une seule relation. *Invent. Math.* **4**(2), 142–158 (1967)
15. P. Linnel, T. Schick, Finite group extensions and the Atiyah conjecture. *J. Am. Math. Soc.* **20**, 1003–1051 (2007)
16. A. Lubotzky, Combinatorial group theory for pro- p -groups. *J. Pure Appl. Algebra* **25**, 311–325 (1982)
17. A. Lubotzky, A. Magid, Cohomology of unipotent and pronipotent groups. *J. Algebra* **74**, 76–95 (1982)
18. J. Lurie, Derived algebraic geometry XIII: rational and p -adic homotopy theory (2011)
19. A. Magid, Identities for pronipotent groups. *Proc. Symp. Pure Math.* **56**, 281–289 (1994)
20. M.A. Mandell, E_∞ -algebras and p -adic homotopy theory. *Topology* **40**(1), 43–94 (2001)
21. O.V. Melnikov, Products of powers and commutators in free pro- p -groups. *Math. Notes* **40**(4), 753–757 (1986)
22. O.V. Melnikov, Aspherical pro- p -groups. *Sb.: Math.* **193**(11), 1639–1670 (2002)
23. A. Mikhovich, Proalgebraic crossed modules of quasirational presentations, in *Extended Abstracts Spring 2015*. Trends in Mathematics, vol. 5, ed. by D. Herbera, W. Pitsch, S. Zarzuela (Birkhäuser, Cham, 2015)
24. A. Mikhovich, Quasirational relation modules and p -adic Malcev completions. *Topol. Appl.* **201**, 86–91 (2016)
25. A. Mikhovich, Quasirationality and aspherical (pro- p)presentations. [arXiv:1704.05515](https://arxiv.org/abs/1704.05515)
26. A. Mikhovich, Quasirationality and pronipotent crossed modules (accepted for publication in *Journal of Knot Theory and Its Ramifications*). *Math. Notes* **105**(4), 68–76 (2019)
27. J. Milne, Algebraic groups, Lie groups and their arithmetic subgroups, <http://www.jmilne.org/math/CourseNotes/ALA.pdf>
28. D. Passman, *The Algebraic Structure of Group Rings*. Pure and Applied Mathematics (Wiley-Interscience, New York, 1977)
29. J.P. Pridham, On the l -adic pro-algebraic and relative pro- l -fundamental groups, *Arithmetics of Fundamental Groups*. Contributions in Mathematical and Computational Sciences, vol. 2 (Springer, Berlin, 2012), pp. 245–279
30. D. Quillen, Rational homotopy theory. *Ann. Math.* **90**(2), 205–295 (1969)
31. L. Ribes, P. Zalesskii, *Profinite Groups*. A Series of Modern Surveys in Mathematics, vol. 40 (Springer, Berlin, 2000)
32. N. Romanovskii, On pro- p -groups with a single defining relator. *Isr. J. Math.* **78**(1), 65–73 (1992)
33. T. Schick, Finite group extensions and the Baum-Connes conjecture. *Geom. Topol.* **11**, 1767–1775 (2007)
34. J.-P. Serre, *Groupes et algèbres de Lie*. Moscow, Mir (1969) (in Russian)

35. J.-P. Serre, *Galois Cohomology*. SMM (Springer, Berlin, 1997)
36. J.-P. Serre, Structure des certains pro- p -groupes (d'après Demushkin). Séminaire Bourbaki. **252**, 1–11 (1962–1963), in Collected papers, vol. 3 (2007) (in Russian)
37. V.M. Tsvetkov, Pro- p -groups with a single defining relation. Math. Notes Acad. Sci. USSR **37**, 273 (1985). <https://doi.org/10.1007/BF01158177>
38. A. Vezzani, The pro-unipotent completion, <http://users.mat.unimi.it/users/vezzani/Files/Research/prounipotent.pdf>
39. W. Waterhouse, *Introduction to Affine Group Schemes* (Springer, Berlin, 1979)

A Survey on Knotoids, Braidoids and Their Applications



Neslihan GÜgümcü, Louis H. Kauffman and Sofia Lambropoulou

Abstract This paper is a survey on the theory of knotoids and braidoids. Knotoids are open ended knot diagrams in surfaces and braidoids are geometric objects analogous to classical braids, forming a counterpart theory to the theory of knotoids in the plane. We survey through the fundamental notions and existing works on these objects as well as their applications in the study of proteins.

Keywords Knotoids · Multi-knotoids · Spherical knotoids · Planar knotoids · Loop bracket polynomial · Arrow loop polynomial · Θ -graphs · Line isotopy · Braidoiding algorithm · L -braidoiding move · Alexander theorem · L -moves · Markov theorem · Proteins

2010 Mathematics Subject Classification 57M27 · 57M25

N. GÜgümcü (✉) · S. Lambropoulou
School of Applied Mathematical and Physical Sciences, National Technical
University of Athens, Zografou Campus, 157 80 Athens, Greece
e-mail: nesli@central.ntua.gr
URL: <http://www.nesligugumcu.weebly.com>

S. Lambropoulou
e-mail: sofia@math.ntua.gr
URL: <http://www.math.ntua.gr/~sofia>

L. H. Kauffman
Department of Mathematics, Statistics, and Computer Science,
University of Illinois at Chicago, 851 South Morgan St., Chicago,
IL 60607-7045, USA
e-mail: kauffman@uic.edu
URL: <http://homepages.math.uic.edu/~kauffman/>

Department of Mechanics and Mathematics,
Novosibirsk State University, Novosibirsk, Russia

© Springer Nature Switzerland AG 2019
C. C. Adams et al. (eds.), *Knots, Low-Dimensional Topology
and Applications*, Springer Proceedings in Mathematics & Statistics 284,
https://doi.org/10.1007/978-3-030-16031-9_19

1 Introduction

The theory of knotoids was introduced by Turaev [31] in 2012. A surface knotoid is an oriented curve with two endpoints, in an oriented surface, having finitely many self-intersections that are endowed with under/over data. The endpoints can be in different regions of the diagram. This definition extends the notion of $(1, 1)$ -tangle whose endpoints can be assumed to be fixed at the boundary of the disk where the tangle lives. The theory of knotoids in the 2-sphere extends the theory of classical knots and also proposes a new diagrammatic approach to classical knot theory [31]. In [31] basic notions of knotoids were studied comprehensively, including the introduction of several invariants of knotoids in the 2-sphere, such as the complexity (or height) and the Jones/bracket polynomial. Knotoids in S^2 were classified by Bartholomew in [5] and up to 5 crossings by using a generalization of the bracket polynomial for knotoids that was defined by Turaev. There is also a recent classification table for prime knotoids of positive height with up to 5 crossings [23] given by Korablev, May and Tarkaev, obtained by using the correspondence between the knotoids in S^2 and the knots in thickened torus. The first and the second listed authors introduced several new invariants in [12, 14] in analogy with invariants from virtual knot theory. Recently, knotoids have been studied in the field of biochemistry as they suggest new topological models for open linear protein chains. The invariants introduced in [12, 14, 31] have been used for determining the topological entanglement of open protein chains in [10, 11]. Some other recent works on knotoids are on biquandle coloring invariants, by the first listed author and Nelson [18], and on the study of knots that are knotoid equivalent, by Adams, Henrich, Kearney and Scoville [1]. See further [15, 19, 22].

Further, in [12, 16, 17] the theory of braidoids is initiated by the first and the last authors in relation to the theory of planar knotoids. A braidoid diagram extends the notion of classical braid diagram [3, 4] with extra ‘free’ strands that initiate/terminate at two endpoints located anywhere in the plane of the diagram. The closure operation for braidoids requires special attention due to the presence of the endpoints and their forbidden moves, while a ‘braidoiding’ algorithm turning any planar knotoid diagram into a braidoid diagram is the proof of an analogue of the classical Alexander theorem [2, 7, 9, 20, 25, 26, 29, 32, 35] for knotoids. With the introduction of L -moves on braidoids, which were originally defined for classical braids by the last author [24–26], a geometric analogue of the classical Markov theorem [6–8, 24–26, 28–30, 33] for braidoids is enabled. In [12, 13, 16] a set of combinatorial elementary blocks for braidoids is also introduced, which are proposed in [16] for an algebraic encoding of the entanglement of open protein chains in 3-dimensional space.

The outline of the paper is as follows. In Sect. 2 we review the basic notions of knotoids and in Sect. 3 we present closure types for knotoids for obtaining knots. In Sect. 3.3 we focus on the spherical knotoids and how they extend the classical knot theory. In Sect. 4 we present geometric interpretations for spherical and planar knotoids. In Sect. 5 we survey through the existing works and results on the invariants of knotoids. In Sect. 6 we review the fundamental notions of braidoids. In Sects. 6.3

and 6.4, we present the key elements for proving an analogue of the Alexander theorem for knotoids/multi-knotoids. In Sect. 6.5 we reprise the definition of the L -moves on braidoid diagrams that give rise to an analogue of the Markov theorem for braidoids. Finally, in Sect. 7 we present the applications of knotoids to the study of proteins where we also review the building blocks for braidoid diagrams, which is proposed to be used in encoding open protein chains by algebraic expressions.

2 Knotoids and Knotoid Isotopy

2.1 Knotoid Diagrams

Let Σ be an oriented surface. A *knotoid diagram* K in Σ [31] is an immersion of the unit interval $[0, 1]$ in Σ with a finite number of double points each of which is a transversal self-intersection endowed with over/under data. Such self-intersections of K are called *crossings* of K . The images of 0 and 1 are two distinct points called the *endpoints* of K and are specifically called the *leg* and the *head*, respectively. A knotoid diagram is naturally oriented from its leg to its head. The trivial knotoid diagram is assumed to be an immersed curve without any self-intersections as depicted in Fig. 1a.

The notion of knotoid can be extended to include more components. A *multi-knotoid diagram* in Σ is a union of a knotoid diagram and a finite number of knot diagrams [31].

2.2 Moves on Knotoid Diagrams

Planar isotopy moves generated by the Ω_0 -move and the Reidemeister moves $\Omega_1, \Omega_2, \Omega_3$ (see Fig. 2) that take place in a local disk free of any endpoints are allowed on knotoid diagrams. A special case of planar isotopy moves that involves an endpoint is a *swing move*, whereby an endpoint can be pulled within its region, without crossing any other arc of the diagram, as illustrated in Fig. 2. We refer to all these moves as Ω -moves of knotoids.

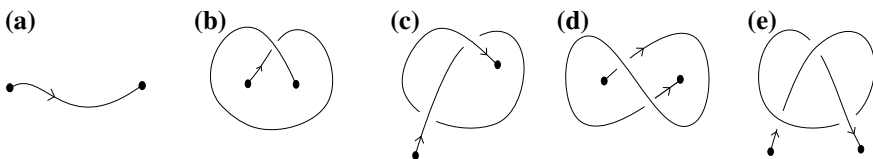


Fig. 1 Examples of knotoid diagrams

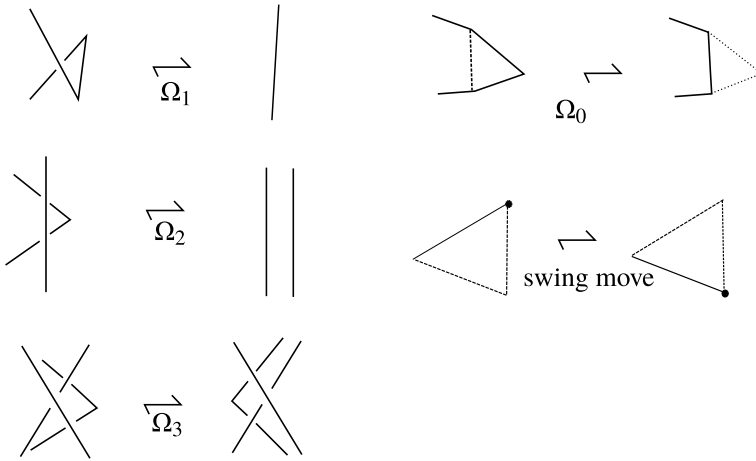
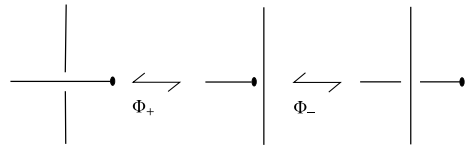


Fig. 2 The moves generating isotopy on knotoid diagrams

Fig. 3 Forbidden knotoid moves



The moves consisting of pulling the arc adjacent to an endpoint over or under a transversal arc, as shown in Fig. 3, are the *forbidden knotoid moves* and are denoted by Φ_+ and Φ_- , respectively. Notice that, if both Φ_+ and Φ_- -moves were allowed, any knotoid diagram in any surface could be clearly turned into the trivial knotoid diagram.

2.3 Knotoids

The Ω -moves generate an equivalence relation on knotoid diagrams in Σ , called *knotoid isotopy*. Two knotoid diagrams are *isotopic* to each other if there is a finite sequence of Ω -moves that takes one to the other. The isotopy classes of knotoid diagrams in Σ are called *knotoids*. The equivalence relation defined on knotoid diagrams applies also to multi-knotoid diagrams, and the corresponding equivalence classes are called *multi-knotoids*.

Let $\mathcal{K}(\mathbb{R}^2)$ and $\mathcal{K}(S^2)$ denote the set of all knotoids in \mathbb{R}^2 and S^2 , respectively. We shall call knotoids in $\mathcal{K}(\mathbb{R}^2)$ *planar* and knotoids in $\mathcal{K}(S^2)$ *spherical*.

There is a surjective map [31]

$$\iota : \mathcal{K}(\mathbb{R}^2) \hookrightarrow \mathcal{K}(S^2),$$

induced by the inclusion $\mathbb{R}^2 \hookrightarrow S^2 = \mathbb{R}^2 \cup \{\infty\}$. However, the map ι is not injective. Indeed, there are knotoid diagrams in the plane representing a nontrivial knotoid while they represent the trivial knotoid in S^2 . For an example, see Fig. 1b. It is well-known that the knot theory of the plane coincides with the knot theory of the 2-sphere, while the non-injectivity of the map ι implies that the theory of knotoids in \mathbb{R}^2 differs from the theory of knotoids in S^2 , also yields a more refined theory than the theory of spherical knotoids.

3 Knotoids, Classical Knots and Virtual Knots

3.1 Classical Knots via Knotoids

In [31] the study of knotoid diagrams is suggested as a new diagrammatic approach to the study of knots in three-dimensional space, as any classical knot can be represented by a knotoid diagram in \mathbb{R}^2 or in S^2 . More precisely, the endpoints of a knotoid diagram can be connected with an arc in S^2 that goes either under each arc it meets or over each arc it meets, as illustrated in Fig. 4. This way we obtain an oriented classical knot diagram in S^2 representing a knot in \mathbb{R}^3 . The connection types are called the *underpass closure* and the *overpass closure*, respectively. The knot that is represented by a knotoid diagram may differ depending on the type of the closure. For example, the knotoid in Fig. 4 represents a trefoil via the underpass closure and the trivial knot via the overpass closure.

In order to have a well-defined representation of knots via knotoids, we should fix the closure type for knotoid diagrams. When we choose the underpass closure as closure type, we have the following proposition. The statement of the proposition is symmetric for the overpass closure.

Proposition 1 ([31]) *Two knotoid diagrams in S^2 or \mathbb{R}^2 represent the same classical knot if and only if they are related to each other by finitely many Ω -moves, swing moves and the forbidden Φ_- -moves.*

Given a knot in S^3 . We can also consider cutting out an underpassing or an overpassing strand of an oriented diagram of the knot. The resulting diagram is clearly a knotoid

Fig. 4 The overpass and the underpass closures of a knotoid diagram resulting in different knots

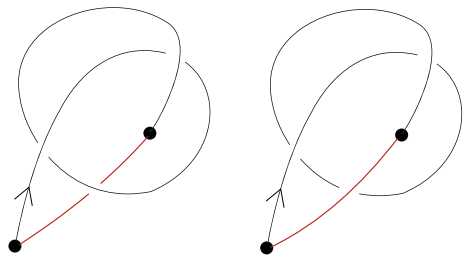


diagram in the plane or the 2-sphere. In fact we can obtain a set of knotoid diagrams by cutting out different strands and the resulting knotoid diagrams all represent the given knot via the underpass or the overpass closure. Knotoid representatives of a knot in S^3 clearly have less number of crossings than any of the diagrams of the knot. For this reason, use of knotoid diagrams to study knots in S^3 provides a considerable amount of simplification for computing knot invariants, such as the knot group [31].

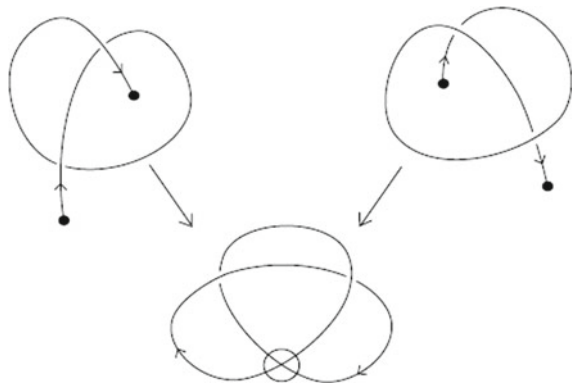
Another interesting question in relation with the knotoid closures has been recently worked in [1]. Two knots K_1, K_2 in S^3 are said to be *knotoid equivalent* if there exists a knotoid κ such that K_1 is the underpass closure of κ and K_2 is the overpass closure of κ . So the question is: *Which pairs of knots are knotoid equivalent?* The authors proved the following theorem.

Theorem 1 ([1, Theorem 2.3]) *Given any two knots K_1, K_2 in S^3 , K_1 is knotoid equivalent to K_2 .*

3.2 Virtual Knots via Knotoids

The endpoints of a knotoid diagram in S^2 can be tied up also in the virtual way. Namely, the endpoints of a knotoid diagram can be connected with an arc by declaring each intersection of the arc with the diagram as a virtual crossing, as illustrated in Fig. 5. This induces a non-injective (e.g. the knotoids in Fig. 5 are different) and non-surjective mapping from the set of knotoids in S^2 to the set of virtual knots of genus 1, called the *virtual closure map* [15]. Being a well-defined map, the virtual closure map provides a way to extract invariants for knotoids from the virtual knot invariants. In fact, most of the new invariants of knotoids that the first and the second authors have discovered in [14] and we briefly mention in Sect. 3.3, are the result of using the principle that the virtual knot class of the virtual closure of a knotoid is an invariant of the knotoid.

Fig. 5 The virtual closure of two knotoids



3.3 Spherical Knotoids Extend the Classical Knot Theory

There is a well-defined injective map from the set of oriented classical knots to $\mathcal{K}(S^2)$ [31]. This map is induced by specifying an oriented diagram for a given oriented knot in S^3 and cutting out an open arc from this diagram that does not contain any crossings. The resulting diagram is a knotoid diagram in S^2 with its endpoints lying in the same local region of S^2 . Such a knotoid diagram is a *knot-type knotoid diagram* and the isotopy class of the diagram is a *knot-type knotoid*. Figure 1a, b and e are some examples of knot-type knotoid diagrams. It is clear that this map gives a one-to-one correspondence between the set of oriented classical knots and the set of knot-type knotoids in S^2 . There are also knotoids that do not lie in the image of this map. They are called *proper knotoids*. The endpoints of any of the representative diagram of a proper knotoid can lie in any but different local regions of the diagram. Figure 1c, d illustrate some examples of proper knotoids.

3.3.1 The Monoid of Knotoids

As Turaev explains in [31], two knotoids K_1, K_2 in S^2 can be concatenated end-to-end in the following way. One can cut out regular disk-neighborhoods of the head of K_1 and the leg of K_2 and identify the remaining surfaces with boundary along their boundaries with an orientation-reversing homeomorphism carrying the unique intersection point of K_1 with the regular neighborhood of the head of K_1 to the unique intersection point of K_2 with the regular neighborhood of the leg of K_2 . The resulting diagram is a composite knotoid diagram in S^2 , denoted by $K_1 \# K_2$. Equipped with the binary operation $\#$, the set of spherical knotoids, $\mathcal{K}(S^2)$, carries a monoid structure [31].

4 Geometric Interpretations of Knotoids

4.1 A Geometric Interpretation of Spherical Knotoids

A Θ -graph is a spatial graph with two vertices v_0, v_1 , called the *leg* and the *head* respectively, and three edges, e_+, e_0, e_- connecting v_0 to v_1 , as exemplified in Fig. 6. The isotopy on Θ -graphs is defined to be the ambient isotopy of the 3-dimensional space preserving the labeling of vertices and the edges, and the set of Θ -graphs consists of the isotopy classes of Θ -graphs.

There is a binary operation on the set of Θ -graphs, called the *vertex multiplication* [34] given as follows. Let Θ_1 and Θ_2 be two Θ -graphs, take out an open 3-disk neighborhood of the head of Θ_1 and an open 3-disk neighborhood of the leg of Θ_2 , each intersecting with the graphs along 3-radii (simple parts from e_0, e_+, e_-). Then identify the remaining manifolds with boundary along their boundaries with an orientation-reversing homeomorphism. With the vertex multiplication, the set of

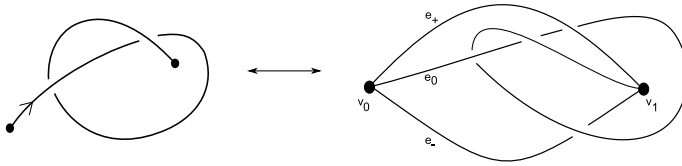


Fig. 6 A knotoid and the corresponding simple Θ -graph

Θ -graphs forms a monoid. A Θ -graph is called *simple* Θ -graph if the union of its edges, e_+ and e_- (the upper and the lower edge, respectively) is the trivial knot. Simple Θ -graphs form a submonoid [31].

Turaev showed the following correspondence between the spherical knotoids and the simple Θ -graphs that gives also rise to a geometric interpretation of spherical knotoids via Θ -curves.

Theorem 2 ([31, Theorem 6.2]) *There is an isomorphism of monoids of spherical knotoids and of simple Θ -graphs.*

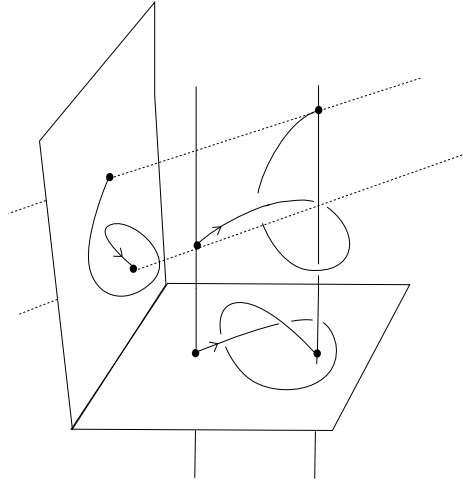
4.2 A Geometric Interpretation of Planar Knotoids

It is explained in [14] that the theory of planar knotoids is related naturally to open space curves on which an appropriate isotopy is defined. An open curve located in \mathbb{R}^3 corresponds to a planar knotoid diagram when projected regularly along the two lines passing through its endpoints and are perpendicular to a chosen projection plane. View Fig. 7. Conversely, an open space curve with two specified parallel lines passing from its endpoints can be viewed as a *lifting* of the related knotoid diagram. A *line isotopy* [14] between two open space curves is an ambient isotopy of \mathbb{R}^3 transforming one curve to the other one in the complement of the lines, keeping the endpoints on the lines and fixing the lines. The isotopy classes of planar knotoids (considered in the chosen projection plane) are in one-to-one correspondence with the line isotopy classes of open space curves [14]. Furthermore, in [21] Kodokostas and the third author make the observation that this interpretation of planar knotoids as space curves is related to the knot theory of the handlebody of genus two and they propose the construction of knotoid invariants through this connection. These ideas are further explored in [22].

5 Invariants of Knotoids

In [14, 31] several invariants for knotoids are introduced. One of the first invariants introduced by Turaev [31] was the the *bracket* and the *Jones polynomial* for knotoids. The bracket polynomial extends to spherical knotoids in the natural way. More

Fig. 7 Projections of an open space curve as a knotoid diagram



precisely, the bracket expansion is directly applied to knotoid diagrams as shown in Fig. 8, and in each state we observe a single long segment component with endpoints and a finite number of circular components. Each circular component contributes to the polynomial by the value $-A^{-2} - A^2$. The initial conditions given in Fig. 8 are sufficient for the computation of the bracket polynomial of a knotoid. The closed formula for the bracket polynomial of knotoids is as follows.

Definition 1 The *bracket polynomial* of a knotoid diagram K is defined as

$$\langle K \rangle = \sum_S A^{\sigma(S)} d^{\|S\|-1},$$

where the sum is taken over all states, $\sigma(S)$ is the sum of the labels of the state S , $\|S\|$ is the number of components of S , and $d = -A^2 - A^{-2}$.

The bracket polynomial of knotoids in S^2 normalized by the writhe factor, $(-A^3)^{-wr(K)}$, generalizes the Jones polynomial with the substitution $A = t^{-1/4}$. Note that the Jones polynomial of the trivial knotoid is trivial. Furthermore, the following conjecture [14] extends the long-standing Jones polynomial conjecture.

Conjecture 1 *The Jones polynomial of spherical knotoids detects the trivial knotoid.*

Some other generalizations of the Jones polynomial are: Turaev’s *2-variable bracket polynomial* [31] that is obtained by a use of the intersection number of the connection arc used in the underpass closure with the rest of the diagram and also with the state components, and the *arrow polynomial* [14] that keeps track of the cusp-like structure (see Fig. 11) arising in the oriented bracket expansion (see Fig. 10 for the oriented state expansion) by assigning new variables namely Λ_i ’s to zig-zag components. There is a special generalization of the bracket polynomial for planar knotoids induced by distinguishing the circular state components nested around the long segment component from the circular state components that do not nest around

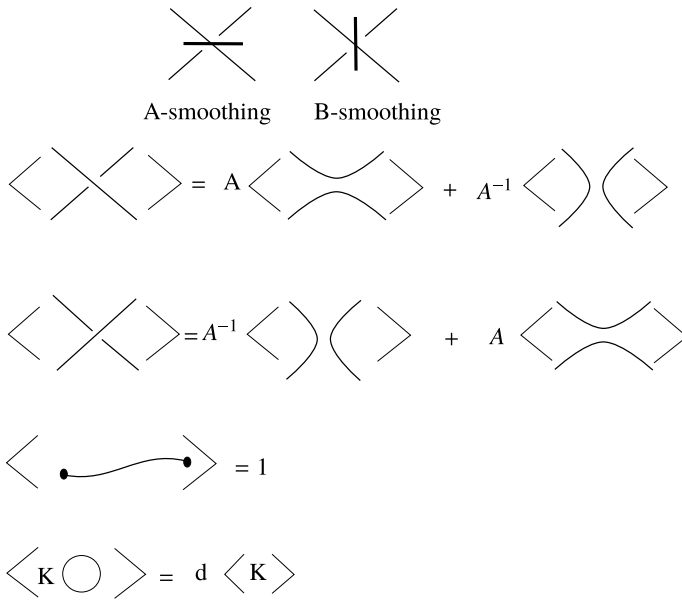
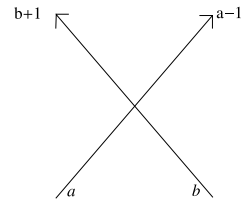


Fig. 8 State expansion of the bracket polynomial

Fig. 9 An affine biquandle coloring on knotoid diagrams



the long segment component. Turaev defined the *3-variable bracket polynomial* [31] for planar knotoids based on this idea and the *loop bracket polynomial*, which is a specialization of the 3-variable bracket polynomial, was utilized in [11] to classify the knotoid models of protein chains (see Sect. 7). Similarly the first and the second listed authors introduce the *arrow loop polynomial* in [15].

Furthermore, the *affine index polynomial*, given in [14], is induced by a non-trivial biquandle structure on knotoid diagrams (see Fig. 9), and a number of biquandle coloring invariants were studied in [18].

There is also a well-defined parity assigned to crossings of (planar or spherical) knotoid diagrams. The *Gaussian parity* is a mapping that assigns each crossing of a knotoid diagram to either 0 or 1. The importance of an existing parity for knotoids comes from the fact that there is no nontrivial parity for classical knot diagrams. Some parity based invariants for knotoids such as the *odd writhe* and the *parity bracket polynomial* [27] were studied in [14].

Fig. 10 Arrow state sum expansion

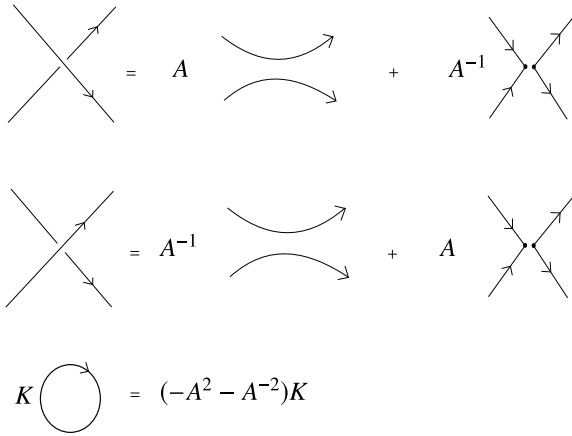
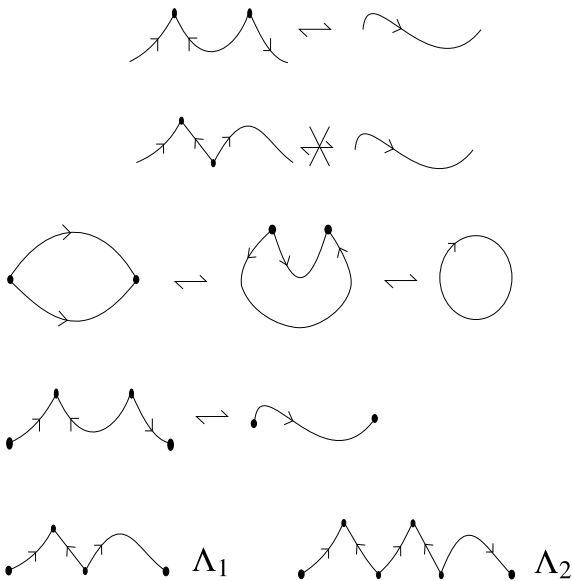


Fig. 11 Cusps



Proper knotoids give rise to interesting questions related to their intrinsic nature, such as the crossing-wise distance between the endpoints, the so-called *height*. More precisely, the *height* of a knotoid diagram in S^2 [31] is the least number of crossings created when the endpoints are joined up by an underpassing strand. The *height* of a knotoid is the minimum of the height of knotoid diagrams in its equivalence class and so forms an invariant for knotoids.

The first and the second listed authors showed that the affine index polynomial and the arrow polynomial establish lower bound estimations for the height of a knotoid. More precisely we have the following lower bound estimations for the height of a knotoid.

Theorem 3 ([14, Theorem 4.12]) *The height of a knotoid is greater than or equal to the maximum degree of its affine index polynomial.*

Theorem 4 ([14, Theorem 5.1]) *The height of a knotoid is greater than or equal to the Λ -degree of its arrow polynomial.*

The interested reader is referred to [15, 19] for ongoing works on knotoids regarding the parity aspect of knotoids and a Khovanov homology construction in analogy with the Khovanov homology for virtual knots/links [19], respectively.

6 The Theory of Braidoids

In this section we reprise the fundamental notions of braidoids introduced by the first and the last listed authors. Braidoids are defined as to form a braided counterpart theory to the theory of planar knotoids.

6.1 Braidoid Diagrams

Let I denote the unit interval $[0, 1] \subset \mathbb{R}$. A *braidoid diagram* B is an immersion of a finite union of arcs into $I \times I \subset \mathbb{R}^2$. The images of arcs are called *strands* of B . There are only finitely many intersection points among the strands of B which are transversal double points endowed with over/under data, the crossings of B . We identify \mathbb{R}^2 with the xt -plane with the t -axis directed downward. Following the orientation of I , each strand is naturally oriented downward, with no local maxima or minima, so that it intersects a horizontal line at most once.

A braidoid diagram has two types of strands, the classical strands and the free strands. A *classical strand* is as a braid strand with two ends, one lying in $I \times \{0\}$ and the other lying in $I \times \{1\}$. A *free strand* is a strand that either has one of its ends lying in $I \times \{0\}$ or in $I \times \{1\}$ and the other end lying anywhere in $I \times I$ or it has two of its ends lying anywhere in $I \times I$. There are two such free ends, called the *endpoints* of B and are denoted by a vertex to be distinguished from the fixed ends. For examples see Fig. 12. The two endpoints are called the *leg* and the *head* and are denoted by l and h respectively, in analogy with the endpoints of a knotoid diagram. The head is the endpoint that is terminal for a free strand while the leg is the starting endpoint for a free strand, with respect to the orientation.

The other ends of the strands of B are named *braidoid ends*. Each braidoid end is numbered accordingly to its order from left to right. Braidoid ends lie equidistantly and two braidoid ends having the same order on $\{t = 0\}$ and $\{t = 1\}$ are vertically aligned. Two braidoid ends whose orders coincide are called *corresponding ends*. See the examples in Fig. 12.

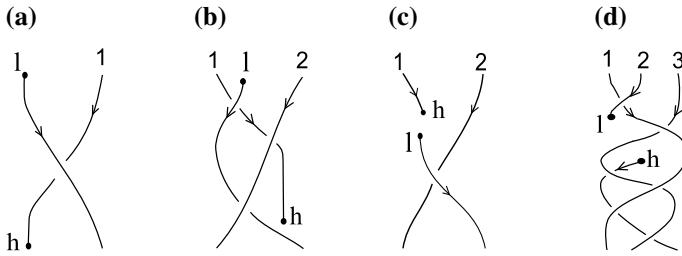


Fig. 12 Some examples of braidoid diagrams

6.2 Isotopy Moves on Braidoid Diagrams

We allow on braidoid diagrams the oriented Reidemeister moves Ω_2 and Ω_3 (recall Fig. 2), which preserve the downward orientation of the arcs in the move patterns. In addition to these moves, the endpoints of a braidoid diagram can be pulled up or down in the vertical direction by a *vertical move*, and right or left in the horizontal direction by a *swing move* in the vertical strip determined by the neighboring corresponding ends, as long as they do not intersect or cross through any strand of the diagram. That is, the pulling of the leg or the head over or under any strand is forbidden. It is clear that allowing both forbidden moves cancels any braiding of the free strands.

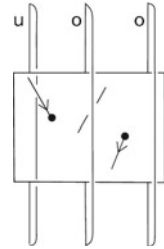
The *braidoid isotopy* is induced by keeping the braidoid ends fixed on the top and bottom lines ($t = 0$ and $t = 1$, respectively) but allowing the Reidemeister moves Ω_2 and Ω_3 and planar Δ -moves, as well as the swing and the vertical moves for the endpoints. Two braidoid diagrams are isotopic if one can be obtained from the other by a finite sequence of the above moves. An equivalence class of isotopic braidoid diagrams is a *braidoid*.

6.3 A Closure on Braidoids

One way to define a closure operation on braidoid diagrams in order to obtain planar (multi)-knotoid diagrams is by adding an extra property to braidoid diagrams. More precisely, each pair of the corresponding ends in a braidoid diagram is labeled either *o* or *u*, standing for ‘over’ or ‘under’, respectively. We attach the labels next to the braidoid ends lying at the top line and call the diagram a *labeled braidoid diagram*. Two labeled braidoid diagrams are called *isotopic* if their braidoid ends possess the same labeling and they are isotopic as unlabeled diagrams. The corresponding equivalence classes are called *labeled braidoids*.

Let B be a labeled braidoid diagram. The *closure* of B , denoted \widehat{B} , is a planar (multi)-knotoid diagram that results from B by the following topological operation: each pair of corresponding braidoid ends of B is joined up with a straight arc (with slightly tilted extremes) that lies on the right of the line of the corresponding braidoid

Fig. 13 The closure of an abstract labeled braidoid diagram



ends in a distance arbitrarily close to this line so that none of the endpoints is located between the line and the closing arc. The closing arc goes entirely over or entirely under the rest of the diagram according to the label of the ends. See Fig. 13 for an abstract illustration of the closure of a labeled braidoid diagram.

Proposition 2 ([16, 17]) *The closure operation induces a well-defined map from the set of labeled braidoids to the set of planar (multi)-knotoids.*

6.4 How to Turn a Knotoid into a Braidoid?

J.W. Alexander proved in 1923 that any oriented classical knot/link can be represented by an isotopic knot/link diagram in braided form [2]. See also [9]. The proof of the Alexander theorem by the last listed author [24–26] utilizes the *L-braiding moves*. In [16, 17] the first and the last listed authors proved the following analogue of the Alexander theorem for (multi)-knotoids by utilizing these moves.

Theorem 5 ([16, 17]) *Any (multi)-knotoid diagram in \mathbb{R}^2 is isotopic to the closure of a labeled braidoid diagram.*

Let K be a (multi)-knotoid diagram whose plane is equipped with the top-to-bottom direction. The basic idea for turning K into a braidoid diagram is to keep the arcs that are oriented downward, with respect to the top-to-bottom direction, and to eliminate the ones that are oriented upward (*up-arcs*), producing at the same time pairs of corresponding braidoid strands, such that the (multi)-knotoid resulting after closure is isotopic to K . The elimination of the up-arcs is done by the braidoiding moves.

An *L-braidoiding move* consists in cutting an up-arc at a point and pulling the resulting two pieces, the upper upward to the line $t = 1$ and the lower downward to the line $t = 0$, both entirely *over* or *under* the rest of the diagram. The resulting pieces are pulled so that their ends are kept aligned vertically with the cut-point. Finally the lower piece is turned into a braidoid strand by Δ -moves. See Fig. 14. For the purpose of closure, the resulting pair of strands is labeled *o* or *u* depending on our choice we make for pulling the upper and lower pieces during the braidoiding move. The reader is referred to Fig. 14 for an illustration of an *L-braidoiding move* where

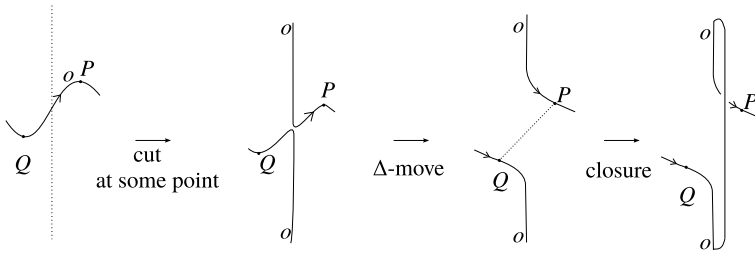


Fig. 14 An L -braidoiding move

it can be also verified that the closure of the resulting strands labeled o is isotopic to the initial up-arc.

Theorem 5 is proved by applying any one of the braidoiding algorithms. These algorithms are both based on the L -braidoiding moves. In Fig. 15 we illustrate the steps of the algorithm that is given in [17]. As for the algorithm in [20] turning any virtual knot/link diagram into a virtual braid diagram, we start by rotating each crossing containing one or two up-arcs by $\frac{\pi}{2}$ or π , respectively, so that we end up with a knotoid diagram whose up-arcs are all free of any crossings. All of these ‘free’ up-arcs are given an order and a labeling of o or u each, and are eliminated by the L -braidoiding moves one by one. The algorithm terminates in finite steps and results in a labeled braidoid diagram in Fig. 15. The algorithm in [17] which is based on [26], uses braidoiding moves for up-arcs in crossings and is more appropriate for establishing Markov-type theorems for braidoids (see Theorem 6). Yet, an added value of the first algorithm is the following consequence: *Any (multi)-knotoid diagram is isotopic to the uniform closure of a braidoid diagram* [12, 17].

6.5 L -Equivalence

It is clear that due to the choices made in order to prepare a (multi)-knotoid diagram for a braidoiding algorithm (such as subdivision and labeling of the up-arcs) as well as knotoid isotopy moves, we obtain different braidoid diagrams with possibly different numbers of strands and labels. The question that would lead to a Markov-like theorem for braidoids is to ask how these braidoid diagrams are related to each other. Clearly, the braidoid isotopy does not change the number of strands nor the labeling, so braidoid isotopy is not sufficient for determining such relations. The first and the last listed authors showed in [16, 17] that the L -moves on braidoid diagrams provide an answer to this question.

An L -move on a braidoid diagram B consists in cutting a strand of B at an interior point, not vertically aligned with a braidoid end or an endpoint or a crossing, and then pulling the resulting ends away from the cutpoint to the top and bottom of B respectively, keeping them aligned with the cutpoint, and so as to create a new pair of

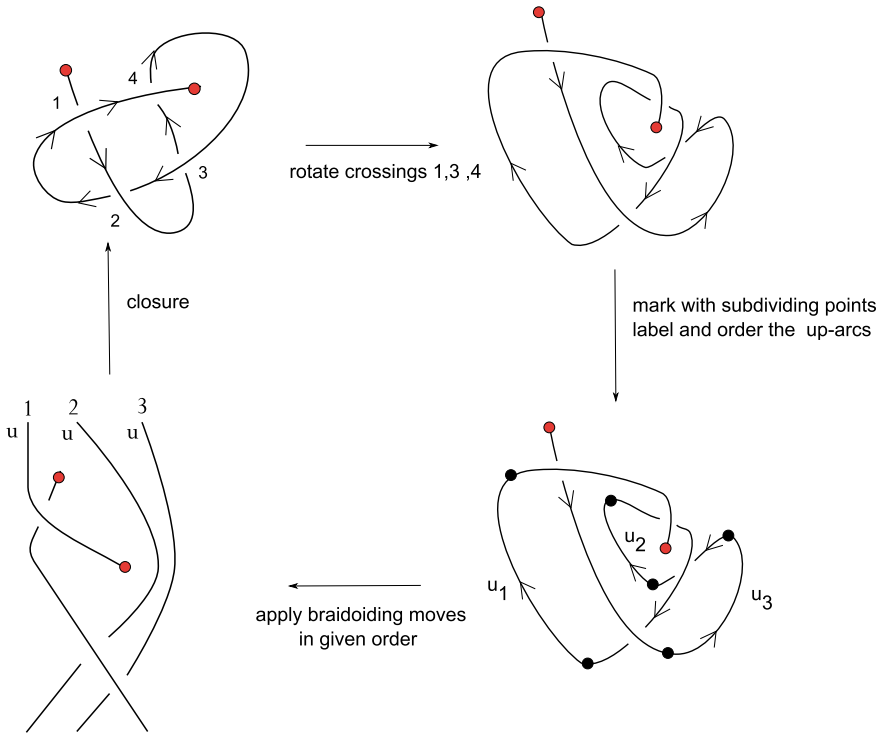
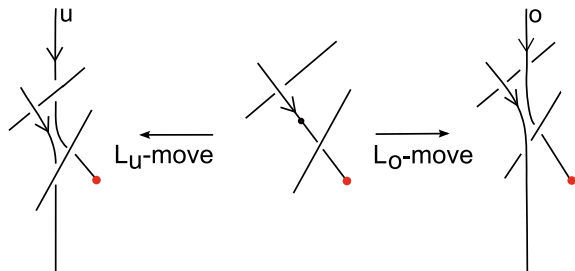


Fig. 15 An example showing how the algorithm works

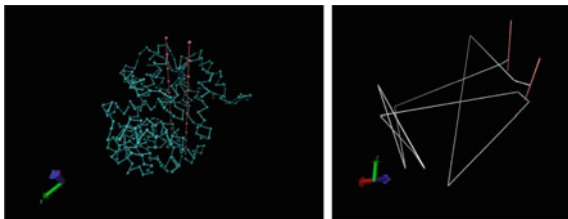
Fig. 16 L -moves



corresponding braidoid strands. See Fig. 16 for an illustration of an L -move. There are two types of L -moves, namely L_o and L_u . For an L_o -move the pulling of the resulting new strands is entirely *over* the rest of the diagram. For an L_u -move the pulling of the new strands is entirely *under* the rest of the diagram. The two resulting strands are both labelled according to the type of the L -move. See Fig. 16.

The above definition provides us with the following result, which is an analogue of the classical Markov theorem.

Fig. 17 The configuration of the backbone of the protein 3KZN in 3D and its simplified configuration; image from Dimos Goundaroulis, private communication



Theorem 6 ([12, Theorem 13]) *The closures of two labeled braidoid diagrams are isotopic (multi)-knotoids in \mathbb{R}^2 if and only if the labeled braidoid diagrams are related to each other by a finite sequence of L-moves and braidoid isotopy moves.*

7 Applications

7.1 Applications to the Study of Proteins

The correspondence of line isotopy classes of open space curves and isotopy classes of planar knotoids suggests that a topological analysis of linear physical structures lying in 3-dimensional space can be done by simulating them by open space curves and by taking their orthogonal projections. Through this idea, knotoids, both in S^2 and \mathbb{R}^2 , have found important applications in the study of open protein chains [10] (see Fig. 17 for an example), as well as of open protein chains with chemical bonds via introducing the notion of *bonded knotoids* [11]. In these papers, open protein chains are studied via their projections into planes. The corresponding knotoid classes are considered in the 2-sphere and in the plane, and they are classified by using the (normalized) bracket polynomial and the Turaev's loop bracket polynomial [11, 31], respectively. In Fig. 18 we see three atlases that contain colored regions. Each of these colored regions corresponds to one topological class of the protein 3KZN when it is closed to some knot, and when it is projected to a knotoid, a spherical knotoid and a planar knotoid, respectively. As seen from Fig. 18, the number of colors increases as we go from the knot representation to the planar knotoid representation. By this data, the authors concluded that planar knotoids yield a more refined analysis for understanding the topological structure of open protein chains than knots or spherical knotoids [11]. This is due to the facts that more knotoids close to the same knot and that the classification of knotoids in the plane is more refined than the classification of spherical knotoids. For example a trivial knotoid in S^2 may happen to be a non-trivial knotoid when considered in \mathbb{R}^2 as we discussed in Sect. 2.3.

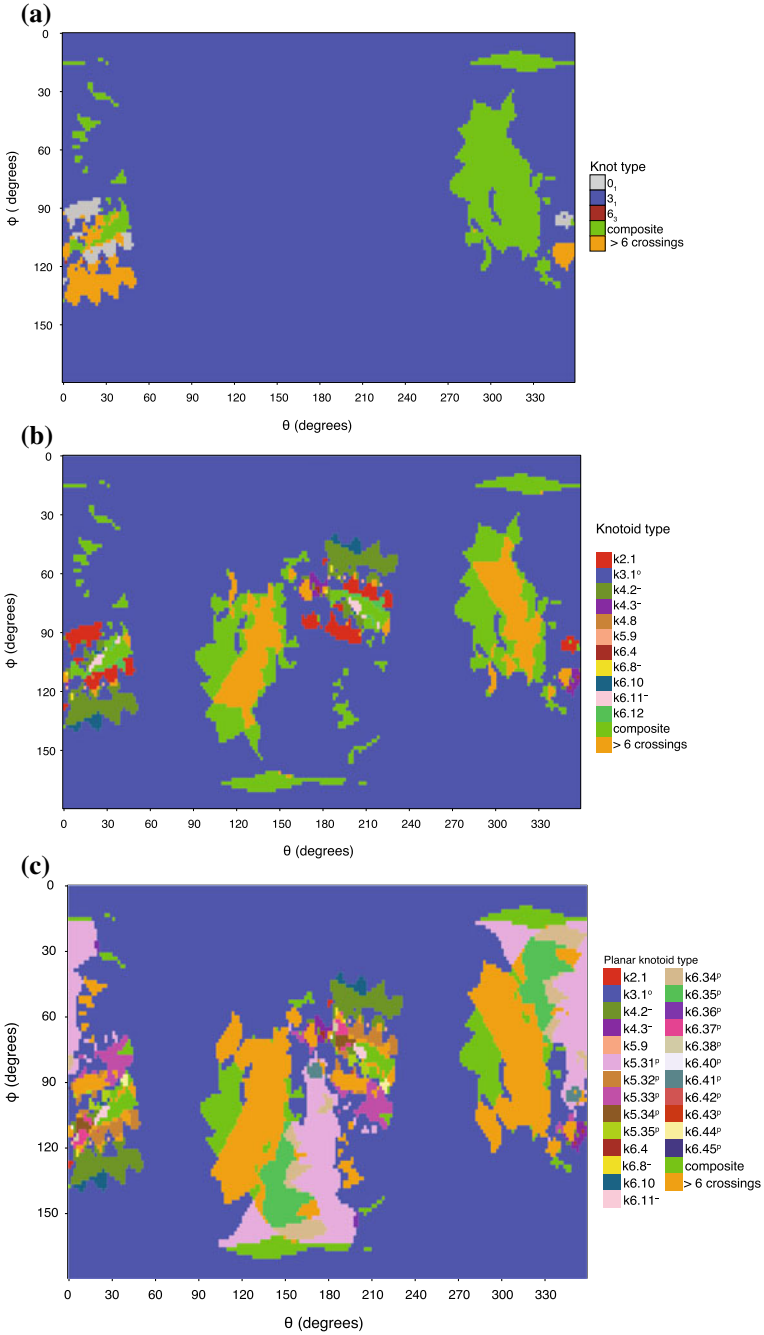


Fig. 18 Atlases showing the topological analysis of 3KZN via knots, spherical knotoids and planar knotoids, image from [11]

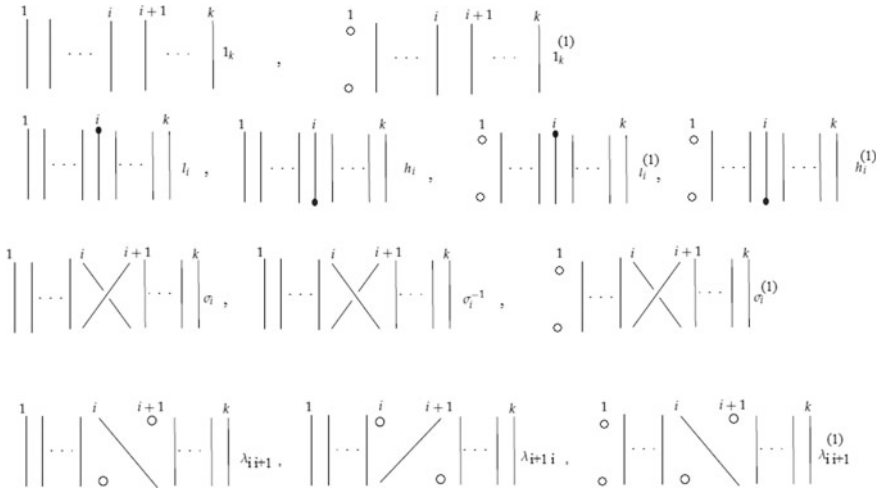


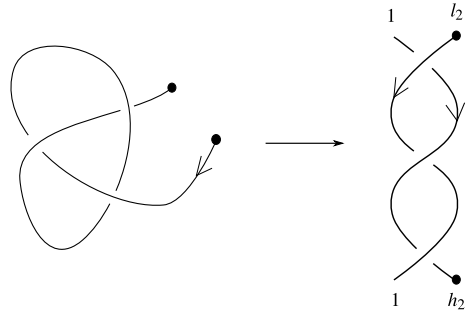
Fig. 19 Elementary k -blocks

7.2 Elementary Blocks and a Proposed Application of Braidoids

As demonstrated in [13, 16], any braidoid diagram can be divided into a finite number of horizontal stripes, each containing one of the blocks that are depicted in Fig. 19. The blocks consist of the classical braid generators, the identity elements containing one endpoint, along with their extensions by the *implicit points*, which are empty nodes put along the vertical direction of the endpoints, and along with the *shifting blocks*, which result from the change of positioning of strands before or after the appearance of an endpoint. A product on the set of elementary n -blocks and relations with respect to this product, induced by the isotopy moves of the braidoid diagrams, is further explored in [13]. Then, any braidoid diagram on n strands can be read, from top to bottom, as a word that corresponds to a combination of finitely many elementary n - or $(n + 1)$ -blocks.

Any planar knotoid diagram can be turned into a (labeled) braidoid diagram by Theorem 5, so it can be represented by an expression in terms of elementary blocks. This suggests an algebraic encoding for open protein chains or, in general, for linear polymer chains: they can be projected to planes and the resulting knotoid diagrams can be turned into braidoid diagrams that have algebraic expressions. An example is illustrated in Fig. 20, where the knotoid corresponding to protein 3KZN is turned into a braidoid diagram, which is represented by the word $l_2\sigma_1^3h_2$ in elementary blocks.

Fig. 20 The knotoid of the protein 3KZN and a corresponding braidoid diagram with algebraic expression $l_2\sigma_1^3h_2$



Acknowledgements The research of Sofia Lambropoulou and Neslihan Gügümcü has been co-financed by the European Union (European Social Fund - ESF) and Greek national funds through the Operational Program IJEducation and Lifelong Learning of the National Strategic Reference Framework (NSRF) - Research Funding Program: THALES: Reinforcement of the interdisciplinary and/or inter-institutional research and innovation, MIS: 380154. Louis H. Kauffman's work was supported by the Laboratory of Topology and Dynamics, Novosibirsk State University (contract no. 14.Y26.31.0025 with the Ministry of Education and Science of the Russian Federation)

References

1. C. Adams, A. Henrich, K. Kearney, N. Scoville, Knots related by knotoids. To appear in *Am. Math. Mon.* (2019)
2. J.W. Alexander, A lemma on systems of knotted curves. *Proc. Natl. Acad. Sci. USA* **9**, 93–95 (1923)
3. E. Artin, Theorie der Zöpfe. *Abh. Math. Semin. Hambg. Univ.* **4**, 47–72 (1926)
4. E. Artin, Theory of braids. *Ann. Math.* **48**, 101–126 (1947)
5. A. Bartholomew, Andrew Bartholomew's mathematics page: knotoids, <http://www.layer8.co.uk/maths/knotoids/index.htm>. Accessed 14 Jan 2015
6. D. Bennequin, Entrelacements et équations de Pfaffé. *Asterisque* **107–108**, 87–161 (1983)
7. J.S. Birman, Braids, links and mapping class groups. *Ann. Math. Stud.* **82** (1974) (Princeton University Press, Princeton)
8. J.S. Birman, W.W. Menasco, On Markov's theorem. *J. Knot Theory Ramif.* **11**(3), 295–310 (2002)
9. H. Brunn, Über verknottete Kurven. *Verh. des Int. Math. Congr.* **1**, 256–259 (1897)
10. D. Goundaroulis, J. Dorier, F. Benedetti, A. Stasiak, Studies of global and local entanglements of individual protein chains using the concept of knotoids. *Sci. Rep.* **7**, 6309 (2017)
11. D. Goundaroulis, N. Gügümcü, S. Lambropoulou, J. Dorier, A. Stasiak, L.H. Kauffman, Topological models for open knotted protein chains using the concepts of knotoids and bonded knotoids, in *Polymers*, Special issue on Knotted and Catenated Polymers, vol. 9(9), ed. by D. Racko, A. Stasiak (2017), p. 444. <https://doi.org/10.3390/polym9090444>
12. N. Gügümcü, On knotoids, braidoids and their applications. Ph.D. thesis, National Technical University of Athens (2017)
13. N. Gügümcü, A combinatorial setting for braidoids. In preparation
14. N. Gügümcü, L.H. Kauffman, New invariants of knotoids. *Eur. J. Comb.* **65C**, 186–229 (2017)
15. N. Gügümcü, L.H. Kauffman, Parity in knotoids. Submitted for publication
16. N. Gügümcü, S. Lambropoulou, Knotoids, braidoids and applications. *Symmetry* **9**(12), 315 (2017). <https://doi.org/10.3390/sym9120315>

17. N. Gügümcü, S. Lambropoulou, Braidoids. Submitted for publication
18. N. Gügümcü, S. Nelson, Biquandle coloring invariants of knotoids. To appear in *J. Knot Theory Ramif.* [arXiv:1803.11308](https://arxiv.org/abs/1803.11308). <https://doi.org/10.1142/S0218216519500299>
19. N. Gügümcü, L.H. Kauffman, D. Goundaroulis, S. Lambropoulou, A Khovanov homology for knotoids. In preparation
20. L.H. Kauffman, S. Lambropoulou, Virtual braids. *Fundam. Math.* **184**, 159–186 (2004)
21. D. Kodokostas, S. Lambropoulou, A spanning set and potential basis of the mixed Hecke algebra on two fixed strands. *Mediterr. J. Math.* **15:192** (2018). <https://doi.org/10.1007/s00009-018-1240-7>
22. D. Kodokostas, S. Lambropoulou, Rail knotoids. Accepted for publication in *J. Knot Theory Ramif*
23. P.G. Korablev, Y.K. May, V. Tarkaev, Classification of low complexity knotoids. *Sib. Electron. Math. Rep.* **15**, 1237–1244 (2018) [Russian, English abstract]. <https://doi.org/10.17377/semi.2018.15.100>
24. S. Lambropoulou, Short proofs of Alexander’s and Markov’s theorems. Warwick preprint (1990)
25. S. Lambropoulou, A study of braids in 3-manifolds. Ph.D. thesis, University of Warwick (1993)
26. S. Lambropoulou, C.P. Rourke, Markov’s theorem in 3-manifolds. *Topol. Appl.* **78**, 95–122 (1997)
27. V. Manturov, Parity in knot theory. *Mat. Sb.* **201**(5), 65–110 (2010)
28. A.A. Markov, Über die freie Äquivalenz geschlossener Zöpfe. *Rec. Math. Mosc.* **1**(43), 73–78 (1936)
29. H.R. Morton, Threading knot diagrams. *Math. Proc. Camb. Philos. Soc.* **99**, 247–260 (1986)
30. P. Traczyk, A new proof of Markov’s braid theorem, preprint (1992), Banach Cent. Publ. **42**, Institute of Mathematics Polish Academy of Sciences, Warszawa (1998)
31. V. Turaev, Knotoids. *Osaka J. Math.* **49**, 195–223 (2012)
32. P. Vogel, Representation of links by braids: a new algorithm. *Comment. Math. Helv.* **65**, 104–113 (1990)
33. N. Weinberg, Sur l’ equivalence libre des tresses fermée. *Comptes Rendus (Doklady) de l’ Académie des Sciences de l’ URSS* **23**(3), 215–216 (1939)
34. K. Wolcott, The knotting of theta curves and other graphs in S^3 . *Geom. Topol.* (Athens, 1985, Lect. Notes Pure Appl. Math. **105**, 325–346 (1987), Dekker, New York)
35. S. Yamada, The minimal number of Seifert circles equals the braid index of a link. *Invent. Math.* **89**, 347–356 (1987)

Regulation of DNA Topology by Topoisomerases: Mathematics at the Molecular Level



Rachel E. Ashley and Neil Osheroff

Abstract Although the genetic information is encoded in a one-dimensional array of nucleic acid bases, three-dimensional relationships within DNA play a major role in how this information is accessed and utilized by living organisms. Because of the intertwined nature of the DNA two-braid and its extreme length and compaction in the cell, some of the most important three-dimensional relationships in DNA are topological in nature. Topological linkages within the two-braid and between different DNA segments can be described in simple mathematical terms that account for both the twist and the writhe in the double helix. Topoisomerases are ubiquitous enzymes that regulate the topological state of the genetic material by altering either twist or writhe. To do so, these enzymes transiently open the topological system by breaking one or both strands of the two-braid. This article will review the mathematics of DNA topology, describe the different classes of topoisomerases, and discuss the mechanistic basis for their actions in both biological and mathematical terms. Finally, it will discuss how topoisomerases recognize the topological states of their DNA substrates and products and how some of these enzymes distinguish supercoil handedness during catalysis and DNA cleavage. These latter characteristics make topoisomerases well suited for their individual physiological tasks and impact their roles as targets of important anticancer and antibacterial drugs.

Keywords DNA topology · DNA topoisomerases · DNA supercoiling · Supercoil handedness

R. E. Ashley · N. Osheroff (✉)
Vanderbilt University School of Medicine, Nashville, TN 37232-0146, USA
e-mail: neil.osheroff@vanderbilt.edu

R. E. Ashley
e-mail: rachel.e.ashley@vanderbilt.edu

N. Osheroff
VA Tennessee Valley Healthcare System, Nashville, TN 37212, USA

© Springer Nature Switzerland AG 2019
C. C. Adams et al. (eds.), *Knots, Low-Dimensional Topology
and Applications*, Springer Proceedings in Mathematics & Statistics 284,
https://doi.org/10.1007/978-3-030-16031-9_20

1 DNA Topology

DNA (deoxyribonucleic acid) encodes all the inheritable genetic information that makes us what we are. Thus, it is arguably the most important biomolecule in the cell. The structure of DNA represents a perfect biological relationship between form and function. The genetic material is contained in a plectonemically coiled two-braid in which the two strands of the double helix are antiparallel and complementary [1]. This structure serves not only as a framework for the organization and expression of the genetic information, but also provides an elegant mechanism for self-replication and repair [1].

The amount of DNA in a human is staggering. The human genome is encoded in ~3 billion base pairs that are contained on 23 individual chromosomes [2]. Because humans are diploid, each of our cells contains ~6 billion base pairs and 46 chromosomes. At actual size, the DNA in a human cell is ~2 m in length and is compressed into a nucleus that is ~5–10 μm in diameter [3]. The human body is comprised of ~30 trillion cells [4, 5] and therefore contains ~180 sextillion base pairs of DNA that would stretch ~60 billion kilometers in length if laid end-to-end.

Although the human genome is linear, the extreme length and cellular compaction of DNA, the high frictional forces associated with a two-braid of that length, and the fact that the DNA is anchored to cellular scaffolds preclude torsional stress from being translated throughout the genetic material by rotation of DNA ends. Therefore, for all practical purposes, human DNA can be considered to be a closed topological system [6–16]. As long as the ends of DNA are “fixed,” topological relationships are defined as those that can be altered only by breaking one or both strands of the double helix. Even though the genetic information contained within DNA is encoded within a linear sequence of bases, the topological structure of the molecule has profound effects on how this information is accessed and used in the cell.

2 Mathematical and Biological Implications of DNA Topology

DNA topology can be defined mathematically by three straightforward concepts: twist (Tw), writhe (Wr), and linking number (Lk) [8–11, 17–22]. Twist is the total number of double helical turns in a defined DNA segment. By convention, positive twist is defined as the right-handed twist observed in the normal Watson-Crick DNA structure. Twist represents torsional stress in the double helix. Writhe is defined as the number of times the double helix crosses itself if the DNA segment is projected in two dimensions and represents axial stress in the molecule. Each writhe is assigned an integral value of -1 or $+1$ based on the handedness of the crossover, which is determined by the direction of rotation that would be required to align the front DNA segment with the back segment without rotating the DNA more than 180° [8, 9]. If the front segment must be rotated clockwise, the writhe is negative (i.e., right-

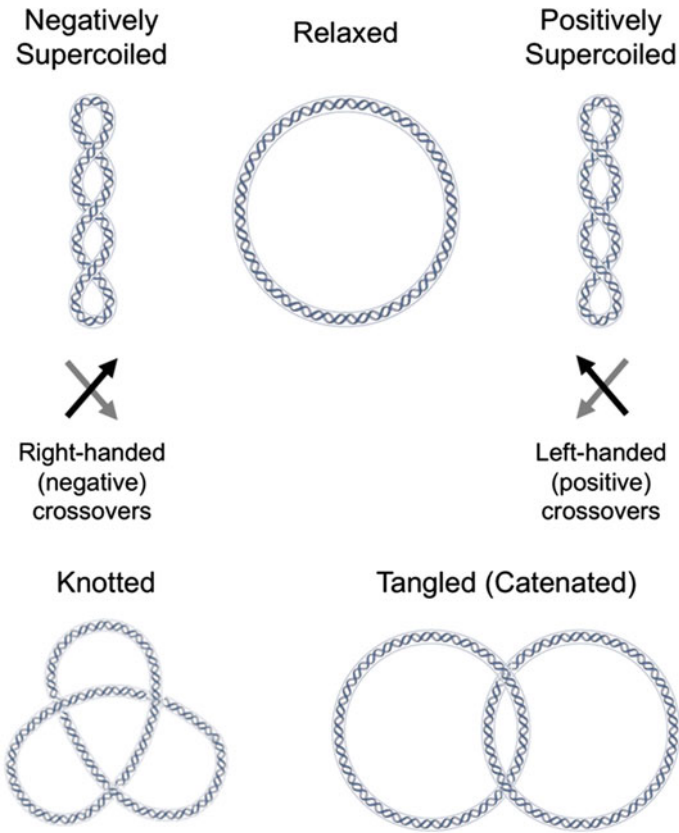


Fig. 1 Topological relationships in DNA. DNA molecules are drawn as circles for simplicity. Top: DNA that is not under torsional stress is referred to as “relaxed” (middle) and is represented as an unknot (or trivial knot). Underwinding or overwinding the DNA results in negatively supercoiled (left) or positively supercoiled (right) DNA, respectively. Supercoiling is depicted here as writhe (DNA crossovers) for visual clarity, but it should be noted that twist and writhe are interconvertible within these molecules. Bottom: Intramolecular knots (left) and intermolecular tangles (catenanes, shown as a hopf link, right) can also form in DNA. In these cases, twist and writhe are not interconvertible

handed); conversely, if it must be rotated counterclockwise, the writhe is positive (i.e., left-handed) (Fig. 1).

Mathematically, DNA twist and writhe are related, and the sum of these two values is expressed as the linking number (Lk):

$$Lk = Tw + Wr \tag{1}$$

Two key concepts associated with this equation should be emphasized. First, in a topologically closed system, the linking number is invariant [8–11, 17–21]. The only

way to alter this value is to open the system by breaking one or both chains of the DNA double helix. Second, in the absence of knots or tangles, twist and writhe are fluid and interconvertible. The classic means of demonstrating this fluidity (although it is becoming increasingly more dated) is a telephone cord [8–11, 17–21]. Another example could be a coiled lock of hair such as those seen on a Greek statue. In its unstretched configuration, the cord (or hair) writhes about itself, forming coils without visible twisting. However, when the cord (or hair) is stretched, the writhes are lost and the cord is visibly twisted. Although the coiled and stretched structures are homeomorphic, they contain very different levels of twist and writhe.

When DNA is not under torsional stress, as observed in the canonical Watson-Crick structure, it is said to be “relaxed.” In this form, the double helix makes one helical turn for every 10.5 base pairs (bp) [23]. Therefore, the linking number of a relaxed DNA molecule of 1050 bp would be 100. The magnitude to which topology has the potential to affect the biological function of DNA becomes obvious in the context of the human organism. Considering only links formed between the strands of the DNA two-braid, there are ~600 million links within the ~6 billion bp genome. Every time the genetic information is duplicated, the cell must remove every one of these links. If even one link remains (or if an additional link is generated), two daughter chromosomes will remain intertwined and will not be properly segregated. In total, the ~30 trillion cells of the human body contain ~18 sextillion DNA links!

2.1 DNA Supercoiling

DNA can contain two different kinds of links: those that are formed between the two strands of the DNA two-braid and those that are formed between two separate segments of double helical DNA. This section will address the topological ramifications of links formed between the strands of the two-braid.

The linking number for a right-handed plectonemically coiled double helix is always positive [8, 9, 11, 18]; $Lk = 0$ would mean that the DNA was completely unwound with no crossings between the two strands of the helix, yielding a paranemic structure. Therefore, DNA topology is often expressed as the change in linking number, ΔLk , which is defined as the difference between the actual Lk of a DNA molecule and the Lk if the molecule were completely relaxed (Lk_0).

$$\Delta Lk = Lk - Lk_0 \quad (2)$$

For example, if the 1050-bp molecule above had an actual Lk of 94, then $\Delta Lk = 94 - 100 = -6$, which would mean that the molecule had 6% fewer links than in relaxed DNA.

A DNA molecule with a $\Delta Lk \neq 0$ is under stress, which can be distributed over the molecule as a combination of torsional and axial stress [8, 9, 11, 18]. Axial stress results in the superhelical twists depicted as crossovers in Fig. 1. Consequently, DNA

in which $\Delta Lk \neq 0$ is referred to as being “supercoiled.” DNA with a *negative* ΔLk is referred to as “underwound” or “negatively supercoiled,” and DNA with a *positive* ΔLk is referred to as “overwound” or “positively supercoiled.”

Because the number of links between the two strands in the DNA two-braid is dependent on the length of a given molecule, ΔLk is also length dependent. Therefore, the term σ (specific linking difference or, more commonly, superhelical density) is utilized to compare levels of supercoiling between DNA molecules of different sizes [8, 9, 11, 18]. The σ value is independent of DNA length and is calculated using the equation

$$\sigma = \Delta Lk \div Lk_0 \quad (3)$$

Thus, for the example discussed above, $\sigma = \Delta Lk(-6) \div Lk_0(100) = -0.06$. The σ value is always negative for underwound DNA and is always positive for overwound DNA.

Although DNA is typically drawn as a relaxed molecule, this topological form does not usually exist in nature. Organisms generally maintain their genome in an ~6% underwound state [8, 11, 15, 16, 18–20], which puts energy into DNA and enhances the opening of the double helix. This negative supercoiling is important because the two-braid is the storage form for the genetic material, and the two strands must be separated in order to express (i.e., transcribe) and duplicate (i.e., replicate) the information encoded in DNA.

While negative supercoiling is beneficial to the cell, DNA overwinding is problematic. Positively supercoiled DNA is generated ahead of replication and transcription machinery, because these tracking systems move through the DNA without rotating [7, 8, 24, 25], thereby pushing extra twists ahead of the replication or transcription bubble (Fig. 2). This overwinding makes it increasingly more difficult to open the double helix and, if unresolved, can block the progression of the tracking system [6–8, 11, 14, 15, 24, 25].

2.2 DNA Knotting and Tangling

This section will address the topological ramifications of links formed between two separate segments of double helical DNA.

As described above, human cells contain ~2 m of DNA (on 46 chromosomes) that is packed into a nucleus that is only 5–10 μm in diameter [3]. Thus, the DNA two-braid falls prey to the same problems as would be expected if a large number of very long ropes were constrained in a small space. Upon movement or manipulation of the ropes, knots (i.e., links formed within a single rope) and tangles (i.e., links formed between different ropes) are routinely formed. Similarly, biological processes that move or manipulate the double helix often induce the formation of knots and

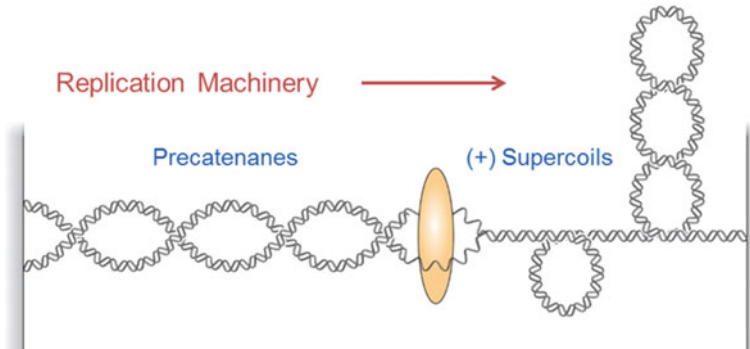


Fig. 2 Moving DNA tracking machinery creates topological problems. As tracking systems move through the DNA, twists are pushed ahead of the fork, resulting in the accumulation of positive supercoils. In the case of replication, precatenanes (links between newly synthesized daughter chromosomes) form behind the fork. Artwork by Ethan Tyler, National Institutes of Health Medical Arts

tangles into the DNA (Fig. 1). If unresolved, DNA knots and tangles can have lethal consequences.

Knots are formed as a result of recombination pathways that are used to increase genetic diversity and repair some types of DNA damage [6, 8, 11, 12, 24, 26, 27]. The presence of knots does not allow the two strands of the double helix to be separated and therefore prevents essential DNA processes such as replication and transcription from taking place.

DNA tangles are routinely formed during replication when some of the torsional stress in front of the fork redistributes behind it, resulting in links between the two newly synthesized DNA molecules (Fig. 2) [6, 8, 12, 24, 26, 27]. This tangling prevents the linked chromosomes from being properly segregated into daughter cells during mitosis or meiosis. Because DNA tangles are most easily represented as concatenated circles (shown in Fig. 1 as a hopf link), tangled DNA molecules are often referred to as being “catenated.”

The ΔLk in DNA knots and tangles is caused by the introduction of writhe. It is notable that these writhes are fundamentally different than those present in supercoiled DNA. Whereas writhes generated during supercoiling can be freely converted to twists, the crossovers observed in DNA knots and tangles are constrained as writhes [10, 11].

2.3 Alteration of DNA Topology by Strand Breakage

Assuming a closed topological system, the linking number of DNA can only be changed if one or both strands of the two-braid are cut [6, 8, 11, 12, 15, 24, 26, 27]. Cutting a single strand can alleviate (or, under some circumstances, induce) torsional

stress or twist within the molecule. Conversely, cutting both strands can alter the axial stress or writhe in the DNA.

In supercoiled DNA, the ΔLk is caused by a change in the number of links formed between the two strands of the double helix, resulting in a molecule in which twist and writhe are interconvertible. Therefore, supercoils within DNA can be removed by cutting either one or both strands of the two-braid [6, 8, 11, 12, 15, 24, 26–28]. In DNA knots and tangles, however, the ΔLk is the result of links between separate segments of DNA two-braids. Thus, the writhes in knots and tangles can only be removed if both strands are broken.

3 Topoisomerases

Cells express multiple enzymes known as topoisomerases that regulate the topological state of the genome [6, 9, 13, 15, 27, 29, 30]. Because DNA topology profoundly affects fundamental cellular processes, topoisomerases are encoded by all species. For simplicity, this article will focus primarily on topoisomerases expressed in humans and bacteria. These enzymes alter the superhelical density of DNA and resolve knots and tangles by creating transient breaks in the DNA backbone, which opens the topological system (Fig. 3) [6, 9, 13, 15, 27–32].

Topoisomerases are divided into two major classes based on how many DNA strands they cut to carry out their functions: type I topoisomerases cut one strand, and type II topoisomerases cut both strands of the two-braid [6, 9, 13, 15, 27, 29, 30]. In order to maintain the integrity of the genetic material while the DNA is cut, topoisomerases remain attached to the newly generated termini until they reseal the strand break(s). The stable complexes formed when these enzymes covalently attach to DNA are called “cleavage complexes” and are a hallmark of topoisomerase activity.

3.1 *Type I Topoisomerases*

There are two subclasses of type I topoisomerases in humans and bacteria: type IA and IB [8, 9, 22, 29, 33–37]. Type I enzymes are denoted by odd numerals and are grouped into the subclasses based on homology and enzymatic mechanism. Type IA topoisomerases use a “single-strand passage” mechanism in which they break one strand of the DNA two-braid, pass the opposite strand through the break, and rejoin the original strand (Fig. 4) [28, 29, 38]. When the enzyme cleaves the DNA, the energy of the broken sugar-phosphate bond is conserved by the formation of a new covalent bond between a tyrosyl residue in the active site of the enzyme and the newly generated 5'-terminal phosphate of the DNA. (DNA strands have a directionality defined by the linkages between the sugar and phosphate groups that make up their backbones. Each phosphate connects the 3'-carbon of one sugar to the 5'

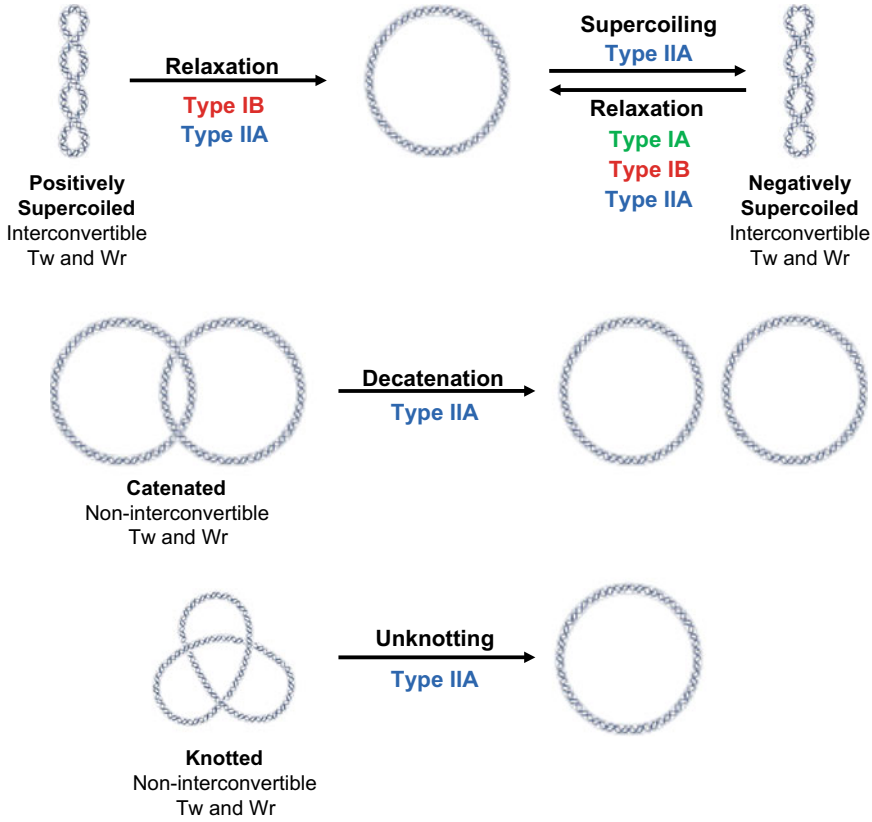


Fig. 3 Actions of type I and type II topoisomerases. The different cleavage activities of type I and type II topoisomerases allow them to work on different topological structures within double-stranded DNA. Because type I enzymes only cut one strand of the DNA, they are restricted to working on twist. Because type II enzymes cut both strands of the DNA, they are able to work on writhe

carbon of the following sugar in the chain.) The corresponding 3'-DNA terminus generated by the cleavage event is prevented from rotating by non-covalent interactions with the enzyme. As a result of the single-strand passage mechanism, every catalytic event mediated by type IA topoisomerases changes the linking number by one [13, 28, 29, 38].

Even though type IB topoisomerases also cut one strand of the DNA two-braid, they act by a very different mechanism than the type IA enzymes. Type IB topoisomerases alter DNA topology using a “controlled rotation” mechanism (Fig. 5) [13, 28, 29, 38]. These enzymes covalently attach to the 3'-terminal phosphate during the cleavage event and allow the 5'-DNA terminus of the cleaved strand to rotate about the intact strand. Each rotation changes the linking number by one. The number

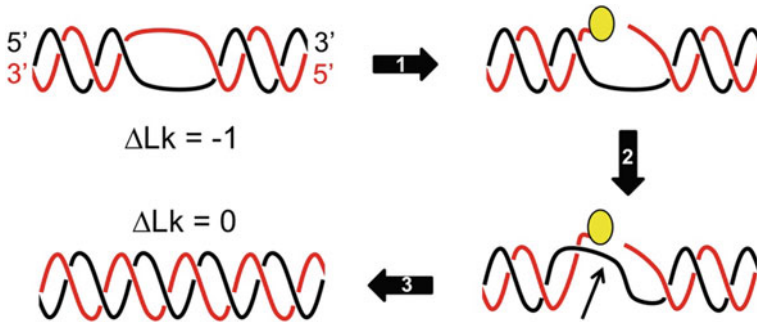


Fig. 4 “Single-strand passage” mechanism of type IA topoisomerases. The two strands of the DNA two-braid are depicted in red and black. The enzyme is drawn as a yellow circle. One enzymatic cycle is shown, during which one negative supercoil is relaxed, causing a change from $\Delta Lk = -1$ to $\Delta Lk = 0$

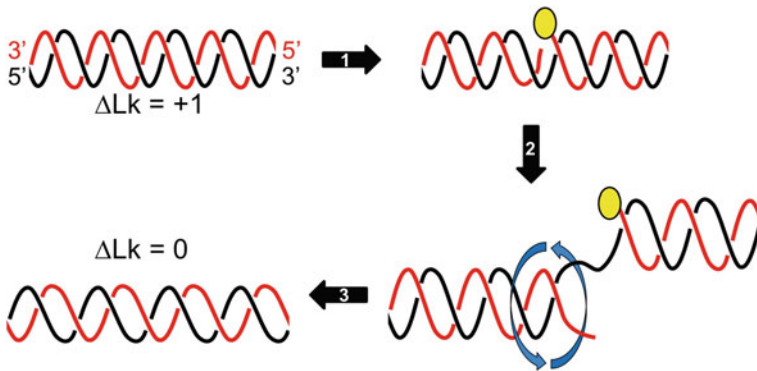


Fig. 5 “Controlled rotation” mechanism of type IB topoisomerases. The two strands of the DNA two-braid are depicted in red and black. The enzyme is drawn as a yellow circle. One enzymatic cycle is shown, during which one positive supercoil is relaxed, causing a change from $\Delta Lk = +1$ to $\Delta Lk = 0$

of strand rotations that occur per catalytic event depends on a number of factors, including the superhelical density of the DNA substrate.

Irrespective of the mechanism used (single-strand passage versus controlled rotation), type I topoisomerases always function by changing the number of links formed between the two strands of the DNA two-braid [13, 28, 29, 38]. Therefore, these enzymes alter DNA topology by changing twist. Consequently, they can alter the superhelical density of DNA, but they cannot resolve DNA knots or tangles formed within double-stranded DNA (Fig. 3).

Humans encode both type IA (topoisomerases III α and III β) and type IB (topoisomerase I) enzymes [6, 13, 14, 28, 29, 38]. Human topoisomerase III contributes to genomic stability and prevents inappropriate recombination by relaxing hyper-negatively supercoiled DNA [29, 33–37]. It also works with other proteins to resolve

recombination intermediates and stalled replication forks [9, 22, 29, 33–37]. In mice, deletion of the α isoform is lethal, while deletion of the β isoform shortens life span and has deleterious effects on fertility. In humans, deletion of topoisomerase III β is also associated with schizophrenia and neurodevelopmental disorders [39].

The major role of topoisomerase I is likely to remove torsional stress that accumulates ahead of replication forks and other DNA tracking systems [6, 13, 14, 28, 29, 38]. Although the enzyme is dispensable at the cellular level (presumably because of functional redundancies with type II topoisomerases), it appears to be necessary for proper development in multicellular organisms [6, 40–42].

Bacteria encode primarily type IA enzymes, topoisomerase I and topoisomerase III. Bacterial topoisomerase I is also known as ω protein and is unrelated to human topoisomerase I. (Unfortunately, a common name was assigned to both proteins before the differences were realized.) Bacterial topoisomerase I works in concert with gyrase (a type II topoisomerase discussed below) to regulate the overall superhelical state of the bacterial chromosome [22, 29, 38]. Bacterial topoisomerase III is a homolog of human topoisomerase III α and III β and also plays important roles in maintaining genomic stability [29, 43].

3.2 *Type II Topoisomerases*

There are two subclasses of type II topoisomerases: type IIA and IIB [9, 12, 29, 33–35, 44, 45]. Type II enzymes are denoted by even numerals (with the exception of gyrase, which is discussed below) and are grouped into the subclasses based on homology and reaction mechanism. To date, functional type IIB topoisomerases have been found only in plant and archaeal species. Therefore, only the type IIA enzymes, which are found in humans and bacteria, will be discussed in this article.

Type IIA topoisomerases alter DNA topology by using a “double-strand passage” mechanism in which they cleave both strands of the DNA two-braid, pass a second intact double-helical segment through the break, and rejoin the cleaved strands (Fig. 6) [12, 15, 26, 27, 29–31, 46]. The cleaved DNA is known as the “gate-” or “G-segment,” and the intact segment that is transported through the break is known as the “transport-” or “T-segment.” Type IIA enzymes in humans function as homodimers, whereas those in bacteria are A₂B₂ heterotetramers (the A and B subunits have fused to form the protomer subunit in the human enzyme) [12, 15, 26, 27, 29–31, 34, 44–46]. The structures of the enzymes have bilateral symmetry that allow for the formation of gated protein annuli at opposite ends. This permits the T-segment to be captured by the protein above the G-segment and exit the protein below it in a controlled fashion (Fig. 6). The double-strand passage reaction involves a series of coordinated protein movements that are coupled to the binding and hydrolysis of the high-energy cofactor ATP.

Due to their bilateral symmetry, type IIA topoisomerases have two active-site tyrosyl residues [29]. When the enzymes cut the double helix, these residues form covalent bonds with the newly generated 5'-terminal phosphates on opposite strands

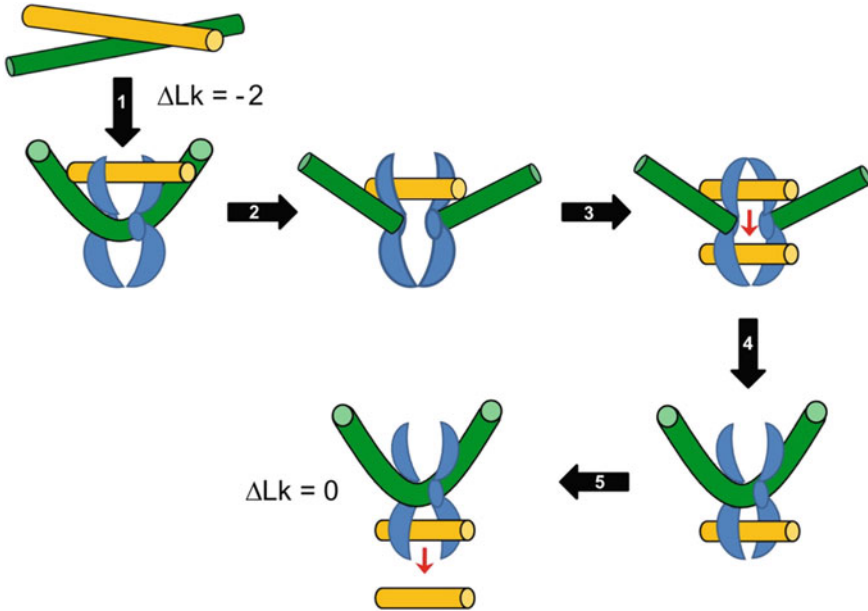


Fig. 6 “Double-strand passage” mechanism of type IIA topoisomerases. The two DNA two-bridges are shown in green (the G-segment) and yellow (the T-segment). The enzyme is shown in blue. One enzymatic cycle is shown, during which two negative supercoils are relaxed, causing a change from $\Delta Lk = -2$ to $\Delta Lk = 0$

of the DNA. The two scissile bonds are located across the major groove of the DNA, resulting in the formation of 4-base-long single-stranded chains on the 5'-end of each strand [26, 27, 29–31, 46–48]. As with the type I enzymes, this linkage preserves both genomic integrity and the energy of the broken sugar-phosphate bond.

Because type IIA topoisomerases act on two distinct DNA segments, they modulate DNA topology by altering writhe (Figs. 3 and 6) [9]. As a result of their reaction, they invert the sign of the writhe formed by the DNA crossover (for example, converting a -1 link to a $+1$ link). Thus, each event catalyzed by type IIA topoisomerases changes the linking number by two. The ability to work on writhe allows type II enzymes to modulate DNA superhelical density. More importantly, it allows them to remove DNA knots and tangles (in which writhe and twist are not interconvertible).

Humans encode two type IIA topoisomerases, topoisomerase II α and topoisomerase II β , which are closely related isoforms [6, 27, 29, 49–57]. (It is notable that vertebrates encode two isoforms of topoisomerase II, while invertebrates and lower eukaryotes encode only a single type II enzyme.) Topoisomerase II α and II β share ~70% of their amino acid sequence, but are encoded by separate genes. Although both use the double-strand passage reaction, they differ in their patterns of expression and their cellular functions [12, 27, 35, 44, 45, 54, 58]. Topoisomerase II α is essential for the survival of proliferating cells (its loss cannot be compensated

for by the β isoform), and its expression increases over the cell cycle, peaking in G2/M [59–61]. Rapidly growing cells contain ~500,000 copies of topoisomerase II α , while quiescent cells and differentiated tissues contain virtually none of the α isoform. Topoisomerase II α is associated with DNA replication complexes and remains bound to chromosomes throughout mitosis, suggesting that it has important functions in growth-related processes such as replication and chromosome segregation [6, 62].

Topoisomerase II β is required for neural development in mammals, but is otherwise dispensable at the cellular level [12, 14, 35, 45, 54, 58, 60, 63]. Unlike topoisomerase II α , topoisomerase II β is expressed at high concentrations in most cell types independent of proliferation status. The physiological functions of the β isoform are not yet fully defined. However, it dissociates from chromosomes during mitosis and seems to have an important role in the transcription of developmentally and hormonally regulated genes [35, 63–65].

With the exception of a few species, bacteria encode two type IIA topoisomerases, gyrase and topoisomerase IV [31, 46, 66, 67]. Gyrase is the only known topoisomerase that is able to introduce negative supercoils into DNA [29, 33, 35, 58]. To accomplish this task, gyrase wraps the DNA around the C-terminal domain of its A subunit in a right-handed fashion, thereby generating a constrained positive supercoil on the enzyme. (It should be noted that, similar to DNA, proteins have directionality. In this case, directionality is defined by the peptide bonds that link the amino acids in the protein chain and goes from the amino- or N-terminus of the protein to the carboxy- or C-terminus.) In mathematical terms, gyrase performs a type I Reidemeister move on the DNA [68, 69]. Because the DNA wrapping does not change the linking number of the molecule, a compensatory (equal but opposite) type I Reidemeister move is induced elsewhere in the DNA molecule [10, 68, 69], which introduces an unconstrained negative supercoil into the unbound portion of the two-braid. When strand passage occurs, the sign of the induced positive supercoil is inverted, causing a net introduction of two negative supercoils per catalytic cycle [8, 9, 12, 58]. Another important implication of this wrapping mechanism is that the G- and T-segments are on the same DNA molecule and are in close proximity [70]. Consequently, even though gyrase works only on writhe, it is much more efficient at relaxing positive supercoils and introducing negative supercoils than it is at decatenating or unknotting DNA, because these latter reactions require the use of G- and T-segments that are on different DNA molecules or are distal to each other on the same DNA molecule [29, 33, 35, 46, 58].

The major cellular roles of gyrase stem from the ability of the enzyme to carry out intramolecular reactions and to actively underwind DNA. Gyrase functions ahead of replication forks and transcription complexes to alleviate torsional stress induced by DNA overwinding [31, 35, 71]. Additionally, acting in conjunction with bacterial topoisomerase I, gyrase modulates the overall level of DNA supercoiling in the bacterial genome by introducing negative supercoils to maintain the genetic material in an underwound state [31, 35, 71].

Topoisomerase IV uses a “canonical” (i.e., non-wrapping) double-strand passage reaction similar to that utilized by the human type II enzymes [9, 29, 31, 46]. Consequently, topoisomerase IV is able to modulate superhelical density and is also able to carry out the intermolecular strand passage reactions required for decatenation and unknotting. Topoisomerase IV and gyrase display sequence homology. However, due to the differences between the canonical and wrapping mechanisms, they have distinct functions in the bacterial cell [12, 29, 31, 33, 35, 46, 58, 72]. While topoisomerase IV may be involved in regulating DNA over- and underwinding [73–75], its primary function is to remove knots and tangles formed by recombination and replication [31, 76–78].

4 Recognition of DNA Topology by Topoisomerases

Early studies on the recognition of DNA topology by topoisomerases were concerned with the ability of the enzymes to differentiate between their substrates and products. Consequently, these studies focused primarily on the distinction between negatively supercoiled and relaxed DNA. All of these studies demonstrated that topoisomerases interacted more tightly with their DNA substrates. For example, gyrase (which introduces negative supercoils into relaxed substrates) binds relaxed DNA ~10-fold more tightly than negatively supercoiled molecules [79]. Conversely, human topoisomerase IB [80] and eukaryotic topoisomerase IIA [81] display much higher affinities for supercoiled compared to relaxed DNA. Topoisomerase IIA also hydrolyzes its ATP cofactor more rapidly with negatively supercoiled substrates [81].

The first evidence for the mechanism by which topoisomerases distinguish supercoiled from relaxed DNA came from an electron microscopy study of topoisomerase-DNA complexes, which demonstrated that eukaryotic topoisomerase II binds at DNA crossovers [82]. A later study showed that topoisomerase II simultaneously binds two double-stranded DNA segments [83]. These findings are consistent with the facts that helix-helix juxtapositions are more prevalent in supercoiled molecules and that the type IIA enzyme acts on DNA writhes.

A surprising result of the electron microscopy study was that mammalian topoisomerase IB also binds at DNA crossovers, despite the fact that the enzyme works on twist [82]. The binding of crossovers as a means to differentiate between relaxed and supercoiled molecules was supported by a later study that demonstrated that the type IB enzyme bound equally well to positively and negatively supercoiled DNA, which eliminated topology recognition based on twist [80]. The binding site for the second DNA helix on type IB topoisomerases was later identified by a crystallographic study [84].

In contrast to topoisomerase IB, bacterial topoisomerase I (a type IA enzyme), which recognizes its supercoiled substrate by the single-strand character of the twist associated with negatively supercoiled DNA [85], does not bind at DNA crossovers [82].

5 Recognition of DNA Supercoil Geometry by Topoisomerases

Whereas the studies described above focused on the ability of topoisomerases to discern DNA substrates from reaction products, later studies recognized the fact that topoisomerases work on two very different supercoiled substrates: positively and negatively supercoiled molecules. As discussed above, DNA in organisms ranging from bacteria to humans is globally underwound by ~6% [8, 15, 16, 18–20]. However, the torsional stress generated by DNA tracking systems such as replication forks and transcription complexes acutely overwinds the DNA ahead of these molecular machines [6–8, 14, 15, 24, 25]. Therefore, these later studies focused on the ability of topoisomerases to discern the geometry (i.e., handedness) of DNA supercoils.

Two different aspects of supercoil geometry recognition by topoisomerases have been examined: the ability to discern supercoil handedness over the entire catalytic event and, more specifically, during the formation of cleavage complexes. Because the mechanisms and ramifications of geometry recognition during these processes differ significantly, they will be discussed separately below.

5.1 Recognition of DNA Supercoil Geometry During Catalysis

This section will discuss the ability of topoisomerases to discern supercoil handedness during catalysis (i.e., the process of changing DNA linking number). For enzymes other than gyrase, studies have examined the removal of positive versus negative supercoils. In the case of gyrase, the removal of positive supercoils has been compared to the introduction of negative supercoils into relaxed DNA.

5.1.1 Type I Topoisomerases

As a result of their mechanisms of action, type IA and type IB topoisomerases recognize DNA supercoil handedness in very different manners. Type IA topoisomerases will not relax positively supercoiled two-braids because they require substantial single-stranded character in their DNA substrate in order to carry out the single-strand passage reaction [85]. The overwinding associated with positive supercoiling impedes this necessary strand separation, whereas negative supercoiling naturally enhances opening of the two strands.

Conversely, type IB topoisomerases, which use a controlled rotation mechanism, can remove both positive and negative supercoils [86]. In fact, human topoisomerase I relaxes positively supercoiled DNA an order of magnitude faster than it does negatively supercoiled substrates [87]. This finding is consistent with simulation studies that suggest mechanistic differences between the removal of positive and negative

supercoils, which require the DNA to rotate in opposite directions within the active site of the enzyme [88]. It is also consistent with the primary physiological function of type IB topoisomerases, which is to remove the positive supercoils that accumulate ahead of DNA tracking systems [6, 13, 14, 28, 29, 38].

5.1.2 Type IIA Topoisomerases

All type IIA topoisomerases that use a canonical double-strand passage reaction (as opposed to wrapping) examined to date can remove both positive and negative supercoils. Topoisomerase IV [75, 89–91] and human topoisomerase II α [92, 93] both relax positively supercoiled DNA considerably faster than they do negatively supercoiled molecules. There are two significant differences between positively and negatively supercoiled DNA that could serve as the basis for this chiral recognition. First, the ΔTw (i.e., the difference in twist between the supercoiled and relaxed molecule) is opposite in positively and negatively supercoiled DNA. As discussed above, the differences in ΔTw that accompany over- and underwinding have significant effects on DNA strand separation. Second, the DNA crossings formed in positive and negative writhe occur with different angles ($\sim 60^\circ$ and $\sim 120^\circ$, respectively) [94]. The development of single-molecule systems in which two DNA segments can be interwound without altering twist allowed the mechanism of chiral recognition to be addressed. Both topoisomerase IV and human topoisomerase II α appear to distinguish between positively and negatively supercoiled substrates based on differences in writhe [90, 93]. This finding suggests that these enzymes can discern crossover angles formed at DNA nodes. Elements in the C-terminal domain of both enzymes are required for this recognition [94, 95].

In contrast to topoisomerase IV and human topoisomerase II α , a number of type IIA topoisomerases cannot discern DNA supercoiling geometry during catalysis and relax positive and negative supercoils at similar rates. Among these are human topoisomerase II β and the type IIA enzymes found in yeast, *Drosophila*, and some viral species [89, 92, 95–97]. It is not obvious why these enzymes do not recognize supercoil geometry. However, this once again seems to be related to the C-terminal domains of the type IIA enzymes, which vary widely between species and are lacking in the viral proteins. As further evidence for the role of this protein domain, replacement of the C-terminal domain of topoisomerase II β with that of topoisomerase II α results in a chimeric enzyme that is capable of distinguishing DNA geometry and relaxes positive supercoils an order of magnitude faster than it does negative supercoils [95].

Gyrase differs from other type IIA topoisomerases in that it does not normally relax negatively supercoiled DNA. Therefore, geometry recognition studies with gyrase have compared its abilities to remove positive supercoils and to introduce negative supercoils into relaxed DNA. These processes correspond to the major cellular roles of the enzyme: to remove positive supercoils ahead of DNA tracking systems and to maintain the negative superhelical density of the bacterial chromosome [31, 35, 71]. Gyrase relaxes positive supercoils ~ 10 -fold faster than it negatively supercoils relaxed DNA [91, 98]. The rapid removal of positive supercoils by gyrase

reflects its acute function of relaxing overwound DNA ahead of tracking systems and once again requires elements in the C-terminal domain of the enzyme. In this case, it is the specific amino acid residues responsible for DNA wrapping that are necessary [91].

5.2 Recognition of Supercoil Geometry During DNA Cleavage

Although critical to the catalytic function of topoisomerases, the formation of DNA cleavage complexes poses a potential danger to the cell (Fig. 7) [9, 14, 44, 57, 99]. When DNA tracking systems attempt to traverse covalent topoisomerase-cleaved DNA roadblocks in the two-braid, strand breaks can no longer be rejoined by the enzyme and require cellular repair pathways to re-establish the integrity of the double helix. If the strand breaks overwhelm the repair processes, they can induce mutations, chromosomal rearrangements, and cell death pathways. Thus, the enzymes that are necessary for modulating the topological state of DNA also have the potential to fragment the genome.

The inherent danger of cleavage complexes has been exploited for the development of important anticancer and antibacterial drugs that act by stabilizing these complexes. Camptothecin-based drugs that target human topoisomerase I are used to treat ovarian, colorectal, and small-cell lung cancers [100]. Etoposide, doxoru-

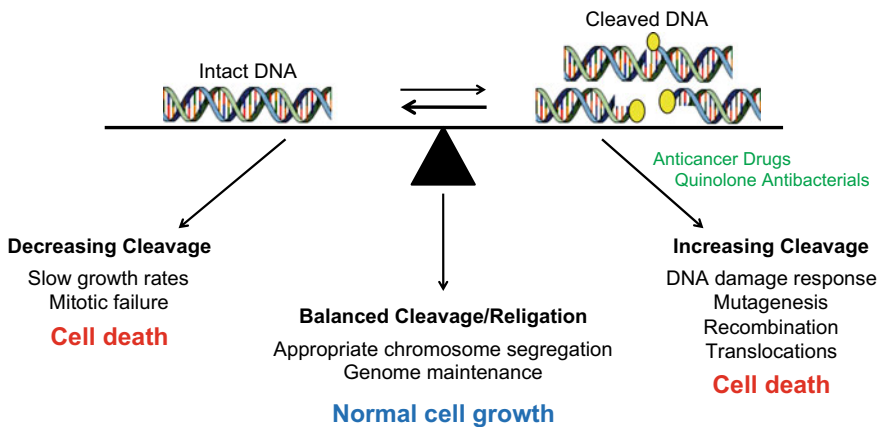


Fig. 7 Critical balance of DNA cleavage and resealing by topoisomerases. The activity of topoisomerases must be tightly controlled in the cell. When an appropriate level of cleavage complexes is maintained, topological problems are resolved and the cell can grow normally. If the levels of cleavage complexes decrease, slow growth rates and mitotic failure can cause cell death. Conversely, if the levels of cleavage complexes are too high, DNA damage can overwhelm the cell and also lead to cell death. Figure adapted from Pendleton et al. [57]

bicin, and mitoxantrone, which are used to treat a wide variety of blood-borne and solid tumors, target human topoisomerase II α and topoisomerase II β [44, 57, 99, 101, 102]. Finally, quinolones, such as ciprofloxacin and levofloxacin, which target gyrase and topoisomerase IV, are among the most widely prescribed antibacterial drugs worldwide [46, 67, 103, 104].

Because DNA cleavage complexes formed ahead of tracking systems are the most likely to be converted to permanent strand breaks, topoisomerase-mediated DNA cleavage events that occur on positively supercoiled DNA pose the greatest danger to the cell. Therefore, the ability of topoisomerases to discern supercoil geometry during the cleavage event has been addressed.

5.2.1 Type I Topoisomerases

No data has been reported for the cleavage of positively supercoiled DNA by type IA topoisomerases (presumably because these enzymes do not function on positively supercoiled molecules).

The only type IB topoisomerase for which geometry recognition during cleavage has been investigated is human topoisomerase I [105, 106]. In both the absence and presence of anticancer drugs, this enzyme maintains ~3-fold higher levels of cleavage complexes on positively as compared to negatively supercoiled DNA. Currently, there are no data that address the mechanistic basis for this distinction. However, this result implies that, while type IB topoisomerases work faster on positively supercoiled DNA, they are also inherently more dangerous to the cell while acting on this substrate.

5.2.2 Type IIA Topoisomerases

Even though human topoisomerase II α is the only eukaryotic type IIA topoisomerase that can recognize supercoil handedness during catalysis, human topoisomerase II α and II β can both discern supercoil geometry during DNA cleavage [105]. A similar result has been found for viral type IIA topoisomerases [96]. All of these enzymes maintain 2–4-fold lower levels of cleavage complexes with positively as compared to negatively supercoiled substrates. Similar results have been found in the absence and presence of anticancer drugs. While this characteristic makes these enzymes safer while operating ahead of DNA tracking systems, it also reduces the potential lethality of chemotherapeutics.

The differential abilities of type IIA enzymes to discern supercoil geometry during catalysis versus cleavage indicates that this recognition must be bimodal in nature. To this point, removal of the C-terminal domain, which is crucial for geometry recognition during catalysis, has no effect on supercoil handedness recognition during cleavage [96, 105]. A later study demonstrated that the ability of human topoisomerase II α to discern supercoil geometry is embedded within its catalytic core (which contains only the elements needed for the enzyme to cleave and rejoin DNA and does not

include either the N-terminal gate or the C-terminal domain) [107]. At the present time, it is not known whether the mechanistic basis for the recognition of supercoil geometry during cleavage is related to the crossover angle of the writhes or the sign of the ΔTw in the DNA.

The effects of supercoil geometry on DNA cleavage mediated by the bacterial type II topoisomerases, gyrase and topoisomerase IV, differ substantially from one another. Gyrase, like the human and viral type IIA enzymes, maintains 2–4-fold lower levels of cleavage complexes on positively supercoiled DNA both in the absence and presence of antibacterial drugs [91, 98, 108]. This recognition is independent of the ability of the enzyme to wrap DNA, which suggests that gyrase also uses a bimodal mechanism to recognize supercoil handedness during catalysis and cleavage. In contrast, topoisomerase IV is the only type IIA enzyme examined to date that does not maintain lower levels of cleavage complexes on positively supercoiled substrates. One study indicated that topoisomerase IV maintains similar levels of cleavage complexes on positively and negatively supercoiled DNA [91], while another suggested that it maintains higher levels of cleavage complexes on overwound substrates [75].

The differential abilities of gyrase and topoisomerase IV to recognize supercoil handedness during cleavage may impact their relative efficacies as targets for quinolone antibacterials. Because gyrase must operate on the overwound DNA formed ahead of replication forks and transcription complexes, it is perfectly positioned to generate cleavage complexes with the potential to be converted to permanent DNA damage. However, the diminished levels of cleavage complexes generated by the enzyme on positively supercoiled DNA may partially abrogate the cytotoxic effects of quinolones. Conversely, topoisomerase IV maintains high levels of cleavage complexes on overwound substrates, but typically acts behind the fork, where cleavage complexes are less likely to be disrupted by tracking systems.

6 Conclusions

DNA topology has a profound effect on how the genetic information is expressed, passed from generation to generation, and recombined in the cell. Topological linkages within the DNA two-braid and between different DNA segments can be described in simple mathematical terms that account for both the twist and the writhe in the double helix. Topoisomerases are enzymes that function as “molecular mathematicians” that regulate the topological state of the genetic material by altering either twist or writhe. To do so, type I and type II topoisomerases transiently open the topological system by breaking one or both strands of the two-braid, respectively.

The importance of topoisomerases is underscored by the fact that they are expressed in all cells and in all species. Topoisomerases can distinguish between the topological states of their substrates and products, which makes them more efficient enzymes. Furthermore, many topoisomerases can distinguish DNA supercoil handedness during catalysis and DNA cleavage, which makes them well suited to

their individual physiological tasks and also impacts their roles as targets of important anticancer and antibacterial drugs.

Acknowledgements Work in the senior author's laboratory was supported by National Institutes of Health grants R01 GM033944 and R01 GM126363 and US Veterans Administration Merit Review award 101 Bx002198. R.E.A. was supported by pre-doctoral fellowship DGE-0909667 from the National Science Foundation. We are grateful to Elizabeth G. Gibson for critical reading of the manuscript.

References

1. J.D. Watson, F.H.C. Crick, Molecular structure of nucleic acids. *Nature* **171**, 737–738 (1953)
2. International Human Genome Sequencing Consortium, Finishing the euchromatic sequence of the human genome. *Nature* **431**, 931–945 (2004)
3. B. Alberts, *Molecular Biology of the Cell*, 6th edn. (Garland Science, Taylor and Francis Group, New York, NY, 2015)
4. E. Bianconi, A. Piovesan, F. Facchin, A. Beraudi, R. Casadei, F. Frabetti, L. Vitale, M.C. Pelleri, S. Tassani, F. Piva et al., An estimation of the number of cells in the human body. *Ann. Hum. Biol.* **40**, 463–471 (2013)
5. R. Sender, S. Fuchs, R. Milo, Revised estimates for the number of human and bacteria cells in the body. *PLoS Biol.* **14**, e1002533 (2016)
6. J.C. Wang, Cellular roles of DNA topoisomerases: a molecular perspective. *Nat. Rev. Mol. Cell Biol.* **3**, 430–440 (2002)
7. O. Espeli, K.J. Marians, Untangling intracellular DNA topology. *Mol. Microbiol.* **52**, 925–931 (2004)
8. A.D. Bates, A. Maxwell, *DNA Topology* (Oxford University Press, New York, USA, 2005)
9. J.E. Deweese, M.A. Osheroff, N. Osheroff, DNA topology and topoisomerases: teaching a “knotty” subject. *Biochem. Mol. Biol. Educ.* **37**, 2–10 (2008)
10. C. Adams, A brief introduction to knot theory from the physical point of view, in *Proceedings of Symposia in Applied Mathematics: Applications of Knot Theory*, vol. 66, eds. by D. Buck, E. Flapan (American Mathematical Society, Providence, 2009), pp. 1–20
11. D. Buck DNA topology, in *Proceedings of Symposia in Applied Mathematics: Applications of Knot Theory*, vol. 66, eds. by D. Buck, E. Flapan (American Mathematical Society, Providence, 2009), pp. 47–80
12. Z. Liu, R.W. Deibler, H.S. Chan, L. Zechiedrich, The why and how of DNA unlinking. *Nucleic Acids Res.* **37**, 661–671 (2009)
13. S.H. Chen, N.L. Chan, T.S. Hsieh, New mechanistic and functional insights into DNA topoisomerases. *Annu. Rev. Biochem.* **82**, 139–170 (2013)
14. Y. Pommier, Y. Sun, S.N. Huang, J.L. Nitiss, Roles of eukaryotic topoisomerases in transcription, replication and genomic stability. *Nat. Rev. Mol. Cell Biol.* **17**, 703–721 (2016)
15. Y. Seol, K.C. Neuman, The dynamic interplay between DNA topoisomerases and DNA topology. *Biophys. Rev.* **8**, 101–111 (2016)
16. L. Finzi, W.K. Olson, The emerging role of DNA supercoiling as a dynamic player in genomic structure and function. *Biophys. Rev.* **8**, 1–3 (2016)
17. F.B. Fuller, The writhing number of a space curve. *Proc. Natl. Acad. Sci. USA* **68**, 815–819 (1971)
18. W.R. Bauer, F.H. Crick, J.H. White, Supercoiled DNA. *Sci. Am.* **243**, 100–113 (1980)
19. J.H. White, N.R. Cozzarelli, A simple topological method for describing stereoisomers of DNA catenanes and knots. *Proc. Natl. Acad. Sci. USA* **81**, 3322–3326 (1984)
20. A.V. Vologodskii, N.R. Cozzarelli, Conformational and thermodynamic properties of supercoiled DNA. *Annu. Rev. Biophys. Biomol. Struct.* **23**, 609–643 (1994)

21. M.R. Dennis, J.H. Hannay, Geometry of Calugareanu's theorem. *Proc. Roy. Soc. A* **461**, 3245–3254 (2005)
22. A.C. Ketrone, N. Osheroff, DNA topology and topoisomerases, in *Molecular Life Sciences: An Encyclopedic Reference*, ed. by E. Bell (Springer, New York, New York, NY, 2014), pp. 1–19
23. D. Shore, R.L. Baldwin, Energetics of DNA twisting. II. Topoisomer analysis. *J. Mol. Biol.* **170**, 983–1007 (1983)
24. A. Falaschi, G. Abdurashidova, O. Sandoval, S. Radulescu, G. Biamonti, S. Riva, Molecular and structural transactions at human DNA replication origins. *Cell Cycle* **6**, 1705–1712 (2007)
25. A. Travers, G. Muskhelishvili, A common topology for bacterial and eukaryotic transcription initiation? *EMBO Rep.* **8**, 147–151 (2007)
26. J.M. Fortune, N. Osheroff, Topoisomerase II as a target for anticancer drugs: when enzymes stop being nice. *Prog. Nucleic Acid Res. Mol. Biol.* **64**, 221–253 (2000)
27. A.K. McClendon, N. Osheroff, DNA topoisomerase II, genotoxicity, and cancer. *Mutat. Res.* **623**, 83–97 (2007)
28. J.B. Leppard, J.J. Champoux, Human DNA topoisomerase I: relaxation, roles, and damage control. *Chromosoma* **114**, 75–85 (2005)
29. J.J. Champoux, DNA topoisomerases: structure, function, and mechanism. *Annu. Rev. Biochem.* **70**, 369–413 (2001)
30. A.J. Schoeffler, J.M. Berger, Recent advances in understanding structure-function relationships in the type II topoisomerase mechanism. *Biochem. Soc. Trans.* **33**, 1465–1470 (2005)
31. C. Levine, H. Hiasa, K.J. Marians, DNA gyrase and topoisomerase IV: biochemical activities, physiological roles during chromosome replication, and drug sensitivities. *Biochim. Biophys. Acta* **1400**, 29–43 (1998)
32. Y. Pommier, Topoisomerase I inhibitors: camptothecins and beyond. *Nat. Rev. Cancer* **6**, 789–802 (2006)
33. K.D. Corbett, J.M. Berger, Structure, molecular mechanisms, and evolutionary relationships in DNA topoisomerases. *Annu. Rev. Biophys. Biomol. Struct.* **33**, 95–118 (2004)
34. P. Forterre, S. Gribaldo, D. Gadelle, M.C. Serre, Origin and evolution of DNA topoisomerases. *Biochimie* **89**, 427–446 (2007)
35. S.M. Vos, E.M. Tretter, B.H. Schmidt, J.M. Berger, All tangled up: how cells direct, manage and exploit topoisomerase function. *Nat. Rev. Mol. Cell Biol.* **12**, 827–841 (2011)
36. T. Viard, C.B. de la Tour, Type IA topoisomerases: a simple puzzle? *Biochimie* **89**, 456–467 (2007)
37. N.M. Baker, R. Rajan, A. Mondragon, Structural studies of type I topoisomerases. *Nucleic Acids Res.* **37**, 693–701 (2009)
38. Y.C. Tse-Dinh, Bacterial and archeal type I topoisomerases. *Biochim. Biophys. Acta* **1400**, 19–27 (1998)
39. G. Stoll, O.P. Pietilainen, B. Linder, J. Suvisaari, C. Brosi, W. Hennah, V. Leppa, M. Tornainen, S. Ripatti, S. Ala-Mello et al., Deletion of TOP3 β , a component of FMRP-containing mRNPs, contributes to neurodevelopmental disorders. *Nat. Neurosci.* **16**, 1228–1237 (2013)
40. J.L. Nitiss, Investigating the biological functions of DNA topoisomerases in eukaryotic cells. *Biochim. Biophys. Acta* **1400**, 63–81 (1998)
41. M.P. Lee, S.D. Brown, A. Chen, T.-S. Hsieh, DNA topoisomerase I is essential in *Drosophila melanogaster*. *Proc. Natl. Acad. Sci. USA* **90**, 6656–6660 (1993)
42. S.G. Morham, K.D. Kluckman, N. Voulomanos, O. Smithies, Targeted disruption of the mouse topoisomerase I gene by camptothecin selection. *Mol. Cell Biol.* **16**, 6804–6809 (1996)
43. C.R. Lopez, S. Yang, R.W. Deibler, S.A. Ray, J.M. Pennington, R.J. Digate, P.J. Hastings, S.M. Rosenberg, E.L. Zechiedrich, A role for topoisomerase III in a recombination pathway alternative to RuvABC. *Mol. Microbiol.* **58**, 80–101 (2005)
44. J.E. Deweese, N. Osheroff, The DNA cleavage reaction of topoisomerase II: wolf in sheep's clothing. *Nucleic Acids Res.* **37**, 738–749 (2009)
45. J.L. Nitiss, DNA topoisomerase II and its growing repertoire of biological functions. *Nat. Rev. Cancer* **9**, 327–337 (2009)
46. N.G. Bush, K. Evans-Roberts, A. Maxwell, DNA topoisomerases. *EcoSal Plus*, **6** (2015)

47. J.M. Berger, Structure of DNA topoisomerases. *Biochim. Biophys. Acta* **1400**, 3–18 (1998)
48. J.C. Wang, Moving one DNA double helix through another by a type II DNA topoisomerase: the story of a simple molecular machine. *Q. Rev. Biophys.* **31**, 107–144 (1998)
49. R. Velez-Cruz, N. Osheroff, DNA topoisomerases: type II, in *Encyclopedia of Biological Chemistry*, eds. by W.J. Lennarz, M.D. Lane (Elsevier, 2004), pp. 806–811
50. F.H. Drake, J.P. Zimmerman, F.L. McCabe, H.F. Bartus, S.R. Per, D.M. Sullivan, W.E. Ross, M.R. Mattern, R.K. Johnson, S.T. Crooke, Purification of topoisomerase II from amsacrine-resistant P388 leukemia cells. Evidence for two forms of the enzyme. *J. Biol. Chem.* **262**, 16739–16747 (1987)
51. F.H. Drake, G.A. Hofmann, H.F. Bartus, M.R. Mattern, S.T. Crooke, C.K. Mirabelli, Biochemical and pharmacological properties of p170 and p180 forms of topoisomerase II. *Biochemistry* **28**, 8154–8160 (1989)
52. M. Tsai-Pflugfelder, L.F. Liu, A.A. Liu, K.M. Tewey, J. Whang-Peng, T. Knutsen, K. Huebner, C.M. Croce, J.C. Wang, Cloning and sequencing of cDNA encoding human DNA topoisomerase II and localization of the gene to chromosome region 17q21-22. *Proc. Natl. Acad. Sci. USA.* **85**, 7177–7181 (1988)
53. J.R. Jenkins, P. Ayton, T. Jones, S.L. Davies, D.L. Simmons, A.L. Harris, D. Sheer, I.D. Hickson, Isolation of cDNA clones encoding the beta isozyme of human DNA topoisomerase II and localisation of the gene to chromosome 3p24. *Nucleic Acids Res.* **20**, 5587–5592 (1992)
54. C.A. Austin, K.L. Marsh, Eukaryotic DNA topoisomerase II β . *BioEssays* **20**, 215–226 (1998)
55. K.B. Tan, T.E. Dorman, K.M. Falls, T.D. Chung, C.K. Mirabelli, S.T. Crooke, J. Mao, Topoisomerase II α and topoisomerase II β genes: characterization and mapping to human chromosomes 17 and 3, respectively. *Cancer Res.* **52**, 231–234 (1992)
56. A.M. Wilstermann, N. Osheroff, Stabilization of eukaryotic topoisomerase II-DNA cleavage complexes. *Curr. Top. Med. Chem.* **3**, 1349–1364 (2003)
57. M. Pendleton, R.H. Lindsey Jr., C.A. Felix, D. Grimwade, N. Osheroff, Topoisomerase II and leukemia. *Ann. NY Acad. Sci.* **1310**, 98–110 (2014)
58. A.C. Gentry, N. Osheroff, DNA topoisomerases: type II, in *Encyclopedia of Biological Chemistry*, 2nd edn., eds. by W.J. Lennarz, M.D. Lane (Academic Press, Waltham, 2013), pp. 163–168
59. M.M. Heck, W.N. Hittelman, W.C. Earnshaw, Differential expression of DNA topoisomerases I and II during the eukaryotic cell cycle. *Proc. Natl. Acad. Sci. USA* **85**, 1086–1090 (1988)
60. R.D. Woessner, M.R. Mattern, C.K. Mirabelli, R.K. Johnson, F.H. Drake, Proliferation- and cell cycle-dependent differences in expression of the 170 kilodalton and 180 kilodalton forms of topoisomerase II in NIH-3T3 cells. *Cell Growth Differ.* **2**, 209–214 (1991)
61. K. Kimura, M. Saijo, M. Ui, T. Enomoto, Growth state- and cell cycle-dependent fluctuation in the expression of two forms of DNA topoisomerase II and possible specific modification of the higher molecular weight form in the M phase. *J. Biol. Chem.* **269**, 1173–1176 (1994)
62. P. Grue, A. Grasser, M. Sehested, P.B. Jensen, A. Uhse, T. Straub, W. Ness, F. Boege, Essential mitotic functions of DNA topoisomerase II α are not adopted by topoisomerase II β in human H69 cells. *J. Biol. Chem.* **273**, 33660–33666 (1998)
63. M.O. Christensen, M.K. Larsen, H.U. Barthelmes, R. Hock, C.L. Andersen, E. Kjeldsen, B.R. Knudsen, O. Westergaard, F. Boege, C. Mielke, Dynamics of human DNA topoisomerases II α and II β in living cells. *J. Cell Biol.* **157**, 31–44 (2002)
64. B.G. Ju, V.V. Lunnyak, V. Perissi, I. Garcia-Bassets, D.W. Rose, C.K. Glass, M.G. Rosenfeld, A topoisomerase II β -mediated dsDNA break required for regulated transcription. *Science* **312**, 1798–1802 (2006)
65. I.G. Cowell, Z. Sondka, K. Smith, K.C. Lee, C.M. Manville, M. Sidorcuk-Lesthuruge, H.A. Rance, K. Padget, G.H. Jackson, N. Adachi et al., Model for MLL translocations in therapy-related leukemia involving topoisomerase II β -mediated DNA strand breaks and gene proximity. *Proc. Natl. Acad. Sci. USA* **109**, 8989–8994 (2012)
66. C. Sissi, M. Palumbo, In front of and behind the replication fork: bacterial type IIA topoisomerases. *Cell. Mol. Life Sci.* **67**, 2001–2024 (2010)

67. V.E. Anderson, N. Osheroff, Type II topoisomerases as targets for quinolone antibacterials: turning Dr. Jekyll into Mr. Hyde. *Curr. Pharm. Des.* **7**, 337–353 (2001)
68. J.W. Alexander, G.B. Briggs, On types of knotted curves. *Ann. Math.* **28**, 562–586 (1926)
69. K. Reidemeister, Elementare begründung der knotentheorie. *Abh. Math. Sem. Univ. Hamburg* **5**, 24–32 (1927)
70. A. Morrison, N.R. Cozzarelli, Contacts between DNA gyrase and its binding site on DNA: features of symmetry and asymmetry revealed by protection from nucleases. *Proc. Natl. Acad. Sci. USA* **78**, 1416–1420 (1981)
71. D.A. Koster, A. Crut, S. Shuman, M.A. Bjornsti, N.H. Dekker, Cellular strategies for regulating DNA supercoiling: a single-molecule perspective. *Cell* **142**, 519–530 (2010)
72. J. Kato, Y. Nishimura, R. Imamura, H. Niki, S. Hiraga, H. Suzuki, New topoisomerase essential for chromosome segregation in *E. coli*. *Cell* **63**, 393–404 (1990)
73. H. Hiasa, K.J. Marians, Topoisomerase IV can support *oriC* DNA replication *in vitro*. *J. Biol. Chem.* **269**, 16371–16375 (1994)
74. E.L. Zechiedrich, A.B. Khodursky, S. Bachellier, R. Schneider, D. Chen, D.M. Lilley, N.R. Cozzarelli, Roles of topoisomerases in maintaining steady-state DNA supercoiling in *Escherichia coli*. *J. Biol. Chem.* **275**, 8103–8113 (2000)
75. N.J. Crisona, T.R. Strick, D. Bensimon, V. Croquette, N.R. Cozzarelli, Preferential relaxation of positively supercoiled DNA by *E. coli* topoisomerase IV in single-molecule and ensemble measurements. *Genes Dev.* **14**, 2881–2892 (2000)
76. X. Wang, R. Reyes-Lamothe, D.J. Sherratt, Modulation of *Escherichia coli* sister chromosome cohesion by topoisomerase IV. *Genes Dev.* **22**, 2426–2433 (2008)
77. M.C. Joshi, D. Magnan, T.P. Montminy, M. Lies, N. Stepankiw, D. Bates, Regulation of sister chromosome cohesion by the replication fork tracking protein SeqA. *PLoS Genet.* **9**, e1003673 (2013)
78. P. Zawadzki, M. Stracy, K. Ginda, K. Zawadzka, C. Lesterlin, A.N. Kapanidis, D.J. Sherratt, The localization and action of topoisomerase IV in *Escherichia coli* chromosome segregation is coordinated by the SMC complex. *MukBEF. Cell Rep.* **13**, 2587–2596 (2015)
79. N.P. Higgins, N.R. Cozzarelli, The binding of gyrase to DNA: analysis by retention by nitrocellulose filters. *Nucleic Acids Res.* **10**, 6833–6847 (1982)
80. K.R. Madden, L. Stewart, J.J. Champoux, Preferential binding of human topoisomerase I to superhelical DNA. *EMBO J.* **14**, 5399–5409 (1995)
81. N. Osheroff, Eukaryotic topoisomerase II. Characterization of enzyme turnover. *J. Biol. Chem.* **261**, 9944–9950 (1986)
82. E.L. Zechiedrich, N. Osheroff, Eukaryotic topoisomerases recognize nucleic acid topology by preferentially interacting with DNA crossovers. *EMBO J.* **9**, 4555–4562 (1990)
83. J. Roca, J.M. Berger, J.C. Wang, On the simultaneous binding of eukaryotic DNA topoisomerase II to a pair of double-stranded DNA helices. *J. Biol. Chem.* **268**, 14250–14255 (1993)
84. A. Patel, L. Yakovleva, S. Shuman, A. Mondragon, Crystal structure of a bacterial topoisomerase IB in complex with DNA reveals a secondary DNA binding site. *Structure* **18**, 725–733 (2010)
85. K. Kirkegaard, J.C. Wang, Bacterial DNA topoisomerase I can relax positively supercoiled DNA containing a single-stranded loop. *J. Mol. Biol.* **185**, 625–637 (1985)
86. J.J. Champoux, R. Dulbecco, An activity from mammalian cells that untwists superhelical DNA—a possible swivel for DNA replication (polyoma-ethidium bromide-mouse-embryo cells-dye binding assay). *Proc. Natl. Acad. Sci. USA* **69**, 143–146 (1972)
87. R.F. Frohlich, C. Veigaard, F.F. Andersen, A.K. McClendon, A.C. Gentry, A.H. Andersen, N. Osheroff, T. Stevnsner, B.R. Knudsen, Tryptophane-205 of human topoisomerase I is essential for camptothecin inhibition of negative but not positive supercoil removal. *Nucleic Acids Res.* **35**, 6170–6180 (2007)
88. L. Sari, I. Andricioaei, Rotation of DNA around intact strand in human topoisomerase I implies distinct mechanisms for positive and negative supercoil relaxation. *Nucleic Acids Res.* **33**, 6621–6634 (2005)

89. G. Charvin, D. Bensimon, V. Croquette, Single-molecule study of DNA unlinking by eukaryotic and prokaryotic type-II topoisomerases. *Proc. Natl. Acad. Sci. USA* **100**, 9820–9825 (2003)
90. K.C. Neuman, G. Charvin, D. Bensimon, V. Croquette, Mechanisms of chiral discrimination by topoisomerase IV. *Proc. Natl. Acad. Sci. USA* **106**, 6986–6991 (2009)
91. R.E. Ashley, A. Dittmore, S.A. McPherson, C.L. Turnbough Jr., K.C. Neuman, N. Osheroff, Activities of gyrase and topoisomerase IV on positively supercoiled DNA. *Nucleic Acids Res.* **45**, 9611–9624 (2017)
92. A.K. McClendon, A.C. Rodriguez, N. Osheroff, Human topoisomerase II α rapidly relaxes positively supercoiled DNA: implications for enzyme action ahead of replication forks. *J. Biol. Chem.* **280**, 39337–39345 (2005)
93. Y. Seol, A.C. Gentry, N. Osheroff, K.C. Neuman, Chiral discrimination and writhe-dependent relaxation mechanism of human topoisomerase II α . *J. Biol. Chem.* **288**, 13695–13703 (2013)
94. K.D. Corbett, A.J. Schoeffler, N.D. Thomsen, J.M. Berger, The structural basis for substrate specificity in DNA topoisomerase IV. *J. Mol. Biol.* **351**, 545–561 (2005)
95. A.K. McClendon, A.C. Gentry, J.S. Dickey, M. Brinch, S. Bendsen, A.H. Andersen, N. Osheroff, Bimodal recognition of DNA geometry by human topoisomerase II α : preferential relaxation of positively supercoiled DNA requires elements in the C-terminal domain. *Biochemistry* **47**, 13169–13178 (2008)
96. A.K. McClendon, J.S. Dickey, N. Osheroff, Ability of viral topoisomerase II to discern the handedness of supercoiled DNA: bimodal recognition of DNA geometry by type II enzymes. *Biochemistry* **45**, 11674–11680 (2006)
97. T.R. Strick, V. Croquette, D. Bensimon, Single-molecule analysis of DNA uncoiling by a type II topoisomerase. *Nature* **404**, 901–904 (2000)
98. R.E. Ashley, T.R. Blower, J.M. Berger, N. Osheroff, Recognition of DNA supercoil geometry by *Mycobacterium tuberculosis* gyrase. *Biochemistry* **56**, 5440–5448 (2017)
99. J.L. Nitiss, Targeting DNA topoisomerase II in cancer chemotherapy. *Nat. Rev. Cancer* **9**, 338–350 (2009)
100. Y. Pommier, DNA topoisomerase I inhibitors: chemistry, biology, and interfacial inhibition. *Chem. Rev.* **109**, 2894–2902 (2009)
101. Y. Pommier, E. Leo, H. Zhang, C. Marchand, DNA topoisomerases and their poisoning by anticancer and antibacterial drugs. *Chem. Biol.* **17**, 421–433 (2010)
102. Y. Pommier, C. Marchand, Interfacial inhibitors: targeting macromolecular complexes. *Nat. Rev. Drug Discov.* **11**, 25–36 (2012)
103. K.J. Aldred, R.J. Kerns, N. Osheroff, Mechanism of quinolone action and resistance. *Biochemistry* **53**, 1565–1574 (2014)
104. D.C. Hooper, G.A. Jacoby, Mechanisms of drug resistance: quinolone resistance. *Ann. N. Y. Acad. Sci.* **1354**, 12–31 (2015)
105. A.K. McClendon, N. Osheroff, The geometry of DNA supercoils modulates topoisomerase-mediated DNA cleavage and enzyme response to anticancer drugs. *Biochemistry* **45**, 3040–3050 (2006)
106. A.C. Gentry, S. Juul, C. Veigaard, B.R. Knudsen, N. Osheroff, The geometry of DNA supercoils modulates the DNA cleavage activity of human topoisomerase I. *Nucleic Acids Res.* **39**, 1014–1022 (2011)
107. R.H. Lindsey Jr., M. Pendleton, R.E. Ashley, S.L. Mercer, J.E. Deweese, N. Osheroff, Catalytic core of human topoisomerase II α : insights into enzyme-DNA interactions and drug mechanism. *Biochemistry* **53**, 6595–65602 (2014)
108. E.G. Gibson, T.R. Blower, M. Cacho, B. Bax, J.M. Berger, N. Osheroff, Mechanism of action of *Mycobacterium tuberculosis* gyrase inhibitors: a novel class of gyrase poisons. *ACS Infect. Dis.* **4**, 1211–1222 (2018)

Topological Entanglement and Its Relation to Polymer Material Properties



Eleni Panagiotou

Abstract In this manuscript we review recent results that show how measures of topological entanglement can be used to provide information relevant to dynamics and mechanics of polymers. We use Molecular Dynamics simulations of coarse-grained models of polymer melts and solutions of linear chains in different settings. We apply the writhe to give estimates of the entanglement length and to study the disentanglement of polymer melts in an elongational flow. Our results also show that our topological measures correlate with viscoelastic properties of the material.

Keywords Topology · Polymers · Inking number · Writhe · Entanglements · Knots · Viscoelasticity · Oscillatory shear · Entanglement length · Periodic linking number · Primitive path · Average crossing number

2010 Mathematics Subject Classification 57M25 · 82D60 · 91A44 · 92E10 · 76A99

1 Introduction

Polymers are macromolecules which cannot cross each other without breaking their bonds. This uncrossability constraint has a significant impact on the mechanical properties of polymeric material and its effects are called polymer entanglement [8, 11, 46]. Edwards suggested that entanglements restrict individual chains in a curvilinear tubelike region enclosing each chain [37]. The axis of the tube is a coarse-grained representation of the chain and it is called the *primitive path* (PP). There are several methods for extracting the PP network, such as the Z1-code [1, 21, 28, 47] and the CReTA algorithm [3, 50, 51]. Edwards also pointed out that one could see the polymer chains as mathematical curves in space and proposed to use topology to

E. Panagiotou (✉)

Department of Mathematics and SimCenter, University of Tennessee at Chattanooga,
Chattanooga, TN 37403, USA

e-mail: eleni-panagiotou@utc.edu

© Springer Nature Switzerland AG 2019

C. C. Adams et al. (eds.), *Knots, Low-Dimensional Topology and Applications*, Springer Proceedings in Mathematics & Statistics 284,
https://doi.org/10.1007/978-3-030-16031-9_21

435

study polymer entanglement [12, 13]. However, the connection between topological entanglement and polymer entanglement remains elusive and the use of topological tools in the study of material properties has not been fully exploited. In this review we present a series of computer simulations of polymeric material which are analyzed using topological tools to provide evidence that they capture information relevant to polymer mechanics.

One of the difficulties in studying topological entanglement in polymers, is that tools of topological complexity traditionally refer to closed curves. A *knot* (resp. *link*) is one (or more resp.) simple closed curve(s) in space without intersections. The complexity of these knots or links can be measured by using *topological invariants* [15, 22, 43]. The topological invariants are properties of knots or links, which remain invariant for isotopic configurations. In the case of linear polymers, the notion of topological invariant does not apply, since linear chains can be continuously deformed to attain any configuration [35, 37]. Recent advances have made it possible to identify knots and links in linear polymers (open chains) [18, 19, 32, 34, 49]. Even though very helpful, it is not known how these methods could be applied to a system of open chains evolving in time. An alternative approach is provided using the Gauss linking integral [35]. For two closed chains (ring polymers) the Gauss linking integral is a topological invariant that measures the algebraic number of times one chain turns around the other. For two open chains (linear polymers), it is a real number that is a continuous function of the chain coordinates. The Gauss linking integral can be also applied to one chain in order to provide measures of self-entanglement of a chain, called *writhe* [2, 7, 9, 25, 30, 31] and *average crossing number* [4–6, 9, 10]. Moreover, the simulation of polymers requires the use of Periodic Boundary Conditions (PBC) to avoid boundary effects, which creates periodic entanglement [35]. For this reason, a new measure of entanglement, the periodic linking number, was introduced in [35] to study linking in PBC. It is an extension of the Gauss linking integral in systems employing PBC that gives a topological invariant in the case of closed chains and a continuous function of the chain coordinates in the case of open chains. In this review we present a series of studies of entanglement in polymers using the Gauss linking integral and the periodic linking number which make a clear connection between polymer entanglement and topological entanglement.

First, we discuss how the writhe of the chains in a melt can be combined with the Z1 algorithm to provide a new estimator of the entanglement length, a key parameter in the tube model [38] and it was shown that this estimator has several advantages compared to estimators based on the output of Z1 only. The Gauss linking integral was used in combination with the Z1 algorithm to understand how the entanglement network deforms with the chains under the influence of a strong deformation [36] and revealed a different local and global behavior of the chains. In [39] we used computer simulations of polymeric weave material in an oscillatory shear experiment and studied their mechanical response and compared it to the complexity of the weaves, as it was measured by the Gauss linking integral. The results therein showed that there is a correlation between the viscoelasticity of the polymeric materials and the writhe and the periodic linking number of the chains. This suggests that one could

control the viscoelastic response of material by controlling the linking and writhe of the original chain conformations.

This paper is organized as follows. In Sect. 2 we introduce approaches to study the topology/geometry of the polymeric chains in a melt. In Sect. 3 we show how topological tools can be combined with contour reduction algorithms to provide information relevant to the tube model. In Sect. 4 we show how the combination of topological measures of entanglement with contour reduction algorithms can provide more insight in the conformational properties of chains under deformation. In Sect. 5 we present results that reveal the relation between the topology of the polymer entanglements and the bulk material mechanics.

2 Measures of Entanglement

2.1 The Gauss Linking Integral and the Periodic Linking Number

A measure of the degree to which polymer chains interwind and attain complex configurations is the Gauss linking integral:

Definition 2.1 (*Gauss Linking Number*) The Gauss *Linking Number* of two disjoint (closed or open) oriented curves l_1 and l_2 , whose arc-length parametrizations are $\gamma_1(t), \gamma_2(s)$ respectively, is defined as the following double integral over l_1 and l_2 [17]:

$$L(l_1, l_2) = \frac{1}{4\pi} \int_{[0,1]} \int_{[0,1]} \frac{(\dot{\gamma}_1(t), \dot{\gamma}_2(s), \gamma_1(t) - \gamma_2(s))}{\|\gamma_1(t) - \gamma_2(s)\|^3} dt ds, \tag{1}$$

where $(\dot{\gamma}_1(t), \dot{\gamma}_2(s), \gamma_1(t) - \gamma_2(s))$ is the *scalar triple product* of $\dot{\gamma}_1(t), \dot{\gamma}_2(s)$ and $\gamma_1(t) - \gamma_2(s)$.

The Gauss Linking Number is a topological invariant for closed chains and a continuous function of the chain coordinates for open chains.

We also define a measure for the degree of intertwining of a chain around itself.

Definition 2.2 (*Writhe*) For a curve ℓ with arc-length parameterization $\gamma(t)$ is the double integral over l :

$$Wr(l) = \frac{1}{4\pi} \int_{[0,1]} \int_{[0,1]} \frac{(\dot{\gamma}(t), \dot{\gamma}(s), \gamma(t) - \gamma(s))}{\|\gamma(t) - \gamma(s)\|^3} dt ds. \tag{2}$$

The Writhe is a continuous function of the chain coordinates for both open and closed chains. The Average Crossing Number (ACN) is obtained when we consider the absolute value of the integrand in the Writhe.

For systems employing Periodic Boundary Conditions (PBC), the linking that is imposed from one simulated chain on another chain propagates in three dimensional space by the images of the other chain. In other words, for a system with PBC each simulated chain gives rise to a *free chain* in the periodic system which consists of an infinite number of copies of the simulated chain. We call each copy of a chain an *image* of the free chain. It has been shown that a measure of entanglement that can capture the global linking in a periodic system is the *periodic linking number* LK_P [35].

Definition 2.3 (*Periodic Linking Number*) Let I and J denote two (closed, open or infinite) free chains in a periodic system. Suppose that I_u is an image of the free chain I in the periodic system. The *Periodic Linking Number*, LK_P , between two free chains I and J is defined as:

$$LK_P(I, J) = \sum_v L(I_u, J_v), \quad (3)$$

where the sum is taken over all the images J_v of the free chain J in the periodic system.

The Periodic Linking Number is a topological invariant for closed chains and a convergent series for open chains that changes continuously with the chain coordinates. For its computation, we use a cutoff, the *local Periodic Linking Number* [35, 40].

2.2 Z1 Algorithm

The Z1 algorithm [1, 28, 47], given a polymer melt configuration, minimizes the total contour length of all chains, while all chain ends remain fixed in space, by moving the beads sequentially in space while maintaining the noncrossability of the chains. In this way the chains become rectilinear strands coming together at kinks where the entanglements occur.

A direct consequence of the specific mathematical formulation is that the Z1 algorithm provides as output the average contour length of a PP, L_{pp} and, by mapping the extracted interior nodes of each PP into kinks, it also returns the average number of interior kinks (entanglements) per chain, \mathcal{Z} .

3 A New Method to Compute N_e -estimators via Writhe and \mathcal{Z}

In the core of the tube model is the notion of *entanglement strand*, N_e . This is a portion of a polymer chain in-between topological constraints in a melt. This length is also related to the radius of the surrounding tube. N_e is very important in characterizing

polymeric material [46] and estimates of N_e from low molecular weight simulations are needed. In this section we suggest a new N_e -estimator for polymer chains in a melt.

To do this, we combine the local entanglement information, provided by the Z1 algorithm, with the global entanglement information given by the writhe of a chain and its primitive path. In [38] a semi-analytical formula for the mean squared writhe of an entanglement strand, \mathcal{W}_e^2 , using only the writhe of the chain and the writhe of its PP was obtained:

$$\mathcal{W}_e^2 \approx \left\langle \frac{[W(I) - W_{pp}(I)]^2}{Z + 1} \right\rangle. \quad (4)$$

where $W(I)$ denotes the writhe of the chain I , $W_{pp}(I)$ denotes the writhe of the PP of the chain I and Z denotes the number of kinks in the PP of I . The average is taken over all chains in a melt.

We find that the mean squared writhe as a function of the length of the chains is very well approximated by:

$$\langle W^2 \rangle \approx 0.03 \left(\frac{N}{\kappa} \right)^{1.18}. \quad (5)$$

where κ is the stiffness parameter of the chains [38].

Since \mathcal{W}_e^2 is the mean squared writhe of polymer chains of length \mathcal{N}_e , one can obtain an estimator of N_e by comparing \mathcal{W}_e^2 to the values of the left hand side of Eq. 5.

Thus, a new N_e -estimator is given by the solution of the following equation:

$$\langle W^2 \rangle \approx 0.03 \left(\frac{\mathcal{N}_e}{\kappa} \right)^{1.18}. \quad (6)$$

for some stiffness parameter κ that depends on the system under study.

We apply the new N_e -estimator to a melt of multibead linear chains interacting via a repulsive Lennard-Jones (LJ) potential by molecular dynamics (MD) and compare our results to those obtained by other N_e -estimators for the same system. This is a classical multibead FENE chain system with a dimensionless number density 0.84 at temperature $T = 1$ [27]. We use a time step $\Delta t = 0.005$ within a velocity Verlet algorithm with temperature control. All samples were pre-equilibrated using a hybrid algorithm [26]. We apply the Z1 algorithm and compute the writhe of the chains and their PPs for various molecular weights N .

The Z1 code returns values for Z , L_{pp} and R_{ee} (end-to-end distance), by which, various estimators $\mathcal{N}_e(N)$ can be computed [20]. These are the *classical S-coil* estimator, the *M-coil* estimator, *classical S-kink* estimator and the *modified S-kink* estimator [20], shown in Fig. 1.

For our systems, where the corresponding stiffness parameter is $\kappa \approx 2.34$, Eq. (6) gives a new N_e -estimator by the solution of the following equation

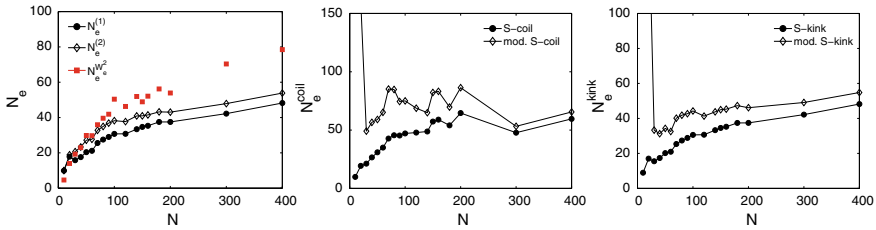


Fig. 1 $\mathcal{N}_e(N)$ obtained by counting beads, $\mathcal{N}_e^{(1)}$, $\mathcal{N}_e^{(2)}$ and via writhe, $\mathcal{N}_e^{\mathcal{W}_e^2}$. We observe that $\mathcal{N}_e^{(1)}(N) := \langle \mathcal{N}_e \rangle_t \approx \langle \mathcal{N}_e \rangle + 5 := \mathcal{N}_e^{(2)}(N) + 5$. Also, we observe that $\mathcal{N}_e^{\mathcal{W}_e^2}(N)$ gives a larger estimate. The data for $\mathcal{N}_e^{\mathcal{W}_e^2}(N)$ is compatible with a limiting value of $N_e \approx 80$ obtained by the M-coil estimator [20]

$$\mathcal{W}_e^2(N) = 0.01 \mathcal{N}_e^{1.18}(N). \tag{7}$$

We denote this estimator by $\mathcal{N}_e^{\mathcal{W}_e^2}$, shown in Fig. 1. The data suggests a limiting value of $N_e \approx 80$, which agrees with the known N_e value reported in experiments [44, 48]. We notice that $\mathcal{N}_e^{\mathcal{W}_e^2}$ is not an ideal estimator, since it converges quite slowly. However, it approaches the M-coil estimator faster than any of the other estimators. We note that the estimates of N_e based on counting the number of beads between kinks and the M-kink estimators give an estimate $N_e \approx 45$ that is almost half of the one reported by using our topological/geometrical methods and that reported in rheological experiments [20, 29, 50, 51]. Our results indicate a transition to the presence of kinks for chains with $N > 45$. These findings suggest that N_e is related to the global topological entanglement of the chains, captured by $\mathcal{N}_e^{\mathcal{W}_e^2}$, while only a fraction of this value, approximately half, seems to be related to the number of local obstacles restricting the local motion of the chains, and is captured by the number of beads between kinks and the M -kink estimators.

4 Topological Entanglement and Disentanglement of Polymer Chains with an Elongational Force

In this work we study the entanglement characteristics of linear chains in a melt under the action of directed forces [36]. We obtain information about the motion of the chains, their PPs and the entanglement strands. To study the pulling-force induced flow behavior of model polymer melts, we have performed nonequilibrium molecular dynamics (NEMD) computer simulations at constant bead number density, volume, and temperature (NVT ensemble) in a cubic cell with PBC. More precisely, we study a classical multibead FENE chain system with a dimensionless number density 0.84 at temperature $T = 1$, with $M = 100$ linear chains, where each chain consists of $N = 100$ beads. All the beads interact with a purely repulsive part of the

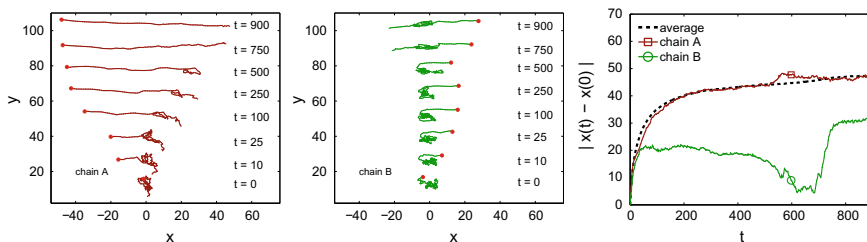


Fig. 2 Selected sequences of snapshots for individual chains contained in the melt, artificially shifted vertically with time. The marked head groups experience a constant force in x -direction. Chains tend to either unravel completely, or to tighten existing knots. The absolute displacement of the force-bearing bead in x -direction for the two chains shown in (a,b), as well as $\langle |x(t) - x(0)| \rangle$ obtained as an average over all chains is shown in the last figure

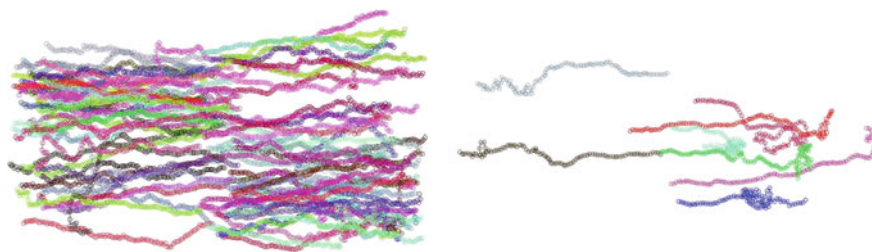


Fig. 3 Visualization of the final elongated melt state. Only the parent images of the in total 100 chains are shown. Left: Subset of chains with $|W| < 0.5$ and Right: $|W| \geq 0.5$. As expected, most of the chains with $|W| > 0.5$ contain local tight knots [42]

Lennard-Jones potential, and all dimensionless values are given in Lennard-Jones (LJ) units. To create samples that largely differ in their number of entanglements, while N and the simulation box size remain constant, we apply a constant force of magnitude $F = 50$ pointing into the negative (positive) x -direction to all those terminal beads (a randomly selected one for each chain) that are initially located in the left (right) half of the simulation box.

With time the chains tend to be pulled straight (while remaining within the periodic simulation box) as a result of the enforced overall deterministic motion of their selected ends (Figs. 2 and 3). A peculiarity of this simulation setup is that one can reach a state of almost fully elongated chains, while going through all intermediate states of partial elongation quickly compared with the situation encountered in conventional elongational flows, where the flow-induced alignment is caused by thermostatting with respect to an affine deformation.

The end-to-end distance, $\mathcal{R}_{ee} = \langle R_{ee}^2 \rangle^{1/2}$, as function of time is shown in Fig. 4a. The plateau value is $\mathcal{R}_{ee} \approx 93$, ie. $\sim 93\%$ of the value corresponding to the fully aligned conformation whose bonds remain at the equilibrium bond length ≈ 1 . We observe that \mathcal{R}_{ee} initially increases rapidly with time, in analogy to the case of

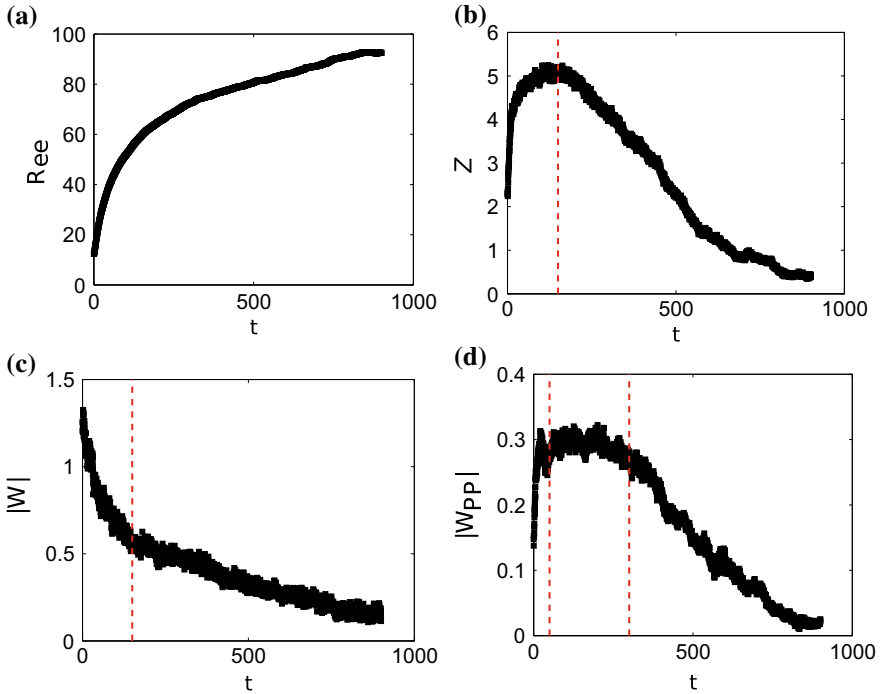


Fig. 4 **a** Square-root of the mean squared end-to-end distance, $\mathcal{R}_{ee} = \langle R_{ee}^2 \rangle^{1/2}$, as a function of time. **b** Number of entanglements computed by the Z1 algorithm. The vertical dashed line is at $t = 150$. **c** Mean absolute writhe, $\langle |W| \rangle$ vs time. The vertical dashed line is at $t = 150$. **d** Mean absolute writhe of the PPs, $\langle |W_{pp}| \rangle$ versus time. The two vertical dashed lines are at $t = 50$ and $t = 300$, respectively

an applied shear or elongational flow. A simultaneous chain alignment is visually obvious from the snapshots in Figs. 2 and 3.

The mean number of kinks \mathcal{Z} as a function of time is shown in Fig. 4b. We observe an initial increase of \mathcal{Z} followed by a decrease until all the kinks are lost. The increase of \mathcal{Z} is a surprising result since one expects that the network will disentangle as the chains stretch in time [23]. This has been observed also before for knotted configurations [24]. The excess in \mathcal{Z} may be an effect of the particular protocol, where the chain ends are pulled into the initially stationary matrix of the other chains and, thus, as the chains stretch out, there is more available length where contacts with other chains can occur.

The mean absolute writhe averaged over all chains in the melt as a function of time is shown in Fig. 4c. The mean absolute writhe of the original FENE chains decreases monotonically with time. This is expected, since the chains stretch and the writhe gives on average smaller absolute value for more extended configurations [45].

The mean absolute writhe of all PPs in the PP network obtained by the application of the Z1 algorithm as a function of time is shown in Fig. 4d. The increase of $\langle |W_{pp}| \rangle$

for $t < 50$ and the decrease for $t > 300$ is in accordance with the behavior of \mathcal{Z} in the same time intervals. This indicates that the created entanglements are not all simple contacts, but that the conformations of the PPs get indeed more complex. But, for $50 < t < 150$, $\langle |W_{pp}| \rangle$ remains almost constant, while \mathcal{Z} continuously increases in this time. In other words, the creation of new kinks in this interval does not affect the global self-entanglement of the PPs. Our results thus demonstrate that only a portion of the newly created entanglements contribute to a more complex global conformation of the tube.

It is worth emphasizing that the behaviors of $\langle |W| \rangle$ and $\langle |W_{pp}| \rangle$ differ substantially. For $t < 150$, $\langle |W| \rangle$ decreases while $\langle |W_{pp}| \rangle$ increases. This indicates that the chains continuously stretch out while the tube gets more entangled. For $t < 350$, $\langle |W| \rangle$ decreases while $\langle |W_{pp}| \rangle$ is almost constant. During that period, the chains continue being stretched while the tube remains in an unaltered conformation. For $t > 450$ both $\langle |W| \rangle$ and $\langle |W_{pp}| \rangle$ follow the same scaling, both decreasing. Interestingly, $\langle |W(t)| \rangle > \langle |W_{pp}(t)| \rangle$, for all t . This suggests that even at large t , when the PPs have stretched out, chains have eventually not stretched out in a comparable fashion due to self-entanglement/knotting of the original chains (chain B in Fig. 2 and also chains shown in Fig. 3).

5 Topological Entanglement and Viscoelastic Properties of Polymers

We investigate the relationship between the writhe and the periodic linking number of the chains in a melt with the viscoelastic parameters of the material, using an oscillatory shear simulation. In order to better control the effects of entanglement and show that the topological measures can reflect material properties even in weakly entangled systems, we use very particular initial configurations. We consider materials that have polymer chains entangled in a weave-like topology, see Fig. 5. We consider weave topologies given by aligned (w0), orthogonal non-interlaced at different densities (wI, wII) and alternating interlacing (wIII). By subjecting the material to oscillatory shear deformations, we can measure the extent the density or the topological complexity affect mechanical responses.

The polymers are treated as elastic macromolecules modeled with harmonic bond potential of energy $E = K_b(r - r_0)^2$, $K_b = 250$, r denotes the length of extension of the polymer bonds and $r_0 = 1$ denotes the rest length of the bond. The polymer bending stiffness is controlled with a harmonic angle potential with energy $E = K_\theta(1 - \cos(\theta - \theta_0))$, with $K_\theta = 8$, where θ is the angle between two consecutive bonds. The rest angle is $\theta_0 = \pi$. The length of the simulation box is approximately 20σ . Each polymer chain has approximately 20 monomers inside the simulation box. The beads of our polymers interact through the Lennard-Jones (LJ) potential with a cutoff of 2.5σ . We simulate the finite temperature and kinetics of the polymer chain

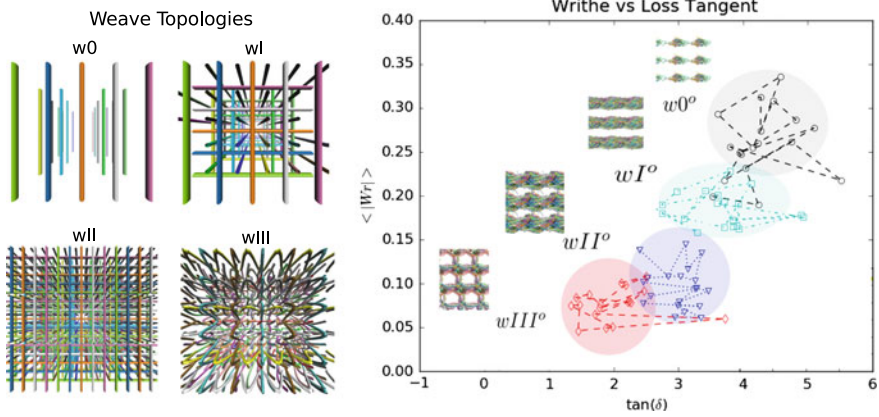


Fig. 5 Left: The different weaves we consider in our studies labelled as weave0 (w0), weaveI (wI), weaveII (wII) and weaveIII (wIII). Shown from top (left to right), bottom (left to right). Right: Writhe and Loss Tangent of open chains for small frequencies of oscillation (frequencies corresponding to periods $T > 6\tau_D$). We find a linear behavior of the Writhe as a function of the Loss Tangent. The data points corresponding to the different weaves form clusters. As the topological complexity of the weave decreases both the Writhe and Loss Tangent increase

dynamics using the Langevin Thermostat [16]. We perform these simulations using LAMMPS [41].

To study the bulk mechanics of the polymeric system, we perform rheological studies using oscillatory shearing motions based on Lees-Edwards boundary conditions [33]. We use a sinusoidal oscillation of the displacement $L(t) = L_0 + A \sin(2\pi t/T_p)$ with amplitude A and time periodicity T_p . This corresponds to a cosine oscillation of the strain with rate $\dot{\gamma} = \dot{\gamma}_0 \cos(\omega t)$ where $\omega = 2\pi/T_p$ and $\dot{\gamma}_0 = A\omega$. As a measure of material response, we consider the dynamic complex modulus $G(\omega) = G_1(\omega) + iG_2(\omega)$. The components are defined from measurements of the stress as the least-squares fit of the periodic stress component σ_{xy} by the function $g(t) = G_1(\omega)\gamma_0 \sin(\omega t) + G_2(\omega)\gamma_0 \cos(\omega t)$. The G_1 is referred as the Elastic Storage Modulus and G_2 is described as the Viscous Loss Modulus. The loss tangent, $\tan(\delta)$, is the ratio of G_2 over G_1 and can be interpreted as reflecting the strength of what is sometimes called “colloidal forces”. In other words, if $\tan \delta < 1$ then the particles are highly associated and sedimentation could occur, representative of a solid-like material. If $\tan \delta > 1$, the particles are highly unassociated, representative of a liquid-like material.

We show the mean absolute Writhe of open chains as a function of the loss tangent for small frequencies of oscillation in Fig. 5. We find a decay of the mean absolute Writhe with the loss tangent and a clustering of the data for each system. These results show a relationship between Writhe and $\tan \delta$ that scales like $\langle |Wr| \rangle \sim \tan \delta^{6/5}$. The responses at small frequencies are clustered and ordered with their Writhe decreasing as $w0 > wI > wII > wIII$. The increase of the writhe with the loss tangent occurs since for less complex weaves, the chains are free from entanglements and can

attain conformations of random coils. On the other hand, the more complex woven configurations, significantly restrict the motion of the chains and keep them together.

Similar results were reported in [39] for the mean absolute Periodic Linking Number of the open systems at small frequencies as a function of the loss tangent. The mean absolute Periodic Linking Number decreases with the loss tangent for $\tan \delta > 1$. For $\tan \delta > 1$ the responses of the open systems are fitted to a relation of the form $\langle |LK_P| \rangle \sim \tan \delta^{-5/4}$. These results show that interactions underlying mechanical responses can be effectively captured by the Periodic Linking Number.

6 Conclusions

The results presented in this review provide strong evidence that topological tools can provide information relevant to polymer mechanics. We showed that the writhe and the periodic linking number are correlate with the viscoelasticity of the material in simple, weakly entangled polymer conformations. Our topological tools can be applied to different length scales to provide information about local and global entanglement. We saw that the writhe in combination with the output of the Z1 code gives an estimator of the entanglement length, a characteristic length scale in polymer physics. Moreover, using the writhe, we were able to better understand the disentanglement process of polymers in a melt. It would be interesting to further explore this in more complicated, realistic systems of polymer melts. Ideally, we would like to include topological parameters in theories of polymer entanglement with the goal of creating new material with desired macroscopic properties by controlling their entanglement [14, 46].

References

1. Z1 is available online at <http://www.complexfluids.ethz.ch/Z1>
2. P.K. Agarwal, H. Edelsbrunner, Y. Wang, Computing the writhing number of a polygonal knot. *Discrete Comput. Geom.*, 32:37–53 (2004)
3. S. Anogiannakis, C. Tzoumanekas, D.N. Theodorou, Microscopic description of entanglements in polyethylene networks and melts. *Macromolecules* **45**, 9475–9492 (2012)
4. J. Arsuaga, Y. Diao, M. Vazquez. Mathematical methods in DNA topology: applications to chromosome organization and site-specific recombination. in *Mathematics of DNA Structure, Functions and Interactions*, eds. by C.J. Benham, S. Harvey, W.K. Olson, D. W. Sumners, D. Swigon (New York: Springer Science + Business Media, 2009), vol. 40, pp. 7–36
5. G.A. Arteca, Self-similarity complexity along the backbones of compact proteins. *Phys. Rev. E*, **56**, 4516–4520 (1997)
6. G.A. Arteca, O. Tapia, Relative measure of geometrical entanglement to study folding-unfolding transitions. *Int. J. Quant. Chem.* **80**, 848–855 (2000)
7. M.A. Berger, C. Prior, The writhe of open and closed curves. *J. Phys. A*, **39**, 8321–8348 (2006)
8. P.G. de Gennes, *Scaling concepts in Polymer Physics* (Cornell University Press, 1979)
9. Y. Diao, A. Dobay, A. Stasiak, The average inter-crossing number of equilateral random walks and polygons. *J. Phys. A Math. Gen.* **38**, 7601–7616 (2005)

10. Y. Diao, R.N. Kushner, K.C. Millett, A. Stasiak, The average crossing number of equilateral random polygons. *J. Phys. A Math. Gen.* **36**, 11561–11574 (2003)
11. M. Doi, S.F. Edwards, *The Theory of Polymer Dynamics* (Clarendon Press, Oxford, 1986)
12. F. Edwards, Statistical mechanics with topological constraints. I *Proc. Phys. Soc.* **91**, 513–9 (1967)
13. F. Edwards, Statistical mechanics with topological constraints: II. *J. Phys. A Gen. Phys.* **1**, 15–28 (1968)
14. G.H. Fredrickson, *The Equilibrium Theory of Inhomogeneous Polymers* (Oxford University Press, 2013)
15. P. Freyd, D. Yetter, J. Hoste, W. Lickorish, K.C. Millett, A. Ocneanu, A new polynomial invariant for knots and links. *Bull. Am. Math. Soc.* **12**, 239–46 (1985)
16. C.W. Gardiner, *Handbook of Stochastic Methods* (Series in Synergetics. Springer, 1985)
17. K.F. Gauss, *Werke* (Kgl. Gesellsch. Wiss., Göttingen, 1877)
18. D. Goundaroulis, N. Gügümcü, S. Lambropoulou, J. Dorier, A. Stasiak, L.H. Kauffman, Topological models for open knotted protein chains using the concepts of knotoids and bonded knotoids. *Polymers* **9**, 444 (2017)
19. N. Gügümcü, S. Lambropoulou, Knotoids, braidoids and applications. *Symmetry* **9**, 315 (2017)
20. R.S. Hoy, K. Foteinopoulou, M. Kröger, Topological analysis of polymeric melts: Chain-length effects and fast-converging estimators for entanglement length. *Phys. Rev. E* **80**, 031803 (2009)
21. N.C. Karayiannis, M. Kröger, Combined molecular algorithms for the generation, equilibration and topological analysis of entangled polymers: Methodology and performance. *Int. J. Mol. Sci.* **10**, 5054–5089 (2009)
22. L.H. Kauffman, *Knots and Physics*, volume 1 of *Series on knots and everything* (World Scientific, 1991)
23. J.M. Kim, D.J. Keffer, B.J. Edwards, M. Kröger, Rheological and entanglement characteristics of linear-chain polyethylene liquids in planar cuette and planar elongational flow. *J. Non-Newtonian Fluid Mech.* **152**, 168–183 (2008)
24. D. Kivotides, S.L. Wilkin, T.G. Theofanous, Entangled chain dynamics of polymer knots in extensional flow. *Phys. Rev. E* **80**, 041808 (2009)
25. K. Klenin, J. Langowski, Computation of writhe in modelling of supercoiled dna. *Biopolymers* **54**, 307–317 (2000)
26. M. Kröger, Efficient hybrid algorithm for the dynamic creation of semiflexible polymer solutions, brushes, melts and glasses. *Comput. Phys. Commun.* **118**, 278–298 (1999)
27. M. Kröger, Simple models for complex nonequilibrium fluids. *Phys. Rep.* **390**, 453–551 (2004)
28. M. Kröger, Shortest multiple disconnected path for the analysis of entanglements in two- and three-dimensional polymeric systems. *Comput. Phys. Commun.* **168**, 209–232 (2005)
29. F. Lahmar, C. Tzoumanekas, D.N. Theodorou, B. Rousseau, Topological analysis of linear polymer melts: a statistical approach. *Macromolecules* **42**, 7485 (2009)
30. C. Laing, D.W. Sumners, Computing the writhe on lattices. *J. Phys. A* **39**, 3535–3543 (2006)
31. C. Laing, D.W. Sumners, The writhe of oriented polygonal graphs. *J. Knot Theor. Ramif.* **17**, 1575–1594 (2008)
32. M. Laso, N.C. Karayiannis, K. Foteinopoulou, L. Mansfield, M. Kröger, Random packing of model polymers: local structure, topological hindrance and universal scaling. *Soft Matter* **5**, 1762–1770 (2009)
33. A.W. Lees, S. Edwards, The computer study of transport processes under extreme conditions. *J. Phys. C: Solid State Phys.* **5**, 1921 (1972)
34. K.C. Millett, A. Dobay, A. Stasiak, Linear random knots and their scaling behavior. *Macromolecules* **38**, 601–606 (2005)
35. E. Panagiotou, The linking number in systems with periodic boundary conditions. *J. Comput. Phys.* **300**, 533–573 (2015)
36. E. Panagiotou, M. Kröger, Pulling-force-induced elongation and alignment effects on entanglement and knotting characteristics of linear polymers in a melt. *Phys. Rev. E* **90**, 042602 (2014)

37. E. Panagiotou, M. Kröger, K. Millett, Writhe versus mutual entanglement of linear polymer chains in a melt. *Phys. Rev. E* **88**, 062604 (2013)
38. E. Panagiotou, M. Kröger, K.C. Millett, Writhe and mutual entanglement combine to give the entanglement length. *Phys. Rev. E* **88**, 062604 (2013)
39. E. Panagiotou, K.C. Millett, P.J. Atzberger, Topological methods for polymeric materials: characterizing the relationship between polymer entanglement and viscoelasticity. *Polymers* **11**(3), 43 (2019)
40. E. Panagiotou, C. Tzoumanekas, S. Lambropoulou, K.C. Millett, D.N. Theodorou, A study of the entanglement in systems with periodic boundary conditions. *Progr. Theor. Phys. Suppl.* **191**, 172–181 (2011)
41. S. Plimpton, Fast parallel algorithms for short-range molecular dynamics. *J. Comput. Phys.* **117**, 1–19 (1995)
42. J. Portillo, Y. Diao, R. Scharein, J. Arsuaga, M. Vazquez, On the mean and variance of the writhe of random polygons. *J. Phys. A Math. Theor.* **44**, 275004 (2011)
43. J. Przytycki, P. Traczyk, Conway algebras and skein equivalence of links. *Proc. Amer. Math. Soc.* **100**, 744–48 (1987)
44. M. Pütz, K. Kremer, What is the entanglement length in a polymer melt? *Europhys. Lett.* **49**, 735–741 (2000)
45. E.J. Rawdon, J.C. Kern, M. Piatek, P. Plunkett, A. Stasiak, K.C. Millett, Effect of knotting on the shape of polymers. *Macromolecules* **41**, 8281–8287 (2008)
46. M. Rubinstein, R. Colby, *Polymer Physics* (Oxford University Press, 2003)
47. S. Shanbhag, M. Kröger, Primitive path networks generated by annealing and geometrical methods: Insights into differences. *Macromolecules* **40**, 2897 (2007)
48. S.K. Sukumaran, G.S. Grest, K. Kremer, R. Everaers, Identifying the primitive path mesh in entangled polymer liquids. *R. J. Polym. Sci. B Polym. Phys.* 43:917–933 (2005)
49. J.I. Sulkowska, E.J. Rawdon, K.C. Millett, J.N. Onuchic, A. Stasiak, Conservation of complex knotting and slipknotting in patterns in proterins. *PNAS* **109**, E1715 (2012)
50. C. Tzoumanekas, F. Lahmar, B. Rousseau, D.N. Theodorou, Topological analysis of linear polymer melts: a statistical approach. *Macromolecules* **42**, 7474 (2009)
51. C. Tzoumanekas, D.N. Theodorou, Topological analysis of linear polymer melts: a statistical approach. *Macromolecules* **39**, 4592–4604 (2006)

Topological Surgery in the Small and in the Large



Stathis Antoniou, Louis H. Kauffman and Sofia Lambropoulou

Abstract We directly connect topological changes that can occur in mathematical three-space via surgery, with black hole formation, the formation of wormholes and new generalizations of these phenomena. This work widens the bridge between topology and natural sciences and creates a new platform for exploring geometrical physics.

Keywords Topological surgery · Topological process · Three-space · Three-sphere · Three-manifold · Handle · Poincaré dodecahedral space · Knot theory · Natural phenomena · Natural processes · Dynamics · Reconnection · Morse theory · Mathematical model · Falaco solitons · Black holes · Wormholes · Einstein-Rosen bridge · Cosmic string · Quantum gravity · Cosmology · ER=EPR · Entanglement · DNA recombination · Biology

2010 Mathematics Subject Classification 57M25 · 57R65 · 83F05

S. Antoniou (✉) · S. Lambropoulou
School of Applied Mathematical and Physical Sciences, National Technical
University of Athens, Athens, Greece
e-mail: santoniou@math.ntua.gr

S. Lambropoulou
e-mail: sofia@math.ntua.gr

L. H. Kauffman
Department of Mathematics, Statistics, and Computer Science,
University of Illinois at Chicago, Chicago, IL, USA
e-mail: kauffman@uic.edu

Department of Mechanics and Mathematics, Novosibirsk State University,
Novosibirsk, Russia

© Springer Nature Switzerland AG 2019
C. C. Adams et al. (eds.), *Knots, Low-Dimensional Topology
and Applications*, Springer Proceedings in Mathematics & Statistics 284,
https://doi.org/10.1007/978-3-030-16031-9_22

1 Introduction

The universe undergoes topological and geometrical changes at all scales. This paper goes to the foundations of these changes by offering a novel topological perspective. The common features of these changes are described via topological surgery, a manifold-changing process which has been used in the study and classification of manifolds. We briefly address small and large scale phenomena exhibiting 1 and 2-dimensional surgery and then focus on large scale cosmic phenomena exhibiting 3-dimensional surgery. More precisely, we describe the formation of black holes and wormholes. Our surgery approach allows the formation of a black hole from the collapse of a knotted cosmic string, without ending up in a singular manifold. It further describes Einstein-Rosen bridges (wormholes) linking the two black holes through a singularity where the disconnected black holes collapse to each other, and the bridge is born topologically. The collapse of a cosmic string can be viewed as an orchestrated creation of bridges that is topologically equivalent to 3-dimensional surgery. We present a rich family of 3-manifolds that can occur and the possible implications of these constructions in quantum gravity and general relativity.

2 The Topological Process of Surgery

Topological surgery is a mathematical technique introduced by Wallace [1] and Milnor [2] which creates new manifolds out of known ones in a controlled way. Given an m -manifold M , an m -dimensional n -surgery consists of removing a thickened sphere $S^n \times D^{m-n}$ and gluing back another thickened sphere $D^{n+1} \times S^{m-n-1}$ using a gluing homeomorphism along the common boundary $S^n \times S^{m-n-1}$, see [3] for details. This operation produces a new m -manifold M' which may, or may not, be homeomorphic to M . Since $(S^n \times D^{m-n}) \cup (D^{n+1} \times S^{m-n-1}) = \partial(D^{n+1} \times D^{m-n}) \cong D^{m+1}$, an m -dimensional n -surgery can be seen as the process of passing from one boundary component of handle D^{m+1} to the other. The extra dimension of the $(m + 1)$ -dimensional handle leaves room for continuously passing from one boundary component of the handle to the other.

For example, the process of 1-dimensional 0-surgery shown in Fig. 1(1) removes the 1-dimensional thickening of a 0-sphere (represented by the two red points) and

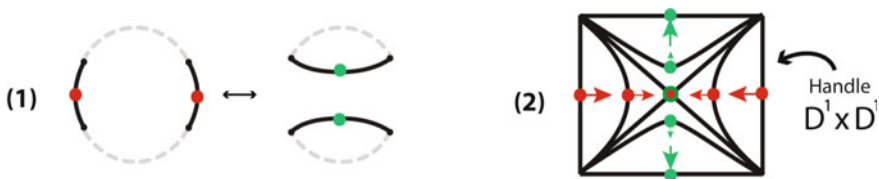


Fig. 1 (1) 1-dimensional surgery (2) 2-dimensional handle

replaces it with the thickening of another 0-sphere (represented by the two green points). Starting with the circle $M = S^1$, this process produces two circles $M' = S^0 \times S^1$. This global change of topology is induced by the local process of collapsing the cores of two segments (the two red points) and uncollapsing the core of the other two segments (the two green points), see Fig. 1(2). As also shown in the figure, this local process happens within a 2-dimensional handle $D^1 \times D^1$. One can provide an algebraic description of this dynamic process by using the local form of a Morse function, see Lemma 2.19 of [3]. For instance, in dimension 1, the local process is described by varying parameter t of the level curves $-x^2 + y^2 = t$ in the range $t \in (-1, 1)$.

3 Small Scale Surgery in Nature

We will briefly present some natural phenomena exhibiting topological surgery in dimensions 1 and 2. All these phenomena happen in small scales, meaning that their characteristic lengths range from the size of a molecule to a few meters.

The process of 1-dimensional surgery is exhibited in various natural phenomena where segments are detached and rejoined such as the crossing over of chromosomes during meiosis, viscous vortex reconnection and site-specific DNA recombination. These phenomena have been detailed in [4–6] where we show that although they are quite different, they undergo a similar topological change which is described using our surgery approach.

If the initial manifold is an embedding of the circle, 1-dimensional 0-surgery can create or destroy a crossing hence producing new knots or links. For example, starting with the circular DNA molecule of Fig. 2, with the help of certain enzymes, site-specific recombination performs a 1-dimensional 0-surgery on the molecule and produces the Hopf link.

Nature is filled with 2-dimensional surgeries too, see [4–6] for details. Examples comprise gene transfer in bacteria, where the donor cell produces a connecting tube called a ‘pilus’ which attaches to the recipient cell, the biological process of mitosis, where a cell splits into two new cells, and the formation Falaco Solitons. We will describe how surgery is exhibited in Falaco Solitons, the dynamics of which are visible to the naked eye. Each Falaco soliton consists of a pair of contra-rotating indentations in the water-air surface of a swimming pool, see Fig. 3(1) and [7]. From the topological viewpoint the surgery consists in taking disk neighborhoods of two points $S^0 \times D^2$ (the indentations in Fig. 3(1)) and joining them via a tube (which is

Fig. 2 DNA recombination as an example of 1-dimensional 0-surgery

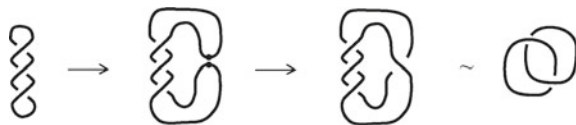
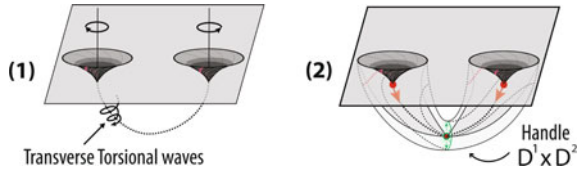


Fig. 3 (1) Falaco topological defects (2) 3-dimensional handle



a thickened circle $D^1 \times S^1$), see Fig. 3(2). Here the tube is the cylindrical vortex made from the propagation of the torsional waves around the singular thread. The 3-dimensional handle containing all the 2-dimensional temporal ‘slices’ of this process is shown Fig. 3(2).

4 Large Scale Surgery in Nature

Large scale phenomena can also exhibit 1- or 2-dimensional surgery. For instance, 1-dimensional surgery happens in magnetic reconnection, the phenomena whereby cosmic magnetic field lines from different magnetic domains are spliced to one another, changing their pattern of conductivity with respect to the sources, see [4] for details. Moving up to 3-dimensional surgery, we have two types of surgery, both of which require four dimensions to be visualized. As we will see, both types describe large scale cosmic phenomena. The first type is exhibited in the creation of entangled black holes while the second one describes the formation of black holes from cosmic strings.

4.1 Types of 3-Dimensional Surgery

Starting with a 3-manifold M , we first have the 3-dimensional 0-surgery, whereby two 3-balls $S^0 \times D^3$ are removed from M and are replaced in the closure of the remaining manifold by a thickened sphere $D^1 \times S^2$:

$$\chi(M) = \overline{M \setminus h(S^0 \times D^3)} \cup_h (D^1 \times S^2)$$

Next, for $m = 3$ and $n = 2$, we have the 3-dimensional 2-surgery, which is the reverse (dual) process of 3-dimensional 0-surgery. Hence we will not consider it a different type of 3-dimensional surgery.

Finally, for $m = 3$ and $n = 1$, we have the 3-dimensional 1-surgery, whereby a solid torus $S^1 \times D^2$ is removed from M and is replaced by another solid torus

$D^2 \times S^1$ (with the factors now reversed) via a homeomorphism h of the common boundary:

$$\chi(M) = \overline{M \setminus h(S^1 \times D^2)} \cup_h (D^2 \times S^1)$$

This type of surgery is clearly self-dual.

4.2 3-Dimensional 0-Surgery and Entangled Black Holes

The process of 3-dimensional 0-surgery joins the spherical neighborhoods of two points via a tube $D^1 \times S^2$ which is one dimension higher than the one shown in Fig. 3(2). If we consider that our initial manifold is the 3-dimensional spatial section of the 4-dimensional spacetime, this tube is what physicists call a wormhole. A connection between Falaco solitons and wormholes has been conjectured by Kiehn [8]. Our surgery description reinforces this connection. Moreover, this change of topology, which, according to J. A. Wheeler, results from quantum fluctuations at the Planck scale [9], can now also be viewed as a result of a ‘classical’ continuous topological change of 3-space.

Let us now consider the $ER = EPR$ hypothesis of Susskind [10], which says that a wormhole is equivalent to the quantum entanglement of two concentrated masses that each forms its own black hole. Adding this hypothesis to our description, the two sites in space are the singularities of the two black holes, shown in red in Fig. 4(1), which will not collapse individually but will become the ends of the wormhole, shown in green in Fig. 4(1). We cannot visualize this process directly but it can be understood by considering that the green arc is the core D^1 of the higher dimensional handle $D^1 \times D^3$ for the wormhole. Note that an observer in our initial 3-space M^3 would not be able to detect the topological change, which occurs across the event horizons.

4.3 3-Dimensional 1-Surgery and Cosmic String Black Holes

The other type of 3-dimensional surgery describes a more subtle topological change. It collapses a solid torus (which is a thickened circle) to a point and uncollapses another solid torus in such way that the meridians are glued to the longitudes and

Fig. 4 (1) Pair of entangled black holes (2) String of entangled black holes

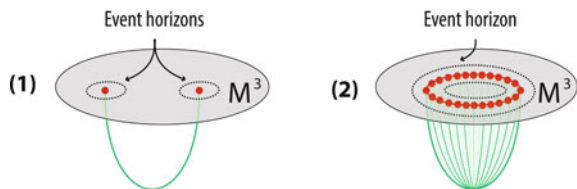
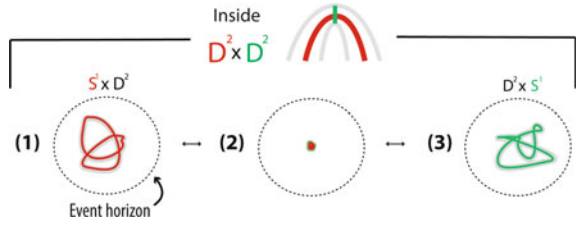


Fig. 5 3-dimensional 1-surgery inside the event horizon



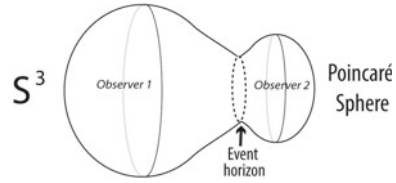
vice-versa. This type of surgery is also called ‘knot surgery’ as the circle can be a knot. Knot surgery is an ideal candidate for describing black holes that are formed via the collapse of cosmic strings. This idea is based on [11] where S.W. Hawking estimates that a fraction of cosmic string loops can collapse to a small size inside their Schwarzschild radius. As cosmic strings are hypothetical topological defects of small (but non-zero) diameter, a cosmic string loop can be considered as a knotted solid torus. As described in [11], the loop collapses to a point thus creating a black hole the center of which contains the singularity. At that point, the 3-space becomes singular, see the passage from Fig. 5(1) to Fig. 5(2).

Our surgery description says more [12]. According to it the process doesn’t stop at the singularity, but continues with the uncollapsing of another cosmic string loop from the singularity, see Fig. 5(3). Thus, the creation of a cosmic string black hole is a 3-dimensional 1-surgery that continuously changes the initial 3-space to another 3-manifold. The process goes through the singular point of the black hole without having a singular manifold in the end. Instead, one ends up with a topologically new universe with a local topology change in the 3-space, which happens within the event horizon.

This type of surgery is also related to the $ER = EPR$ hypothesis. Consider a cosmic string made of pairs of entangled concentrated masses. When each pair of masses collapse, they become connected by a wormhole as previously shown in Fig. 4(1). Given that all these pairs of masses have started on the same cosmic string, the distinct wormholes merge and the entire collection of wormhole cores (the green arcs in Fig. 4(1)) forms a 2-disc D^2 , see Fig. 4(2), which is the core of the higher dimensional handle $D^2 \times D^2$ containing the temporal ‘slices’ of the process. Our surgery description generalizes having a separate Einstein-Rosen bridge for each pair of black holes and amalgamates these bridges to form a new manifold in three dimensions. The effect of surgery is that, from any black hole location on the cosmic string to any other, there is a ‘bridge’ through the new 3-manifold. As this process joins the neighborhood of a circle instead of two points, one can rotate Fig. 4(1) to receive Fig. 4(2).

Another advantage of knot surgery is that it is able produce a great variety of 3-manifolds. In fact, according to a theorem by Wallace [1] and Lickorish [13]

Fig. 6 Observer 1 in S^3 and Observer 2 in the Poincaré dodecahedral space



knot surgery can create all closed, connected, orientable 3-manifolds. One such 3-manifold, which is of great interest to physicists, is the Poincaré dodecahedral space, that has been proposed as possible shape for the geometric universe [14–16]. This manifold can be obtained by doing knot surgery on the trefoil knot (with the right framing, see [17]). Did the shape of the universe come about via the collapse of a trefoil cosmic string?!

Suppose there are observers in an initial spherical universe $M^3 = S^3$ containing a trefoil cosmic string. After surgery, a ‘mathematical’ observer would be able to see the Poincaré dodecahedral space and detect the topology change. However, a physical observer, who is subject to the restrictions of physical laws, would only see towards the event horizon in which the trefoil cosmic string has collapsed. Let us call this observer, *Observer 1*, see Fig. 6. After surgery, *Observer 1* would see the same universe S^3 , the only change being the formation of the event horizon. On the other side of the event horizon, a new universe emerges in which new observers might evolve. Such an observer, say *Observer 2*, will see a Poincaré dodecahedral space and the event horizon from the other side, unaware that the original S^3 universe is behind it, see Fig. 6. Finding the Poincaré dodecahedral space (or some other non-trivial 3-manifold) in our universe may indicate that we are observers that evolved inside the event horizon of a collapsed trefoil cosmic string (or some other cosmic string).

5 Conclusion

The surgery approach provides continuous paths to wormhole and cosmic string black hole formation. If one adds the $ER = EPR$ hypothesis, surgery also describes the entanglement of a pair or a string of black holes. Our topological perspective offers a process producing black holes and new non-singular 3-manifolds from cosmic strings, binding entanglement and the connectivity of space with the rich structure of three- and four-dimensional manifolds.

Acknowledgements Kauffman’s work was supported by the Laboratory of Topology and Dynamics, Novosibirsk State University (contract no. 14.Y26.31.0025 with the Ministry of Education and Science of the Russian Federation).

References

1. A.H. Wallace, Modifications and cobounding manifolds. *Canad. J. Math.* **12**, 503–528 (1960)
2. J. Milnor, A procedure for killing the homotopy groups of differentiable manifolds. *Symposia in Pure Math. Amer. Math. Soc.* **3**, 39–55 (1961)
3. A. Ranicki, *Algebraic and Geometric Surgery* (Clarendon Press, Oxford Mathematical Monographs, 2002)
4. S. Antoniou, S. Lambropoulou, Extending topological surgery to natural processes and dynamical systems. *PLoS one* **12**(9). <https://doi.org/10.1371/journal.pone.0183993> (2017)
5. S. Antoniou, *Mathematical Modeling Through Topological Surgery and Applications*. Springer Theses Book Series. Springer International Publishing. <https://doi.org/10.1007/978-3-319-97067-7> (2018)
6. S. Antoniou, S. Lambropoulou, Topological Surgery in Nature. Book ‘Algebraic Modeling of Topological and Computational Structures and Applications’, Springer Proceedings in Mathematics and Statistics, vol. 219. <https://doi.org/10.1007/978-3-319-68103-0>(2017)
7. R.M. Kiehn, Non-equilibrium systems and irreversible processes—adventures in applied topology, vol. 1—Non equilibrium thermodynamics, pp. 147, 150 University of Houston Copyright CSDC Inc. (2013)
8. R.M. Kiehn, F. Solitons, *Cosmic Strings in a Swimming Pool*. Preprint (2001). <http://arxiv.org/pdf/gr-qc/0101098v1>
9. J.A. Wheeler, On the nature of quantum geometrodynamics. *Ann. Phys.* **2**, 604–614 (1957). [https://doi.org/10.1016/0003-4916\(57\)90050-7](https://doi.org/10.1016/0003-4916(57)90050-7)
10. L. Susskind, Copenhagen vs Everett, Teleportation, and ER = EPR. *Fortschr. Phys.* **64**(6–7), 551–564 (2016). <https://doi.org/10.1002/prop.201600036>
11. S.W. Hawking, Black holes from cosmic strings. *Phys. Lett. B* **231**(237) [https://doi.org/10.1016/0370-2693\(89\)90206-2](https://doi.org/10.1016/0370-2693(89)90206-2) (1989)
12. S. Antoniou, L.H. Kauffman, S. Lambropoulou, *Topological surgery in cosmic phenomena* (in preparation)
13. W.B.R. Lickorish, A representation of orientable combinatorial 3-manifolds, *Ann. of Math.* **2**(76), 531–540 (1962)
14. J.R. Weeks, *The Shape of Space* (CRC Press, 2001)
15. J.-P. Luminet, J.R. Weeks, A. Riazuelo, R. Lehoucq, J.-P. Uzan, Dodecahedral space topology as an explanation for weak wide-angle temperature correlations in the cosmic microwave background. *Nature* **425**, 593–595 (2003)
16. J. Levin, Topology and the cosmic microwave background. *Phys. Rep.* **365**, 251–333 (2002)
17. V.V. Prasolov, A.B. Sossinsky, Knots, links, braids and 3-manifolds. *AMS Transl. Math. Monogr.* **154**, (1997)

Conference Program

Saturday 16 July

16:00–21:00 Arrivals

Sunday 17 July

07:30–08:30 Breakfast

08:45–12:30 Registration

12:45–13:45 Lunch

16:00–17:10 Arrivals/Registration

Amphitheatre D. Vikelas

17:15–17:45 Welcomes

17:45–18:15 Dionyssis Gangas

The International Olympic Academy and the dissemination of the Olympic values

18:15–18:45 Sofia Lambropoulou

Homage to Christos Papakyriakopoulos

18:50–19:35 **Link invariants:** Vaughan F.R. Jones

Knots and links from the Thompson groups

19:40–21:00 Welcome Reception

Monday 18 July

07:30–08:30 Breakfast

Plenary talks: Amphitheatre D. Vikelas

- 08:45–09:30 **Virtual Knot Theory:** Louis H. Kauffman
Invariants in Virtual Knot Theory
- 09:45–10:30 **Geometry of knots and manifolds:** Colin Adams
Multi-crossing number of knots and relations with other invariants
- 10:30–11:00 Coffee break

Session 1: Amphitheatre D. Vikelas

- 11:00–11:40 **Geometry of knots and manifolds:** Joshua Howie
A characterisation of alternating knot exteriors
- 11:55–12:35 **Geometry of knots and manifolds:** Effie Kalfagianni
Geometric estimates from knot spanning surfaces
- 12:45–13:45 Lunch
- 16:00–16:20 **Geometry of knots and manifolds:** Nikolay Abrosimov
Volumes of polyhedra related with links and knots
- 16:25–16:45 **Geometry of knots and manifolds:** Evgeny Fominykh
Complexity of virtual 3-manifolds
- 16:50–17:10 **Geometry of knots and manifolds:** Stefanos Gialamas
Determining Vanishing Massey Triple Products in the Complement of a Link with more than two components
- 17:15–17:35 **Geometry of knots and manifolds:** Catherine Gille
Klein branched covers of spatial trivalent graphs and surgery
- 17:35–18:00 Coffee break
- 18:00–18:20 **Geometry of knots and manifolds:** Delphine Moussard
Finite type invariants of rational homology 3-spheres
- 18:25–18:45 **Geometry of knots and manifolds:** Tom Needham
The Geometry of the Shape Space of Framed Loops
- 18:50–19:10 **Geometry of knots and manifolds:** Joao M. Nogueira
Knot complement with all possible meridional essential surfaces

Session 2: Conference Hall Otto Szymiczek

- 11:00–11:40 **Invariants of knots in 3-manifolds/Skein modules:** Thang Le
Triangular decomposition of skein algebras and quantum Teichmuller spaces
- 11:55–12:35 **Invariants of knots in 3-manifolds/Skein modules:** Uwe Kaiser
Skein theory of links in hyperbolic 3-manifolds
- 12:45–13:45 Lunch
- 16:00–16:40 **Invariants of knots in 3-manifolds/Skein modules:** Hugh Morton
A skein theoretic model for the double affine Hecke algebras
- 16:50–17:10 **Invariants of knots in 3-manifolds/Skein modules:** Ioannis Diamantis
On the Homflypt skein module of the lens spaces $L(p, 1)$ via braids

- 17:15–17:35 **Invariants of knots in 3-manifolds/Skein modules:** Boštjan Gabrovšek
Knots in Seifert Fibered Spaces
- 17:35–18:00 Coffee break
- 18:00–18:20 **Invariants of knots in 3-manifolds/Skein modules:** Enrico Manfredi
Diffeomorphic vs isotopic knots in lens spaces
- 18:25–18:45 **Invariants of knots in 3-manifolds/Skein modules:** Alessia Cattabriga
Representations and invariants of links in lens spaces

Session 3: Conference Room C. Diem

- 11:00–11:40 **Braids:** Jinseok Cho
Cluster algebra on the braids
- 11:55–12:35 **Braids:** Mauro Spera
Geometry of unitary Riemann surface braid group representations and Laughlin-type wave functions
- 12:45–13:45 Lunch
- 16:00–16:40 **Braids:** Vladimir Vershinin
Brunnian and Cohen braids and Lie algebras
- 16:50–17:10 **Braids:** Usman Ali
On the Gröbner-Shirshov basis of 3-braids
- 17:15–17:35 **Braids:** Zaffar Iqbal
Hilbert series of right-angled affine Artin monoids $M(\tilde{A}_n^\infty)$
- 17:35–18:00 Coffee break
- 18:00–18:20 **Braids:** Joseph Ricci
Congruence subgroups and low-dimensional representations of the braid group B_3
- 19:15–20:00 Poster session
- 20:00–21:00 Dinner

Tuesday 19 July

- 07:30–08:30 Breakfast

Plenary talks: Amphitheatre D. Vikelas

- 08:45–09:30 **Geometry of knots and manifolds:** Cameron Gordon
Left-orderability and cyclic branched covers of knots
- 09:45–10:30 **Khovanov homology and categorification:** Radmila Sazdanovic
Khovanov homology: an introduction
- 10:30–11:00 Coffee break

- 11:00–11:40 **Knot algebras/Link invariants:** Sofia Lambropoulou
A new skein invariant for classical links from the Yokonuma–Hecke algebras

Session 1: Amphitheatre D. Vikelas

- 11:55–12:35 **4-dimensional topology:** Anthony Bosman
Shake Slice and Shake Concordant Links
- 12:45–13:45 Lunch
- 16:00–16:40 **4-dimensional topology:** Samuel J. Lomonaco
The Geometry of the Fox Free Calculus with Applications to Higher Dimensional Knot Theory
- 16:50–17:10 **4-dimensional topology:** Celeste Damiani
Alexander invariants for ribbon tangles
- 17:15–17:35 **Geometry of knots and manifolds:** Shawn Rafalski
Volume bounds for certain hyperbolic 3-orbifolds
- 17:35–18:00 Coffee break
- 18:00–18:20 **Geometry of knots and manifolds:** António Salgueiro
Actions of 3-manifolds with the same quotient
- 18:25–18:45 **Geometry of knots and manifolds:** Anastasiia Tsvietkova
The number of surfaces of fixed genus in an alternating link complement
- 18:50–19:10 **Geometry of knots and manifolds:** Christine Ruey Shan Lee
The colored Jones polynomial and slopes of pretzel knots
- 19:15–19:35 **Geometry of knots and manifolds:** Byunghee An
Chekanov–Eliashberg DGAs for singular Legendrian knots

Session 2: Conference Hall Otto Szymiczek

- 11:55–12:35 **Knot algebras/Link invariants:** Mikami Hirasawa
Interlacing zeros of Alexander polynomials of links
- 12:45–13:45 Lunch
- 16:00–16:20 **Knot algebras/Link invariants:** Dimos Goundaroulis
A new 2-variable generalization of the Jones polynomial
- 16:25–16:45 **Knot algebras/Link invariants:** Fathi Ben Aribi
Detecting knots with the L_2 -Alexander invariant
- 16:50–17:10 **Knot algebras/Link invariants:** Nafaa Chbili
Polynomial invariants of Quasi-Alternating links
- 17:15–17:35 **Knot algebras/Link invariants:** Zhiqing Yang
Multi-skein equation knot invariant
- 17:35–18:00 Coffee break
- 18:00–18:20 **Virtual Knot Theory:** Neslihan Güğümçü
How to estimate the height of a knotoid
- 18:25–18:45 **Knot algebras/Link invariants:** Hwa Jeong Lee
On the arc index of Kanenobu knots

- 18:50–19:10 **Knot algebras/Link invariants:** John Bryden
Abelian quantum knot Invariants
- 19:15–19:35 **Knot algebras/Link invariants:** Alexander Stoimenow
On coefficients and roots of the Alexander-Conway polynomial

Session 3: Conference Room C. Diem

- 11:55–12:35 **Khovanov homology and categorification:** Alexander Shumakovitch
Knot invariants arising from homological operations on Khovanov homology
- 12:45–13:45 Lunch
- 16:00–16:20 **Khovanov homology and categorification:** Dan Scofield
Torsion in Khovanov link homology via chromatic graph cohomology
- 16:25–16:45 **Khovanov homology and categorification:** Marithania Silvero
Studying torsion of extreme Khovanov homology
- 16:50–17:10 **Khovanov homology and categorification:** Hoel Queffelec
HOMFLY-PT and Alexander polynomials from a doubled Schur algebra
- 17:15–17:35 **Khovanov homology and categorification:** Abdul Rauf Nizami
Khovanov Homology of the Braid Link $x_1x_2x_1 \dots$
- 17:35–18:00 Coffee break
- 18:00–18:20 **Braids:** Matthieu Calvez
Towards an algebraic Nielsen-Thurston classification of braids
- 18:25–19:05 **Topological spaces:** Ruth Lawrence
Explicit DGLA models of simple chain complexes and their properties
- 19:30–20:00 Poster session
- 20:00–21:00 Dinner

Wednesday 20 July

- 07:30–08:30 Breakfast

Plenary talks: Amphitheatre D. Vikelas

- 08:45–09:30 **Knot algebras/Link invariants:** Dror Bar-Natan
The brute and the hidden paradise
- 09:45–10:30 **Knots in Nature—Physical Sciences:** Kenneth C. Millett
Random sampling spaces of thick polygons
- 10:30–11:00 Coffee break

Session 1: Amphitheatre D. Vikelas

- 11:00–11:40 **Khovanov homology and categorification:** Anna Beliakova
Quantum Link Homology via Trace Functor
- 11:55–12:35 **Khovanov homology and categorification:** Paul Wedrich
Some differentials on colored Khovanov-Rozansky link homology

Session 2: Conference Hall Otto Szymiczek

- 11:00–11:40 **Virtual Knot Theory:** Valeriy Bardakov
Some representations of virtual braid group
- 11:55–12:35 **Virtual Knot Theory:** Paolo Bellingeri
Local moves for welded knotted objects
- 12:45–13:45 Lunch
- 14:00–20:00 Excursion: sightseeing at the Kaiafas lake and thermal springs & swimming at the beach of Zaharo
- 20:00–21:00 Dinner

Thursday 21 July

- 07:30–08:30 Breakfast

Plenary talks: Amphitheatre D. Vikelas

- 08:45–09:30 **TQFTs and the volume conjecture:** Stavros Garoufalidis
Nahm sums, the Bloch group and quantum topology
- 09:45–10:30 **Distributive structures and Yang-Baxter homology:** Jozef H. Przytycki
Knot Theory: from Fox 3-colorings of links to Yang-Baxter homology
- 10:30–11:00 Coffee break

Session 1: Amphitheatre D. Vikelas

- 11:00–11:40 **Knots in Nature—Physical Sciences:** Renzo L. Ricca
Knots cascade detected by a monotonically decreasing sequence of HOMFLYPT values
- 11:55–12:35 **Knots in Nature—Physical Sciences:** Mark Dennis
Knotted Vortices in Light
- 12:45–13:45 Lunch
- 15:00–15:20 **Knots in Nature—Physical Sciences:** Benjamin Bode
Knotted fields and real algebraic links
- 15:25–15:45 **Knots in Nature—Physical Sciences:** David Foster
Knotted Resonances
- 15:50–16:30 **Knots in Nature—Physical Sciences:** Rafal Komendarczyk
Ropelength, crossing number and finite-type invariants

- 16:35–17:00 Coffee break
- 17:00–17:20 **Knots in Nature—Physical Sciences:** Stathis Antoniou
The dynamics of topological surgery
- 17:25–17:45 **Knots in Nature—Physical Sciences:** Xin Liu
On the derivation of HOMFLYPT as a new invariant of topological fluid mechanics
- 17:50–18:10 **Knots in Nature—Physical Sciences:** Ljubica S. Velimirovic
Infinitesimal bending of knots
- 18:15–18:35 **Invariants of knots in 3-manifolds/Skein modules:** Dimitrios Kodokostas
Algebras of Hecke type on the mixed braid group with two fixed strands

Session 2: Conference Hall Otto Szymiczek

- 11:00–11:40 **Distributive structures and Yang-Baxter homology:** Masahico Saito
Topological quandles and cocycle knot invariants
- 11:55–12:35 **Distributive structures and Yang-Baxter homology:** Takefumi Nosaka
Twisted cohomology pairings of knots
- 12:45–13:45 Lunch
- 15:00–15:20 **Distributive structures and Yang-Baxter homology:** Jim Hoste
Knots with finite n -quandles
- 15:25–15:45 **Distributive structures and Yang-Baxter homology:** Seung Yeop Yang
Annihilation of rack and quandle homology groups of finite quandles
- 15:50–16:10 **Distributive structures and Yang-Baxter homology:** Witold Rosicki
Cocycle invariants of codimension 2 embeddings of manifolds
- 16:15–16:35 **Distributive structures and Yang-Baxter homology:** Xiao Wang
Equivalence of two definitions of set-theoretic Yang-Baxter homology
- 16:35–17:00 Coffee break
- 17:00–17:20 **Distributive structures and Yang-Baxter homology:** Sam Nelson
Biquandle Brackets
- 17:25–17:45 **Distributive structures and Yang-Baxter homology:** Seonmi Choi
On quandle homology groups of finite quandles
- 17:50–18:10 **Distributive structures and Yang-Baxter homology:** Sujoy Mukherjee
The role of associativity in the homology of self-distributive algebraic structures

- 18:15–18:35 **Distributive structures and Yang-Baxter homology:** Byeorhi Kim
On decomposition of finite quandles

Session 3: Conference Room C. Diem

- 11:00–11:40 **TQFTs and the volume conjecture:** Christian Blanchet
Modified trace on quantum $sl(2)$ and logarithmic invariants
- 11:55–12:35 **Khovanov homology and categorification:** Piotr Sulkowski
Knot invariants and BPS states
- 12:45–13:45 Lunch
- 15:00–15:40 **TQFTs and the volume conjecture:** Hitoshi Murakami
Colored Jones polynomial and $SL(2;C)$ representations of a knot group
- 15:50–16:10 **TQFTs and the volume conjecture:** Tian Yang
Volume Conjectures for Reshetikhin-Turaev and Turaev-Viro invariants
- 16:15–16:35 **TQFTs and the volume conjecture:** Renaud Detcherry
Curve operators in TQFT as Toeplitz operators
- 16:35–17:00 Coffee break
- 17:00–17:20 **TQFTs and the volume conjecture:** Wade Bloomquist
Asymptotic Faithfulness of Quantum $SU(3)$ Representations
- 17:25–17:45 **Knots in Nature—Life Sciences:** Pawel Dabrowski-Tumanski
Topology of proteins with complex lasso structure
- 17:50–18:10 **Knots in Nature—Life Sciences:** Candice Price
A Discussion on the Tangle Model: An Application of Topology
- 18:15–18:35 **Knots in Nature—Life Sciences:** Alexander Taylor
Virtual knotting expressed in proteins
- 20:00–21:00 Conference Dinner
- 21:00–23:00 Greek dances—Music & Party

Friday 22 July

- 07:30–08:30 Breakfast

Plenary talks: Amphitheatre D. Vikelas

- 08:45–09:30 **Knots in Nature—Life Sciences:** Neil Osheroff
Recognition of DNA Topology by Topoisomerases
- 09:45–10:30 **Knots in Nature—Physical Sciences:** Dmitry Sokoloff
Classical helicity and higher helicity invariants in astrophysical dynamos
- 10:30–11:00 Coffee break

Session 1: Amphitheatre D. Vikelas

- 11:00–11:40 **Knots in Nature—Life Sciences:** Lynn Zechiedrich
Effect of DNA Supercoiling on DNA Dynamics
- 11:55–12:35 **Knots in Nature—Life Sciences:** Joanna Sulkowska
Entanglement in proteins: knots, slipknots and lassos

Session 2: Conference Hall Otto Szymiczek

- 11:00–11:40 **Knots in Nature—Physical Sciences:** Philipp Reiter
Elastic knots
- 11:55–12:35 **Topological spaces:** Andrey Mikhovich
Schematization, QR-presentations and Conjuring(s)
- 12:45–13:45 Farewell Lunch
- 20:00–21:00 Dinner

Saturday 23 July

- 07:00–12:00 Departures

List of Participants

Nikolay Abrosimov

Sobolev Institute of Mathematics, Russia

E-mail: abrosimov@math.nsc.ru

Colin Adams

Williams College, USA

E-mail: cadams@williams.edu

Usman Ali

CASPAM, Bahauddin Zakariya University Multan, Pakistan

E-mail: usman76swat@yahoo.com

Daniel Amankwah

TU Chemnitz, Germany

E-mail: daniel.amankwah@aims-senegal.org

Byunghee An

Institute for Basic Science, Center for Geometry and Physics, South Korea

E-mail: anbyhee@ibs.re.kr

Cristina Ana-Maria Anghel

Université Paris Diderot, France

E-mail: simple_words91@yahoo.com

Stathis Antoniou

National Technical University of Athens, Greece

E-mail: stathis.antoniou@gmail.com

Dror Bar-Natan

University of Toronto, Canada

E-mail: drorbn@math.toronto.edu

Valeriy Bardakov

Sobolev Institute of Mathematics, Russia

E-mail: bardakov@math.nsc.ru

Anna Beliakova

Universität Zürich, Switzerland

E-mail: anna@math.uzh.ch

Giulio Belletti

Scuola Normale Superiore, Pisa, Italy

E-mail: gbelletti451@gmail.com

Paolo Bellingeri

University of Normandy, Caen, France

E-mail: paolo.bellingeri@unicaen.fr

Fathi Ben Aribi

University of Geneva, Switzerland

E-mail: fathi.benaribi@unige.ch

Sylvia Benvenuti

Università di Camerino, Italy

E-mail: sylvia.benvenuti@unicam.it

Christian Blanchet

IMJ-PRG, Université Paris Diderot, France

E-mail: christian.blanchet@imj-prg.fr

Wade Bloomquist

University of California Santa Barbara, USA

E-mail: bloomquist@math.ucsb.edu

Benjamin Bode

University of Bristol, United Kingdom

E-mail: benjamin.bode@bristol.ac.uk

Anthony Bosman

Rice University, USA

E-mail: anthony.bosman@rice.edu

John Bryden

PMU, Saudi Arabia

E-mail: jmbryden@mac.com

Matthieu Calvez

Universidad de Santiago de Chile USACH, Chile

E-mail: calvez.matthieu@gmail.com

Alessia Cattabriga

University of Bologna, Italy

E-mail: alessia.cattabriga@unibo.it

Mustafa Cengiz

Boston College, USA

E-mail: mustafa.cengiz@bc.edu

Alex Chandler

North Carolina State University, USA

E-mail: alexchandler100@gmail.com

Nafaa Chbili

UAEU, United Arab Emirates

E-mail: nafaachbili@uaeu.ac.ae

Maria Chlouveraki

University of Versailles, France

E-mail: maria.chlouveraki@uvsq.fr

Jinseok Cho

Pohang Mathematics Institute, POSTECH, South Korea

E-mail: dol0425@gmail.com

Sangbum Cho

Hanyang University, South Korea

E-mail: scho2007@gmail.com

Seonmi Choi

Kyungpook National University, South Korea

E-mail: [csm123c@gmail.com](mailto:csml23c@gmail.com)

Bruno Aarón Cisneros de la Cruz

CONACyT—UNAM Oaxaca, Mexico

E-mail: brunoc@matem.unam.mx

Amanda R. Curtis

University of California, Santa Barbara, USA

E-mail: arcurtis@math.ucsb.edu

Pawel Dabrowski-Tumanski

Faculty of Chemistry and Centre of New Technologies, University of Warsaw, Poland

E-mail: p.dabrowski@cent.uw.edu.pl

Celeste Damiani

Université de Caen Normandie, France

E-mail: celeste.damiani@unicaen.fr

Marco De Renzi

Université Paris Diderot, France

E-mail: marco.de-renzi@imj-prg.fr

Mark Dennis

University of Bristol, United Kingdom

E-mail: mark.dennis@bristol.ac.uk

Renaud Detcherry

Michigan State University, USA

E-mail: renaud.detcherry@gmail.com

Ioannis Diamantis

International College Beijing, China Agricultural University, China

E-mail: diamantis@math.ntua.gr

Andrew Fish

University of Brighton, United Kingdom

E-mail: Andrew.fish@brighton.ac.uk

Nathan Fisher

Tufts University, USA

E-mail: nathan.fisher@tufts.edu

Marcelo Flores

Universidad de Valparaiso, Chile

E-mail: marcelo.flores@uv.cl

Evgeny Fominykh

Chelyabinsk State University, Russia

E-mail: efominykh@gmail.com

David Foster

University of Bristol, United Kingdom

E-mail: dave.foster@bristol.ac.uk

David Freund

Dartmouth College, USA

E-mail: dfreund@math.dartmouth.edu

Boštjan Gabrovšek

University of Ljubljana, Faculty of Mathematics and Physics, Slovenia

E-mail: bostjan.gabrovsek@fmf.uni-lj.si

Stavros Garoufalidis

Georgia Institute of Technology, USA

E-mail: stavros@math.gatech.edu

Anne Isabel Gaudreau

McMaster University, Canada

E-mail: gaudreai@mcmaster.ca

Stefanos Gialamas

American Community Schools of Athens, Greece

E-mail: gialamas@acs.gr

Catherine Gille

IMJ-PRG, Université Paris Diderot, France

E-mail: catherine.gille@imj-prg.fr

Dimos Goundaroulis

National Technical University of Athens, Greece

E-mail: dground@mail.ntua.gr

Cameron Gordon

University of Texas at Austin, USA

E-mail: gordon@math.utexas.edu

Neslihan Gügümcü

National Technical University of Athens, Greece

E-mail: nesli@central.ntua.gr

Carl Hammarsten

Lafayette College, USA

E-mail: hammarsc@lafayette.edu

Mikami Hirasawa

Nagoya Institute of Technology, Japan

E-mail: hirasawa.mikami@nitech.ac.jp

Cynthia Hog-Angeloni

Gutenberg University, Mainz, Germany

E-mail: hogangel@uni-mainz.de

Jim Hoste

Pitzer College, Claremont, USA

E-mail: jhoste@pitzer.edu

Joshua Howie

University of Melbourne, Australia

E-mail: josh.howie@gmail.com

Zaffar Iqbal

University of Gurat, Pakistan

E-mail: zaffar.iqbal@uog.edu.pk

Michal Jablonowski

University of Gdańsk, Poland

E-mail: michal.jablonowski@gmail.com

Gyo Taek Jin

KAIST, South Korea

E-mail: trefoil@kaist.ac.kr

Vaughan F.R. Jones

Vanderbilt University, USA

E-mail: vaughan.f.jones@vanderbilt.edu

Jesus Juyumaya

Universidad de Valparaiso, Chile

E-mail: juyumaya@uvach.cl

Uwe Kaiser

Boise State University, USA

E-mail: ukaiser@boisestate.edu

Effie Kalfagianni

Michigan State University, USA

E-mail: kalfagia@math.msu.edu

Konstantinos Karvounis

Universität Zürich, Switzerland

E-mail: konstantinos.karvounis@math.uzh.ch

Louis H. Kauffman

University of Illinois at Chicago, USA

E-mail: kauffman@uic.edu

Ulgen Kilic

Bogazici University, Turkey

E-mail: ulgenklc@gmail.com

Byeorhi Kim

Kyungpook National University, South Korea

E-mail: kbrdooly@naver.com

Dimitrios Kodokostas

National Technical University of Athens, Greece

E-mail: dkodokostas@gmail.com

Rafal Komendarczyk

Tulane University, USA

E-mail: rako@tulane.edu

Andrew Kriker

Nanyang Technological University, Singapore

E-mail: ajkriker@ntu.edu.sg

Yevhen (Evgeniy) Kurianovych

University of Minnesota, Twin Cities, USA

E-mail: kuria014@umn.edu

Sofia Lambropoulou

National Technical University of Athens, Greece

E-mail: sofia@math.ntua.gr

Ruth Lawrence

Hebrew University, Jerusalem, Israel

E-mail: ruthel@ma.huji.ac.il

Thang Le

Georgia Institute of Technology, USA

E-mail: letu@math.gatech.edu

Christine Ruey Shan Lee

University of Texas at Austin, USA

E-mail: clec@math.utexas.edu

Hwa Jeong Lee

Daegu Gyeongbuk Institute of Sciences & Technology, South Korea

E-mail: hjwith@dgist.ac.kr

Sangyop Lee

Chung-Ang University, South Korea

E-mail: sylee@cau.ac.kr

Xin Liu

Beijing University of Technology, China

E-mail: xin.liu@bjut.edu.cn

Samuel J. Lomonaco

University of Maryland Baltimore County (UMBC), USA

E-mail: lomonaco@umbc.edu

Enrico Manfredi

Università di Bologna, Italy

E-mail: enrico.manfredi3@unibo.it

Daniel Mathews

Monash University, Australia

E-mail: Daniel.Mathews@monash.edu

Katie McCallum

University of Brighton, United Kingdom

E-mail: katiemccallum@live.co.uk

Andrey Mikhovich

MSU, Moscow, Russia

E-mail: mikhandr@mail.ru

Kenneth C. Millett

University of California, Santa Barbara, USA

E-mail: millett@math.ucsb.edu

Hugh Morton

University of Liverpool, United Kingdom

E-mail: morton@liverpool.ac.uk

George Moulantzikos

University of Crete, Greece

E-mail: mulangik@gmail.com**Delphine Moussard**

Université de Bourgogne, France

E-mail: Delphine.Moussard@u-bourgogne.fr**Sujoy Mukherjee**

The George Washington University, USA

E-mail: sujoymukherjee@gwu.edu**Hitoshi Murakami**

Tohoku University, Japan

E-mail: starshea@tky3.3web.ne.jp**Tom Needham**

University of Georgia, USA

E-mail: tneedham@math.uga.edu**Sam Nelson**

Claremont McKenna College, USA

E-mail: Sam.Nelson@cmc.edu**Wanda Niemyska**

University of Silesia and University of Warsaw, Poland

E-mail: wniemyska@cent.uw.edu.pl**Abdul Rauf Nizami**

University of Education, Lahore, Pakistan

E-mail: arnizami@ue.edu.pk**Joao M. Nogueira**

University of Coimbra, Portugal

E-mail: joaomdfn@gmail.com**Takefumi Nosaka**

Kyushu University, Japan

E-mail: nosaka@math.kyushu-u.ac.jp**Neil Osheroff**

Vanderbilt University School of Medicine, USA

E-mail: neil.osheroff@vanderbilt.edu**Martin Palmer**

Université Paris 13, France

E-mail: palmer.martin.d@gmail.com**Petros Pantavos**

University of Athens, Greece

E-mail: posidrop@gmail.com**Carlo Petronio**

Università di Pisa, Italy

E-mail: petronio@dm.unipi.it**Candice Price**

University of San Diego, USA

E-mail: candice.r.price@gmail.com

Jozef H. Przytycki

George Washington University, USA & University of Gdansk, Poland

E-mail: przytyck@gwu.edu

Hoel Queffelec

CNRS and U. Montpellier, France

E-mail: hoel.queffelec@umontpellier.fr

Shawn Rafalski

Fairfield University, USA

E-mail: srafalski@fairfield.edu

Philipp Reiter

University of Duisburg-Essen, Germany

E-mail: philipp.reiter@uni-due.de

Alessandra Renieri

University of Camerino, Italy

E-mail: alessandra.renieri@unicam.it

Renzo L. Ricca

U. Milano-Bicocca, Italy

E-mail: renzo.ricca@unimib.it

Joseph Ricci

University of California Santa Barbara, USA

E-mail: ricci@ucsb.edu

Witold Rosicki

University of Gdansk, Poland

E-mail: wrosicki@mat.ug.edu.pl

Masahico Saito

University of South Florida, USA

E-mail: saito@usf.edu

António Salgueiro

University of Coimbra, Portugal

E-mail: ams@mat.uc.pt

Radmila Sazdanovic

North Carolina State University, USA

E-mail: rsazdanovic@math.ncsu.edu

Nancy Scherich

University of California, Santa Barbara, USA

E-mail: nscherich@math.ucsb.edu

Franz Wilhelm Schlöder

University of Heidelberg, Germany

E-mail: franz.schloeder@googlemail.com

Dan Scofield

North Carolina State University, USA

E-mail: dscofie@ncsu.edu

Bruno Sévennec

CNRS, France

E-mail: sevennec@ens-lyon.fr

Alexander Shumakovitch

The George Washington University, USA

E-mail: Shurik@gwu.edu

Marithania Silvero

Universidad de Sevilla, Spain

E-mail: marithania@us.es

Ourania Siskoglou

University of Crete, Greece

E-mail: ourania.nia@gmail.com

Dmitry Sokoloff

Moscow State University and IZMIRAN, Russia

E-mail: sokoloff.dd@gmail.com

Mauro Spera

Dipartimento di Matematica e Fisica Niccolo Tartaglia, Universita Cattolica del Sacro Cuore, Italy

E-mail: mauro.spera@unicatt.it

Petros Stefaneas

National Technical University of Athens, Greece

E-mail: petrosstefaneas@gmail.com

Alexander Stoimenow

Gwangju Institute of Science and Technology, School of General Studies, GIST College, South Korea

E-mail: stoimeno@yahoo.com

Isidoros Strouthos

University College London, United Kingdom

E-mail: i.strouthos@ucl.ac.uk

Charalampos Stylianakis

University of Glasgow, United Kingdom

E-mail: c.stylianakis.1@research.gla.ac.uk

Joanna Sulkowska

University of Warsaw, Faculty of Chemistry and Centre of New Technologies, Poland

E-mail: jsulkows@gmail.com

Piotr Sulkowski

University of Warsaw, Poland & Caltech, USA

E-mail: psulkows@gmail.com

Ryoto Tange

Kyushu University, Japan

E-mail: r-tange@math.kyushu-u.ac.jp

Alexander Taylor

University of Bristol, United Kingdom

E-mail: alexanderjohntaylor@gmail.com

Michel Thomé

SMF and EMS, France

E-mail: michelmthome@free.fr

Anastasiia Tsvietkova

University of California, Davis, USA

E-mail: n.tsvet@gmail.com

Ljubica S. Velimirovic

Faculty of Science and Mathematics, University of Nis, Serbia

E-mail: vljubica@pmf.ni.ac.rs

Vladimir Vershinin

Université de Montpellier, France

E-mail: Vladimir.verchinine@univ-montp2.fr

Xiao Wang

The George Washington University, USA

E-mail: wangxiao@gwmail.gwu.edu

Paul Wedrich

Imperial College London, United Kingdom

E-mail: p.wedrich@gmail.com

Simon Willerton

University of Sheffield, United Kingdom

E-mail: S.Willerton@shef.ac.uk

Seung Yeop Yang

The George Washington University, USA

E-mail: syyang@gwu.edu

Tian Yang

Stanford University, USA

E-mail: yangtian@math.stanford.edu

Zhiqing Yang

Dalian University of Technology, China

E-mail: yangzhq@dlut.edu.cn

Lynn Zechiedrich

Baylor College of Medicine, Houston, Texas, USA

E-mail: elz@bcm.edu